Nanotechnology in the Life Sciences

Muthupandian Saravanan
Hamed Barabadi *Editors*

Cancer Nanotheranostics

Volume 1

Springer

Nanotechnology in the Life Sciences

Series Editor

Ram Prasad
Department of Botany
Mahatma Gandhi Central University
Motihari, Bihar, India

Nano and biotechnology are two of the 21st century's most promising technologies. Nanotechnology is demarcated as the design, development, and application of materials and devices whose least functional make up is on a nanometer scale (1 to 100 nm). Meanwhile, biotechnology deals with metabolic and other physiological developments of biological subjects including microorganisms. These microbial processes have opened up new opportunities to explore novel applications, for example, the biosynthesis of metal nanomaterials, with the implication that these two technologies (i.e., thus nanobiotechnology) can play a vital role in developing and executing many valuable tools in the study of life. Nanotechnology is very diverse, ranging from extensions of conventional device physics to completely new approaches based upon molecular self-assembly, from developing new materials with dimensions on the nanoscale, to investigating whether we can directly control matters on/in the atomic scale level. This idea entails its application to diverse fields of science such as plant biology, organic chemistry, agriculture, the food industry, and more.

Nanobiotechnology offers a wide range of uses in medicine, agriculture, and the environment. Many diseases that do not have cures today may be cured by nanotechnology in the future. Use of nanotechnology in medical therapeutics needs adequate evaluation of its risk and safety factors. Scientists who are against the use of nanotechnology also agree that advancement in nanotechnology should continue because this field promises great benefits, but testing should be carried out to ensure its safety in people. It is possible that nanomedicine in the future will play a crucial role in the treatment of human and plant diseases, and also in the enhancement of normal human physiology and plant systems, respectively. If everything proceeds as expected, nanobiotechnology will, one day, become an inevitable part of our everyday life and will help save many lives.

More information about this series at http://www.springer.com/series/15921

Muthupandian Saravanan • Hamed Barabadi
Editors

Cancer Nanotheranostics

Volume 1

Springer

Editors
Muthupandian Saravanan
AMR and Nanomedicine Lab
Department of Pharmacology
Saveetha Dental College
Saveetha Institute of Medical and
Technical Sciences (SIMATS)
Chennai, India

Hamed Barabadi
Department of Pharmaceutical
Biotechnology, School of Pharmacy,
Shahid Beheshti University
of Medical Science
Tehran, Iran

ISSN 2523-8027 ISSN 2523-8035 (electronic)
Nanotechnology in the Life Sciences
ISBN 978-3-030-74329-1 ISBN 978-3-030-74330-7 (eBook)
https://doi.org/10.1007/978-3-030-74330-7

This Springer imprint is published by the registered company Springer Nature Switzerland AG
The registered company address is: Gewerbestrasse 11, 6330 Cham, Switzerland

Preface

Nanotechnology is an interdisciplinary research field that integrates chemistry, engineering, biology, and medicine. Nanomaterials offer tremendous opportunities as well as challenges for researchers. Of course, cancer is one of the world's most common health problems, responsible for many deaths. Exploring efficient anticancer drugs could revolutionize treatment options and help manage cancer mortality. Nanomedicine plays a significant role in developing alternative and more effective treatment strategies for cancer theranostics. This book mainly focuses on the emerging trends using nanomaterials and nanocomposites as alternative anticancer materials. The book is divided into three main topic areas: how to overcome existing traditional approaches to combat cancer, applying multiple mechanisms to target the cancer cells, and how nanomaterials can be used as effective carriers. The contents highlight recent advances in interdisciplinary research on processing, morphology, structure, and properties of nanostructured materials and their applications to combat cancer.

Cancer Nanotheranostics is comprehensive in that it discusses all aspects of cancer nanotechnology. Because of the vast amount of information, it was decided to split this material into two volumes. In the first volume of Cancer Nanotheranostics, we discuss the role of different nanomaterials for cancer therapy, including lipid-based nanomaterials, protein and peptide-based nanomaterials, polymer-based nanomaterials, metal-organic nanomaterials, porphyrin-based nanomaterials, metal-based nanomaterials, silica-based nanomaterials, exosome-based nanomaterials, and nano-antibodies. In the second volume, we discuss the nano-based diagnosis of cancer, nano-oncology for clinical applications, nano-immunotherapy, nano-based photothermal cancer therapy, nano-erythrosomes for cancer drug delivery, regulatory perspectives of nanomaterials, limitations of cancer nanotheranostics, the

safety of nano-biomaterials for cancer nanotheranostics, multifunctional nanomaterials for targeting cancer nanotheranostics, and the role of artificial intelligence in cancer nanotheranostics.

Mekelle, Ethiopia — Muthupandian Saravanan
Tehran, Iran — Hamed Barabadi

Contents

Chapter 1
Targeted Nanotheranostic Systems in Cancer Therapy

Avneet Kour, Aman Tiwari, Jiban Jyoti Panda, and Jibanananda Mishra

Contents

1.1 Introduction

Cancer is an unconquerable ailment due to its multitudinous characteristics that might be triggered by various endogenous and exogenous factors. It is the second major cause of the mortality worldwide accounting for approximately 9.6 million deaths in 2018, which is prognosticated to exceed cardiac complications, considered to be the major reason for death worldwide (WHO). The predominant cause of cancer-related death worldwide accounts to lung cancer that causes approximately 1.76 million deaths followed by colorectal cancer (862,000 deaths), stomach cancer (783,000 deaths), liver cancer (782,000 deaths), and breast cancer (627,000 deaths). In low- and middle-income countries, approximately 70% of deaths occur due to cancer, and the number of cancer patients is speculated to rise to 21 million by 2030 (WHO; Bhakta-Guha et al., 2015). Cancer causes a huge financial burden due to the economic cost of treatment and palliative concern. The yearly economic cost of cancer in 2015 was estimated to be approximately US$ 100 billion (Herper, 2015).

A. Kour · A. Tiwari · J. J. Panda (✉)
Institute of Nano Science and Technology, Punjab, India
e-mail: jyoti@inst.ac.in

J. Mishra (✉)
AAL Biosciences Research Pvt. Ltd., Haryana, India

M. Saravanan, H. Barabadi (eds.), *Cancer Nanotheranostics*, Nanotechnology in the Life Sciences, https://doi.org/10.1007/978-3-030-74330-7_1

Thus, these demand for the exploration of better, safer, and more efficient therapeutic and diagnostic approaches for combating the disease.

There have been significant advancements in cancer therapy, and various advanced treatment procedures have decreased the number of cancer deaths (Roy Chowdhury et al., 2016). Conventional cancer treatment procedures involve surgery (thoracoscopic, laparoscopic, endoscopic, laser), immunotherapy, chemotherapy, stem cell transplant therapy, and radiotherapy (Howell & Valle, 2015). Chemotherapy combats cancers (lung cancer, sarcoma, breast cancer, myeloma) by the intake of the drugs. Radiotherapy (image-guided, four-dimensional conformal and intensity-modulated) interferes in the progression of various types of cancers (prostate, head, breast, neck) (Bucci et al., 2005). Various cancer immunotherapeutics modulate the immune systems which are responsible for causing the malignancy. However, these treatment approaches suffer from manifold side effects. The current-day treatment approaches for the disease often entail invasive methods and exhibit drug resistance and systemic toxicity.

Apart from therapeutics, various approaches have been developed for the diagnosis of the tumors so that effective therapeutic regimen can be proposed like x-ray, ultrasonography, computed tomography (CT), magnetic resonance imaging (MRI), and nuclear scan. Regardless of the numerous approaches for the diagnosis of cancer, there are still various limitations that need to be addressed before realizing the proper and early detection of the disease. However, ameliorated diagnostic and therapeutic perspectives have increased the survival rate of patients suffering from cancer, but still complete riddance of the disease is improbable. Therefore, it becomes inevitable to explore and find novel approaches to diagnose and treat cancer more effectively. One such novel arena for effective treatment as well as diagnosis of cancer is nanotheranostics.

1.2 Nanotheranostics

A nanoparticle carries great potential in cancer due to their selectivity and tumor-homing approaches. These can be easily surface fabricated with the cancer-targeting ligands, thereby reducing side effects. These have enhanced in vivo circulation duration that reduces the frequency of administration and thus improves patient compliance. Thus, owing to these benefits, nanoparticles are considered as a potential therapeutic platform for the therapy of cancer.

In 2002, John Funkhouser coined the term “theranostics” to represent the diagnosis and therapeutic activity simultaneously to cure the ailment (Wang et al., 2012; Kelkar & Reineke, 2011). These modalities provide targeted drug delivery to tumor tissues and analyze the response generated by the released active moieties to the desired organ or tissue while minimizing toxic effects (Sahoo et al., 2014). The amalgamation of nanoparticles and theranostics is known to develop nanotheranostics. These nanotheranostic tools are stratagem to extirpate cancer cells and simultaneously analyze the drug activity. The nanotheranostic agents consist of a

therapeutic moiety such as nucleic acids (miRNA and siRNA), proteins, and targeting ligands that can be linked covalently or noncovalently to the delivery entity (Nabil et al., 2019) (Fig. 1.1).

Nanotheranostics can be used in early-stage detection and treatments for patients suffering from cancer. Multifunctional hybrid nanotheranostics help in treatment planning, online tracking of therapeutic response, and further enabling personalized medicine (Anselmo & Mitragotri, 2016). These nanotheranostics systems are used for imaging, for instance, as optical guiding moieties during the surgical resection of breast cancer and melanoma (Blau et al., 2018).

Many parameters such as particle size, loading capacity, and surface interactions with the biological milieu are vital to be considered for any nanotheranostic design. Nanoparticulate system with an optimal size between 5 nm and 200 nm is effective for tumor targeting (Lammers et al., 2010). For instance, it was observed that smaller-sized nanoparticles exhibit enhanced stability and extravasation to tumor sites, whereas liposomes larger in size demonstrated better loading properties but were unstable and easily approachable by the reticuloendothelial system and are further cleared from blood circulation (Cruz et al., 2016; Perrie & Ramsay, 2017). The size of nanoparticles also affects their interaction with biosurface, loading efficiency, stability, and biodistribution index of the loaded drugs. The morphology, surface charge, and composition of the nanoparticles have been different and can be linked to different nanoparticles, i.e., stability, penetration inside the cells, and toxicity (Grumezescu, 2018).

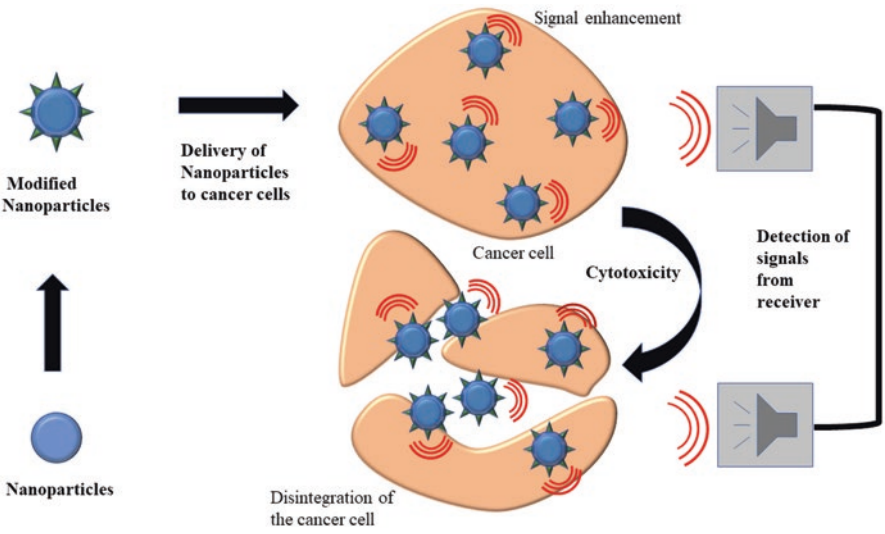

Fig. 1.1 Scheme demonstrating nanotheranostic particles entering a cancer cell for therapeutically killing the cell. These particles further emit signs that can be analyzed utilizing a diagnostic probe

1.2.1 Different Types of Nanotheranostics

Nanoplatforms are the vital component of theranostic systems that act as a scaffold to integrate imaging and therapeutic systems in single moiety and simultaneously realize their activities. Various materials are used for the construction of nanotheranostic scaffolds, and these are mentioned below (Fig. 1.2). Different applications of these theranostic systems are further listed in Table 1.1

1.2.1.1 Magnetic Nanoparticles

Magnetic nanotheranostics have attained significant heed in the region of cancer therapy. Magnetic nanoparticles facilitate MRI, positron emission tomography (PET), optical imaging, and additionally promote effective delivery of gene(s) as well as conventional chemotherapies. Magnetic nanoparticles also enable hyperthermia-based killing of cancerous cells. Magnetic nanoparticle-associated hyperthermia produces local heat and thus results in the release of active moieties either bound to the magnetic nanoparticles or encapsulated within polymeric matrices (Kumar & Mohammad, 2011; Xie & Jon, 2012; Singh & Sahoo, 2014). These theranostic agents are smaller in size, up to ~100 nm, allowing better penetration in the tumor tissues and promoting enhanced delivery (Draz et al., 2014). Magnetic nanoparticles particularly iron oxide nanoparticles (IONPS) can be surface functionalized with chemotherapeutic agents, other targeting entities, and biocompatible polymers due to their large surface area-to-volume ratio to reduce the cytotoxicity of the nanoparticles (Xie et al., 2011; Yoo et al., 2013). To improve the multifunctional capabilities of iron oxide nanoparticles, the biphasic system consisted of PEGylated terbium along with the $GdPO_4$ nanorice sensitized with cerium and

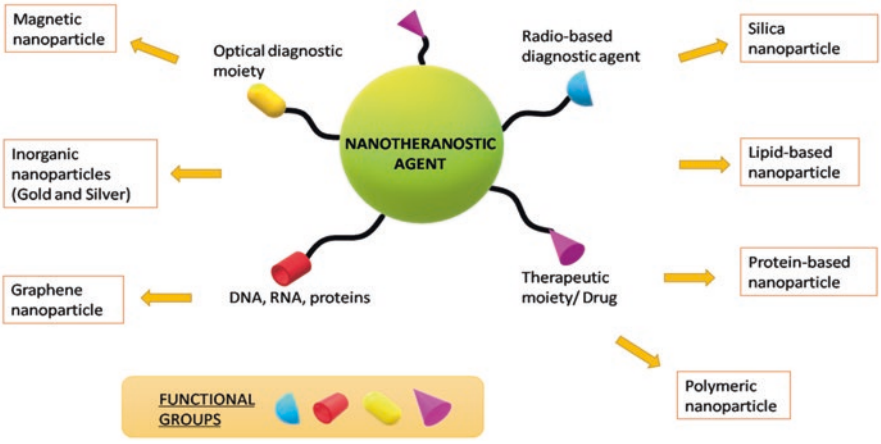

Fig. 1.2 Various types of cancer nanotheranostics

Table 1.1 Type of cancer nanotheranostics and their applications

Nanotheranostic agents	Applications/advantages	References
Magnetic	Multimodal imaging Hyperthermia Methodical gene and drug delivery Thermal cell apoptosis Enhanced cell penetration	Sahu et al. (2014) Kumar and Mohammad (2011); Xie and Jon (2012); Singh and Sahoo (2014) Patra et al. (2014) Huang et al. (2015) Yu et al. (2015)
Gold/silver	Multimodal imaging Easy to synthesize Cell apoptosis by PTT and PDT	Sahoo et al. (2014); Boisselier and Astruc (2009) Boisselier and Astruc (2009); Natarajan et al. (2009) Dixit et al. (2015); Liu et al. (2015a); Shi et al. (2014); Mukherjee et al. (2014)
Graphene	Large surface area, colloidal stability Image-assisted photothermal activity Super-paramagnetism, optical absorbance	Draz et al. (2014) Miao et al. (2015b) Shi et al. (2013)
Silica	Higher porosity Image-assisted drug delivery	Wang et al. (2015) Gao et al. (2013)
Lipid/polymeric	Ease of fabrication Longer duration of circulation Higher specificity and low toxicity	Gu et al. (2007) Luk et al. (2012); Makino and Kimura (2014) Draz et al. (2014); Schroeder et al. (2010)
Protein	Enables both internal and external surface modification Ferritin nanocages have a natural affinity for human transferrin receptor-1	Lim et al. (2013) Lim et al. (2013); Ren et al. (2014); Truffi et al. (2016); Wang et al. (2016)

glutamic acid. This biphasic system with the iron oxide nanoparticles exhibited green light luminescence characteristics with efficient aqueous stability. This was loaded with anticancer drug doxorubicin and demonstrated cell killing in vitro using cell lines like HeLa and MCF-7. This multimodal system was considered as a powerful tool for imaging and collaborative chemo-thermal cancer therapy (Sahu et al., 2014). PEGylated molybdenum disulfide flakes amalgamated with iron oxide nanoparticles have been utilized as a theranostic platform in vivo. These molybdenum disulfide flakes carry photothermal properties to convert near-infrared light into thermal and iron oxide magnetic characteristics, which were used to analyze the transport of the particle to the tissue via an external magnetic field (Yu et al., 2015). Superparamagnetic iron oxide nanotheranostics conjugated with the amphiphilic poly(styrene)-b-poly(acrylic acid) doxorubicin and folic acid were used as nanotheranostic component, and this nanoparticulate system was used for targeted anticancer activity in human breast cancer and colon cancer cell line (Patra et al.,

2014). SPIO nanotheranostic platform was fabricated and was further labelled with the fluorescent dye 5-FAM and antibody HuCC49ΔCH$_2$. Anticancer drugs such as doxorubicin, azido-doxorubicin, MI-219, and 17-DMAG were encapsulated into nanoparticles. pH-based release of the drug, distribution at the cellular level, and cytotoxicity of the drug-loaded SPIO-nanotheranostic was analyzed utilizing fluorescence microscopy and MTS assay. The structures exhibited enhanced targeting and uptake in HuCC49ΔCH$_2$-SPIO cells, as evidenced by various imaging techniques (fluorescent imaging, MRI, and Prussian blue staining). It was observed that HuCC49ΔCH$_2$-SPIO nanotheranostics got accumulated in endosomes/lysosomes where the encapsulated doxorubicin was released due to acidic environment persisting in the lysosomes and from here further got diffused to the cytosol and nuclei. In contrast, the encapsulated Adox demonstrated limited release in the endosomes/lysosomes. Thus, HuCC49ΔCH$_2$-SPIO-based nanotheranostics served as a platform for cancer cell imaging and targeted anticancer therapy (Zou et al., 2010). The anticancer activity of the well-known anticancer drug doxorubicin was also found to increase when conjugated with the human serum albumin-templated iron oxide nanoparticles. These nanotheranostic systems demonstrated anticancer potential in 4T1 cells when being analyzed via MRI (Quan et al., 2011). A triple modality nanoparticle system composed of the iron oxide@Au nanostar (gold shell, Fe_3O_4 core) was used for the MRI, CT scanning, and thermal imaging of tumor cells (Wang et al., 2005). Iron oxide cluster-structured nanoparticle platform templated with hydrazine, ferrous chloride, and ligands have demonstrated photothermal therapy-based anticancer activity in HeLa cells and were monitored utilizing optical coherence tomography microscopy (OCTM) (Huang et al., 2015). These nanostructures were claimed for the imaging and exhibited enhanced therapeutic efficacy than cetuximab only, in A431 and 32D/EGFR overexpressed epidermal growth factor receptor (EGFR) cell lines (Tseng et al., 2015) (Fig. 1.3).

1.2.1.2 Gold- and Silver-Based Nanotheranostics

Apart from iron, many other nanoparticles, composed of gold and silver, can be easily fabricated with various surface modifications, more biocompatible, and less cytotoxic (Boisselier & Astruc, 2009). Gold nanoparticle conjugated with microRNA, quantum dots, and streptavidin/biotin adhered with a chimeric mouse-human IgG1 monoclonal antibody (mAb) ChL6 (MAb-ChL6) were developed for the therapy of the breast cancer. This system inhibited breast cancer by inhibiting proliferation of the cell and thus leading to the apoptosis with no effect on normal cells and was analyzed using microscopic techniques (Natarajan et al., 2009). Gold nanobeacons conjugated with the 30-Cy3 and 50-thiol-C6 were used for mRNA silencing in HCT 116 cells (Conde et al., 2013). Fluorescent gold nanoclusters encapsulated with suicidal gene CD_UPRT (cytosine deaminase-uracil phosphoribosyltransferase) and prodrug 5-fluorocytosine were used for the targeted inhibition of the HeLa cells (Sahoo et al., 2014). Nanosystems comprising the gold nanoparticles with the biodegradable liposomes have shown therapeutic effect via

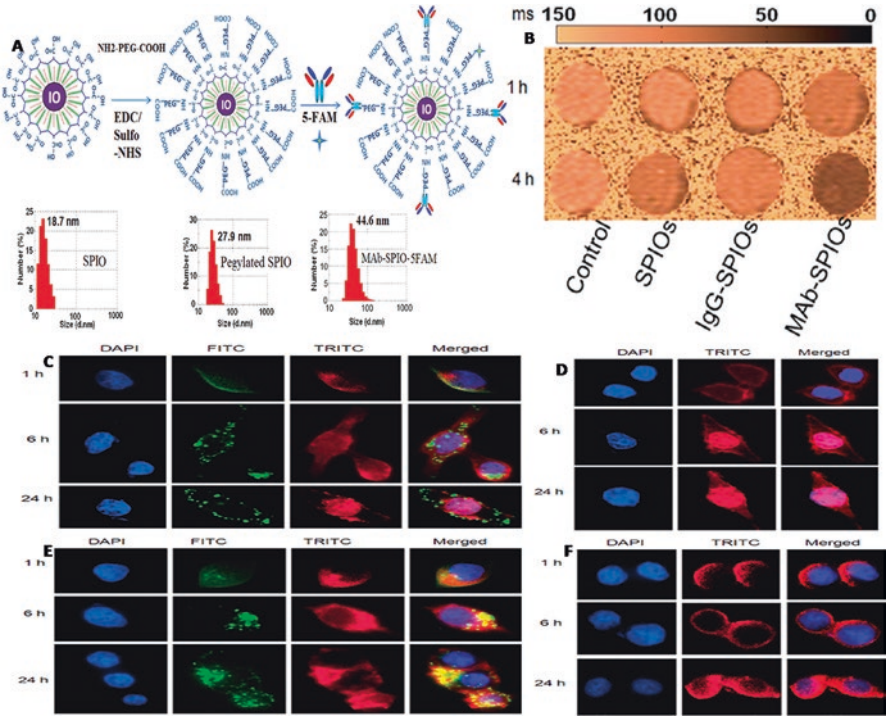

Fig. 1.3 (**a**) Schematic representation demonstrating superparamagnetic iron oxide nanoparticle PEGylation and conjugation with antibody (HuCC49ΔCH$_2$) and dye, fluorescein amidites (5-FAM), (**b**) *T*2-weighted spin-echo magnetic resonance phantom images of LS174T cells incubated with superparamagnetic iron oxide nanoparticles, nonspecific IgG labeled SPIOs, and HuCC49ΔCH$_2$ labelled SPIOs, (**c**) intracellular distribution of doxorubicin (Dox), inLS174T cells, (**d**) HuCC49ΔCH$_2$-SPIOs loaded with Adox, (**e**) Adox, and (**f**) HuCC49ΔCH$_2$-SPIOs loaded with doxorubicin. Green color depicted the localization of SPIOs (5-FAM). Nuclei were stained in blue color. Red color depicted the distribution profile of Dox or Adox. The yellow color in the merged images demonstrated co-localization of SPIOs and Dox or Adox. (Reprinted with permission from Zou et al. (2010). Copyright (2010) from American Chemical Society (ACS))

photothermal therapy in breast cancer cells, and optical analysis can be carried via multispectral imaging and tri-modality microphoton emission tomography imaging (Rengan et al., 2013). Gold nanostructures conjugated with anti-mucin 7 antibodies can specifically target urothelial tumor cells photothermally (Chen et al., 2015a). A nanotheranostic platform consisting of the gold nanoparticles, graphene oxide, and aptamer (Apt-AuNP-GO) was generated to enhance targeted therapy of the breast cancer MCF-7 cell line by near-infrared (NIR) light activatable photothermal therapy without exerting any effect on the normal cells even in the low doses as shown in Fig. 1.4 (Yang et al., 2015). This nanoplatform had advantages such as specific targeting ability, improved biocompatibility, and tumor cell apoptosis. The self-assembled aptamer conjugated gold nanoparticle graphene oxide nanoplatform targeted MUC1-positive human breast cancer cells (MCF-7) due to the interaction

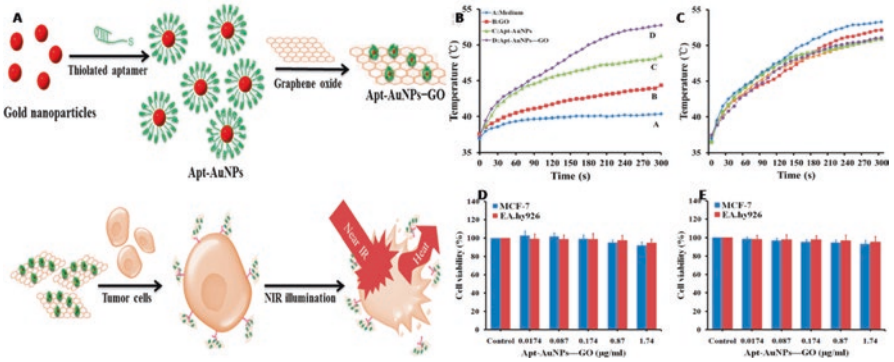

Fig. 1.4 (**a**) Schematic illustration of the fabrication of the Aptamer-gold nanoparticle hybridized graphene oxide (Apt-AuNP–GO) nanocomposite and for photothermal ablation of the cancer cells under near-infrared illumination, (**b**) photothermal heating curve effect of the nanocomposite, (**c**) photothermal stability of nanocomposite irradiated by the near-infrared laser. Cytotoxicity of Apt-AuNP–GO was analyzed by (**d**) MTT assay and (**e**) LDH assay. (Reprinted with permission from Yang et al. (2015). Copyright (2015) from American Chemical Society (ACS))

between the MUC1-binding-aptamer and the MUC1 (type I transmembrane mucin glycoprotein) on the cell membrane. Due to the near-infrared radiation, Apt-AuNP-GO induced transient enhancement in HSP70 expression, which declined after that, resulting in irreversible cell death. It was demonstrated that the cumulative therapy of heat and HSP70 inhibitor synergistically generated breast cancer apoptosis. So, this can lead to the fabrication of the potential HSP70 inhibitors-loaded Apt-AuNP-GO that may generate heat and the HSP70 inhibitor to breast cancer cells and further enhance therapeutic properties with fewer side effects. Gold nanoparticles templated with peptides, EGFR and photosensitizer (Pc 4) were used as therapeutic agents in U87-MG human glioma cells (Dixit et al., 2015). Multifunctional gold nanostars (AuNS) has been demonstrated to inhibit sarcoma in a xenograft tumor model via PTT, and the process was analyzed using surface-enhanced Raman spectroscopy (SERS), two-photon luminescence (TPL) imaging, and X-ray CT (Liu et al., 2015a). Gold-core gold-shell or gold-core silver-shell nanoparticles conjugated with activatable aptamer probes have exhibited efficient site-specific activity via PTT in A549 cells guided by high contrast imaging systems (Shi et al., 2014). Biosynthesized silver nanoparticles fluoresce bright red inside cells and have elicited anticancer activity in human lung cancer, mouse melanoma, and human breast cancer cells (Mukherjee et al., 2014).

1.2.1.3 Lipid and Polymers Nanoparticle-Based Systems as Nanotheranostics

Lipids and polymers have been employed as nanocarriers, due to their enhanced circulation duration, improved targeting ability, and diagnostic ability (Gu et al., 2007; Luk et al., 2012; Makino & Kimura, 2014). Lipid- and polymer-based

nanotheranostic components provide cellular compatibility and improved cellular uptake (Draz et al., 2014; Schroeder et al., 2010). Zhang et al. exhibited that PEGylated liposomes linked with iron oxide nanoparticles and infrared dye were used as nanotheranostic agents that inhibited the growth of the breast cancer cells and can be analyzed via in vivo imaging modes, superparamagnetic MRI, and fluorescence imaging in NIR (Zhang et al., 2014a). Multifunctional lipid nanoparticles in conjugation with trastuzumab, rapamycin, and quantum dots inhibited HER2-positive breast cancer cells. Nanocapsule coated with the surfactants bearing chemotherapeutic agents colchicine and fluorescent moiety, coumarin-6 have been utilized simultaneously for bioimaging and treatment of various cancer cells such as MCF-7, A549, and melanoma cell (Bazylińska et al., 2016). Polymeric nanoparticles such as nanospheres and micelles are linked with functionalized probes for targeted activity and analysis of photodynamic therapy reduction in tumor size (Luk & Zhang, 2014). Du et al. reported that the poly(lactic acid) nanoparticles loaded recombinant human endostatin linked with GX1 peptide, a targeted antiangiogenic agent and near-infrared dye, 800 CW as a potential nanotheranostic platform for treatment and observation of the colorectal cancer cells (Du et al., 2015). PEGylated Mn^{2+}-chelated polydopamine (PMPDA) nanostructures were fabricated as a promising nanotheranostic platform via the introduction of the Mn^{2+} and SH-polyethylene glycol onto polydopamine nanomoieties without any extrinsic chelators. These were considered as the potential nanotheranostic agents via photothermal therapy-induced ablation for 10 min in HeLa cells and exhibited improved MRI signal increment for both in vitro as well as in vivo imaging because of intrinsic manganese-chelating factors, and the value of longitudinal relativity coefficient was 6.55 mM^{-1} s^{-1} at 9.4 T. The improved biocompatibility of PMPDA nanostructures was due to the use of Mn^{2+} ions as diagnostic agents and biocompatible polydopamine as photothermal agents and was assessed by the MTT assay. Therefore, the fabricated PMPDA nanostructures were used as a promising theranostic platform for MRI-assisted photothermal ablation of the cancer cells, as shown in Fig. 1.5 (Miao et al., 2015a). One of the research group reported that redox-responsive nanoparticles encapsulating L-cysteine-associated poly (disulfide amide) and docetaxel as a nanotheranostic platform were efficient in killing HeLa, A549, MCF-7, and DU145 cell lines (Wu et al., 2015).

1.2.1.4 Protein-Based Nanotheranostic Systems

Protein-based nanotheranostic agents have been utilized as vehicles for therapeutic and diagnostic approaches (Lim et al., 2013; Ren et al., 2014; Truffi et al., 2016; Wang et al., 2016; Huang et al., 2014; Chen et al., 2015b). Engineered protein nanocages can be fabricated on their internal (drugs/aptamers/contrast agents) and external surfaces (ligand) due to their proteinaceous nature (Lim et al., 2013). Ferritin nanocages have also been used as potential cancer theranostics (Lim et al., 2013; Ren et al., 2014; Truffi et al., 2016; Wang et al., 2016; Huang et al., 2014; Chen et al., 2015b) as the ferritin heavy (H)-chain has a high affinity toward human

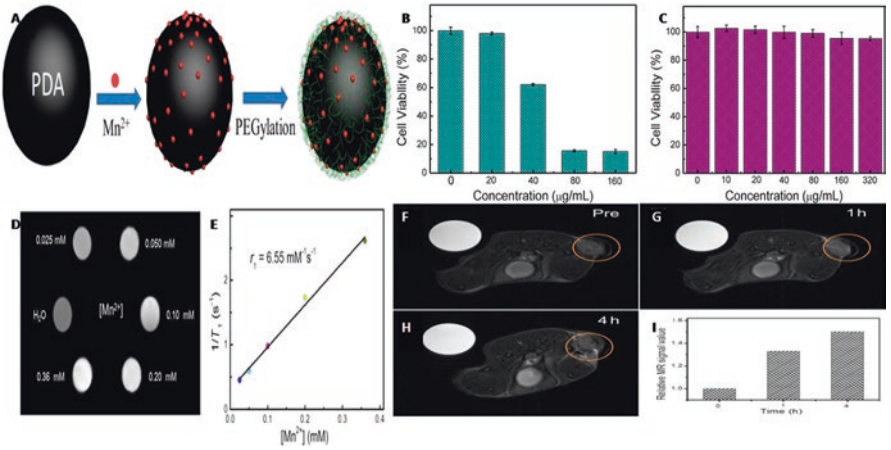

Fig. 1.5 (**a**) Schematic representation demonstrating the fabrication of theranostic PEGylated Mn^{2+} polydopamine nanostructures (PMPDA), (**b**) viability of HeLa cells treated with various concentrations of PMPDA nanoparticles with laser illumination for 10 min, (**c**) viability of HUVEC cells treated with various concentrations of PMPDA nanostructures for 24 h, (**d**) MRI (in vitro assay) of PMPDA nanoparticle in aqueous solution with different Mn^{2+} concentrations, (**e**) corresponding T1 relaxation study of the nanostructures as a function of Mn^{2+} concentration, (**f**–**h**) in vivo T1-weighted magnetic resonance imaging of 4T1 tumor-bearing mouse at different time duration after the administration of the intravenous tail injection of PMPDA theranostics. The orange circles depicted tumor issues. The big white spots in the top-left corner are pure water as background, (**i**) corresponding intensity of the signal of T1-weighted magnetic resonance signals at the tumor site at different intervals. (Reprinted with permission from Miao et al. (2015a). Copyright (2015) from American Chemical Society (ACS))

transferrin receptor-1 (CD71) (Li et al., 2010), that is overexpressed in tumor cells (Truffi et al., 2016; Wang et al., 2016; Huang et al., 2014). Nanoradiopeptides and fluorescent peptide nanoprobes are reported to be efficient theranostic agents (Okarvi, 2004; Luo et al., 2012). Lipoprotein-based nanoparticles have been used as theranostic agents in cancer treatment (Ng et al., 2011). A multifunctional albumin-based nanotheranostics has been developed for tumor-associated targeted delivery and dual-modal imaging-assisted combination therapy of cancer. Human serum albumin (HSA) was pre-modified with a photosensitizer moiety chlorine e6 (Ce6), which also served as a chelating entity for Mn^{2+} to enable magnetic resonance imaging. Then the anticancer drug paclitaxel was used to induce the self-assembly of Ce6 modified HAS along with the tumor-targeting peptide Arg-Gly-Asp (cRGDyK) that target αvβ3-integrin overexpressed on tumor angiogenic endothelium. Two types of nanostructures were developed, one either by the simultaneous co-assembly of both HSA-Ce6 and HSA-RGD or the second one forming an HSA-Ce6@HSA-RGD core-shell structure. These structures enabled both chemo- and photodynamic therapy, and synergistic cancer cell apoptosis was observed when HSA-Ce6-PTX-RGD-treated cells were exposed to light irradiation. On administration via systemic mode, excellent tumor targeting of RGD adhered nanoparticles was revealed by

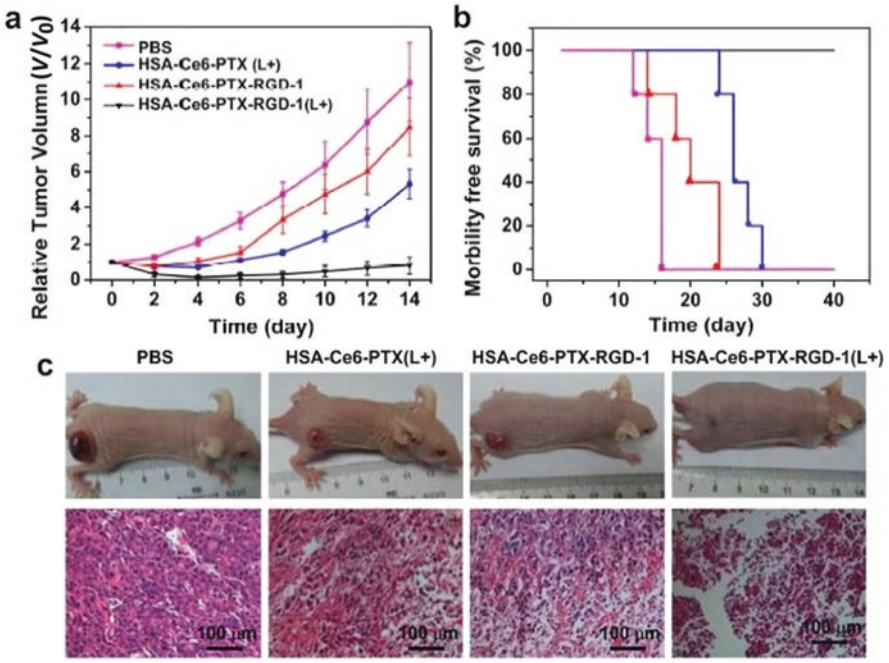

Fig. 1.6 In vivo tumor-targeted combination therapy of albumin-based nanotheranostic and laser irradiation. (**a**) Relative tumor volume curves of different groups of mice after treatments are shown; mice with PBS injection, mice administered with human serum albumin-chlorine e6-paclitaxel and illuminated with 660-nm laser, mice administered with HSA-Ce6-PTX-RGD-1 without or with the 660-nm laser illumination, (**b**) curves elicited the survival rate of mice with U87MG tumors after treatments, (**c**) representative images of mice from different groups taken at the 14th day (the upper row) and H&E-stained tumor pieces taken from different groups of mice after being treated with various drug molecules (the bottom row). (Reprinted with permission from Chen et al. (2015c). Copyright (2015) from American Chemical Society (ACS))

in vivo dual-modal fluorescence/MR imaging. The HSA-Ce6-PTX-RGD-1 nanoformulation inhibited tumor growth after i.v. injection and exhibited combined photodynamic and chemotherapy, as shown in Fig. 1.6. The combined photo- and chemotherapy was also more effective as compared to individual monotherapies (Chen et al., 2015c). A protein-based nanoreactor-assisted fabrication of semiconductor nanocrystals has demonstrated the ability to act as potential cancer theranostic agents (Yang et al., 2016).

1.2.1.5 Graphene-Based Nanotheranostics

Graphene-based nanotheranostic agents have exhibited various advantages such as easy surface modification, enhanced surface area, colloidal stability, and improved electrical and mechanical properties (Draz et al., 2014). Graphene sheets have exhibited death in CD^{44+} KB carcinoma cells utilizing image-guided photothermal

therapy (Miao et al., 2015b). A positively charged nanocomposite-bearing dendrimer-coated nanographene conjugated with gadolinium interacted with the negatively charged Let–7 g miRNA, thus forming Gd-NGO/Let–7 g complexes that exhibited anticancer activity. This complex was also loaded with anthracycline anticancer drug epirubicin and further simultaneously demonstrated effective contrasting agent and better antineoplastic activity as compared to the single conjugates (Yang et al., 2014). Graphene gold nanoconjugates have demonstrated efficient photothermal properties (Zedan et al., 2013; Huang et al., 2011). A multifunctional moiety consisting of GO-Au-IONP has demonstrated increased superparamagnetism, photothermal therapeutic property, and optical absorbance in NIR laser irradiation therapies (Shi et al., 2013).

1.2.1.6 Silica-Based Nanotheranostics

Porous silica nanoparticles conjugated with dibenzocyclooctyne Alexa Fluor 488, iRGD peptide, were used as theranostic entities (Wang et al., 2015). Multifunctional nanotheranostic silica rattles bioconjugated with luteinizing hormone-releasing hormone-*Pseudomonas aeruginosa* exotoxin 40 (LHRH-PE40) fusion protein and co-loaded with docetaxel was used for image-assisted cancer-specific drug delivery and therapy (Gao et al., 2013). Silica nanoclamps were used as potential nanotheranostic agents when conjugated with camptothecin, doxorubicin, and quantum dots to treat the pancreatic cancer cells (Muhammad et al., 2014). Chan et al. reported that the mesoporous silica nanoparticle adhered with lanthanide ions such as europium and gadolinium was used as potential theranostic agents to select cancer cells simultaneously diagnosing via MRI and fluorescence imaging (Chan & Lin, 2015). Another group reported that mesoporous silica nanoparticles combined with hyaluronic acid and PEGylated phospholipid-loaded carbon and silica nanocrystals could inhibit breast cancers that overexpress CD44, causing photothermal ablation (He et al., 2012). These mesoporous silica nanoparticles were used as potential nanotheranostic agents when conjugated with the hematoporphyrin and docetaxel with trifunctional therapy and bifunctional imaging system (Fan et al., 2013, 2014).

1.3 Specific Applications of Cancer-Targeted Nanotheranostics

1.3.1 Nanotheranostics Application in Personalized Cancer Therapy

Treating cancer entirely is still contentious because certain issues such as tumor cells are similar to normal human cells; therapeutic efficacy changes significantly with stage and type of cancer due to which continuous monitoring of therapy is

mandatory. For example, doxil and abraxane are the drugs approved for the treatment of solid tumors; they act by enhanced permeability and retention (EPR) mechanism (Northfelt et al., 1998; O'Brien et al., 2004; Gradishar et al., 2005; Hassan et al., 2004; Emoto et al., 1998). However, the EPR effect does not remain constant and varies with the type and stage of cancers (e.g., pancreatic adenocarcinoma and gastric cancer) (MacKenzie, 2004; Fuchs & Mayer, 1995). Various anticancer agents exhibited good results in vitro but failed in vivo due to development of desmoplasia around tumor cells, which resist drug accumulation within it. Additionally, there is high interpatient variability observed among the same tumor type due to the difference in structural complexity and vascular leakage. Thus, probable outcomes of therapy vary from patient to patient, and hence continuous observation of drug accumulation and leakage is needed to define the proper outcome of any anticancer therapy (Harrington et al., 2001; Yang et al., 2010a). In a nutshell, "one-fits-all" type of strategy cannot be adopted in cancer treatment, leading to individualization of therapy, i.e., personalized therapy (Kim et al., 2013).

Personalized cancer therapy can be adopted using nanotheranostics; both diagnostic and therapeutic entities are introduced into a single platform. Nanotheranostics can be the solution to all problems mentioned above – (a) nanosize ease journey of therapeutic agents up to the tumor tissues; (b) after reaching the tumor tissues, the therapeutic agents treat the tumor; and (c) the diagnostic enabling continuous surveillance of the therapeutic progress (Tsai et al., 2010; Cabral et al., 2007; Itaka et al., 2010). When adhered to the targeting agents, these synergistic combinations can be crucial for the management of cancer. For instance, Luo et al. designed targeted therapy for prostate cancer using gold nanoparticles as a radiosensitizer and prostate-specific membrane antigen (PSMA-1) as targeting agent which significantly enhanced gold nanoparticle uptake in PSMA overexpressed in prostate cancer cells (Luo et al., 2019).

1.3.1.1 Nanotheranostics for Targeting Tumor Microenvironment (TME)

Exploring the tumor microenvironment is a very necessary aspect of tumor management. The microenvironment of tumor cells distinguishes it from normal cells. However, these distinguishing characteristics of the tumor microenvironment can also be used for targeting the tumor. Main tumor microenvironment components are hypoxia, pH, enzymatic processing, calcium level, lymphangiogenesis, aerobic glycolysis, immune system activation, inflammation, desmoplasia, and exosomes (Jin & Jin, 2020). The tumor microenvironment has played a crucial role in designing and developing targeted and specific nanotherapies. The tumor microenvironment has certain distinguishing components that can be targeted by proper modification of the delivery system, such as the hypoxic nature of tumor microenvironment which provides an aid to design a system that gets activated when exposed to hypoxic (reductive) conditions (Renfrew et al., 2013). Higher enzymatic activity in tumors leads to design enzyme responsive drug delivery (Mizukami et al., 2008). Lower pH of TME leads to the development of pH-responsive drug delivery system

(Li et al., 2019a). In such a way, improved targeted therapy can be designed with lesser side effects in cancer treatment (Fig. 1.7).

It has been observed that the proliferative tumor cells possess disorganized vasculature and need more oxygen. Thus, solid tumors remain hypoxic. These hypoxic tumor cells show resistance to chemotherapeutic and radiotherapeutic options (Davda & Bezabeh, 2006). Diepart et al. had proved diversity in oxygen content found within tumor and affirmed to predict resistance shown to therapy by hypoxic area in tumor (Diepart et al., 2011). To determine the oxygen level in the tumor region, F19MRI and perfluorocarbon (PFC) were used in combination as it possessed the ability to dissolve oxygen. Oxygen possesses paramagnetic property (Parhami & Fung, 1983); PFCs19F longitudinal relaxivity (r1) is linearly correlated to PFCs partial pressure of dissolved O_2 (pO_2) at a given temperature. Oximetry study had also been performed using hexafluorobenzene (Liu et al., 2011) either solely or in combination with perfluorooctyl bromide (PFOB) or perfluorodecalin encapsulated within nanoemulsion (Mason & Antich, 1994). Also, proteins in the extracellular matrix of tumours get modified due to the inflammation, which

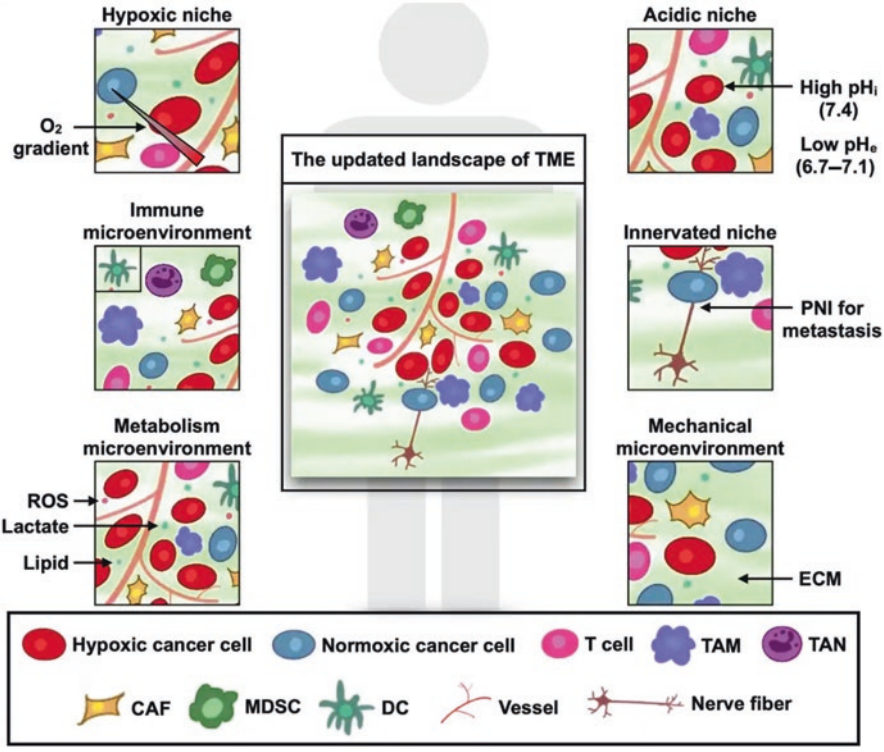

Fig. 1.7 Schematic description of the tumor microenvironment. It consists of tumor cells, stromal cells, blood vessels, nerve fibers, extracellular matrix, and associated acellular components. It can be distinct into microenvironments that include hypoxic, acidic, innervated, immune, metabolism and mechanical. (Reproduced with permission from Jin and Jin (2020). Copyright, 2020 Springer)

consequently develops desmoplasia. Abdolahinia et al. designed collagenase and metformin-conjugated gold nanoparticle (GNP); those demonstrated enhanced permeation and cytotoxicity in breast cancer spheroids. Collagenase enhanced permeation into tumor cells via desmoplasia, and metformin suppressed cancer stem cells (CSC) (Abdolahinia et al., 2019).

Tumors also demonstrate high enzymatic activity and produce a high number of protons because of high metabolic activity such as glycolysis, hydrolysis, etc. Mizukami et al. attempted to evaluate metabolic activity of protease enzyme and thus designed F19 MRI probe with Gd-chelate (gadolinium chelate) cleaved by hydrolase cleavable linker (DEVD peptide linkage) which was specifically cleaved by caspase-3. Initially, the interaction between Gd and F19 causes paramagnetic relaxation which produced short T2 (transverse relaxation time) and hence gave low MRI signal on the other hand after separation of the linker by caspase-3; it produced long T2 and hence exhibited enhanced MRI signal (Mizukami et al., 2008). Yang et al. designed nanotheranostics for intracellular delivery of the drugs and imaging of tumor cells. Herein, doxorubicin was conjugated with a dipeptide H-Phe-Lys-OH using para-amino-benzyloxy carbonyl (PABC) linker. This conjugation was tethered to the silica-coated magnetic nanoparticle (SMNP). H-Phe-Lys-OH peptide sequence gets selectively cleaved by the protease cathepsin B found in various malignant tumors. Additionally, both cancer cell specific imaging and the real-time intracellular release of doxorubicin from the nanosystems could be monitored by the combined use of MRI and fluorescence technique (Yang et al., 2011).

TME is acidic due to the high production rate of protons and lower lymphatic drainage in tumor tissues. Also, due to the Warburg effect, the amount of lactate secretion in tumor tissues is enhanced, leading to an acidic pH environment there (Roma-Rodrigues et al., 2019). This acidic pH environment can help design pH-responsive anticancer therapy. Song et al. developed gold nanoparticles functionalized with citraconic anhydride ligand for pH-responsive aggregation in tumor cells and photoacoustic imaging (Song et al., 2013). Li et al. attempted to develop gold nanoparticles which were functionalized with 4-(2-(5-(1,2-dithiolan-3-yl) pentanamide) ethylamino) 2methyl-4-oxobut-2-enoic acid (LSC) and RGDyK peptide conjugation using 16mercaptohexadecanoic acid (MHDA). LSC had citraconic ion responsive to pH and c(RGDyK)-MHDA ligand specifically targeted to tumor tissues due to their high affinity toward overexpressed αvβ3 integrin in angiogenic vessels (He et al., 2010).

1.3.1.1.1 Monitoring Drug/Therapeutic Molecule Biodistribution

Antitumor drugs are usually very toxic to normal cells due to which person under the therapy suffers more because of the therapy instead of the tumor burden itself. Hence, drug accumulation specifically into the tumor cells and tissue is the dire need to eliminate the unwanted side effects of many potent but toxic chemotherapeutics. Thus, it also becomes very important to monitor the organ and tumor distribution of the chemotherapeutic molecules which can be achieved by the use of

nanotheranostic-based approach (He et al., 2010). Many nanotheranostics have been developed for this purpose. Glycol chitosan nanoparticles (CNPs) were explored for their specific accumulation within tumor cells (Kim et al., 2010; Min et al., 2008; Kim et al., 2008). The tumor homing characteristic, i.e., the biodistribution of CNP within the body was monitored by attaching NIR fluorescent dye CY5.5 to paclitaxel (PTX) containing CNPs (PTX-CNP-CY5.5). When this PTX-CNP-CY5.5 nanotheranostic combination was injected intravenously to SSC-7 xenograft mice, it demonstrated high stability, deformability and a potential near-infrared fluorescent signal were observed in the tumor region indicating cancer cell-specific accumulation (Runciman et al., 2011; Fokong et al., 2012; Nam et al., 2009).

1.3.1.1.2 Therapeutic Efficacy Measurement

Therapeutic response of any therapy can be measured by using various imaging techniques. When apoptosis occurs, certain changes in the plasma membrane and enzymes occur, which can be detected using imaging probes. Thus, the efficacy of ongoing therapy can be measured (Ehling et al., 2013; Brindle, 2008; Riedl & Shi, 2004). Caspase is one of the overexpressing enzymes during cell death. Reidl et al. prepared hyaluronic acid-containing NPs with CY5.5(NIR dye) and BHQ (Black Hole Quencher). CY5.5 and BHQ are linked together with DEVD caspase-cleavable peptide. At the time of cell death, caspases get overexpressed, and they break the peptide linkage DEVD. Consequently, CY5.5 shows strong fluorescence signals confirming cell death (Riedl & Shi, 2004).

1.3.1.2 Photothermal-Based Cancer Therapy

It is a specific kind of therapeutic approach for cancer that involves the killing of tumor cells by thermal heating in the presence of light. Designing photothermal-based therapeutic systems for cancer involve incorporating heat-generating material susceptible to electromagnetic radiation such as NIR light (Boisselier & Astruc, 2009). NIR-responsive photothermal agents show high absorption along with low fluorescence emission in NIR range to release absorbed light in the form of heat energy and cause local cell destruction. Some organic dyes and inorganic NPs like ICG, Prussian blue, Cypate, IR825, IR780 (Hong et al., 2013; Chen et al., 2014; Yue et al., 2013; Cheng et al., 2014) and graphene (Orecchioni et al., 2015; Yang et al., 2010b), carbon nanotubes (Lin et al., 2015), and gold nanoparticles (nanorod, nanocage, nanotube, nanoshell) (Wang et al., 2013) are widely studied for this purpose. The photothermal effect helps the drug to release rapidly and to accumulate intracellularly (Chen et al., 2017; Yang et al., 2012). The light-guided thermal therapy gives better control over therapy, and hence healthy tissue damage is greatly reduced (Benov, 2015; Wilson & Patterson, 2008). A multifunctional nanotheranostic platform has been constructed to integrate nanomaterial-increased computed tomography imaging and integrate photothermal therapy with radiation therapy. These

results demonstrated that Au@Platinum nanodendrites exhibited absorbance in the near-infrared region because of the dendritic structure and improved radiosensitizing effect due to the composition of gold and platinum. Au@Pt NDs demonstrated anticancer activity; cancer cells apoptosis occurred at a low near-infrared laser power and X-ray radiation dose via the synergistic activity of PTT and RT, as shown in Fig. 1.8. The computed tomography imaging demonstrated by Au@Pt NDs determined the origin of cancer and thus assisted in the PTT/RT (Liu et al., 2017). Tian et al. produced a nanoparticle (Fe_3O_4@$Cu_{2-x}S$) with strong absorption and better control over photothermal property by tuning Cu level (Tian et al., 2013). Zhou et al. designed a nanoparticle having combined PTT-radiotherapeutic action. CuS nanoparticle developed here comprises both radioactive and non-radioactive "Cu." Such CuS nanoparticles emit radiation as well as heat for local cellular damage (Zhou et al., 2015). Shao et al. designed a nanosphere containing black phosphorus quantum dots wrapped in poly(lactic-co-glycolic acid) as a photothermal agent. Biocompatible and biodegradable poly(lactic-co-glycolic acid) controls the degradation rate of black phosphorus by reducing its access towards water (Shao et al., 2016). Fang et al. designed a nanosystem for combined PTT and chemotherapeutic effect by utilizing NIR responsive hollow mesoporous carbon nanoparticles as carriers for doxorubicin. Further, the system was modified using graphene quantum dots that aided in preventing premature drug release, and hyaluronic acid for achieving higher tumor cell uptake (Fang et al., 2018). Huang et al. successfully utilized gold nanoparticles (plasmonic nanoparticle) as photo absorbing agents for photothermal therapy with better targeting and photothermal properties (Huang et al.,

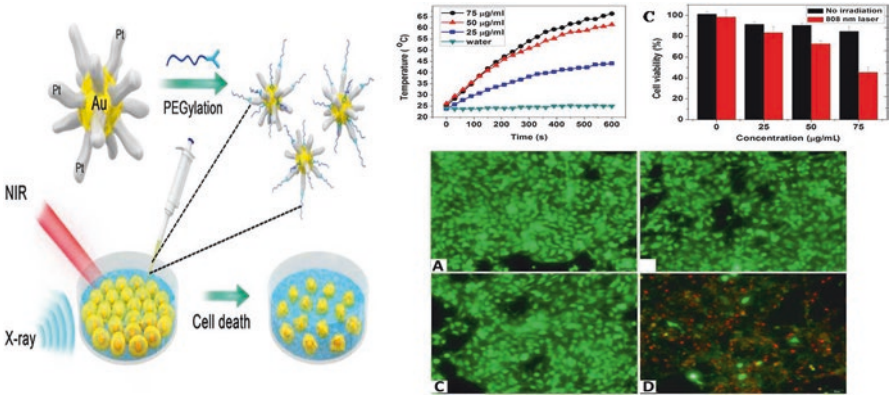

Fig. 1.8 (**a**) Scheme illustrating PEGylation and photothermal-/radiation-based synergistic therapeutic application of the Gold@Platinum nanodendrites, (**b**) photothermal effects demonstrated by Au@PtNDs after illuminated with the 808 nm laser at power 1 W/cm^2 for 10 min, (**c**) cell viability of 4T1 cells after treatment with the Au@Pt NDs and near-infrared laser irradiation. (**d**) Live/dead staining images of 4T1 cells after nanotheranostic treatment and laser illumination: (**A**) without treatment; (**B**) laser irradiation with 808 nm at 1 W/cm^2 for 10 min; (**C**) Au@Pt NDs alone (**D**) Au@Pt NDs and laser irradiation. Live and dead cells were expressed as green (live cells) and red (dead cells) colors, respectively, in the above images. (Reprinted with permission from Liu et al. (2017). Copyright (2017) from American Chemical Society (ACS))

2008a). Although PTT has shown better therapeutic efficacy in many cases, still there are many shortcomings associated with this that need attention. This involves the limited penetration depth of light, which constricts the potential use of PTT effectively for surface-exposed skin cancer only and not suitable for deep-seated tumours. Along with PTT, there are some other thermal therapies available such as magnetically induced and microwave-induced hyperthermia (Gupta & Gupta, 2005; Mashal et al., 2010).

1.3.1.3 Photodynamic Therapy for Cancer

This involves the use of photosensitizer materials for therapy. When irradiated with suitable laser light, photosensitizers transfer their light to the surrounding media to produce reactive oxygen species that cause apoptosis (Huang et al., 2008b). PDT has various advantages over PTT such as it requires a lower density of light to generate the therapeutic effect, unlike PTT, which requires high power density light. It also demonstrates less adverse effects and exhibits low cumulative toxicity and enhances the quality of life of patients (Ng et al., 2013). Clinically PDT is found to be effective in various types of tumors like oral, esophageal, nasopharyngeal, lung and bladder tumors (Lucky et al., 2015). Some of the photosensitizers approved by the FDA for cancer treatments are Photofrin, Visudyne, Levulan, Metvix, Hexvix, Foscan, Laserphyrin, etc. (Chilakamarthi & Giribabu, 2017). Wang et al. improved PDT effect in catalase entrapped nanocapsules using porphyrin as photosensitizers (Wang et al., 2018). Zhang et al. developed doxorubicin-loaded in mesoporous silica-coated gold cube nanocomposite that used phthalocyanine as a photosensitizer material for enhanced PDT effect (Zhang et al., 2019a). Wan et al. designed a system for enhanced PDT effect by preparing nano-RBC carriers containing oxyhemoglobin and ammonium bicarbonate (gas generating system) for co-action of ICG and DOX. With the help of oxyhemoglobin, PDT efficiency is improved (Wan et al., 2018). Xianchun Zhu et al. developed a system (5,10,15,20-Tetrakis(N-(2-(1H-imidazole-4-yl)ethyl)benzamide)-porphyrin); thereby photosensitizers were activated only when they reach the target tumor cells. Porphyrin was used as a photosensitizer which helps to generate singlet oxygen and causes cell death. In this case, the photosensitized singlet oxygen gets released in the acidic environment only. This control is achieved by imidazole protonation, which leads to forming an aggregation in the weak alkaline condition, causing quenching of the singlet oxygen (Zhu et al., 2011).

Apart from single-photon excitation, two-photon PDT is also explored in PDT, where two photons are utilized to enable energy absorption at low energy NIR region, further giving better depth of penetration and accurate targeting in tumor tissues. Li et al. used a two-photon approach to improve PDT effect. Tetraphenylporphyrin (TPP) was conjugated with [9,9′-bis(6″-bromohexyl) fluorene-2,7-ylenevinylene-co-alt-1,4-phenylene] (PFV) as two-photon synthesizers for enhanced PDT action. Conjugate was then covalently adhered to gold nanorods coated with mesoporous silica. Surface plasmon resonance properties of

gold and fluorescence energy transfer from PFV improved TPP's two photon-PDT effects. The combined action of two-photon imaging and two photon-PDT was studied in vitro using HeLa cells (Li et al., 2019b).

1.3.1.4 Nanotheranostics in Radiotherapy of Cancer (RT)

Radiotherapy constitutes an important aspect of cancer therapy. It is used to treat various cancers as they directly damage the DNA. However, RT has several adverse effects as they damage normal human cells also, and the generation of radiation resistance is being observed in many cases (Roy Chowdhury et al., 2016). RT has been found to enhance survival after surgical resection (Koshy et al., 2010). To enhance the effectiveness of RT additional metallic NPs, having strong photoelectric absorption ability is being employed. For example, GNPs can be used for these purposes owing to their stronger ability to absorb and transfer photoelectrons, Auger electrons, and X-rays (Hainfeld et al., 2008). Polyethylene glycosylation of GNP(P-GNP) has been further proven to enhance the circulation time of RT (Joh et al., 2013). Geng et al. demonstrated that gold nanostructures when adhered with thioglucose enhanced radiation-induced toxicity in ovarian cancer cells. Tumor cells require high glucose due to enhanced metabolic rate, and hence thioglucose conjugated gold nanoparticles were utilized as a sensitizer to increase ovarian cancer radiotherapy (Geng et al., 2011).

1.3.1.5 Cancer Immunotherapy-Mediated Through Nanotheranostic Systems

Immunotherapy is an advanced technology which does not directly kill the cancer cells but targets it indirectly by activating the immune system against it. Immunoadjuvant antigen and nucleic acid vaccine-loaded nanoparticles have been found to improve the efficacy of anticancer therapy (Ma et al., 2016). Lee et al. designed gold nanoparticles vaccines as immunotherapy for lymph node (Lee et al., 2012). Cao et al. designed ultrasmall GO-GNP as an immunoadjuvant in immunotherapy (Cao et al., 2014). Wang et al. developed MnO_2–CpG-silver nanoclusters (AgNCs)-doxorubicin (DOX) conjugate in which MnO_2 served as a support system for both the chemotherapeutic molecule doxorubicin and immunomodulatory agent CpG–AgNCs. The Dox-MnO_2 conjugation caused immunogenic cytotoxicity producing tumor-specific immune response and abrogated immunosuppressive activity of regulatory T-cells. This overall enhanced T-cell-associated tumor-specific immune response of CPG-AgNc and significantly enhanced their antitumor activity even for solid tumors (Wang et al., 2017). Recently, photoimmunotherapy (a combination of phototherapy and immunotherapy) developed as a promising therapeutic option for cancer ailment. Mitsunaga et al. conjugated a monoclonal antibody, anti-HER1 MAb, Panitumumab, with a phototoxic dye, phthalocyanine dye, IR700, for gaining synergistic antitumor activity. The system could specifically target HER1

overexpressing tumor tissues utilizing the conjugated antibody, and when being activated by NIR light, it produced phototherapy induced necrotic cell death. It was found that fractionate administration of Panitumumab-IR700 and orderly repetitive NIR irradiation demonstrated better cytotoxicity in the HER-1 overexpressing cell line, A431 (Mitsuanga et al., 2012).

1.3.1.6 Combinatorial Cancer Therapy Achieved by Means of Nanotheranostic Systems

Conventional therapies are unable to tackle cancer efficiently. This led to the development of a combinatorial approach which involves amalgamating two or more therapeutic approaches within a single system (e.g., photothermalphotodynamic, chemophotodynamic, chemophotothermal) for combating the disease more effectively. This combination gives synergistic cytotoxic effects a more precisely in nature and with fewer side effects (Zhang et al., 2014b; Liu et al., 2015b; Sahu et al., 2013). In 2014, Zhang et al. constructed a theranostic system where surface-enhanced Raman scattering (SERS) was used as an imaging technique for diagnosis, DOX for chemotherapy and gold nanorods as a tool for photothermal therapy. These combinations of therapies demonstrated synergistic effects when combined together as compared to the case when they were being used alone (Zhang et al., 2014b). Using PTT-PDT simultaneously enhanced therapeutic efficacy as well as reduced laser exposure period. This combination damaged tumor cells from the surface and internally overcame each other's pitfalls (Sahu et al., 2013; Gong et al., 2014). Tarantula et al. designed a system to activate both PTT as well as PDT with the same radiation light, where he developed silicon naphthalocyanine nanoplatform which upon enhancing power density from 0.3 to 1.3 W/cm^2 shifted from PDT to PTT-PDT (Taratula et al., 2015). Zhang et al. designed a system (AuNR@SiO_2-TCPP) for combined PTT-PDT action. Herein, silica-coated gold nanorods (photothermal agent for PTT action) were conjugated with 4-carboxyphenyl porphyrin (photosensitizer for PDT action). Silica coating enhanced the loading of the photosensitizer into the system. This synergistic combination (PDT-PTT) demonstrated significant tumor load reduction compared to alone therapy of PDT or PTT (Zhang et al., 2019b). Lv et al. fabricated GdOF: Ln@SiO_2_ZnPc-DCs mesoporous microcapsules with the assistance of efficient upconversion luminescent gadolinium oxyfluorides: Ln as cores with the mesoporous silica layer as a shell with hollow cavities and this platform was utilized simultaneously for various imaging systems such as CT, MRI, UCL, photothermal and multiple therapies such as PDT, PTT, and chemotherapy as shown in Fig. 1.9 (Lv et al., 2015). Thus, combinational therapy achieved by means of nanotheranostics enhanced therapeutic efficacy, reduced dose regimen, and minimized side effects and MDR (Scheinberg et al., 2010; Park et al., 2009). Hence, this undoubtedly can be considered as the future of cancer therapy.

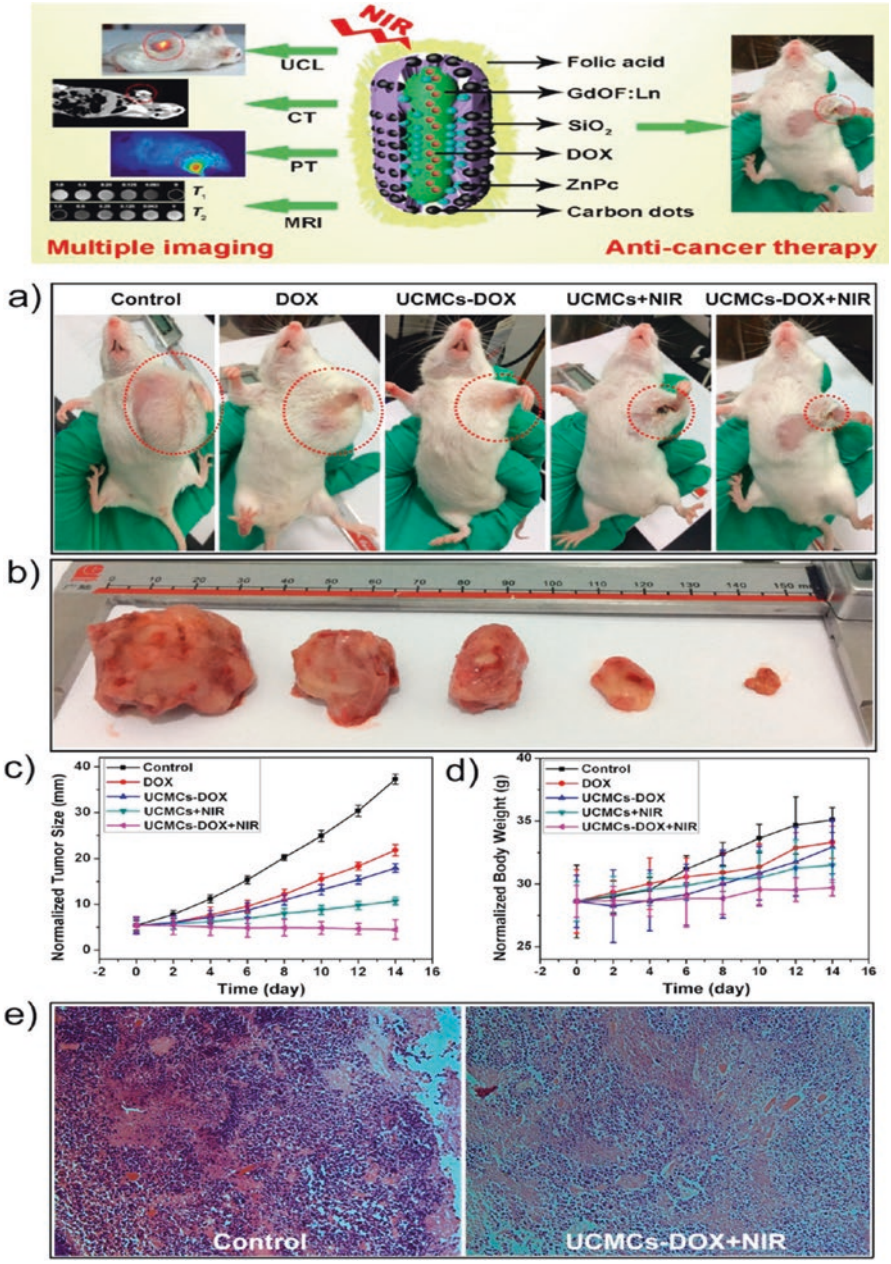

Fig. 1.9 Combinatorial therapy achieved when the anticancer drug was combined with PTT and PDT agents. (**a**) Images of mice after treatment with the various drugs, (**b**) image of tumor tissue obtained after 14 days, (**c**) size of the tumor, (**d**) body weight of H22 tumor in various groups after treatment with the molecule, and (**e**) H&E-stained photographs of tumors from the control group and the UCMCs-doxorubicin irradiated with the laser. (Reproduced with permission from Lv et al. (2015). Copyright (2015), American Chemical Society)

1.4 Conclusion

Nanotheranostic systems are smart platforms for achieving improved cancer imaging and therapy. Nanotheranostics facilitate targeted therapy, improve drug efficacy, enable real-time treatment monitoring and understanding of cancer treatment at molecular levels, and are used in personalized medicine with minimal treatment and cost. Nevertheless, the development of the theranostic system still meets with certain shortcomings, leading to their limited hit in the clinical trials. Major difficulties being observed in the field of nanotheranostics involve their complex nature arising due to the presence of multiple therapeutic and imaging entities in a single system, which in many cases makes them less predictable in terms of treatment outcome. Thus, many of the theranostic agents present at the conceptualization stage need to be explored in greater details.

References

Abdolahinia, E. D., et al. (2019). Enhanced penetration and cytotoxicity of metformin and collagenase conjugated gold nanoparticles in breast cancer spheroids. *Life Sciences, 231*, 116545.

Anselmo, A. C., & Mitragotri, S. (2016). Nanoparticles in the clinic. *Bioengineering & Translational Medicine, 1*, 10–29.

Bazylińska, U., Zieliński, W., Kulbacka, J., Samoć, M., & Wilk, K. A. (2016). New diamidequat-type surfactants in fabrication of long-sustained theranostic nanocapsules: Colloidal stability, drug delivery and bioimaging. *Colloids and Surfaces. B, Biointerfaces, 137*, 121–132.

Benov, L. (2015). Photodynamic therapy: Current status and future directions. *Medical Principles and Practice, 24*(Suppl 1), 14–28.

Bhakta-Guha, D., Saeed, M. E. M., Greten, H. J., & Efferth, T. (2015). Dis-organizing centrosomal clusters: Specific cancer therapy for a generic spread? *Current Medicinal Chemistry, 22*, 685–694.

Blau, R., et al. (2018). Image-guided surgery using near-infrared Turn-ON fluorescent nanoprobes for precise detection of tumor margins. *Theranostics, 8*, 3437–3460.

Boisselier, E., & Astruc, D. (2009). Gold nanoparticles in nanomedicine: Preparations, imaging, diagnostics, therapies and toxicity. *Chemical Society Reviews, 38*, 1759–1782.

Brindle, K. (2008). New approaches for imaging tumour responses to treatment. *Nature Reviews. Cancer, 8*, 94–107.

Bucci, M. K., Bevan, A., & Roach, M. (2005). Advances in radiation therapy: Conventional to 3D, to IMRT, to 4D, and beyond. *CA: A Cancer Journal for Clinicians, 55*, 117–134.

Cabral, H., Nishiyama, N., & Kataoka, K. (2007). Optimization of (1,2-diamino-cyclohexane) platinum(II)-loaded polymeric micelles directed to improved tumor targeting and enhanced aantitumoractivity. *Journal of Controlled Release, 121*, 146–155.

Cao, Y., et al. (2014). Ultrasmall graphene oxide supported gold nanoparticles as adjuvants improve humoral and cellular immunity in mice. *Advanced Functional Materials, 24*, 6963–6971.

Chan, M.-H., & Lin, H.-M. (2015). Preparation and identification of multifunctional mesoporous silica nanoparticles for in vitro and in vivo dual-mode imaging, theranostics, and targeted tracking. *Biomaterials, 46*, 149–158.

Chen, Q., et al. (2014). Near-infrared dye bound albumin with separated imaging and therapy wavelength channels for imaging-guided photothermal therapy. *Biomaterials, 35*, 8206–8214.

Chen, C. H., Wu, Y.-J., & Chen, J.-J. (2015a). Gold nanotheranostics: Photothermal therapy and imaging of Mucin 7 conjugated antibody nanoparticles for urothelial cancer. *BioMed Research International, 2015*, 813632.

Chen, Q., et al. (2015b). Sortase A-mediated multi-functionalization of protein nanoparticles. *Chemical Communications, 51*, 12107–12110.

Chen, Q., et al. (2015c). Drug-induced self-assembly of modified albumins as nano-theranostics for tumor-targeted combination therapy. *ACS Nano, 9*, 5223–5233.

Chen, M.-M., et al. (2017). NIR responsive liposomal system for rapid release of drugs in cancer therapy. *International Journal of Nanomedicine, 12*, 4225–4239.

Cheng, L., et al. (2014). PEGylated Prussian blue nanocubes as a theranostic agent for simultaneous cancer imaging and photothermal therapy. *Biomaterials, 35*, 9844–9852.

Chilakamarthi, U., & Giribabu, L. (2017). Photodynamic therapy: Past, present and future. *The Chemical Record, 17*, 775–802.

Conde, J., Rosa, J., de la Fuente, J. M., & Baptista, P. V. (2013). Gold-nanobeacons for simultaneous gene specific silencing and intracellular tracking of the silencing events. *Biomaterials, 34*, 2516–2523.

Cruz, M. E. M., Simoes, S. I., Corvo, M. L., Martins, M. B. F., & Gaspar, M. M. (2016). Formulation of NPDDS for macromolecules. In *Drug delivery nanoparticles formulation and characterization* (pp. 55–70). CRC Press. https://doi.org/10.3109/9781420078053-7

Davda, S., & Bezabeh, T. (2006). Advances in methods for assessing tumor hypoxia in vivo: Implications for treatment planning. *Cancer Metastasis Reviews, 25*, 469–480.

Diepart, C., et al. (2011). In vivo mapping of tumor oxygen consumption using (19)F MRI relaxometry. *NMR in Biomedicine, 24*(5), 458–463.

Dixit, S., et al. (2015). Dual receptor-targeted theranostic nanoparticles for localized delivery and activation of photodynamic therapy drug in glioblastomas. *Molecular Pharmaceutics, 12*, 3250–3260.

Draz, M. S., et al. (2014). Nanoparticle-mediated systemic delivery of siRNA for treatment of cancers and viral infections. *Theranostics, 4*, 872–892.

Du, Y., et al. (2015). GX1-conjugated poly(lactic acid) nanoparticles encapsulating Endostar for improved in vivo anticolorectal cancer treatment. *International Journal of Nanomedicine, 10*, 3791–3802.

Ehling, J., Lammers, T., & Kiessling, F. (2013). Non-invasive imaging for studying antiangiogenic therapy effects. *Thrombosis and Haemostasis, 109*, 375–390.

Emoto, M., et al. (1998). The blood flow characteristics in borderline ovarian tumors based on both color Doppler ultrasound and histopathological analyses. *Gynecologic Oncology, 70*, 351–357.

Fan, W., et al. (2013). Rattle-structured multifunctional nanotheranostics for synergetic chemo−/radiotherapy and simultaneous magnetic/luminescent dual-mode imaging. *Journal of the American Chemical Society, 135*, 6494–6503.

Fan, W., et al. (2014). A smart upconversion-based mesoporous silica nanotheranostic system for synergetic chemo-/radio-/photodynamic therapy and simultaneous MR/UCL imaging. *Biomaterials, 35*, 8992–9002.

Fang, J., et al. (2018). Graphene quantum dots-gated hollow mesoporous carbon nanoplatform for targeting drug delivery and synergistic chemo-photothermal therapy. *International Journal of Nanomedicine, 13*, 5991–6007.

Fokong, S., et al. (2012). Image-guided, targeted and triggered drug delivery to tumors using polymer-based microbubbles. *Journal of Controlled Release, 163*, 75–81.

Fuchs, C. S., & Mayer, R. J. (1995). Gastric carcinoma. *The New England Journal of Medicine, 333*, 32–41.

Gao, F., et al. (2013). LHRH-PE40 fusion protein tethered silica nanorattles for imaging-guided tumor-specific drug delivery and bimodal therapy. *Advanced Materials, 25*, 5508–5513.

Geng, F., et al. (2011). Thio-glucose bound gold nanoparticles enhance radio-cytotoxic targeting of ovarian cancer. *Nanotechnology, 22*, 285101.

Gong, H., et al. (2014). Engineering of multifunctional nano-micelles for combined photothermal and photodynamic therapy under the guidance of multimodal imaging. *Advanced Functional Materials, 24*(41), 6492–6502. https://doi.org/10.1002/ADFM.201401451

Gradishar, W. J., et al. (2005). Phase III trial of nanoparticle albumin-bound paclitaxel compared with polyethylated castor oil-based paclitaxel in women with breast cancer. *Journal of Clinical Oncology, 23*, 7794–7803.

Grumezescu, A. M. (2018). *Design of nanostructures for theranostics applications* (1st ed.). William Andrew Applied Science Publishers. https://www.elsevier.com/books/design-of-nanostructures-for-theranostics-applications/grumezescu/978-0-12-813669-0

Gu, F. X., et al. (2007). Targeted nanoparticles for cancer therapy. *Nano Today, 2*, 14–21.

Gupta, A. K., & Gupta, M. (2005). Synthesis and surface engineering of iron oxide nanoparticles for biomedical applications. *Biomaterials, 26*, 3995–4021.

Hainfeld, J., Dilmanian, F., Slatkin, D., & Smilowitz, H. (2008). Radiotherapy enhancement with gold nanoparticles. *The Journal of Pharmacy and Pharmacology, 60*(8), 977–985. https://doi.org/10.1211/jpp.60.8.0005

Harrington, K. J., et al. (2001). Effective targeting of solid tumors in patients with locally advanced cancers by radiolabeled pegylated liposomes. *Clinical Cancer Research, 7*, 243–254.

Hassan, M., et al. (2004). Quantitative assessment of tumor vasculature and response to therapy in kaposi's sarcoma using functional noninvasive imaging. *Technology in Cancer Research & Treatment, 3*, 451–457.

He, X., Wang, K., & Cheng, Z. (2010). In vivo near-infrared fluorescence imaging of cancer with nanoparticle-based probes. *Wiley Interdisciplinary Reviews. Nanomedicine and Nanobiotechnology, 2*, 349–366.

He, Q., Ma, M., Wei, C., & Shi, J. (2012). Mesoporous carbon@silicon-silica nanotheranostics for synchronous delivery of insoluble drugs and luminescence imaging. *Biomaterials, 33*, 4392–4402.

Herper, M. (2015, May 5). The cancer drug market just hit $100 billion and could jump 50% in four years. *Forbes*. https://www.forbes.com/sites/matthewherper/2015/05/05/cancer-drug-sales-approach-100-billion-and-could-increase-50-by-2018/

Hong, Y., et al. (2013). Micelles assembled with carbocyanine dyes for theranostic near-infrared fluorescent cancer imaging and photothermal therapy. *Biomaterials, 34*, 9124–9133. https://pubmed.ncbi.nlm.nih.gov/24008037/

Howell, M., & Valle, J. W. (2015). The role of adjuvant chemotherapy and radiotherapy for cholangiocarcinoma. *Best Practice & Research. Clinical Gastroenterology, 29*, 333–343.

Huang, X., Jain, P. K., El-Sayed, I. H., & El-Sayed, M. A. (2008a). Plasmonic photothermal therapy (PPTT) using gold nanoparticles. *Lasers in Medical Science, 23*, 217–228.

Huang, Z., et al. (2008b). Photodynamic therapy for treatment of solid tumors--potential and technical challenges. *Technology in Cancer Research & Treatment, 7*, 309–320.

Huang, X., et al. (2011). Synthesis of hexagonal close-packed gold nanostructures. *Nature Communications, 2*, 292.

Huang, P., et al. (2014). Dye-loaded ferritin nanocages for multimodal imaging and photothermal therapy. *Advanced Materials, 26*, 6401–6408.

Huang, C.-C., et al. (2015). New insight on optical and magnetic Fe_3O_4 nanoclusters promising for near infrared theranostic applications. *Nanoscale, 7*, 12689–12697.

Itaka, K., et al. (2010). Polyplex nanomicelle promotes hydrodynamic gene introduction to skeletal muscle. *Journal of Controlled Release, 143*, 112–119.

Jin, M.-Z., & Jin, W.-L. (2020). The updated landscape of tumor microenvironment and drug repurposing. *Signal Transduction and Targeted Therapy, 5*, 166.

Joh, D. Y., et al. (2013). Theranostic gold nanoparticles modified for durable systemic circulation effectively and safely enhance the radiation therapy of human sarcoma cells and tumors. *Translational Oncology, 6*, 722–731.

Kelkar, S. S., & Reineke, T. M. (2011). Theranostics: Combining imaging and therapy. *Bioconjugate Chemistry, 22*, 1879–1903.

Kim, J.-H., et al. (2008). Antitumor efficacy of cisplatin-loaded glycol chitosan nanoparticles in tumor-bearing mice. *Journal of Controlled Release, 127*, 41–49.
Kim, K., et al. (2010). Tumor-homing multifunctional nanoparticles for cancer theragnosis: Simultaneous diagnosis, drug delivery, and therapeutic monitoring. *Journal of Controlled Release, 146*, 219–227.
Kim, T. H., Lee, S., & Chen, X. (2013). Nanotheranostics for personalized medicine. *Expert Review of Molecular Diagnostics, 13*, 257–269.
Koshy, M., Rich, S. E., & Mohiuddin, M. M. (2010). Improved survival with radiation therapy in high grade soft tissue sarcomas of the extremities: A SEER analysis. *International Journal of Radiation Oncology, Biology, Physics, 77*(1), 203–209.
Kumar, C. S. S. R., & Mohammad, F. (2011). Magnetic nanomaterials for hyperthermia-based therapy and controlled drug delivery. *Advanced Drug Delivery Reviews, 63*, 789–808.
Lammers, T., Kiessling, F., Hennink, W. E., & Storm, G. (2010). Nanotheranostics and image-guided drug delivery: Current concepts and future directions. *Molecular Pharmaceutics, 7*, 1899–1912.
Lee, I.-H., et al. (2012). Imageable antigen-presenting gold nanoparticle vaccines for effective cancer immunotherapy in vivo. *Angewandte Chemie International Edition, 51*, 8800–8805.
Li, L., et al. (2010). Binding and uptake of H-ferritin are mediated by human transferrin receptor-1. *PNAS, 107*, 3505–3510.
Li, S., et al. (2019a). pH-responsive targeted gold nanoparticles for in vivo photoacoustic imaging of tumor microenvironments. *Nanoscale Advances, 1*, 554–564.
Li, S., et al. (2019b). Gold nanorod enhanced conjugated polymer/photosensitizer composite nanoparticles for simultaneous two-photon excitation fluorescence imaging and photodynamic therapy. *Nanoscale, 11*, 19551–19560.
Lim, S., Peng, T., & Sana, B. (2013). Protein cages as theranostic agent carriers. In M. Long (Ed.), *World Congress on Medical Physics and Biomedical Engineering May 26–31, 2012, Beijing, China* (pp. 321–324). Springer. https://doi.org/10.1007/978-3-642-29305-4_86
Lin, Z., et al. (2015). Photothermal ablation of bone metastasis of breast cancer using PEGylated multi-walled carbon nanotubes. *Scientific Reports, 5*, 11709.
Liu, S., et al. (2011). Quantitative tissue oxygen measurement in multiple organs using 19F MRI in a rat model. *Magnetic Resonance in Medicine, 66*, 1722–1730.
Liu, Y., et al. (2015a). A plasmonic gold nanostar theranostic probe for in vivo tumor imaging and photothermal therapy. *Theranostics, 5*, 946–960.
Liu, J., et al. (2015b). Mesoporous silica coated single-walled carbon nanotubes as a multi-functional light-responsive platform for cancer combination therapy. *Advanced Functional Materials, 25*, 384–392.
Liu, X., et al. (2017). PEGylated Au@PtNanodendrites as novel theranostic agents for computed tomography imaging and photothermal/radiation synergistic therapy. *ACS Applied Materials & Interfaces, 9*, 279–285.
Lucky, S. S., Soo, K. C., & Zhang, Y. (2015). Nanoparticles in photodynamic therapy. *Chemical Reviews, 115*, 1990–2042.
Luk, B. T., & Zhang, L. (2014). Current advances in polymer-based nanotheranostics for cancer treatment and diagnosis. *ACS Applied Materials & Interfaces, 6*, 21859–21873.
Luk, B. T., Fang, R. H., & Zhang, L. (2012). Lipid- and polymer-based nanostructures for cancer theranostics. *Theranostics, 2*, 1117–1126.
Luo, H., et al. (2012). An (125)I-labeled octavalent peptide fluorescent nanoprobe for tumor-homing imaging in vivo. *Biomaterials, 33*, 4843–4850.
Luo, D., et al. (2019). Prostate-specific membrane antigen targeted gold nanoparticles for prostate cancer radiotherapy: Does size matter for targeted particles? *Chemical Science, 10*, 8119–8128.
Lv, R., et al. (2015). A yolk-like multifunctional platform for multimodal imaging and synergistic therapy triggered by a single near-infrared light. *ACS Nano, 9*, 1630–1647.
Ma, Y., Huang, J., Song, S., Chen, H., & Zhang, Z. (2016). Cancer-targeted nanotheranostics: Recent advances and perspectives. *Small, 12*, 4936–4954.

MacKenzie, M. J. (2004). Molecular therapy in pancreatic adenocarcinoma. *The Lancet Oncology, 5*, 541–549.

Makino, A., & Kimura, S. (2014). Solid tumor-targeting theranostic polymer nanoparticle in nuclear medicinal fields. *ScientificWorldJournal, 2014*, 424513.

Mashal, A., et al. (2010). Toward carbon-nanotube-based theranostic agents for microwave detection and treatment of breast cancer: Enhanced dielectric and heating response of tissue-mimicking materials. *IEEE Transactions on Biomedical Engineering, 57*, 1831–1834.

Mason, R. P., & Antich, P. P. (1994). Tumor oxygen tension: Measurement using Oxygent as a 19F NMR probe at 4.7 T. *Artificial Cells, Blood Substitutes, and Immobilization Biotechnology, 22*, 1361–1367.

Miao, Z.-H., et al. (2015a). Intrinsically Mn^{2+}-chelated polydopamine nanoparticles for simultaneous magnetic resonance imaging and photothermal ablation of cancer cells. *ACS Applied Materials & Interfaces, 7*(31), 16946–16952. https://doi.org/10.1021/acsami.5b06265, https://pubs.acs.org/doi/pdf/10.1021/acsami.5b06265

Miao, W., et al. (2015b). Image-guided synergistic photothermal therapy using photoresponsive imaging agent-loaded graphene-based nanosheets. *Journal of Controlled Release, 211*, 28–36.

Min, K. H., et al. (2008). Hydrophobically modified glycol chitosan nanoparticles-encapsulated camptothecin enhance the drug stability and tumor targeting in cancer therapy. *Journal of Controlled Release, 127*, 208–218.

Mitsuanga, M., Nakajima, T., Sano, K., Choyke, P. L., & Kobayashi, H. (2012). Near infrared theranostic photoimmunotherapy (PIT): Repeated exposure of light enhances the effect of immunoconjugate. *Bioconjugate Chemistry, 23*, 604–609.

Mizukami, S., et al. (2008). Paramagnetic relaxation-based 19F MRI probe to detect protease activity. *Journal of the American Chemical Society, 130*, 794–795.

Muhammad, F., et al. (2014). Responsive delivery of drug cocktail via mesoporous silica nanolamps. *Journal of Colloid and Interface Science, 434*, 1–8.

Mukherjee, S., et al. (2014). Potential theranostics application of bio-synthesized silver nanoparticles (4-in-1 system). *Theranostics, 4*, 316–335.

Nabil, G., et al. (2019). Nano-engineered delivery systems for cancer imaging and therapy: Recent advances, future direction and patent evaluation. *Drug Discovery Today, 24*, 462–491.

Nam, H. Y., et al. (2009). Cellular uptake mechanism and intracellular fate of hydrophobically modified glycol chitosan nanoparticles. *Journal of Controlled Release, 135*, 259–267.

Natarajan, A., Venugopal, S. K., Denardo, S. J., & Zern, M. A. (2009). Breast cancer targeting novel microRNA-nanoparticles for imaging. In *Multimodal biomedical imaging IV* (International Society for Optics and Photonics) (Vol. 7171). Society of Photo-Optical Instrumentation Engineers.

Ng, K. K., Lovell, J. F., & Zheng, G. (2011). Lipoprotein-inspired nanoparticles for cancer theranostics. *Accounts of Chemical Research, 44*, 1105–1113.

Ng, K. K., Lovell, J. F., Vedadi, A., Hajian, T., & Zheng, G. (2013). Self-assembled porphyrin nanodiscs with structure-dependent activation for phototherapy and photodiagnostic applications. *ACS Nano, 7*, 3484–3490.

Northfelt, D. W., et al. (1998). Pegylated-liposomal doxorubicin versus doxorubicin, bleomycin, and vincristine in the treatment of AIDS-related Kaposi's sarcoma: Results of a randomized phase III clinical trial. *Journal of Clinical Oncology, 16*, 2445–2451.

O'Brien, M. E. R., et al. (2004). Reduced cardiotoxicity and comparable efficacy in a phase III trial of pegylated liposomal doxorubicin HCl (CAELYX/Doxil) versus conventional doxorubicin for first-line treatment of metastatic breast cancer. *Annals of Oncology, 15*, 440–449.

Okarvi, S. M. (2004). Peptide-based radiopharmaceuticals: Future tools for diagnostic imaging of cancers and other diseases. *Medicinal Research Reviews, 24*, 357–397.

Orecchioni, M., Cabizza, R., Bianco, A., & Delogu, L. G. (2015). Graphene as cancer theranostic tool: Progress and future challenges. *Theranostics, 5*, 710–723.

Parhami, P., & Fung, B. M. (1983). Fluorine-19 relaxation study of perfluoro chemicals as oxygen carriers. *The Journal of Physical Chemistry, 87*, 1928–1931.

Park, H., et al. (2009). Multifunctional nanoparticles for combined doxorubicin and photothermal treatments. *ACS Nano, 3*, 2919–2926.

Patra, H. K., et al. (2014). MRI-visual order-disorder micellar nanostructures for smart cancer theranostics. *Advanced Healthcare Materials, 3*, 526–535.

Perrie, Y., & Ramsay, E. (2017). Nanomedicines: Exploring the past, present and future. *Drug Discovery World, 18*, 17–22.

Quan, Q., et al. (2011). HSA coated iron oxide nanoparticles as drug delivery vehicles for cancer therapy. *Molecular Pharmaceutics, 8*, 1669–1676.

Ren, D., Kratz, F., & Wang, S.-W. (2014). Engineered drug-protein nanoparticle complexes for folate receptor targeting. *Biochemical Engineering Journal, 89*, 33–41.

Renfrew, A. K., Bryce, N. S., & Hambley, T. W. (2013). Delivery and release of curcumin by a hypoxia-activated cobalt chaperone: A XANES and FLIM study. *Chemical Science, 4*, 3731–3739.

Rengan, A. K., Jagtap, M., De, A., Banerjee, R., & Srivastava, R. (2013). Multifunctional gold coated thermo-sensitive liposomes for multimodal imaging and photothermal therapy of breast cancer cells. *Nanoscale, 6*, 916–923.

Riedl, S. J., & Shi, Y. (2004). Molecular mechanisms of caspase regulation during apoptosis. *Nature Reviews. Molecular Cell Biology, 5*, 897–907.

Roma-Rodrigues, C., et al. (2019). Nanotheranostics targeting the tumor microenvironment. *Frontiers in Bioengineering and Biotechnology, 7*, 197.

Roy Chowdhury, M., Schumann, C., Bhakta-Guha, D., & Guha, G. (2016). Cancer nanotheranostics: Strategies, promises and impediments. *Biomedicine & Pharmacotherapy, 84*, 291–304.

Runciman, A., Xu, D., Pelton, A. R., & Ritchie, R. O. (2011). An equivalent strain/Coffin-Manson approach to multiaxial fatigue and life prediction in superelastic Nitinol medical devices. *Biomaterials, 32*, 4987–4993.

Sahoo, A. K., Banerjee, S., Ghosh, S. S., & Chattopadhyay, A. (2014). Simultaneous RGB emitting Au nanoclusters in chitosan nanoparticles for anticancer gene theranostics. *ACS Applied Materials & Interfaces, 6*, 712–724.

Sahu, A., Choi, W. I., Lee, J., & Tae, G. (2013). Graphene oxide mediated delivery of methylene blue for combined photodynamic and photothermal therapy. *Biomaterials, 34*(26), 6239–6248. https://doi.org/10.1016/j.biomaterials.2013.04.066

Sahu, N. K., Singh, N. S., Pradhan, L., & Bahadur, D. (2014). Ce3+ sensitized GdPO4:Tb3+ with iron oxide nanoparticles: A potential biphasic system for cancer theranostics. *Dalton Transactions, 43*, 11728–11738.

Scheinberg, D. A., et al. (2010). Conscripts of the infinite armada: Systemic cancer therapy using nanomaterials. *Nature Reviews Clinical Oncology, 7*(5), 266–276. https://www.nature.com/articles/nrclinonc.2010.38

Schroeder, A., Levins, C. G., Cortez, C., Langer, R., & Anderson, D. G. (2010). Lipid-based nanotherapeutics for siRNA delivery. *Journal of Internal Medicine, 267*, 9–21.

Shao, J., et al. (2016). Biodegradable black phosphorus-based nanospheres for in vivo photothermal cancer therapy. *Nature Communications, 7*, 12967.

Shi, X., et al. (2013). Graphene-based magnetic plasmonic nanocomposite for dual bioimaging and photothermal therapy. *Biomaterials, 34*, 4786–4793.

Shi, H., et al. (2014). Au@Ag/Au nanoparticles assembled with activatable aptamer probes as smart "nano-doctors" for image-guided cancer thermotherapy. *Nanoscale, 6*, 8754–8761.

Singh, A., & Sahoo, S. K. (2014). Magnetic nanoparticles: A novel platform for cancer theranostics. *Drug Discovery Today, 19*, 474–481.

Song, K., et al. (2013). Smart gold nanoparticles enhance killing effect on cancer cells. *International Journal of Oncology, 42*, 597–608.

Taratula, O., Schumann, C., Duong, T., Taylor, K. L., & Taratula, O. (2015). Dendrimer-encapsulated naphthalocyanine as a single agent-based theranostic nanoplatform for near-infrared fluorescence imaging and combinatorial anticancer phototherapy. *Nanoscale, 7*, 3888–3902.

Tian, Q., et al. (2013). Sub-10 nm Fe_3O_4@Cu(2–*x*)S core-shell nanoparticles for dual-modal imaging and photothermal therapy. *Journal of the American Chemical Society, 135*, 8571–8577.
Truffi, M., et al. (2016). Ferritin nanocages: A biological platform for drug delivery, imaging and theranostics in cancer. *Pharmacological Research, 107*, 57–65.
Tsai, H.-C., et al. (2010). Graft and diblock copolymer multifunctional micelles for cancer chemotherapy and imaging. *Biomaterials, 31*, 2293–2301.
Tseng, S.-H., Chou, M.-Y., & Chu, I.-M. (2015). Cetuximab-conjugated iron oxide nanoparticles for cancer imaging and therapy. *International Journal of Nanomedicine, 10*, 3663–3685.
Wan, G., et al. (2018). Nanoscaled red blood cells facilitate breast cancer treatment by combining photothermal/photodynamic therapy and chemotherapy. *Biomaterials, 155*, 25–40.
Wang, L., et al. (2005). Monodispersed core–shell Fe_3O_4@Au nanoparticles. *The Journal of Physical Chemistry. B, 109*, 21593–21601.
Wang, L.-S., Chuang, M.-C., & Ho, J. A. (2012). Nanotheranostics – A review of recent publications. *International Journal of Nanomedicine, 7*, 4679–4695.
Wang, Y., et al. (2013). Comparison study of gold nanohexapods, nanorods, and nanocages for photothermal cancer treatment. *ACS Nano, 7*, 2068–2077.
Wang, C.-F., et al. (2015). Multifunctional porous silicon nanoparticles for cancer theranostics. *Biomaterials, 48*, 108–118.
Wang, Z., et al. (2016). Biomineralization-inspired synthesis of copper sulfide-ferritin nanocages as cancer theranostics. *ACS Nano, 10*, 3453–3460.
Wang, Z., et al. (2017). A bifunctional nanomodulator for boosting CpG-mediated cancer immunotherapy. *Nanoscale, 9*, 14236–14247.
Wang, H., et al. (2018). Photosensitizer-crosslinked in-situ polymerization on catalase for tumor hypoxia modulation & enhanced photodynamic therapy. *Biomaterials, 181*, 310–317.
WHO. *Cancer*. https://www.who.int/news-room/fact-sheets/detail/cancer
WHO. *World cancer report 2014*. https://www.who.int/cancer/publications/WRC2014/en/
Wilson, B. C., & Patterson, M. S. (2008). The physics, biophysics and technology of photodynamic therapy. *Physics in Medicine and Biology, 53*, R61–R109.
Wu, J., et al. (2015). Hydrophobic cysteine poly(disulfide)-based redox-hypersensitive nanoparticle platform for cancer theranostics. *Angewandte Chemie (International Ed. in English), 54*, 9218–9223.
Xie, J., & Jon, S. (2012). Magnetic nanoparticle-based theranostics. *Theranostics, 2*, 122–124.
Xie, J., Liu, G., Eden, H. S., Ai, H., & Chen, X. (2011). Surface-engineered magnetic nanoparticle platforms for cancer imaging and therapy. *Accounts of Chemical Research, 44*, 883–892.
Yang, R., et al. (2010a). Dissecting variability in responses to cancer chemotherapy through systems pharmacology. *Clinical Pharmacology and Therapeutics, 88*(1), 34–38.
Yang, K., et al. (2010b). Graphene in mice: Ultrahigh in vivo tumor uptake and efficient photothermal therapy. *Nano Letters, 10*, 3318–3323.
Yang, Y., et al. (2011). Enzyme-responsive multifunctional magnetic nanoparticles for tumor intracellular drug delivery and imaging. *Chemistry – An Asian Journal, 6*, 1381–1389.
Yang, X., et al. (2012). Near-infrared light-triggered, targeted drug delivery to cancer cells by aptamer gated nanovehicles. *Advanced Materials, 24*, 2890–2895.
Yang, H.-W., et al. (2014). Gadolinium-functionalized nanographene oxide for combined drug and microRNA delivery and magnetic resonance imaging. *Biomaterials, 35*, 6534–6542.
Yang, L., et al. (2015). Photothermal therapeutic response of cancer cells to aptamer-gold nanoparticle-hybridized graphene oxide under NIR illumination. *ACS Applied Materials & Interfaces, 7*, 5097–5106.
Yang, T., et al. (2016). Protein-nanoreactor-assisted synthesis of semiconductor nanocrystals for efficient cancer theranostics. *Advanced Materials, 28*, 5923–5930.
Yoo, H., et al. (2013). Multifunctional magnetic nanoparticles modified with polyethylenimine and folic acid for biomedical theranostics. *Langmuir, 29*, 5962–5967.
Yu, J., et al. (2015). Smart MoS_2/Fe_3O_4 nanotheranostic for magnetically targeted photothermal therapy guided by magnetic resonance/photoacoustic imaging. *Theranostics, 5*, 931–945.

Yue, C., et al. (2013). IR-780 dye loaded tumor targeting theranostic nanoparticles for NIR imaging and photothermal therapy. *Biomaterials, 34*, 6853–6861.

Zedan, A. F., Moussa, S., Terner, J., Atkinson, G., & El-Shall, M. S. (2013). Ultrasmall gold nanoparticles anchored to graphene and enhanced photothermal effects by laser irradiation of gold nanostructures in graphene oxide solutions. *ACS Nano, 7*, 627–636.

Zhang, L., Zhou, H., Belzile, O., Thorpe, P., & Zhao, D. (2014a). Phosphatidylserine-targeted bimodal liposomal nanoparticles for in vivo imaging of breast cancer in mice. *Journal of Controlled Release, 183*, 114–123.

Zhang, W., Wang, Y., Sun, X., Wang, W., & Chen, L. (2014b). Mesoporous titania based yolk–shell nanoparticles as multifunctional theranostic platforms for SERS imaging and chemo-photothermal treatment. *Nanoscale, 6*, 14514–14522.

Zhang, X., et al. (2019a). Gold cube-in-cube based oxygen nanogenerator: A theranostic nanoplatform for modulating tumor microenvironment for precise chemo-phototherapy and multimodal imaging. *ACS Nano, 13*, 5306–5325.

Zhang, S., Lv, H., Zhao, J., Cheng, M., & Sun, S. (2019b). Synthesis of porphyrin-conjugated silica-coated Au nanorods for synergistic photothermal therapy and photodynamic therapy of tumor. *Nanotechnology, 30*, 265102.

Zhou, M., et al. (2015). Single agent nanoparticle for radiotherapy and radio-photothermal therapy in anaplastic thyroid cancer. *Biomaterials, 57*, 41–49.

Zhu, X., et al. (2011). Imidazole-modified porphyrin as a pH-responsive sensitizer for cancer photodynamic therapy. *Chemical Communications, 47*, 10311–10313.

Zou, P., et al. (2010). Superparamagnetic iron oxide nanotheranostics for targeted cancer cell imaging and pH-dependent intracellular drug release. *Molecular Pharmaceutics, 7*, 1974–1984.

Chapter 2
Dual Targeting Drug Delivery for Cancer Theranostics

Ghassem Amoabediny, Ghazal Rastegar, Mahin Maleki, Dina Jafari, Zeynab Amoabediny, Fardin Rahimi, and Mina Khodarahmi

Contents

G. Amoabediny (✉)
Chemical Engineering Faculty, University of Tehran, Tehran, Iran

Research Center for New Technologies in Life Science Engineering (UTLSE), University of Tehran, Tehran, Iran

College of Engineering, Department of Chemical Engineering, University of Tehran, Tehran, Iran
e-mail: amoabediny@ut.ac.ir; http://utlse.ir

G. Rastegar · M. Maleki · D. Jafari · Z. Amoabediny
Chemical Engineering Faculty, University of Tehran, Tehran, Iran

Research Center for New Technologies in Life Science Engineering (UTLSE), University of Tehran, Tehran, Iran

F. Rahimi · M. Khodarahmi
Research Center for New Technologies in Life Science Engineering (UTLSE), University of Tehran, Tehran, Iran

Faculty of New Sciences and Technologies, University of Tehran, Tehran, Iran

M. Saravanan, H. Barabadi (eds.), *Cancer Nanotheranostics*, Nanotechnology in the Life Sciences, https://doi.org/10.1007/978-3-030-74330-7_2

Abbreviations

BBB	Blood-brain barrier
BPA	Borono phenylalanine
BSH	Sodium boro captate
c(RGDyC)	Cyclic arginine-glycine-aspartic acid-tyrosine-cysteine
CNT	Carbon nanotubes
DOX	Doxorubicin
EGFP	Enhanced green fluorescent protein
EGFR	Epidermal growth factor receptor
EPR	Permeability and retention effect
FA	Folate
FDA	US Food and Drug Administration
GBM	Glioblastoma multiforme
Glu-VC	Glucose and vitamin C
GO	Graphene oxide
HA	Hyaluronic acid
HAP	Hydroxyapatite
HepG2	Hepatocellular carcinoma cell line
HIV	Human immunodeficiency virus
IL-4R	Interleukin-4 receptor
MGO	Magnetic graphene oxide
OA	Oleanolic acid
O-MWNT	Oxidized multi-walled carbon nanotube
PAMAM	Poly(amidoamine)
PCL	Poly(3-caprolactone)
PLA	Polylactic acid
PLGA	Polylactic-co-glycolic acid
PNAL	Poly[(N isopropylacrylamide-r-acrylamide)-b-L-lactic acid]
PTX	Paclitaxel
RAGE	Receptors for advanced glycation end products
RGD	Arginine-glycine-aspartic acid
Tf	Transferrin
TfR	Tf receptor
WGA	Wheat germ agglutinin

2.1 Introduction to Dual Targeting

Over the recent years, designed nanoparticle vehicles had a significant effect in cancer treatment and diagnosis. In this area, researchers have designed and developed new delivery vehicles for therapeutics and diagnostics purposes (Donahue et al., 2019). Nanomedicine has come up to reduce unfavorable conditions such as

low solubility of drugs, cytotoxicity, and bioavailability of them which influence the effectiveness of drugs. The most studied drug delivery systems include lipid-based, polymer-based, and carbon-based vehicles (Amoabediny et al., 2018a; Anarjan, 2019). Nanocarriers' characteristics such as surface charge, shape, chemical structure, and mechanical strength can change and improve to increase nanomedicines efficacy using nanotechnology (Kydd et al., 2017).

Previously, permeability and retention (EPR) effect was assumed to be a major underlying mechanism for internalization of most nanocarriers used for drug delivery to cancerous cells. However, further investigations showed the less important role of EPR in human cells. Also, in spite of the better efficacy of nano-formulated drugs than free drugs, problems like unwanted normal cells death because of their lack of selectivity for cancer cells led to more research on active-targeted nanocarriers (Lammers et al., 2012). After that, several active targeted nano-formulations have developed and introduced in literature and some succeed to the clinical trials (van der Meel et al., 2013).

Active-targeting strategies are based on developing a nanocarrier modified with ligands or particular physical or chemical characteristics to specifically bind to surface markers of cancer cells and deliver therapeutic imaging and diagnostic agents or all of them to cancer cells. To now, different ligands were used to actively target nanocarriers. Antibodies, aptamers, folic acid, transferrin, and arginine-glycine-aspartic acid (RGD) tripeptides are of the most studied ligands used for active targeting (Anarjan, 2019). Haghiralsadat et al. synthesized liposomal carriers for co-delivery of siRNA and DOX to osteosarcoma (OS) cells. They functionalized PEGylated liposomes by conjugation of an YSA peptide, a ligand for the EphA2 receptor, highly upregulating on osteosarcoma cells, to specifically target OS cells. Their results showed that targeted delivery systems have strong cytotoxic effects against SaOs-2 and MG-63 cells while showing less toxicity to primary bone cells (Haghiralsadat et al., 2018). Besides using ligands to selectively deliver nanocarriers, some delivery systems benefit from magnetic fields to localized nanocarriers in the tumor environment (Rezayan et al., 2016; Zhang et al., 2017).

In active-targeting strategy, cancer cell surface markers affinity to the ligand-modified nanocarriers and consequently markers expression play an important role. It is well-known that tumor cell surface markers are not constant and dynamically change with tumor stages. Also, sometimes various markers are upregulated on tumor cells and upregulation of compensatory receptors are the main reasons for drug resistance. Additionally, the ligand-receptor binding process is a saturable process. These are some processes involved in reducing the mono-targeted nanomedicine efficiency which motivates to develop dual-targeted cancer nanotheranostics (Zhu et al., 2018). Dual-targeting therapy demonstrates superior efficacy over single-targeting in terms of cellular uptake, cell selectivity, and penetration into the tumor. In the study of Taili Zong et al., a dual-targeting nanovehicle is presented by two ligands, TAT and T7, with different targets. In this study, the ligand T7 targets blood-brain barrier (BBB), and the ligand TAT targets brain glioma tumor and affects drug penetration into the tumor cells. This dual-targeted liposomal system enhanced cellular uptake, passed better through BBB, targeted brain glioma, and

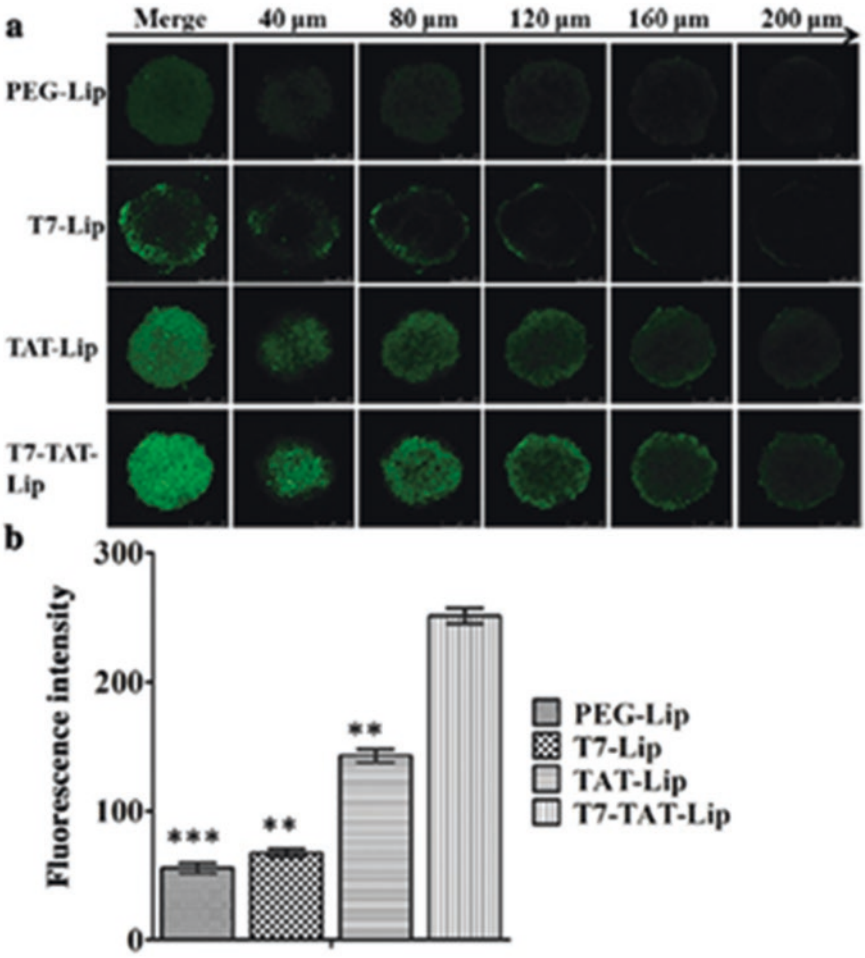

Fig. 2.1 Comparing dual-targeted (by using two ligands, TAT and T7), single-targeted and non-targeted coumarin-6-labeled liposomal systems uptake on C6 tumor spheroids. (**a**) Representative CLSM images of liposome uptake by tumor spheroid within different depths. Scale bars represented 250 μm. (**b**) Quantitative determinations by flow cytometry (Zong et al., 2014). With permission from Elsevier Copyright, 2014

penetrated into the tumor. Figure 2.1 demonstrates significantly higher cellular uptake of these dual targeted systems (Zong et al., 2014).

However, none of the dual-targeted drug delivery systems have entered clinical practice and researches are ongoing. The dual-targeted nanocarriers can be categorized to five groups as demonstrated in Fig. 2.2. Some nano-formulations have two different ligands on their surface targeting two different receptors of one kind of cancerous cells. Second type is systems with two different ligands which target two different markers of two different cells. Another category is using a ligand for

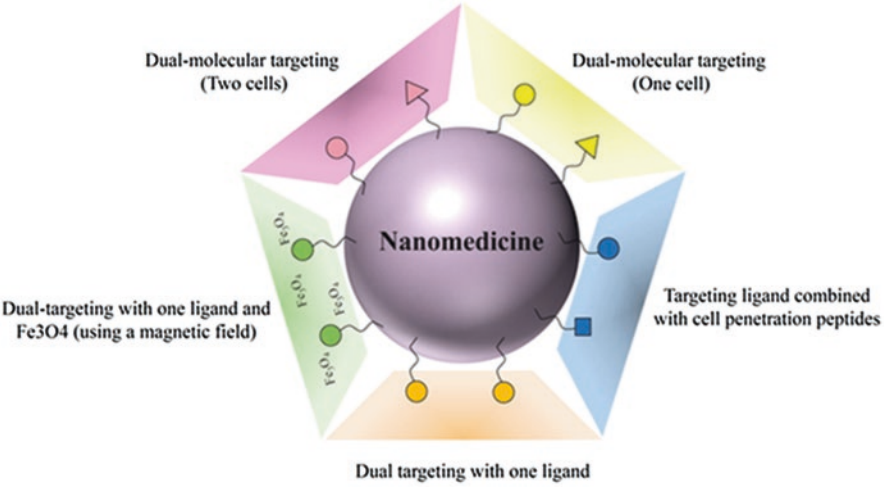

Fig. 2.2 Potential dual-targeting strategies

targeting and a peptide to increase cell penetration of drug delivery nano-systems. The fourth type is implementation of a magnetic nanoparticle and a ligand to design a carrier which can be targeted by a ligand and magnetic force. And the last one is targeting an overexpressed receptor which is the same in two different cell types by means of one kind of ligand.

This chapter will focus on dual-targeted nanomedicine developed for cancer therapy. The most investigated carriers which developed and implemented dual-targeting strategy are lipid-based, polymer-based, and carbon-based carriers. Some great examples of dual-targeting strategies are presented in Table 2.1. The chapter will discuss different dual-targeted nano-formulations based on mentioned carriers' categories.

2.2 Dual-Targeted Nanovehicles

2.2.1 Lipid-Based Vehicles

The most investigated lipid-based carrier in drug delivery systems is liposome. Liposomes are self-assembled spherical vesicles constructed from an aqueous core and lipid bilayer membranes, meaning that both hydrophilic and hydrophobic drug molecules can incorporate in liposomes. Liposomes were the very first type of nanoparticle drug delivery systems to be applied for biomedical purposes and have continued to be in the spotlight of research up until this day. Liposomes have many advantages in drug delivery, such as biocompatibility, biodegradability, and enhanced therapeutic index (Amoabediny et al., 2018a). Being a doxorubicin

Table 2.1 Examples of dual targeting strategies for the purpose of cancer therapy

Carrier type	Ligands	Encapsulated drug	Target cells	References
Liposome	Tf-TAT	DOX-PTX	B16 melanoma cells	Yuan et al. (2016)
Liposome	RGD-Tf	PTX	BBB-C6 glioma cells	Qin et al. (2014)
Liposome	Biotin-glucose	PTX	MCF7 Breast Cancer Cells	Huang et al. (2020)
Liposome	c(RGDyC)	boron-containing agents	U87 glioma cells- HUVECs	Kang et al. (2017)
Liposome	HA-FA	PTX	B16 melanoma cells- HepG2 carcinoma cells	Liu et al. (2014)
Liposome	RGD	PTX	MDA-MB-231 breast cancer	Zhao et al. (2019)
Liposome	Glucose- Vitamin C	PTX	C6 glioma cells	Peng et al. (2018)
Liposome	Fe_3O_4	Oleic Acid	A549 adenocarcinoma cells-HeLa cells	Li et al. (2018b)
Liposome	TAT-T7	DOX	BBB-C6 glioma cells	Zong et al. (2014)
Liposome	FA-Asp8	DOX	MDA-MB-231 breast cancer	Ke et al. (2017)
Liposome	YSA peptide	DOX	SaOs-2 and MG-63	Haghiralsadat et al. (2018)
Liposome	Antibody	Silibinin and glycyrrhizic acid	HepG2	Amoabediny et al. (2018b)
Polymeric	RGD-Tf	PTX	HUVECs-HeLa cells	Xu et al. (2012)
Polymeric	AP1	DOX	C6 glioma cells-HUVECs	Sun et al. (2017)
Polymeric	CGKRK peptide	PTX	U87MG cells-HUVECs	Sun et al. (2017)
Polymeric	IRNPs-RGD	DOX	C6 glioma cells-HUVECs	Gao et al. (2014)
Polymeric	Tf-WGA	DOX	BBB-C6 glioma cells	He et al. (2011)
Polymeric	ANG	PTX	U87 MG cells	Xin et al. (2011)
Polymeric	FA-RGD	DOX	KB carcinoma cells	Lin et al. (2015a, 2015b)
Polymeric	Angiopep-2 peptide- AS1411 aptamer	DOX	BCECs- C6 Cells	Wang et al. (2018)
multi-walled carbon nanotube	Angiopep-2	PTX	BCECs- C6 Cells	Ren et al. (2012)
multiwall carbon nanotube	Folate-iron	DOX	HeLa cells	Li et al. (2011)

(continued)

Table 2.1 (continued)

Carrier type	Ligands	Encapsulated drug	Target cells	References
Graphene oxide nanocarriers	Aptamer	PTX	MCF-7 cancer cells- L-929 fibroblast cell	Hussien et al. (2018)
Graphene oxide nanocarriers	FA	DOX	–	Li et al. (2018a)
Graphene oxide nanocarriers	EGFR	DOX	CT-26 cells	Lu et al. (2018)
Graphene oxide nanocarriers	Fe_3O_4-FA	DOX	HeLa cells	Yang et al. (2011)
Graphene oxide nanocarriers	Fe_3O_4-FA	DOX	HeLa Cells	Du et al. (2020)

(Dox)-encapsulating PEGylated liposome, Doxil® was the first nano-therapeutic drug which the US Food and Drug Administration (FDA) approved for treatment of cancer (Danhier et al., 2010). Even though non-targeting nanocarriers such as Doxil® seemed to have satisfactory results in the past, some drawbacks have limited their applications, the most significant one being their nonspecific targeting (Liu et al., 2014). In order to overcome this issue, many researchers have reported the design and synthesis of dual-targeting liposomes, having optimized features and superior therapeutic outcomes.

Mingqing Yuan et al. (Yuan et al., 2016) have used transferrin (Tf) and a type of cell penetrating peptide, TAT, to modify liposomes for dual-delivery of two anticancer drugs, namely DOX and Paclitaxel (PTX), for treatment of melanoma. Being the trans-activator protein of the human immunodeficiency virus (HIV) type-1, TAT is crucial for viral duplication. Two lysine and six residues arginine exist in TAT peptide. Due to cationic charges of them, their interplay with the negatively charged cell membrane are facilitated, increasing permeability of the cell membrane. Therefore, TAT could enter cells when it conjugates with either large or small molecules and can deliver them into the targeted cells efficiently through both receptor-/transporter-independent and unsaturated pathways (Kluza et al., 2012).

PTX interferes with the normal process of microtubule breakdown, while DOX interacts with DNA through inhibition of macromolecular biosynthesis. The in vitro cellular uptake study of B16 cells was investigated using flow cytometry. Based on the results, dual-modified liposomes had higher cellular uptake: 14-, 8.7-, and 2.8-fold higher than non-modified, Tf-modified, and TAT-modified liposomes, respectively. Furthermore, based on apoptosis assays, liposomes dual modified by Tf and TAT showed higher necrotic and apoptosis effect (88.1% of the cells detected in the necrotic and apoptosis quadrants) in comparison to non-modified (4.1%), Tf-modified (14.2%), and TAT-modified liposomes (Yuan et al., 2016).

In another report, Li Qin et al. developed dual-targeting PTX-loaded liposomes decorated with RGD and Tf for targeting glioblastoma multiform (GBM). GBM explains 70% of all malignant gliomas and is exceedingly aggressive with 5%

survival rate. RGD has high affinity toward αvβ3 integrin that is highly expressed in glioma, and Tf is a special ligand for the TF receptor (TFR) existing with high density in both the BBB and the surface of the tumor cells. C6 and b.End.3 cell lines were used to evaluate the cellular uptake and the cytotoxicity of the dual-modified liposomes. In both types of cells, dual-modified liposome uptake was 8.6- and 3.2-fold higher than that of non-decorated liposomes, respectively. In the cytotoxicity experiment, the cell viability of all types of liposomes was dependent to time and the dose of PTX. The non-modified liposome formulation reached the highest cell viability amid of the four liposome formulations in all equivalent drug concentrations that were used. For example, after 24 hours and at PTX concentration of 300 μg/ml, the non-modified liposomes showed almost twice higher cell viability in comparison to the RGD-Tf-modified liposomes (Qin et al., 2014).

Another study elaborated on designing biotin-glucose branched ligand-conjugated, dual-targeting liposomes. When compared to the regular carriers, biotin-modified, glucose-modified, and dual-modified liposomes had much higher cellular uptake in both 4T1 cells and in MCF-7 cells. In the cytotoxicity assay, the dual-targeting liposomes exhibited the highest growth inhibition in all types of liposomes (non-modified and single modified). Nevertheless, free PTX showed the highest inhibition rate, because the transport of free drugs into the cells is directly and also via passive diffusion, without a drug release process (Huang et al., 2020).

Another liposomal dual-targeting system was reported by Weirong Kang et al. who developed cyclic arginine-glycine-aspartic acid-tyrosine-cysteine (c(RGDyC)) conjugated carriers for in vitro boron neutron capture therapy. Two agents which are containing boron, sodium borocaptate (BSH), and boronophenylalanine (BPA) are clinically approved in most countries; however, both of them lack tumor selectivity, which is the reason for their limited therapeutic outcome. Overexpression of αvβ3 in glioblastoma cells (U87) and human umbilical vein endothelial cells (HUVEC) has categorically been proven. So far, to target many types of tumors, both linear and cyclic RGD have been implemented as ligands. However, cyclic RGD peptides are more stable and have more tendency to αvβ3 compared to linear RGD peptides. In U87 and HUVEC cells, cellular uptake of c(RGDyC)-covered carriers was more than of non-covered liposomes. For example, in HUVEC cells, the cellular uptake of modified liposomes was 2.5-fold more than the non-modified ones after 3 hours, and more than 4-fold higher after 16 hours. In addition, cell viability of both U87 and HUVEC cells was remarkably lower when treated with c(RGDyC)-covered liposomes compared to that of regular liposomes. For instance, in U87 cells case, when treated with modified carriers, cell viability was almost 2-fold lower than when treated with non-modified liposomes. All in all, it was concluded that cyclic RGD peptide-conjugated boron encapsulating liposomes cause a dual targeting approach with utilizing the high expression of αvβ3 in glioblastoma cells and tumor vasculature resulting in more impressive boron neutron capture therapy (Kang et al., 2017).

In another report, Guo-Xia Liu et al. reported a dual-targeting nanocarrier composed of liposomes loaded with PTX and the plasmid pCMV-EGFP (pEGFP-N1)

which green fluorescent protein (EGFP) exists in it, modified by folate (FA), and coated with hyaluronic acid (HA). FA-modified liposomes have a positive charge, which makes them interact with serum complexes compound, and form aggregates. To prevent this from happening, HA, a negatively charged component of the extracellular matrix was coated on the surface of FA-modified liposomes. HA coated liposomes bound to CD44, which is highly expressed in many types of cancer cells. Furthermore, the HA layer on the surface of the liposomes would undergo an enzyme degradation, which exposes the FA moiety and targets the cancer cells. Using MTT assay, the in vitro cytotoxicity of HA/FA/liposomes and FA/liposomes at several concentrations of DNA (1.0, 2.0, 3.0, 4.0, and 5.0 μg/mL) was studied on murine malignant melanoma cell line (B16), which is CD44-positive and FR-positive, as well as human hepatocellular carcinoma cell line (HepG2), which is CD44-positive and FR-negative. Cell viabilities of both cell types treated with drug-free HA/FA/liposome was more than of drug free FA/liposomes. For example, in B16 cells case, at DNA concentration of 5.0 μg/mL, the cell viability of those treated by paclitaxel-free HA/FA/liposomes was twice more than the cells treated with FA/liposomes. Which demonstrates that the HA shell could obviously affect the cytotoxicity of the nanovehicles and reduce it. Moreover, the IC50 values of HA/FA/liposomes and non-modified liposomes on B16 cells were 1.92 and 3.96 μg/mL and on HepG2 cells were 3.28 and 5.02 μg/mL. The higher cytotoxicity is ascribed to better delivery of the HA/FA/liposomes. Compared to non-modified vehicles, FA/liposomes showed higher internalization rates in B16 cells at 0.5 and 2 h, respectively, which was affected by the overexpression of folate receptors on the surface of B16 cells. Moreover, in comparison to FA/liposomes, HA/FA/liposomes represented more cellular uptake rates at 0.5 h, which indicated that HA was a biocompatible layer, and also enhanced the rates of internalization (Liu et al., 2014).

In another study, PTX-loaded liposomes co-modified with glutamic oligopeptide and RGD were developed to effectively target bone metastases. Hydroxyapatite (HAP) is an inorganic compound and the main component of bone. It is reported that HAP can be the best target in selective drug delivery to bone; this characteristic of HAP was utilized in this study. Glutamic acid oligopeptides, in addition, have excellent bone-targeted ability, which is due to their ionic interaction with $Ca2^{+}$. In MTT assay which is applied to evaluate the different liposomes cytotoxicity on MDA-MB-231 cells, the co-modified liposomes exhibited lower cell viability compared to that of non-modified carriers. For example, at drug concentration of 16 ng/ml, the cell viability of co-modified carriers was 1.8-fold lower than that of the regular ones. HAP binding assay demonstrated that dual-modified liposomes had threefold and more than eightfold higher HAP binding efficiency compared to that of RGD-modified and non-modified liposomes, respectively. In vivo tumor targeting was investigated by injecting MDA-MB-231 cancer cells into BALB/c nude mice. The results showed that dual-modified carriers had higher affinity toward cancer cells in comparison to that of ordinary cells. For example, after 2 hours, paclitaxel concentration in MDA-MB-231 cells was more than twice higher than that of normal cells. Furthermore, the drug concentration in MDA-MB-231 cells was the highest in mice remedied with co-modified carriers: 5–8 times higher than that of mice

remedied with free drug, 3–5 times higher than that following non-modified liposome injection, and 1–3-fold more than that following Glu_6/liposomes (Zhao et al., 2019).

Another interesting study has to do with Yao Peng et al. who designed and synthesized liposomes improved by glucose and vitamin C (Glu-VC) for delivery of PTX to the brain. GLUT1 and SVCT2 are physiological transport systems for glucose and vitamin C, respectively, which are expressed on the brain capillary endothelial cells and also choroid plexus epithelium cells, respectively. VC has a significant brain targeting capability, since the highest amount of VC is found in the brain (up to 10-times higher than the others). The cellular uptake of the modified liposomes on C6 cells (GLUT1- and SVCT2-overexpressed cells) was 4.79, 1.95, and 4.00 times higher than that of non-modified liposomes, Glu-modified liposomes, and VC-modified liposomes, respectively. Furthermore, the relative uptake efficiencies of Glu-VC liposomes were 6.12-fold higher than that of non-modified liposomes. In vivo imaging further indicated that the co-modified liposomes showed the best capability of accumulating in the cancer cells with much amount of fluorescence than single-modified and non-modified liposomes (Peng et al., 2018).

Another article elaborated on magnetic octreotide-modified and Fe_3O_4-coated liposomes loaded with oleanolic acid (OA), in which the coated Fe_3O_4 nanoparticles result in a magnetic targeting property. Drug delivery carriers formulated to magnetic targeting using magnetic field source outside of the tumor site can enhance the drugs accumulation in tumor sites. However, high accumulation of drug incorporated nanoparticles in tissue of tumor is not a harbinger of great therapeutic effect. Rather, it is the efficient intracellular uptake of drugs by the tumor cells which leads to high therapeutic effect. Although to reach high cellular uptake, the modified Octreotide was located on the surface of the liposomes. At first, the Oct-modified carriers connect to the surface of SSTR2 overexpressed cells. After that, a clathrin-coated pit forms in the cell membrane. Further, the pit forms a clathrin-coated vesicle to enter the cells. As a result, Oct can function as both a tumor-targeting and tumor-penetrating peptide of a tumor. Cytotoxicity assay conducted in in vitro condition, intracellular uptake, and antitumor effects of the developed nanocarrier, on A549 (SSTRs overexpression) and human cervical carcinoma cells (HeLa cells, SSTRs low expression) were investigated. In case of A549 cells, it was seen that in the cells treated with both Oct-modified liposomes and magnetic Oct-modified liposomes, there was stronger intracellular fluorescence than in those treated with non-modified carriers. However, for HeLa cells there was no considerable difference between all the groups. In addition, there was no eye-catching difference in the antitumor effects between Oct-modified liposomes and magnetic Oct-modified liposomes for both of A549 and HeLa cells. The Oct-modified liposomes showed a significant increased inhibitory effect for A549 cells compared to non-modified liposomes: The mean inhibition rates caused by non-modified, Oct-modified, and magnetic Oct-modified liposomes at OA concentration of 100 μg/ml were 82.51, 90.06, and 89.76%, respectively. However, no significant difference in inhibition rate for HeLa cells is reported under the same conditions, their mean inhibition rates were 83.82, 85.18, and 84.68%, respectively, further demonstrating the role of

receptor-mediated internalization in growth inhibition. Mice which had S180 tumor were applied to investigate the in vivo targeted therapeutic effect. Volumes of the tumor of mice treated with Oct-modified liposomes were significantly smaller than those of mice-treated non-modified liposomes. For example, the tumor volumes of all kinds of Oct-modified liposomes were more than twofold smaller than that of naked liposomes groups, after 10 days. In addition, the body weight of animals treated with different types of liposomes exhibited no significant variation during the treatment. These results further indicate the role of octreotide in receptor-mediated targeting and Fe_3O_4 in enhancing nanocarriers accumulation (Li et al., 2018b).

Taili zong et al. also reported a system of dual-targeting drug delivery constructed from liposomes improved with dual peptides, T7 and TAT. The uptake of modified liposome with T7 and TAT was 2.8, 11.4, and 13.9 times more than by C6 cells and 2.4, 11.0, and 14.1 times higher by bEnd.3 cells than those of modified separately with TAT, with T7, and non-regular liposomes. These outcomes demonstrate that the distance of co-modified liposome (with both TAT and T7) to the target glioma cells were less and TAT was able to arrive the membrane of cancerous cells and raise the cellular uptake. Compared with the regular carriers, the uptake of tumor had increased 4.5, 2.6, and 1.2, times by co-modified liposome, liposome modified with TAT, and liposome modified with T7 (Zong et al., 2014).

Xianzhu Ke et al. designed a dual-targeting liposomal system which loaded DOX, for targeting cancerous cells in bone modified with FA and Asp8, that Asp8 targets the bone and FA targets the bone cancerous cells. The in vitro cytotoxicity results demonstrated that both FA/liposomes and FA/Asp8/liposomes had significantly higher cytotoxicity (with an IC_{50} of 15.3 μg/mL for FA/Asp8/liposomes, 100.5 μg/mL for Asp8/liposomes, 17.8 μg/mL for FA/liposomes, and 94.9 μg/mL for non-modified liposomes), which clearly confirms the effect of FA on the anti-proliferative activities in FR over-expressed cells (MDA-MB-231). In vivo screening showed that treatment with dual-conjugated carriers in the tumor bearing mice increases the median survival time (27 days), which was 1.2, 1.3, and 1.4 times more than that of DOX-loaded modified liposome with Asp8, DOX-loaded modified liposome with F, and free DOX. Furthermore, according to imaging of whole body, the liposomes modified with Asp8 and co-modified liposomes with FA and Asp8 showed higher accumulation in the right back limb of mice. However, there were no observed signs in the bone of mice treated with non-conjugated carriers. These results confirm that Asp8 functionalized liposomes do enjoy well bone-targeting ability in vivo (Ke et al., 2017).

2.2.2 Polymer-Based Vehicles

Using of biodegradable polymers in drug delivery systems has experienced rapid growth in the past decade, and many research articles have reported the use of pharmaceutical agents capable of conjugating to the polymeric vehicles to increase their circulation half-life as well as their targeting abilities.

In one report, nanoparticles constructed from hyperbranched amphiphilic poly[(amine-ester)-co-(D,L-lactide)]/1,2-dipalmitoyl-sn-glycero-3-phosphoethanolamine copolymer (HPAE-co-PLA/DPPE) functionalized by RGD, and Tf was used for chemotherapy of HUVECs and HeLa cells. Co-modification of the nanoparticles with Tf and RGD led to active targeting of the tumor cells: RGD enhanced the targeting, transportation, and nanoparticle gathering to tumor vasculature, expressing integrin, and Tf enhanced the cellular uptake of nanoparticles in TfR-expressing cancerous cells. By applying RGD, the cytotoxic yield increased 10 times in α5β3 integrin overexpressed HUVECs, but cytotoxicity in Tf receptor overexpressed HeLa cells, improved twice by using Tf. For HUVECs cells, the nanoparticles modified with RGD and dual-modified formulations had a lower IC_{50} than non-modified, Tf-modified nanoparticles, and the free-PTX. However, for HeLa cells, in comparison to free-PTX, non-modified and RGD-modified nanoparticles, the IC_{50} of dual-modified and Tf-modified nanoparticles reduced. This result is elucidated by the reality that the surface of HUVECs expresses abundant α5β3 integrin receptors but few TfR; hence the RGD-modified nanoparticles would enjoy a higher cell toxicity. On the other hand, Tf-modified nanoparticles effected better on HeLa cells and were more toxic to it, the surface of which is covered with Tf receptors, rather than α5β3 integrin receptors. Furthermore, dual-modified nanoparticles showed 1.4-times and 1.7-times higher uptake by HeLa cells and HUVECs compared to non-modified nanoparticles, respectively (Xu et al., 2012).

In the study of Sun et al., they developed nanocarriers including DOX-loaded polylactic acid (PLA) nanoparticles and a tumor homing peptide (AP1) for targeting brain tumor cells. AP1 joined to interleukin-4 receptor (IL-4R), which is expressed on glioma cells and also vascular endothelial cells. As expected, AP1-covered nanocarriers showed more cellular uptake, which was also related to the nanoparticles concentration. For instance, the uptake of AP1-modified carriers in C6 cells was about twice more than that of non-modified particles. In addition, the amount of IC50 in any formulation of DOX was 48.68 ng/mL for AP1-modified carriers, 114.8 ng/mL for non-modified carriers, and 194.3 ng/mL for free DOX in C6 cells. The amount of IC50 in any formulation of DOX was 57.49 ng/mL for AP1-modified carriers, 125.8 ng/mL for non-modified carriers and 232.2 ng/mL for free DOX in HUVEC cells. Regarding the in vivo studies, mice treated with AP1-decorated carriers achieved higher survival time (47 days) in comparison to mice that were treated with non-modified particles (35 days), which further confirms the superiority of dual-targeting strategies (Sun et al., 2017).

Quanyin Hu et al. presented another polymer-based dual-targeting drug delivery system constructed from CGKRK peptide-modified MePEG-PCL and maleimide-PEG-PCL nanoparticles, targeting tumor cells, and tumor angiogenic blood vessels. Despite the fact that angiogenesis inhibitors which stop tumor growth are established to reach high efficacy in animal models as well as pre-clinical use, their actual clinical use entails low survival rate. One of the main reasons attributed to this phenomenon is called “evasive resistance”: when oxygen and nutrient leave the body after antiangiogenic therapy, tumors could reconcile and even go forward to steps of more intense malignancy. CGKRK peptide specially binds to neovascular

endothelial cells and tumor cells with high dependency. Sulfated polysaccharide exists on the surface of tumor cells and neovascular endothelial cells which is called the CGKRK receptor. Interestingly, CGKRK peptides do not recognize the vessels in normal tissues; rather, they only recognize them in tumors. Hu et al. used HUVEC cells and U87MG cells as a model of neovascular endothelial cells and tumor cell model, respectively, based on their overexpressed heparan sulfate. The cellular incorporation of CGKRK-modified nanocarriers in both types of cells was more than that of unmodified carriers: in HUVEC cells 2.2, 2.3, 2.5, 2.7, and 2.8 times higher and in U87MG cells 1.7, 1.5, 1.8, 1.8, and 2 times higher. Furthermore, flow cytometry results demonstrated that CGKRK-modified particles loaded with PTX had significantly higher apoptosis (18.35% for HUVECs and 22.25% for U87MG) when compared to that of non-modified ones (10.19% for HUVECs and 9.46% for U87MG). In addition, the IC_{50} value for HUVEC and U87MG cells are reported to be 96.95 ng/ml and 52.51 ng/ml, which are much lower than that of non-modified particles (163.1 ng/ml for HUVEC cells and 107.3 ng/ml for U87MG cells). In vivo antitumor growth effect evaluations indicated that 14 days post injection, the tumor bulk size of mice which were given treatment with modified particles was 2.2-fold smaller than tumor size of mice treated with non-modified carriers (Sun et al., 2017).

In another report, polymeric nanoparticles were immobilized with interleukin-13 peptide (IRNPs) and RGD to establish a delivery system of dual targeting for treatment of cancer cells, in which RGD targeted αvβ3, and IL13Rα2 receptors was targeted by interleukin-13 peptide on GBM cells. To clarify the ability of targeting, cellular uptake on C6 and HUVEC cells was investigated by in vitro analyzing. The results indicated that in order to modify endocytosis pathways, the main endocytosis pathways changed from macropinocytosis in non-modified nanoparticles to clathrin-mediated endocytosis in the modified ones. Because of the combination of the effect of RGD and IL-13p, dual-modified carriers demonstrated a better localization in GBM cells. They were clearly noticed in neovessels and GBM cells suggesting their successful dual targeting effect (Gao et al., 2014).

Hai He et al. reported a carrier by using dual-targeting concept which was loaded with DOX and consisted of wheat germ agglutinin (WGA) and Tf functionalized PEGylated Poly(amidoamine) (PAMAM) dendrimers. Dendrimers are promising new scaffolds for polymeric drug delivery systems owing to their distinctive properties, such as their intensive branching. Wheat germ agglutinin (WGA) and lectins have shown a strong affinity for cerebral capillary endothelium, decreased toxicity to normal cells, and increased binding towards malignant tumor cells. The constructed dual-targeting carriers did obviously reduce the cytotoxicity of DOX for the normal cells and, simultaneously, stopped the growth of C6 cells efficiently. The results of transportion through the BBB indicated that PEGylated dendrimers co-modified with Tf and WGA delivered 13.5% of the whole DOX during 2 hours, representing an increase transportation in comparison to that of free DOX (5%), PEGylated dendrimers modified with WGA (8%) and PEGylated dendrimers modified with Tf (7%) during the same time. Moreover, because of the targeting effects of Tf and WGA, the amount of DOX localization in the cancer cells was increased, causing thorough breakage of the avascular C6 glioma spheroids at in vitro conditions (He et al., 2011).

In another study, a PTX-loaded dual-targeting carrier was introduced by immobilizing Angiopep with poly(3-caprolactone) (PCL) nanoparticles (ANG-NP). PCL is a biodegradable polymer which has FDA approval and vastly used in drug delivery applications. The cellular internalization of ANG-NP in U87 MG cells exhibited both a time-dependent as well as an energy-dependent mode. Incubation with Filipin and Genistein (inhibitors of caveolae-mediated endocytosis) did reduce the cellular intake of ANG-NP to 84.3% and 74.5%, respectively, which demonstrated the role of caveolae-mediated endocytosis in the cellular internalization process of ANG-NP. Furthermore, the IC_{50} value of PTX nanoparticles modified with Angiopep was 3.4 and 3.8 times lower than that of Taxol® and non-modified carriers, respectively, which indicated that the antiproliferative impact of the polymeric vehicles was significantly elevated by being conjugated with angiopep. In order to imitate the dual barrier (BBB and tumor barrier) of glioma in vivo, a BCECs-U87MG glioma co-culture model was investigated to monitor the dual-targeting effects of ANG/PTX/NP. The transport ratios of nanoparticles across the BCECs monolayer model in vitro indicated that after 8 h transport from the donor chamber, the concentration of PTX in basolateral compartment could reach median lethal dose toward U87MG cells (Xin et al., 2011).

Formed from the self-assembly of amphiphilic copolymer building blocks, polymeric micelles have been significantly exploited in the drug delivery arena. They provide a core-shell particle in which the hydrophobic core encapsulates either imaging agents or hydrophobic therapeutics, while the shell gives the carriers the capability of maintaining their stability in aqueous solutions. However, it is noteworthy that micelles not modified by targeting molecules cannot target tumor sites with high efficiency. Therefore, studies regarding ways to enhance the tumor targeting of polymeric micelles are growing rapidly.

With that being said, in a related study, DOX-loaded magnetic polymeric micelles composed of copolymers of PEG and PCL modified with FA and encapsulating superparamagnetic iron oxide (SPIO) nanoparticles were reported for dual-targeting KB cells, derived from human oral cavity squamous carcinoma. The cellular uptake screening revealed that when the strength of the external magnetic field was reduced to 0 G from 4150 G, cell internalization of the FA-modified and the non-modified micelles decreased 84% and 92%, respectively. At high magnetic field strength (4150 G), the magnetic targeting effect was more conspicuous than that of FA targeting. On the other hand, at weaker magnetic field strength (450 G), results indicated no eye-catching magnetic-induced targeting effect on the KB cells internalization. In addition, FA-mediated cell targeting was more obvious when the external magnetic field was weakened: in a 4150 G magnetic field, FA targeting resulted in 1.2-fold increase in the DOX fluorescence in cells, whereas in 450 G and 0 G magnetic fields, the same targeting strategy led to 2.3- and 2.4-fold increase in drug fluorescence, respectively (Yang et al., 2008).

In another study, PTX-loaded magnetic micelles constructed of amphiphilic polymer poly[(N isopropylacrylamide-r-acrylamide)-b-L-lactic acid] (PNAL) and modified by RGD was reported. In water, PNAL is able to form micelles above

certain concentrations. Confocal microscopy image screening indicated that the uptake of the carriers in HeLa cells increased 7.8-fold after 6 h incubation, when both RGD and magnetic force attraction were applied on the micelles (Lin et al., 2015a, 2015b).

In another remarkable report, a polymer (PLGA)-lipid (lecithin) nanocarrier was reported which was conjugated to angiopep-2 and an aptamer (AS1411). Being a G-rich DNA aptamer, AS1411 is capable of attaching to nucleolin, a nucleus-located protein which exists in high quantities in the plasma membrane of numerous cancer cells including glioma. It has been indicated that the surface of BCECs is rich in LRP. Knowing this, ANG-2 is easily able to connect to LRP for transcytosis of the brain delivery. Therefore, BCECs were applied as a model to investigate the targeting capability of ANG-2. The results indicated that carriers decorated with ANG-2 displayed significantly higher cellular uptake than unmodified vehicles (1.7-fold higher). Furthermore, the efficiency of the AS1411-immobolized carriers was studied. In which case, aptamer-modified vehicles displayed much higher red fluorescence in comparison to other carriers, indicating that the cellular association of the carriers was enhanced due to the interaction between AS1411 and nucleolin. Using flow cytometry, they also investigated the relative cell uptake of the decorated carriers. The results showed that ANG-2-modified vehicles also displayed higher fluorescence when compared to unmodified carriers (1.5-fold higher). Therefore, they claimed that modification by ANG-2 enhances nanoparticles uptake by glioma cells as well. By decorating the vehicles with aptamer, the carriers displayed even more intensity within C6 cells (2.4-fold higher). As a result, it is safe to say that in comparison to ANG-2, AS14111 enjoys quite higher binding affinity toward glioma cells. In vitro evaluation of BBB penetration further demonstrated that the delivery of free DOX was the lowest since it was passively diffused into the BBB and could be effluxed by active transporters quite easily (Wang et al., 2018).

2.2.3 Carbon-Based Vehicles

The most common carbon-based nanocarriers are carbon nanotubes and graphene oxide nanoparticles.

Recently, the rate of investigation in carbon nanotubes (CNT) as drug delivery carriers has obviously increased owing to their unique physical and chemical properties. CNTs have very high surface area which allows substantial levels of therapeutic loading within the nanotube wall. In addition, supramolecular binding of aromatic molecules such as DOX are easily bound by π- π stacking on the polyaromatic surface of CNTs.

This being said, an oxidized multi-walled carbon nanotube (OMWNT) conjugated by angiopep-2 (OMWNT/ANG) was designed and reported for the purpose of treating brain glioma. To evaluate the capability of glioma targeting of the O-MWNT/ANG in vivo, the fluorescence image of glioma-bearing mice after administrating the carriers was investigated. The results showed that the fluorescence intensity of

the group treated with OMWNT/ANG was much higher than that of those treated with OMWNT at 2 h and 24 h post injection, indicating that OMWNT did accumulate in glioma in a much higher fashion and that OMWNT/ANG did reinforce the potential of glioma targeting (Ren et al., 2012).

In a similar study, folate- and iron-modified multiwall carbon nanotube (FA-MWCNT-Fe) was designed as a dual-targeting vehicle for delivering DOX into HeLa cells using an external magnetic field. Due to being conjugated by folate and the iron particles, the FA-MWCNT-Fe recognized HeLa cells through an active targeted pathway and connected to the cells via a passive targeted manner, respectively. The use of iron modification and magnetic field led to 2–3-fold improvement of the cytotoxicity caused by FA-MWCNT-Fe compared to that of iron-lacking carriers, demonstrating that even though the magnetically targeted nanocarriers targeting delivery is passive, they do enhance the targeting efficiency eye-catchingly (Li et al., 2011).

Since its discovery in 2004, graphene has been exploited for gene and drug delivery as well as intracellular tracking because of its ability to traverse the plasma membrane and improve the cellular uptake of a wide variety of molecules. More importantly, since all its atoms are exposed on its surface, graphene displays very high surface area, causing quite enhanced binding and loading of various types of molecules. When being exploited as a drug carrier, graphene is often transformed to graphene oxide (GO) to improve the carrier hydrophilicity by introducing functional groups which contain oxygen. One of its major advantages is that graphene oxide (GO) is highly dispersed in aqueous environments owing to its numerous hydrophilic groups, such as hydroxyl, epoxide, and carboxylic groups. Moreover, its significant biocompatibility makes GO a promising vehicle for drug/gene delivery systems (Xiong et al., 2010).

More importantly, it has been indicated that the adsorption between GO and DOX is pH-sensitive, offering low rate of drug release when circulating in blood (pH ~ 7.4) and a bursting release after cellular internalization into the endosomes (pH ~5). GO also has powerful optical absorption in the near-infrared (NIR) tissue transparency window, which enables its application as a photothermal therapy agent (the use of light absorbents for absorbing 808 nm NIR light and to transform it into thermal energy in order to kill cancer cells). (Wang et al., 1995; Obraztsov et al., 2007).

In one study, it was established that PTX-loaded aptamer-conjugated magnetic graphene oxide (MGO) nanocarriers, prepared by binding Fe_3O_4 on the layer of GO and then being linked to aptamer (targeting moiety), enjoyed high biocompatibility based on cellular toxicity assay. Furthermore, flow cytometry investigation showed that the MGOs could specifically bind to MCF-7 cancer cells. Besides, the cytotoxic effect of PTX-loaded MGO on MCF-7 cancer cells (at various drug doses) was significantly higher than that of both non-magnetic carriers and aptamer-deprived carriers (Hussien et al., 2018).

In another report, heparin and polyethyleneimine-folic acid immobilized GO was constructed in order to encapsulate DOX for enhanced cellular uptake. Heparin is utilized not only as a therapeutic vehicle, but as a targeting substance as well,

since it is capable of competitively attaching to receptors for advanced glycation end products on the membrane. The GO surface was charged negatively on the grounds of the high amount of both hydrophilic carboxyl and sulfonate groups in heparin. Therefore, the constructed carriers enjoyed prolonged circulation time. More notably, heparin did improve both the stability as well as the drug-loading capacity due to the large number of hydrophilic carboxyl and sulfonate groups, which increases the hydrophilic chain of GO and sets up hydrogen-bonds with DOX. Therefore, it was indicated that heparin played a crucial role in enhancing the stability and the drug loading capability of GO carriers (Li et al., 2018a).

In recent years, many reports have categorically demonstrated that if exposed to NIR, GO is capable of demolishing cancer cells in vitro and decreasing tumor size in vivo. With this in mind, a magnetic GO nanocarrier, which was both pH-sensetive and dual-targeting, was prepared for chemo-phototherapy of CT-26 cells. It was modified with PEG and a type of epidermal growth factor receptor (EGFR) monoclonal antibody (cetuximab), since EGFR exists in high quantities on the surface of CT-26 cells. In vitro cytotoxicity data showed that the IC_{50} value of modified-GO particles toward CT-26 cells was 1.48 μg/mL, being lower than that of non-modified ones (2.64 μg/mL). More importantly, the IC_{50} value was further reduced to 1.17 μg/mL after employing photothermal therapy by NIR laser light exposure. In vivo antitumor studies in BALB/c mice showed that at day 14, the relative tumor volumes for mice treated by the dual-targeting method was 22.6-fold lower than that of mice treated by regular DOX-loaded GO nanocarriers and 13.8-fold lower when compared to mice treated by magnetic DOX loaded GO nanocarriers (without utilizing phototherapy) (Lu et al., 2018).

Xiaoying Yang et al. reported a magnetic dual-targeting drug delivery and pH-sensitive controlled release system based on Dox-loaded graphene oxide (GO) functionalized with Fe_3O_4 and folate. The drug was released quite slowly from GO carriers at neutral conditions, and only a small amount of the total Dox was released after 80 h at pH = 7 and pH = 9 (7.5% and 11%, respectively). In addition, HeLa cell viability (after being treated by Fe_3O_4/f/GO) was 1.5-fold lower than that of non-modified carriers. Lastly, the cellular uptake screening confirmed that dual-modified nanoparticles had significantly higher uptake in HeLa cells compared to that of regular carriers (Yang et al., 2011).

Another magnetic GO nanocarrier was reported by Jinglei Du et al. They developed dual-targeting Dox-loaded nanocarriers by utilizing both magnetic targeting and folate active targeting. The carriers were constructed of magnetic ordered mesoporous carbon nanospheres. The dual-targeting nanoparticles induced higher cell death compared to that of the regular carriers. In addition, the biosafety of the vehicles has been demonstrated: at carrier concentration of 100 μg/ml, the cell viability is 76.05%. (Du et al., 2020).

2.2.4 Other Vehicles

Apart from previously discussed three main categories, some other carriers have been developed with the aim of developing dual-targeted nanomedicines for cancer therapy. These mainly consist of inorganic materials such as silica nanoparticles and gold nano-structures (Liu et al., 2015; Chen et al., 2016). Liu et al. synthesized hollow mesoporous silica nanocarriers (HMSN) conjugated with tLyp-1 peptide (tHMSN) for targeting both tumor and angiogenic blood vessel cells. They compared the cellular uptake rate between targeted and non-targeted formulations using doxorubicin as model drug. Their results show that the targeted sample has more cytotoxicity on both angiogenic blood vessels and cancerous cells probably due to higher endocytosis rate (Liu et al., 2015).

2.3 Conclusion and Outlook

The researches described in this chapter focus attention on developed dual-targeted nanocarriers in site-specific drug delivery to cancerous cells. Different targeting strategies and nanocarriers have been applied to reach dual-targeted drug delivery systems with increased therapeutic efficacy by delivering their cargo more selectively not only to specific organs but to cancerous cells populations and even specific organelles. Based on the discussed carriers, it seems that the biosafety of polymers and liposomes are more than that of inorganic materials; therefore systematic studies on inorganic materials long-term biosafety profiles are needed.

Despite persuasive results of preclinical researches regarding the superiority of dual-targeting strategies over single-targeting, there is still a wide range of obstacles to deal with before their clinical development. Some of these challenges are the same among all active targeting strategies (Zhang et al., 2020). (1) One of the issues attributed to all active-targeted complex systems is difficulty to adapt to large-scale production in the pharmaceutical industry because of the complex preparation process. Almost all the clinically approved nanomedicines such as Doxil are not so complicated in their composition, structure, and production process. (2) The characterization of dual and multi-targeted systems face some challenges. In most of the studies, the theoretical value of conjugated ligands density is reported. However, in these nano-formulations, determination of practical value of ligands conjugation and ligands attachment stoichiometry are key parameters. (3) Most of researches testing dual-targeted nano-medicines efficacy have been conducted in in vitro condition using 2D tumor models and in in vivo condition using nude mice. The complex and dynamic condition in the human body and high level of variability observed between different cancer stages and cancers reveals the need for sophisticated cancer models. Developing 3D cell cultures with patient-derived cell lines and using cancer models in immunocompetent animals can lead to more precise assessment of patient response to new dual-targeted nanomedicines. However, the fate of drug

delivery systems in the body, their integrity, ligands attachment and function, their circulation time and clearance characteristics and off-target possibility are still important questions (Belfiore et al., 2018). (4) Developing these complicated dual and multi-targeted nano-formulations needs proper and optimized combination of ligands because due to the steric hindrance, unbalanced ligands density can hamper targeting (Luo et al., 2020).

Cancer theranostic formulations constructed by combining different nanoparticles, to achieve a combination of therapeutics, such as photothermal therapy, photodynamic therapy, and chemotherapy as well as imaging and diagnostics functions at the same time, can accelerate new dual-targeted drug delivery systems movement to clinical phases. Also advances in technologies of nanomaterials large-scale production and utilization of models that better mimic in vivo tumor condition, in vitro multicellular tumor spheroid models, co-culture models, tumor models in microfluidic systems and patient-derived xenografts will help to overbear some of the challenges regarding the differences between the body condition and available models in the evaluation of dual-targeted theranostics. Such insights can pave the way for the progress of the next-generation dual-targeting nanomedicine approaches to the clinic.

References

Amoabediny, G., Haghiralsadat, F., Naderinezhad, S., Helder, M. N., Akhoundi Kharanaghi, E., Mohammadnejad Arough, J., & Zandieh-Doulabi, B. (2018a). Overview of preparation methods of polymeric and lipid-based (niosome, solid lipid, liposome) nanoparticles: A comprehensive review. *International Journal of Polymeric Materials and Polymeric Biomaterials, 67*(6), 383–400.

Amoabediny, G., Ochi, M. M., Rezayat, S. M., Akbarzadeh, A., & Ebrahimi, B. (2018b). *Targeted nano-liposome co-entrapping anti-cancer drugs.* Google patent US20160228362A1.

Anarjan, F. S. (2019). Active targeting drug delivery nanocarriers: Ligands. *Nano-Structures & Nano-Objects, 19*, 100370.

Belfiore, L., Saunders, D. N., Ranson, M., Thurecht, K. J., Storm, G., & Vine, K. L. (2018). Towards clinical translation of ligand-functionalized liposomes in targeted cancer therapy: Challenges and opportunities. *Journal of Controlled Release, 277*, 1–13.

Chen, D., Li, B., Cai, S., Wang, P., Peng, S., Sheng, Y., He, Y., Gu, Y., & Chen, H. (2016). Dual targeting luminescent gold nanoclusters for tumor imaging and deep tissue therapy. *Biomaterials, 100*, 1–16.

Danhier, F., Feron, O., & Préat, V. (2010). To exploit the tumor microenvironment: Passive and active tumor targeting of nanocarriers for anti-cancer drug delivery. *Journal of Controlled Release, 148*(2), 135–146.

Donahue, N. D., Acar, H., & Wilhelm, S. (2019). Concepts of nanoparticle cellular uptake, intracellular trafficking, and kinetics in nanomedicine. *Advanced Drug Delivery Reviews, 143*, 68–96.

Du, J., Li, Q., Chen, L., Wang, S., Zhang, L., Yu, S., Yang, Y., & Liu, X. (2020). In vitro cytotoxicity and antitumor activity of dual-targeting drug delivery system based on modified magnetic carbon by folate. *Journal of Nanomaterials, 2020*, 1.

Gao, H., Xiong, Y., Zhang, S., Yang, Z., Cao, S., & Jiang, X. (2014). RGD and interleukin-13 peptide functionalized nanoparticles for enhanced glioblastoma cells and neovasculature dual targeting delivery and elevated tumor penetration. *Molecular Pharmaceutics, 11*(3), 1042–1052.

Haghiralsadat, F., Amoabediny, G., Naderinezhad, S., Zandieh-Doulabi, B., Forouzanfar, T., & Helder, M. N. (2018). Codelivery of doxorubicin and JIP1 siRNA with novel EphA2-targeted PEGylated cationic nanoliposomes to overcome osteosarcoma multidrug resistance. *International Journal of Nanomedicine, 13*, 3853.

He, H., Li, Y., Jia, X.-R., Du, J., Ying, X., Lu, W.-L., Lou, J.-N., & Wei, Y. (2011). PEGylated poly (amidoamine) dendrimer-based dual-targeting carrier for treating brain tumors. *Biomaterials, 32*(2), 478–487.

Huang, M., Pu, Y., Peng, Y., Fu, Q., Guo, L., Wu, Y., & Zheng, Y. (2020). Biotin and glucose dual-targeting, ligand-modified liposomes promote breast tumor-specific drug delivery. *Bioorganic & Medicinal Chemistry Letters, 30*(12), 127151.

Hussien, N. A., Işıklan, N., & Türk, M. (2018). Aptamer-functionalized magnetic graphene oxide nanocarrier for targeted drug delivery of paclitaxel. *Materials Chemistry and Physics, 211*, 479–488.

Kang, W., Svirskis, D., Sarojini, V., McGregor, A. L., Bevitt, J., & Wu, Z. (2017). Cyclic-RGDyC functionalized liposomes for dual-targeting of tumor vasculature and cancer cells in glioblastoma: An in vitro boron neutron capture therapy study. *Oncotarget, 8*(22), 36614.

Ke, X., Lin, W., Li, X., Wang, H., Xiao, X., & Guo, Z. (2017). Synergistic dual-modified liposome improves targeting and therapeutic efficacy of bone metastasis from breast cancer. *Drug Delivery, 24*(1), 1680–1689.

Kluza, E., Jacobs, I., Hectors, S. J., Mayo, K. H., Griffioen, A. W., Strijkers, G. J., & Nicolay, K. (2012). Dual-targeting of αvβ3 and galectin-1 improves the specificity of paramagnetic/fluorescent liposomes to tumor endothelium in vivo. *Journal of Controlled Release, 158*(2), 207–214.

Kydd, J., Jadia, R., Velpurisiva, P., Gad, A., Paliwal, S., & Rai, P. (2017). Targeting strategies for the combination treatment of cancer using drug delivery systems. *Pharmaceutics, 9*(4), 46.

Lammers, T., Kiessling, F., Hennink, W. E., & Storm, G. (2012). Drug targeting to tumors: Principles, pitfalls and (pre-) clinical progress. *Journal of Controlled Release, 161*(2), 175–187.

Li, R., Wu, R. A., Zhao, L., Hu, Z., Guo, S., Pan, X., & Zou, H. (2011). Folate and iron difunctionalized multiwall carbon nanotubes as dual-targeted drug nanocarrier to cancer cells. *Carbon, 49*(5), 1797–1805.

Li, J., Liang, X., Zhang, J., Yin, Y., Zuo, T., Wang, Y., Yang, X., & Shen, Q. (2018a). Inhibiting pulmonary metastasis of breast cancer based on dual-targeting graphene oxide with high stability and drug loading capacity. *Nanomedicine: Nanotechnology, Biology and Medicine, 14*(4), 1237–1248.

Li, L., Wang, Q., Zhang, X., Luo, L., He, Y., Zhu, R., & Gao, D. (2018b). Dual-targeting liposomes for enhanced anticancer effect in somatostatin receptor II-positive tumor model. *Nanomedicine, 13*(17), 2155–2169.

Lin, M. M., Kang, Y. J., Sohn, Y., & Kim, D. K. (2015a). Dual targeting strategy of magnetic nanoparticle-loaded and RGD peptide-activated stimuli-sensitive polymeric micelles for delivery of paclitaxel. *Journal of Nanoparticle Research, 17*(6), 1–18.

Lin, M. M., Kang, Y. J., Sohn, Y., & Kim, D. K. (2015b). Dual targeting strategy of magnetic nanoparticle-loaded and RGD peptide-activated stimuli-sensitive polymeric micelles for delivery of paclitaxel. *Journal of Nanoparticle Research, 17*(6), 248.

Liu, G.-X., Fang, G.-Q., & Xu, W. (2014). Dual targeting biomimetic liposomes for paclitaxel/DNA combination cancer treatment. *International Journal of Molecular Sciences, 15*(9), 15287–15303.

Liu, Y., Chen, Q., Xu, M., Guan, G., Hu, W., Liang, Y., Zhao, X., Qiao, M., Chen, D., & Liu, H. (2015). Single peptide ligand-functionalized uniform hollow mesoporous silica nanoparticles achieving dual-targeting drug delivery to tumor cells and angiogenic blood vessel cells. *International Journal of Nanomedicine, 10*, 1855.

Lu, Y.-J., Lin, P.-Y., Huang, P.-H., Kuo, C.-Y., Shalumon, K., Chen, M.-Y., & Chen, J.-P. (2018). Magnetic graphene oxide for dual targeted delivery of doxorubicin and photothermal therapy. *Nanomaterials, 8*(4), 193.

Luo, Y., Yang, H., Zhou, Y.-F., & Hu, B. (2020). Dual and multi-targeted nanoparticles for site-specific brain drug delivery. *Journal of Controlled Release, 317*, 195–215.

Obraztsov, A., Obraztsova, E., Tyurnina, A., & Zolotukhin, A. (2007). Chemical vapor deposition of thin graphite films of nanometer thickness. *Carbon, 45*(10), 2017–2021.

Peng, Y., Zhao, Y., Chen, Y., Yang, Z., Zhang, L., Xiao, W., Yang, J., Guo, L., & Wu, Y. (2018). Dual-targeting for brain-specific liposomes drug delivery system: Synthesis and preliminary evaluation. *Bioorganic & Medicinal Chemistry, 26*(16), 4677–4686.

Qin, L., Wang, C. Z., Fan, H. J., Zhang, C. J., Zhang, H. W., Lv, M. H., & Cui, S. D. (2014). A dual-targeting liposome conjugated with transferrin and arginine-glycine-aspartic acid peptide for glioma-targeting therapy. *Oncology Letters, 8*(5), 2000–2006.

Ren, J., Shen, S., Wang, D., Xi, Z., Guo, L., Pang, Z., Qian, Y., Sun, X., & Jiang, X. (2012). The targeted delivery of anticancer drugs to brain glioma by PEGylated oxidized multi-walled carbon nanotubes modified with angiopep-2. *Biomaterials, 33*(11), 3324–3333.

Rezayan, A. H., Mousavi, M., Kheirjou, S., Amoabediny, G., Ardestani, M. S., & Mohammadnejad, J. (2016). Monodisperse magnetite (Fe3O4) nanoparticles modified with water soluble polymers for the diagnosis of breast cancer by MRI method. *Journal of Magnetism and Magnetic Materials, 420*, 210–217.

Sun, Z., Yan, X., Liu, Y., Huang, L., Kong, C., Qu, X., Wang, M., Gao, R., & Qin, H. (2017). Application of dual targeting drug delivery system for the improvement of anti-glioma efficacy of doxorubicin. *Oncotarget, 8*(35), 58823.

van der Meel, R., Vehmeijer, L. J., Kok, R. J., Storm, G., & van Gaal, E. V. (2013). Ligand-targeted particulate nanomedicines undergoing clinical evaluation: Current status. *Advanced Drug Delivery Reviews, 65*(10), 1284–1298.

Wang, X., Lin, X., Dravid, V. P., Ketterson, J. B., & Chang, R. P. (1995). Carbon nanotubes synthesized in a hydrogen arc discharge. *Applied Physics Letters, 66*(18), 2430–2432.

Wang, S., Zhao, C., Liu, P., Wang, Z., Ding, J., & Zhou, W. (2018). Facile construction of dual-targeting delivery system by using lipid capped polymer nanoparticles for anti-glioma therapy. *RSC Advances, 8*(1), 444–453.

Xin, H., Jiang, X., Gu, J., Sha, X., Chen, L., Law, K., Chen, Y., Wang, X., Jiang, Y., & Fang, X. (2011). Angiopep-conjugated poly (ethylene glycol)-co-poly (ε-caprolactone) nanoparticles as dual-targeting drug delivery system for brain glioma. *Biomaterials, 32*(18), 4293–4305.

Xiong, X.-B., Uludağ, H., & Lavasanifar, A. (2010). Virus-mimetic polymeric micelles for targeted siRNA delivery. *Biomaterials, 31*(22), 5886–5893.

Xu, Q., Liu, Y., Su, S., Li, W., Chen, C., & Wu, Y. (2012). Anti-tumor activity of paclitaxel through dual-targeting carrier of cyclic RGD and transferrin conjugated hyperbranched copolymer nanoparticles. *Biomaterials, 33*(5), 1627–1639.

Yang, X., Chen, Y., Yuan, R., Chen, G., Blanco, E., Gao, J., & Shuai, X. (2008). Folate-encoded and Fe3O4-loaded polymeric micelles for dual targeting of cancer cells. *Polymer, 49*(16), 3477–3485.

Yang, X., Wang, Y., Huang, X., Ma, Y., Huang, Y., Yang, R., Duan, H., & Chen, Y. (2011). Multi-functionalized graphene oxide based anticancer drug-carrier with dual-targeting function and pH-sensitivity. *Journal of Materials Chemistry, 21*(10), 3448–3454.

Yuan, M., Qiu, Y., Zhang, L., Gao, H., & He, Q. (2016). Targeted delivery of transferrin and TAT co-modified liposomes encapsulating both paclitaxel and doxorubicin for melanoma. *Drug Delivery, 23*(4), 1171–1183.

Zhang, W., Yu, Z.-L., Wu, M., Ren, J.-G., Xia, H.-F., Sa, G.-L., Zhu, J.-Y., Pang, D.-W., Zhao, Y.-F., & Chen, G. (2017). Magnetic and folate functionalization enables rapid isolation and enhanced tumor-targeting of cell-derived microvesicles. *ACS Nano, 11*(1), 277–290.

Zhang, Y., Cao, J., & Yuan, Z. (2020). Strategies and challenges to improve the performance of tumor-associated active targeting. *Journal of Materials Chemistry B, 8*(18), 3959–3971.

Zhao, Z., Zhao, Y., Xie, C., Chen, C., Lin, D., Wang, S., Cui, X., Guo, Z., & Zhou, J. (2019). Dual-active targeting liposomes drug delivery system for bone metastatic breast cancer: Synthesis and biological evaluation. *Chemistry and Physics of Lipids, 223*, 104785.

Zhu, Y., Feijen, J., & Zhong, Z. (2018). Dual-targeted nanomedicines for enhanced tumor treatment. *Nano Today, 18*, 65–85.

Zong, T., Mei, L., Gao, H., Shi, K., Chen, J., Wang, Y., Zhang, Q., Yang, Y., & He, Q. (2014). Enhanced glioma targeting and penetration by dual-targeting liposome co-modified with T7 and TAT. *Journal of Pharmaceutical Sciences, 103*(12), 3891–3901.

Chapter 3
Cancer Nanotechnology for Drug Targeting and Delivery Approaches

Vadivel Siva, Chunchana Kuppe Renuka Prasad Ravikumar, Ponnusamy Thillai Arasu, Nagendra Nath Yadav, Arumugam Murugan, Hardeo Singh Yadav, Sultan Asath Bahadur, and Saminathan Balamurali

Contents

V. Siva · S. A. Bahadur
Department of Physics, Condensed Matter Physics Laboratory, International Research Centre, Kalasalingam Academy of Research and Education, Krishnankoil, Tamil Nadu, India

Chunchana Kuppe Renuka Prasad Ravikumar
Department of Chemistry, East West Institute of Technology, Bangalore, Karnataka, India

P. T. Arasu
Department of Chemistry, College of Natural and computational Sciences, Wollega University, Nekemte, Ethiopia

N. N. Yadav · A. Murugan (✉) · H. S. Yadav
Department of Chemistry, North Eastern Regional Institute of Science and Technology, Itanagar, Arunachal Pradesh, India
e-mail: amu@nerist.ac.in

S. Balamurali
Department of Computer Applications, Kalasalingam Academy of Research and Education, Krishnankoil, Tamil Nadu, India

M. Saravanan, H. Barabadi (eds.), *Cancer Nanotheranostics*, Nanotechnology in the Life Sciences, https://doi.org/10.1007/978-3-030-74330-7_3

3.1 Introduction

Cancer is a wide tenure; it describes the illness that results from cellular change and source the unrestrained development and separation of cells, which is also called malignancy, i.e., an irregular development of cells. The normal cells become abnormal and grow beyond their usual boundaries that can affect any part of the body; it can also invade nearest body parts and spread to other organs (Anand et al., 2008). The normal cells transform into cancer cells through a multistage process that develops a malignant tumor from the precancerous lesion. Presently more than 100 types, together with lung cancer, lymphoma, breast, skin, prostate, colon cancer, and many symptoms, exists based on the type of cancer. Curing of cancer may be done based on the treatments using chemotherapy, radiation, and/or surgery. In that, a few kinds of cancer cause quick cell development, while others cause cells to develop and partition at a slower rate (Ghoncheh et al., 2015). Malignant growth is a significant general medical issue around the world. Worldwide segment attributes and anticipate an expanding disease frequency in the following for many years, with >20 million new malignancy cases every year expected by 2025. Cancer disease is the second most common reason for death internationally, representing an expected 9.6 million passings in 2018. In the next few decades, it is projected that low and center pay nations will be hit by the increment in cases and passings. Many of those cases can be prevented, or at the very least treated effectively, when there is an early diagnosis. By ranking, five most frequent cancers in the World are lung, prostate, colorectum, stomach, and liver in males and breast, colorectum, lung, cervix uteri, and stomach in females (Kolonel et al., 2004; Jemal et al., 2007). Nowadays, lung cancer is a more common cause of deaths found in both women and men, and out of these, women are leading in number of deaths due to the cancer in many countries.

The maximum passing cases in women are reported in North America, Western and Northern Europe, Australia, China, and New Zealand. It remains the 1st or 2nd foremost reason for early passing (i.e., at ages 30–69 years) in 134 countries out of 184. It positions 3rd or quarter in remaining 45 nations. Of the 15.2 million premature deaths from non-communicable diseases worldwide in 2018, 36% was due to the cancer. The estimate of global cancer-related problems by 2040 is predictable to surpass 27 million (Lowy & Collins, 2016; Bray et al., 2018). Cancer is a disease of concerning international issue and is another foremost purpose of loss of life. The USA remnants one of the nations with the very best prevalence quotes of prostate cancers. Historically, 93% of prostate cancer occurs as acinar adenocarcinoma. The last 7% of prostate cancers are different like neuroendocrine tumors, basal cellular carcinoma, and ductal adenocarcinoma (Davis et al., 2012). Post-cancerous effects are not as mutual in the early stages of prostate cancer as in ascites adenocarcinoma. Acinar adenocarcinoma and intraocular carcinoma are difficult to distinguish because they are often seen together. This cancer cell achieving abnormal growth due to a genetic mutation that promotes cancer is called cancer cells. Therefore, to diagnose cancer, it is more important to classify the description of the cancer cells and/or biomarkers exclusively articulated in cancer cells. For example, specific proteins (e.g., Matrix metalloproteinase) are expressed to promote irregular development on cancer cells, which characterize the diagnosis and classification of cancer cells such proteins and their function. Cancer is characterized by individuality after development signs, irresponsibility to indications that inhibit uncontrolled replication, cell division, prolonged angiogenesis apoptosis, and lastly the ability to pierce into additional tissues recognized as metastasis (Hanahan & Weinberg, 2011; Siegel et al., 2020). The microenvironment of the benign tumor reveals variations in extracellular environment and different regulatory proteins, which play an important role in the origin and expansion of cancers (Pavlova & Thompson, 2016). Prior to 1950, surgery was considered as the only favored treatment for cancer. After 1960, radiation therapy was introduced to regulate resident sicknesses. Over a period of time, it was thought that individual cure of surgical therapy and radiation could now not be viable contrasted with their utilization to control most malignant growths. Currently, biological molecules, drugs, and immune mediators are used for remedy. To date, we've no longer reached the level of first-rate treatment that counteracts the mortality charge and shortens the long-time period survival fee for metastatic cancer. The trials and features of dissimilar tumor agencies have been decided to create a new revolution in neoplastic cancer or to target drugs for tumors. Energy remedy is based totally on the usage of physical objects consisting of protons, electrons, and diverse ions to killing cancer cells (Nagai & Kim, 2017). The instrument overdue therapy using radiation is that huge power radiations which inhibit cell separation and their capacity to multiply with the aid of their negative inherited cloth. If that is complete earlier surgery, therapy using radiation is assumed through the aim of shrinking the tumor. If achieved afterward with surgical treatment, the radiation will destroy the left facet in the back of the tumor cells and decrease the recurrence of most cancers. Because radiation remedy works in a localized manner to treat universal cancers, chemotherapy may be used single or with radiation remedy (Culp et al.,

2020), which is measured to be the maximum operative and widely used technique in maximum kinds of cancer. Chemotherapy medicines aim tumor cells and produce mostly sensitive O_2 types, which often finish tumor cells through genetic toxicity (DeVita & Chu, 2008; Aslam et al., 2014). However, chemotherapy affects normal cells, leading to varying degrees of adjacent belongings such as hair loss, nausea, fatigue, and death in so many belongings (Aslam et al., 2014).

3.2 Classification of Cancers

Cancers can be classified as squamous cells or epithelial cells based on their cellular origin. There are certain types of cancer that start from a specific type of cell. The most common type of cancer, "carcinomas," originates from epithelial cells. These cells are found mainly on the outside and inside of the human body (Visvader, 2011; Thun et al., 2010; Kotnis et al., 2005). There are different types of epithelial cells with specific names for cancer.

3.2.1 Squamous Cell Carcinoma

The type of cancer that occurs in squamous cells located underneath the external surface of human skin (Blackadar, 2016). Squamous cells include numerous tissues, such as the lungs, intestines, kidneys, stomach, and bladder.

3.2.2 Transitional Cell Carcinoma

This type of cancer arises from a kind of epithelial material called the transitional epithelium. These are mainly found on the outer surface of the bladder, uterus, kidneys, and some other organs (Hassanpour & Dehghani, 2017).

3.2.3 Adenocarcinoma

Adenocarcinoma forms in glandular epithelial cells which secrete fluids or mucus. Epithelial cells are also called glandular tissues. Adenocarcinoma mainly involves breast, prostate, and colon cancers (Moreira-Nunes et al., 2020).

3.2.4 Basal Cell Carcinoma

When cancer develops under the epidermis or from the basal layer, the outer layer of human skin, when cancer begins in soft tissues and bones such as blood vessels, fat, muscle, fibrous tissue and lymph vessels, it is referred to as sarcomas. On the other hand, cancer of the blood-forming tissues found in the bone marrow is called leukemia. In this type of cancer, abnormal white blood cells are formed in the blood and bone core (Blackadar, 2016). Dependent on the nature of the blood cells that cause cancer, they can be divided into lymphoma and myeloid (American Cancer Society).

3.2.5 Lymphoma

Cancer that arises in lymphocyte cells (T cells or B cells) (Yuen et al., 2016).

3.2.6 Myeloma

It is a cancer that occurs in plasma cells. These are part of the immune system. When plasma cells become abnormal, they are called myeloma cells (Hassanpour & Dehghani, 2017). The five most common cancers are breast, prostate, lung, colorectum, and cervix uteri (Chiang & Massague, 2008). The most widely recognized reason for cancer mortality for men was lung, liver, stomach, colon and prostate while for women they were breasts, lung, colon, cervix and stomach. Cancer deaths in both sexes include lung, liver, stomach, colon, and breast (Vos et al., 2016). Cancer is emerging as a major health problem in low- and middle-income republics in the Asia-Pacific region, including India, and is the leading cause of death (21%) worldwide from non-communicable diseases (Pavlova & Thompson, 2016). The cancer profile varies in different populations; the evidence is that this variation is mainly the result of different lifestyle and environmental factors, which may be affected by preventive interventions (Parkin et al., 2002).

3.3 Classification by Grade

There is an irregularity which persists inside the cells with admiration to the nearby usual matters. A growth in irregularity will increase the exceptional from one to four. Well-differentiated cells carefully look like regular cells and fit to cheap grade tumors. Unsuitably distinguished cells are identical eccentric with admiration to the encompassing tissues. This is the aberration in cells which growth to their nearby

usual tissues (Rosai & Ackerman, 1979). Upsurge in irregularity raises the rating, from one to four. Well-differentiated cells sensibly look like average cells and fit to inferior growths. Unsuitably distinguished cells are particularly extraordinary which recognition to the nearby matters (Jemal et al., 2007). These are well-graded tumors including:

(a) This comprises well-distinguished cells with minor abnormalities.
(b) These cells are temporarily distinguished and slightly irregular.
(c) In an environment containing mutated chromosomes, the cells are abnormally different and very abnormal and crop some destructive chemicals that can infect neighboring cells and arrive in the bloodstream (Carbone, 2020).
(d) Cells are undeveloped, rude, and undistinguishable (Oluogun et al., 2019).

3.4 Causes of Cancer

The beginning and progression of most cancers relies upon numerous issues in the cell (immune situations, hormones, and mutations) as well as outside elements from the environment (smoking, chemical substances, infectious organism, and radiation). These complete additives composed motivate bizarre cellular conduct and uncontrolled proliferation (Amador et al., 2019). As a result, abnormal cell mass grows in the form and distresses the normal tissues around them, sometimes spreading to other parts of the body (Fig. 3.1).

As indicated by the greatest natural model for malignant growth, tumor suppression and mutations in many cancers are the primary factors mainly to the improvement of cancer. Another version suggests that some mutations in a number one gene that regulates mobile department may additionally feed normal cells closer to unusual chromosome replication, subsequent in deletion or replication of whole chromosomes segments (Ames et al., 1995). These alternate in gene contented in cells creates ordinary tiers of a selected protein regardless of definite necessity. If slightly chromosomal mutation touches a protein that performs an essential role inside the mobile cycle, qualitatively or quantitatively, it may motivate most cancers (Idikio, 2011). Nearby is likewise robust suggestion that undesirable totaling (hypermethylation) or removal of organizations (hypomethylation) to genes worried within the guideline of cell series, apoptosis, and DNA repair is related to a few cancers, which is crucial to remember that cancers container take years or few months to add enough DNA mutations to come across the cancer form. Consequently, there can be various mechanisms that bring about the improvement of malignant growth. This further darkens the troublesome errand of characterizing the genuine reason for malignant growth (Golemis et al., 2018).

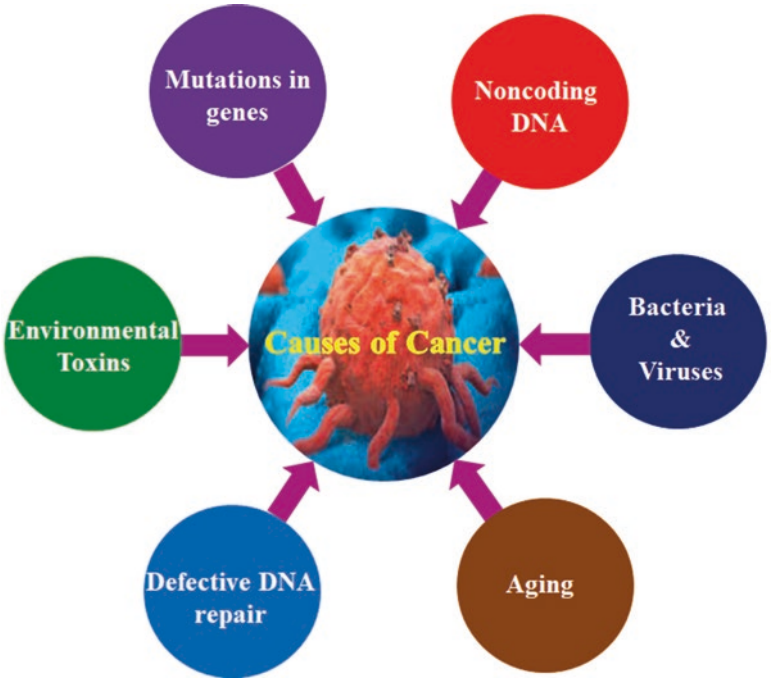

Fig. 3.1 Factors involved in causing cancer

3.4.1 Cause of Cancer Through Infectious Agents

Development of tumor through infectious agents has three primary types. The first type is the acceptance of ongoing irritation because of a proceeding with safe reaction to a determined contamination. This happens, for instance, on account of hepatitis C infection (HCV), related with cancer for liver, which ceaselessly imitates in the liver, located up an ongoing condition of aggravation there. Another example is *H. pylori*. There is a tall predominance of tenacious disease with *H. pylori*: around the world, 75% of persons is tainted, with commonness actuality advanced in sub-Saharan Africa; anywhere *H. pylori* is related with 63.4% of all stomach cancer growths (Griffin & Kellam, 2009). Nonetheless, the way that not all people affected with *H. pylori* create cancer due gastric obviously shows that the irresistible specialist is a danger factor, yet that other natural and hereditary impacts are associated with disease arrangement (Ataollahi et al., 2015). Second kind, oncogenesis can happen via infection instigated exchange. This is because of the estimation of the pathological genome in a dormant structure in an inflamed cell, both without duplication, likewise with Epstein-Barr infection (EBV), which contaminates B lymphocytes, or through joining of the pathological genome into a host-mobile chromosome, similarly as with humanoid papilloma virus (HPV), the reason for cervical malignant growth. EBV is an awful lot of the time outstanding in teenagers Burkitt's

lymphoma, put up-relocate non-Hodgkin's lymphoma, B-cell lymphomas, nasopharyngeal carcinoma, and Hodgkin's contamination (Griffin & Kellam, 2009). The third type is the consistent concealment of the invulnerable scheme by way of the transferrable agent, for instance, the immunodeficiency like AIDS brought approximately through HIV disease. The presence of regular mechanisms of immune commentary for cancer cells, which is due to an infectious etiology will similarly envelop safe structures that frequently control the contamination, recommends why microbes with oncogenic capacity don't quickly motivate malignancy. An undermined resistant scheme can bring about a multiplied price of disease pushed tumors with the aid of debilitating the secure management. Such a diffusion is visible, as an instance, in transplant sufferers, who're being handled with immune suppressants, or in humans with AIDS (Stein et al., 2008). Microorganisms related with malignant growth represent a significant number of these types; tenacious infection includes sidestepping the insusceptible reaction just as ongoing irritation, which even in the invulnerable skilled prompts chronic cell propagation and a more serious danger of oncogenic conversion. Nonetheless, numerous non-oncogenic microbes are similarly capable at these cycles, showing that different components must be included (Shaco-Levy et al., 2010). For instance, the danger of a transferable agent producing malignancy may likewise rely upon the cell type diseased, as convinced cell heredities might be additionally "inclined" to change than others. These instances, the expanded commonness of leukemias and lymphomas in kids and youthful grownups, recommendsthat lymphocytes are more powerless to change.

3.5 Early Diagnosis and Screening

Early analysis is described as early detection of cancer in patient's symptoms of the disease. This is in assessment to the cancer check that seeks to pick out unauthorized (pre-scientific) cancer or pre-cancerous lesions which are apparently healthy goal populace. Early diagnosis and screening of cancer are crucial components of complete management of cancer, but they fluctuate in resource content material and infrastructure requirements, effect, and fee (Loud & Murphy, 2017; Shieh et al., 2016). The recognition of early diagnosis of most cancers is on those with signs and symptoms with most cancers. The aim is to link the diagnosis at an early level to the diagnosis and remedy at once. When accomplished right now, cancer may be diagnosed at a curable degree, improving existence and high-quality of existence. There are three steps to early diagnosis including (a) access to consciousness and care about tumor signs; (b) experimental assessment, diagnosis, and stabilization; (c) and admittance to action including ache release (Loud & Murphy, 2017).

The average fame of early analysis and screening programs may be assessed inside the distribution of most cancers reputed in diagnosis and traits through the years. For example, an area that has excessive incidence costs of advanced cancers may be lower than the early diagnostic capability (Nersesyan & Slavin, 2007).

3.6 Existing Technology

3.6.1 Types of Cancer Treatment

Since the acknowledgment of cancer, the target of remarkable research is to find novel techniques for quality therapy approaches for malignancy. Currently, more than 60% of all continuous clinical quality therapy preliminaries overall are focusing on cancer (Wu et al., 2006). The variety of therapies and its improvement depend on the type of cancer, its locality, and stage of progression. Some are "local" treatments like surgery and radiation therapy, which are used to treat a specific tumor or area of the body. Drug treatments (such as chemotherapy, immunotherapy, or targeted therapy) are often called "systemic" treatments because they can affect the entire body. Chemotherapy, surgical removal of tumors, radiation therapy, and its techniques are discussed in this section.

3.6.1.1 Chemotherapy

Chemotherapy, surgical treatment, and radiotherapy are a number of the most cancers remedies available in recent times (Morrison et al., 2011). The records of chemotherapy dates returned to the early twentieth century; however, its usage in cancer treating commenced within the thirties. The word "chemotherapy" was invented by Paul Ehrlich, a scientist belonging to German, who had a specific hobby in agents of alkalis and got up with this word to explain the chemical remedy for the ailment. Chemotherapy is a drug remedy that uses effective chemicals to kill the quick growing cells in the human body (Wang et al., 2016; Su et al., 2016). Chemotherapy works here to result in modifications inside the tumor cells in order that they break rising or expire. Subsequently, the two parts of chemotherapy drugs are cytostatic and cytotoxic, individually. Chemotherapy is regularly used to treat cancer due to the fact that most cancer cells grow and grow tons quicker than the most cells in the frame. The kind of chemotherapy case is to be had. Chemotherapy drugs can be used alone or in combination to deal with extraordinary sorts of cancer (Wan et al., 2012). Although chemotherapy is a notable way to treat many sorts of cancer, chemotherapy also contains the hazard of aspect results. Some chemotherapy aspect results are moderate and treatable, while others can be a reason for serious headaches. Another approach of remedy is neoadjuvant treatment, which objectives to decrease the scale of the number one growth and stop micro metastasis. This kind of action recovers the most conventional medical strategies in retaining the feature of important organs (Mouw et al., 2017). Neoadjuvant chemotherapy is indicated for cancer of the breast, anal, lungs, gastrointestinal rectal, bladder, neck and head, and a few kinds of sarcoma. Nearby are some cancers on which adjuvant chemotherapy has been installed with healing results, and the prices of therapy with new effective pills and mixtures are predicted to increase in addition (Roeder et al., 2020). Chemotherapy can be used for (a) neoadjuvant chemotherapy – shrink a tumor

before radiation treatment or medical procedure; (b) adjuvant chemotherapy, abolish cancer cells outstanding after surgery or therapy using radiation; (c) the other treatments (radiation or biological) may be additional active; and (d) abolishing tumor cells that reappear or feast to additional portions of your body (Roeder et al., 2020).

3.6.1.2 Surgical Removal of Tumors

Resection or operation surgery is considered to be the maximum hopeful and ordinary remedy of many kind and malevolent tumors because it guarantees minimum harm to the encompassing tissues as compared to radiotherapy and chemotherapy (Tohme et al., 2017; Benjamin, 2014). Another cause to recall surgical treatment as a desired treatment choice is that the tumor can be eliminated without undue threat of tissue injury (Demicheli et al., 2008). Dissimilar varieties of open or minimally invasive surgical procedures may be executed relying on different factors including a) the cause for the surgery; b) patient's preference; c) the portion of the body somewhere operation is to be achieved; and d) the tumor mass to be detached (Demicheli et al., 2008). Operations also differ in contingent on the phase of the tumor (Tian et al., 2018). Surgery may be done for the cases including (a) Eliminate the whole growth from a specific area; (b) Debulk removes a growth that can cause damage to a specific organ; (c) A large tumor eases the symptoms of cancer when it causes pain or severe pressure on any part of the body (Tian et al., 2018). During open surgical treatment, a large reduction is made, and that is normally accompanied with the aid of elimination of the tumor and wholesome tissue related to approximately carefully current lymph bulges. In assessment, for less aggressive surgical treatment, the general practitioner types a few small incisions instead of an adult, after which with the help of a laparoscope, a thin tube is connected to a camera, which sees the tumor in detail. The diagram presentations of the image on a screen, which lets in the health care professional to display the operation in quite good. The tumor, with a small amount of healthful tissue, is cautiously eliminated with the help of special surgical equipments (Wagner et al., 1995).

3.6.1.3 Radiation-Based Surgical Knife

3.6.1.3.1 Gamma Knife Systems

There is no real operation in a gamma knife technique; the gamma knife is not really a knife. Gamma Knife a medical procedure is a therapy strategy that utilizations radiation and computer-guided planning to treat brain tumors, vascular malformations and other different irregularities in the brain. The Gamma knife is really a therapy that carries light emissions centered radiation. Many radiation beams focus on the cell mass under treatment, which produces exceptionally high levels of radiation without a surgical incision or opening (Kano et al., 2017).

3.6.1.3.2 Stereotactic Radiosurgery

Stereotactic radiosurgery (SRS) is a type of healing radiology that uses ionizing radiation to damage and spoil decisions on parts within a tissue or organ. This method discloses a minor portion of the body to a totally excessive quantity of radiation. Nevertheless, no incision or blade changed into use within the complete way, but it's far nonetheless known as a surgery due to the fact the consequences of this treatment are similar to a normal operation. Since the administered radiation beam may be very high, it's vital to pay extra consideration to the radiation beam in order that the peripheral tissues are left unaffected. It is commonly applied in brain tumors that are hard or hazardous to use traditional surgical techniques or where a patient's health does no longer support a surgical procedure (Andrews et al., 2004).

3.6.1.3.3 Proton Beam Therapy

Cyclotron or proton beam therapy is a type of molecular radiation therapy. Instead of using beams of radiation, gamma beams, or X-beams, molecular radiation therapy uses particles such as protons or neutrons (Galluzzi et al., 2017).

3.6.1.4 Radiation Therapy

Radiation therapy plays an important role as the primary or adjunctive treatment for many gynecological cancers (Rosenfeld et al., 2014). There are many side effects related to the use of radiation therapy. It is a form of most cancer treatment that uses beams of excessive strength to kill the cancer cells. Radiation remedy often makes use of X-rays, however can also use protons or different kinds of strength. The term "radiation therapy" frequently mentions exterior beam radiation remedy. During this sort of radiation, excessive power beams come from a device outside your frame that are aimed at the beams at a specific point on your frame. During a special kind of radiation remedy referred to as brachytherapy, the radiation is placed inside your body (Roeder et al., 2020). Radiation therapy damages cells through extinguishing the gene that panels how cells produce and division. Although each healthy and most cancer cells are broken via energy remedy, the goal of radiation remedy is to spoil as many regular, healthful cells as imaginable. Normal cells often repair damage as a result of radiation (Baskar et al., 2014).

3.6.1.5 Radiation Therapy Techniques Fractionation

Fractionated transport of radiation therapy utilizes the radiological organic differentiation of cancer cells, multiplying the survival margin of normal cells over the most cancers' cells means of various occasions since they have an entire re-establish

design brought by way of the supplemental degrees of radiation (Balukrishna et al., 2015).

3.6.1.5.1 3D Conformal Radiotherapy

The use of 2D square fields in therapy has arisen as outdated, making CT scan primarily based on 3D radiation therapy (Read, 1998), the primary technique, for detecting cancerous hundreds, heading off vital organs, and target selection for radiation remedy.

3.6.1.5.2 Image-Guided Radiotherapy

The use of pre-treatment imaging techniques such as image-guided radiotherapy helps to accurately stabilize the radiation, divert the radiation from the complex organs, and target only the tumor masses, thus minimizing organ damage resulting from objective errors (Chen et al., 2009).

3.6.1.5.3 Intensity-Modulated Radiation Therapy

This innovation utilizes an opposite scheduling software that modifies the intensity of the beam radiation used through treatment, subsequent in the indiscretion of the radiation levels, which distinguishes the target from the vital organs (Jalil ur Rehman et al., 2018).

3.7 Drawbacks of Existing Cancer Treatments

Cancer cures may result in numerous side consequences. A side effect occurs when the treatment harms healthy cells. Side effect outcomes may range from man or woman to person and from person to person of remedy. In trend, chemotherapy is a remedy that makes use of chemical sellers to break all of the dividing cells. Therefore, chemotherapy is a particular, non-molecular therapy. Most chemotherapy agents kill most cancer cells by means of interacting with DNA synthesis or cell function (Chakraborty & Rahman, 2012). Disadvantages of chemotherapy encompass the development of poisonous facet results, resistance to chemical agents, and the want for other treatment in combination with chemotherapy in an effort to cure the affected person (Schirrmacher, 2019). These atoms are the reason sub-atomic-based medicines are so cherished. Most molecular-based therapies are designed to ruin handiest cancer cells. Since atomic-based cures are specific, they're not related with poisonous side results, for example, chemotherapy. Some types of

chemotherapy can cause your hair to fall out. This condition is called alopecia. Hair usually grows back two to three months after treatment (Chakraborty & Rahman, 2012). Cancer treatments may make the stomach feel debilitated and may upchuck (Chakraborty & Rahman, 2012; Nurgali et al., 2018). Some of the time, disease patients become ill from considering malignancy treatment. Medications used to treat cancer can cause some people to have difficulty concentrating or remembering things (Chakraborty & Rahman, 2012). Cancer and its treatment can cause pain. Pain can make it difficult to do normal activities. In surgical treatments, the inability to kill the microorganism around the edges of the tumor may leave the patient's tumor cells after surgery (Chakraborty & Rahman, 2012).

3.8 Benefits of Nanotechnology in Cancer Treatments

To obtain lengthy-term survival benefits, a couple of molecular adjustments or drug mixtures targeting cancer markers can be required (Jin et al., 2020). This could be one of the maximum difficult but promising precision most cancers treatment strategies in the destiny. Nanotechnology can offer rapid and sensitive uncovering of maximum cancer-associated particles, and scientists can come across molecular variations once they happen in a minor proportion of cells. Nanotechnology has the capacity to create absolutely novel and especially effective therapeutic sellers (Jaishree & Gupta, 2012). Eventually and exclusively, the use of nanosized merchandise for cancer reduces its potential to act straight away and repair without problems; ability to provide and/or deal with remedy, prognosis, or both; and the potential to passively accumulate on the tumor web page, actively concentrated on cancer cells and turning in conventional biological barriers inside the body, together with the dense stromal tissue of the pancreas or the blood-brain barrier that substantially restricts the distribution of living cells to our central nervous system (Jin et al., 2020).

3.9 Tools of Nanotechnology for Cancer Diagnosis and Therapy

Cancer diagnosis and therapy research activity in the area of nanotechnology are powered by recent advances in the development of various vehicles for efficient drug delivery. Various vehicles such as liposomes, nanoshells, quantum dots, gold nanoparticles, dendrimers, nanowires, solid lipid nanoparticles (SLNs), and carbon nanotube have been developed so far and described below (Jin et al., 2020).

3.9.1 Liposomes

Liposome is colloidal drug carrier applied in gene therapy and utilized for drug targeting due to their remarkable capability of solubilizing the water-insoluble herbal substance and along these traces suitable for remedy of cancer. Liposomes are measured ≥400 nm and consist of phospholipids. It is a cholesterol bilayer layer (Chaturvedi et al., 2019). Structure of liposomes has a structure of hydrophilic heads settled through surfactants and numerous hydrophobic tails (Fig. 3.2) (Juri et al., 2017). Because of this shape, fluid hydrophilic segments can be trapped in the internal, at the same time as the lipophilic segments may be mixed between the lipid bilayers (Yue & Dai, 2018; Bozzuto & Molinari, 2015; Akbarzadeh et al., 2013; Allen & Cullis, 2013; Zhang et al., 2008). In liposomes, the attention of drugs within the membrane is associated with exclusive advantages, for instance, protection of medication from degradation, negligible indistinct poisonousness, and simple conveyance to the centered accessible. Liposomes are biodegradable, biocompatible, and more consistent in colloidal answers and include the assets to target most cancer cells. In normal sound tissues, the liposome is held within the bloodstream due to the fact the tight intersections in endothelial cells do not permit any molecule spill out of vessel but rather than veins in stable tissue; tumor vessels are leakier that permit the nanosized liposome to spill out from blood to focused tumor website. In any case, liposomes have some drawbacks, for example, low encapsulation efficiency, terrible storage stability, simple oxidation of liposomal

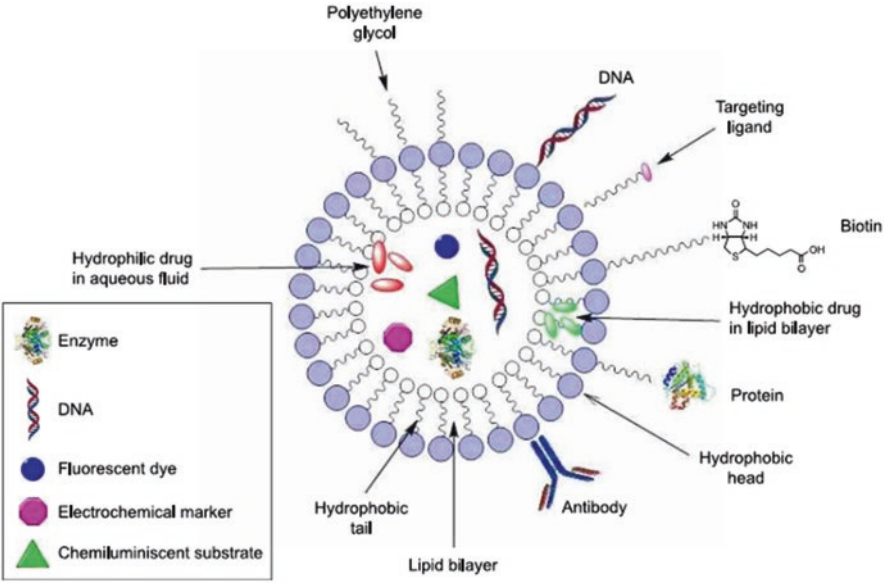

Fig. 3.2 Structure of liposomes. (Adapted with permission from Juri et al. (2017) Copyright © 2017, Dove Medical Press Limited)

phospholipids, and short transport time. Conveyance to tumor locations and decrease the effects of chemotherapy or antimicrobial treatments, just as to enhance explicitness to harmful locations. The tremendous drawback of liposomes is its quick degradation and freedom by way of the liver macrophages (MeCormack & Gregoriadis, 1994), consequently lessening the term of pastime of the medication it bears. This can be decreased partly with the appearance of secrecy liposomes wherein the liposomes are blanketed with substances like polyoxyethylene (IIlum & Dacis, 1984) which forestalls opsonization of the liposome and their take-up by macrophages (Senior et al., 1999; Anajwala et al., 2010).

The steadiness of liposomes is impacted by means of the lipid composition and shape, and this provides the improvement of liposomal product design. The stability of liposomal nanostructures includes several perspectives, for instance, colloidal and biological stability should colloidal protection need, liposomes structure larger-sized particles, and their productivity as transport systems are decreased. Encapsulation of medicine into liposomes has accredited the therapeutic retailers to the target and furthermore evaded their take-up by way of the reticuloendothelial system (Constantinidou et al., 2009; Ananda et al., 2011; Juri et al., 2017). Because of specific enhancements given at the tumor web page, the liposomes can go to the tumor cells and transport the chemotherapeutic sellers, which are compressed into the nanoparticles (Liu & Xu, 2015).

3.9.2 Nanoshells

The size of nanoshells is around 10–300 nm (Fig. 3.3). It includes insulator central which is normally composed of silica enclosed by a tiny gold outer case (Hirsch et al., 2003; Loo et al., 2004). These nanoshells translate plasmon-interceded electrical energy into light and are likewise adaptable to optical tuning with an emanation/retention exhibit from the UV to the infrared which is valuable in upgrading imaging properties (Kim, 2007; Alper, 2005). Nanoshells are engaging as they offer imaging and therapeutic opportunities in the medical care area without being related with substantial metal poisonousness.

3.9.3 Quantum Dots

Quantum dots (QDs) were exposed by Alexie Ekimov and Louis E Brus in 1980. Quantum dots are nanoparticles within size of 2–10 nm which is shown in Fig. 3.4 (Maiti & Bhattacharyya, 2013). Quantum dot acts as small semiconductors. A property of semiconductors lies between bulk semiconductors and discrete molecules because nanoparticles have the properties of high surface-to-volume proportions. The determination of nanoparticles absorption and emission properties may be controlled accurately due to their sizes and shapes (Morrow et al., 2007). Nanocrystals

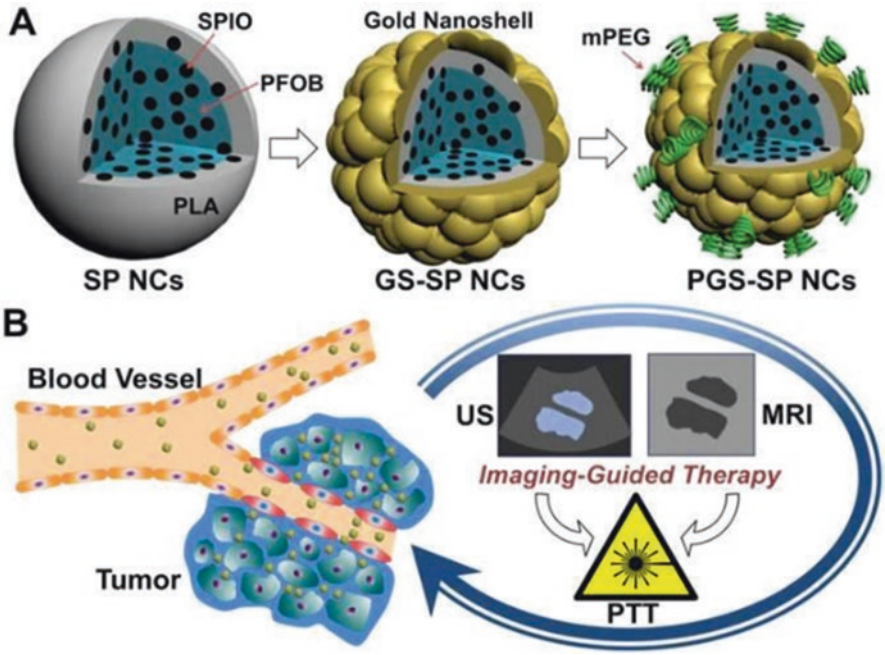

Fig. 3.3 Silica core-gold shell nanoshells. (Reproduced from Open Access journal under the term of Creative Commons Attribution License (Abshikbayeva et al. 2019) Copyright © 2019)

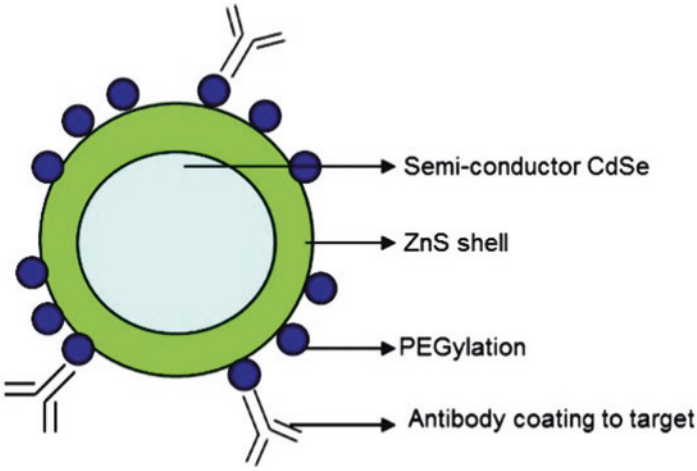

Fig. 3.4 Quantum dot. (Reproduced from Open Access journal under the term of Creative Commons Attribution License (Krishanan & George 2014) Copyright © 2014)

of quantum dots have luminescent, optical, and chemical properties due to their size and surface (Fang et al., 2012). Quantum dot acts as an efficient fluorescent probe due to size and high stability. Due to quantum confinement effects, quantum dot has the unique property of photophysical as a colloidal nanocrystalline semiconductor (Shao et al., 2011; Kashyap et al., 2019). Quantum dot may be useful to find the molecule biomarkers for cancer diagnosis and treatment. Quantum dot plays an essential role for detection of cancer which is helpful for diagnostics, imaging, targeted drug delivery, and phototherapy. The quantum dot designs of cadmium selenide (CdSe), cadmium telluride (CdTe), indium phosphide (InP), and indium arsenide (InAs) are used in biological applications (Bharali & Mousa, 2010). The inorganic core is enclosed by an inorganic shell, which shows higher photostability and increases the fluorescence properties of the core. The surface of the shell is coated with another layer that enhances solubility and stability of quantum dots in the blood (Madani et al., 2013).

Use of QDs in cancer identity was set up by Gao and co-workers (2002) when they named human prostate Cancer boom cells with QDs shaped with an immunizer for Prostate-Specific Membrane Antigen (PSMA). Bostick et al. (2006) diagnosed five biomarkers on a similar tissue slide with the aid of QD-based multiplexed imaging, from which more biomarkers will be expected utilizing diverse slides each stained with the five diverse biomarkers. Ruan et al. (2011) demonstrated that QD-based totally safe marking has extra constant picture force contrasted with conventional fluorescent immunolabeling. QDs can be moreover used to perceive the ovarian carcinoma marker CA125 in diverse classes of examples, for example, fixed cells, tissue regions, and xenograft portions. Moreover, the photostability of QD indicators is greater explicit and more extremely good than that of normal herbal color (Wang et al., 2004). Another studies deal with specifically mark MCF-7 and BT-474 BC cells for HER2, epidermal growth factor receptor (EGFR), estrogen receptor (ER), progesterone receptor (PR), and mammalian target of rapamycin (m-TOR) through visible and NIR QDs which confirmed that QD-based nanotechnology is an effective way to deal with proposal multiplexed disease biomarker imagery in situ on unblemished tumor tissue examples for tumor pathology study on the histological and sub-atomic levels on the identical time (O'Connor et al., 2009). Kawashima et al. (2010) efficiently centered on EGFR single-atoms in hominoid ovarian epidermal carcinoma cells (A431).

3.9.4 Gold Nanoparticles

Gold nanoparticles are playing a very important role in cancer diagnosis and treatment due to their belongings such as amphiphilicity, shape, biocompatibility size, carrier capabilities, and surface area (Fig. 3.5). Colloidal gold nanoparticles used as contrast agents due to their properties of high surface area-to-volume ratio, biological inertness, broad optical properties, low toxicity, resistance to corrosion, and good antimicrobial efficacy. Gold nanoparticles are used in bioimaging and

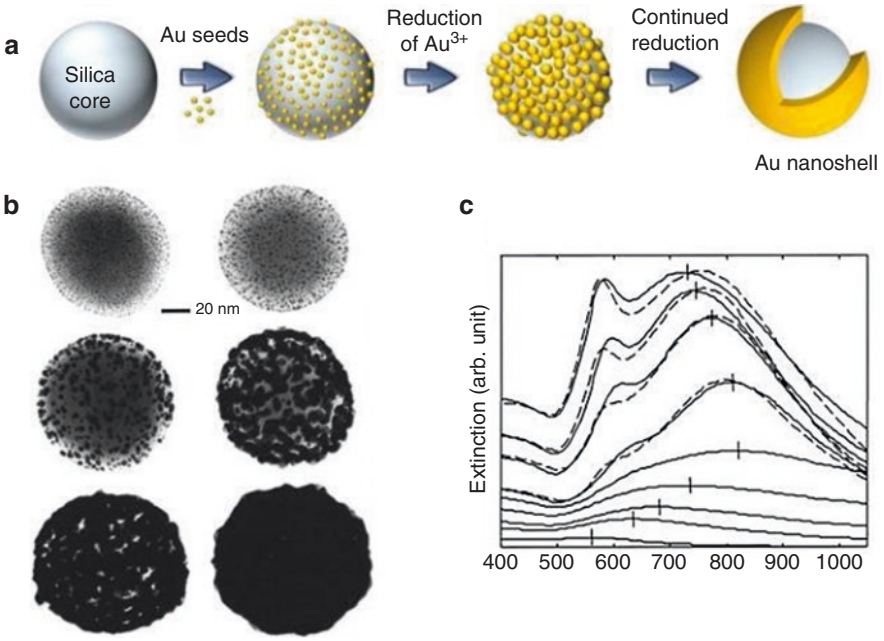

Fig. 3.5 Silica core-gold nanoshells. (Reproduced from Open Access journal under the term of Creative Commons Attribution License (Abshikbayeva et al., 2019) Copyright © 2019)

photothermal therapy because they are conjugated with antibodies to discover cervical and pancreatic cancers. Gold nanoparticles act as diagnostic agents in various cancers (Purohit & Singh, 2018). Gold nanoparticles have been exploited as a cargo for drug delivery. Due to surface properties of light scattering, gold nanoparticles bind with biomaterials for drug delivery (Liong et al., 2008). Light scattering properties of gold nanoparticles are altered due to their size and shape and have greater photostability (Huang et al., 2007).

3.9.5 Dendrimers

Dendrimers are polymers with distinctly branched round structure which is shown in Fig. 3.6 (Riggio et al., 2011). Dendrimers have an inner center, which may be inspired to exchange its form and size, enclosed with the aid of chains of branches with surface reactive web sites. Due to diverse surface functional agencies gift in the surface of dendrimers, various therapeutic agents can be loaded on the surface of dendrimers efficiently through conjugation like hydrophobic interaction, hydrogen bonds, or chemical linkage (Oerlemans et al., 2010). They are used for focusing on specific therapeutic drugs and molecules. Dendrimers have properties of excessive water solubility, described molecular weight, polyvalence, and biocompatibility.

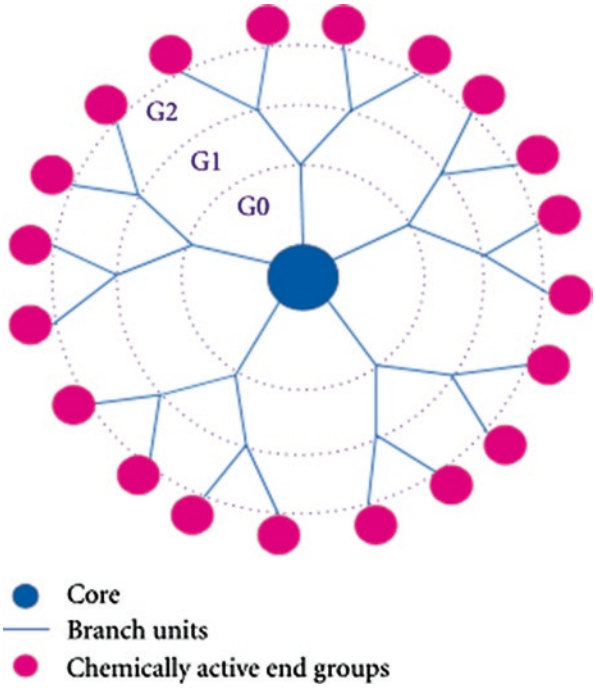

Fig. 3.6 Structure of a dendrimer. (Reproduced from Open Access journal under the term of Creative Commons Attribution License (Riggio et al., 2011) Copyright © 2011)

They have performed a very vital role inside the field of nanomedicine. Dendrimer is a nanoparticle with size around 1–15 nm. They can interface with cell membranes, mobile organelles, and proteins. Moreover, dendrimers with cationic surfaces will be in trendy collaboration with the lipid bilayer, encouraging elevated penetrability and faded trustworthiness of herbal membranes (Riggio et al., 2011).

Cooperation among dendrimers and cell membranes make a decision about a mechanism that reasons the spillage of cytosol proteins. Through bodily and chemical bonds, dendrimers collaborate with diverse types of drug, and they can be utilized for the becoming a member of hydrophobic/hydrophilic particles in their vacant cavities through nonbonding cooperation. Another option is to attach the drug particle to its fringe, ultimately obtaining a complicated system. The complication is shaped because of the electrostatic connections or formation between the drug and the dendrimers. Additionally, the covalent formation of drug to dendrimers may additionally incorporate PEG, p-amino benzoic acid, p-amino hippuric acid, and lauryl chains or biodegradable linkages which include amide or ester bonds. These bureaucracies were discovered to construct the dependability of drug and blood resistance time, and reason raised healing interest (Madaan et al., 2014). One extra favorable advantage of the dendrimer is that it can gather with DNA in the cluster model that is DNA-polyamidoamine in the cluster as an example

DNAPAMAM. This complex proficiently destroys malignant cells which have specific folic acid receptors extraordinarily. Dendrimer-antibody conjugates bind successfully with prostate-unique membrane antigen tremendous (LNCaP.FGC) cells while they do now not to bind with ordinary cells and the uptake of the conjugate was additionally much greater than unconjugated dendrimer in tumor cells. Additional period of dendrimer, for instance, glycodendrimers, is glycopeptide dendrimers formed to the anti-mitotic agent colchicine and dendrimers that can be part of sugar moieties into their improvement (Woller & Cloninger, 2001; Roy & Baek, 2002). Recently, a G5-PAMAM dendrimer has been prepared with a diameter of 5 nm and in excess of 100 functional amines at the surface. This nano-transporter was utilized for the delivery of methotrexate in a preclinical record. The dendrimer floor fee was first moderated via converting peripheral amines with acetyl organizations. At that point, the G5-PAMAM dendrimer turned into shaped with methotrexate (as the cytotoxic agent) and with folate as the focusing on atom. A biodistribution observed in mice with subcutaneous tumors validated cover and intracellular addition of dendrimers in xenograft human KB tumors that overexpressed folate receptors. The in vivo transport of the G5-PAMAM dendrimer formed with methotrexate initiated ten times lower in tumor length contrasted and observed after essential corporation of unfastened methotrexate at a similar molar attention (Kukowska-Latallo et al., 2005).

3.9.6 Nanowires

Nanowires are glowing silica wires in nanoscale folded over unmarried aspects of human hairs (Fig. 3.7). The sizes of the nanowires are very smaller than viruses but stronger than spider silk. Nanowire-based businesses are playing essential functions for diagnosis and remedy of most cancers. Due to residences of nanowires, it may be changed to experience molecular markers of cancer cells. Also, it could use the studies of kinetics of biomolecular reactions (Zheng et al., 2006). Protein covered nanowires have anticipated packages in most cancers imaging like prostate ailment, breast, and ovarian cancers (Anajwala et al., 2010). Proteins that are connected to the antibody will makeover the nanowires electrical conductance and this will be analyzed by way of a detector. Accordingly, proteins added by using malignancy cells may be identified and before evaluation of tumor may be done. They are set down throughout a small fluidic channel and that they allow cells or particles to transport via it. Nanowires can be covered with an antibody or oligonucleotide, a short stretch of DNA that may be utilized to perceive (Ravindran, 2011). In $_2O_3$ nanowires (NW), silicon nanowires (SiNW), and gold-conducting polymer NW (AuNW) may be independently altered for figuring out malignancy biomarkers (Choi et al., 2010; Hu et al., 2011), specifically, SiNWs for VEGF identity; peptide nucleic acid (PNA-altered SiNW for RNA malignancy biomarkers; SiO_2-NW IL-10 for alkaline phosphatase sandwich insusceptible measure of interleukin10; and osteopontin (OPN) cell breakdown within the lungs biomarkers. AuNW polymers

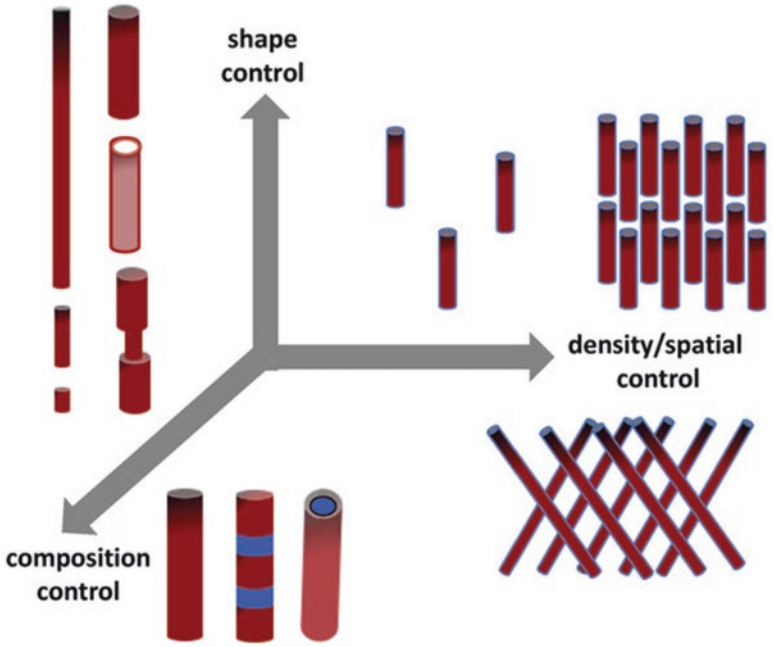

Fig. 3.7 Illustration of the versatility of the template-assisted synthesis of nanowires. (Reproduced from Open Access journal under the term of Creative Commons Attribution License (Piraux, 2020) Copyright © 2020)

were applied as formats for CK-7, epithelial cellular marker, enzymatic immunoassay, and polypyrrole-(Ppy-) NW, which have been included into the sphere impact transistor (FET) device, as a semiconducting material for the most cancers antigen 125 (CA 125) check (Fruscella et al., 2016).

3.9.7 Solid Lipid Nanoparticles (SLNs)

SLNs are of size in the range of 10–1000 nm and are used as a nanocarrier with packages focused on drug delivery. SLNs are organized with solid lipids which are solids at outline temperature (diglycerides, triglycerides, steroids, monoglycerides, fatty acids, or waxes) (Martinelli et al., 2019; Sonali et al., 2018). The high hydrophobicity of lipids has formed by addition of small part of surfactants or polymeric stabilizers in the aqueous medium with a purpose to have an impact on the physicochemical properties of the molecule (Waghmare et al., 2012). Hydrophobic drugs are condensed throughout the practice, even though hydrophilic drugs must be either synthetically appended to the elements or dissolve within the hydrophilic PEG shell (Liu et al., 2004). Compared to liposomes, lipid nanoparticles assure

higher drug stability and not on time delivery because of their crystalline structure. Also, in regard to other organic nanoparticles, they needn't issue with organic solvents for the duration of their manufacture, making them more noteworthy comfortable to utilize. Nonetheless, the high crystallinity of sturdy lipid nanoparticles can serve low drug loading effectiveness and additionally moderate drug discharge profiles. Consequently, nanostructured lipid transporters (NLCs) that contain as a minimum one lipids liquid at room temperature (like oleic corrosive, as an instance) are frequently appreciated (Muller et al., 2002). Solid lipid nanoparticle affiliation is the blessings of liposomes and PNPs and displays high balance within the physiological surroundings. Further, there may be no want of harmful organic solvent within the manufacturing of SLNs which makes them alright to be used. They can upload each hydrophilic and hydrophobic agent, mainly demonstrating favorable circumstances in proteins or peptides shipping (Ekambaram et al., 2012). Martins et al. (2013) have discussed the ability of camptothecin-loaded SLNs into the brain parenchyma subsequent to navigating through the blood-brain barrier (BBB). For this reason, they organized camptothecin-loaded SLNs for brain concentrated on and installation the gainful impact of SLNs on mind concentrated on when contrasted with the non-encapsulated (Fig. 3.8).

3.9.8 Carbon Nanotube

The shape of carbon nanotubes is cylindrical. Carbon nanotubes are allotropes form fullerene groups of carbon which are made up of layers of hexagonal association of graphite sheet via sp^2-hybridized carbon atoms (Fig. 3.9). Carbon nanotubes have two sorts, i.e., unmarried-walled CNTs (SWNTs) and multiwalled CNTs (MWNTs).

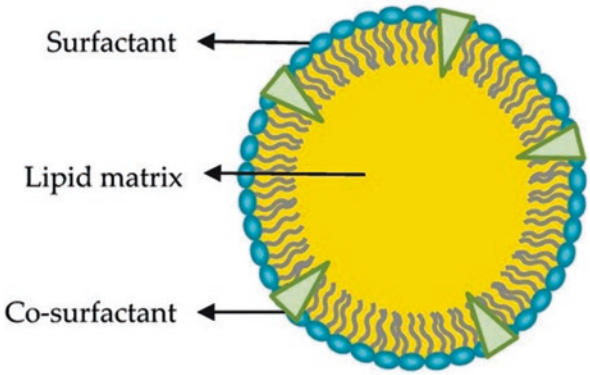

Fig. 3.8 Proposed model of solid lipid nanoparticles structure. Schematic representation of solid lipid nanoparticle (SLN) structure, showing the surfactant, cosurfactant and the solid lipid matrix. (Reproduced from Open Access journal under the term of Creative Commons Attribution License (Bayon-Cordero et al., 2019) Copyright © 2019)

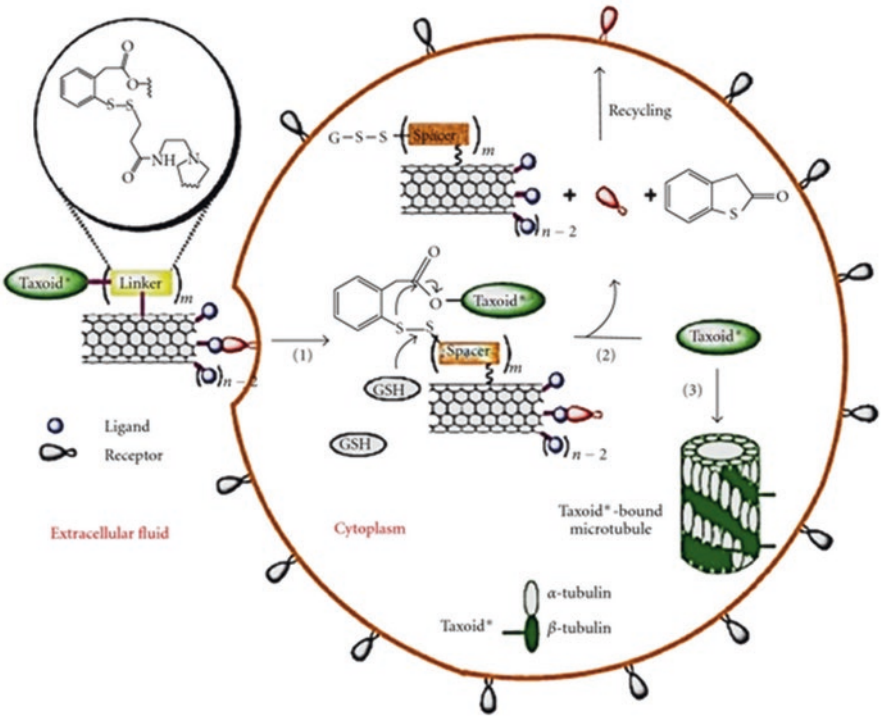

Fig. 3.9 (1) Internalization of the CNTs carried conjugate into the tumor cell via receptor-mediated endocytosis. (2) Taxoid was released by the cleavage of the chemical linker. (3) The free taxoid molecules were bound to microtubules to form stabilized microtubes, resulting in arrest of cell mitosis and induction of apoptosis. (Reproduced from Open Access journal under the term of Creative Commons Attribution License (Elhissi et al., 2012) Copyright © 2012)

Single-walled CNTs consist of a unmarried sheet of cylindrical graphene with width of 0.4–2 nm, and multiwalled carbon nanotubes consist of numerous concentric graphene sheets with inward breadth of 1–3 nm and outside distance across of 2–100 nm (Kesharwani & Iyer, 2015). The layers are folded right into a constant cylinder that may be open finished or protected on the limits with a greenback. CNTs have mild biodegradation and coffee biocompatibility. The physical and substance houses of CNTs are related with the structure, surface region, mechanical energy, excessive mechanical behavior, excessive electrical and high thermal conductivity and extremely-light-weight; they could offer a promising technique for gene and drug delivery for most cancers treatment (Tanaka et al., 2004) CNTs are an affordable contender for large biomedical applications because of an enormous range of trademark bodily and substance homes (Bianco et al., 2005; Ji et al., 2010). CNTs show capacities for drug loading on a superficial stage or in the inward middle through covalent and non-covalent connections. These nanoparticles can immobilize healing retailers, for example, tablets, proteins, DNA, and antibodies on the outer wall, or exemplify them inside the nanotubes, diminishing the cytotoxicity for

wholesome tissues. Due to their nano-needle-like shape, carbon nanoparticles are efficiently taken up and moved into the cytoplasm of goal cells without causing mobile dying. Their packages are confined because of the manner that CNTs are hydrophobic in nature and insoluble in water and are accrued in inward organs, having a low degradation charge (Gherman et al., 2015). A multifunctional dendrimer-altered multiwalled CNT for focusing on the folic acid (FA) receptor, which is overexpressed in malignant boom cells, a single-walled CNT combined with electrochemiluminescent silica NPs for identifying PSA within the blood, and, at last, a multilayered catalyst included CNT for excessive touchy chemiluminescent immunoassay of serum AFP. CNT, due to their herbal capacity to go into the mobile layer to supply drugs interior centered changed cells and to trade over optical electricity into thermal energy, may be provided to NIR to thermally weigh down cancer cells. Formation of QD to CNT has empowered confining disorder cells within the patients, by QD imaging, and resulting cellular demolition by means of drug delivery or thermal inactivation (Madani et al., 2013). This methodology can open up new skylines on multimodal nanoplatforms in oncology. CNTs produce deadly warmness upon NIR irradiation. Whenever they are taken up with the aid of the cells, they may likewise collaborate with proteins and DNA to disturb the mobile signaling or factor of different treatments (Ren et al., 2012; Chakrabarti et al., 2015). The essential NIR light absorption assets of CNTs have been applied to destruct malignant increase cells in vitro, while their NIR photoluminescence belongings have been utilized for in vitro cell imaging and analyzing. Robinson and co-workers (2010) have clarified the utility of i.v., agency of single-walled carbon nanotubes (SWCNTs) as image luminescent probes for in vivo tumor imaging. The investigation tested sizeable favorable instances of misusing the intrinsic characteristics of SWCNTs for theranostic programs. CNTs can enhance the chemotherapy of brain growths which proposal healthier submissions in scientific performs.

3.10 Drug-Targeting Approaches for Cancer Therapy

3.10.1 Active Targeting

The vigorous directing of the drug is the maximum appropriate targeting technique for powerful delivery of nanoparticles in harmful cells without bringing approximately any poisonousness. The lively concentration on the drug can be carried through molecular popularity of the most cancers' cells both through antibody-antigen or ligand-receptor interactions (Fig. 3.10). Nanoparticles and different polymer drug conjugates provide diverse open-door probabilities so far focused on tumors through surface changes which permit precise biochemical communications with the proteins/receptors communicated heading in the right direction cells. The folate receptor (FR) is a profoundly particular tumor marker often overexpressed in over 90% of ovarian carcinoma sufferers and in several different malignancy kinds

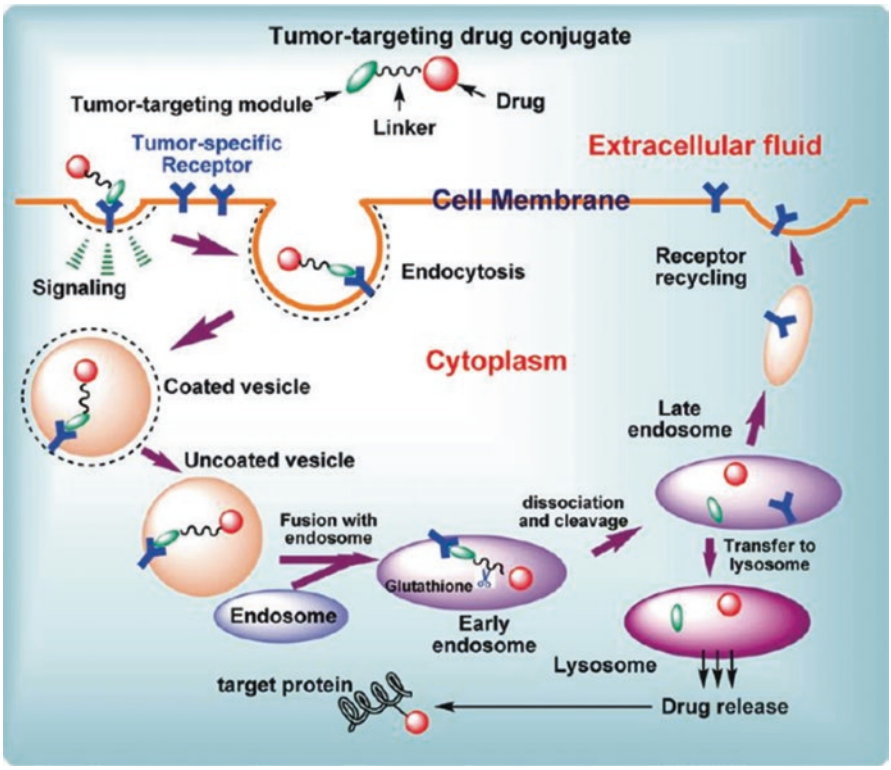

Fig. 3.10 Schematic representation of the RME of a tumor-targeting drug conjugate, drug release, and drug-binding to the target protein. (Adapted with permission from Chen et al. (2010) Copyright © 2010, American Chemical Society)

(choriocarcinomas, uterine sarcomas, osteosarcomas). Folate receptors are normally overexpressed by means of most cancer cells due to the upgraded necessity of folate for DNA instruction. The interplay of a folate moiety with the folate receptor on tumor cells prompts an endocytic shipping which ends up in cytosolic accumulating. It is studied that folate-protected liposomes boost the aggregation of chemotherapy retailers in a diverse kinds of tumor cells and on this manner upgrades their cytotoxicity (Pan & Lee, 2005). In addition, folate-included liposomes were utilized as a codelivery automobile for DOX and causes enhance in vitro take-up of DOX in KB (human epidermal carcinoma) and HeLa (cervical malignancy) cells as those cells overexpress folate receptors (Gerasimov et al., 1999).

Dimensions of nanoparticles simply as their superficial attributes are the important boundaries which can exchange the biodistribution of nanoparticles. Particles decreased than one hundred nm and covered with hydrophilic polymers, as an example, amphiphilic polymeric compounds which can be product of polyethylene oxide, for instance, poloxamers, poloxamines, or polyethylene glycol (PEG) are being researched to break out their take-up by means of the RES. To enhance the

viability of focused cancer chemotherapeutics to the tumor, a mix of passive and energetic targeting method is being researched wherein long-flowing drug companies are shaped to tumor cellular specific antibody reaction or peptides (Vasir & Labhasetwar, 2005). In another methodology of lively targeting of anticancer drug, nanoparticle fashioned integrin ligand has been proposed for gene delivery specifically to the angiogenic blood vessels in tumor-bearing mice as the integrins are vital for cell invasion and migration. Hood and co-worker (2002) mounted a DNA encapsulated cationic polymerized liposome carrying avb3 ligand and utilized it to target on the integrins of M21-cancer xenograft tumors. Results confirmed specifically enhancement in gene expression within the tumor and that the delivery of a mutant Raf gene avoided the endothelial cell signaling and angiogenesis, inflicting big tumor harm after just one injection.

3.10.2 Passive Targeting

Passive targeting suggests the gathering of drug or drug-provider machines at a particular website due to physicochemical or pharmacological components. Penetrability of the tumor vasculature increments to where particulate conveys, as an instance, nanoparticles can extravasate from blood route and restriction inside the tumor tissue. This occurs considering the fact that as tumors increase and crush the reachable delivery of oxygen and nutrients, they discharge cytokines and other signaling particles that enroll fresh blood vessels to the tumor, a cycle referred to as angiogenesis. Angiogenic blood vessels, distinctive to the tight blood vessels in maximum ordinary tissues, have cavities as tremendous as 600–800 nm among adjoining endothelial cells. Drug transporters within the nanometer size reach can extravasate through those cavities into the tumor interstitial area (Anajwala et al., 2010).

The drug transporter complex courses operate in the circulatory system, and it is to be taken to the objective receptor. Different properties of drug transporter complex, for example, atomic weight, surface charge, hydrophobic or hydrophilic nature of the surface, and its size, are key for efficient passive targeting of drugs. For example, PEG-included covertness liposomes float within the blood and its lifestyles span within the stream device is notably contributed by means of the surface price on PEG containing liposomes. The passive mode focused on the most commonly implemented method for drug shipping in most cancers mobile. As a producing tumor contains broken vasculature and subsequently activates structure one hundred-800 nm measured pores in blood vessels and receives leakier. Alongside this disfigurement in the vasculature, poor lymphatic waste aids in penetration and renovation of nanoparticles on the tumor web page and this is called as the enhanced permeability and retention (EPR) sway (Chaturvedi et al., 2019). Ordinary tumor vasculatures are lined by using near endothelial cells, hence forestalling nanoparticle drug from getting away or extravasation, even though tumor tissue vasculatures are spilling and hyperpermeable permitting specific amassing of nanoparticles

within the tumor interstitial space (referred to as aloof nanoparticle tumor specializing in) (Fig. 3.11) (La Van et al., 2003).

3.11 Use of Nanotechnology in Conventional Cancer Therapy

Recent developments in nanotechnology have extended its uses in conventional cancer therapies, i.e., photothermal and gene therapy.

3.11.1 Photothermal Therapy

Photothermal treatment is a measured and successful cancer treatment which includes photothermal agents for precise warming of the target most cancers location quarter causes thermal destruction of tumor as expressed in Fig. 3.12 (Montaseri et al., 2020). These photothermal retailers are both steel nanoparticles or function chromophores or mild soaking up colors, for instance, indocyanine green,

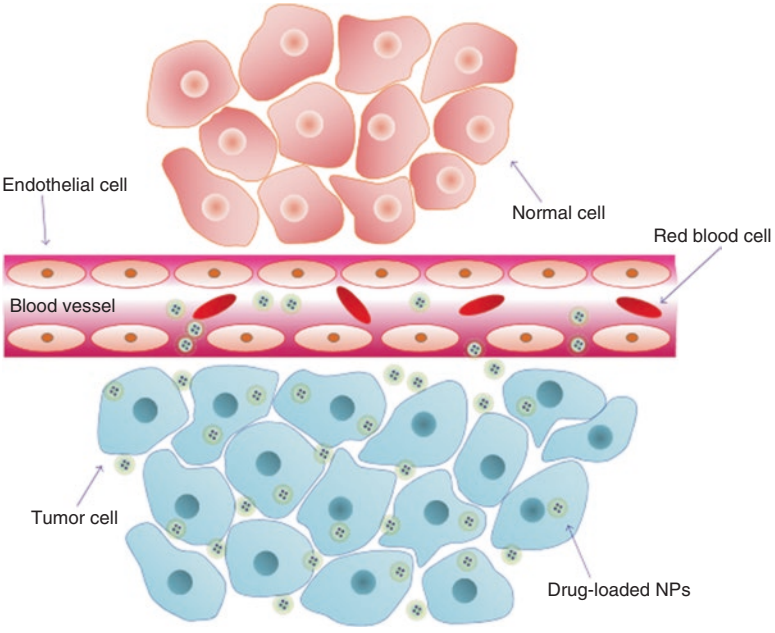

Fig. 3.11 Schematic diagram of enhanced permeation and retention (EPR) effect. (Reproduced from Open Access journal under the term of Creative Commons Attribution License (Yu et al., 2016) Copyright © 2016)

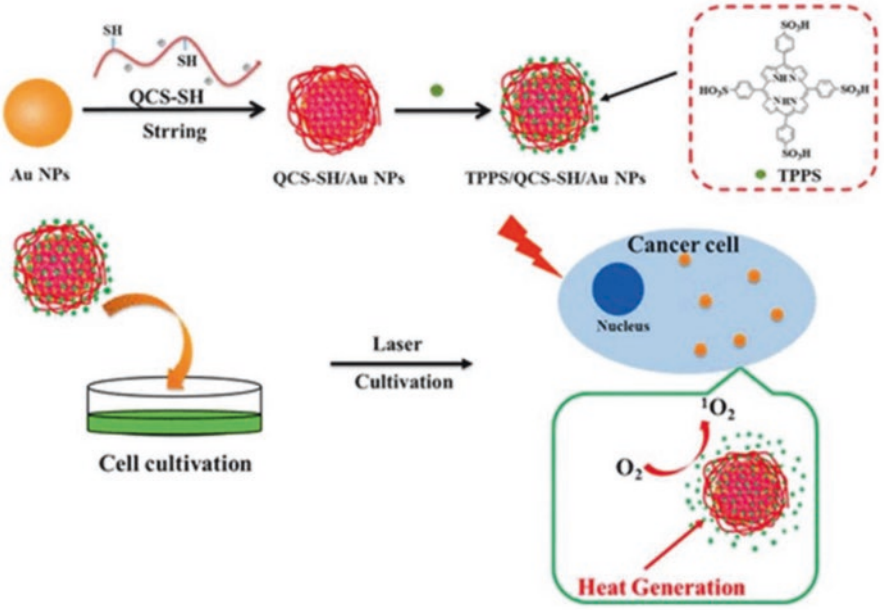

Fig. 3.12 Proposed fabrication of meso-tetrakis (4-sulphonatophenyl) porphyrin (TPPS)/QCS-SH/gold nanoparticles (AuNPs) for dual mode photodynamic therapy (PDT)/photothermal therapy (PTT) treatment of cancer. (Reproduced from Open Access journal under the term of Creative Commons Attribution License (Montaseri et al., 2020) Copyright © 2020)

porphyrin conjugated with transition metallic, naphthalocyanine, and so forth. In the thermal remedy of tumors, electromagnetic energies, for instance, microwaves and radiowaves, cause mobile destruction just like the denaturation of protein and membrane, in this way severe final results in cell demise. Photothermal treatment exactly targets the tumor cells due to the fact tumor cells are heat sensitive without frightening normal cells (Huang et al., 2006). Photothermal marketers like gold nanoparticle, carbon nanotubes (CNT), and nanorods sporting pills take in around 650–900 nm in near-infrared (NIR) place and convert into warmness. Iron oxide nanoparticle is like other mostly applied photothermal agent with control absorption potential ability as they've high molecule density within the water consequently brings about the big floor region. Water-suspended iron oxide nanoparticles have been regarded to supply heat while vaccinated immediately into the tumors inside the sight of applied oscillating magnetic appealing subject (Wang et al., 2017).

3.11.2 Gene Therapy

Gene therapy has been placed in a critical position in cancer treatment. Normally, in gene therapy processes, the genetic material is transported through the intravenous route; as nucleic acids are liable to degradation with the aid of nucleases and speedy clearance in systemic circulate move, a vector is wanted to percentage, ensure and shipping the genetic fabric to its web page of interest (Juri et al., 2017). This treatment can possibly get freed off the diminished viability and stale-goal harmfulness of chemotherapy and gives a superb asset for disease treatment both by way of regulating the outflow of tumor genes or via moving the genes that produce healing proteins or convert a non-poisonous compound right into a lethal drug. On the righteousness of this, numerous methodologies of most cancers gene remedy include gene silencing method making use of siRNA/shRNA, miRNA intervened gene treatment method and self-destruction gene treatment technique utilizing the transgene that causes disabled tumor development within the wake of being brought into tumor cells were grown so far (Wang et al., 2016). Concealment of tumor-specific oncogenes and changed tumor suppressor genes using the little interfering RNA (siRNA) and quick clip RNA (shRNA) facilitates in express targeting of tumor cells and ultimately evades the systemic poisonousness (Ameres et al., 2007). SiRNA is short 20–25 nucleotides in period dsRNA framed from ribonuclease, dicer intervened separate of twofold stranded RNA. SiRNA interfaces with a multifunctional

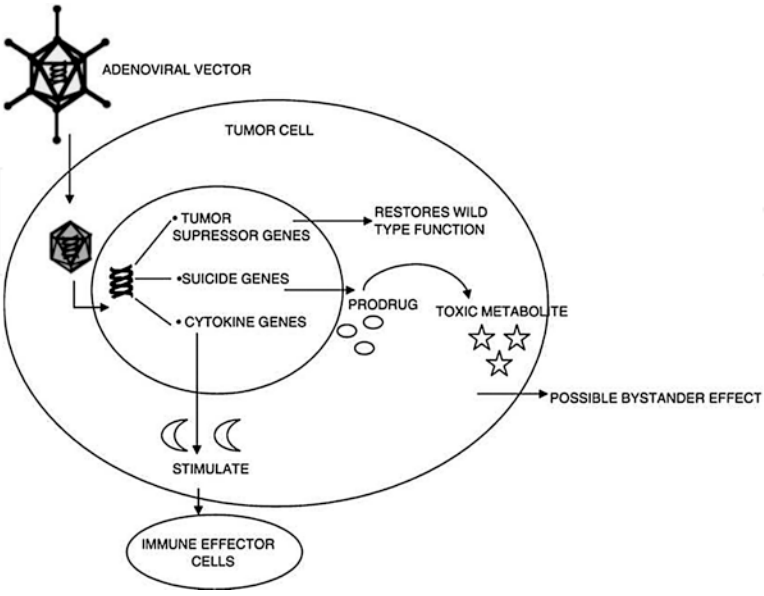

Fig. 3.13 Gene therapy strategies, mutation compensation, suicide gene therapy and immunopotentiation. (Reproduced from Open Access journal under the term of Creative Commons Attribution License (Cevher et al., 2012) Copyright © 2012)

protein, Argonaute, and systems RNA Induced Silencing Complex (RISC) which degrades vacationer RNA strand after the binding of centered corresponding mRNA as referenced in Fig. 3.13 (Cevher et al., 2012).

Genes and little RNAs may be appended to NPs by way of electrostatic interaction or conjugated onto the floor of NPs. In another way, applied nanocarriers for malignant boom genes remedy, polymeric nanoparticles, and inorganic nanoparticles had been used broadly in one of a kind most cancers remedy research. Polymer-based nanoparticles have many advantages which include small size, slender distribution, the potential to epitomize a big collection of great therapeutics, and deliver assurance from enzymatic degradation and their significant balance (Wang et al., 2015). Mattheolabakis et al. (2016) prepared a PEI-based hybrid polymer nanoparticle that blanketed HA and polyethylene glycol (PEG) and framed a polyplex by way of mixing it in with surviving silencing siRNA. Cotransfection of polyplex with CCD-C8 in most cancers breakdown inside the lungs cells indicated important restraint in tumor development. Besides, inorganic nanoparticles together with carbon nanotubes, gold nanoparticles, quantum spots, and so forth have been utilized in most cancers gene therapy. Oishi and co-employees (2006) preliminary located the inclusion of siRNA into gold nanoparticles and added it into liver carcinoma mobile line HuH7.

3.12 Future Research

Nanotechnology has been utilized widely in an enormous number of malignant growth diagnosis and therapeutic studies by numerous researchers and could be the following large thing in fighting cancer. Many research works were carried out so far in the area of cancer nanotechnology yet at the same time much more is yet to see the light of the day. Regarding manufacturing of nanomaterials, novel preparation ways are as yet should have been investigated to improve the issues with the current techniques. To fulfil different application needs, nanoparticle-circle composites with various morphology, various sizes (from nanometer to micrometer range), and various measures of nanoparticles have consistently been sought after. In the interim, more helpful activity methods and large-scale manufacturing are another significant improvement heading. For the alteration of the circle, direction formation of practical atoms and exact control of their number are the primary difficulties. Furthermore, appropriate surface covering has been attempted to improve the biocompatibility, specificity, and selectivity of the nanoparticle-circle composites. Concerning their pragmatic application, from one viewpoint, it's basic to build up a sound knowledge of the thermodynamics and kinetics energy of the limiting response at circle/arrangement interface, which will give a theoretical establishment to managing their application experimentally, for example, better controlling the development of the circle biomolecule forms, all the more effectively streamlining the working conditions in focused organic applications, etc. Then again, to guarantee the smooth change from seat to the bedside, numerous issues should be tended

to before the nanoparticle-circle composites can be utilized in people, including their biocompatibility, in vivo focusing on adequacy, pharmacokinetics, biodistribution, poisonousness, and so on. Numerous scientists have consistently been dedicating themselves to these examinations, and some even had made extraordinary advances, in spite of the fact that which are a long way from being ideal show a much brilliant application prospect (Wen et al., 2016). Notwithstanding the characteristic disadvantages, the capability of DNA-based nanomaterial in malignancy treatment is past the shadow of uncertainty, and further headway in the territory of DNA nanomaterial would give a considerable cancer analysis and treatment approach. In addition, preparation of a skilled multimodal nanoparticle should be stressed that could give a twofold punch to cancer in type of brisk conclusion and successful treatment. So obviously malignant growth nanotechnology will positively give a productive, powerful, and safe disease determination and treatment strategy not long from now (Chaturvedi et al., 2019).

3.13 Conclusions

Utilization of nanomaterials in various fields of science, designing, and innovation has gotten exceptionally well known for the most recent couple of years. Nanomedicine depends on different nanostructure proposals, which are formed with a wide scope of explicit targeting agents utilized for clinical applications, as early cancer diagnosis and therapy. The particular agents are joined to the nanoparticles; surface, which help the growth and distribution of those specialists in the neoplastic tissue. In present day, nanoparticles are being utilized broadly in biomedical research as a drug delivery system or as a treatment approach. Reliable with this reality, utilization of nanotechnology in cancer diagnostics and treatment has unlocked the road for new exploration region for example nano-oncology. Throughout the long term, research action in nano-oncology territory is fuelled by late advances in nanotechnology and set up the nano-oncology as a potential cancer treatment approach. Similarly, an incredible potential is accessible by biochemical alterations that expansion the potency and reduction the off-target impacts and opposite symptoms of restorative medications, permitting the execution of new customized drugs in medical use. Causes of cancer, treatment of cancer with limitation of exiting technology, and advantage of cancer nanotechnology for drug targeting and delivery methods of various vehicles such as liposomes, nanoshells, quantum dots, gold nanoparticles, dendrimers, nanowires, SLNs, and carbon nanotube were explained in the chapter. In general, we can infer that nano-oncology has opened a limitless method to look and design drug and drug delivery system for therapy of cancer. A constant and broad exploration in nano-oncology will build up as a conspicuous cancer treatment approach in the not-so-distant future.

References

Abshikbayeva, Z., Tosi, D., Balmassov, D., Schena, E., Saccomandi, P., & Inglezakis, V. (2019). Application of nanoparticles and nanomaterials in thermal ablation therapy of cancer. *Nanomaterials, 9*, 1195.

Akbarzadeh, A., Rezaei-Sadabady, R., Davaran, S., Joo, S. W., Zarghami, N., Hanifehpour, Y., Samiei, M., Kouhi, M., & Nejati Koshki, K. (2013). Liposome: Classification, preparation, and applications. *Nanoscale Research Letters, 8*, 102.

Allen, T. M., & Cullis, P. R. (2013). Liposomal drug delivery systems: From concept to clinical applications. *Advanced Drug Delivery Reviews, 65*, 36–48.

Alper, J. (2005). Shining a Light on Cancer Research. In *NCI Alliance for Nanotechnology in Cancer*. National Cancer Institute. USA Report 49, January/February, 1-3, 2005.

Amador, C., Greiner, T. C., Heavican, T. B., Smith, L. M., Galvis, K. T., Lone, W., Bouska, A., D'Amore, F., Pedersen, M. B., Pileri, S., et al. (2019). Reproducing the molecular subclassification of peripheral T-cell lymphoma-NOS by immunohistochemistry. *Blood, 134*, 2159–2170.

Ameres, S. L., Martinez, J. M., & Schroeder, R. (2007). Molecular basis for target RNA recognition and cleavage by human RISC. *Cell, 130*, 101–112.

Ames, B. N., Gold, L. S., & Willett, W. C. (1995). The causes and prevention of cancer. *Proceedings of the National Academy of Sciences of the United States of America, 92*(12), 5258–5265.

Anajwala, C. C., Jani, G. K., & Swamy, S. M. V. (2010). Current trends of nanotechnology for cancer therapy. *International Journal of Pharmaceutical Sciences and Nanotechnology, 3*, 1043–1056.

Anand, P., Kunnumakara, A. B., Sundaram, C., Harikumar, K. B., Tharakan, S. T., Lai, O. S., Sung, B., & Aggarwal, B. B. (2008). Cancer is a preventable disease that requires major lifestyle changes. *Pharmaceutical Research, 25*(9), 2097–2116.

Ananda, S., Nowak, A. K., Cher, L., Dowling, A., Brown, B., Simes, J., Rosenthal, M. A., & COGNO. (2011). Phase 2 trial of temozolomide and pegylated liposomal doxorubicin in the treatment of patients with glioblastoma multiforme following concurrent radiotherapy and chemotherapy. *Journal of Clinical Neuroscience, 18*, 1444–1448.

Andrews, D. W., Scott, C. B., Sperduto, P. W., Flanders, A. E., Gaspar, L. E., Schell, M. C., Werner-Wasik, M., Denas, W., Ryu, J., Bahary, J. P., Souhami, L., Rotman, M., Mehta, M. P., & Curran, J. R. W. J. (2004). Whole brain radiation therapy with or without stereotactic radiosurgery boost for patients with one to three brain metastases: Phase III results of the RTOG 9508 randomised trial. *The Lancet, 363*(9422), 1665–1672.

Aslam, M. S., Naveed, S., Ahmed, A., Abbas, Z., Gull, I., & Atha, M. A. (2014). Side effects of chemotherapy in cancer patients and evaluation of patients opinion about starvation based differential chemotherapy. *Journal of Cancer Therapy, 5*, 817–822.

Ataollahi, M. R., Sharifi, J., Paknahad, M. R., & Paknahad, A. (2015). Breast cancer and associated factors: A review. *Journal of Medicine and Life, 8*(4), 6–11.

Balukrishna, S., Pilaka, V. K. R., Michael, R. C., Samuel, P., & Ravindran, P. B. (2015). Hyperfractionated Intensity Modulated Radiation Therapy (HF-IMRT) in head and neck cancer: The technical feasibility and results of a short clinical series. *Journal of Clinical and Diagnostic Research, 9*(5), XR01–XR04.

Baskar, R., Dai, J., Wenlong, N., Yeo, R., & Yeoh, K. W. (2014). Biological response of cancer cells to radiation treatment. *Frontiers in Molecular Biosciences, 1*, 24.

Bayon-Cordero, L., Alkorta, I., & Arana, L. (2019). Application of solid lipid nanoparticles to improve the efficiency of anticancer drugs. *Nanomaterials, 9*, 474.

Benjamin, D. J. (2014). The efficacy of surgical treatment of cancer – 20 years later. *Medical Hypotheses, 82*(4), 412–420.

Bharali, D. J., & Mousa, S. A. (2010). Emerging nanomedicines for early cancer detection and im- proved treatment: Current perspective and future promise. *Pharmacology & Therapeutics, 128*, 324–35.10.

Bianco, A., Kostarelos, K., & Prato, M. (2005). Applications of carbon nano tubes in drug delivery. *Current Opinion in Chemical Biology, 9*, 674–679.

Blackadar, C. B. (2016). Historical review of the causes of cancer. *World Journal of Clinical Oncology, 7*(1), 54–86.

Bostick, R. M., Kong, K. Y., Ahearn, T. U., Chaudry, Q., Cohen, V., & Wang, M. D. (2006). Detecting and quantifying biomarkers of risk for colorectal cancer using quantum dots and novel image analysis algorithms. *Conference Proceedings: Annual International Conference of the IEEE Engineering in Medicine and Biology Society, 1*, 3313–3316.

Bozzuto, G., & Molinari, A. (2015). Liposomes as nanomedical devices. *International Journal of Nanomedicine, 10*, 975.

Bray, F., Ferlay, J., Soerjomataram, I., Siegel, R. L., Torre, L. A., & Jemal, A. (2018). Global cancer statistics 2018: GLOBOCAN estimates of incidence and mortality worldwide for 36 cancers in 185 countries. *CA: A Cancer Journal for Clinicians, 68*, 394–424.

Carbone, A. (2020). Cancer classification at the crossroads. *Cancers (Basel), 12*(4), 980.

Cevher, E., Sezer, A. D., & Caglar, E. S. (2012). Gene delivery systems: Recent progress in viral and non-viral therapy. In A. D. Sezer (Ed.), *Recent advances in novel drug carrier systems* (pp. 437–470). IntechOpen.

Chakrabarti, M., Kiseleva, R., Vertegel, A., & Ray, S. K. (2015). Carbon nanomaterials for drug delivery and cancer therapy. *Journal of Nanoscience and Nanotechnology, 15*, 5501–5511.

Chakraborty, S., & Rahman, T. (2012). The difficulties in cancer treatment. *Ecancermedicalscience, 6*, ed16.

Chaturvedi, V. K., Singh, A., Singh, V. K., & Singh, M. P. (2019). Cancer nanotechnology: A new revolution for cancer diagnosis and therapy. *Current Drug Metabalism, 20*, 416–429.

Chen, G. T. Y., Sharp, G. C., & Mori, S. (2009). A review of image-guided radiotherapy. *Radiological Physics and Technology, 2*, 1–12.

Chen, S., Zhao, X., Chen, J., Chen, J., Kuznetsova, L., Wong, S. S., & Ojima, I. (2010). Mechanism-based tumor-targeting drug delivery system. Validation of efficient vitamin receptor-mediated endocytosis and drug release. *Bioconjugate Chemistry, 21*, 979–987.

Chiang, A. C., & Massague, J. (2008). Molecular basis of metastasis. *The New England Journal of Medicine, 359*, 2814–2823.

Choi, Y.-E., Kwak, J.-W., & Park, J. W. (2010). Nanotechnology for early cancer detection. *Sensors, 10*, 428–455.

Constantinidou, A., Jones, R. L., Scurr, M., Al-Muderis, O., & Judson, I. (2009). Pegylated liposomal doxorubicin, an effective, well-tolerated treatment for refractory aggressive fibromatosis. *European Journal of Cancer, 45*, 2930–2934.

Culp, M. B., Soerjomataram, I., Efstathiou, J. A., Bray, F., & Jemal, A. (2020). Recent global patterns in prostate cancer incidence and mortality rates. *European Urology, 77*, 38–52.

Davis, F. G., Dolecek, T. A., McCarthy, B. J., & Villano, J. L. (2012). Toward determining the lifetime occurrence of metastatic brain tumors estimated from 2007 United States cancer incidence data. *Neuro-Oncology, 14*, 1171–1177.

Demicheli, R., Retsky, M. W., Hrushesky, W. J. M., Baum, M., & Gukas, I. D. (2008). The effects of surgery on tumor growth: A century of investigations. *Annals of Oncology, 19*(11), 1821–1828.

DeVita, V. T., & Chu, E. (2008). A history of cancer chemotherapy. *Cancer Research, 68*, 8643–8653.

Ekambaram, P., Sathali, A. A. H., & Priyanka, K. (2012). Solid lipid nanoparticles: A review. *Scientific Reviews & Chemical Communications, 2*, 80–102.

Elhissi, A. M. A., Ahmed, W., Hassan, I. U., Dhanak, V. R., & D'Emanuele, A. (2012). Carbon nanotubes in cancer therapy and drug delivery. *Journal of Drug Delivery, 2012*, 837327.

Fang, M., Peng, C. W., Pang, D. W., & Li, Y. (2012). Quantum dots for cancer research: Current status, remaining issues, and future perspectives. *Cancer Biology & Medicine, 9*, 151–163.

Fruscella, M., Ponzetto, A., Crema, A., & Carloni, G. (2016). The extraordinary progress in very early cancer diagnosis and personalizes therapy: The role of oncomarkers and nanotechnology. *Journal of Nanotechnology, 2016*, Article ID 3020361. https://doi.org/10.1155/2016/3020361

Galluzzi, L., Pedro, J. M. B. S., Demaria, S., Formenti, S. C., & Kroemer, G. (2017). Activating autophagy to potentiate immunogenic chemotherapy and radiation therapy. *Nature Reviews. Clinical Oncology, 14*, 247–258.

Gao, Z., Lukyanov, A. N., Singhal, A., & Torchilin, V. P. (2002). Diacyllipidpolymer micelles as nanocarriers for poorly soluble anticancer drugs. *Nano Letters, 2*, 979–982.

Gerasimov, O. V., Boomer, J. A., Qualls, M. M., & Thompson, D. H. (1999). Cytosolic drug delivery using pH-and light-sensitive liposomes. *Advanced Drug Delivery Reviews, 38*, 317–338.

Gherman, C., Tudor, M. C., Constantin, B., Flaviu, T., Stefan, R., Maria, C. S., Braicu, C., Pop, L., Petric, R. C., & Neagoe, I. B. (2015). Pharmacokinetics evaluation of carbon nanotubes using FTIR analysis and histological analysis. *Journal of Nanoscience and Nanotechnology, 15*, 2865–2869.

Ghoncheh, M., Mirzaei, M., & Salehiniya, H. (2015). Incidence and mortality of breast cancer and their relationship with the Human Development Index (HDI) in the world in 2012. *Asian Pacific Journal of Cancer Prevention, 16*(18), 8439–8443.

Golemis, E. A., Scheet, P., Beck, T. N., Scolnick, E. M., Hunter, D. J., Hawk, E., & Hopkins, N. (2018). Molecular mechanisms of the preventable causes of cancer in the United States. *Genes & Development, 32*, 868–902.

Griffin, L. D., & Kellam, P. (2009). Infectious causes of cancer and their detection. *Journal of Biology, 8*, article no.67. http://jbiol.com/content/8/7/67

Hanahan, D., & Weinberg, R. A. (2011). Hallmarks of cancer: The next generation. *Cell, 144*, 646–674.

Hassanpour, S. H., & Dehghani, M. (2017). Review of cancer from perspective of molecular. *Journal of Cancer Research and Practice, 4*, 127–129.

Hirsch, L. R., Stafford, R. J., Bankson, J., Sershen, S. R., Rivera, B., Price, R., Hazle, J. D., Halas, N. J., & West, J. L. (2003). Nanoshellmediated near-infrared thermal therapy of tumors under magneticresonance guidance. *Proceedings of the National Academy of Sciences of the United States of America, 100*, 13549–13554.

Hood, J. D., Bednarski, M., Frausto, R., Guccione, S., Reisfeld, R., Xiang, R., & Cheresh, D. A. (2002). Tumor regression by targeted gene delivery to the neovasculature. *Science, 296*, 2404–2407.

Hu, Y., Fine, D. H., Tasciotti, E., Bouamrani, A., & Ferrari, M. (2011). Nanodevices in diagnostics, Wiley interdisciplinary reviews. *Nanomedicine and Nanobiotechnology, 3*, 11–32.

Huang, X., Jain, P. K., El-Sayed, I. H., & El-Sayed, M. A. (2006). Determination of the minimum temperature required for selective photothermal destruction of cancer cells with the use of immunotargeted gold nanoparticles. *Journal of Photochemistry and Photobiology B: Biology, 82*, 412–417.

Huang, X., Jain, P. K., El-Sayed, I. H., & El-Sayed, M. A. (2007). Gold nanoparticles: Interesting optical properties and recent applications in cancer diagnostics and therapy. *Nanomedicine (London, England), 2*, 681–693.

Idikio, H. A. (2011). Human cancer classification: A systems biology-based model integrating morphology, cancer stem cells, proteomics, and genomics. *Journal of Cancer, 2*, 107–115.

Illum, L., & Dacis, S. S. (1984). The organ uptake of intravenously administered colloidal particles can be altered using a nonionic surfactant (Poloxamer 338). *FEBS Letters, 167*, 79–82.

Jaishree, V., & Gupta, P. D. (2012). Nanotechnology: A revolution in cancer diagnosis. *Indian Journal of Clinical Biochemistry, 27*(3), 214–220.

Jemal, A., Siegel, R., Ward, E., Murray, T., Xu, J., & Thun, M. J. (2007). Cancer statistics, 2007. *CA: a Cancer Journal for Clinicians, 57*(1), 43–66.

Ji, S. R., Liu, C., Zhang, B., Yang, F., Xu, J., Long, J., Jin, C., Fu, D. L., Ni, Q. X., & Yu, X. J. (2010). Carbon nanotubes in cancer diagnosis and therapy. *Biochimica et Biophysica Acta, 1806*, 9–35.

Jin, C., Wang, K., Oppong-Gyebi, A., & Hu, J. (2020). Application of nanotechnology in cancer diagnosis and therapy - a mini-review. *International Journal of Medical Sciences, 17*(18), 2964–2973.

Juri, A., Braicu, C., Pop, L. A., Tomuleasa, C., Gherman, C. D., & Neagoe, I. B. (2017). The new era of nanotechnology, an alternative to change cancer treatment. *Drug Design, Development and Therapy, 11*, 2871–2890.

Kano, H., Flickinger, J. C., Tonetti, D., Hsu, A., Yang, H. C., Flannery, T. J., Niranjan, A., & Lunsford, L. D. (2017). Estimating the risks of adverse radiation effects after gamma knife radiosurgery for arteriovenous malformations. *Stroke, 48*, 84–90.

Kashyap, M., Tiwari, A., Arya, K., & Saxena, V. L. (2019). Quantum dot: An emerging nanocrystal for cancer diagnosis and therapy. *Research Journal of Life Sciences, Bioinformatics, Pharmaceutical and Chemical Sciences, 5*, 320–330.

Kawashima, N., Nakayama, K., Itoh, K., Itoh, T., Ishikawa, M., & Biju, V. (2010). Reversible dimerization of EGFR revealed by single molecule fluorescence imaging using quantum dots. *European Journal of Organic Chemistry, 16*, 1186–1192.

Kesharwani, P., & Iyer, A. K. (2015). Recent advances in dendrimer-based nanovectors for tumor-targeted drug and gene delivery. *Drug Discovery Today, 20*, 536–547.

Kim, K. Y. (2007). Nanotechnology platforms and physiological challenges for cancer thera- peutics. *Nanomedicine: Nanotechnology, Biology and Medicine, 3*(2), 103–110.

Kolonel, L. N., Altshuler, D., & Henderson, B. E. (2004). The multiethnic cohort study: Exploring genes, lifestyle and cancer risk. *Nature Reviews. Cancer, 4*, 519–527.

Kotnis, A., Sarin, R., & Mulherkar, R. (2005). Genotype phenotype and cancer: Role of low penetrance genes and environment in tumor susceptibility. *Journal of Biosciences, 30*, 93–102.

Krishanan, S. R., & George, S. K. (2014). Nanotherapeutics in cancer prevention, diagnosis and treatment. In S. J. T. Gowder (Ed.), *Pharmacology and therapeutics* (pp. 235–253). IntechOpen. https://doi.org/10.5772/58419

Kukowska-Latallo, J. F., Candido, K. A., Cao, Z., Nigavekar, S. S., Majoros, I. J., Thomas, T. P., Balogh, L. P., Khan, M. K., & Baker, J. J. R. (2005). Nanoparticle targeting of anticancer drug improves therapeutic response in animal model of human epithelial cancer. *Cancer Research, 65*, 5317–5324.

La Van, D. A., McGuire, T., & Langer, R. (2003). Small-scale systems for in vivo drug delivery. *Nature Biotechnology, 21*, 1184–1191.

Liong, M., Lu, J., Kovochich, M., Xia, T., Ruehm, S. G., Nel, A. E., Tamanoi, F., & Zink, J. I. (2008). Multifunctional inorganic nanoparticles for imaging, targeting, and drug delivery. *ACS Nano, 2*, 889–896.

Liu, C., & Xu, X. Y. (2015). A systematic study of temperature sensitive liposomal delivery of doxorubicin using a mathematical model. *Computers in Biology and Medicine, 60*, 107–116.

Liu, J., Xiao, Y., & Allen, C. (2004). Polymer-drug compatibility: A guide to the development of delivery systems for the anticancer agent, ellipticine. *Journal of Pharmaceutical Sciences, 93*, 132–143.

Loo, C., Lin, A., Hirsch, L., Lee, M. H., Barton, J., Halas, N., West, J., & Drezek, R. (2004). Nanoshell-enabled photonics-based imaging and therapy of cancer. *Technology in Cancer Research & Treatment, 3*, 33–40.

Loud, J. T., & Murphy, J. (2017). Cancer screening and early detection in the 21st century. *Seminars in Oncology Nursing, 33*(2), 121–128.

Lowy, D. R., & Collins, F. S. (2016). Aiming high--changing the trajectory for cancer. *The New England Journal of Medicine, 374*, 1901–1904.

Madaan, K., Kumar, S., Poonia, N., Lather, V., & Pandita, D. (2014). Dendrimers in drug delivery and targeting: Drug-dendrimer interactions and toxicity issues. *Journal of Pharmacy & Bioallied Sciences, 6*, 139–150.

Madani, S. Y., Shabani, F., Dwek, M. V., & Seifalian, A. M. (2013). Conjugation of quantum dots on carbon nanotubes for medical diagnosis and treatment. *International Journal of Nanomedicine, 8*, 941–950.

Maiti, A., & Bhattacharyya, S. (2013). Quantum dots and applications in medical science. *International Journal of Chemical Science and Chemical Engineering, 3*, 37–42.

Martinelli, C., Pucci, C., & Ciofani, G. (2019). Nanostructured crriers as innovative tools for cancer diagnosis and therapy. *APL Bioengineering*. 3.011502. 0. https://doi.org/10.1063/1.5079943

Martins, S. M., Sarmento, B., Nunes, C., Lucio, M., Reis, S., & Ferreira, D. C. (2013). Brain targeting effect of camptothecin-loaded solid lipid nanoparticles in rat after intravenous administration. *European Journal of Pharmaceutics and Biopharmaceutics, 85*(3 Pt A), 488–502.

Mattheolabakis, G., Ling, D., Ahmad, G., & Amiji, M. (2016). Enhanced anti-tumor efficacy of lipid-modified platinum derivatives in combination with survivin silencing sirna in resistant non-small cell lung cancer. *Pharmaceutical Research, 33*, 2943–2953.

MeCormack, B., & Gregoriadis, G. (1994). Drugs-in-cyclodextrins-inliposomes a novel concept in drug delivery. *International Journal of Pharmaceutics, 112*, 249–258.

Montaseri, H., Kruger, C. A., & Abrahamse, H. (2020). Recent advances in porphydrin-based inorganic nanoparticles for cancer treatement. *International Journal of Molecular Sciences, 21*, 3358.

Moreira-Nunes, C. A., Mesquita, F. P., Portilho, A. J. D., Junior, F. A. R. M., Maues, J. H. D. S., Pantoja, L. D. C., Wanderley, A. V., Khayat, A. S., Zuercher, W. J., Montenegro, R. C., Moraes-Filho Mod, & Moraes, M. E. A. D. (2020). Targeting aurora kinases as a potential prognostic and therapeutical biomarkers in pediatric acute lymphoblastic leukaemia. *Scientific Reports, 10*, 21272.

Morrison, R., Schleicher, S. M., Sun, Y., Niermann, K. J., Kim, S., Spratt, D. E., Chung, C. H., & Lu, B. (2011). Targeting the mechanisms of resistance to chemotherapy and radiotherapy with the cancer stem cell hypothesis. *Journal of Oncology, 2011*, 941876.

Morrow, K. J., Bawa, J. R., & Wei, C. (2007). Recent advances in basic and clinical nanomedicine. *Medical Clinics of North America, 91*, 805–843.

Mouw, K. W., Cleary, J. M., Reardon, B., Pike, J., Braunstein, L. Z., Kim, J., Amin-Mansour, A., Miao, D., Damish, A., Chin, J., Ott, P. A., Fuchs, C. S., Martin, N. E., Getz, G., Carter, S., Mamon, H. J., Hornick, J. L., Allen, E. M. V., & D'Andrea, A. S. (2017). Genomic evolution after chemoradiotherapy in anal squamous cell carcinoma. *Clinical Cancer Research, 23*(12), 3214–3222.

Muller, R. H., Radtke, M., & Wissing, S. A. (2002). Nanostructured lipid matrices for improved microencapsulation of drugs. *International Journal of Pharmaceutics, 242*, 121–0128.

Nagai, H., & Kim, Y. H. (2017). Cancer prevention from the perspective of global cancer burden patterns. *Journal of Thoracic Disease, 9*(3), 448–451.

Nersesyan, H., & Slavin, K. V. (2007). Current aproach to cancer pain management: Availability and implications of different treatment options. *Therapeutics and Clinical Risk Management, 3*(3), 381–400.

Nurgali, K., Jagoe, R. T., & Abalo, R. (2018). Editorial: Adverse effects of cancer chemotherapy: Anything new to improve tolerance and reduce sequelae? *Frontiers in Pharmacology, 9*, 245.

O'Connor, A. E., Gallagher, W. M., & Byrne, A. T. (2009). Porphyrin and nonporphyrin photosensitizers in oncology: Preclinical and clinical advances in photodynamic therapy. *Photochemistry and Photobiology, 85*, 1053–1074.

Oerlemans, C., Bult, W., Bos, M., Storm, G., Nijsen, J. F. W., & Hennink, W. E. (2010). Polymeric micelles in anticancer therapy: Targeting, imaging and triggered release. *Pharmaceutical Research, 27*, 2569–2589.

Oishi, M., Nakaogami, J., Ishii, T., & Nagasaki, Y. (2006). Smart PEGylated gold nanoparticles for the cytoplasmic delivery of siRNA to induce enhanced gene silencing. *Chemistry Letters, 35*, 1046–1047.

Oluogun, W. A., Adedokun, K. A., Oyenike, M. A., & Adeyeba, O. A. (2019). Histological classification, grading, staging, and prognostic indexing of female breast cancer in an African population: A 10-year retrospective study. *International Journal of Health and Science (Qassim), 13*(4), 3–9.

Pan, X. Q., & Lee, R. J. (2005). In vivo antitumor activity of folate receptortargeted liposomal daunorubicin in a murine leukemia model. *Anticancer Research, 25*, 343–346.

Parkin, D. M., Bray, F., Ferlay, J., & Pisani, P. (2002). Global cancer statistics, 2002. *CA: a Cancer Journal for Clinicians, 55*, 74–108.

Pavlova, N. N., & Thompson, C. B. (2016). The emerging hallmarks of cancer metabolism. *Cell Metabolism, 23*, 27–47.

Piraux, L. (2020). Magnetic nanowires. *Applied Science, 10*, 1832.

Purohit, R., & Singh, S. (2018). Fluorescent gold nanoclusters for efficient cancer cell targeting. *International Journal of Nanomedicine, 13*, 15–17.

Ravindran, R. (2011). Nano technology in cancer diagnosis and treatment: An overview. *Oral & Maxillofacial pathology Journal, 2*, 101–106.

Read, G. (1998). Conformal radiotherapy: A clinical review. *Clinical Oncology, 10*(5), 288–296.

Rehman, J., Zahra, A. N., Khalid, M., Asghar, H. M. N. H. K., Gilani, Z. A., Ullah, I., Nasar, G., Akhtar, M. M., & Usmani, M. N. (2018). Intensity modulated radiation therapy: A review of current practice and future outlooks. *Journal of Radiation Research and Applied Sciences, 11*(4), 361–367.

Ren, J., Shen, S., Wang, D., Xi, Z., Guo, L., Pang, Z., Qian, Y., Sun, X., & Jiang, X. (2012). The targeted delivery of anticancer drugs to brain glioma by PEGylated oxidized multi-walled carbon nanotubes modified with angiopep-2. *Biomaterials, 33*, 3324–3333.

Riggio, C., Pagni, E., & Raffa, C. A. (2011). Nano-oncology: Clinical application for cancer therapy and future perspectives. *Journal of Nanomaterials, 2011*. Article ID 164506, 10 pages. https://doi.org/10.1155/2011/164506

Robinson, J. T., Welsher, K., Tabakman, S. M., Sherlock, S. P., Wang, H., Luong, R., & Dai, H. (2010). High performance in vivo near-IR (>1 μm) imaging and photothermal cancer therapy with carbon nanotubes. *Nano Research, 3*, 779–793.

Roeder, F., Meldolesi, E., Gerum, S., & ValentiniV, R. C. (2020). Recent advances in (chemo-) radiation therapy for rectal cancer: A comprehensive review. *Radiation Oncology, 15*, 262.

Rosai, J., & Ackerman, L. V. (1979). The pathology of tumors, part III: Grading, staging & classification. *CA: a Cancer Journal for Clinicians, 29*, 66–77.

Rosenfeld, M. R., Ye, X., Supko, J. G., Dasideri, S., Grossman, S. A., Bream, S., Mikkelson, T., Wang, D., Chang, Y. C., Hu, J., McAfee, Q., Fisher, J., Troxel, A. B., Piao, S., Heitjan, D. F., Tan, K. S., Pontiggia, L., O'Dwyer, P. J., Davis, L. E., & Amaravadi, R. K. (2014). A phase I/II trial of hydroxychloroquine in conjunction with radiation therapy and concurrent and adjuvant temozolomide in patients with newly diagnosed glioblastoma multiforme. *Autophagy, 10*, 1359–1368.

Roy, R., & Baek, M. G. (2002). Glycodendrimers: Novel glycotope isosteres unmasking sugar coding. Case study with T-antigen markers from breast cancer MUC1 glycoprotein. *Reviews in Molecular Biotechnology, 90*, 291–309.

Ruan, Y., Yu, W., Cheng, F., Zhang, X., Rao, T., Xia, Y., & Larre, S. (2011). Comparison of quantum-dots-and fluorescein-isothiocyanate-based technology for detecting prostate-specific antigen expression in human prostate cancer. *IET Nanobiotechnology, 5*, 47–51.

Schirrmacher, V. (2019). From chemotherapy to biological therapy: A review of novel concepts to reduce the side effects of systemic cancer treatment (review). *International Journal of Oncology, 54*(2), 407–419.

Senior, J., Delgado, C., Fisher, D., Tilcock, C., & Gregoriadis, G. (1999). Influence of surface hydrophilicity of liposomes on their interaction with plasma-protein and clearance from the circulation studies with poly (ethylene glycol)-coated vesicles. *Biochimica et Biophysica Acta, 1062*, 77–87.

Shao, L., Gao, Y., & Yan, F. (2011). Semiconductor quantum dots for biomedical applications. *Sensors, 11*, 11736–11751.

Shieh, Y., Eklund, M., Sawaya, G. F., Black, W. C., Kramer, B. S., & Esserman, L. J. (2016). Population-based screening for cancer: Hope and hype. *Nature Reviews. Clinical Oncology, 13*(9), 550–565.

Siegel, R. L., Miller, K. D., & Jemal, A. (2020). Cancer statistics, 2020. *CA: a Cancer Journal for Clinicians, 70*, 7–30.

Sonali, V. M. K., Singh, R. P., Agrawal, P., Mehata, A. K., Pawde, D. M., Narendra, S. R., & Muthu, M. S. (2018). Nanotheranostics: Emerging strategies for early diagnosis and therapy of brain cancer. *Nano, 2*, 70–86.

Stein, L., Urban, M. I., O'Connell, D., Yu, X. Q., Beral, V., Newton, R., Ruff, P., Donde, B., Hale, M., Patel, M., & Sitas, F. (2008). The spectrum of human immunodeficiency virus-associated cancers in a South African black population: Results from a case-control study, 1995-2004. *International Journal of Cancer, 122*, 2260–2265.

Stelow, E. B., Shaco-Levy, R., Bao, F., Garcia, J., & Klimstra, D. (2010). Pancreatic acinar cell carcinomas with prominent ductal differentiation: Mixed acinar ductal carcinoma and mixed acinar endocrine ductal carcinoma. *American Journal of Surgical Pathology, 34*(4), 510–518.

Su, P. J., Wu, M. H., Wang, H. M., Lee, C. L., Huang, W. K., Wu, C. E., Chang, H. K., Chao, Y. K., Tseng, C. K., Chiu, T. K., Lin, N. M. J., Ye, S. R., Lee, J. Y. C., & Hsieh, C. H. (2016). Circulating tumour cells as an independent prognostic factor in patients with advanced Oesophageal squamous cell carcinoma undergoing chemoradiotherapy. *Scientific Reports, 6*, 31423.

Tanaka, T., Shiramot, S., Miyashita, M., Fujishima, Y., & Kaneo, Y. (2004). Tumor targeting based on the effect of enhanced permeability and retention (EPR) and the mechanism of receptor-mediated endocytosis (RME). *International Journal of Pharmacy, 277*, 39–61.

Thun, M. J., De Lancey, J. O., Center, M. M., Jemal, A., & Ward, E. M. (2010). The global burden of cancer: Priorities for prevention. *Carcinogenesis, 31*, 100–110.

Tian, X., Liu, K., Hou, Y., Cheng, J., & Zhang, J. (2018). The evolution of proton beam therapy: Current and future status. *Molecular and Clinical Oncology, 8*(1), 15–21.

Tohme, S., Simmons, R. L., & Tsung, A. (2017). Surgery for cancer: A trigger for metastases. *Cancer Research, 77*(7), 1548–1552.

Vasir, J. K., & Labhasetwar, V. (2005). Targeted drug delivery in cancer therapy. *Technology in Cancer Research & Treatment, 4*, 363–374.

Visvader, J. E. (2011). Cells of origin in cancer. *Nature, 469*, 314–322.

Vos, T., et al. (2016). Global, regional, and national incidence, prevalence, and years lived with disability for 310 diseases and injuries, 1990-2015: A systematic analysis for the Global Burden of Disease Study 2015. *Lancet, 388*, 1545–1602.

Waghmare, A. S., Grampurohit, N. D., Gadhave, M. V., Gaikwad, D. D., & Jadhav, S. L. (2012). Solid lipid nanoparticles: A promising drug delivery system. *International Research Journal of Pharmacy, 3*, 100–107.

Wagner, A., Ploder, O., Enislidis, G., Truppe, M., & Ewers, R. (1995). Virtual image guided navigation in tumor surgery-technical innovation. *Journal of Cranio-Maxillofacial Surgery, 23*, 271–273.

Wan, S., Pestka, S., Jubin, R. G., Lyu, Y. L., Tsai, Y. C., & Liu, L. F. (2012). Chemotherapeutics and radiation stimulate MHC class I expression through elevated interferon-beta signaling in breast cancer cells. *PLoS One, 7*, e32542.

Wang, H. Z., Wang, H. Y., Liang, R. Q., & Ruan, K. C. (2004). Detection of tumor marker CA125 in ovarian carcinoma using quantum dots. *Acta Biochimica et Biophysica Sinica, 36*, 681–686.

Wang, C. E., Stayton, P. S., Pun, S. H., & Convertine, A. J. (2015). Polymer nanostructures synthesized by controlled living polymerization for tumor-targeted drug delivery. *Journal of Controlled Release, 219*, 345–354.

Wang, K., Kievit, F. M., & Zhang, M. (2016). Nanoparticles for cancer gene therapy: Recent advances, challenges, and strategies. *Pharmacological Research, 114*, 56–66.

Wang, Z., Qiao, R., Tang, N., Lu, Z., Wang, H., Zhang, Z., Xue, X., Huang, Z., Zhang, S., Zhang, G., & Li, Y. (2017). Active targeting theranostic iron oxide nanoparticles for MRI and magnetic resonance guided focused ultrasound ablation of lung cancer. *Biomaterials, 127*, 25–35.

Wen, C. Y., Xie, H. Y., Zhang, Z. L., Wu, L. L., Hu, J., Tang, M., Wu, M., & Pang, D. W. (2016). Fluorescent/magnetic micro/nano-spheres based on quantum dots and/or magnetic nanoparticles: Preparation, properties and their applications in cancer studies. *Nanoscale, 8*, 12406–12429.

Woller, E. K., & Cloninger, M. J. (2001). Mannose functionalization of a sixth generation dendrimer. *Biomacromolecules, 2*, 1052–1054.

Wu, H. C., Chang, D. K., & Huang, C. T. (2006). Targeted therapy for cancer. *Journal of Cancer Molecules, 2*(2), 57–66.

Yu, X., Trase, I., Ren, M., Duval, K., Guo, X., & Chen, Z. (2016). Design of nanoparticle-based carriers for targeted drug delivery. *Journal of Nanomaterials, 2016*. Article ID 1087250, 15 pages.

Yue, X., & Dai, Z. (2018). Liposomal nanotechnology for cancer theranostics. *Current Medicinal Chemistry, 25*, 1397–1408.

Yuen, G. J., Demissie, E., & Pillai, S. (2016). B lymphocytes and cancer: A love-hate relationship. *Trends Cancer, 2*(12), 747–757.

Zhang, L., Gu, F., Chan, J., Wang, A., Langer, R., & Farokhzad, O. (2008). Nanoparticles in medicine: Therapeutic applications and developments. *Clinical Pharmacology and Therapeutics, 83*, 761–769.

Zheng, G., Patolsky, F., & Lieber, C. M. (2006). Nanowire biosensors: A tool for medicine and life sciene. *Nanomedicine: Nanotechnology, Biology and Medicine, 2*, 277. https://doi.org/10.1016/j.nano.2006.10.050

Chapter 4
Camelid Single-Domain Antibodies for Targeting Cancer Nanotheranostics

Sepideh Khaleghi, Shahryar Khoshtinat Nikkhoi, and Fatemeh Rahbarizadeh

Contents

Sepideh Khaleghi and Shahryar Khoshtinat Nikkhoi contributed equally.

S. Khaleghi
Department of Biotechnology, Faculty of Advanced Science and Technology, Tehran Medical Sciences, Islamic Azad University, Tehran, Iran

S. Khoshtinat Nikkhoi
Department of Pharmaceutics, Rutgers the State University of New Jersey, Piscataway, NJ, USA

F. Rahbarizadeh (✉)
Department of Medical Biotechnology, Faculty of Medical Sciences, Tarbiat Modares University, Tehran, Iran
e-mail: rahbarif@modares.ac.ir

M. Saravanan, H. Barabadi (eds.), *Cancer Nanotheranostics*, Nanotechnology in the Life Sciences, https://doi.org/10.1007/978-3-030-74330-7_4

4.1 Specific Characteristics of VHH

Antibodies are undoubtedly one of the crucial macromolecules in the immune system. Human antibodies are categorized based on the type of heavy chain, alpha (α), delta (δ), gamma (γ), epsilon (ε), and mu (μ) which give rise to IgA, IgD, IgG, IgE, and IgM, respectively. Among different types of antibodies, IgG plays an important role in passive immunotherapy for a wide span of maladies, especially cancer and autoimmunity. Human IgGs comprise four distinct polypeptide chains, two heavy chains and two light chains, H_2L_2 antibodies. The heavy chain is made of four domains, NH3–VH–CH1–CH2–CH3–COOH. The CH3 and CH2 establish antibody Fc, which interact with different immune effector cells, such as natural killer cells in antibody-dependent cell cytotoxicity (ADCC), or collaborate with serum protein such as complements in opsonization of invaders. There is no or little evidence regarding the interaction of IgG light chains with immune cells.

Unlike the heavy chain, the IgG light chain consists of two domains, CL1 and VL, which bind to their heavy chain counterpart and collectively shape the Fab fragment. The SDS-PAGE pattern of antibodies usually shows two bands, one heavy chain (50 kDa) and one light chain (25 kDa). The whole IgG molecule is gigantic, 150 kDa, with dimensions of 14.2 nm × 8.2 nm × 3.8 nm. The size of the IgG is a big issue in terms of antibody therapy and drug delivery. Whole IgG tumor penetration is low as the core of the tumor is extensively dense with minimal leakage. It is estimated that the penetration of monoclonal antibodies into the solid tumor is around 0.001–0.1% of injected dose (Marcucci et al., 2013; Thurber et al., 2008; Christiansen & Rajasekaran, 2004). Among the six aforementioned domains, only VH and VL engage together and generate scFv, which is the smallest fragment derived from H_2L_2 antibody with the ability to bind to the target of interest. Even though there are many products based on the scFv on the market, some disadvantages have been associated with this type of molecule. Firstly, the CDR3 length is comparatively small; hence it would not be able to recognize and bind to protein cavities or clefts. Secondly, due to reducing tumor microenvironments, scFvs disulfide bond may become broken, which significantly hamper the binding. All scFvs have two domains, VH and VL, which are usually locked together through a disulfide bond and a linker, usually $glycin_4serin$. Thirdly, the scFv solubility is usually low. The residues in the interface of VH and VL are mostly composed of hydrophobic amino acids helping to keep two domains of scFv together through hydrophobic interactions. In prokaryotic expression, sometimes these hydrophobic amino acids of VH cannot thoroughly cover VL hydrophobic patches. Consequently, exposed hydrophobic amino acids cause extensive aggregation.

In cancer antibody therapy, antibody exerts its efficacy in three ways, first by blocking the receptor, and second by antibody-dependent cell cytotoxicity or ADCC. Upon binding to the target of interest, the natural killer cell binds to the Fc of the bound antibody through Fcγ receptor III a (CD16a) and kills the tumor. It is observed that cells with even a low density of receptor of interest are as good targets as cells overexpressing that receptor. The side effect of anti-HER2 antibody therapy

attests to this claim. Cardiomyocytes express a very low level of the HER2 receptor. There are some reports of cardiotoxicity of Herceptin (anti-HER2 antibody) in breast cancer patients. This toxicity emanates from NK cell ADCC of cardiomyocyte and damages the heart tissue (Leemasawat et al., 2020; Herrmann, 2020; Padegimas et al., 2020). Last but not least, bound antibody can activate complement system to lyse the target cells.

In the early 1990s, scientists serendipitously came across a Camelidae IgG antibody with a different SDS-PAGE pattern (Hamers-Casterman et al., 1993). This pattern attested to the lack of a light chain. Later, this kind of antibody was named as *H*eavy-*C*hain only *A*nti*b*ody or HCAb with the molecular weight of 95 kDa. Further rummage into HCAbs revealed that lacking a light chain is not the only difference. This antibody also lacks the CH1 domain. Camelidae IgG has three subclasses, IgG1, IgG2, and IgG3. The IgG1 is identical to human IgGs with a heavy chain and light chain. But IgG2 and IgG3 are the ones called HCAb, solely composed of a heavy chain. The variable fragment of HCAb, which binds to the target of interest, is called the *V*ariable of *H*eavy chain *H*CAb or VHH. Unlike scFv, VHH is composed of a single-domain antigen-binding fragment. For the very same reason, this molecule also is called either single-domain antibody (sdAb) or nanobody. VHH has many advantages over scFv. The most conspicuous advantage of VHH compared to the whole IgG is the petite size. The molecular weight of VHH is around 12–15 kDa with dimensions of 4 nm × 2.5 nm × 3 nm. Due to its small size, VHHs are able to penetrate the solid tumor, far more efficient than the whole antibody. VHHs are resistant to reducing tumor microenvironment. Besides, VHHs are very thermostable due to one or two intramolecular disulfide bonds (Muyldermans, 2020).

4.2 Structure of VHH

The secondary structure of VHH is very similar to both VH and VL domians of a conventional antibody. VHH consists of nine antiparallel β strands, A–B–C–C′–C″–D–E–F–G. These β strands are connected through several loops, three of the them participate in binding to the targets, H1, H2, and H3, which connects B–C, C′–C″, and F–G, respectively. From an immunological perspective, VHH structure includes four frameworks (FR 1–4) and three complementarity-determining regions (CDR), CDR 1–3 (Fig. 4.1). Frameworks are the platform of the molecule, which are conserved and work as a backbone of the entire molecule. This part of the molecule does not take part in binding directly but has a direct impact on the correct folding of CDRs. Hence the sequence of the frameworks could be effective on VHH affinity. The frameworks are connected via CDRs, which are hypervariable. This part of the molecule is responsible for binding specifically to the target of interest. Aligning immunological with biochemical secondary structure together, CDR1–3 are actually the loops 1–3 (H1, H2, H3). One of the disadvantages of VHH is inefficient binding to non-proteaceous targets, such as small molecules, and carbohydrates. By

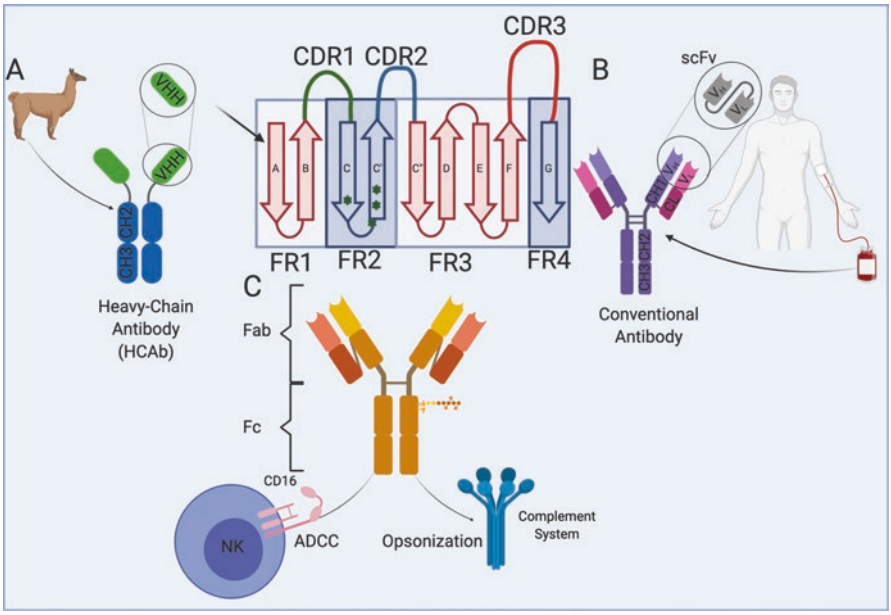

Fig. 4.1 (**a**) Camelidae antibodies are devoid of the light chain. VHH, the variable of the heavy chain of HCAb, is the smallest natural binding moiety. VHH has an elongated CDR3, which is able to penetrate protein cavities and clefts. By comparing the sequence of VHH with human VH, four residues, denoted with green stars, are replaced in VHH by small and hydrophilic amino acids. These residues play an important role in VHH solubility. (**b**) Human antibody is composed of two heavy chains and two light chains. The variable domain is composed of two different domains, VH and VL, also called scFv. (**c**) The Fc region of antibody plays a vital role in cancer therapy. This domain interacts with natural killer cells through CD16 (FcγRIIIa) to exert ADCC. Besides, antibody-coated invaders are opsonized by the complement system which facilitates phagocytosis

structural analysis of anti-methotrexate, anti-triclocarban, and anti-cortisol VHHs, Arabi-Ghahroudi et al. found out that the non-hypervariable loop between D and E β strands, within FR3, works as a CDR4 and plays an important role in binding to non-proteinaceous targets. They observe that this loop is 14 residues longer in anti-hapten VHHs compared to normal VHHs (Henry et al., 2019).

As mentioned earlier, CDR3 connects F–G β strands, is longer than CDRs in convention antibodies. The length of CDR3 in VHH is on average 18 residues, but in humans and mice, VH CDR3 is 14 or 12 residues, respectively. Scientists found out CDR3 plays the most vital role in the affinity and specificity of the VHH. It is assumed that, during evolution, the length of CDR3 becomes longer to compensate for the absence of the light chain (Kubala et al., 2010). There are some reports that even VHH can reach enzyme active sites and either play an agonist or antagonist role. It is important to mention that CDR1 and CDR2 also form flat paratopes to bind to convex and concave epitopes. Hence, VHH can reach out to both protein cavities, clefts (through protruded CDR3) and convex, concave paratope (through CDR1 and CDR2), while VH and VL CDRs are shorter than VHH CDR3 and only

recognize flat, convex, and concave epitopes. In another word, the epitopes that are inaccessible by scFv are accessible via protruded VHH CDR3 (Harmsen & De Haard, 2007).

But elongated CDR3 is not the only difference between VHH and VH. VHHs are very soluble proteins due to their hydrophilic amino acid composition. This feature makes VHH ideal for heterologous protein expression. As mentioned above, scFv solubility is lower than VHH. With a closer look at the VHH and VH structure and amino acid composition, it is observed that the second framework of VH is composed of hydrophobic amino acids. These amino acids form a hydrophobic patch that binds to the VL through hydrophobic interaction and stabilize the molecule. These hydrophobic amino acids are replaced by small and hydrophilic ones in VHH. The most notable substitutions are V37F/Y (in the strand C), G44E, L45R, and W47G (in the stand C′) (the exact number may be different based on the algorithm of antibody residues numbering). VHH is a very stable molecule. This stability is another distinction of VHH. Most of the VHH has an intramolecular disulfide bond to connect CDR1 (in camels) or CDR2 (in llamas) to CDR3 (Manglik et al., 2017). This bond helps to stabilize elongated CDR3. To produce disulfide-bonded VHH in a prokaryote, this molecule must be expressed and ushered to the periplasmic space. The *E. coli* cytoplasm environment is reducing and is not suitable for disulfide bond formation. But the periplasmic space is an oxidizing environment and also benefited from some foldase and chaperone to establish disulfide bonds. In the periplasmic space, *DsbA* and *DsbB* carry out the de novo disulfide bond formation and *DsbC* and *DsbD* proofread the bond. *DsbA* is a potent oxidase that oxidizes the cysteine residues in the periplasmic space. But the only oxidizing space and/or presence of *DsbA* is not enough for correct disulfide bond formation (Hatahet et al., 2010; Nguyen et al., 2011). *DsbC* is a V shape disulfide isomerase which ensures the correct S–S formation and folding. Besides, there are some engineered strains of *E. coli* with reducing cytoplasms, such as *Origami B* (DE3) (Kaplan et al., 2016) and *SHuffle*® (Lobstein et al., 2012). The advantage of *SHuffle*® is that *DsbC* is constitutively expressed in the cytoplasm. This ensures that the disulfide bond is established correctly, which is vital for protein folding and function. Based on our data, the expression of the *SHuffle*® is lower than BL21 Star (DE3) (Nikkhoi et al., 2017). The first reason is that due to the expression of some extra protein including *DsbC*, *SHuffle*® is metabolically more burdened than *BL21 Star* (DE3). The second reason is that the doubling time is *SHuffle*® in longer. It is noteworthy to mention that the inclusion body in *BL21 Star* (DE3) was higher than *SHuffle*®. Consequently, although the yield is lower in *SHuffle*®, the expressed VHH is soluble and in native conformation. In a recent study, scientists found out VHHs expressed in *SHuffle*® are heterogeneous in terms of disulfide bridge formation. This means the efficiency of disulfide bridge formation is not absolute, and still some proteins are expressed without an S–S bond. Conversely, VHH expressed in the periplasmic space revealed a more homogeneous disulfide-bonded protein (Chabrol et al., 2020).

4.3 VHH Cell Penetration

Due to the petite dimension, VHH can also be used to penetrate the cell as either agonist or antagonist of key enzymes, signaling molecules, or even viral enzymes inside cells. VHHs are unable to penetrate the cell without being fused to *C*ell-*P*enetrating *P*eptide (CPP). CPPs, 5–30 amino acids, are the sequence that gives rise to enhanced cellular uptake. One of the biggest disadvantages of CPP is that cargoes are delivered to any type of cell without discrimination (Böhmová et al., 2018). One of the efficient CPP is called penetratin. NS5B is pivotal RNA-dependent RNA polymerase which is crucial for the hepatitis C virus (HCV) replication. NS5B is a promising target in HCV therapy. Blocking this enzyme may end up suppressing virus replication. Hence, scientists developed a penetrable anti-NS5B VHH to block the RNA polymerase. To do so, anti-NS5B VHH was fused to penetratin to be able to enter the contaminated cells. Using this technique, they efficiently block the HCV replication inside the contaminated cells (Thueng-In et al., 2012). Cell-penetrating VHHs are ideal tools for tracing a molecule inside the cell. Chromobody, VHH fused to a fluorescent protein, is fully functional even in the reducing environment of cytoplasm. Li et al. used cell chromobody, anti-GFAP (glial fibrillary acidic protein) VHH fused to CPP and GFP, to track and image astrocytes (Li et al., 2012). In another study, a group of scientists used two cell-permeable chromobodies to show a protein-protein interaction. In this study, two VHHs against p53 and PCNA (proliferating cell nuclear antigen) were fused to arginine-rich CPP. They chose VHH since the molecular weight of the cargo of CPPs is a decisive factor in internalization efficiency. Using this technique, they were able to study the interaction of P53 and PCNA in the nucleus (Li et al., 2012).

4.4 Humanization of VHH

Humanization of antibodies is the best way to eliminate immune response when administering antibodies raised in different species. There are many humanized monoclonal antibodies with FDA approval, such as paliviz*umab*, trastuz*umab*, natalizumab, and bevaciz*umab* (-zumab suffix in antibody nomenclature denotes to humanized antibodies). To humanize the VHHs, the rule of thumb is that CDRs should be left intact. Any change to this part of VHHs may disrupting the affinity. The only parts that should be subjected to humanization are frameworks. It must be noted that the four residues in FR2, V37, G44, L45, and W47 are key for solubility, affinity, and stability; hence changing these residues must be done carefully. Totally there are ten amino acid difference between VHH and human VH, including four key amino acids mentioned above. Humanizing VHH should be neutral to affinity and stability. There is a report regarding changing amino acids in frameworks that may be detrimental to the folding of CDRs, especially CDR3, which is a

consequence of loss of binding (Vincke et al., 2009). To circumvent this problem, humanization is partially done to prevent significant changes in affinity (Dong et al., 2020).

4.5 VHH-Based Therapeutic Systems

4.5.1 VHH-Drug Conjugates

One of the perks of VHHs is the ease of production and satisfactory penetration in solid tumors. These features make this molecule an ideal candidate for antibody-drug conjugate (ADC). In ADC, a drug is conjugated to an antibody binding to a tumor marker. The antibody moiety works as a vehicle to deliver cargo to the tumor microenvironment and target cells. Using this system, the cargo is localized to the tumor site and accumulates the therapeutic agent close to cancer cells. This system not only improves the efficiency of therapy but also curtails the side effects and toxicities.

There are many different compounds used to conjugate to an antibody to develop ADC. One of which is inhibitors, which block a vital biochemical process inside a cell. In 2015, Fang et al. generated ADC using VHH7, anti-MHC-II, and Mertansine (DM1) (Fang et al., 2016). The DM1 is a potent inhibitor of microtubule polymerization but with a narrow therapeutic window when used alone. A therapeutic window is a range of concentrations that the drug is effective with low toxicity. According to their results, DM1 toxicity was 20 times lower in HEK293 and HeLa (MHC-II negative cells) compared to A20 cells (MHC-II positive). Cucurmosin (CUS), extracted from pumpkin pulp, is a strong ribosome inhibitor. Deng et al. fused the anti-EGFR to CUS and showed improved targeted toxicity in HepG2 and A549 cell lines compared to SUC alone (Deng et al., 2017).

Enzymes also can be used in ADC. One of the widely used enzymes is urease, which converts urea to ammonia that is toxic for cancer cells (Tian et al., 2015). In a study, urease was conjugated to anti-vascular endothelial growth factor receptors (VEGFRs) VHH to deliver the enzyme to the tumor site. VEGFR is a hub receptor for angiogenesis in a tumor (Tian et al., 2017). Without angiogenesis, the tumor dies due to a lack of nutrients and oxygen. The results showed significant targeted toxicity in cells expressing VEGFR.

The other option to generate ADC is bacterial toxins. *Pseudomonas* exotoxin A, a bacterial toxin, fused to anti-CD7 VHH to induce apoptosis in CD7+ cells including Jurkat, CEM, T-cell acute lymphoblastic leukemia (T-ALL), and acute myeloid leukemia (AML) (Tang et al., 2016). In another study, PE38, also *Pseudomonas* exotoxin A (PE38), fused to anti-CD38 VHH (Wang et al., 2016). This immunotoxin showed great selective toxicity in several multiple myeloma cell lines. A similar study was also conducted by Li et al. using PE38 to VHH targeting vascular endothelial growth factor receptor 2 (VEGFR2) (Behdani et al., 2013).

4.5.2 VHH in Cancer Immune Cell Therapy

Adaptive immunotherapy is now the brightest road to contain cancer. Immunotherapy is a very broad field of study that is beyond the scope of this chapter. Although T cells are grouped as adaptive immunity and NK cells as innate immunity, both cells have a lot in common, especially in terms of immunotherapy (Mikkilineni & Kochenderfer, 2021). Both cells get activated upon encountering cancer cells (Galluzzi et al., 2020) and secretes perforin and granzyme B to kill tumor cells. Besides, both cells, upon activation, also secrete some cytokine and interleukin to boost the immune system to fight cancer more efficiently (Waldman et al., 2020). Here, we explain the recent advances in T and NK cell-based immunotherapy using VHH as a targeting moiety.

4.5.2.1 CAR T Cell Therapy

Chimeric antigen receptor (CAR) T cell has revolutionized adoptive immunotherapy. A chimeric antigen receptor comprises five distinct parts, 1) antigen-binding fragment, 2) spacer between antigen binding fragment and cell membrane, 3) transmembrane, 4) co-stimulatory, and 5) activator (CD3ζ) domain(s). Upon facing tumor cells, the antigen-binding domain engages the target of interest and an activatory signal relay to the immune cells. Co-stimulatory domains, such as CD28, OX40, 4-1BB, and many more, boost the signal to CD3ζ which subsequently activates T cells more robustly. Activated T cell secretes granzyme B and perforin into the immunological synapse. Perforins generate pores on the target cell which serves as a safe passage for granzyme B to get into the cell. Granzyme B activates Caspase cascades and subsequently leads to apoptosis that kills the cancerous cell. Here we mainly focus on CAR T cells having VHH as an antigen-binding domain. Utilizing CAR T cells has been very efficient in hematological malignancies, especially multiple myeloma. One of the important tumor markers in multiple myeloma is CD38. Anti-CD38-based CAR T cells therapy has been promising due to low side effects (Drent et al., 2016, 2017). VHH-based anti-CD38 CAR T cell was developed in 2018 by Chinese scientists (An et al., 2018). This engineered T cell was very efficient in secreting IL-2, TNF-α, and IFN-γ upon encountering the target cells. Besides, anti-CD38 CAR T cells showed little off-target toxicity.

Utilizing CAR T cells in solid tumors is not as efficient as in hematological malignancies. The reason is that solid tumors are quite dense and hard to penetrate. Most of the activated T cells are trapped on the edge of tumors. There are many undergoing pieces of research to increase the efficiency of solid tumor immunotherapy. In 2018, Munter et al. generated a dual CAR T cell. As an antigen-binding fragment, they used anti-HER2 and anti-CD20 VHH fused through Llama IgG2a hinge. The results showed that the bivalent VHH was able to bind to HER2 and CD20 simultaneously. Besides, the dual CAR T cells were able to kill both HER2+ and CD20+ cell lines (De Munter et al., 2018). The next important tumor biomarker

is VEGFR2, which plays a central role in cancer progression and metastasis. This receptor facilitates angiogenesis which increases the nutrient and oxygen in the tumor site. Using anti-VEGFR2-based CAR T cells, not only VHH was able to bind and block this receptor but also kill the cells expressing this tumor biomarker (Hajari Taheri et al., 2019). Rajabzadeh et al. developed second-generation CAR T cells using anti-MUC1 VHH and CD28 as the co-stimulatory domain. According to their results, after co-culturing CAR T cell with $MUC1^+$ cell lines, MCF-7 and T47D, the secretion of TNF-α and IFN-γ were increased several folds compared to co-culturing with untransduced T cell (Rajabzadeh et al., 2018, 2021). One of the disadvantages of monotherapy is that cancer cells may become resistant through different mechanisms, such as genetic drift. One approach to circumvent this dilemma is to use oligoclonal VHH as the binding domain. Oligoclonal VHH includes more than two nonoverlapping VHH binding to different epitopes, either on the same receptor, which is monovalent, or on the different receptors which are oligospecific. In 2014, Jamnani et al. generated an oligoclonal VHH-based CAR T cell using nonoverlapping anti-HER2 VHH. The results showed that oligoclonal VHH illustrated better toxicity toward HER2+ breast cancer cell line compared to monovalent CAR T cells (Jamnani et al., 2014). There are many studies using VHH-based CAR T cells in solid tumor immunotherapy such as breast cancer (Khaleghi et al., 2012; Iri-Sofla et al., 2011), prostate cancer (Hassani et al., 2019), and many more.

There is a new concept in CAR T cell therapy, so-called Universal CAR, or UniCAR. The difference between UniCAR to usual CAR lies in the extracellular antigen-binding fragment (Bachmann et al., 2018). In UniCAR the antigen-binding domain is against a unique epitope, not a tumor biomarker (Loureiro et al., 2018). Then the antibody, binding to the tumor biomarker, is fused to the epitope that is specific for UniCAR. The fused antibody is used to make a bridge between immune effector cells and target cells (Bachmann, 2019). One of the widely used epitopes in UniCAR is E5B9 which is not immunogenic and is not expressed on the surface of normal cells. The UniCAR is equipped with anti-E5B9 scFv, which binds to E5B9-tagged antibody to elicit an immune response. One of the leading scientists working in this field is Dr. Michael Bachmann. He has published several articles regarding VHH-based UniCAR. He generated a UniCAR expressing anti-E5B9 scFv as an extracellular binding moiety and then fused the anti-EGFR VHH to E5B9 tag. The fused VHH binds to the target of interest, EGFR, and UniCAR binds to E5B9 tag (Jureczek et al., 2020; Albert et al., 2017, 2018). Consequently, the effector immune cell can attack the target cell. The advantage of this system is that there is no need to develop new CAR T cells for different types of cancer. It is noteworthy to stipulate that transfecting and engineering an immune cell is very laborious, expensive, and time-consuming. Using UniCAR, different types of cancer can be treated just by changing the E5B9-tagged VHH or scFv (Bachmann et al., 2018).

CAR T cells are not always used to attack tumor cells. In 2019, a group of scientists at MIT developed a new CAR T cell directed toward the tumor microenvironment (Xie et al., 2019). Through this strategy, not only engineered T cells were ushered to the tumor site but also trapped there and remained for a longer time (Xie et al., 2019, 2020). Besides, they engineered T cells to secrete anti-CD47 and

anti-PD-1 VHH to overcome the immunosuppressive tumor microenvironment. The CD47 is a “don’t eat me” signal expressed by tumor cells to evade immune response (Eladl et al., 2020). The PD-1 is an inhibitory receptor expressed on T cells. When engaged to PD-L1, which is expressed on tumor cells, T cells become deactivated (Barclay et al., 2018; Havel et al., 2019). Hence, using the aforementioned strategy, T cells not only could be enriched in the tumor microenvironment but also escape the immune-suppressive tumor milieu.

4.5.2.2 CAR NK Cell Therapy

Unlike T cells, natural killer (NK) cells are part of the innate immune system, meaning NK cells recognize tumor cells or foreign invaders without undergoing somatic recombination (Shimasaki et al., 2020). One of the eye-catching advantages of NK cells is the lack of graft-versus-host disease (GVHD) response in patients (Guillerey et al., 2016). This means if an NK is administered to multiple patients, no toxic immune response will be raised against the estrange NK cells. This has helped the scientists to come up with an off-the-shelf immunotherapy system, which means the optimized NK cell can be prepared and administered to multiple patients without any host immune response. On the opposite side, GVHD is a big problem with T cell therapy. To address this concern, to prepare CAR T cell dose, PBMCs are collected from each patient, engineered by viral vectors to express CAR, and then reinfused to patients. This process makes the CAR T cells therapy pricey (Myers & Miller, 2021).

A group of scientists from Germany and the UK developed anti-CD38 VHH-based CAR NK. CD38 is NAD-hydrolyzing ectoenzyme, which is overexpressed in hematological malignancies, especially multiple myeloma. In this study, NK 92, an immortalized NK cell, was transduced virally to stably express CAR construct. Then, they used bone marrow samples of eight patients to test the CAR NK cell. The results were promising since anti-CD38 CAR NK was able to eliminate CD38+ cells from bone marrow samples (Hambach et al., 2020). In a similar study, anti-CD7 VHH-based CAR NK-cell was used for acute lymphoblastic leukemia (T-ALL) therapy. Using CAR NK cells to eradicate CD7+ T-ALL resulted in an elevated level of Granzyme B and interferon γ (IFN-γ) following co-culture of NK and T-ALL cells (Fig. 4.2).

4.5.3 Targeted Cancer Therapy by VHH-Armed Nanoparticles

One of the breakthroughs in cancer therapy developed almost two decades ago. The rapid expansion of using nanotechnology in medicine, nanomedicine, has opened a new and promising window in fighting cancer. Nanoparticles can be targeted toward tumor microenvironments by either passive or active targeting. Passive targeting means selective delivery of nanoparticles using a unique feature of the tumor

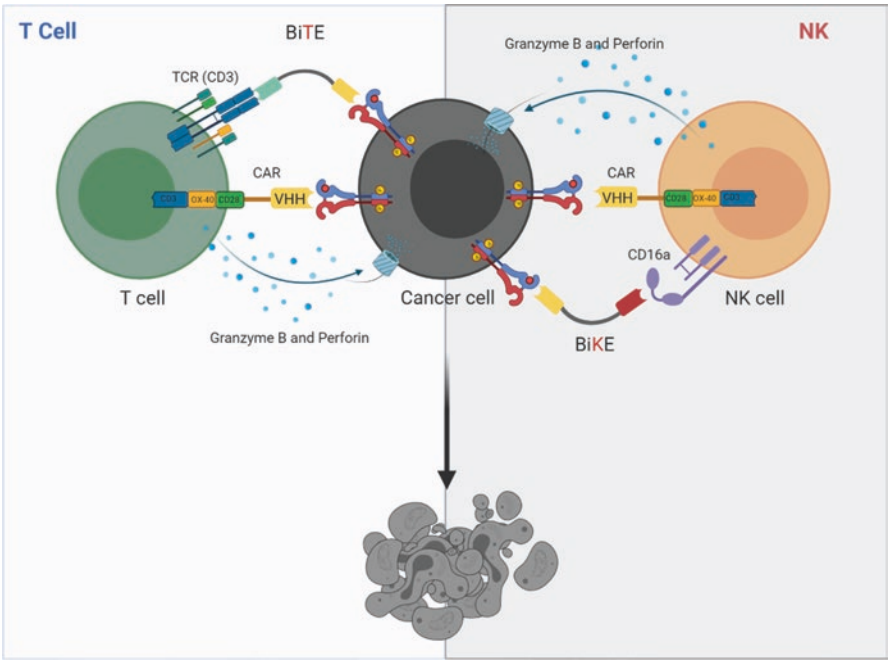

Fig. 4.2 Different strategies of adoptive immunotherapy. Chimeric antigen receptor (CAR) is a novel approach to direct NK and T cell activity toward specific cancer cells. Upon binding to the target of interest, CARs relay the activating signal to either NK or T cells. Consequently, after secretion of granzyme B and perforin, cancer cells start apoptosis. The second strategy to harness immune cell activity is a bivalent antibody. A bivalent antibody is composed of two antibodies, the first one binds to tumor-associated antigen (TAA) and the second one binds to either CD16 or CD3 on NK and T cells, respectively. The bivalent antibody works as a bridge between the target cell and immune effector cell. Upon immunological synapse formation, the effector cell lyses the tumor cells

microenvironment. There are many ways of passively targeting the drugs to the tumor site, one of which is enhanced permeation and retention (EPR). To expand very fast, tumors must be provided with sufficient amounts of nutrients and oxygen to generate enough energy (Lugano et al., 2020). To achieve this, cancer cells start establishing a neovascular vessel inside a solid tumor through a process called angiogenesis, which is fast and imperfect (Folkman, 2006). Newly established vessels have many pores in nanometer diameter, which is not seen in normal vessels (Fig. 4.3). These pores significantly increase the permeation of nanoparticles. It is observed that nanoparticles around 20–500 nm can pass through the pores in the leaky vessels but not in normal vessels (Kalyane et al., 2019). The other characteristic of a solid tumor is longer retention of drugs inside the tumor before being drained through the lymphatic system. The reason is that the solid tumor is tremendously dense in the core which causes the lymphatic vessels to collapse and block the drainage. It is noteworthy to mention longer retention does not apply to small

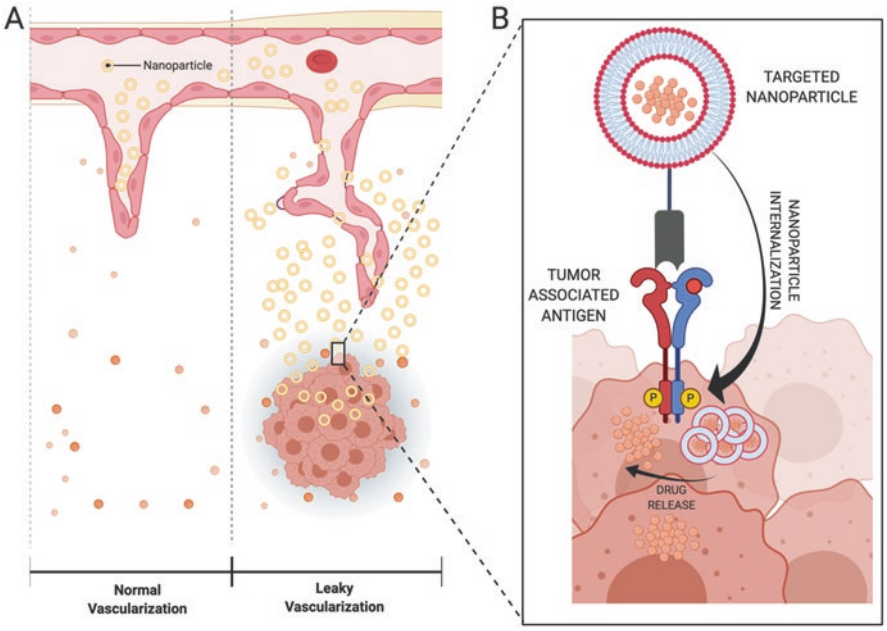

Fig. 4.3 (**a**) Throughout the body, normal vessels are sealed; only nutrients and oxygen may pass through endothelial cells, from blood to tissue. But solid tumors demand more oxygen and nutrients, which leads to angiogenesis. Angiogenesis is the hallmark of all solid tumors. Newly established vessels are leaky; there are many nanodiameter-sized pores in these vessels, which are nanomedicine's central dogma. The nanoparticle can go through these pores and get into a tumor microenvironment. As normal vessels are devoid of such pores, this is called passive targeting. (**b**) Nanoparticles also can be decorated with wide range of targeting moieties, such as VHH, to target and deliver the cargo of interest to specific tumor cells

molecule drugs since they are rapidly cleared from the blood through the renal system but encapsulating them inside a nanoparticle facilitate the delivery to the cancer cells. There are two FDA-approved nanoparticle-based drugs on the market, Doxil© and Caelyx©, which make most of the EPR effect. As the surface of most nanoparticles is hydrophobic, they tend to elicit immune response and aggregation (Osman et al., 2018). Attaching PEG on the surface of the nanoparticle makes the surface much more hydrophilic, which subsequently reduces immune response and aggregation. PEGylation also improves pharmacodynamic and pharmacokinetics features (Liu et al., 2018).

Although nanoparticle delivery to peripheral tumor cells has been successful, delivery to the tumor core has been a big failure. Tumor cell proliferation rates are heterogeneous. The cells close to newly established vessels receive enough nutrients and oxygen, so they grow faster. The cells in the core are hypoxic/necrotic since the blood vessels in this area collapse due to condensed cells and high pressure. The penetration of nanoparticles is even hampered at the tumor core. There are some innovative approaches to boost the tumor perfusion, such as using bradykinin

(kinin) (Qin et al., 2009; Emerich et al., 2001), nitric oxide (Ng et al., 2007; Sonveaux et al., 2005), peroxynitrite (Cooke & Davidge, 2002), prostaglandins (Emerich et al., 2001), vascular permeability factor (VPF)/vascular endothelial growth factor (VEGF) (Brown et al., 1993) and other cytokines. The shortcoming of all these approaches is a temporary increase in tumor perfusion. There are other approaches like radiation (Wang et al., 2009), ultrasound (Gee et al., 2001; Hoyt et al., 2015), hyperthermia (Song et al., 1984; Koning et al., 2010), and many more, but none of them are impeccable. The other problem associated with PEGylated nanoparticle delivery is that PEG can activate the complement system, which can further lower the efficiency of the delivery of therapeutic reagent to the tumor site (Pannuzzo et al., 2020).

The efficiency of passive targeting is around 20%. Encapsulation of toxic chemotherapeutic agents both reduces the toxicity and therapeutic effect. There is another layer of targeting called active targeting which refines the targeting efficiency. Active targeting is defined as decorating the surface of the nanoparticle with antibody/antibody fragment (Hervé-Aubert et al., 2020), VHH (D'Hollander et al., 2017; Wu et al., 2019), peptide (Sun et al., 2016), affibody (Akhtari et al., 2016; Jia et al., 2020), aptamer (Xu et al., 2016), and ligand (Xu et al., 2020) binding to cancer biomarkers. A biomarker is any feature to distinguish cancer cells from normal cells encompassing DNA, RNA, and protein (Lassere, 2008). For instance, some cancer cells express and/or overexpress a cell surface receptor. This receptor either is absent on normal cells or is expressed at a negligible level. Active targeting means aiming a nanoparticle to specific cells with specific characteristics (Slamon et al., 2001; Behr et al., 2001). Active targeting adds up some perks to passive targeting. Firstly, active targeting improves the accumulation of drugs in the tumor microenvironment. This could lead to further reduce the toxicity of the drug to undesired organs (Vong & Nagasaki, 2020). Secondly, targeted drug delivery would increase drug uptake which concludes in improved therapeutic characteristics (Huda et al., 2020). Finally, as the receptor engaged with surface-modified nanoparticles becomes internalized, it helps to reduce the density of cell surface oncogene receptors, such as HER2 (Li et al., 2016) (Fig. 4.3).

4.5.3.1 Immunoliposome

The most objective of nanomedicine is characteristic mimetics in nanoparticles for decreasing cytotoxicity and a few side impacts in vitro and in vivo. Nanoparticles can overcome a few impediments in medicate organization such as quick clearance within the kidney and clearance through reticuloendothelial framework (RES) as well as factors such as drug plasma fluctuation, high toxicity of certain medicinal products, poor solubility of hydrophobic medicinal products, drug resistance, and the inactivation of certain medicinal products by acidic endolysosomal and tumor microenvironment, even ineffective drug penetration to the target tissue (Beltrán-Gracia et al., 2019). In order to increase the therapeutic effect, the arrival of nanotechnology has led to the discovery of many nano-based drug carriers, such as

nanospheres, nanocapsules, polymeric nanoparticles, liposomes, and fullerenes (Eloy et al., 2017). Liposomes nanoparticles are the best example of cell membrane biomimetics, whereas lipids are main mammalian cell membrane compounds. In the 1960s, liposomes were first prepared, but it was known as a nanoparticle until the year 2000. Therefore, a fundamental target for the preparation of liposome nanoparticles is the types of phospholipids and cell membrane composition. As the activity and properties of liposomes depend on the physicochemical interactions between the different lipid species within the lipid composition. The presence of charges on the lipids, for example, is known to decrease the probability of aggregation and increase the overall efficiency of encapsulation (Eroğlu & İbrahim, 2020). Liposomes are used to encapsulate cosmetics, medications, and fluorescent detection reagents and to transport nucleic acids, peptides, and proteins in vivo to cellular sites as delivery devices. It is possible to bind targeting components such as antibodies to liposomal surfaces and use them to generate large antigen-specific complexes. So, over the past few years, liposomes have become a valuable method in drug delivery for the treatment of many diseases. Moreover, the biocompatibility and use of these nanoparticles can be improved by trapping other particle forms in the center of liposomes or between two layers of liposomes, such as iron oxide magnetic nanoparticles (Prasad et al., 2020), quantum dots (Sercombe et al., 2015), and polyethyleneimine (Patel, 2020). The development of bimodal nanoparticles with efficient imaging techniques and advanced responsive contrast agents for cell labeling and their clinical application have contributed to the advancement of these research activities (Prasad et al., 2020). In addition, liposomes are able to trap water-soluble drugs that otherwise do not easily move through the bilayer membrane and can also load lipophilic drugs into the lipid layers to make them dispersible in an aqueous medium. To date, liposomes have remained the most scientifically proven nanocarriers, owing to their improved bioavailability, biocompatibility, biodegradability, and low toxicity (due to their phospholipid content and high capacity for encapsulation) (Sercombe et al., 2015). Efforts have been made over the last four decades since the beginning of 1970 to maximize the stability of liposomes as well as to increase the capacity of encapsulation. In the year 1995, a revolution took place in which AmBisome® and Doxil® were approved for clinical trials (Patel, 2020). Over the past 30 years, active targeting by the use of bioconjugation techniques to bind peptides, antibodies, or aptamers to the liposome surface has been widely studied in order to enhance personalized medicine, despite passive targeting based on physical and chemical characteristics of liposomes. In this respect, the polar head group of lipids found in liposomes is very important because it enables the reactive group to be derivatized or chemically modified. Lipid activation may be achieved either prior to integration into the structure of the bilayer or after the intact liposome is formed. To activate the lipids in the liposome, sulfhydryl and amine-reactive crosslinking agents such as SPDP, MBS, SMPB, and SMCC might be used. The amine group on the phosphatidylethanolamine (PE) glycerol phosphate head is most widely found in liposome conjugates, while lipids such as PE and stearyl amine-containing amine groups can also be used in crosslinker nucleophilic reactions or modification reagents such as glutaraldehyde. In the same way, phosphatidylglycerol (PG) and

carboxyl-containing phosphatidylserine (PS)-related aldehyde groups can be used to react with amine-containing ligands by reductive amination and carbodiimide reaction, respectively. The periodate-oxidation of carbohydrate or glycerol groups on lipid components accompanied by subsequent bonding with the amine-containing ligand requires reduction of amination-mediated conjugation (Khaleghi et al., 2017). The conjugation of thiolated VHHs (by 2-iminothiolane) to maleimide-PEG2000-DSPE of liposomes was performed covalently, according to Khaleghi et al. Targeted imaging of anti-HER2 VHH-conjugated magnetoliposomes for breast cancer was the objective of this research. Polyethylene glycol (PEG) may also be used to couple two molecules together as a spacer. In general, PEG spacers are heterobifunctional in nature in the sense that there are two groups at both ends that connect with the liposome and the attaching moiety. Alternatively, the liposomes may also be adjusted to hold SH groups that are guided by disulfide and thioether reactions to react with maleimide, vinyl sulfone, or orthopyridyl disulfide bearing PEG. In order to form such conjugate systems, such as ligand-Mal-PEG-DSPE conjugates, ligand-Hz-PEG-DSPE conjugates, ligand-amino-PEG-DSPE conjugatesm and ligand-carboxyl-PEG-DSPE conjugates, the other end of the PEG containing reactive groups could be used to bind the ligand to the shaped PEG lipid during liposome preparation or post-insertion (Khaleghi et al., 2017). In 2018, four types of non-overlapping monoclonal VHHs were developed by Nikkhoiee et al. to target the HER2 receptor ectodomain via methotrexate-loaded PEGylated liposomes. In this study, the functional assay of thiolated VHHs against HER2 antigen and flow cytometry against HER2 positive breast cancer cell lines were confirmed by ELISA (SK-BR-3, BT-474). The attachment was made according to the conjugates of ligand-Mal-PEG-DSPE (Fig. 4.4) (Nikkhoi et al., 2018). In 2018, doxorubicin-loaded PEGylated liposome nanoparticles targeted by anti-HER2 VHHs fragments suppressed HER2-positive breast cancer cell lines by Farasat et al. (2019). The VHHs can be a great tool for the targeted delivery of theranostic nanoparticles because of their small size and advanced physical characterization. Compared with trastuzumab targeted nanoparticles, the functional assay of VHH targeted nanoparticles showed more efficient penetration of internal cellular components and low side effects on the physical properties of nanoparticles, such as relaxivity, size, and stability (Khaleghi et al., 2016).

4.5.3.2 PAMMAM

Many different types of dendrimers are available, such as peptide dendrimers (PPI), poly(l-lysine) dendrimers, dendrimers of polyamidamine (PAMAM), PAMAM organosilicon dendrimers (PAMAMOS), etc. (Luong et al., 2016). Among these dendrimers, however, PAMAM has been widely studied as a carrier for the delivery of genes and therapeutic molecules. PAMAM dendrimers are a class of synthetic macromolecules with strongly branched and monodisperse, with well-defined structures and compositions. Their center is normally ethylenediamine, which is repeatedly added to methyl acrylate and ethylenediamine (EDTA) according to the

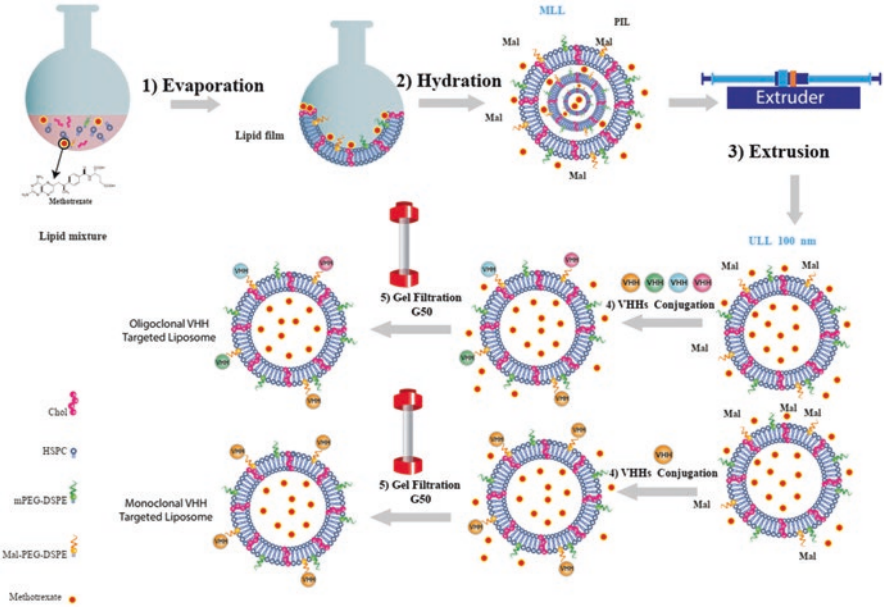

Fig. 4.4 The procedure of methotrexate containing VHH-targeted immunoliposome. (1) Evaporation: The lipids must first be dissolved and blended into an organic solvent to ensure a homogeneous mixture of lipids when preparing liposomes with a mixed lipid composition. Usually, chloroform/methanol mixtures are used to perform this method. The aim is to obtain a clear lipid solution for full lipid mixing. Usually 20 mg lipid/ml organic solvent is prepared with lipid solutions, but higher concentrations can be used if lipid solubility and mixing are appropriate. (2) Hydration: By simply applying an aqueous medium (containing methotrexate) to the container of dry lipid and agitating, hydration of the dry lipid film/cake is achieved. Until adding to the dry lipid, the temperature of the hydrating medium should be above the temperature of the gel-liquid crystal transition (Tc or Tm) of the lipid with the highest Tc. The lipid suspension should be maintained above Tc throughout the hydration cycle after the addition of the hydrating medium. (3) Extrusion: Lipid extrusion is a technique in which a lipid suspension is forced to yield particles with a diameter close to the pore size of *t* thumbnail through a polycarbonate filter with a fixed pore size. (4) VHHs conjugation: The conjugation of thiolated VHHs (by 2-iminothiolane) to maleimide-PEG2000-DSPE of liposomes was performed covalently. (5) Gel filtration G50: The separation of conjugated immunoliposomes containing methotrexate was done by size exclusion chromatography

desired number of generations, G0, G1, G2, G3, G4, etc. Various feature groups, including NH2, OH, CHO, COOMe, Boc, COONa, or CH3 groups, could be terminated by superficial divisions of PAMAM. Usually, the NH2 community is employed to bring genetic material into cells. Because of certain flexible PAMAM properties, such as non-immunogenicity, water-solubility, spherical shape, and controlled release of drugs, they are ideal carriers of genes and drugs for bimodal co-delivery systems. The efficacy of drug loading could be influenced by numerous factors, including functional surface groups, size, chemical structure, generation numbers,

degree of PAMAM PEGylation, loaded drug molecular weight, pH, solvent form, and temperature (Fana et al., 2020). Without sacrificing the spherical geometry of PAMAM dendrimers in solution, the surface groups of PAMAM dendrimers provide a flexible attachment point for the conjugation of multiple therapeutic agents from anticancer drugs to image reporters. The most effective ligand for attacking cancer cells is potentially monoclonal antibodies by binding to a particular cognate antigen overexpressed on cancer cells (Abedi-Gaballu et al., 2018). Antibody conjugation to the dendrimer surface has also been used for tumor targeting, although the key drawback is the high molecular weight of antibodies (150 kDa). Folic acid (FA) is another well-studied cancer targeting ligand, and transferrin, low-density lipoprotein, integrins, and other adhesion molecules are favored in some studies. The functionality of PAMAM nanoparticles can as described above be affected by attached particle surface groups. The findings of selective PAMAM nanoparticles with small targeting modalities such as folic acid, ferritin, Aptamers, RGD, etc. are more advanced in many forms of research compared to traditional antibodies with enormous size and susceptibility to covalent conjugation (Li et al., 2018). For the active targeting of PAMAM nanoparticles, single-chain antibodies with small sizes and greater stability in various physical and chemical environments may be the correct option. There is a low risk of self-immunogenicity in repeated in vivo therapies due to the low immunogenicity of VHHs. In various delivery systems consisting of chemotherapeutic drugs (methotrexate, 5-FU, docetaxel, cisplatin, doxorubicin, paclitaxel), genes (DNA or RNA), and two forms of theranostic agents, PAMAM nanoparticles due to porous structures are acceptable. In order to prevent nuclease action, PAMAM dendrimers are able to create stable PAMAM-nucleic acid complexes. Via interactions with the major and minor grooves and the backbone of phosphate groups, the PAMAM dendrimers can strongly interact with DNA. In addition, the stability tests of the PAMAM/DNA complexes clearly showed that the PAMAM-G4 dendrimer was more stable than the others. Therapeutic nucleic acids are intended to activate or inhibit the expression of particular genes responsible for the biosynthesis and alteration of various proteins that can play a crucial role in the battle against a wide range of diseases such as cancer (Xiao et al., 2020). Jafari Iri Sofla et al. stabilize the targeted G5-PAMAM-dependent gene delivery mechanism against HER2-positive cancer cells by covalently binding anti-HER2 VHHs to the distal ends of polyethylene glycols in the framework of PAMAM-polyethylene glycol. In relation to condensed gene construction, this targeted PAMAM can effectively cause apoptosis, encoding a transcriptionally targeted truncated-Bid killer gene under the influence of the promoter of breast cancer-specific MUC1 (transmembrane glycoprotein mucin 1). Efficient targeted gene delivery by luciferase assay was seen in the cellular uptake assay and the apoptotic cells were measured by Annexin/PI flow cytometry (Jafari Iri Sofla et al., 2019).

4.5.3.3 PEI

There are many benefits to non-viral gene delivery agents over viral vectors, including their ability to directly target, inability to incorporate into the host genome, low immunogenicity, unrestricted transfection of DNA and ease of production/synthesis (Saqafi & Rahbarizadeh, 2019). Among non-viral vectors, due to its high DNA condensing and transfection ability, positively charged polyethyleneimine (PEI), a synthetic polymer, is most extensively evaluated. Successful electrostatic interactions with the anionic charges of DNA molecules can be encouraged by the strong cationic surface charge of PEI. The PEI polymer is ideal for the coupling of targeting ligands, including small peptides or antibodies, due to its large number of primary functional surface amine groups. Due to their negatively charged cell surface, positively charged nano-carriers such as PEI typically show higher cell surface binding and internalization skills. So, in the use of PEI nanoparticles, non-specific attachment is prevalent. This downside can be overcome by PEGylation and targeting of nanoparticles. While PEGylation increases the biocompatibility of PEI polycation, the transfection capacity of this nanoparticle is reduced. Targeting ligands should be used in the PEI-PEG copolymer to increase their specificity and gene transfection capacity in order to address this barrier. However, basic binding and cellular internalization may be influenced by the percentage of conjugation and the size of targeting agent molecules (Wagner et al., 2002). In 2018, Saqafi et al. prepared PEI nanoparticles targeting anti-HER2 VHH as compacting agents for the construction of the transcriptionally targeted tBid killer gene. In addition, as its tumor specificity and elevated protein expression capabilities in breast cancer have been confirmed, the MUC1 gene promoter has been used for transcriptional targeting. The conjugation of huge targeting agents such as traditional antibodies will promote immunological obstruction and induce self-immunogenicity, as with other delivery nanoparticles, the 25 kDa branched polyethyleneimine polymer conjugated with 15 kDa anti-HER2 VHHs has a low probability of immunological reactions compared to 150 kDa whole antibody (Saqafi & Rahbarizadeh, 2018).

4.6 VHH: The "Magic Bullet" for Molecular Imaging and Diagnosis

Therapeutic radiolabeled molecules such as mAbs, mAb fragments, peptides, or synthetic proteins that interact with tumor-associated membrane proteins are deployed through targeted radionuclide therapy (TRNT) and target both the primary tumor site and metastases. Molecular imaging integration can help to predict a good TRNT. To predict targeting and possible toxicity to healthy tissues, this theranostic approach aims to use an equivalent imaging compound. One mAb-based TRNT agent, anti-CD20mAb90Y-ibritumomab, is currently being commercially used to treat B cell non-Hodgkin lymphoma (Wagner et al., 2002). Peptide radionuclide

receptor therapy (PRRNT) has been shown to be effective in neuroendocrine tumor patients and is currently being studied in prostate and pancreatic carcinomas (Iezzi et al., 2018). Camelid single-domain antibody (VHH) fragments, also known as VHHs or nanobodies, can resolve some of the problems associated with the use of other targeting vehicles, such as mAbs, for theranosis. VHHs have become useful theranosis drugs due to their smaller scale, high stability, and extremely precise targeting. In preclinical studies, VHHs targeting a variety of membrane-bound cancer biomarkers such as CEA (D'Huyvetter et al., 2017), EGFR (Iqbal et al., 2010), HER2 (Mir et al., 2020), and PSMA (Oliveira et al., 2013) were successfully assessed as in vivo theranostic tracers using a variety of radionuclides. In the treatment of HER2-overexpressing cancer, D'Huyvetter et al. developed a131I-labeled VHH as a theranostic medication. The results show the potential of SGMIB-2Rs15d for theranosis. A low radioactive SGMIB-2Rs15d initial scan enables patient selection and dosimetry calculations for subsequent therapeutic SGMIB-2Rs15d and may thus influence the outcome of therapy for $HER2^{+}$ breast cancer (D'Huyvetter et al., 2017).

Li et al. prepared glial fibrillary acid protein (GFAP) and fluorescent protein (GFP) monomeric fusion VHHs to demonstrate that recombinant VHH-GFP complexes have substantial potential for a one-step fluorescent detection assay that can be used in brain imaging. These "fluobodies" explicitly labeled GFAP on murine brain parts and were able to cross the BBB and mark astrocytes in vivo with a simple version (pI = 9.3) of the fusion protein VHH-GFP (Li et al., 2012).

Iqbal et al. compared the ability of VHHs to bind single-domain antibody (EG2) (15 kDa), bivalent EG2-hFC (80 kDa) and pentavalent V2C-EG2 (128 kDa) using surface plasmon resonance and cell binding tests in vitro and in vivo using pharmacokinetics, biodistribution, optical imaging, and fluorescent microscopy studies for their binding affinities. The results showed that among the three constructs studied, the EG2-hFc VHH construct had the highest apparent affinity for EGFR/EGFRvIII receptors, the longest half-life of circulation, and the best glioblastoma-targeting properties, indicating that it can grow into a molecular imaging and/or therapeutic agent for EGFR-overexpressed tumors, including glioblastoma (Iqbal et al., 2010). For the diagnosis and stage of cancer, six imaging modalities can currently be used, namely, x-ray (computed tomography, CT), magnetic resonance imaging (MRI), single-photon emission tomography (SPECT), positron emission tomography (PET), ultrasound (US), and, more recently, optical imaging clinical evaluation (Mir et al., 2020).

4.6.1 Optical Imaging

Molecular imaging of cell surface markers has become an increasingly effective cancer imaging technique, which can be used for diagnosis, therapy response assessment, and surgical resection guidance. Recent developments in the production of targeted probes have prompted further advancements in Cat, SPECT, and,

more recently, optical imaging as well. Recently, optical molecular imaging has gained a lot of interest because the probes used are non-radioactive, and in addition, recent camera systems allow high-resolution imaging, no ionizing radiation, so no need for workers protection; no radioactive decay of the probe, thus, longer stability. Limited sensitivity is one of the problems posed by optical molecular imaging, owing to limited light penetration into the tissue, which prohibits whole-body imaging applications. However, optical imaging is suitable for noninvasive identification of superficial tumors (e.g., breast or head and neck cancers) or endoscope-accessible tumors (e.g., lung cancer, tumors located in the gastrointestinal tract or abdominal cavity) (Oliveira et al., 2013).

4.6.1.1 Fluorescent Fusion VHH

Originally isolated from jellyfish, green fluorescent protein (GFP) is commonly used to observe the cellular location of proteins in cultured cell lines as a protein tag. In a large range of sources, including different A equorea species and reef corals, GFP variants have recently been discovered. The vivid, monomeric green fluorescent protein m Wasabi is a monomeric mTFP1 engineered variant originally derived from Clavularia sp. tetrameric cyan fluorescent protein cFP484. Coral. Coral. Li et al. used recombinant VHH directed against a particular marker of astrocytes, the human glial fibrillary acid protein (GFAP). Only simple VHHs (e.g., pI = 9.4) were able in vitro to cross the BBB (7.8 vs. 0% with pI = 7.7 for VHH). The findings showed that these simple VHHs are capable of crossing the BBB in vivo, diffusing into the brain tissue, penetrating astrocytes and explicitly labeling GFAP by intracarotid and intravenous injections into live mice (Li et al., 2012). For precise protein localization and molecular optical imagery, Shufeng Li et al. developed mWasabi fluorescent protein-binding VHHs. The bright, monomeric green fluorescent protein m Wasabi is a monomeric mTFP1 engineered version originally derived from the *Clavularia* sp. tetrameric cyan fluorescent protein cFP484. With coral. mWasabi is roughly 2 times brighter than EGFP. mWasabi is a true monomer and is most likely not to interfere with the function or localization of its fusion partner, unlike many fluorescent proteins widely used. With standard GFP filter sets, mWasabi can be easily detected and can be used as a direct substitute for EGFP or other GFPs. Nanobodies provide excellent alternatives to traditional antibodies, with reduced size, increased solubility, and higher development of less costly bacteria in their valued characteristics (Farasat et al., 2017). In addition, nanobodies are exceptionally high in thermostability and acid tolerance (maintaining intense heat and pH treatment functions) and can also be conveniently customized for their single domain format into a variety of constructs. It has few interactions with host proteins for which Wasabi are freely diffusible in the cytoplasm. For enhanced protein tagging and identification, mWasabi has proven to be very useful. mWasabi fusions are also more soluble than traditional GFP fusions, and blue and red fluorescent labels can be co-imaged. Nanobodies are also used to improve GFP fluorescence or to dim the signal from the fluorescence. The choice of camelid-derived

single-domain antibodies (nanobodies) that modulate the conformation and spectral properties of the green fluorescent protein was reported by Kirchhofer et al. (GFP). More recently, as an approach to purifying the GFP from total protein extracts, anti-GFP nanobodies directly coupled to Sepharose produce a trap column-based purification system. A method that uses a YFP fusion-tag to produce recombinant proteins using suspension-cultured HEK293F cells was developed by Schellenberg et al. YFP is a dual-function tag that allows high-expressing clones to be directly visualized and fluorescence-based selected for rapid purification using a high-stringency high-affinity anti-GFP/YFP VHH support (Kirchhofer et al., 2010).

4.6.1.2 Near-Infrared/Fluorescent Fusion VHH

The foundation of optical imaging lies in the detection of fluorophore-emitted light, making it a cost-effective, non-radioactive cancer detection imaging modality, both in screening and intra-operative environments. The production of near-infrared (NIR) fluorophores is the subject of recent developments in optical imaging probes. Fluorophores that emit light in the spectrum's NIR range (e.g., 700 and 800 nm) allow deeper tissue penetration than fluorophores that emit in the normal range of 400–600-nm (Bannas et al., 2014). These benefits are the result of lower absorption of light by the blood and other components of the tissue, as well as minimal autofluorescence of the tissue in this spectrum range. Optical molecular imaging requires high tumor specificity in addition to an effective NIR fluorophore and an imaging device capable of detecting the light emitted by this fluorophore, which can be achieved by using fluorescent probes targeting tumor-specific markers that are preferably (over) expressed strictly in cancerous tissues and not in normal tissues. Several biomarkers have been identified and cancer progression has been correlated with their (over) expression. In order to allow tumor targeting, various targeting moieties have been used, such as affibodies, peptides, traditional monoclonal antibodies (mAbs), or antibody fragments (De Meyer et al., 2014). VHHs penetrate successfully across the mass of the tumor and are maintained by the tumor. Due to the rapid accumulation of these nanobodies into the tumor and their rapid removal (1–2 h half-life), 2–4 h post-injection visualization is already possible (p.i.). In comparison, to accumulate in the tumor, mAbs can take more than 24–48 h and provide comparable contrast. For effective and accurate tumor detection through imaging, adequate signal (described as contrast or tumor-to-background ratio, i.e., T/B ratio) and a clear tumor delineation are necessary (Mir et al., 2020). Taking into account the heterogeneity of cancers (e.g., breast cancers), supplying an adequate signal for optical imaging of early-stage cancers can be a challenge for a specific probe. We proposed that two tumor-specific probes could be combined to increase the T/B ratio and thus promote the identification of tumors. In addition, by using dual-spectral imaging, knowledge on the degree of expression of various tumor markers within the same tumor can be obtained, which could speed up tumor characterization (De Meyer et al., 2014). Kijanka et al. investigated whether an optical imaging combination of two optical probes that explicitly identify two independent markers

of breast cancer may enhance tumor detection. For this, VHH B9 targeting CAIX, which localizes to peri-necrotic regions of tumors, and VHH 11A4 targeting HER2, which is known to have a more homogeneous distribution across the tumor tissue, were used as a bimodal targeting agent. The findings showed that VHHs at earlier time points p.i. have better T/B ratios than traditional antibodies. VHHs grow faster in the tumor as a result of their small size, and the non-bound fraction is cleared faster. In reality, the first report on the phase I clinical trial of VHH targeting HER2 for the evaluation of HER2 expression in breast cancer by PET was published quite recently. In a phase II trial, the promising results obtained warrant further evaluation and highlight the potential of the VHHs as probes, even for whole-body imaging when combined with various modalities of imaging. The conjugation was performed using maleimide-modified fluorophores which bind directly to the C-terminal cysteine at the VHH to avoid any detrimental effects of fluorophore conjugation on the binding ability of the VHH. The findings showed that two tumor-specific VHHs bearing the same NIR fluorophore results were injected at a higher T/B ratio than a single tumor-specific VHH injection combined with an unrelated VHHH injection (Kijanka et al., 2016).

4.6.2 PET/CT/SPECT

The noninvasive quantitation and visualization of tumors in vivo is made possible by molecular imaging techniques, commonly used in the clinic, and VHHs have become promising, small-sized high-affinity tracers. In both single-photon emission computed tomography (SPECT) and positron emission tomography, nuclear imaging probes associated with VHHs have been evaluated (PET). Nanobodies have a higher penetration rate in tissues compared with monoclonal antibodies and can be cleared easily via the kidney. Nanobodies are now used extensively in molecular imaging (De Meyer et al., 2014; Bala et al., 2019). Radiolabeled VHHs penetrate tumors and tissues effectively and bind biomarkers very easily and very precisely expressed on cells, whereas unbound VHH is rapidly cleared from non-target organs and tissues. Broos K and his team have carried out noninvasive SPECT/CT imaging murine tumor models with positive PD-L1 expression using 99mTc-labeled PD-L1-specific VHHs; when coupled to a diagnostic radionuclide, this allows generating high contrast images as quickly as 1 h after tracer administration, for example (Bridoux et al., 2020). The 68Ga-labeled anti-HER2 VHH 2Rs15d probe, developed to screen candidates who qualify for treatment with antiHER2 therapeutics, is the most advanced VHH under clinical evaluation. Via conjugation of a residualized prosthetic agent that was synthesized by copper-catalyzed azide-alkyne cycloaddition, Zhou et al. evaluated a HER2-VHH 2Rs15d labeled with 18F. There is great interest in developing improved methods for labeling fast-clearing biomolecules with 18F that can be performed efficiently under physiological conditions because of the short half-life, widespread availability, and favorable radiation dosimetry properties of 18F (Zhao et al., 2016). A fusion VHHs called Nb6 (relative molecular

mass is 77837.357 Da) was prepared by Jiang et al., which are two anti-hPD-L1VHHs connected to Fcc6 (Huang et al., 2019). In addition, the I-124 radio-label PD-L1 Nb6 was stated by Huang HF et al. to be useful for non-invasive PET imaging in osteosarcoma tumor mode (Huang et al., 2019). Molecular imaging of immune checkpoints was the subject of Lecocq et al. Nanobodies, the smallest functional fragments of camelid heavy-chain-only antibodies, were produced in this research to noninvasively evaluate the expression of mouse LAG-3 using single-positron emission computed tomography (SPECT)/CT imaging. Injection of 99mTechnetium-labeled nanobodies in healthy mice demonstrated specific absorption in peripheral immune organs, such as the spleen and lymph nodes, not found in knock-out mice of the LAG-3 gene. In addition, using SPECT/CT, VHH uptake could be visualized and compared to the existence of LAG-3 as evaluated in flow cytometry and immunohistochemistry. The diagnostic ability of nanobodies was further confirmed by SPECT/CT scans of tumor-bearing mice (Lecocq et al., 2019). Verhelle et al. showed that 99mTc can be labeled with VHHs raised against the 8-kDa amyloidogenic gelsolin peptide and used in vivo as amyloidogenic gelsolin imaging agents. In addition, there has been some evidence that this can be accomplished with a low background signal and high specificity. This and other VHH-based imaging agents can be helpful in drug screening research and clinical application, especially in situations where their limits are revealed by current imaging platforms (Verhelle et al., 2016).

4.7 Conclusion

In short, this chapter describes the role of VHHs in various fields of biotechnology, such as diagnostics and therapy. Single-domain antibodies are soluble, stable with unique attachment flexibility and deep penetration capabilities in solid tumors. An effective tiny protein in molecular imaging with non-invasive in vivo imaging due to rapid kidney clearance. In addition, VHHs can fold independently so that many forms of conjugation with dyes, peptides, radioisotopes as tracing elements or attachment as targeting agents to the surface of nanoparticles have no effect on the 3D structure of VHHs so that many tags can be fused in their tertiary structure, such as His-tag or even fluorescent labels such as green fluorescent protein (GFP). Compared to traditional antibodies, the use of VHHs for therapeutic applications, blocking the interaction between the target and the corresponding receptor, or disrupting the signal transduction cascade caused after their detection shows many advantages, the most powerful distinction being the small size and simple 3D structure of VHHs. In addition, VHHs in the bacterial host can be produced on a large scale with good yields. VHHs are smaller (15 kDa) than standard fragments of IgGs (150 kDa) or their corresponding fragments of Fab (55 kDa) or scFv (28 kDa) that can be chemically or recombinantly prepared. In most commercial diagnostic studies, VHHs can be a good alternative to traditional antibodies for their tolerance and stability over long periods of time until immobilized in solid support. Fortunately,

nanomedicine will enhance the clinical and diagnostic skills and capabilities of VHHs. The integration of VHHs into various nanotechnology systems, such as nanocarriers or biosensors, would strengthen some of the disadvantages observed in the currently elevated VHHs, such as the decrease in renal clearance or the effective refolding and functionalization of the transducer, in order to improve sensing affinity. In addition, to further maximize their solubility, VHHs may be encapsulated, adding drugs or radio labels for therapy.

References

Abedi-Gaballu, F., Dehghan, G., Ghaffari, M., Yekta, R., Abbaspour-Ravasjani, S., Baradaran, B., et al. (2018). PAMAM dendrimers as efficient drug and gene delivery nanosystems for cancer therapy. *Applied Materials Today, 12*, 177–190.

Akhtari, J., Rezayat, S. M., Teymouri, M., Alavizadeh, S. H., Gheybi, F., Badiee, A., et al. (2016). Targeting, bio distributive and tumor growth inhibiting characterization of anti-HER2 affibody coupling to liposomal doxorubicin using BALB/c mice bearing TUBO tumors. *International Journal of Pharmaceutics, 505*(1–2), 89–95.

Albert, S., Arndt, C., Feldmann, A., Bergmann, R., Bachmann, D., Koristka, S., et al. (2017). A novel nanobody-based target module for retargeting of T lymphocytes to EGFR-expressing cancer cells via the modular UniCAR platform. *Oncoimmunology, 6*(4), e1287246.

Albert, S., Arndt, C., Koristka, S., Berndt, N., Bergmann, R., Feldmann, A., et al. (2018). From mono-to bivalent: Improving theranostic properties of target modules for redirection of UniCAR T cells against EGFR-expressing tumor cells in vitro and in vivo. *Oncotarget, 9*(39), 25597.

An, N., Hou, Y. N., Zhang, Q. X., Li, T., Zhang, Q. L., Fang, C., et al. (2018). Anti-multiple myeloma activity of nanobody-based anti-CD38 chimeric antigen receptor T cells. *Molecular Pharmaceutics, 15*(10), 4577–4588.

Bachmann, M. (2019). The UniCAR system: A modular CAR T cell approach to improve the safety of CAR T cells. *Immunology Letters, 211*, 13–22.

Bachmann, D., Aliperta, R., Bergmann, R., Feldmann, A., Koristka, S., Arndt, C., et al. (2018). Retargeting of UniCAR T cells with an in vivo synthesized target module directed against CD19 positive tumor cells. *Oncotarget, 9*(7), 7487.

Bala, G., Crauwels, M., Blykers, A., Remory, I., Marschall, A. L., Dübel, S., et al. (2019). Radiometal-labeled anti-VCAM-1 nanobodies as molecular tracers for atherosclerosis–impact of radiochemistry on pharmacokinetics. *Biological Chemistry, 400*(3), 323–332.

Bannas, P., Well, L., Lenz, A., Rissiek, B., Haag, F., Schmid, J., et al. (2014). In vivo near-infrared fluorescence targeting of T cells: Comparison of nanobodies and conventional monoclonal antibodies. *Contrast Media & Molecular Imaging, 9*(2), 135–142.

Barclay, J., Creswell, J., & León, J. (2018). Cancer immunotherapy and the PD-1/PD-L1 checkpoint pathway. *Archivos Espanoles de Urologia, 71*(4), 393–399.

Behdani, M., Zeinali, S., Karimipour, M., Khanahmad, H., Schoonooghe, S., Aslemarz, A., et al. (2013). Development of VEGFR2-specific nanobody Pseudomonas exotoxin A conjugated to provide efficient inhibition of tumor cell growth. *New Biotechnology, 30*(2), 205–209.

Behr, T., Behe, M., & Wörmann, B. (2001). Trastuzumab and breast cancer. *The New England Journal of Medicine, 345*(13), 995–996.

Beltrán-Gracia, E., López-Camacho, A., Higuera-Ciapara, I., Velázquez-Fernández, J. B., & Vallejo-Cardona, A. A. (2019). Nanomedicine review: Clinical developments in liposomal applications. *Cancer Nanotechnology, 10*(1), 11.

Böhmová, E., Machová, D., Pechar, M., Pola, R., Venclíková, K., Janoušková, O., et al. (2018). Cell-penetrating peptides: A useful tool for the delivery of various cargoes into cells. *Physiological Research, 67*, S267–SS79.

Bridoux, J., Broos, K., Lecocq, Q., Debie, P., Martin, C., Ballet, S., et al. (2020). Anti-human PD-L1 nanobody for immuno-PET imaging: Validation of a conjugation strategy for clinical translation. *Biomolecules, 10*(10), 1388.

Brown, L. F., Berse, B., Jackman, R. W., Tognazzi, K., Manseau, E. J., Senger, D. R., et al. (1993). Expression of vascular permeability factor (vascular endothelial growth factor) and its receptors in adenocarcinomas of the gastrointestinal tract. *Cancer Research, 53*(19), 4727–4735.

Chabrol, E., Stojko, J., Nicolas, A., Botzanowski, T., Fould, B., Antoine, M., et al. (2020). VHH characterization. Recombinant VHHs: Production, characterization and affinity. *Analytical Biochemistry, 589*, 113491.

Christiansen, J., & Rajasekaran, A. K. (2004). Biological impediments to monoclonal antibody–based cancer immunotherapy. *Molecular Cancer Therapeutics, 3*(11), 1493–1501.

Cooke, C.-L. M., & Davidge, S. T. (2002). Peroxynitrite increases iNOS through NF-κB and decreases prostacyclin synthase in endothelial cells. *American Journal of Physiology-Cell Physiology, 282*(2), C395–C402.

D'Hollander, A., Jans, H., Velde, G. V., Verstraete, C., Massa, S., Devoogdt, N., et al. (2017). Limiting the protein corona: A successful strategy for in vivo active targeting of anti-HER2 nanobody-functionalized nanostars. *Biomaterials, 123*, 15–23.

D'Huyvetter, M., De Vos, J., Xavier, C., Pruszynski, M., Sterckx, Y. G., Massa, S., et al. (2017). 131I-labeled anti-HER2 camelid sdAb as a theranostic tool in cancer treatment. *Clinical Cancer Research, 23*(21), 6616–6628.

De Meyer, T., Muyldermans, S., & Depicker, A. (2014). Nanobody-based products as research and diagnostic tools. *Trends in Biotechnology, 32*(5), 263–270.

De Munter, S., Ingels, J., Goetgeluk, G., Bonte, S., Pille, M., Weening, K., et al. (2018). Nanobody based dual specific CARs. *International Journal of Molecular Sciences, 19*(2), 403.

Deng, C., Xiong, J., Gu, X., Chen, X., Wu, S., Wang, Z., et al. (2017). Novel recombinant immunotoxin of EGFR specific nanobody fused with cucurmosin, construction and antitumor efficiency in vitro. *Oncotarget, 8*(24), 38568–38580.

Dong, J., Huang, B., Jia, Z., Wang, B., Kankanamalage, S. G., Titong, A., et al. (2020). Development of multi-specific humanized llama antibodies blocking SARS-CoV-2/ACE2 interaction with high affinity and avidity. *Emerging Microbes & Infections, 9*(1), 1034–1036.

Drent, E., Groen, R. W., Noort, W. A., Themeli, M., van Bueren, J. J. L., Parren, P. W., et al. (2016). Pre-clinical evaluation of CD38 chimeric antigen receptor engineered T cells for the treatment of multiple myeloma. *Haematologica, 101*(5), 616–625.

Drent, E., Themeli, M., Poels, R., de Jong-Korlaar, R., Yuan, H., de Bruijn, J., et al. (2017). A rational strategy for reducing on-target off-tumor effects of CD38-chimeric antigen receptors by affinity optimization. *Molecular Therapy, 25*(8), 1946–1958.

Eladl, E., Tremblay-LeMay, R., Rastgoo, N., Musani, R., Chen, W., Liu, A., et al. (2020). Role of CD47 in hematological malignancies. *Journal of Hematology & Oncology, 13*(1), 1–14.

Eloy, J. O., Petrilli, R., Trevizan, L. N. F., & Chorilli, M. (2017). Immunoliposomes: A review on functionalization strategies and targets for drug delivery. *Colloids and Surfaces B: Biointerfaces, 159*, 454–467.

Emerich, D. F., Dean, R. L., Snodgrass, P., Lafreniere, D., Agostino, M., Wiens, T., et al. (2001). Bradykinin modulation of tumor vasculature: II. Activation of nitric oxide and phospholipase A2/prostaglandin signaling pathways synergistically modifies vascular physiology and morphology to enhance delivery of chemotherapeutic agents to tumors. *Journal of Pharmacology and Experimental Therapeutics, 296*(2), 632–641.

Eroğlu, İ., & İbrahim, M. (2020). Liposome–ligand conjugates: A review on the current state of art. *Journal of Drug Targeting, 28*(3), 225–244.

Fana, M., Gallien, J., Srinageshwar, B., Dunbar, G. L., & Rossignol, J. (2020). PAMAM dendrimer nanomolecules utilized as drug delivery systems for potential treatment of glioblastoma: A systematic review. *International Journal of Nanomedicine, 15*, 2789.

Fang, T., Duarte, J. N., Ling, J., Li, Z., Guzman, J. S., & Ploegh, H. L. (2016). Structurally defined αMHC-II nanobody–drug conjugates: A therapeutic and imaging system for B-cell lymphoma. *Angewandte Chemie International Edition, 55*(7), 2416–2420.

Farasat, A., Rahbarizadeh, F., Ahmadvand, D., & Yazdian, F. (2017). Optimization of an anti-HER2 nanobody expression using the Taguchi method. *Preparative Biochemistry and Biotechnology, 47*(8), 795–803.

Farasat, A., Rahbarizadeh, F., Ahmadvand, D., Ranjbar, S., & Khoshtinat, N. S. (2019). Effective suppression of tumour cells by oligoclonal HER2-targeted delivery of liposomal doxorubicin. *Journal of Liposome Research, 29*(1), 53–65.

Folkman, J. (2006). Angiogenesis. *Annual Review of Medicine, 57*(1), 1–18.

Galluzzi, L., Humeau, J., Buqué, A., Zitvogel, L., & Kroemer, G. (2020). Immunostimulation with chemotherapy in the era of immune checkpoint inhibitors. *Nature Reviews Clinical Oncology, 17*(12), 725–741.

Gee, M. S., Saunders, H. M., Lee, J. C., Sanzo, J. F., Jenkins, W. T., Evans, S. M., et al. (2001). Doppler ultrasound imaging detects changes in tumor perfusion during antivascular therapy associated with vascular anatomic alterations. *Cancer Research, 61*(7), 2974–2982.

Guillerey, C., Huntington, N. D., & Smyth, M. J. (2016). Targeting natural killer cells in cancer immunotherapy. *Nature Immunology, 17*(9), 1025–1036.

Hajari Taheri, F., Hassani, M., Sharifzadeh, Z., Behdani, M., Arashkia, A., & Abolhassani, M. (2019). T cell engineered with a novel nanobody-based chimeric antigen receptor against VEGFR2 as a candidate for tumor immunotherapy. *IUBMB Life, 71*(9), 1259–1267.

Hambach, J., Riecken, K., Cichutek, S., Schütze, K., Albrecht, B., Petry, K., et al. (2020). Targeting CD38-expressing multiple myeloma and Burkitt lymphoma cells in vitro with nanobody-based chimeric antigen receptors (Nb-CARs). *Cell, 9*(2), 321.

Hamers-Casterman, C., Atarhouch, T., Muyldermans, S., Robinson, G., Hammers, C., Songa, E. B., et al. (1993). Naturally occurring antibodies devoid of light chains. *Nature, 363*(6428), 446–448.

Harmsen, M., & De Haard, H. (2007). Properties, production, and applications of camelid single-domain antibody fragments. *Applied Microbiology and Biotechnology, 77*(1), 13–22.

Hassani, M., Hajari Taheri, F., Sharifzadeh, Z., Arashkia, A., Hadjati, J., van Weerden, W. M., et al. (2019). Construction of a chimeric antigen receptor bearing a nanobody against prostate a specific membrane antigen in prostate cancer. *Journal of Cellular Biochemistry, 120*(6), 10787–10795.

Hatahet, F., Nguyen, V. D., Salo, K. E., & Ruddock, L. W. (2010). Disruption of reducing pathways is not essential for efficient disulfide bond formation in the cytoplasm of E. coli. *Microbial Cell Factories, 9*(1), 67.

Havel, J. J., Chowell, D., & Chan, T. A. (2019). The evolving landscape of biomarkers for checkpoint inhibitor immunotherapy. *Nature Reviews Cancer, 19*(3), 133–150.

Henry, K. A., Hussack, G., Kumaran, J., Gilbert, M., MacKenzie, C. R., Sulea, T., et al. (2019). Role of the non-hypervariable FR3 D-E loop in single-domain antibody recognition of haptens and carbohydrates. *Journal of Molecular Recognition, 32*(11), e2805.

Herrmann, J. (2020). Adverse cardiac effects of cancer therapies: Cardiotoxicity and arrhythmia. *Nature Reviews Cardiology, 17*(8), 474–502.

Hervé-Aubert, K., David, S., Lautram, N., Passirani, C., Chourpa, I., Aubrey, N., et al. (2020). Targeted nanomedicine with anti-EGFR scFv for siRNA delivery into triple negative breast cancer cells. *European Journal of Pharmaceutics and Biopharmaceutics, 157*, 74–84.

Hoyt, K., Umphrey, H., Lockhart, M., Robbin, M., & Forero-Torres, A. (2015). Ultrasound imaging of breast tumor perfusion and neovascular morphology. *Ultrasound in Medicine & Biology, 41*(9), 2292–2302.

Huang, H.-F., Zhu, H., Li, G.-H., Xie, Q., Yang, X.-T., Xu, X.-X., et al. (2019). Construction of anti-hPD-L1 HCAb Nb6 and in situ 124I labeling for noninvasive detection of PD-L1 expression in human bone sarcoma. *Bioconjugate Chemistry, 30*(10), 2614–2623.

Huda, S., Alam, M. A., & Sharma, P. K. (2020). Smart nanocarriers-based drug delivery for cancer therapy: An innovative and developing strategy. *Journal of Drug Delivery Science and Technology, 60*, 102018.

Iezzi, M. E., Policastro, L., Werbajh, S., Podhajcer, O., & Canziani, G. A. (2018). Single-domain antibodies and the promise of modular targeting in cancer imaging and treatment. *Frontiers in Immunology, 9*, 273.

Iqbal, U., Trojahn, U., Albaghdadi, H., Zhang, J., O'Connor-McCourt, M., Stanimirovic, D., et al. (2010). Kinetic analysis of novel mono-and multivalent VHH-fragments and their application for molecular imaging of brain tumours. *British Journal of Pharmacology, 160*(4), 1016–1028.

Iri-Sofla, F. J., Rahbarizadeh, F., Ahmadvand, D., & Rasaee, M. J. (2011). Nanobody-based chimeric receptor gene integration in Jurkat cells mediated by PhiC31 integrase. *Experimental Cell Research, 317*(18), 2630–2641.

Jafari Iri Sofla, F., Rahbarizadeh, F., Ahmadvand, D., Nomani, A., & Vernet, E. (2019). Anti–HER2 single domain antibody-conjugated dendrimers for targeted delivery of truncated-bid transgene to breast cancer cells. *Journal of Bioactive and Compatible Polymers, 34*(1), 39–57.

Jamnani, F. R., Rahbarizadeh, F., Shokrgozar, M. A., Mahboudi, F., Ahmadvand, D., Sharifzadeh, Z., et al. (2014). T cells expressing VHH-directed oligoclonal chimeric HER2 antigen receptors: Towards tumor-directed oligoclonal T cell therapy. *Biochimica et Biophysica Acta (BBA)-General Subjects, 1840*(1), 378–386.

Jia, D., Yang, Y., Yuan, F., Fan, Q., Wang, F., Huang, Y., et al. (2020). Increasing the antitumor efficacy of doxorubicin liposomes with coupling an anti-EGFR affibody in EGFR-expressing tumor models. *International Journal of Pharmaceutics, 586*, 119541.

Jureczek, J., Feldmann, A., Bergmann, R., Arndt, C., Berndt, N., Koristka, S., et al. (2020). Highly efficient targeting of EGFR-expressing tumor cells with UniCAR T cells via target modules based on Cetuximab®. *OncoTargets and Therapy, 13*, 5515–5527.

Kalyane, D., Raval, N., Maheshwari, R., Tambe, V., Kalia, K., & Tekade, R. K. (2019). Employment of enhanced permeability and retention effect (EPR): Nanoparticle-based precision tools for targeting of therapeutic and diagnostic agent in cancer. *Materials Science and Engineering: C, 98*, 1252–1276.

Kaplan, O., Zarubova, J., Mikulova, B., Filova, E., Bártová, J., Bačáková, L., et al. (2016). Enhanced mitogenic activity of recombinant human vascular endothelial growth factor VEGF121 expressed in E. coli origami B (DE3) with molecular chaperones. *PLoS One, 11*(10), e0163697.

Khaleghi, S., Rahbarizadeh, F., Ahmadvand, D., Rasaee, M. J., & Pognonec, P. (2012). A caspase 8-based suicide switch induces apoptosis in nanobody-directed chimeric receptor expressing T cells. *International Journal of Hematology, 95*(4), 434–444.

Khaleghi, S., Rahbarizadeh, F., Ahmadvand, D., Malek, M., & Madaah Hosseini, H. R. (2016). The effect of superparamagnetic iron oxide nanoparticles surface engineering on relaxivity of magnetoliposome. *Contrast Media & Molecular Imaging, 11*(5), 340–349.

Khaleghi, S., Rahbarizadeh, F., Ahmadvand, D., & Hosseini, H. R. M. (2017). Anti-HER2 VHH targeted magnetoliposome for intelligent magnetic resonance imaging of breast cancer cells. *Cellular and Molecular Bioengineering, 10*(3), 263–272.

Kijanka, M. M., van Brussel, A. S., van der Wall, E., Mali, W. P., van Diest, P. J., van Bergen En Henegouwen, P. M., et al. (2016). Optical imaging of pre-invasive breast cancer with a combination of VHHs targeting CAIX and HER2 increases contrast and facilitates tumour characterization. *EJNMMI Research, 6*(1), 14.

Kirchhofer, A., Helma, J., Schmidthals, K., Frauer, C., Cui, S., Karcher, A., et al. (2010). Modulation of protein properties in living cells using nanobodies. *Nature Structural & Molecular Biology, 17*(1), 133.

Koning, G. A., Eggermont, A. M., Lindner, L. H., & ten Hagen, T. L. (2010). Hyperthermia and thermosensitive liposomes for improved delivery of chemotherapeutic drugs to solid tumors. *Pharmaceutical Research, 27*(8), 1750–1754.

Kubala, M. H., Kovtun, O., Alexandrov, K., & Collins, B. M. (2010). Structural and thermodynamic analysis of the GFP: GFP-nanobody complex. *Protein Science, 19*(12), 2389–2401.

Lassere, M. N. (2008). The Biomarker-Surrogacy Evaluation Schema: A review of the biomarker-surrogate literature and a proposal for a criterion-based, quantitative, multidimensional hierarchical levels of evidence schema for evaluating the status of biomarkers as surrogate endpoints. *Statistical Methods in Medical Research, 17*(3), 303–340.

Lecocq, Q., Zeven, K., De Vlaeminck, Y., Martens, S., Massa, S., Goyvaerts, C., et al. (2019). Noninvasive imaging of the immune checkpoint LAG-3 using nanobodies, from development to pre-clinical use. *Biomolecules, 9*(10), 548.

Leemasawat, K., Phrommintikul, A., Chattipakorn, S. C., & Chattipakorn, N. (2020). Mechanisms and potential interventions associated with the cardiotoxicity of ErbB2-targeted drugs: Insights from in vitro, in vivo, and clinical studies in breast cancer patients. *Cellular and Molecular Life Sciences, 77*(8), 1571–1589.

Li, T., Bourgeois, J. P., Celli, S., Glacial, F., Le Sourd, A. M., Mecheri, S., et al. (2012). Cell-penetrating anti-GFAP VHH and corresponding fluorescent fusion protein VHH-GFP spontaneously cross the blood-brain barrier and specifically recognize astrocytes: Application to brain imaging. *The FASEB Journal, 26*(10), 3969–3979.

Li, J. Y., Perry, S. R., Muniz-Medina, V., Wang, X., Wetzel, L. K., Rebelatto, M. C., et al. (2016). A biparatopic HER2-targeting antibody-drug conjugate induces tumor regression in primary models refractory to or ineligible for HER2-targeted therapy. *Cancer Cell, 29*(1), 117–129.

Li, J., Liang, H., Liu, J., & Wang, Z. (2018). Poly (amidoamine) (PAMAM) dendrimer mediated delivery of drug and pDNA/siRNA for cancer therapy. *International Journal of Pharmaceutics, 546*(1–2), 215–225.

Liu, S., Pan, J., Liu, J., Ma, Y., Qiu, F., Mei, L., et al. (2018). Dynamically PEGylated and borate-coordination-polymer-coated polydopamine nanoparticles for synergetic tumor-targeted, chemo-photothermal combination therapy. *Small, 14*(13), 1703968.

Lobstein, J., Emrich, C. A., Jeans, C., Faulkner, M., Riggs, P., & Berkmen, M. (2012). SHuffle, a novel Escherichia coli protein expression strain capable of correctly folding disulfide bonded proteins in its cytoplasm. *Microbial Cell Factories, 11*(1), 753.

Loureiro, L., Feldmann, A., Bergmann, R., Koristka, S., Berndt, N., Arndt, C., et al. (2018). Development of a novel target module redirecting UniCAR T cells to Sialyl Tn-expressing tumor cells. *Blood Cancer Journal, 8*(9), 1–6.

Lugano, R., Ramachandran, M., & Dimberg, A. (2020). Tumor angiogenesis: Causes, consequences, challenges and opportunities. *Cellular and Molecular Life Sciences, 77*(9), 1745–1770.

Luong, D., Kesharwani, P., Deshmukh, R., Amin, M. C. I. M., Gupta, U., Greish, K., et al. (2016). PEGylated PAMAM dendrimers: Enhancing efficacy and mitigating toxicity for effective anticancer drug and gene delivery. *Acta Biomaterialia, 43*, 14–29.

Manglik, A., Kobilka, B. K., & Steyaert, J. (2017). Nanobodies to study G protein–coupled receptor structure and function. *Annual Review of Pharmacology and Toxicology, 57*, 19–37.

Marcucci, F., Bellone, M., Rumio, C., & Corti, A. (2013). Approaches to improve tumor accumulation and interactions between monoclonal antibodies and immune cells. *MAbs, 5*(1), 34–46. Taylor & Francis.

Mikkilineni, L., & Kochenderfer, J. N. (2021). CAR T cell therapies for patients with multiple myeloma. *Nature Reviews Clinical Oncology, 18*(2), 71–84.

Mir, M. A., Mehraj, U., Sheikh, B. A., & Hamdani, S. S. (2020). Nanobodies: The “magic bullets” in therapeutics, drug delivery and diagnostics. *Human Antibodies, 28*(1), 29–51.

Muyldermans, S. (2020). A guide to: Generation and design of nanobodies. *The FEBS Journal*. https://doi.org/10.1111/febs.15515

Myers, J. A., & Miller, J. S. (2021). Exploring the NK cell platform for cancer immunotherapy. *Nature Reviews Clinical Oncology, 18*(2), 85–100.

Ng, Q.-S., Goh, V., Milner, J., Stratford, M. R., Folkes, L. K., Tozer, G. M., et al. (2007). Effect of nitric-oxide synthesis on tumour blood volume and vascular activity: A phase I study. *The Lancet Oncology, 8*(2), 111–118.

Nguyen, V. D., Hatahet, F., Salo, K. E., Enlund, E., Zhang, C., & Ruddock, L. W. (2011). Pre-expression of a sulfhydryl oxidase significantly increases the yields of eukaryotic disulfide bond containing proteins expressed in the cytoplasm of E. coli. *Microbial Cell Factories, 10*(1), 1–13.

Nikkhoi, S. K., Rahbarizadeh, F., & Ahmadvand, D. (2017). Oligo-clonal nanobodies as an innovative targeting agent for cancer therapy: New biology and novel targeting systems. *Protein Expression and Purification, 129*, 115–121.

Nikkhoi, S. K., Rahbarizadeh, F., Ahmadvand, D., & Moghimi, S. M. (2018). Multivalent targeting and killing of HER2 overexpressing breast carcinoma cells with methotrexate-encapsulated tetra-specific non-overlapping variable domain heavy chain anti-HER2 antibody-PEG-liposomes: In vitro proof-of-concept. *European Journal of Pharmaceutical Sciences, 122*, 42–50.

Oliveira, S., Heukers, R., Sornkom, J., Kok, R. J., & van Bergen En Henegouwen, P. M. (2013). Targeting tumors with nanobodies for cancer imaging and therapy. *Journal of Controlled Release, 172*(3), 607–617.

Osman, G., Rodriguez, J., Chan, S. Y., Chisholm, J., Duncan, G., Kim, N., et al. (2018). PEGylated enhanced cell penetrating peptide nanoparticles for lung gene therapy. *Journal of Controlled Release, 285*, 35–45.

Padegimas, A., Clasen, S., & Ky, B. (2020). Cardioprotective strategies to prevent breast cancer therapy-induced cardiotoxicity. *Trends in Cardiovascular Medicine, 30*(1), 22–28.

Pannuzzo, M., Esposito, S., Wu, L.-P., Key, J., Aryal, S., Celia, C., et al. (2020). Overcoming nanoparticle-mediated complement activation by surface PEG-pairing. *Nano Letters, 20*(6), 4312–4321.

Patel, V. (2020). Liposome: A novel carrier for targeting drug delivery system. *Asian Journal of Pharmaceutical Research and Development, 8*(4), 67–76.

Prasad, R., Jain, N. K., Yadav, A. S., Chauhan, D. S., Devrukhkar, J., Kumawat, M. K., et al. (2020). Liposomal nanotheranostics for multimode targeted in vivo bioimaging and near-infrared light mediated cancer therapy. *Communications Biology, 3*(1), 1–14.

Qin, L.-J., Gu, Y.-T., Zhang, H., & Xue, Y.-X. (2009). Bradykinin-induced blood–tumor barrier opening is mediated by tumor necrosis factor-α. *Neuroscience Letters, 450*(2), 172–175.

Rajabzadeh, A., Hamidieh, A. A., & Rahbarizadeh, F. (2018). Cytotoxic function of chimeric antigen receptor (CAR) T cells redirected by anti-Muci nanobody. *Biology of Blood and Marrow Transplantation, 24*(3), S474.

Rajabzadeh, A., Rahbarizadeh, F., Ahmadvand, D., Kabir, S. M., & Hamidieh, A. A. (2021). A VHH-based anti-MUC1 chimeric antigen receptor for specific retargeting of human primary T cells to MUC1-positive cancer cells. *Cell Journal, 22*(4), 502.

Saqafi, B., & Rahbarizadeh, F. (2018). Specific targeting of human epidermal growth factor receptor 2 (HER2) overexpressing breast cancer cells by polyethylene glycol-grafted polyethyleneimine modified with anti-HER2 single-domain antibody. *Journal of Bioactive and Compatible Polymers, 33*(1), 17–37.

Saqafi, B., & Rahbarizadeh, F. (2019). Polyethyleneimine-polyethylene glycol copolymer targeted by anti-HER2 nanobody for specific delivery of transcriptionally targeted tBid containing construct. *Artificial Cells, Nanomedicine, and Biotechnology, 47*(1), 501–511.

Sercombe, L., Veerati, T., Moheimani, F., Wu, S. Y., Sood, A. K., & Hua, S. (2015). Advances and challenges of liposome assisted drug delivery. *Frontiers in Pharmacology, 6*, 286.

Shimasaki, N., Jain, A., & Campana, D. (2020). NK cells for cancer immunotherapy. *Nature Reviews Drug Discovery, 19*(3), 200–218.

Slamon, D. J., Leyland-Jones, B., Shak, S., Fuchs, H., Paton, V., Bajamonde, A., et al. (2001). Use of chemotherapy plus a monoclonal antibody against HER2 for metastatic breast cancer that overexpresses HER2. *The New England Journal of Medicine, 344*(11), 783–792.

Song, C. W., Lokshina, A., Rhee, J. G., Patten, M., & Levitt, S. H. (1984). Implication of blood flow in hyperthermic treatment of tumors. *IEEE Transactions on Biomedical Engineering, 1*, 9–16.

Sonveaux, P., Kaz, A. M., Snyder, S. A., Richardson, R. A., Cárdenas-Navia, L. I., Braun, R. D., et al. (2005). Oxygen regulation of tumor perfusion by S-nitrosohemoglobin reveals a pressor activity of nitric oxide. *Circulation Research, 96*(10), 1119–1126.

Sun, Y., Kang, C., Yao, Z., Liu, F., & Zhou, Y. (2016). Peptide-based ligand for active delivery of liposomal doxorubicin. *Nano Life, 6*(03n04), 1642004.

Tang, J., Li, J., Zhu, X., Yu, Y., Chen, D., Yuan, L., et al. (2016). Novel CD7-specific nanobody-based immunotoxins potently enhanced apoptosis of CD7-positive malignant cells. *Oncotarget, 7*(23), 34070.

Thueng-In, K., Thanongsaksrikul, J., Srimanote, P., Bangphoomi, K., Poungpair, O., Maneewatch, S., et al. (2012). Cell penetrable humanized-VH/VHH that inhibit RNA dependent RNA polymerase (NS5B) of HCV. *PLoS One, 7*(11), e49254.

Thurber, G. M., Schmidt, M. M., & Wittrup, K. D. (2008). Antibody tumor penetration: Transport opposed by systemic and antigen-mediated clearance. *Advanced Drug Delivery Reviews, 60*(12), 1421–1434.

Tian, B., Wong, W. Y., Hegmann, E., Gaspar, K., Kumar, P., & Chao, H. (2015). Production and characterization of a camelid single domain antibody–urease enzyme conjugate for the treatment of cancer. *Bioconjugate Chemistry, 26*(6), 1144–1155.

Tian, B., Wong, W. Y., Uger, M. D., Wisniewski, P., & Chao, H. (2017). Development and characterization of a camelid single domain antibody–urease conjugate that targets vascular endothelial growth factor receptor 2. *Frontiers in Immunology, 8*, 956.

Verhelle, A., Van Overbeke, W., Peleman, C., De Smet, R., Zwaenepoel, O., Lahoutte, T., et al. (2016). Non-invasive imaging of amyloid deposits in a mouse model of AGel using 99m Tc-modified nanobodies and SPECT/CT. *Molecular Imaging and Biology, 18*(6), 887–897.

Vincke, C., Loris, R., Saerens, D., Martinez-Rodriguez, S., Muyldermans, S., & Conrath, K. (2009). General strategy to humanize a camelid single-domain antibody and identification of a universal humanized nanobody scaffold. *Journal of Biological Chemistry, 284*(5), 3273–3284.

Vong, L. B., & Nagasaki, Y. (2020). Nitric oxide nano-delivery systems for cancer therapeutics: Advances and challenges. *Antioxidants, 9*(9), 791.

Wagner, H. N., Wiseman, G. A., Marcus, C. S., Nabi, H. A., Nagle, C. E., Fink-Bennett, D. M., et al. (2002). Administration guidelines for radioimmunotherapy of non-Hodgkin's lymphoma with 90Y-labeled anti-CD20 monoclonal antibody. *Journal of Nuclear Medicine, 43*(2), 267–272.

Waldman, A. D., Fritz, J. M., & Lenardo, M. J. (2020). A guide to cancer immunotherapy: From T cell basic science to clinical practice. *Nature Reviews Immunology, 20*(11), 651–668.

Wang, J., Wu, N., Cham, M. D., & Song, Y. (2009). Tumor response in patients with advanced non–small cell lung cancer: Perfusion CT evaluation of chemotherapy and radiation therapy. *American Journal of Roentgenology, 193*(4), 1090–1096.

Wang, Y., Fan, Z., Shao, L., Kong, X., Hou, X., Tian, D., et al. (2016). Nanobody-derived nanobiotechnology tool kits for diverse biomedical and biotechnology applications. *International Journal of Nanomedicine, 11*, 3287.

Wu, T., Liu, J., Liu, M., Liu, S., Zhao, S., Tian, R., et al. (2019). A nanobody-conjugated DNA nanoplatform for targeted platinum-drug delivery. *Angewandte Chemie International Edition, 58*(40), 14224–14228.

Xiao, T., Li, D., Shi, X., & Shen, M. (2020). PAMAM dendrimer-based nanodevices for nuclear medicine applications. *Macromolecular Bioscience, 20*(2), 1900282.

Xie, Y. J., Dougan, M., Jailkhani, N., Ingram, J., Fang, T., Kummer, L., et al. (2019). Nanobody-based CAR T cells that target the tumor microenvironment inhibit the growth of solid tumors

in immunocompetent mice. *Proceedings of the National Academy of Sciences, 116*(16), 7624–7631.

Xie, Y. J., Dougan, M., Ingram, J. R., Pishesha, N., Fang, T., Momin, N., et al. (2020). Improved antitumor efficacy of chimeric antigen receptor T cells that secrete single-domain antibody fragments. *Cancer Immunology Research, 8*(4), 518–529.

Xu, G., Yu, X., Zhang, J., Sheng, Y., Liu, G., Tao, W., et al. (2016). Robust aptamer–polydopamine-functionalized M-PLGA–TPGS nanoparticles for targeted delivery of docetaxel and enhanced cervical cancer therapy. *International Journal of Nanomedicine, 11*, 2953.

Xu, Y., Wu, H., Huang, J., Qian, W., Martinson, D. E., Ji, B., et al. (2020). Probing and enhancing ligand-mediated active targeting of tumors using sub-5 nm ultrafine iron oxide nanoparticles. *Theranostics, 10*(6), 2479–2494.

Zhao, J., Zhou, M., & Li, C. (2016). Synthetic nanoparticles for delivery of radioisotopes and radiosensitizers in cancer therapy. *Cancer Nanotechnology, 7*(1), 1–23.

Chapter 5
Emerging Lipid-Based Nanomaterials for Cancer Theranostics

Humzah Jamshaid and Fakhar-ud-Din

Contents

5.1 Cancer: A Gruesome Disease

Appearing as a global health problem, cancer is accompanied with a significant mortality ratio across the globe. In fact, it is a second leading death cause around the world with a death toll of 9.5 million in 2018 (ud Din et al., 2017). According to *GLOBOCAN* statistics, the ten most common types of cancer, their reported cases, and deaths occurred in 2018 are stated in Table 5.1. The associated challenges of this diverse diseased state do not end up here. The "financial toxicity," in addition, appears to be another insurmountable plight – high budgeted diagnostic and

H. Jamshaid · Fakhar-ud-Din (✉)
Nanomedicine Research Group, Department of Pharmacy, Quaid-i-Azam University Islamabad, Islamabad, Pakistan
e-mail: fudin@qau.edu.pk

M. Saravanan, H. Barabadi (eds.), *Cancer Nanotheranostics*, Nanotechnology in the Life Sciences, https://doi.org/10.1007/978-3-030-74330-7_5

Table 5.1 Number of cases and death toll of ten most common types of cancer according to GLOBOCAN-2018 (Bray et al., 2018; Goodarzi et al., 2019)

Type of cancer	Diagnosed cases in 2018 (million)	Number of deaths reported (million)
Lungs	2.093	1.76
Breast	2.088	0.627
Colorectal	1.800	0.862
Prostate	1.276	o.359
Stomach	1.003	0.783
Liver	0.841	0.782
Esophagus	0.572	0.508
Cervix uteri	0.569	0.311
Thyroid	0.567	0.041
Bladder	0.549	0.200

treatment strategies associated with cancer management (Carrera et al., 2018; Zugazagoitia et al., 2016). According to WHO cancer profile 2020, the total mortality with cancer was ten million approximately and overall cancer cases were estimated above 18 million. All these troublesome statistics persuading toward opportune diagnosis and treatment to effectively manage this fatal disease (Mir et al., 2017). Successful curbing of cancer depends mainly upon the timely diagnosis and simultaneous initiation of treatment. Major cancer diagnostics consists of invasive techniques including the determination of blood biomarkers and tissue biopsies as well as non-invasive imaging techniques – magnetic resonance (MR) imaging, computed tomography (CT) imaging, positron emission tomography (PET) scan, and various fluorescence and photoacoustic imaging (Hamilton, 2010). In addition, common management options include radiotherapy, chemotherapy, immunotherapy, and hormonal, photodynamic (PDT), and photothermal therapy (PTT) (Obeid et al., 2018). However, in this chapter, our major focus is generally toward cancer theranostics and particularly toward lipid-based nanomaterials for cancer theranostics.

5.2 Theranostics: An Emerging Modality to Curb Cancer

Expedient diagnosis and treatment are directly related to appropriate cancer prognosis and restrain the catastrophe associated with this fatal disease. Owing to rapid division and metastasis of tumor, the lag period between confirmed diagnosis and initiation of treatment should be avoided (Miller, 2013). Heading toward simultaneous diagnosis and therapeutic delivery of anti-tumor agents, scientists have developed a dual package of diagnostics and therapeutics – the "theranostics" (Kaur et al., 2020). This emerging technology is basically game-changer system properties with concomitant administration of imaging agent, for non-invasive diagnostics,

and anti-tumor agent aimed for synchronized monitoring of drug pharmacokinetics and targeting along with its response in terms of tumor suppression (Ding & Wu, 2012). Furthermore, when nanoparticles are employed for theranostic purposes, they are referred to as "nanotheranostics." Not limited only to cancer diagnosis, they can be employed for biodistribution determination of administered cancer nanomedicine (Muthu et al., 2014). Problems associated with conventional therapeutics and diagnostics, systemic toxicity and inadequate efficacy, can also be tackled using nanotheranostics. To date, numerous types of nanoparticles (NPs) have been designed for cancer theranostics. These include metallic NPs, polymeric NPs, lipid-based NPs, nanocrystals, niosomes, and the list goes on. However, in this chapter, our discussion will be focused towards lipid-based cancer nanotheranostics and their constructive units are shown in Fig. 5.1.

5.2.1 *Unfettered Access of Nanotheranostics to Tumor Site Through EPR Effect*

Conventional anti-cancer agents with molecular weight less than *1000 Da* are associated with myriad use limiting factors and reduction of efficacy. Rapid renal, non-renal clearance and excretion of these agents are among the limiting parameters. Owing to their miniature size, these drugs can also get accumulated in the normal body tissues which is, in fact, a reason for systemic toxicity such as

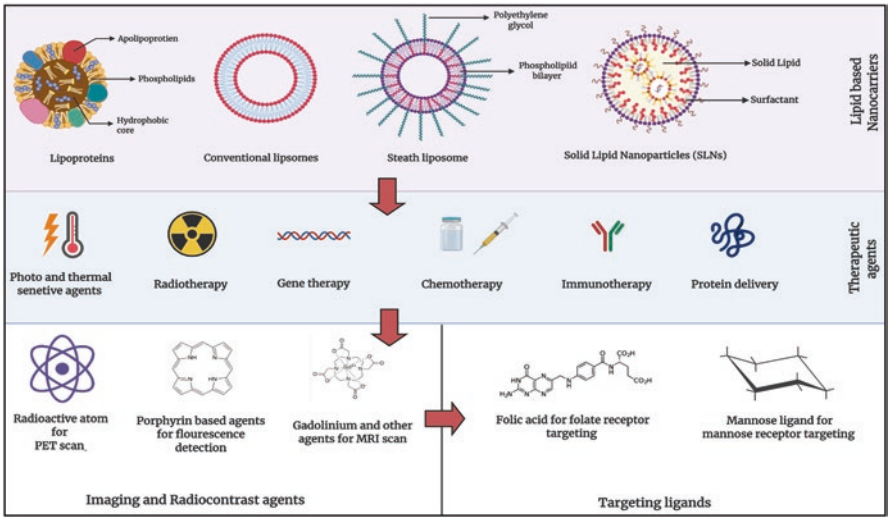

Fig. 5.1 Major components of lipid-based nanotheranostics including lipid NP/nanocarrier, therapeutic agent, diagnostic agent, and surface attached ligand for tumor targeting

myelosuppression, *alopecia*, *nephrotoxicity*, and *mucositis*. These stated problems can be resolved by selectively delivering the therapeutic and diagnostic agents to the tumor cells (de Jonge & Verweij, 2006). The coating or enclosing of these small molecular weight drugs and diagnostics is an optimal approach which could prevent the unfettered access to normal body cells and tissues. *Enhanced permeation and retention* (EPR) phenomenon in tumor micro-environment provide an opportunity to passively target the tumor site using various nanosystems (size ranges from 50 to 200 nm) (Shi et al., 2020). EPR is the set of pathological events that take place to improve the mobility of macromolecules and other substances toward tumor micro-environment in order to meet up the requirements of rapidly dividing cancerous cells. Neo-angiogenesis, in tumor surroundings, with defective, fenestrated and leaky vascular endothelium, together with improper lymphatic drainage are the major pathological defects that give rise to EPR (Prabhakar et al., 2013). Theranostics nanosystems are unable to permeate through healthy vascular beds because of tight endothelial junctions. However, they efficiently permeated through defective vascular epithelium of tumor micro-environment (Golombek et al., 2018; Yhee et al., 2013). To sum up the discussion, EPR prevents the drastic effects of theranostics and facilitates the nanotheranostic retention in tumor surroundings; it is illustrated in Fig. 5.2.

5.2.2 Intracellular Trafficking of Lipid Nanotheranostics

Nanotheranostics and other nanosystems, post-EPR facilitated accumulation in tumor-microenvironment, are usually followed by the internalization in tumor cells. Endocytosis is the actual process responsible for nanosystems internalization inside any cell either normal or cancerous. Large-sized particles, in micron range, are mobilized by micropinocytosis mechanism in which membrane extension wraps the particles and engulf it (Lim & Gleeson, 2011). Nanosystems usually follow the two mechanisms for their cellular internalization, either *caveolin-mediated endocytosis* or *clathrin-mediated endocytosis*. The details of both mechanisms are shown in Fig. 5.3. Lipid nanotheranostics and nanosystems undergo cellular penetration and accumulation through clathrin-mediated endocytosis. This mode of transportation utilized clathrin which is a protein with six amino acid chains – three heavy and three light chains. In addition, dynein receptors are the reason for the clathrin protein enrichment in plasma membranes. Initially, the dynein after binding with the nanosystem attracts the clathrin molecules that form membrane invagination. This membrane invagination gives rise to the formation of endosomes. After possessing nanosystem in endosomes, the entrapped content gets released in cytosol (Behzadi et al., 2017; Foroozandeh & Aziz, 2018).

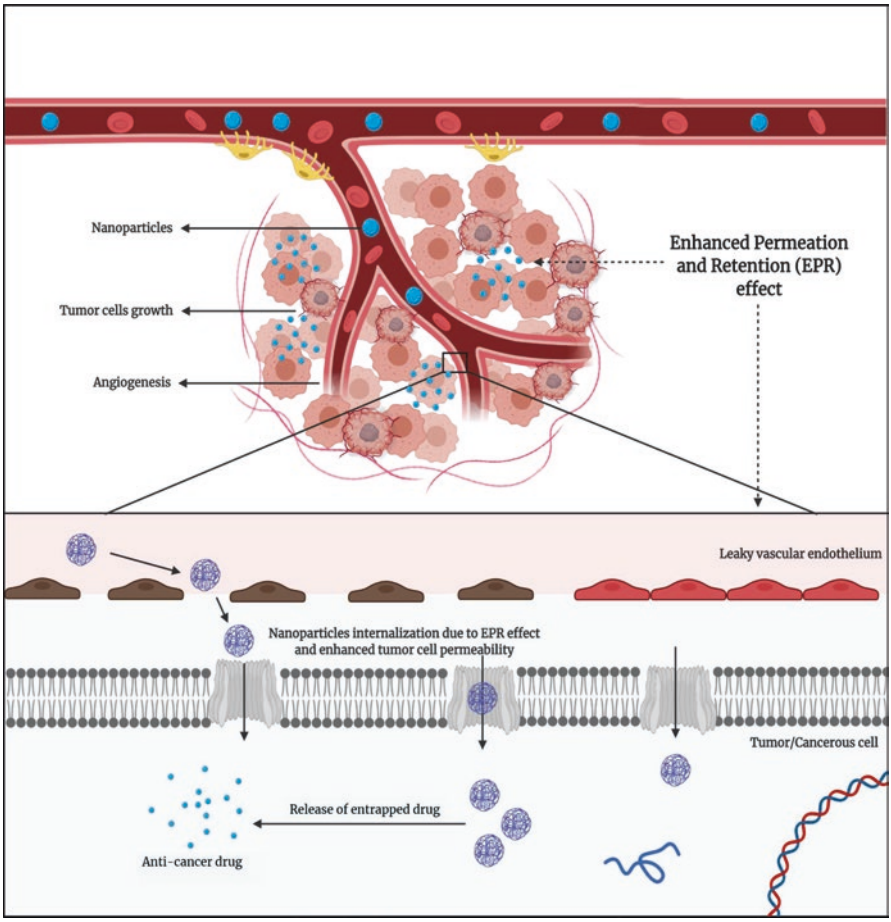

Fig. 5.2 Enhanced permeability and retention (EPR) facilitating the accumulation of nanosystems in tumor micro-environment and tumor cells

5.3 Lipid NPs: The Promising Cancer Theranostic Modality and Their Existing Technology

5.3.1 Liposomes

Nanosystems composed of phospholipid bilayer and cholesterol, the liposomes, are the most adaptable lipid-based NPs adopted for cancer nanotheranostics. The suitability of these nanocarriers is by virtue of several attributes such as biocompatibility, biodegradability, low production cost, as well as the low toxicity (Beltrán-Gracia

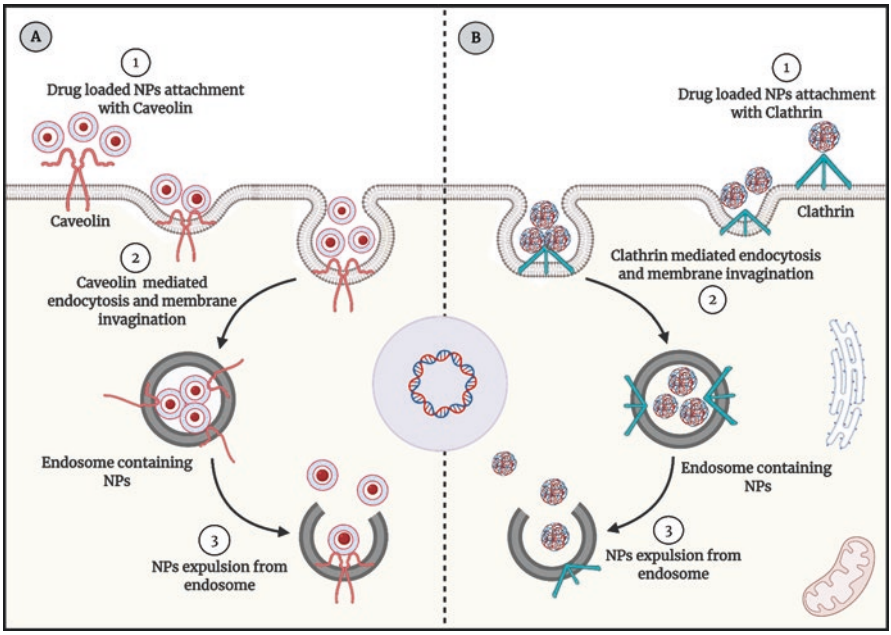

Fig. 5.3 Caveolin (**a**) and clathrin (**b**) facilitated endocytosis for nanosystems and nanotheranostics

et al., 2019). Liposomes have extensively been investigated for several biomedical applications and a number of them are currently enrolled in clinical trials (Beltrán-Gracia et al., 2019). Fortunately, myriad liposomal-based nano-formulations have got approval by FDA such as Lip-Amp-B for fungal infections and Lip-Doxorubicin for ovarian cancer, breast cancer, and against Kaposi's sarcoma (Bulbake et al., 2017). These nanocarriers are, merely, effective in the provision of control and protective delivery of therapeutic agents, proteins, peptides, vaccines, and the diagnostic (imaging) agent as well. For highly water loving agents, with rapid plasma clearance and elimination, the liposomes increase the circulation time and increase plasma half-life. Similarly, liposomes also appear to modify the pharmacokinetic properties and particularly the absorption of lipophilic agents (Torchilin, 2005; Zylberberg & Matosevic, 2016). Structurally, liposomes are composed of phospholipid bilayers, composed of phosphatidylcholine (PC), phosphatidylglycerol (PG), and phosphatidylserine (PS), and the cholesterol to enhance their stability. The therapeutic agent or imaging agent, depending upon its nature, can either be intercalated inside phospholipid layer systems or loaded inside the hydrophilic core, illustrated in Fig. 5.4. In fact, amphiphilic substances can be partitioned between the bilayer and the aqueous core (Pattni et al., 2015). The lipid layer's charge influences greatly the drug delivery and nanosystem internalization. Particularly, cationic liposomes get attracted toward negatively charged surfaces of tumor cells. Furthermore, these positively charged liposomal nanotheranostics are used for the targeting of

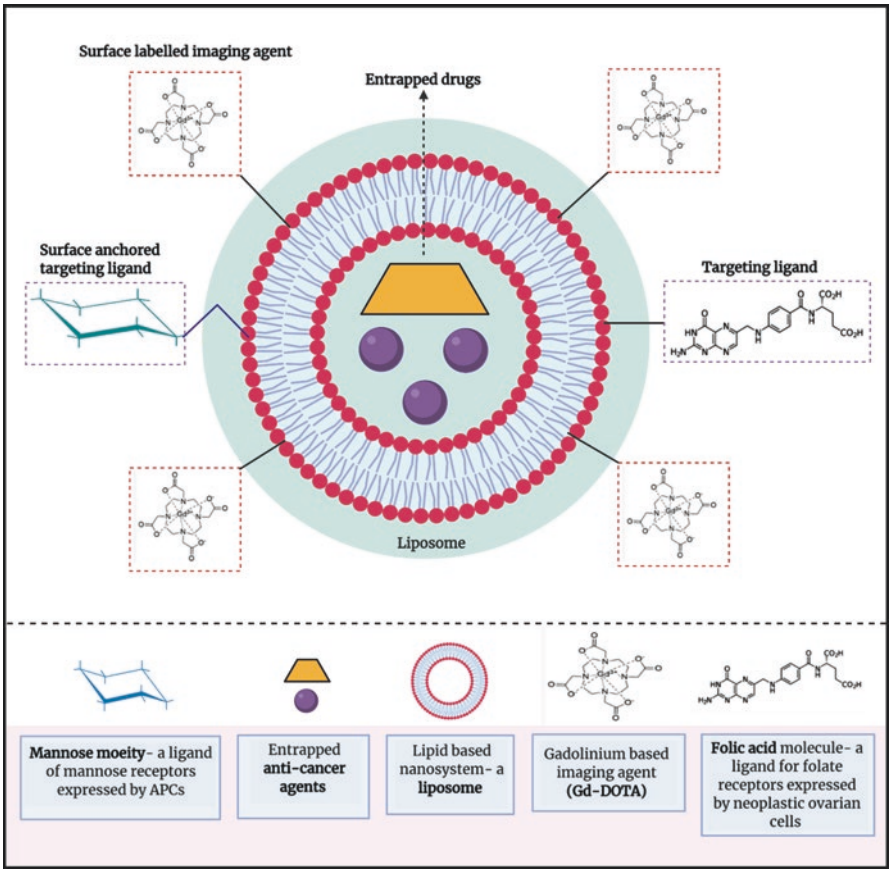

Fig. 5.4 General scheme and structure of liposomal nanotheranostics conjugated with Gd-based MR contrast agent, folic acid, and mannose molecules (for targeting purpose), loaded with anti-cancer agents

angiogenic tumor blood vessels as well as associated with high intra-tumor accumulation (Krasnici et al., 2003). To concise our discussion toward liposomal cancer nanotheranostics, the types of liposomes currently being employed, their structure and properties and investigational candidates are discussed with detail below.

5.3.1.1 Simple Stealth Liposomes

In addition to the phospholipid component and cholesterol, stealth liposomes possess a polymeric layer coating the lipid structure. Contrary to ordinary liposomes, these polymerically protected liposomes provide better protection against core substance leakage and enhance its steric stability. Body defense system, complement system and macrophages, is, fortunately, unable to opsonize and phagocytose these

liposomes. This is another positive aspect of stealth liposomes. The polymeric layers usually do not interfere with the fluidity and functioning of liposome and entrapped drug release mechanism. The fact is these are the most acceptable lipid-based nanomaterial used for drug delivery and theranostics as well (Mineart et al., 2018). The most appropriate polymer owing to its biocompatibility and hydrophilicity is the polyethylene glycol abbreviated commonly as PEG (Immordino et al., 2006).

Stealth liposomes have diverse and versatile applications in the field of nanomedicine. But, in the past few years, this nanosystem has also gained adequate acceptability for simultaneous delivery of therapeutic and the diagnostic agent – the cancer nanotheranostics. Safe and effective tumor site delivery of quantum dots (QDs), fluorescent probes, radioisotopes, and gadolinium (Gd)-based contrast agents along with the therapeutics, are possible using stealth liposomes. Several theranostics liposomes have undergone preclinical investigations and shown to have valuable results to be recruited for clinical studies (Madamsetty et al., 2019). The details of various studies carried out for formulation and evaluation of PEG-coated liposomal theranostics are stated in Table 5.2.

5.3.1.1.1 Stealth Liposomes for Cancer Nanotheranostics

Delivery of QDs

Quantum dots (QDs) are the nanocrystals, comprising semiconductors, CdTe, CdSe, and other compounds, with significant bandgap energy responsible for its photon-emitting properties. Specific amount of energy is required to generate the hole-electron pair and for conversion into an excited state. Along the way of relaxation, the fluorescent photon of characteristic wavelength emits out depending upon the size and nature of QD. These nanocrystals appeared with unprecedented applications in biomedical imaging. Furthermore, these nanocrystals also appeared to possess significant anti-tumor activity through their ability to generate reactive oxygen species (ROS) by photosensitization (Wagner et al., 2019). Despite the myriad benefits of these quantum nanoparticles, these are often associated with some unwanted events including cytotoxicity and accumulation in liver and spleen (Hardman, 2006). Stealth liposomes, however, can be utilized for safer and targeted delivery of QDs to the tumor sites. Against the melanoma tumor C57BL6 mice model, the theranostic ability of PEG-liposomal entrapped QDs. Results were found satisfactory in terms of prolonged plasma circulation time and toxicity reduction. Overall, these QDs-liposomal hybrids were stated to be potentially beneficial in oncology theranostics (Al-Jamal et al., 2009).

Table 5.2 Promising PEG-coated liposomes for tumor theranostics

Diagnostic agent/imaging technique	Therapeutic agent	Cancer targeted	Animal model used for investigation	Findings of investigation	References
Quantum dots (QDs)	–	Melanoma	C57BL6 mice	Prolonged circulation time	Al-Jamal et al. (2009)
^{186}Rh/SPECT	Doxorubicin	Head and neck small cell carcinoma	Xenografted nude rat model	Improved pharmacokinetics, tumor localization and imaging ability	Soundararajan et al. (2009)
Gd-DOTAMA $(C_{18})_2$/MRI	Prednisolone	Melanoma	C57BL6 mice	No pronounced effect on drug therapeutic efficacy circulation life was increased	Cittadino et al. (2012)
^{64}Cu/PET scan-fluorescent imaging	AQ4N	4 T1 tumor	BALB/c mice	Improved biodistribution, tumor internalization and anti-tumor response evidenced by PET scan and fluorescent imaging in 4 T1 tumor bearing BALB/c mice	Feng et al. (2017)
Fe_3O_4/MRI	JPM-565	Breast cancer	MMTV-PyMT mouse model	JPM-565-loaded ferri-liposomes are associated with significant tumor size reduction along with real time MRI monitoring of tumor targeting	Mikhaylov et al. (2011)
Gd based contrast agent/MRI	Anti-survivin SiRNA	Ovarian cancer	Nude female BALB/c mice	Protected SiRNA delivery to the tumor cells evidenced by MRI technique post administration of fabricated liposomes	Kenny et al. (2011)
Fe_3O_4/MRI-US imaging	H_2S	HepG2	Nude female BALB/c HepG2 xenograft model	Effective targeting and tumor killing through H_2S microbubbles visualized by MR and US imaging	Liu et al. (2017)

Radioisotope and Gd-Based Contrast Agent Delivery Along with Chemotherapeutic

The liposomal Doxorubicin is, in fact, the first approved anti-cancer nano-formulation. Vincristine has also got FDA approval in 2013. These developments have opened the new horizons for anti-cancer chemotherapy – the use of nano-formulations (Xing et al., 2016). In the past few years, stealth liposomes have been employed for the simultaneous delivery of therapeutic and imaging agents. Intermediate half-life, β-radiations emitting radioelement, Rhenium-186 (^{186}Rh), have been entrapped inside liposomes already containing anti-tumor antibiotic, doxorubicin (Doxil). This designed nanotheranostics was evaluated in head and neck squamous cell carcinoma nude rat xenograft model, and imaging capability was assessed using single positron emission computed tomography (SPECT) technique. Findings of the study, however, revealed 20 times improved %ID with (^{186}Rh)-labelled Doxil as compared to (^{186}Rh)-labelled PEG liposomes. Moreover due to high labelling efficiency, improved biodistribution and tumor targeting was observed (Soundararajan et al., 2009). Cancer chemotherapy is associated with a number of side effects. The most common among them is chemotherapy-induced nausea and vomiting. Glucocorticoids are proved to be effective in curbing the unwanted emesis (Hesketh, 2017; Vayne-Bossert et al., 2017). In addition, these agents also possess pain relieving property, owing to which they can be used as adjuvant for tumor pain management (Lossignol, 2016). Co-administration of glucocorticoid, prednisolone, and the gadolinium-based MRI contrast agent using stealth liposomes has been carried out and evaluated in C57BL6 mouse models possessing the melanoma tumor – B16 syngeneic tumor. The imaging agent has been utilized to track the anti-cancer biodistribution and tumor cell internalization of the loaded agent (Cittadino et al., 2012).

Later, the group of US and Chinese scientists have designed the novel photodynamic therapy-based, isotope-chelated liposomal nanosystem. Fabricated liposomes are composed of AQ4N – a prodrug usually gets activated in hypoxic cellular environment, hexadecylamine chlorin e6- a photosensitive agent which get activated using light and generate ROS and tumor site (O_2 deficiency) hypoxia. The photosensitizing agent was chelated with radioisotope ^{64}Cu which was used for the in vivo tracking (through PET scan) of PDT-induced chemotherapeutic agents. The results concluded to be greatly improved in terms of nanotheranostics biodistribution, tumor accumulation, and treatment efficiency as compared to alone PDT therapy (Feng et al., 2017). This innovative triple moiety-loaded liposomal nanotheranostics is explained graphically in Fig. 5.5.

Co-delivery of Magnetic NPs and Chemotherapeutic Agent

Supermagnetic properties of iron-based NPs make them suitable candidates for MR imaging used for real time imaging of anti-cancer targeted delivery (Javed et al., 2017). Ferri-liposomes, the ferric oxide magnetic NPs entrapped inside a liposome, were designed for real-time evaluation of tumor targeted delivery of anti-tumor

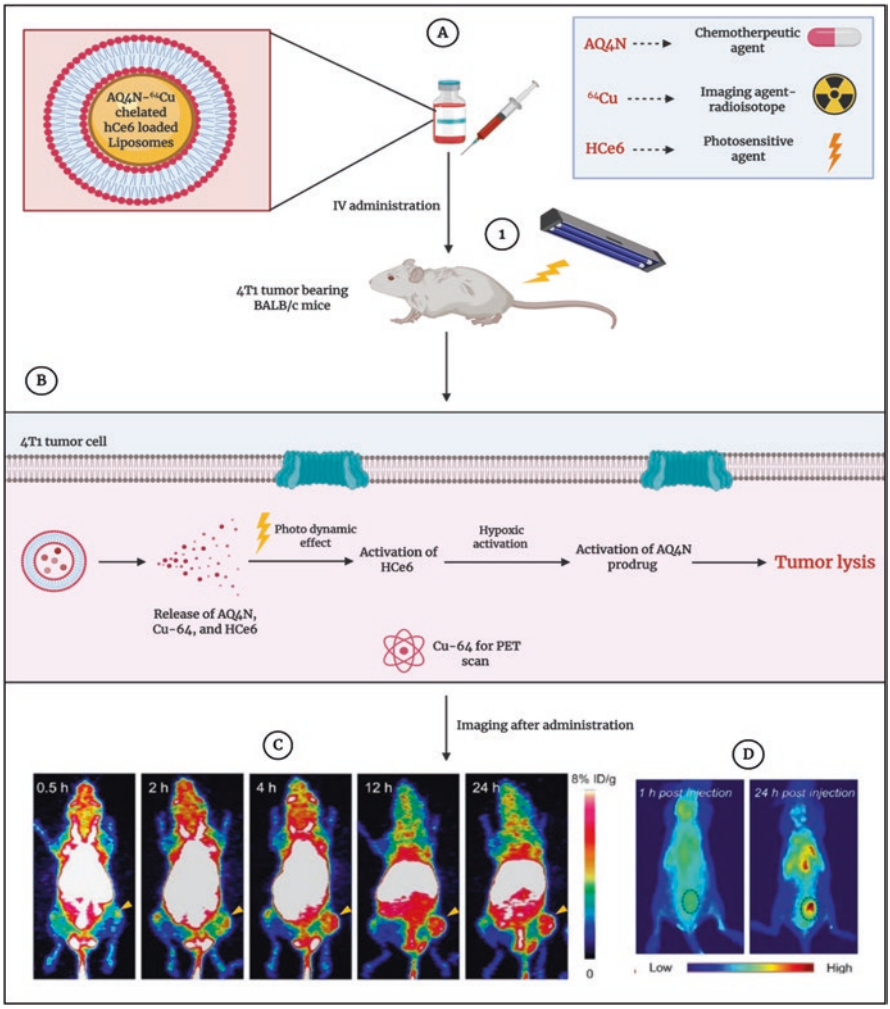

Fig. 5.5 (**a**) Composition of AQ4N-^{64}Cu chelated hCe6 stealth liposomes and its administration in 4 T1 tumor bearing BALB/c mice. (1) Light irradiation was used for activation of hCe6. (**b**) Mechanism of imaging and anti-tumor activity of designed liposomes. (**c**) PET imaging post AQ4N-^{64}Cu chelated hCe6 stealth liposomes administration to 4 T1 tumor-bearing mice model at different time gaps. (Reprinted with Permission from Feng et al., 2017). (**d**) Fluorescence imaging of 4 T1 tumor bearing mice model at 1 h and 24 h post injection. (Reprinted with Permission from Feng et al., 2017). Both (**c**) and (**d**) showing enhanced tumor targeting and accumulation of designed nanotheranostic

agent – the cathepsin inhibitor (JPM-565). This mode of delivery was superior to the stereotyped delivery system of similar agents (Mikhaylov et al., 2011). Another study has also reported the engineering of PEGylated liposomes loaded with stimuli sensitive H_2S precursor, anethole dithiolethione, and magnetic nanoparticle for the

purpose of real time MR imaging. These designed nanotheranostics were tested on HepG2 xenograft mice models. The bio-conversion and formation of H2S and tumor internalization of these nanocarriers were evaluated using ultrasound and MR imaging respectively (Liu et al., 2017).

Co-delivery of SiRNA and Gd-Based Contrast Agent

Small interfering RNA (SiRNA) is an important therapeutic strategy for targeted gene silencing (Guo et al., 2013). However, the negative charge of SiRNA and its hydrophilicity are the responsible factors for poor cell penetration. Short serum half-life and some toxic effects are also listed up in use limiting parameters of unprotected SiRNA (Singh et al., 2018). To overcome these problems, anti-survivin SiRNA is entrapped inside the long-circulating stealth liposomes. This designed nanocarrier is also loaded with gadolinium-based MRI contrast agents. The results of the study showed enhanced ovarian tumor cells distribution and tumor size reduction in mice models followed by IV administration of designed liposomal theranostics (Kenny et al., 2011).

5.3.1.2 Surface-Engineered Stealth Liposomes

Among myriad targeting approaches, receptor-based recognition of tumor cells is the most suitable strategy owing to the receptor overexpression by the unimpededly dividing tumor cells. Nanocarriers are attached with the ligand molecules which are, in fact, the substrate of the receptor experienced targeting. Some commonly targeted tumor cells receptors are folate, riboflavin, estrogen, HER2, integrin, endothelin, interleukin, ICAM-1, and the list goes on (Large et al., 2019), mentioned briefly with their selective ligands in Table 5.3. The ligands of the previously mentioned receptors are intercalated or attached chemically over the lipid NPs superficially. This decoration would ultimately lead to considerable internalization into the receptor expressing tumor cells (Darguzyte et al., 2020; Singh et al., 2017). This technology has currently ameliorated the challenges associated with cancer theranostics; more adequate and effective tumor targeting is achievable. In this section, the existing receptor-mediated targeting approaches, attempts, and studies for cancer theranostics have been discussed.

5.3.1.2.1 Significance of Surface-Engineered Stealth Liposomes

Despite the administration of therapeutic and imaging moieties laden NPs, the cancer management still encounters few challenges such as minimal tumor damage and systemic toxicity. However, all erstwhile mentioned studies have clearly concluded the superiority of ligand labeled liposomal theranostics to their un-labeled counterpart in terms of safety, efficacy, targeting, and real-time monitoring as well.

Table 5.3 Receptors overexpressed by various types of cancer and their respective ligands

Receptor	Ligand	Tumor cells expressing the receptor	Reference
HER2	Antibody (trastuzumab) Scfv Fab Small affibody	Breast cancer Gastric cancer Ovarian cancer Non-small cell carcinoma of lung	Tai et al. (2010)
Estrogen	17β-estradiol Diethylstilbestrol 4-OH tamoxifen	HR+ breast cancer Ovarian cancer Colon cancer Prostate cancer	Nasrazadani et al. (2018); Shanle and Xu (2010)
LHRH	D-Lys^6	Prostate cancer, endometrial cancer Ovarian cancer, pancreatic cancer glioblastoma, melanoma	Li et al. (2017)
Endothelin	ET-1 ET-2 ET-3	Bladder cancer, bone cancer Breast cancer, cervical cancer Kaposi sarcoma, prostate cancer Ovarian cancer, osteosarcoma	Wang and Dashwood (2011)
Folate	Folic acid	Expressed by various carcinomas including Breast carcinoma Lungs carcinoma Renal carcinoma Ovarian carcinoma	Fernández et al. (2018)
Integrin	RGD tripeptides-(fibronectin, osteopontin, vitronectrin, laminin, cilengitide) Non-RGD peptides-(AC-PHSCN-NH_2, JSM6427)	Triple negative breast cancer (TNBC)	Dai et al. (2014); Wu et al. (2019)

5.3.1.3 Stimuli-Responsive (Smart) Stealth Liposomes

Functionality of the "smart" liposomal system usually depends upon the triggering factors of tumor microenvironment. In other words, these liposomes are modified with stimulus sensitive materials which upon exposure cause liposomal membrane de-stabilization and release of entrapped content. The release signal or stimulus is usually of two types – *endogenous stimuli* and *external stimuli*. Internal or endogenous stimulus could be of variant nature such as pH, temperature, and presence of specific enzyme or redox environment. However, the external or foreign stimulus includes temperature, light, magnetic field, or ultrasound waves as well (Lee &

Thompson, 2017; Zangabad et al., 2018). These smart-triggered release liposomes have been found to possess valuable importance and significance in cancer nanomedicine and nanotheranostics which is discussed in the current section.

5.3.1.3.1 Thermosensitive Liposomal Theranostics (TSL-Ts)

Co-utilization of ERP effect and mild hyperthermia stimulus and thermosensitive liposomes (TSL-Ts) undergo degradation and release of entrapped contents. Most importantly, the composition and the phospholipid employed for liposomal construction are critical parameters for thermally induced membrane destabilization. Phospholipid transition temperature (T_m) is the temperature at which the gel-like solid state of phospholipid is transformed into a crystalline liquid state. Thus, the thermosensitive liposomes should be engineered using those phospholipids having T_m slightly higher than body temperature. Dipalmitoyl-phosphatidylcholine (DPPC) is the most suitable candidate in this case with T_m of 41.4 °C. However, drug leakage and hiding from opsonization are refrained by mixing of phospholipids with high T_m and coating with PEG, respectively (Kneidl et al., 2014). This nominal hyperthermia can be induced by focused, high-intensity ultrasound waves, radio waves ablation or through NIR irradiation (Al-Jamal et al., 2009; Gasselhuber et al., 2012). Indocyanine green (ICG)-loaded thermosensitive liposomes was shown to have improved tumor biodistribution and anti-tumor activity evaluated in TNBC xenograft mice models. The release was triggered by NIR laser radiation-induced mild hyperthermia (Shemesh et al., 2015). Combination of DPPC and hydrogenated phosphatidylcholine could provide liposomal stability up to 40 °C. However, using high-intensity focused ultrasound (HIFU) mid hyperthermia (42 °C) can be induced followed by the complete released of entrapped anti-cancer drug, doxorubicin, and the MR contrast agent, gadoteridol. This study was carried out and evaluated in gliosarcoma-bearing Fischer 344 rats. The MR-images have revealed the considerable uptake of doxorubicin and contrast agent followed by hyperthermic induction (de Smet et al., 2011). Generation of TSL-Ts is also possible by loading the PEG-coated liposomes with ammonium bicarbonate. This stabilized system (at optimum body temperature) can cause abrupt release of entrapped imaging and therapeutic agents when exposed to mild hyperthermic conditions approx. at 42 °C. Bubble CO_2 generation usually damages the lipid bilayer system followed by release of the entrapped contents (Xia et al., 2017). The release mechanism of TSL-Ts is illustrated in Fig. 5.6.

5.3.1.3.2 Redox-Responsive Liposomal Theranostics

ROS are, merely, the by-products produced in a result of electron transport chain and protein folding process. Hydrogen peroxide (H_2O_2), a ROS, is considered exhibiting a vital role in cell differentiation and proliferation; however, its excess levels could be responsible for cellular apoptosis. Thus, there is definite presence of

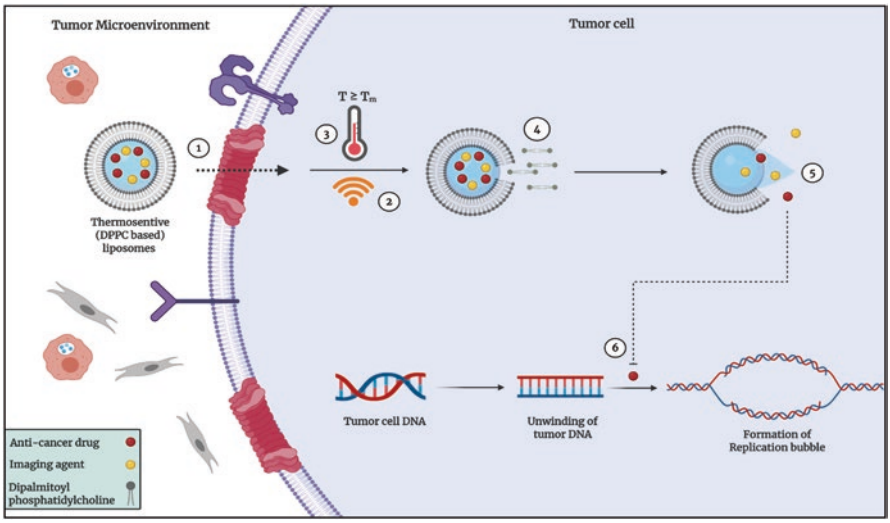

Fig. 5.6 DPPC-based TSL for targeted and intra-tumor delivery of theranostics. (1) ERP mediated TSL internalization in tumor cells. (2) Incidence of high-frequency focused ultrasound (HIFU). (3) HIFU-mediated mild hyperthermia to achieve temperature about 42 °C > T_m. (4) Hyperthermia (42 °C) causes either the transition of gel phase DPPC into a crystalline liquid state or the formation of CO_2 bubbles that disrupt lipid bilayer. (5) Release of entrapped content due to membrane destabilization owing to erstwhile mentioned DPPC transition. (6) Inhibition of tumor cell DNA replication through the release of entrapped anti-cancer drugs

H_2O_2 in tumor cells which is required to be regulated in certain limits owing to the harmful effects of its high concentration (Lennicke et al., 2015). Chen et al. have fabricated novel H_2O_2-responsive pegylated liposomes. In detail, they have formulated horseradish peroxidase (HRP) and its substrate- 2,2′-azino-bis(3-ethylbenzothiazoline-6-sulfonic acid) (ABTS)-loaded stealth liposomes. Liposomal-loaded HRP, in the presence of H_2O_2, stimulates the conversion of colorless ABTS into the greenish ABTS which are capable to absorbing NIR radiations. In response, it emits back-radiations, detected by PA imaging, and heat, both are responsible for cancer theranostic properties (Chen et al., 2017). These redox-sensitive liposomes are, however, tested against breast cancer and brain glioma grafted BALB/c mice models.

5.3.1.3.3 pH-Sensitive Liposomal Theranostics

The concept of pH-sensitive drug delivery arose due to the acidic environment of infected, inflamed, injured, and cancerous cells/tissues. This “smart” drug delivery system was proved to be an efficient tool for targeted delivery of therapeutic as well as diagnostic agents. Generally, the stabilized pH sensitive liposomes (stable at neutral or physiological pH) are constructed using two core

components, viz., amphiphilic stabilizers and pH-responsive lipids (Paliwal et al., 2015). These core components are enlisted in Box 5.1. The mechanism of drug released from pH sensitive liposomal theranostics depends upon the target environment pH, lipid employed for construction, and stabilizer used. The chief lipid imparting pH-sensitive characteristics to the designed liposomes is dioleyl-phosphatidy lamine (DOPE). It is often intercalated with amphiphilic stabilizers or acids. At neutral pH and in presence of amphiphilic stabilizer, the DOPE forms a stabilized lipid bilayer. However, when pH drops down (becomes acidic), i.e., in cellular lysosomes or endosomes, the protonation of amphiphilic stabilizer leads to the transformation of lipid into inverted lamellar layer. Ultimately, the membrane destabilization would cause the release of entrapped materials (Kanamala et al., 2019; Paliwal et al., 2015).

Box 5.1: pH-Responsive Molecules

pH-responsive lipid moieties

- Di-oleoyl-phosphatidylethanolamine (DOPE)
- Egg Phosphatidylcholine (EPC)
- Palmitoyl homocysteine (PHC)
- Poly- oleoyl-phosphatidylethanolamine (POPE)
- Di-palmitoyl-phosphatidylcholine (DPPC)
- Monophosphoryl Lipid A
- Gemini Palmitoyl homocysteine (GPHC)

pH sensitive peptides and polymers

- $H_7K(R_2)_2$ peptide
- Succinylated poly (glycidol)

Amphiphilic stabilizer

- Acidified PEG
- Tween 80

Due to the comparative acidic pH (6.5) of solid tumor microenvironment, the pH-responsive liposomes can be considered as an effective theranostic tool in oncology owing to their targeted delivery characteristics. An attempt was made to fabricate $H_7K(R_2)_2$ peptide conjugated with egg phosphatidylcholine and 1,2-distearoyl-sn-glycero-3-phosphocholine (DSPC)-based liposomes loaded with paclitaxel and iron oxide magnetic NPs for MRI monitoring of tumor biodistribution and anti-tumor activity against nude BALB/c mice bearing MDA-MB-231 breast carcinoma model (Zheng et al., 2018). The results of the study were clear indicative of pH responsiveness of the designed nanosystem.

5.3.1.3.4 Significance of Stimuli-Responsive "Smart" Liposomal Theranostics

The exposure of anti-cancer agents and imaging agents to the normal body cells are associated with few un-avoidable consequences. They get accumulation inside rapidly dividing body cells, irrespective whether they are tumor cells or normal body cells. Many solid tumors have comparatively slower cell division than the bone marrow and epithelial cells. Thus, the chances of their toxicity are high even at therapeutic dosing regimen (Remesh, 2012). Smart liposomes provide targeted tumor cell internalization of theranostics and eschew the anti-cancer associated toxicity.

5.3.1.4 Liposomal Nanotheranostics in Clinical Trials

In the process of drug/formulation discovery and approval, every step owns a specific significance. Pre-clinical or animal studies usually provide preliminary information about the safety and efficacy of designed formulation or drug. Thus, successful preclinical studies are followed by the set of human trials to assess efficacy and safety in the human population (Akhondzadeh, 2016). In context to lipid-based cancer nanotheranostics, vast pre-clinical research, discussed in previous sections, has been carried out and forwarded some of the candidates in human clinical trials enlisted in Table 5.4.

Table 5.4 Liposomal nanotheranostics under clinical trials

Designed liposomes	Imaging agents	Imaging technique	Target tumor	Sponsor/ location	Phase/type of trial	Trial no. reference
Dox-loaded HER-2 labelled stealth liposomes (MM-302)	Cu-64	PET scan	Metastatic breast cancer	Merrimack pharma./ multiple cancer centers of USA	Phase-1/ open label, multi-center human study	NCT01304797 Lee et al. (2017)
Dox-loaded thermosensitive liposomes	–	Focused USG	Hepatic cancer	University of Oxford/ Churchill Hospital, UK	Phase-1/ open label, single center human study	NCT02181075 Lyon et al. (2018)
Dox-loaded stealth liposomes	Tc-99 m	SPECT	Ovarian cancer	Lineberger comprehensive cancer center[a]	–	– Giovinazzo et al. (2016)
Stealth liposomes	Re-188	–	Solid metastatic cancer	Institute of Nuclear Research, Taiwan	Phase-1/ open label, single group assignment	NCT02271516 Madamsetty et al. (2019)

[a]And few other institutes as well. For detail information view reference no. [58]

5.3.2 Solid Lipid Nanoparticles (SLNs)

Solid lipid NPs are another lipid-based, colloidal nanocarriers employed for the purpose of theranostic delivery. They are constructed using solid lipids and surfactant to form solid lipid core and coat, respectively. Both hydrophilic and lipophilic moieties can be incorporated in solid lipid core or intercalated in outer surfactant layers (Paliwal et al., 2020). These nanocarriers provide adequate protection to degradable substances including proteins, vaccines, RNA, and acid labile therapeutics and diagnostics. In addition, entities with poor intestinal absorption also appeared to exhibit significantly improved bioavailability using SLN-mediated delivery (Ganesan et al., 2018). In fact, these nanocarriers have superior stability over liposomes owing to their duo ingredients – lipids and surfactants. In other words, they possess characteristics of both liposomes and niosomes. Furthermore, it is not associated with entrapped contents leakage. These nanosize ranged carriers (50–200 nm) can be modified either by the attachment of ligands, for targeting, or polymerically coated to veil these nanocarriers from the body's innate immune response (Sajid et al., 2019). The general structure and composition of SLNs theranostics have been graphically represented in Fig. 5.2.

5.3.2.1 SLNs: A Vehicle for Cancer Theranostics

In comparison to liposomes, they are less investigated for theranostic purpose. Kuang et al. have designed an admirable cancer nanotheranostic through utilization of NIR based iodinated dye other than ICG- the IR-780. Due to its hydrophobicity, cRGD-labeled SLNs have been used as a drug delivery system. This technique was found to be valuable owing to its imaging-guided photothermal therapy (PTT) against U87MG tumor cells incorporated in nude mice. Results of this study was clearly showing the enhanced biodistribution, integrin receptor (expressed by tumor cells) targeting evaluated through NIR fluorescence imaging, and tumor size reduction followed by designed SLNs delivery (Kuang et al., 2017). SLNs can also hold QDs, in addition to the anti-cancer agents, with surface-attached siRNA. This was another SLN-based approach for optically detectable cancer therapeutics fabricated, studied, and evaluated by Bae and co-workers (Bae et al., 2013). Solid lipid nanoparticles are the appropriate drug delivery system owing to their passive cancer targeting due to EPR of tumor microenvironment (Bayón-Cordero et al., 2019). In addition, the other positive parameters of SLNs are discussed in Sect. 5.6. The SLN-based cancer theranostics are under preclinical investigation and yet to be recruited for clinical trials.

5.3.3 Nanostructured-Lipid Carriers (NLCs)

Nanostructured-lipid carriers (NLCs) are a biocompatible nanosystem formed by the binary combination of solid and liquid lipids. This combination of lipids with different physical states are beneficial in terms of good loading efficacy and sustain

release profile of entrapped contents rather than the expulsive release which is observed with SLNs (Müller et al., 2002). Unlike liposomes, they are also quite stable at room temperature (Haider et al., 2020; Müller et al., 2000). Because of these positive aspects, NLCs are another optimal candidate for the delivery of cancer theranostics.

5.3.3.1 NLCs for Cancer Theranostics

In an attempt of designing NLCs for cancer theranostics, L.D. Olerile et al. have fabricated QD and paclitaxel co-loaded NLCs. This designed nanosystem was found to have better entrapment and loading efficacy with biphasic content release pattern. Moreover, the current nanotheranostics was also shown to be capable of killing and detecting, through NIR fluorescence imaging technique, of H22 hepatocellular carcinoma in female Kunming mice models (Olerile et al., 2017). The results of this study have demonstrated that NLCs are another convenient approach for theranostics delivery. In addition to loading, therapeutic and imaging agents can also be coated over NLCs. To demonstrate this proof of concept, AMD-3100-coated, IR-780-loaded NLCs have been fabricated. AMD-3100, a chemokine receptor inhibitor, prevents the invasion of breast cancer to its myriad metastasis locations. IR-780, however, is a NIR fluorescence dye with an excessive stability profile than ICG. Thus, the prepared NLCs have appeared as a suitable strategy for multimodal theranostics having characteristics of metastasis inhibition, PTT against tumor and NIR fluorescence detection (Olerile et al., 2017). Both of these studies are providing clear evidence regarding benefits of NLCs as cancer theranostics.

5.3.4 Lipoprotein-Based Nanocarriers

5.3.4.1 Lipoprotein Nanocarriers: Natural Nanoparticles

Lipoproteins are the endogenous nano-carriage system for fat molecules (cholesterols and acyl triglycerides) trafficking across the body tissues and cells because they are unable to move freely in plasma. The basic structure of natural bodily lipoproteins consists of phospholipid monolayer with embedded apolipoprotein molecules mentioned in Fig. 5.2. Chylomicrons, low-density lipoproteins (LDL), high-density lipoproteins (HDL), and very low-density lipoproteins (VLDL) are the most common examples of natural lipoproteins. Using this natural approach, the successful and efficacious delivery of hydrophobic, i.e., poorly aqueous soluble anti-cancer entity and imaging moiety is possible. Their entrapment inside the lipoprotein facilitates conveyance to their respective tumor sites. Myriad cancer cell studies have shown that only the nanoparticles with diameter less than 40 nm are capable of surpassing neoplastic cells. Contrary to the previously discussed lipid nanotheranostics, the lipoprotein nanoassemblies are the promising carriers, owing to their easily attainable small diameter – less than 40 nm. Moreover, the problem of instability of phospholipid NPs can also be overruled by utilizing lipoprotein NPs; the

incorporation of α-helical apolipoproteins provides ultrastability to the designed NPs (Kuai et al., 2016; Ng et al., 2011). Among erstwhile mentioned lipoproteins, LDL and HDL (small-sized, approx. 12 nm, lipoproteins) are the appropriate choice for cancer nanotheranostics.

5.3.4.2 Natural Lipoprotein Modification: Strategies for Designing of Delivery System

Usually several strategies can be used to modify natural lipoproteins into an appropriate nanosized carrier system. Amino acid-mediated covalent attachment of imaging agent, therapeutic agent, and the targeting moiety to the apolipoproteins is one of the suitable methods for lipoprotein alteration. In addition to the protein molecules, phospholipid polar heads can also be another appropriate site for covalently bonding of abovementioned crucial components. Furthermore, the targeting, imaging, and therapeutic moiety can also be intercalating these substances in between the superficial lipid layers. Lastly, the core loading of drug which the fabrication of reconstituted lipoprotein is the modest approach for hydrophobic drug and imaging agent delivery (Kornmueller et al., 2019; Ng et al., 2011). Existing technology of lipoprotein nanotheranostics are discussed in the next section. The core components of reconstituted HDL and LDL nanocarriers are stated in Table 5.5.

5.3.4.3 Lipoprotein Nanocarriers: A Tumor-Targeted Delivery System

It has been evaluated that cancer patients fall short in plasma cholesterol levels. The reason behind this reduction is the utilization of the body's cholesterol by explosively dividing tumor cells. Cholesterol is usually acquired by tumor cells for angiogenesis, metastasis, and cell membrane development, as cholesterol is an essential component of biological membranes. To fulfil the demand of cancer cells,

Table 5.5 Core structural components of "reconstituted lipoprotein nanocarriers"

Type of Lipoprotein	Phospholipid	Apoprotein	Reference
HDL	Dimyristoyl-phosphatidylcholine	Apolipoprotein A-I	Cao et al. (2009); Lin et al. (2014)
	Egg phosphatidylcholine		Corbin et al. (2007); Shahzad et al. (2011)
	–	Apolipoprotein A-Π	McMahon et al. (2015)
LDL	1,2-hexadecanediol	Apolipoprotein A-I	Glickson et al. (2008)
	1,2-disteraoyl-phosphatidylethanolamine	Apolipoprotein B	Jasanada et al. (1996)

endogenous lipoproteins provide cholesterol to them (Brown, 2007; Cruz et al., 2013; Simons & Ikonen, 2000). These lipoproteins, mainly HDL, undergo tumor cell internalization and accumulation through particular types of surface receptors expressed by the tumor cells. These receptors are referred as Scavenger receptor type B1 (SR-B1) (Danilo et al., 2013; Shahzad et al., 2011). This approach can be beneficial for selective tumor delivery of therapeutics and diagnostics. Fabricated lipoprotein NPs can deliver exogenous imaging agents and therapeutics specifically to the tumor cell, merely, through SR-B1 receptors mediated active targeting and other surfaced attached receptors, like folate receptors (FR) (Gorin et al., 2012).

5.3.4.4 Lipoprotein Nanocarriers for Cancer Theranostics

Liposomes and other lipid nanocarriers should be required to coat with polymers to make them biocompatible. However, these apolipoprotein-based lipid nanocarriers are biocompatible owing to their structure analogy with naturally occurring fat carriers – HDL and LDL. These nanosystems have been reconstituted for drug delivery as mentioned in previous sections. Various studies have been conducted to deliver cancer therapeutics as they are internalized in tumor cells through LDL and scavenger receptors (McMahon et al., 2015). To maximize its tumor targeting ability, surface modification using FR receptor is an appropriate approach (Corbin et al., 2007). An analogue of naturally derived NIR fluorescent dye, bacteriochlorin e6 bisoleate, was incorporated inside DMPC and Apo-A1 reconstituted HDL lipoproteins to selectively target tumor cells. This designed nanosystem proved to have enhanced LDL receptor mediated tumor internalization evaluated through NIR imaging. These nanoparticles were also claimed to possess ROS generation ability and PDT anti-tumor activity (Cao et al., 2009). Radiolabeled reconstituted LDL nanosystem has also been designed for the purpose of targeted delivery and tumor localization of imaging and contrast agents, however, to the best of our knowledge very less data is available regarding LDL-based nanotheranostics (Jasanada et al., 1996).

5.4 Distinctive Lipid-Based Nanotheranostics

5.4.1 Porphysomes: The Porphyrin-Lipid Hybrid Nanocarriers

Porphysomes are phospholipid and porphyrin hybrid, spherical nanostructures consisting of pyro-lipids and cholesterol. Pyro-lipid is the combination of phosphatidylcholine-based lipids and porphyrin (Huynh & Zheng, 2014; Tang et al., 2018). To understand the functionality of porphysomes, the role of porphyrins in cancer phototherapy must be discussed. *Porphyrins* are the organic substances with proven clinical significance in myriad types of biomedical noninvasive imaging technologies including magnetic resonance, nuclear, and fluorescent imaging. Not

only limited to diagnosis, they also possess PDT-mediated anti-tumor properties (Gomes et al., 2018). Structurally, this class of organic compounds is composed of four pyrrole rings merged through methine linkages having 22-Π electrons. These photosensitizers are luckily soluble in water and administered intravenously for imaging and PDT (Dougherty et al., 1998). Targeting potential of porphysomes can be further enhanced by labeling the surface with certain ligands of the receptors, particularly FR, overexpressed by the tumor cells (Jin et al., 2014).

5.4.1.1 Porphyrin-Loaded Lipid Nanocarriers and Porphysomes

It should be kept in mind that porphysomes are distinct from porphyrin lipid NPs. In porphyrin-loaded lipid nanocarriers, as mentioned in Sect. 5.4, bacteriochlorin, a porphyrin-based fluorescent dye and other porphyrins, are encapsulated inside the rHDL and other lipid nanocarriers for targeted tumor accumulation (Cao et al., 2009; Jin & Zheng, 2011). In contrast, porphysomes are the hybrid structure in which phospholipids are conjugated with porphyrins, as illustrated graphically in Fig. 5.7a, b.

5.4.1.2 Mechanism for Tumor Imaging and Anti-tumor Activity

Porphyrin-laden liposomes and other nanocarriers possess PDT-based tumoricidal characteristics only (Richter et al., 1993). But when porphyrins are conjugated with phospholipid molecules to form pyro-lipids liposomes, they appear to exhibit multifunctional imaging as well as PDT- and PTT-mediated anti-tumor properties. But membrane incorporation should be limited to molar fractions of total phospholipid content, for the purpose to avoid nanosystem instability (Lovell et al., 2011). Free pyro-lipids are also lacking with theranostic properties. Porphysomes, upon light irradiation, transform light energy into heat energy via fluorescence quenching. The heat energy generated causes the destruction of tumor cells. This phenomenon is referred to as photothermal therapy. Furthermore, they also promote the ROS and singlet oxygen genesis which could cause PDT destruction of tumor cells. The detection of porphysomes is usually carried out through PA imaging. These characteristics of porphysomes are shown in Fig. 5.7. Thus, porphysomes are the suitable nano-candidates due to their PDT- and PTT-mediated cytotoxicity and PA imaging for diagnosis and assessing its biodistribution (Lovell et al., 2011; Tang et al., 2018).

5.4.1.3 Porphysomes for Cancer Theranostics

As stated earlier, porphysomes can be used for optical visualization of targeted anti-tumor PTT. The research group of Canada and China have designed the porphyrin-lipid hybrid liposomal mimicking nanocarriers – the porphysomes. This nanosystem was found to be beneficial in terms of selective assassination of tumor cells via PDT

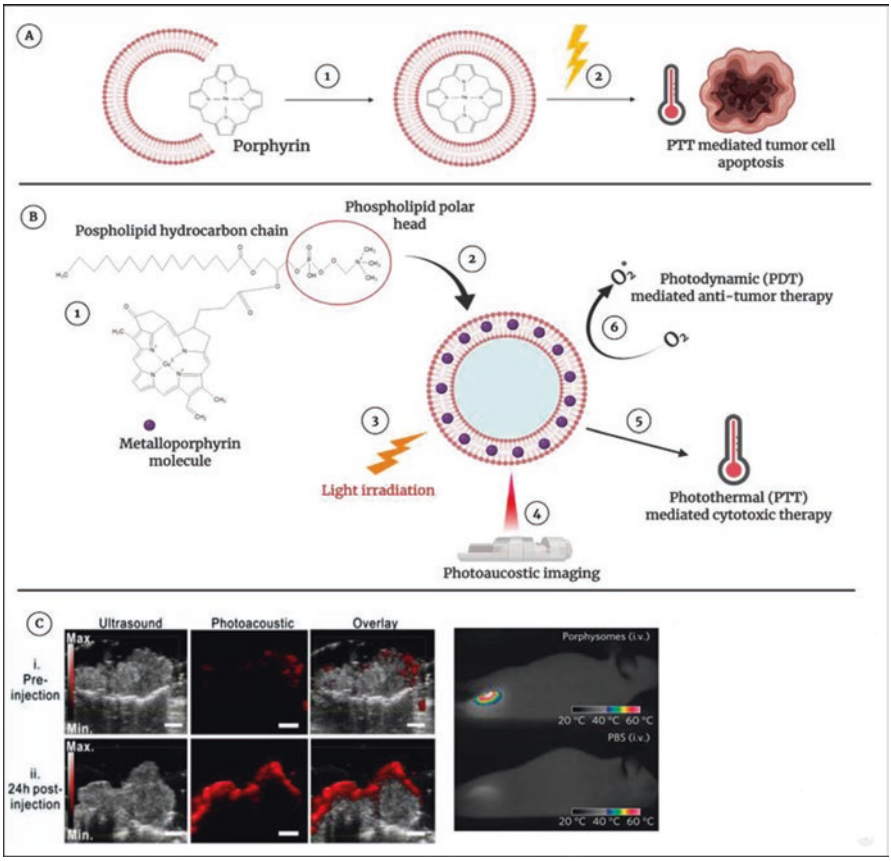

Fig. 5.7 (**a**) Porphyrin-loaded liposomes mediated PTT for tumor apoptosis. (1) Liposomes are passively loaded with porphyrin. (2) Light irradiation cause fluorescence quenching and increase in temperature which ultimately results in tumor destruction. (**b**) Porphysomes mediated PTT, PDT, and PA imaging. (1) Formation of pyro-lipids by the conjugation of metalloporphyrin and phospholipids. (2) Self-assembling of liposome like nanocarrier. (3) Light irradiation to porphysomes results in (4) fluorescent quenching and generation of laser used in PA imaging, (5) surge in temperature of tumor microenvironment above 40 °C (PTT), and (6) production of singlet oxygen for PDT. (**c**) PA-guided PTT therapy against oral carcinoma in Hamster models using novel pyro-lipid-based nanocarrier – porphysomes. (Reprinted with Permission from Muhanna et al., 2015)

and PTT. In addition, these pyro-lipids spherical nano-structures can be superficially modified and attached with certain ligands to maximize the tumor targeting (Jin et al., 2014). Apolipoprotein-E modified pyro-lipids nanocarrier has also been designed to target U87 glioblastoma cells. Analysis was made using NIR fluorescence imaging and tumor cells have shown to exhibit higher concentration of nanocarriers. In addition, the targeted PTT and PDT therapy was found to be associated with approx. 80% reduction in live tumor cells (Rajora et al., 2017). The porphysomes are, in fact, multimodal imaging systems similar to that of inorganic

nanoparticles. These are capable not only for eradication of primary tumors but also clear the metastasized lymph nodes without damaging the adjacent tissues (Muhanna et al., 2015). Following all-in-one strategy, radionuclide labeled ^{64}Cu-porphysomes has been designed and evaluated against orthotopic prostate and bony metastatic cancers. The results have shown targeted tumor killing which has been evaluated through PET and fluorescence imaging (Liu et al., 2013).

5.4.2 Lipid-Protected Calcium Phosphate NPs

Alkylating agents, nucleic acid-based cancer therapeutics, i.e., siRNA, other small molecule chemotherapeutics and theranostics, can be delivered safely through calcium phosphate (CaP) NPs. However, their formulation encounters troublesome precipitation that prevents the formation or alters the stability of its colloidal dispersion. To avoid it, CaP NPs are usually shielded inside a lipid or polymeric casing. In this section, we will focus toward lipid-protected (L) CaP NPs (Huang et al., 2018). General structure of L-CaP NPs consists of inorganic CaP core surrounded by the cationic lipids, i.e., DOPA molecules, in bilayer pattern as shown in Fig. 5.8. In addition, some stabilizers are also incorporated to tackle the suspected aggregation (Li et al., 2010; Tang et al., 2015). In comparison to other inorganic NPs, this nanosystem is safe and tolerable owing the functional Ca^{2+} efflux pumps expressed by cells which prevents Ca^{2+} intracellular accumulation and ultimately Ca^{2+} induced cytotoxicity (Tseng et al., 2013).

5.4.2.1 L-CaP NPs for Cancer Theranostics

Theranostic loading inside L-CaP NPs is usually attained through co-precipitation method. In other words, the loading candidate forms co-precipitate and form complex inside CaP core. L-CaP nanosystems can attain multimodal imaging and therapeutic characteristics through the incorporation of myriad agents inside the CaP core. Furthermore, these nanocarriers exhibit pH sensitive release (at acidic pH) of their payloads (Bisht et al., 2005; Li et al., 2010). Tri-modal imaging CaP nanosystems have been designed to detect the tumor through MR, fluorescence, and nuclear imaging in animal models. This was achieved by incorporation of Gd contrast agent, indocyanine green and 99 m-Tc, respectively. The radio-isotope would possibly impart anti-tumor properties to the designed nanosystem (Ashokan et al., 2013; Wang et al., 2018). Lutetium-177 loaded L-CaP nanosystem designing was another step forward toward cancer theranostics. This radioisotope encapsulated nanosystem emits γ-radiations which are responsible for biodistribution and pharmacokinetic determination through SPECT and Cerenkov imaging. However, the emittance of β-radiation will cause tumor cell destruction and inhibition of tumor growth in the xenograft mice model. The comparison between the plain ^{177}Lu and ^{177}Lu-L-CaP NPs in terms of anti-tumor activity was also made which is clearly indicating

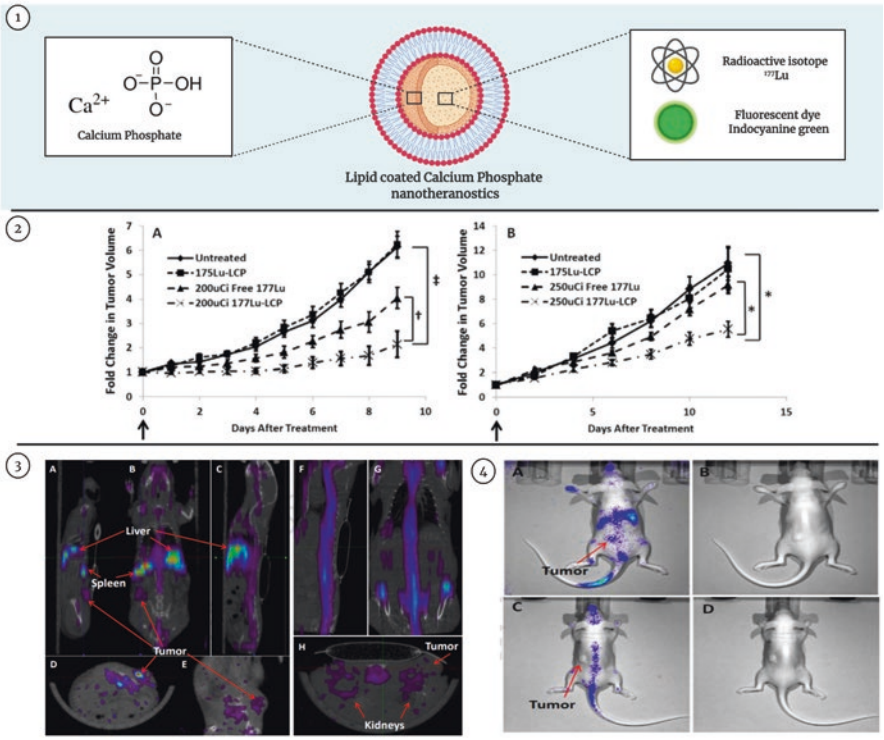

Fig. 5.8 (**1**) General structure of Lipid protected calcium phosphate nanotheranostic. (**2**) Increase in tumor volume followed by treatment with placebo (untreated), ^{175}LU-L-CaP, 200nCi free ^{177}Lu and 200uCi ^{177}Lu-L-CaP (Satterlee et al., 2015). (**3**) SPECT imaging obtain 24 hours post injection of ^{177}Lu-L-CaP showing the improved accumulation of nanosystem (A–E) in tumor, liver, and spleen, whereas plain ^{177}Lu (F–H) was concentrated in bone and kidneys. (Reprinted with Permission from Satterlee et al., 2015). (**4**) Cerenkov luminescence imaging post treatment showing liver, spleen, and tumor accumulation of ^{177}Lu-L-CaP (A). Whereas free ^{177}Lu (C) accumulates in bone and particularly spine. (Reprinted with Permission from Satterlee et al., 2015)

nanosystem superiority owing to targeted tumor accumulation (Satterlee et al., 2015) Fig. 5.8 is showing the biodistribution results of ^{177}Lu-L-CaP NPs evaluated through SPECT and Cerenkov imaging. Moreover, the intensity of tumor volume reduction is also shown graphically in the same figure.

5.5 Superiority of Lipid-Based Nanotheranostics

As discussed erstwhile, conventional theranostics are usually encountered with myriad problems that are limiting their use. Employment of nanomaterials in cancer theranostics is valuable because of targeted tumor delivery, monitoring, and reduced toxicity profile. Among various types of nanomaterials, lipid-based nanomaterials

are one of the suitable options for increasing efficacy and use of theranostics, owing to its size range. They are only capable of crossing tumor cells but unable to penetrate inside the normal cells. The most investigated lipid-based nanosystem, *liposomes*, are capable for provision of guarded and targeted theranostics delivery to the tumor site. Apart from naturally derived phospholipid-liposomes, synthetic liposomal formulations were found to be more stable (Grit & Crommelin, 1993). Moreover, cationic and surface modified liposomes have potential for targeted drug delivery to tumor sites – merely a reason for low toxicity (Mahira et al., 2019; Singh et al., 2016; Trubetskoy et al., 1992). Smart phospholipid carriers are also considered as an efficient delivery tool for Gd-based contrast media, radioisotopes, fluorescent, and NIR dyes as well, along with therapeutic anti-cancer agents. SLNs-based theranostics have improved stability along with the entrapped content expulsion at slow or controlled rate. Just like liposomes, *SLNs* are biocompatible and biodegradable drug delivery systems. SLNs encapsulated theranostics can be administered through a variety of routes including oral, parenteral, intranasal, and ocular (Bayón-Cordero et al., 2019). *NLCs*, as mentioned erstwhile, are constructed by the combination of solid and liquid lipids which imparts numerous beneficial characteristics to them. These nanocarriers overcome the use limiting factors of both liposomes and SLNs. In fact, they have good content loading ability, sustain release characteristics, as well as improved stability at room temperature (Haider et al., 2020). *Lipoproteins (HDL and LDL) nanosystems* are advantageous owing to their structure similarity with endogenous cholesterol carriers. Another positive point is the tumor targeting through SR-B1 receptors. Both are the valuable points for utilization of these NPs for cancer theranostics (McMahon et al., 2015). *Porphysomes* are the innovative nanotheranostic vehicle with myriad benefits. In contrast to conventional theranostic approaches, they are associated with simultaneous PTT- and PDT-based tumor killing and PA imaging-based therapy monitoring. They are superior to the inorganic and metallic NPs in terms of better safety profile (Lovell et al., 2011; Tang et al., 2018). Protected delivery of small molecule chemotherapeutics, alkylating agents, and siRNA along with radiolabeled and other imaging agents can be achieved through employing *L-CaP NPs*. They also hold a better safety profile in comparison to other metallic and inorganic nanotheranostics (Tseng et al., 2013).

5.6 Drawbacks Associated with Lipid-Based Nanotheranostics

Despite their benefits, the lipid nanomaterials are also associated with multiplex challenges and possess few drawbacks as well. In this section, we are going to discuss these limitations. Liposomal nano-formulation experience several stability problems such as leakage of entrapped moieties due to hydrolysis and oxidation of bilayer (Crommelin et al., 1986). Moreover, as a result of the body's response, they undergo rapid degradation, plasma clearance, and elimination. The reason behind is

that the body considers liposomes as foreign harmful materials and triggers the defense mechanism particularly opsonization and reticuloendothelial system (Sercombe et al., 2015). SLNs associated problems, low content loading and an expulsive release pattern, are already mentioned. Associated challenges with lipoprotein nanotheranostics are the isolation of lipoprotein nanosystem constituents, particularly apolipoproteins, which is the problematic task. If apolipoproteins are obtained through bacterial culture, the microbial contamination is a challenging factor. Proper isolation and post-isolation purification should be done with appropriate care and protocols in order to avoid the expected microbial contamination (Nykiforuk et al., 2011). Porphysomes administration in animal models have been found to cause some damaging effects which include alteration in liver enzymes and blood cells profile. Furthermore, this nanosystem also gets accumulation in several organs including heart, spleen, kidneys, and lungs. Conjugation of excessive porphyrin with phospholipids can cause the instability of nano-formulation (Lovell et al., 2011). Overall, the lipid-based nanomaterials are safe to be used for cancer theranostics in comparison to carbon nanotubes and inorganic and metallic nanosystems (Kobayashi et al., 2017; Sawicki et al., 2019). The stability problem of liposomes can be overcome by the addition of cholesterol or the adoption of SLNs or NLCs.

5.7 Future Perspective and Conclusion

Cancer nanotheranostics are associated with targeted treatment and real time simultaneous diagnosis and monitoring. In the domain of lipid nanomaterials, liposomal formulations are thoroughly investigated, on pre-clinical grounds, for their cancer theranostic application with enrollment of some candidates in clinical trials mentioned erstwhile in Table 5.4. Through critical evaluation of available literature, it has been concluded that lipid nanotheranostics are able for provision of improved tumor targeting, reduced toxicity profile, and enhanced theranostic efficacy. In addition, the targeting potential can be maximized by the employment of surface engineered liposomes and other smart liposomal nanosystems. In fact, the smart liposomal nanotheranostics are the suitable candidate to be investigated in the human, owing to their satisfactory pre-clinical results. Porphysomes, because of their inherent properties, are also found to possess valuable theranostic properties and high-quality PA detection. Lipoproteins and L-CaP nanosystems are newly explored nanomaterials for cancer theranostic applications. Just like liposomes, they can hold a variety of anti-cancer agents- chemotherapeutics, immunotherapeutics and SiRNA, along with co-loading of MRI contrast agents, QDs, radioactive isotopes and fluorescence dyes. Despite the promising results of pre-clinical investigations, there is an utmost requirement for academia and industry research collaboration to facilitate further explorations and promotion of valuable nanotheranostics candidates towards clinical trials.

References

Akhondzadeh, S. (2016). The importance of clinical trials in drug development. *Avicenna Journal of Medical Biotechnology, 8*(4), 151.

Al-Jamal, W. T., Al-Jamal, K. T., Tian, B., Cakebread, A., Halket, J. M., & Kostarelos, K. (2009). Tumor targeting of functionalized quantum dot−liposome hybrids by intravenous administration. *Molecular Pharmaceutics, 6*(2), 520–530. https://doi.org/10.1021/mp800187d

Ashokan, A., Gowd, G. S., Somasundaram, V. H., Bhupathi, A., Peethambaran, R., Unni, A. K. K., et al. (2013). Multifunctional calcium phosphate nano-contrast agent for combined nuclear, magnetic and near-infrared in vivo imaging. *Biomaterials, 34*(29), 7143–7157. https://doi.org/10.1016/j.biomaterials.2013.05.077

Bae, K. H., Lee, J. Y., Lee, S. H., Park, T. G., & Nam, Y. S. (2013). Optically traceable solid lipid nanoparticles loaded with siRNA and paclitaxel for synergistic chemotherapy with in situ imaging. *Advanced Healthcare Materials, 2*(4), 576–584. https://doi.org/10.1002/adhm.201200338

Bayón-Cordero, L., Alkorta, I., & Arana, L. (2019). Application of solid lipid nanoparticles to improve the efficiency of anticancer drugs. *Nanomaterials, 9*(3), 474. https://doi.org/10.3390/nano9030474

Behzadi, S., Serpooshan, V., Tao, W., Hamaly, M. A., Alkawareek, M. Y., Dreaden, E. C., et al. (2017). Cellular uptake of nanoparticles: Journey inside the cell. *Chemical Society Reviews, 46*(14), 4218–4244. https://doi.org/10.1039/c6cs00636a

Beltrán-Gracia, E., López-Camacho, A., Higuera-Ciapara, I., Velázquez-Fernández, J. B., & Vallejo-Cardona, A. A. (2019). Nanomedicine review: Clinical developments in liposomal applications. *Cancer Nanotechnology, 10*(1), 11. https://doi.org/10.1186/s12645-019-0055-y

Bisht, S., Bhakta, G., Mitra, S., & Maitra, A. (2005). pDNA loaded calcium phosphate nanoparticles: Highly efficient non-viral vector for gene delivery. *International Journal of Pharmaceutics, 288*(1), 157–168. https://doi.org/10.1016/j.ijpharm.2004.07.035

Bray, F., Ferlay, J., Soerjomataram, I., Siegel, R. L., Torre, L. A., & Jemal, A. (2018). Global cancer statistics 2018: GLOBOCAN estimates of incidence and mortality worldwide for 36 cancers in 185 countries. *CA: A Cancer Journal for Clinicians, 68*(6), 394–424. https://doi.org/10.3322/caac.21492

Brown, A. J. (2007). Cholesterol, statins and cancer. *Clinical and Experimental Pharmacology and Physiology, 34*(3), 135–141. https://doi.org/10.1111/j.1440-1681.2007.04565.x

Bulbake, U., Doppalapudi, S., Kommineni, N., & Khan, W. (2017). Liposomal formulations in clinical use: an updated review. *Pharmaceutics, 9*(2), 12. https://doi.org/10.3390/2Fpharmaceutics9020012

Cao, W., Ng, K. K., Corbin, I., Zhang, Z., Ding, L., Chen, J., et al. (2009). Synthesis and evaluation of a stable bacteriochlorophyll-analog and its incorporation into high-density lipoprotein nanoparticles for tumor imaging. *Bioconjugate Chemistry, 20*(11), 2023–2031. https://doi.org/10.1021/bc900404y

Carrera, P. M., Kantarjian, H. M., & Blinder, V. S. (2018). The financial burden and distress of patients with cancer: Understanding and stepping-up action on the financial toxicity of cancer treatment. *CA: A Cancer Journal for Clinicians, 68*(2), 153–165. https://doi.org/10.3322/caac.21443

Chen, Q., Liang, C., Sun, X., Chen, J., Yang, Z., Zhao, H., et al. (2017). H2O2-responsive liposomal nanoprobe for photoacoustic inflammation imaging and tumor theranostics via in vivo chromogenic assay. *Proceedings of the National Academy of Sciences, 114*(21), 5343–5348. https://doi.org/10.1073/pnas.1701976114

Cittadino, E., Ferraretto, M., Torres, E., Maiocchi, A., Crielaard, B. J., Lammers, T., et al. (2012). MRI evaluation of the antitumor activity of paramagnetic liposomes loaded with prednisolone phosphate. *European Journal of Pharmaceutical Sciences, 45*(4), 436–441. https://doi.org/10.1016/j.ejps.2011.08.022

Corbin, I. R., Chen, J., Cao, W., Li, H., Lund-Katz, S., & Zheng, G. (2007). Enhanced cancer-targeted delivery using engineered high-density lipoprotein-based nanocarriers. *Journal of Biomedical Nanotechnology, 3*(4), 367–376. https://doi.org/10.1166/jbn.2007.053

Crommelin, D. J. A., Fransen, G. J., & Salemink, P. J. M. (1986). Stability of liposomes on storage. In *Targeting of drugs with synthetic systems* (pp. 277–287). Springer.

Cruz, P. M., Mo, H., McConathy, W., Sabnis, N. A., & Lacko, A. G. (2013). The role of cholesterol metabolism and cholesterol transport in carcinogenesis: A review of scientific findings, relevant to future cancer therapeutics. *Frontiers in Pharmacology, 4*, 119. https://doi.org/10.3389/fphar.2013.00119

Dai, W., Yang, F., Ma, L., Fan, Y., He, B., He, Q., et al. (2014). Combined mTOR inhibitor rapamycin and doxorubicin-loaded cyclic octapeptide modified liposomes for targeting integrin α3 in triple-negative breast cancer. *Biomaterials, 35*(20), 5347–5358. https://doi.org/10.1016/j.biomaterials.2014.03.036

Danilo, C., Gutierrez-Pajares, J. L., Mainieri, M. A., Mercier, I., Lisanti, M. P., & Frank, P. G. (2013). Scavenger receptor class B type I regulates cellular cholesterol metabolism and cell signaling associated with breast cancer development. *Breast Cancer Research, 15*(5), R87. https://doi.org/10.1186/bcr3483

Darguzyte, M., Drude, N., Lammers, T., & Kiessling, F. (2020). Riboflavin-targeted drug delivery. *Cancers, 12*(2), 295. https://doi.org/10.3390/cancers12020295

de Jonge, M. J. A., & Verweij, J. (Eds.). (2006). *Renal toxicities of chemotherapy. Seminars in oncology*. Elsevier.

de Smet, M., Heijman, E., Langereis, S., Hijnen, N. M., & Grüll, H. (2011). Magnetic resonance imaging of high intensity focused ultrasound mediated drug delivery from temperature-sensitive liposomes: An in vivo proof-of-concept study. *Journal of Controlled Release, 150*(1), 102–110. https://doi.org/10.1016/j.jconrel.2010.10.036

Ding, H., & Wu, F. (2012). Image guided biodistribution and pharmacokinetic studies of theranostics. *Theranostics, 2*(11), 1040. https://doi.org/10.7150/thno.4652

Dougherty, T. J., Gomer, C. J., Henderson, B. W., Jori, G., Kessel, D., & Korbelik, M. (1998). Photodynamic therapy. *Journal of the National Cancer Institute, 90*, 889. https://doi.org/10.1093/jnci/90.12.889

Feng, L., Cheng, L., Dong, Z., Tao, D., Barnhart, T. E., Cai, W., et al. (2017). Theranostic liposomes with hypoxia-activated prodrug to effectively destruct hypoxic tumors post-photodynamic therapy. *ACS Nano, 11*(1), 927–937. https://doi.org/10.1021/acsnano.6b07525

Fernández, M., Javaid, F., & Chudasama, V. (2018). Advances in targeting the folate receptor in the treatment/imaging of cancers. *Chemical Science, 9*(4), 790–810.

Foroozandeh, P., & Aziz, A. A. (2018). Insight into cellular uptake and intracellular trafficking of nanoparticles. *Nanoscale Research Letters, 13*(1), 339. https://doi.org/10.1186/s11671-018-2728-6

Ganesan, P., Ramalingam, P., Karthivashan, G., Ko, Y. T., & Choi, D.-K. (2018). Recent developments in solid lipid nanoparticle and surface-modified solid lipid nanoparticle delivery systems for oral delivery of phyto-bioactive compounds in various chronic diseases. *International Journal of Nanomedicine, 13*, 1569. https://doi.org/10.2147/IJN.S155593

Gasselhuber, A., Dreher, M. R., Partanen, A., Yarmolenko, P. S., Woods, D., Wood, B. J., et al. (2012). Targeted drug delivery by high intensity focused ultrasound mediated hyperthermia combined with temperature-sensitive liposomes: Computational modelling and preliminary in vivo validation. *International Journal of Hyperthermia, 28*(4), 337–348. https://doi.org/10.3109/02656736.2012.677930

Giovinazzo, H., Kumar, P., Sheikh, A., Brooks, K. M., Ivanovic, M., Walsh, M., et al. (2016). Technetium Tc 99m sulfur colloid phenotypic probe for the pharmacokinetics and pharmacodynamics of PEGylated liposomal doxorubicin in women with ovarian cancer. *Cancer Chemotherapy and Pharmacology, 77*(3), 565–573. https://doi.org/10.1007/s00280-015-2945-y

Glickson, J. D., Lund-Katz, S., Zhou, R., Choi, H., Chen, I. W., Li, H., et al. (2008). Lipoprotein nanoplatform for targeted delivery of diagnostic and therapeutic agents. *Molecular Imaging, 7*(2), 7290–2008. https://doi.org/10.2310/7290.2008.0012

Golombek, S. K., May, J.-N., Theek, B., Appold, L., Drude, N., Kiessling, F., et al. (2018). Tumor targeting via EPR: Strategies to enhance patient responses. *Advanced Drug Delivery Reviews, 130*, 17–38. https://doi.org/10.1016/j.addr.2018.07.007

Gomes, A. T. P. C., Neves, M. G., & Cavaleiro, J. A. S. (2018). Cancer, photodynamic therapy and porphyrin-type derivatives. *An. Acad. Brasil. Ciênc, 90*(1), 993–1026. https://doi.org/10.1590/0001-3765201820170811

Goodarzi, E., Moslem, A., Feizhadad, H., Jarrahi, A. M., Adineh, H. A., Sohrabivafa, M., et al. (2019). Epidemiology, incidence and mortality of thyroid cancer and their relationship with the human development index in the world: an ecology study in 2018. *Advances in Human Biology, 9*(2), 162. https://doi.org/10.4103/AIHB.AIHB_2_19

Gorin, A., Gabitova, L., & Astsaturov, I. (2012). Regulation of cholesterol biosynthesis and cancer signaling. *Current Opinion in Pharmacology, 12*(6), 710–716. https://doi.org/10.1016/j.coph.2012.06.011

Grit, M., & Crommelin, D. J. A. (1993). Chemical stability of liposomes: Implications for their physical stability. *Chemistry and Physics of Lipids, 64*(1–3), 3–18. https://doi.org/10.1016/0009-3084(93)90053-6

Guo, W., Chen, W., Yu, W., Huang, W., & Deng, W. (2013). Small interfering RNA-based molecular therapy of cancers. *Chinese Journal of Cancer, 32*(9), 488. https://doi.org/10.5732/cjc.012.10280

Haider, M., Abdin, S. M., Kamal, L., & Orive, G. (2020). Nanostructured lipid carriers for delivery of chemotherapeutics: A review. *Pharmaceutics, 12*(3), 288. https://doi.org/10.3390/pharmaceutics12030288

Hamilton, W. (2010). Cancer diagnosis in primary care. *British Journal of General Practice, 60*(571), 121–128. https://doi.org/10.3399/bjgp10X483175

Hardman, R. (2006). A toxicologic review of quantum dots: Toxicity depends on physicochemical and environmental factors. *Environmental Health Perspectives, 114*(2), 165–172. https://doi.org/10.1289/ehp.8284

Hesketh, P. J. (2017). Prevention and treatment of chemotherapy-induced nausea and vomiting in adults. UpDate, Jan. 2017.

Huang, J.-L., Chen, H.-Z., & Gao, X.-L. (2018). Lipid-coated calcium phosphate nanoparticle and beyond: A versatile platform for drug delivery. *Journal of Drug Targeting, 26*(5–6), 398–406. https://doi.org/10.1080/1061186x.2017.1419360

Huynh, E., & Zheng, G. (2014). Porphysome nanotechnology: A paradigm shift in lipid-based supramolecular structures. *Nano Today, 9*(2), 212–222. https://doi.org/10.1016/j.nantod.2014.04.012

Immordino, M. L., Dosio, F., & Cattel, L. (2006). Stealth liposomes: Review of the basic science, rationale, and clinical applications, existing and potential. *International Journal of Nanomedicine, 1*(3), 297.

Jasanada, F., Urizzi, P., Souchard, J. P., Favre, G., Boneu, A., & Nepveu, F. (1996). Indium-111 labeling of low density lipoproteins (LDL) with the DTPA-bis (stearylamide) for tumor localization: First imaging and biodistribution in B16 tumored mice. *Journal de Chimie Physique, 93*, 128–131. https://doi.org/10.1051/jcp/1996930128

Javed, Y., Akhtar, K., Anwar, H., & Jamil, Y. (2017). MRI based on iron oxide nanoparticles contrast agents: Effect of oxidation state and architecture. *Journal of Nanoparticle Research, 19*(11), 366. https://ui.adsabs.harvard.edu/link_gateway/2017JNR....19..366J. https://doi.org/10.1007/s11051-017-4045-x

Jin, C. S., Cui, L., Wang, F., Chen, J., & Zheng, G. (2014). Targeting-triggered porphysome nanostructure disruption for activatable photodynamic therapy. *Advanced Healthcare Materials, 3*(8), 1240–1249. https://doi.org/10.1002/adhm.201300651

Jin, C. S., & Zheng, G. (2011). Liposomal nanostructures for photosensitizer delivery. *Lasers in Surgery and Medicine, 43*(7), 734–748. https://doi.org/10.1002/lsm.21101

Kanamala, M., Palmer, B. D., Jamieson, S. M. F., Wilson, W. R., & Wu, Z. (2019). Dual pH-sensitive liposomes with low pH-triggered sheddable PEG for enhanced tumor-targeted drug delivery. *Nanomedicine, 14*(15), 1971–1989. https://doi.org/10.2217/nnm-2018-0510

Kaur, C. D., Mishra, K. K., Sahu, A., Panik, R., Kashyap, P., Mishra, S. P., et al. (2020). Theranostics: New era in nuclear medicine and radiopharmaceuticals. In *Medical isotopes*. IntechOpen.

Kenny, G. D., Kamaly, N., Kalber, T. L., Brody, L. P., Sahuri, M., Shamsaei, E., et al. (2011). Novel multifunctional nanoparticle mediates siRNA tumour delivery, visualisation and therapeutic tumour reduction in vivo. *Journal of Controlled Release, 149*(2), 111–116. https://doi.org/10.1016/j.jconrel.2010.09.020

Kneidl, B., Peller, M., Winter, G., Lindner, L. H., & Hossann, M. (2014). Thermosensitive liposomal drug delivery systems: State of the art review. *International Journal of Nanomedicine, 9*, 4387. https://doi.org/10.2147/IJN.S49297

Kobayashi, N., Izumi, H., & Morimoto, Y. (2017). Review of toxicity studies of carbon nanotubes. *Journal of Occupational Health*, 17–0089. https://doi.org/10.1539/joh.17-0089-ra

Kornmueller, K., Vidakovic, I., & Prassl, R. (2019). Artificial high density lipoprotein nanoparticles in cardiovascular research. *Molecules, 24*(15), 2829. https://doi.org/10.3390/molecules24152829

Krasnici, S., Werner, A., Eichhorn, M. E., Schmitt-Sody, M., Pahernik, S. A., Sauer, B., et al. (2003). Effect of the surface charge of liposomes on their uptake by angiogenic tumor vessels. *International Journal of Cancer, 105*(4), 561–567. https://doi.org/10.1002/ijc.11108

Kuai, R., Li, D., Chen, Y. E., Moon, J. J., & Schwendeman, A. (2016). High-density lipoproteins: nature's multifunctional nanoparticles. *ACS Nano, 10*(3), 3015–3041. https://doi.org/10.1021/acsnano.5b07522

Kuang, Y., Zhang, K., Cao, Y., Chen, X., Wang, K., Liu, M., et al. (2017). Hydrophobic IR-780 dye encapsulated in cRGD-conjugated solid lipid nanoparticles for NIR imaging-guided photothermal therapy. *ACS Applied Materials & Interfaces, 9*(14), 12217–12226. https://doi.org/10.1021/acsami.6b16705

Large, D. E., Soucy, J. R., Hebert, J., & Auguste, D. T. (2019). Advances in receptor-mediated, tumor-targeted drug delivery. *Advanced Therapeutics, 2*(1), 1800091. https://doi.org/10.1002/adtp.201800091

Lee, H., Shields, A. F., Siegel, B. A., Miller, K. D., Krop, I., Ma, C. X., et al. (2017). 64Cu-MM-302 positron emission tomography quantifies variability of enhanced permeability and retention of nanoparticles in relation to treatment response in patients with metastatic breast cancer. *Clinical Cancer Research, 23*(15), 4190–4202. https://doi.org/10.1158/1078-0432.ccr-16-3193

Lee, Y., & Thompson, D. H. (2017). Stimuli-responsive liposomes for drug delivery. *Wiley Interdisciplinary Reviews: Nanomedicine and Nanobiotechnology, 9*(5), e1450. https://doi.org/10.1002/wnan.1450

Lennicke, C., Rahn, J., Lichtenfels, R., Wessjohann, L. A., & Seliger, B. (2015). Hydrogen peroxide–production, fate and role in redox signaling of tumor cells. *Cell Communication and Signaling, 13*(1), 1–19. https://doi.org/10.1186/s12964-015-0118-6

Li, J., Chen, Y.-C., Tseng, Y.-C., Mozumdar, S., & Huang, L. (2010). Biodegradable calcium phosphate nanoparticle with lipid coating for systemic siRNA delivery. *Journal of Controlled Release, 142*(3), 416–421. https://doi.org/10.1016/j.jconrel.2009.11.008

Li, X., Taratula, O., Taratula, O., Schumann, C., & Minko, T. (2017). LHRH-targeted drug delivery systems for cancer therapy. *Mini Reviews in Medicinal Chemistry, 17*(3), 258–267. https://doi.org/10.2174/1389557516666161013111155

Lim, J. P., & Gleeson, P. A. (2011). Macropinocytosis: An endocytic pathway for internalising large gulps. *Immunology and Cell Biology, 89*(8), 836–843. https://doi.org/10.1038/icb.2011.20

Lin, Q., Jin, C. S., Huang, H., Ding, L., Zhang, Z., Chen, J., et al. (2014). Nanoparticle-enabled, image-guided treatment planning of target specific RNAi therapeutics in an orthotopic prostate cancer model. *Small, 10*(15), 3072–3082. https://doi.org/10.1002/smll.201303842

Liu, T. W., MacDonald, T. D., Jin, C. S., Gold, J. M., Bristow, R. G., Wilson, B. C., et al. (2013). Inherently multimodal nanoparticle-driven tracking and real-time delineation of orthotopic prostate tumors and micrometastases. *ACS Nano, 7*(5), 4221–4232. https://doi.org/10.1021/nn400669r

Liu, Y., Yang, F., Yuan, C., Li, M., Wang, T., Chen, B., et al. (2017). Magnetic nanoliposomes as in situ microbubble bombers for multimodality image-guided cancer theranostics. *ACS Nano, 11*(2), 1509–1519. https://doi.org/10.1021/acsnano.6b07525

Lossignol, D. (2016). A little help from steroids in oncology. *Journal of Translational Internal Medicine, 4*(1), 52–54. https://doi.org/10.1515/jtim-2016-0011

Lovell, J. F., Jin, C. S., Huynh, E., Jin, H., Kim, C., Rubinstein, J. L., et al. (2011). Porphysome nanovesicles generated by porphyrin bilayers for use as multimodal biophotonic contrast agents. *Nature Materials, 10*(4), 324–332. https://doi.org/10.1038/nmat2986

Lyon, P. C., Gray, M. D., Mannaris, C., Folkes, L. K., Stratford, M., Campo, L., et al. (2018). Safety and feasibility of ultrasound-triggered targeted drug delivery of doxorubicin from thermosensitive liposomes in liver tumours (TARDOX): a single-centre, open-label, phase 1 trial. *The Lancet Oncology, 19*(8), 1027–1039. https://doi.org/10.1016/S1470-2045(18)30332-2

Madamsetty, V. S., Mukherjee, A., & Mukherjee, S. (2019). Recent trends of the bio-inspired nanoparticles in cancer theranostics. *Frontiers in Pharmacology, 10*. https://doi.org/10.3389/fphar.2019.01264

Mahira, S., Kommineni, N., Husain, G. M., & Khan, W. (2019). Cabazitaxel and silibinin co-encapsulated cationic liposomes for CD44 targeted delivery: A new insight into nanomedicine based combinational chemotherapy for prostate cancer. *Biomedicine & Pharmacotherapy, 110*, 803–817. https://doi.org/10.1016/j.biopha.2018.11.145

McMahon, K. M., Foit, L., Angeloni, N. L., Giles, F. J., Gordon, L. I., & Thaxton, C. S. (2015). Synthetic high-density lipoprotein-like nanoparticles as cancer therapy. In *Nanotechnology-based precision tools for the detection and treatment of cancer* (pp. 129–150). Springer.

Mikhaylov, G., Mikac, U., Magaeva, A. A., Itin, V. I., Naiden, E. P., Psakhye, I., et al. (2011). Ferri-liposomes as an MRI-visible drug-delivery system for targeting tumours and their microenvironment. *Nature Nanotechnology, 6*(9), 594–602. https://doi.org/10.1038/nnano.2011.112

Miller, A. D. (2013). Lipid-based nanoparticles in cancer diagnosis and therapy. *Journal of Drug Delivery, 2013*. https://doi.org/10.1155/2013/165981

Mineart, K. P., Venkataraman, S., Yang, Y. Y., Hedrick, J. L., & Prabhu, V. M. (2018). Fabrication and characterization of hybrid stealth liposomes. *Macromolecules, 51*(8), 3184–3192. https://doi.org/10.1021/acs.macromol.8b00361

Mir, M., Ishtiaq, S., Rabia, S., Khatoon, M., Zeb, A., Khan, G. M., et al. (2017). Nanotechnology: From in vivo imaging system to controlled drug delivery. *Nanoscale Research Letters, 12*(1), 500. https://doi.org/10.1186/s11671-017-2249-8

Muhanna, N., Jin, C. S., Huynh, E., Chan, H., Qiu, Y., Jiang, W., et al. (2015). Phototheranostic porphyrin nanoparticles enable visualization and targeted treatment of head and neck cancer in clinically relevant models. *Theranostics, 5*(12), 1428. https://doi.org/10.7150/thno.13451

Müller, R. H., Mäder, K., & Gohla, S. (2000). Solid lipid nanoparticles (SLN) for controlled drug delivery–a review of the state of the art. *European Journal of Pharmaceutics and Biopharmaceutics, 50*(1), 161–177. https://doi.org/10.1016/s0939-6411(00)00087-4

Müller, R. H., Radtke, M., & Wissing, S. A. (2002). Nanostructured lipid matrices for improved microencapsulation of drugs. *International Journal of Pharmaceutics, 242*(1–2), 121–128. https://doi.org/10.1016/s0378-5173(02)00180-1

Muthu, M. S., Leong, D. T., Mei, L., & Feng, S.-S. (2014). Nanotheranostics - Application and further development of nanomedicine strategies for advanced theranostics. *Theranostics, 4*(6), 660. https://doi.org/10.7150/thno.8698

Nasrazadani, A., Thomas, R. A., Oesterreich, S., & Lee, A. V. (2018). Precision medicine in hormone receptor-positive breast cancer. *Frontiers in Oncology, 8*, 144. https://doi.org/10.3389/fonc.2018.00144

Ng, K. K., Lovell, J. F., & Zheng, G. (2011). Lipoprotein-inspired nanoparticles for cancer theranostics. *Accounts of Chemical Research, 44*(10), 1105–1113. https://doi.org/10.1021/ar200017e

Nykiforuk, C. L., Shen, Y., Murray, E. W., Boothe, J. G., Busseuil, D., Rheaume, E., et al. (2011). Expression and recovery of biologically active recombinant apolipoprotein AIMilano from transgenic safflower (Carthamus tinctorius) seeds. *Plant Biotechnology Journal, 9*(2), 250–263. https://doi.org/10.1111/j.1467-7652.2010.00546.x

Obeid, M. A., Tate, R. J., Mullen, A. B., & Ferro, V. A. (2018). Lipid-based nanoparticles for cancer treatment. In *Lipid nanocarriers for drug targeting* (pp. 313–359). Elsevier.

Olerile, L. D., Liu, Y., Zhang, B., Wang, T., Mu, S., Zhang, J., et al. (2017). Near-infrared mediated quantum dots and paclitaxel co-loaded nanostructured lipid carriers for cancer theragnostic. *Colloids and Surfaces B: Biointerfaces, 150*, 121–130. https://doi.org/10.1016/j.colsurfb.2016.11.032

Paliwal, R., Paliwal, S. R., Kenwat, R., Kurmi, B. D., & Sahu, M. K. (2020). Solid lipid nanoparticles: A review on recent perspectives and patents. *Expert Opinion on Therapeutic Patents, 30*(3), 179–194. https://doi.org/10.1080/13543776.2020.1720649

Paliwal, S. R., Paliwal, R., & Vyas, S. P. (2015). A review of mechanistic insight and application of pH-sensitive liposomes in drug delivery. *Drug Delivery, 22*(3), 231–242. https://doi.org/10.3109/10717544.2014.882469

Pattni, B. S., Chupin, V. V., & Torchilin, V. P. (2015). New developments in liposomal drug delivery. *Chemical Reviews, 115*(19), 10938–10966. https://doi.org/10.1021/acs.chemrev.5b00046

Prabhakar, U., Maeda, H., Jain, R. K., Sevick-Muraca, E. M., Zamboni, W., Farokhzad, O. C., et al. (2013). Challenges and key considerations of the enhanced permeability and retention effect for nanomedicine drug delivery in oncology. AACR. *Cancer Research, 73*(8), 2412–2417.

Rajora, M. A., Ding, L., Valic, M., Jiang, W., Overchuk, M., Chen, J., et al. (2017). Tailored theranostic apolipoprotein E3 porphyrin-lipid nanoparticles target glioblastoma. *Chemical Science, 8*(8), 5371–5384. https://doi.org/10.1039/C7SC00732A

Remesh, A. (2012). Toxicities of anticancer drugs and its management. *International Journal of Basic & Clinical Pharmacology.* 2012 Aug;1(1):2–12.

Richter, A. M., Waterfield, E., Jain, A. K., Canaan, A. J., Allison, B. A., & Levy, J. G. (1993). Liposomal delivery of a photosensitizer, benzoporphyrin derivative monoacid ring A (BPD), to tumor tissue in a mouse tumor model. *Photochemistry and Photobiology, 57*, 1000–1006. https://doi.org/10.1111/j.1751-1097.1993.tb02962.x

Sajid, M., Cameotra, S. S., Khan, M. S. A., & Ahmad, I. (2019). Nanoparticle-based delivery of phytomedicines: Challenges and opportunities. In *New look to phytomedicine* (pp. 597–623). Elsevier.

Satterlee, A. B., Yuan, H., & Huang, L. (2015). A radio-theranostic nanoparticle with high specific drug loading for cancer therapy and imaging. *Journal of Controlled Release, 217*, 170–182. https://doi.org/10.1016/j.jconrel.2015.08.048

Sawicki, K., Czajka, M., Matysiak-Kucharek, M., Fal, B., Drop, B., Męczyńska-Wielgosz, S., et al. (2019). Toxicity of metallic nanoparticles in the central nervous system. *Nanotechnology Reviews, 8*(1), 175–200. https://doi.org/10.1515/ntrev-2019-0017

Sercombe, L., Veerati, T., Moheimani, F., Wu, S. Y., Sood, A. K., & Hua, S. (2015). Advances and challenges of liposome assisted drug delivery. *Frontiers in Pharmacology, 6*, 286. https://doi.org/10.3389/fphar.2015.00286

Shahzad, M. M. K., Mangala, L. S., Han, H. D., Lu, C., Bottsford-Miller, J., Nishimura, M., et al. (2011). Targeted delivery of small interfering RNA using reconstituted high-density lipoprotein nanoparticles. *Neoplasia, 13*(4), 309–IN8. https://doi.org/10.1593/neo.101372

Shanle, E. K., & Xu, W. (2010). Selectively targeting estrogen receptors for cancer treatment. *Advanced Drug Delivery Reviews, 62*(13), 1265–1276. https://doi.org/10.1016/j.addr.2010.08.001

Shemesh, C. S., Moshkelani, D., & Zhang, H. (2015). Thermosensitive liposome formulated indocyanine green for near-infrared triggered photodynamic therapy: In vivo evaluation for triple-negative breast cancer. *Pharmaceutical Research, 32*(5), 1604–1614. https://doi.org/10.1007/s11095-014-1560-7

Shi, Y., van der Meel, R., Chen, X., & Lammers, T. (2020). The EPR effect and beyond: Strategies to improve tumor targeting and cancer nanomedicine treatment efficacy. *Theranostics, 10*(17), 7921. https://doi.org/10.7150/thno.49577

Simons, K., & Ikonen, E. (2000). How cells handle cholesterol. *Science, 290*(5497), 1721–1726. https://doi.org/10.1126/science.290.5497.1721

Singh, A., Trivedi, P., & Jain, N. K. (2018). Advances in siRNA delivery in cancer therapy. *Artificial Cells, Nanomedicine, and Biotechnology, 46*(2), 274–283. https://doi.org/10.1080/21691401.2017.1307210

Singh, R. P., Sharma, G., Kumari, L., Koch, B., Singh, S., Bharti, S., et al. (2016). RGD-TPGS decorated theranostic liposomes for brain targeted delivery. *Colloids and Surfaces B: Biointerfaces, 147*, 129–141. https://doi.org/10.1016/j.colsurfb.2016.07.058

Singh, S. K., Singh, S., Lillard, J. W., Jr., & Singh, R. (2017). Drug delivery approaches for breast cancer. *International Journal of Nanomedicine, 12*, 6205. https://doi.org/10.2147/IJN.S140325

Soundararajan, A., Bao, A., Phillips, W. T., Perez Iii, R., & Goins, B. A. (2009). [186Re] Liposomal doxorubicin (Doxil): In vitro stability, pharmacokinetics, imaging and biodistribution in a head and neck squamous cell carcinoma xenograft model. *Nuclear Medicine and Biology, 36*(5), 515–524. https://doi.org/10.1016/j.nucmedbio.2009.02.004

Tai, W., Mahato, R., & Cheng, K. (2010). The role of HER2 in cancer therapy and targeted drug delivery. *Journal of Controlled Release, 146*(3), 264–275. https://doi.org/10.1016/j.jconrel.2010.04.009

Tang, J., Li, L., Howard, C. B., Mahler, S. M., Huang, L., & Xu, Z. P. (2015). Preparation of optimized lipid-coated calcium phosphate nanoparticles for enhanced in vitro gene delivery to breast cancer cells. *Journal of Materials Chemistry B, 3*(33), 6805–6812. https://doi.org/10.1039/C5TB00912J

Tang, W.-L., Tang, W.-H., & Li, S.-D. (2018). Cancer theranostic applications of lipid-based nanoparticles. *Drug Discovery Today, 23*(5), 1159–1166. https://doi.org/10.1016/j.drudis.2018.04.007

Torchilin, V. P. (2005). Recent advances with liposomes as pharmaceutical carriers. *Nature Reviews Drug Discovery, 4*(2), 145–160. https://doi.org/10.1038/nrd1632

Trubetskoy, V. S., Torchilin, V. P., Kennel, S., & Huang, L. (1992). Cationic liposomes enhance targeted delivery and expression of exogenous DNA mediated by N-terminal modified poly (L-lysine)-antibody conjugate in mouse lung endothelial cells. *Biochimica et Biophysica Acta (BBA)-Gene Structure and Expression, 1131*(3), 311–313. https://doi.org/10.1016/0167-4781(92)90030-4

Tseng, Y.-C., Yang, A., & Huang, L. (2013). How does the cell overcome LCP nanoparticle-induced calcium toxicity? *Molecular Pharmaceutics, 10*(11), 4391–4395. https://doi.org/10.1021/mp400028m

ud Din, F., Aman, W., Ullah, I., Qureshi, O. S., Mustapha, O., Shafique, S., et al. (2017). Effective use of nanocarriers as drug delivery systems for the treatment of selected tumors. *International Journal of Nanomedicine, 12*, 7291. https://doi.org/10.2147/IJN.S146315

Vayne-Bossert, P., Haywood, A., Good, P., Khan, S., Rickett, K., & Hardy, J. R. (2017). Corticosteroids for adult patients with advanced cancer who have nausea and vomiting (not related to chemotherapy, radiotherapy, or surgery). *Cochrane Database of Systematic Reviews, 7*. https://doi.org/10.1002/14651858.CD012002.pub2

Wagner, A. M., Knipe, J. M., Orive, G., & Peppas, N. A. (2019). Quantum dots in biomedical applications. *Acta Biomaterialia, 94*, 44–63. https://doi.org/10.1016/j.actbio.2019.05.022

Wang, H., Li, X., Tse, B. W.-C., Yang, H., Thorling, C. A., Liu, Y., et al. (2018). Indocyanine green-incorporating nanoparticles for cancer theranostics. *Theranostics, 8*(5), 1227. https://doi.org/10.7150/thno.22872

Wang, R., & Dashwood, R. H. (2011). Endothelins and their receptors in cancer: Identification of therapeutic targets. *Pharmacological Research, 63*(6), 519–524. https://doi.org/10.1016/j.phrs.2011.01.002

Wu, P.-H., Opadele, A. E., Onodera, Y., & Nam, J.-M. (2019). Targeting integrins in cancer nanomedicine: Applications in cancer diagnosis and therapy. *Cancers, 11*(11), 1783. https://doi.org/10.3390/cancers11111783

Xia, J., Feng, G., Xia, X., Hao, L., & Wang, Z. (2017). NH4HCO3 gas-generating liposomal nanoparticle for photoacoustic imaging in breast cancer. *International Journal of Nanomedicine, 12*, 1803. https://doi.org/10.2147/IJN.S113366

Xing, H., Hwang, K., & Lu, Y. (2016). Recent developments of liposomes as nanocarriers for theranostic applications. *Theranostics, 6*(9), 1336. https://doi.org/10.7150/thno.15464

Yhee, J. Y., Son, S., Son, S., Joo, M. K., & Kwon, I. C. (2013). The EPR effect in cancer therapy. In *Cancer targeted drug delivery* (pp. 621–632). Springer.

Zangabad, P. S., Mirkiani, S., Shahsavari, S., Masoudi, B., Masroor, M., Hamed, H., et al. (2018). Stimulus-responsive liposomes as smart nanoplatforms for drug delivery applications. *Nanotechnology Reviews, 7*(1), 95–122. https://doi.org/10.1515/ntrev-2017-0154

Zheng, X.-C., Ren, W., Zhang, S., Zhong, T., Duan, X.-C., Yin, Y.-F., et al. (2018). The theranostic efficiency of tumor-specific, pH-responsive, peptide-modified, liposome-containing paclitaxel and superparamagnetic iron oxide nanoparticles. *International Journal of Nanomedicine, 13*, 1495. https://doi.org/10.2147/IJN.S157082

Zugazagoitia, J., Guedes, C., Ponce, S., Ferrer, I., Molina-Pinelo, S., & Paz-Ares, L. (2016). Current challenges in cancer treatment. *Clinical Therapeutics, 38*(7), 1551–1566. https://doi.org/10.1016/j.clinthera.2016.03.026

Zylberberg, C., & Matosevic, S. (2016). Pharmaceutical liposomal drug delivery: A review of new delivery systems and a look at the regulatory landscape. *Drug Delivery, 23*(9), 3319–3329. https://doi.org/10.1080/10717544.2016.1177136

Chapter 6
Emerging Protein and Peptide-Based Nanomaterials for Cancer Therapeutics

Samraggi Choudhury, Nidhi Aggarwal, Jiban Jyoti Panda, and Jibanananda Mishra

Contents

6.1 Introduction

In normal or controlled physiological conditions, human cells divide and differentiate to form new cells. When cells become old, they die and are removed; then, new cells take their place to maintain an uninterrupted and seamless body function. Uncontrolled division of cells is referred to as cancer; it can originate anywhere in the human body (Walter et al., 2010). Cancerous tumors are dangerous as they can spread into nearby or distant tissues in the body. As these tumors advance, few cancer cells dislodge and proceed to other parts of the body through the blood and create new tumors away from the site of origin (DeGregori & Eldredge, 2020). For a

S. Choudhury · N. Aggarwal · J. J. Panda (✉)
Institute of Nano Science and Technology, Punjab, India
e-mail: jyoti@inst.ac.in

J. Mishra (✉)
AAL Biosciences Research Pvt. Ltd., Panchkula, Haryana, India

M. Saravanan, H. Barabadi (eds.), *Cancer Nanotheranostics*, Nanotechnology in the Life Sciences, https://doi.org/10.1007/978-3-030-74330-7_6

quick proliferation of cancer cells, there is a need for exceptional energy metabolism too. Anaerobic glycolysis is a unique quality of cancer under normal oxygen conditions, known as the Warburg effect, responsible for this proliferation (Yaku et al., 2018).

For the proper treatment of cancer, it is very essential to diagnose it in its initial stages (Agrawal & Agrawal, 2015). The survival of a cancer patient is the likelihood to live for a particular time after the disease is diagnosed (Trama et al., 2018). Every year, only in the United States, ~70,000 adolescent and young adults (AYA) are diagnosed with cancer. There is a decline of about 10–20 years of survival rates for AYAs. For instance, the survival rate of 20 years for people falling in the age group 15–29 years diagnosed with cancer is just 20–27% (Wiener et al., 2015). Disease adjusted life years (DALY) have been progressively used to predict a load of disease globally. In middle-income countries like China, the years lived with a disability included 26% and 12% of the complete DALYs related to breast cancer and colorectal cancer. In males, the primary contributor to DALY is liver cancer (Fitzmaurice et al., 2017). In many countries, the consumption of disinfection byproducts (DBPs) through drinking water has been found to be the primary cause of cancer. The DALY from groundwater desalinated water and blend water was ~5.8, 27.0, and 39.9 years, respectively (Chowdhury et al., 2020). Early recognition of people at risk permits an expanded clinical observation; it may aid value in identifying the cause of development and more aggressive prevention methodologies, such as prophylactic surgery or chemoprevention (Buys et al., 2017). Currently, chemotherapeutic agents used to treat cancer have certain limitations as they are cytotoxic to both cancerous and healthy cells (Raju et al., 2019). The molecular characteristics of the tumor in a patient usually impact its clinical outcomes, which can be utilized to manage treatment by diminishing systemic toxicity and successful treatment (Behan et al., 2019). Cancer has emerged as a major concern for death (Weinberg et al., 2015). In 2012, 8 million deaths were reported out of 14 million cases, and it is estimated that by 2030 the death toll will increase by 70% (Antoni et al., 2016). As per reports of the World Health Organization (WHO), in 2015, cancer was responsible for the most deaths in people below the age of 70 in 91 countries. An increase in cancer incidences worldwide is said to be due to the westernization of lifestyle, but every country has different cancer profiles (Siegel et al., 2019). In the United States, 16,85,210 new cancer cases and 5,95,690 cancer deaths were reported as per the data collected by the National Center for Health Statistics. In the women-to-men ratio, cancer cases seemed to be constant in women, but a decline of 31% was observed in men per year (Siegel et al., 2019). The death rate is continuously decreasing since 1991. In underdeveloped countries, death rates are two times more for cervical cancer in females and lung and liver cancer in males compared to developed countries (Siegel et al., 2019). In 2018, 2.2 million cancer patients were prone to other diseases, which constituted 13% of all the cancers. The major cause of cancer was *Helicobacter pylori,* which contributed to 8,10,000 cases; the human papilloma virus caused 6,90,000 cases, and the hepatitis C virus caused 1,60,000 cases (Plummer et al., 2016). In high-income countries, a considerable amount of money is utilized in health care (De Souza et al., 2016). High-income countries have

a high recovery rate than low and middle-income countries. The survival rate of patients >65 years of age is 59.3% and 73.9% in younger patients. According to the American Cancer Society reports the biggest cause of cancer in these countries was cigarette smoking and obesity (McCormick, 2018). Low-income group countries have an increased rate of breast cancer cases in women than other group countries and are more common in >25 years of age (Balekouzou et al., 2016). A high number of prostate cancer cases are also reported in men in these countries. Further, it has been observed that many people are not aware of cancer in these countries. An increasing burden of cancer worldwide demands innovative, affordable, and effective approaches to combat the disease progression and related mortalities, which has led to the basis for the development of nano-drug delivery systems (Bugoye et al., 2019).

Substances with dimensions ranging from 10 to 1000 nm in the nanoscale are said to be nanomaterials (NMs). NMs are formulated and utilized on a small scale. NMs are designed to express unique features inclusive of greater strength, reaction, or conductivity (Mohanraj & Chen, 2007). The properties of NM, such as smaller size, greater surface area, etc. offer preferred and precise biological effects. NMs have become a part of our daily lives by finding applications in medications, diagnosis, aerospace, electronic equipment, construction, eatables, agriculture, cosmetic products, optics, textiles, automobiles, and many more. Industries use NMs in the various formulations of paints, pigments, and pharmaceuticals. In biomedical field, NMs are widely being utilized for their advanced therapeutic properties. Other than the use of NMs in medicine, it is highly employed in the early identification of diseases and aids values in predicting an effective therapeutic regimen (Saifi et al., 2018). Over the past many years, NMs have been observed to be used vigorously in various biomedical applications like targeted drug delivery, bioimaging, and biosensors (McNamara & Tofail, 2017).

Scientists worldwide have been working consistently on various NMs to utilize them in various biomedical applications such as detecting pathogenicity at the onset of a disease or disease site, cancer diagnosis and therapy, design vaccines, etc. The entry of NMs into cells plays a vital role in augmenting treatment efficiency. Bioactive molecules are often observed to be conjugated with NMs to promote their targetability to specific cells (Zhao & Stenzel, 2018). Advanced research has fetched several options for diagnosis and therapy, including magnetic resonance imaging (MRI), computed tomography (CT), biosensing, radiation therapy, chemotherapy, gene therapy, and immunotherapy (Nazir et al., 2014). For example, Bismuth sulfide (Bi_2S_3) NMs are rising as a better theranostic for CT imaging (Cheng et al., 2018). Fluorescent silicon NMs have essentially demonstrated to be effective for long-term bioimaging applications due to their ultrahigh photostability and ideal biocompatibility (Peng et al., 2014). Radiotherapy depends on the accumulation of energy in cancer cells by irradiating high energy photons (X-rays or gamma rays) capable of damaging cancerous cells and their vasculature (Haume et al., 2016), whereas chemotherapy utilizes powerful chemicals to destroy cancer cells in the body (Beaver et al., 2013).

Conventional anticancer therapy, including chemo- and radiotherapy, has displayed certain shortcomings, such as the non-specific mechanism of action, limiting their use in cancer therapy. However, nanotechnology has been realized to encompass a tremendous potential to facilitate targeted drug delivery into the body, which allows us to target the cancerous cells anywhere in the body by increasing the bioavailability of drugs at the specific site without harming the healthy cells. Gene therapy in cancer treatment is based on genetically modifying cells by inserting genes, segments of genes, or oligonucleotides in the patient's body; there are indications that it can also be successfully achieved through nanotechnology (Amer, 2014). Furthermore, to obtain higher intra-tumoral drug concentration, nanovehicles can be targeted precisely to reduce the peripheral or systemic adverse effects related to the drugs along with a site-specific delivery. To increase the specificity of the drug-loaded nanocarriers, they can be conjugated with various ligands, ranging from antibodies, cytokines, aptamers, protein, and peptides; these ligands help in actively targeting the cancer cells. Already, a variety of drug delivery systems, including polymeric nanoparticles, polymer-micelle structures, polymer-drug conjugates, liposomes, lipid drug conjugates, have been established, as briefly discussed in the subsequent section (Fig. 6.1). Some of these nanoparticle-based drug delivery systems are commercially available in the market (Table 6.1), and some are still in clinical trial phases (Tiwari et al., 2012).

To cope with the ever-increasing burden of cancer, conventional drug delivery and diagnostic approaches need to be modulated by incorporating a nanotechnological basis to achieve superior cancer management.

6.2 Different Types of Nanosystems Used in the Field of Cancer Therapy

6.2.1 Liposome-Mediated Drug Delivery Systems

Liposomes are artificially synthesized spherical structures formed by the self-assembly of amphiphilic phospholipids and cholesterol to give rise to a bilayer encircling an aqueous core. Liposomes were discovered by Bangham around 40 years ago and are still being used widely (Bangham & Horne, 1964). Liposomes can entrap water soluble drugs in the aqueous core, whereas the hydrophobic drugs are loaded onto the lipid bilayer of the liposomes. Liposomes can be synthesized to vary in size based on the drug molecule; the lipid composition can be modified to cause an effective release of the drugs (Sapra & Allen, 2003).

Liposomes can be classified based on their size and the number of lipid bilayer present, viz., large unilamellar vesicles (LUV), small unilamellar vesicles (SUV), and multilamellar vesicle (MLV). Based on the composition, they can be organized as conventional liposomes, pH-sensitive liposomes, immunoliposomes, cationic liposomes, long-circulating liposomes. Based on the method chosen for

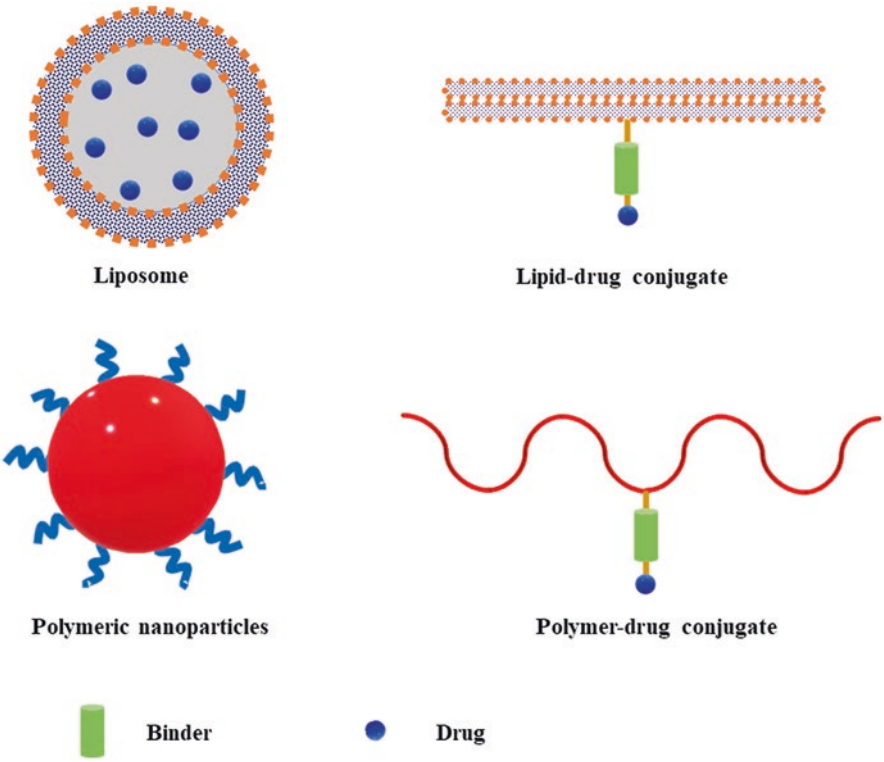

Fig. 6.1 Representation of the structure of various nanodrug delivery systems used in cancer therapy

preparation, they can be classified as French press vesicles, reverse phase vesicles, and injection phase vesicles (Akbarzadeh et al., 2013).

So far, only four liposome-mediated drug delivery formulations have been clinically approved: Doxil®, DanuXome®, Myocet®, and DepoCyt (Hofheinz et al., 2005). The drug component present in Doxil and Myocet is doxorubicin, which exhibits cardiac toxicity effect. Doxil is a PEGylated form of doxorubicin, which increases the circulation time and reduces its toxicity. Doxil is being used to treat metastatic breast and ovarian cancer and AIDS-related Kaposi's sarcoma (Gaitanis & Staal, 2010). Apart from the previously mentioned anticancer formulations, there are many nanoformulations in the clinical trial phase. During the clinical trial phase, the compositions of the nano-drug are being monitored for higher antitumor activities, higher bioavailability, lower toxicity, and to check for potential efficacy is determined.

Table 6.1 Nanoparticle-based drug delivery systems currently available in the market or under clinical trials for cancer therapy (Egusquiaguirre et al., 2012)

Nano vehicle	Generic name	Formulation	Drug	Status
Polymeric nanoparticles	Abraxane®	Albumin conjugated nanoparticles	Paclitaxel	Market
	Docetaxel-PNP	Polymer-coated nanoparticles	Docetaxel	Phase I
	BIND-014	PEG-PLGA nanoparticles	Docetaxel	Phase I
	CRLX101	Cyclodextrin-PEG nanoparticles	Camptothecin	Phase II
Polymeric micelle structures	Paclical®	Polymeric micelle	Paclitaxel	Phase III
	NK911	PEG-PAA micelle	Doxorubicin	Phase III
	NK012	PE-PGA micelle	SN-38	Phase II
	NC-6004 (Nanoplain™)	PEG-polyglutamic acid micelle	Cisplatin	Phase I/II
Polymer-drug conjugated nanoparticles	Oncaspar®	PEG + drug	L-asparaginase	Market
	ProLindac™	HPMA-DACH + drug	Oxaliplatin	Phase II
	DOX-ODX	Dextran + drug	Doxorubicin	Phase I
	Delimotecan	Polyglutamic acid + drug	Camptothecin	Phase I/II
Liposomes	Doxil®	PEGylated liposome	Doxorubicin	Market
	Myocet®	Non-PEGylated liposomes	Doxorubicin	Market
	DepoCyt®	Non-PEGylated liposomes	Cytarabine	Market
	Thermodox™	Heat-activated PEGylated liposomes	Doxorubicin	Phase III
	MBP-426	Tf-NGPE-liposome	Oxaliplatin	Phase II
	CPX-351	Liposome	Cytarabine and daunorubicin	Phase II
Lipid drug conjugates	DE-310	Carboxymethyl dextran polyalcohol polymer	DX-8951	Phase I/II
	ALN-VSP	Lipid conjugated antiSKP and antiVEGF	antiSKP and antiVEGF siRNA	Phase I
	C-VISA-BikDD	Lipid-conjugated plasmid C-VISA-BikDD	Proapototic gene (BikDD)	Phase I

Abbreviations: *PLGA* Poly(D, L-lactic-co-glycolic acid), *PEG* poly(ethylene glycol), *PAA* poly aspartate, *HPMA* N-(2-hydroxypropyl) methacrylamide co-polymer, *DACH*- diaminocyclohexane, *NGPE*- N-glutaryl phosphatidylethanolamine

6.2.2 Lipid Drug-Conjugated Nanoparticle Delivery Systems

These conjugates are lipid moieties linked to chemotherapeutic drug molecules, most of which are in phase I clinical trials such as C-VISA-BikDD, a liposome conjugated with plasmid C-VISA-BikDD. It possesses antineoplastic properties specific to pancreatic cancer. Lipoplatin is liposome-encapsulated cisplatin, which is 110 nm in size. Lipoplatin had shown successful cellular transfer in Phase I and Phase II clinical trials for pancreatic, breast, and head and neck cancer. In phase III, the side effects of cisplatin were lowered (Stathopoulos & Boulikas, 2012).

6.2.3 Polymeric Nanoparticle-Mediated Drug Delivery Systems

Polymeric nanoparticles are made up of biodegradable solid colloids ranging in the submicron range and are used for increasing the biocompatibility of the drug. The drug can be either attached, loaded, dissolved, adsorbed, or entrapped onto the nanoparticles (Sahoo & Labhasetwar, 2003). Polymeric nanoparticles can be natural or synthetic in nature; some of the widely used natural polymers are chitosan, heparin, dextran, albumin, alginate, and synthetic polymers are polyethylene glycol (PEG), polyglycolic acid (PGA), poly (D, L lactide-co-glycolic acid) (PLGA), and polyaspartate (PAA) (Wang et al., 2009). Many cationic polymers are being studied for drug delivery, detection, and imaging of metastatic cancer.

Paclitaxel faces a significant disadvantage regarding its solubility in an aqueous medium, and it needs to be administered along with a solvent. CALAA-01 is under phase I clinical trials, which utilizes cyclodextrin conjugated nanoparticles utilizing anti RRM2 siRNA for ligand-based targeting of tumor cells. siRNA can be used for silencing gene expression, which acts as a promising technique for cancer therapy; however, siRNA suffers certain shortcomings such as degradation in the cellular environment, poor cellular uptake, and rapid clearance. Hence, they need to be protected by conjugating it with nanoparticles (Whitehead et al., 2009). Polymeric micelles are formed as amphiphilic copolymer immersed in an aqueous solution, which leads to the formation of a hydrophobic core and a hydrophilic shell; the drug moieties can be enveloped either in the hydrophobic core or attached to the hydrophilic shell (Bawarski et al., 2008). A plethora of studies and trials are being done to incorporate anticancer drugs into the polymeric micelles; NK 911 incorporated doxorubicin and qualified the phase I trial proving potential anticancerous potential, drug retention in the tumor region, as well as lower neurotoxicity as compared to conventional cancer therapeutics (Matsumura et al., 2004).

6.2.4 Metallic Nanoparticles Used in Cancer Therapy

Metallic nanoparticles have gained much attention in various biomedical applications owing to their optical, thermal, electrical, magnetic, and catalytic properties; their properties majorly depend on their size, shape, and compositions. Metal nanoparticles reduce the toxic effects caused by chemotherapeutics and also aids in site-specific delivery of therapeutic agents, surpassing the biological barriers (Gil & Parak, 2008). Due to their unique structures, metal nanoparticles facilitate vascular permeability into the tumor cells; also, the presence of hydrophilic molecules on the surface of the nanoparticles increases the solubility and half-life of the drug molecule in the system (Minelli et al., 2010). Metal nanoparticles also induces hyperthermia, which increases the internal temperature in the cells beyond its threshold; cancer cells have a lower threshold for tolerating heat than healthy cells. Iron oxide nanoparticles are widely used for hyperthermia therapy for cancer cells due to their higher magnetic and radiofrequency properties. Iron oxide nanoparticles, when incorporated intravenously in squamous epithelial cells, present in a carcinoma mouse model; tumor specific distribution was observed (Torti et al., 2007). Gold silica nanoshells coated with antibodies against medulloblastoma cells and glioma cells to effectively target tumor conditions in vitro. These cells overexpress the interleukin 13 receptor, which acts as the antigen. The cells which expressed higher HER 2 level showed high tumor aggregation (Toub et al., 2006).

6.2.5 Inorganic Nanoparticles for Cancer Therapy

Recently, evidence has suggested the use of inorganic nanoparticles such as quantum dots (QDs) and carbon nanotubes (CNTs) for cancer cell imaging and therapy. QDs help in imaging cancer cells due to their autofluorescent properties both in vivo and in vitro. They are semiconductor nanomaterials with fluorescence properties spanning from the UV region to the near-infrared (NIR) region (Mulder et al., 2009). QDs are conjugated with appropriate peptides or monoclonal antibodies for the tumor environment, which facilitates imaging the tumor angiogenesis using MRI. Carbon nanotubes belong to the fullerene family; they are of two kinds single-walled and multiwalled. CNTs have shown their application in various biomedical processes other than cancer cell imaging; they also act as suitable carriers for therapeutic drug delivery (Lau & Hui, 2002). CNTs in their natural form are insoluble and tend to aggregate in the biological surroundings; they are PEGylated or associated with lipids or DNA to make them more compatible. A novel delivery system was designed which used a magnetic field that facilitates the delivery of nickel-embedded CNTs into the cells, which enhances the cellular delivery (Cai et al., 2005); they also can be functionalized with targeting agents which are designed to kill the cancerous cells (Ou et al., 2009).

Various strategies have been opted to functionalize the aforementioned nanosystems with protein/peptide ligands to achieve a targeted delivery in cancer, as discussed in Sect. 6.3. Also, the capability of peptides to self-assemble into nanocarriers has been summarized for its application in cancer therapy.

6.3 Protein and Peptide-Based Nanoparticles in Cancer Therapy

Though various nanomaterials explored to date have contributed significantly to the field of cancer nanomedicine, the use of protein and peptide-based nanostructures is specifically alluring because protein and peptides can exhibit great potential as therapeutic agents. These naturally occurring biomolecules offer high biocompatibility. Thus, they can act as excellent templates for the synthesis of nanomaterials with potential biomedical applications, specifically in the field of cancer therapy. Protein-based nanostructures would increase the bioavailability of anticancer drugs as well as decrease their toxicity. They are also amphiphilic in nature, which allows them to interact with the drugs as well as the solvents, making them an ideal choice for nanoconjugate formulation, which is capable of crossing biological and cellular barriers (Lohcharoenkal et al., 2014).

Peptides are small molecular structures that can be natural or synthetic in nature and play an essential role in various biological applications. The major goal of peptide-based nanostructures is to encapsulate antineoplastic drugs and release the drugs at their targeted location. Peptides can be good baits for targeted drug delivery as they can bind to many of the receptors overexpressed on the surface of the tumorous cells.

Thus, both proteins and peptides can act as suitable templates for the fabrication of nanostructures to find potential applications in cancer therapy.

6.3.1 Protein-Based Nanodelivery Systems

An urge for accomplishing a successful active drug-targeting to the cancer site has driven the research scientists to exploit various NPs for their surface functionalization ability. The idea of using protein-based nano-delivery systems in cancer management has been flourishing rapidly ever since the tremendous success of the first albumin-coated paclitaxel nanoparticles (PTX-NPs), Abraxane®, in 2005 for managing metastatic as well as recurring breast cancer (Yu et al., 2016; Sorolla et al., 2020a). Protein NPs form a considerable market for therapeutics and diagnostics in oncology due to enhanced selectivity and diminished toxicity characteristics (Yu et al., 2016; Sandra et al., 2019). Due to its amphiphilic nature, protein molecules can interact with both hydrophilic as well as hydrophobic moieties making it an

attractive choice for fabricating NPs (Lohcharoenkal et al., 2014). Protein monomers possess an ability to co-assemble and spontaneously form NPs with a hollow core arrangement for drug accommodation. With versatile and highly tunable surface properties, various modifications/functionalizations can be introduced in protein NPs, thereby modulating their cancer-targetabilities (Lohcharoenkal et al., 2014; Sandra et al., 2019). However, protein-based delivery faces significant limitations of the short half-life, degradation by enzymes, poor uptake in tumor tissue, and inferior barrier traversing potential (Yu et al., 2016). To deal with the aforementioned drawbacks associated with proteins, intelligent approaches must be developed modulating its entry into the systemic circulation and eventually attaining therapeutic effect at the target tumor site. Figure 6.2 describes the probable fate of protein NPs once inside the human body and approaches associated with developing a smart protein-based nano-delivery system (Sandra et al., 2019). This section mainly focuses on recent innovations and advancements made in protein-mediated nano-delivery for cancer therapy.

BBB is a major challenge in controlling glioma and metastatic spinal tumors. Wang and associates developed doxorubicin (DOX) encapsulated ferritin-HREV107-Angiopep-2 (Fn-Rev-Ang)-based NPs for targeting the brain. Ferritin, a naturally occurring protein, is a specific ligand for transferrin receptors-1(TfR1) further involved in cell growth via maintaining iron supply. However, TfR1 is overexpressed on the cancer cell surface. Ferritin NP when combined with angiopep-2 (lipoprotein receptor-related protein-1 ligand) produced Fn-Rev-Ang, which depicted improved migration across BBB as observed by in vivo fluorescence

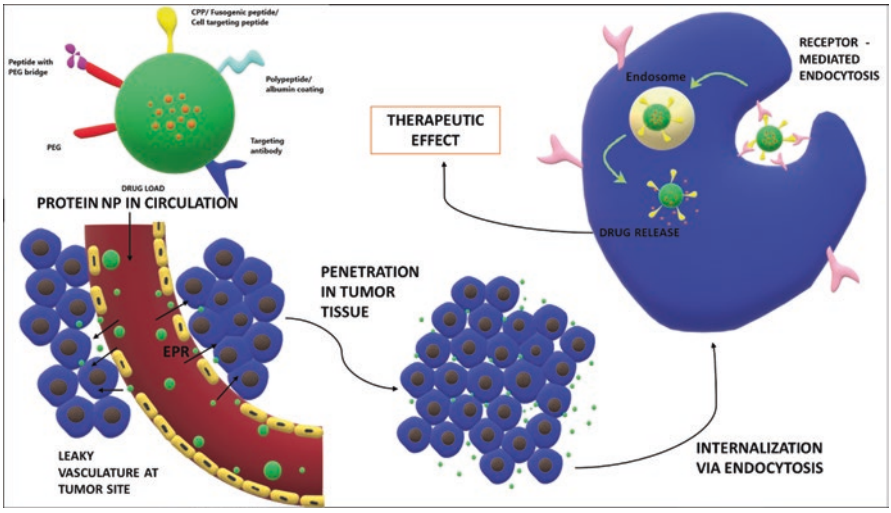

Fig. 6.2 Fate of protein NP inside the human body. PEGylation, serum-albumin coating, and peptide coating on a protein NP can help to escape phagocytosis and rapid clearance from the body. Additions of vasodilators can improve passive targeting involving the EPR mechanism. CPPs/fusogenic peptide addition also prevents lysosomal degradation of protein NP

imaging of Cy5.5 labeled Fn-Rev-Ang NPs. Due to the overexpression of specific angiopep-2 binding receptors, the glioma cell line (U87MG cells) presented higher Fn-Rev-Ang-DOX-Cy5.5 uptake as compared to the kidney epithelium cell line (HEK293T cells). This observation confirmed a significant accumulation of Fn-Rev-Ang NPs in glioma with a negligible effect on normal cells. Bioluminescence imaging with Fn-Rev-Ang-DOX revealed no signs of tumor metastasizing in the spinal cord along with approx. 2.1-times improved survival of mice. Also, Magnevist (a contrast agent), when bound to Fn-Rev-Ang, depicted high distribution in the brain with no signs of altered BBB integrity on H&E imaging. The results conclusively established that Fn-Rev-Ang NPs were able to target glioma by promoting BBB binding and penetration (Wang et al., 2020).

Gregory and associates developed synthetic protein nanoparticles (SPNPs) for combating highly vigorous GBM. Amid various pathways aggravating the disease, the Signal Transducer and Activator of Transcription 3 (STAT3) pathway contributes majorly to the tumor's progression and worsening. Human serum albumin (HSA)-based SPNPs were constructed by encapsulating the STAT3 inhibitor, further decorated with a CPP iRGD to target GBM tissue (Fig. 6.3a) selectively. In vitro studies depicted a 96% encapsulation and a sustained release profile over 3 weeks, along with lowered STAT3 protein levels (Fig. 6.3b). A twofold decrease in the expression of STAT3 level was observed in a dose-dependent fashion with SPNPs. Improved biodistribution, enhanced penetration, and accumulation in brain tissue were observed with SPNPs relative to CPP free nanoformulation in the tumor-bearing mouse. The therapeutic efficacy of siRNA-loaded SPNPs was evaluated in combination with radiotherapy in vivo, which depicted an increased survival time and decreased STAT3 levels in the GBM GL26 mice model. Furthermore, no

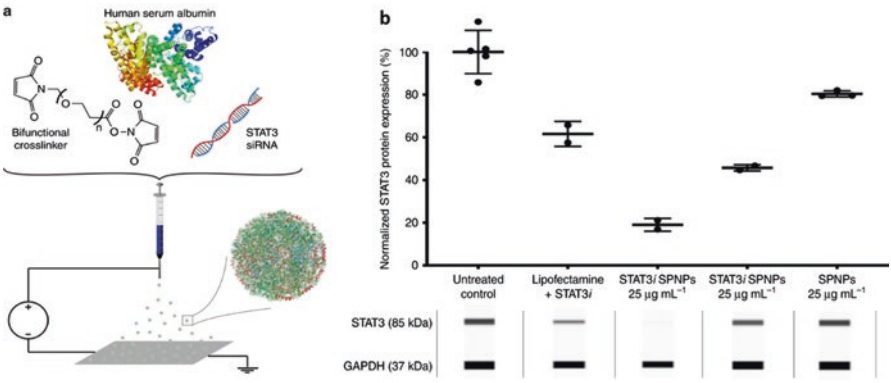

Fig. 6.3 (**a**) Schematic of the jetting formulation for crosslinked, STAT3i-loaded, iRGD-conjugated, targeted albumin NPs (STAT3iSPNPs), (**b**) STAT3 siRNA-loaded SPNPs significantly reduce in vitro expression of target protein in GL26 glioma cells compared to untreated and empty particle control groups. Data are presented as mean values ± s.d. (SPNPs, $n = 3$; Lipofectamine + STAT3i, STAT3i SPNPs (25 and 2.5 μg mL^{-1}, $n = 2$ biological replicates). (Excerpted from an open-access source under the terms of Creative Commons CC BY license, Gregory et al., 2020)

evidence of toxicity was observed with the synthetic nanoformulation. Thereby, SPNPs proved to be successful in providing a targeted drug delivery approach against GBM along with the merits of the RNA interference technique (Gregory et al., 2020).

Magneto-heavy chain ferritin (M-HFn) molecules were developed by Cheng and associates for loading an anticancer drug (DOX) to attain successful therapeutic outcomes in gastric cancer (GC). The group elucidated the clinical potential of targeting TfR1 in treating GC. It was observed that in such a diverse cancer environment, cells without TfR1 depicted tumor-initiating characters, while cells with TfR1 depicted increased proliferation. The GC-PDX mouse model revealed that the rate of tumor inhibition was 2.1 times higher for HFn-DOX than the free drug. Histological evaluation in GC-PDX tumor tissue further confirmed the antitumor action of HFn-DOX by impeding proliferation and inducing death of cancer cells to a larger extent than free drug and free HFn as observed by PCNA and Ki67 (proliferation markers) and TUNEL staining for apoptosis determination. Thus, HFn nanocarriers can be used for treating GC by TfR1 targeted delivery (Cheng et al., 2020).

Mie and associates developed PTX-loaded protein NPs conjugated with MUC1 aptamers via ss-fusion protein for breast cancer therapy. Protein NPs were fabricated by combining elastin-like polypeptides (ELPs) and fused poly-aspartic acid chains (ELP-D). The aptamer selected was S2.2 possessing targetability toward overexpressed MUC1 glycoproteins on the cancer cell. The fusion protein, Gene A*, did not show any evidence of altered activity upon covalent binding with ELP-D as observed by fluorescence images. A targeted delivery of protein NPs conjugated with MUC1 was observed, as shown by the intense fluorescence obtained from protein NP treated MCF-7 cells.

In contrast, protein NP with no MUC1 aptamer depicted nil fluorescence. It was inferred that a high abundance of MUC1 glycoproteins on breast cancer surfaces provides a binding site for MUC1 aptamer, thereby ensuring targeted delivery. Fluorescence imaging with calcein-AM and PI staining depicted a significant cancer cell death post-3 days after being endocytosed by the cancer cell. Thereby, protein NP conjugated with targeting DNA aptamers could target MCF-7 breast cancer cells more effectively than aptamer free preparations (Mie et al., 2019).

Attributed to its potential for prolonged circulation, another group of researchers exploited high-density lipoprotein (HDL) nanodiscs for co-delivery of a TLR-9 targeting ligand (CpG) and chemotherapeutic agent docetaxel (DTX) in GBM. DTX-lipids and ApoA1 peptide were self-assembled to form DTX-sHDL nanodiscs, which was further incubated with CpG-cholesterol in order to obtain DTX-sHDL-CpG nanodiscs (Fig. 6.4). In vitro cellular uptake and in vivo biodistribution studies of HDL nanodiscs established an enhanced intratumoral targeting ability of the DTX-sHDL-CpG nanodiscs as compared to DTX-CpG alone. The therapeutic efficacy of the prepared nanodiscs was confirmed as almost two-times elevated survival was observed in groups treated with DTX-sHDL-CpG nanodiscs. Also, chemotherapy in conjunction with radiotherapy depicted approximately 80% higher survival with no evidence of tumor relapse. Immunohistochemical analysis depicted no

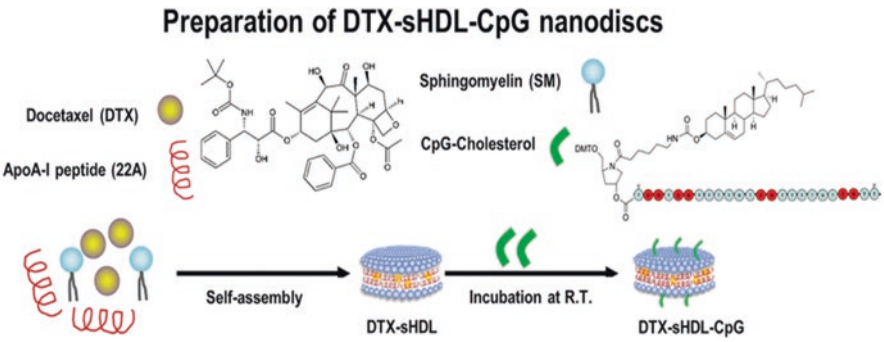

Fig. 6.4 Preparation of DTX-sHDL-CpG nanodiscs by incubating lipid-DTX with CpG and preforming sHDL. (Adapted with permission from Kadiyala et al., 2019. Copyright 2019 American Chemical Society)

toxicity along with retained integrity of brain tissue. Therefore, DTX-sHDL-CpG nanodiscs can offer a better alternative for selectively targeting GBM and aids in a successful therapeutic outcome (Kadiyala et al., 2019).

Yang and associates investigated the potential of a peptide-anchored dual-drug delivery nanosystem consisting of a combination of PTX and YAP siRNA to achieve both BBB permeation and tumor targeting simultaneously. Among numerous delivery vectors available, the research group opted for hepatitis B core protein-virus-like particle (HBc-VLP) functionalized with a brain targeting TGNYKALHPHNG (TGN) and a tumor-targeting arginine-glycine-aspartic acid (RGD) peptide to achieve site-specific delivery to the tumor tissue. The in vitro cellular uptake of TGN/RGD VLP on U87 cells was found to be significantly higher than the in vivo uptake of TGN-VLP across BBB. Also, fluorescence microscopy depicted enhanced accumulation of siRNA from TGN/RGD VLP in the cytoplasm, indicating the potential to deliver the therapeutic gene to the target site explicitly. The carrier system was found to be non-cytotoxic. Immunohistochemical studies of tumor tissue depicted a significant drop in YAP protein levels with siRNA-loaded TGN/RGD VLP compared to the control group. A synergistic anti-tumoral outcome was observed with a low dose of PTX/siRNA-loaded TGN/RGD VLP in U87-Luci tumor-bearing mice due to greater necrosis and apoptosis. Therefore, it was concluded that a peptide-functionalized carrier system could accurately target the tumor tissue providing an effective treatment regimen for glioblastoma (Yang et al., 2020).

To effectively deliver water-insoluble PTX, Park and associates fabricated albumin-bound nanocrystals (NC) for a carrier-independent delivery in cancer treatment. The carrier-based NP system faces limitations of inadequate drug loading and reticuloendothelial system (RES)-mediated clearance from the body leading to feeble therapeutic response. Thereby, carrier-independent PEGylated albumin-NC was developed to prevent phagocytosis and increase its circulation time. Also, albumin bears an innate ability to target cancer cells via interacting with SPARC (secreted protein acidic and rich in cysteine), thereby contributing to a site-selective delivery. Cim-F-alb and Cim-C-alb were developed via crystallization in Pluronic F127 and

hexadecyltrimethylammonium bromide medium, respectively. Cim-F-alb was selected due to its smaller size and enhanced tendency to circumvent phagocytosis. Rapid in vitro dissolution with amorphous Abraxane was suggestive of its low serum stability, whereas slower dissolution of Cim-C-alb due to its crystalline nature indicated high stability and prolonged circulation in plasma. In vivo investigation on intravenous administration in C57BL/6 mice infected with B16F10 tumor demonstrated increased apoptosis with Cim-F-alb compared to marketed standard Abraxane and buffer control. Moreover, drug reaching tumor tissue with Cim-F-alb was significantly higher than with Abraxane, i.e., 27.4 ± 22μg/g and 13.8 ± 6μg/g, respectively, indicating higher drug loading and accumulation.

Conclusively, a protein-based carrier-independent delivery system needs to go a long way in developing a therapeutically effective approach in treating cancers (Park et al., 2017).

6.3.2 Peptide-Based Nanodelivery Systems

Ornamenting NPs with peptides due to their abundant occurrence in nature and inherent biocompatibility led to a major revolution in cancer therapy (Chhikara et al., 2019). A higher degree of expression of many receptors on the surface of the cancer cells makes them hostile for receptor-ligand interactions facilitating internalization and targeting a drug candidate to the site of action (Jiang et al., 2019a). Among numerous ligands available, peptides have marked their significant role as therapeutics by targeting tumor receptors (Raucher, 2019). Capable of adventive structural modifications by the inclusion of non-peptide moieties and its effortless synthesis rendered peptides as the most adaptable group of ligands (Jiang et al., 2019a; Kurrikoff et al., 2019). Conjugation of a peptide to another peptide molecule, a drug moiety, or a nanocarrier provides a platform to develop a peptide-based drug delivery system (Guo et al., 2020). Peptides allow for biological interactions due to their mesial size ranging between large protein ligands and small-molecule ligands. Peptides can be optimized to develop a system inclusive of both smart receptor binding affinity and improved penetrability in solid tumors (Kurrikoff et al., 2019). The development of distinctly conserved biomimetic peptides has been shown to circumvent the glitches linked to the complex nature and toxicity profile of using proteins as ligands (Zhao et al., 2020). Metabolism of peptides by proteolysis followed by its rapid clearance from the body constraints toxic accumulation and related side effects. Additionally, amino acids being their natural degradation products are non-toxic to the body and offer a clinically safe approach for developing a drug delivery system (Hoppenz et al., 2020).

A pronounced development in a peptide-based nano-drug delivery system offers considerable success in the arena of cancer therapeutics. Peptides have evolved into distinct classes, viz., tumor homing peptides (THP), cell-penetrating peptides (CPP), and peptide-targeting altered signaling pathways. The aforementioned classes of peptides have been explored for their potential as a nano-drug delivery

system in cancers (Raucher, 2019). CPPs have mainly been investigated for their potential role in gene therapy for treating cancer (Alhakamy et al., 2020). CPPs primarily consist of a small chain of basic amino acids (<30), rendering them a net positive charge. Till 2003, CPPs were thought to follow non-endocytic internalization via direct but energy-reliant penetration pathway. Later, several processes were investigated to be involved in the passage of CPPs across the membrane. The studies reveal that CPPs are taken up either by phagocytosis or pinocytosis to form endosomes. Subsequent degradation of endosomes is a prerequisite for the CPPs to gain access to the site of action. The endosomal escape may be promoted by a variety of factors, viz., low pH conditions, various lysosomotropic compounds, or due to an interplay between negatively charged vesicle membranes and positively charged CPPs. Furthermore, endosomal escape can also be encouraged by adding various amino acid sequences and their derivatives (Silva et al., 2019). Some of the recent developments in the peptide-based nano-delivery system have been reviewed in this section.

Yan and associates developed a peptide-based delivery system for effectively targeting a nucleic acid-based therapeutic agent to the tumor site. Conventionally used cationic carriers for nucleic acid delivery across the membrane bear the demerits of toxicity. Thereby, an arginine-rich peptide-based delivery system was devised conjugated with fluorous moieties on both the peripheral ends imparting it a bridged conformation, eventually self-aggregating into concentric NPs (NPT) (Fig. 6.5a). Enhanced cellular uptake attributed to its bridged conformation (Fig. 6.5b) was confirmed by CLSM and flow cytometric studies. NPTs promoted the transfer of the therapeutic nucleic acid across MCF7/HeLa cell lines in vitro, indicating a successful cell internalization. The therapeutic efficacy of NPTs was studied in vivo with

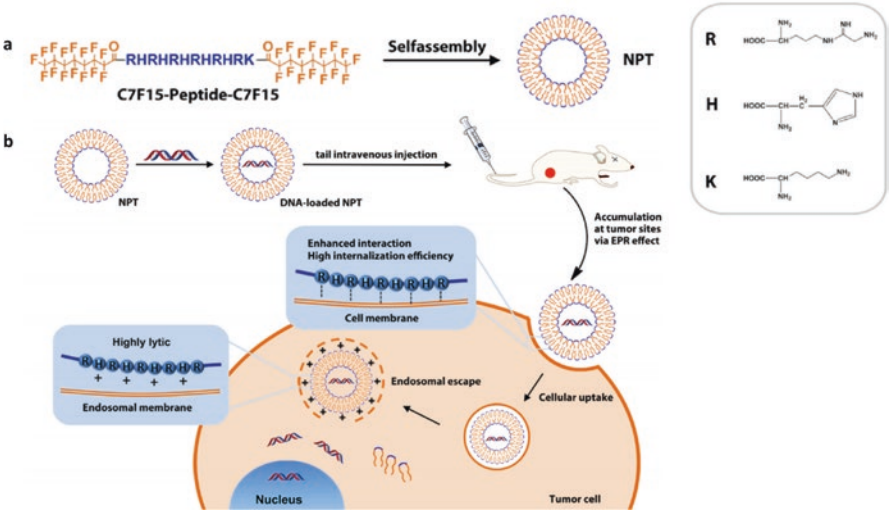

Fig. 6.5 (**a**) Structural details of NPT; (**b**) The process of NPT to transport DNA into tumor cells and escape from endosomes. (Adapted with permission from Yan et al., 2020)

MCF-7 tumor-bearing BALB/c nude mice. Following the fluorescence studies, a prolonged systemic signal for more than 24 h and an enhanced accumulation of NPTs was observed. A superior tumor suppression on iv administration of NPTs confirmed its antitumor efficacy. Thereby, this peptide-based delivery system can offer a promising approach in targeting tumors by improving the transport of nucleic acids across the cell membrane (Yan et al., 2020).

Ruan and associates applied a stapling technique to develop stapled receptor-associated protein-derived peptide (R8AKIEKHS5HYQK), i.e., ST-RAP12, which was further polymerized into micelles loaded with PTX for targeting glioma. Stapling was done by inserting hydrocarbon linkage in the peptide to confer an α-helical configuration necessary for ligand-receptor binding. Stapling of RAP12 rendered it with an improved stability characteristic with twofold more residual peptide content after 4 h compared to non-stapled RAP12. The rate of transcytosis across BBB and blood-brain tumor barrier (BBTB) was found to be improved for ST-RAP12 than RAP12 as observed by confocal laser scanning microscopy (CLSM), indicating a higher penetration in glioma. Moreover, Coumarin-laden ST-RAP12 micelles functionalized with PEG-PLA depicted excellent biocompatibility and a superior in vitro BBB-BBTB penetration. In vivo biodistribution studies using intracranial U87 cells showed a higher accumulation of DiR tagged ST-RAP12-PEG-PLA micelles in the brain than non-stapled as well as non-peptide containing micelles. Immunofluorescence assay depicted an approx. 1.5-fold enhanced co-localization of ST-RAP12-PEG-PLA micelles than RAP12-PEG-PLA micelle with the tumor cells indicating a targeted delivery to glioma. In vitro and in vivo evaluation for antitumor activity revealed increased apoptosis with ST-RAP12-PEG-PLA micelles indicative of an effective anti-glioma function. Thereby, it was concluded that stapling the peptide conferred the micelles with an improved receptor binding ability to target BBB/BBTB in glioma (Ruan et al., 2021).

Recently, another group of researchers elucidated the anti-metastatic potential of RelA siRNA (siRelA) when conjugated with a functional-peptide nano-micelle via systemic administration. siRelA acts against NF-κB mediated metastasis, which is majorly responsible for inflammation-induced neovascularization at tumor sites. The nano-micellar formulation was developed by conjugating methoxy-polyethylene glycol combined polycaprolactone and a functional peptide CH2R4H2C (MPEG-PCL-CH2R4H2C) housed with siRelA was investigated for its role against B16F10 melanoma in mice. Flow cytometry studies revealed a substantial uptake of siRNA from MPEG-PCL-CH2R4H2C micelles compared to naked siRNA by B16F10 cells. Additionally, it was observed that siRNA uptake increases with an increased polymer to the siRNA ratio. Upon CCK-8 assay on rat retinal pigment epithelial cells (RPE-J), a comparable count of viable cells was observed between control and MPEG-PCL-CH2R4H2C, indicating the non-cytotoxic nature of the polymeric micelles. The ability of siRelA/MPEG-PCL-CH2R4H2C to halt themigration of cancer cells into the wounded cell layer demonstrated its anti-metastatic character. Further, the anti-metastatic nature was confirmed in vivo by estimating lung nodule formation in B16F10 cell-based metastasis model. Intravenously administered

siRelA/MPEG-PCL-CH2R4H2C depicted negligible nodule count compared to untreated, si control with MPEG-PCL-CH2R4H2C, and in the group treated with siRelA and without MPEG-PCL-CH2R4H2C subjects. Thus, the above outcomes depicted enhanced localization of CH2R4H2C-based micelles in tumor sites and superior anti-metastatic ability in the lung melanoma (Ibaraki et al., 2020).

A targeted delivery against triple-negative breast cancers (TNBCs) was designed by utilizing the interference peptides (iPeps) approach for delivering chemotherapeutic taxol, docetaxel (DTX). ENGRAILED1 (EN1) is majorly overexpressed in TNBCs. Sorolla and associates aimed to combat TNBC by developing a bi-functional peptide formulation. EN1-iPeps for inhibiting EN1 accompanied with RGD sequence (HGRGDLGRLKK) for its ability to target integrin receptors were used to fabricate EN1-RGD-iPeps-DTX containing NPs. In vitro, immunofluorescence assay depicted a caspase-3-dependent death of TNBC cell lines with no toxicity towards normal cells. RGD peptides led to increased cellular uptake by TNBC cell lines due to the abundance of integrins present on its surface. A 2.2% increased accumulation of dual-peptide functionalized NPs was observed at tumor sites in T11 and SUM149 cell lines compared to non-functionalized NPs. Furthermore, a tenfold less dose of DTX in EN1-RGD-iPeps functionalized NPs demonstrated in vivo anti-tumoral response than with non-functionalized NPs. Thus, bi-functional peptide-functionalized DTX-NPs offered a targeted drug delivery in TNBC with negligible off-site effects (Sorolla et al., 2019).

Li and associates developed a PTX + tetrandrine-loaded micelles functionalized with hyaluronic acid (HA) and a CPP for treating gastric cancer. The positively charged CPP (RRRRRRRRRPVGLIG) on the surface of the micelle promoted its interaction with the negatively charged biological membrane. However, increased RES mediated clearance of the resultant positively charged complex was attenuated by further enveloping it with a negatively charged HA enabling the nanoformulation to escape RES uptake. The HA-CPP decorated 90 nm-sized nanocarriers could accumulate in tumor tissue passively via enhanced penetration and retention (EPR) effect. The HAase-mediated degradation of HA rendered CPP surface-exposed, eventually leading to active tumor targeting action of CPP. Another polymer, TPGS-1000 was used to improve solubility characteristics of the anticancer agents loaded in micelles. Fluorescence microscopic studies revealed an improved uptake of coumarin tagged HA-CPP-dual drug-loaded micelles by BGC-823 cells compared to control groups. HA-CPP conjugated micellar preparation depicted attenuated levels of invasive proteins and improved the level of apoptotic factors in the BGC-823 cell line indicating destructive action toward cancer cells. The therapeutic antitumor potential of HA-CPP-bound nanoformulation was established in vivo after observing negligible tumor volume post-22 days of administration. Thus, the innovatively designed HA-CPP conjugated dual drug-loaded micelles followed passive and active uptake to carry out a successful tumor-targeted treatment (Li et al., 2020)

6.3.3 Self-Assembled Peptide Nanocarriers

Self-assembled delivery systems have been much explored to carry a therapeutically effective amount of drug cargo and release it precisely at the target site. Self-assembly is a spontaneous formation of definite structures under spatial interactions (Habibi et al., 2016). Self-assembled nanocarriers are liable to undergo structural changes in response to altered physiological state, particularly in tumor tissue resulting in a controlled or prompt release of drugs at the tumor site (Jiang et al., 2019b). As mentioned in Sect. 6.5, peptides are the ligands of choice due to too well biocompatibility and natural origin (Cao et al., 2019). By virtue of great diversity in the amino-acid side-chains, it makes peptide molecules capable of interacting with the surroundings. Non-covalent interactions, including hydrogen bonding, halogen bonding, π-π interactions, etc., contribute majorly towards the self-assembly of short peptide sequences (Hu et al., 2020). Electrostatic forces of attraction and repulsion, as well as metal-ion complexes, also drive the self-assembly of peptides into nanostructures. Several reactive functional groups flanking from peptide side-chains also allows for surface functionalization via covalent bond formation with various receptor-targeting ligands (Cao et al., 2019; Hu et al., 2020). Environmental factors such as pH change, radiations, polarity, enzymatic state, etc., often trigger the formation of self-assembled structures (Hu et al., 2020). Peptide-mediated self-assembled nanocarriers possess various structural and physicochemical characteristics making it an important therapeutic system (Cao et al., 2019). Peptide amphiphiles (PA) have been largely employed for therapeutically effective delivery of drugs as well as gene products. Cyclic peptides have also presented a tendency to self-assemble as nanotubes, whereas micelles are generally obtained from branched peptides (Cao et al., 2019).

Rapidly emerging in cancer therapy, self-assembled peptide nanocarriers can target the tumor site passively via the EPR effect via in situ self-assembly, responding to the extrinsic stimulus. The functionalized moieties attached can promote active targeting in the tumor. Self-assembled peptide nanocarriers offer an edge over merits due to their convenient and easy assembly even when conjugated with numerous functional moieties as well as its biocompatible nature (Ren et al., 2020). Multiple research studies have been undertaken for self-assembled peptide nanocarriers in cancer therapy. Some of the significantly relevant studies are discussed in the following segment and Table 6.2.

Zhang and associates carried out groundbreaking research by designing in situ transformable supramolecular peptides to treat Human epidermal growth factor receptor 2-positive (HER2+) tumors. Such tumors generally depict a feeble response to monotherapy due to largely augmented genetic factors leading to overexpression of receptors on their surface. A triple domain peptide molecule was designed containing a bis-pyrene (BP) moiety, a reverse KLVFF peptide (FFVLK), and a cyclic HER2 binding peptide (YCDGFYACYMDV) with an affinity to self-assemble as NPs in a polar medium. After intravenous (IV) administration, already self-assembled into NPs were eventually transformed to nanofibrils on binding with

Table 6.2 Self-assembled peptide-based nanocarriers in cancer therapy

Self-assembled nanosystem	General comments	Important outcomes	References
5-ALA loaded bola-peptide hydrogels	Self-assembled intertwined nanofibrillar structure with an average particle size of 12 nm was obtained due to hydrophobic interactions.	In vivo studies depicted a localized and sustained action of hydrogels, indicating improved drug bioavailability. An absolute suppression of tumors with no signs of reappearance was observed with 5-ALA-loaded bola-peptide hydrogels combined with 635 nm radiation therapy.	Zou et al. (2020)
L_6K_4 (amphiphilic peptide) self-assembled DOX-containing NPs	Self-assembly proceeds via an altered charged state of L_6K_4 in varying pH conditions causing hydrophobic interactions. A higher zeta potential value in acidic medium indicated stronger repulsions, eventually disassembling NPs.	pH-sensitive drug release was observed in vitro with a rapid release under acidic and prolonged release in neutral pH. CLSM studies showing higher drug uptake in HeLa cells than NIH 3T3 cell line indicated that drug readily acts at the peripheral sites of tumor. Also, low pH at the tumor sites may favor superior drug release by disaggregating the NPs.	Gong et al. (2020)
Fulvestrant loaded Fmoc-L-S-G-C-G-N-S (FLS) self-assembled gold nanorods	Multiple interactions by amino acid sequences resulted in self-assembled FLS formation. G and S residues lead to the formation of hydrogen bonds. Disulfide bond formation by C favored crosslinking.	A four-fold higher drug release was observed at higher temperatures when irradiated with NIR compared to non-NIR-induced nanorods. In vitro data suggests that irradiated Fulvestrant-FLS-nanorods were cytotoxic to breast cancer MCF-7 cell line. A disrupted cancer cell morphology was also observed after irradiated Fulvestrant-FLS-nanorods.	Daso and Banerjee (2020)
PTX loaded TRAIL-PA self-assembled supramolecular nanostructure	Self-assembled nanostructure was formed via covalent interactions between TRAIL-mimetic peptide and PA. TRAIL-peptide can selectively target death receptors (DR5), which are over-expressed in breast cancer.	In vivo tumor volume in the MDA-MB-231 cell implanted model was found to be the lowest for the PTX-TRAIL-PA nanostructures as compared to the free drug as well as the non-assembled nanostructures. Caspase-mediated cell death was confirmed in vitro in the MDA-MB-231 cell line due to a higher DR5 targeting by TRAIL-peptide.	Moyer et al. (2019)

Abbreviations: *L_6K_4* Ac-Leu-Leu-Leu-Leu-Leu-Lys-Lys-Lys-Lys-NH_2, *Fmoc-L-S-G-C-G-N-S (FLS)* Fluorenylmethyloxycarbonyl-Leu-Ser-Gly-Cys-Gly-Asn-Ser, *NIR* Near-infrared, *TRAIL* Tumor necrosis factor related apoptosis-inducing ligand, *PA* peptide amphiphile

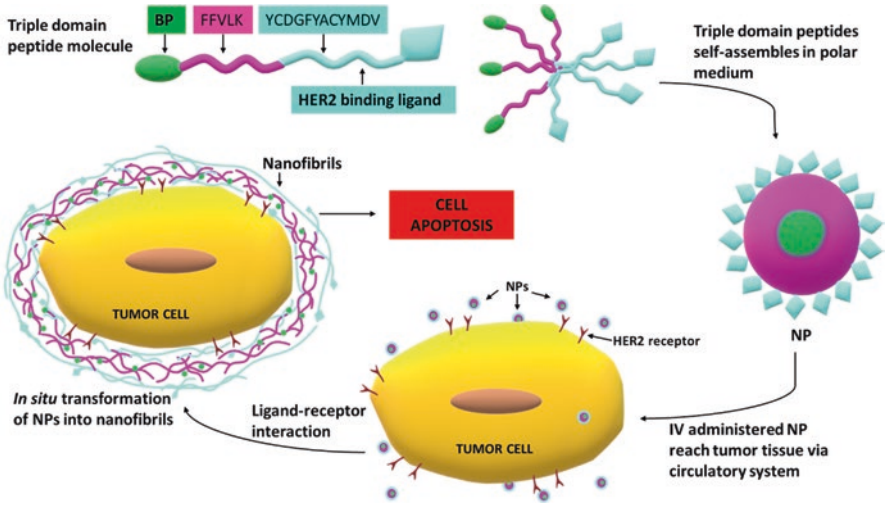

Fig. 6.6 In situ transformable supramolecular peptide to treat Human epidermal growth factor receptor 2 positive ($HER2^+$) tumors

HER2, which interfered with the signaling of HER2 as represented in Fig. 6.6. In vivo investigations depicted no cytotoxicity and a prolonged systemic residence of NPs. The antitumor effect of NPs was attributed to the bursting of tumor cells caused by nanofibrillar structures. A significant depletion in tumor volume was observed without any episodes of recurrence. Furthermore, preclinical and clinical studies are desirable to validate the efficacy of transformable peptide containing NP in $HER2^+$ tumors (Zhang et al., 2020).

In another study, methotrexate (MTX) conjugated with CPPs was self-assembled into NPs in the presence of polyglutamate. Zakeri-Milani and associated designed two CPPs, i.e., R2W4R2 (RRWWWWRR) and W3R4W3 (WWWRRRRWWW), and converted them to form MTX-loaded self-assembled peptide NPs to investigate for its anticancer potential. Self-assembly into rod-like NPs was carried out due to the formation of salt bridges via electrostatic interactions between cationic CPPs and anionic polyglutamate molecules. High free energy values for R2W4R2 as measured by the Wimley-White Scale indicate that it can readily interact with polyglutamate to cause self-assembly. At lower concentrations, E12 did not show significant in vitro cytotoxicity. However, cytotoxicity was observed to increase proportionally with increased dose concentration. Higher cellular uptake of R2W4R2 conjugated self-assembled NPs was confirmed by flow cytometry and fluorescence microscopy in MCF-7 cell lines compared with W3R4W3 conjugated self-assembled NPs. Also, R2W4R2-NPs depicted a better MTX loading (1.1-fold higher) than W3R4W3-NPs. Thus, R2W4R2 self-assembled-NPs loaded with MTX was concluded to have a better uptake and targeting ability at the tumor site with enhanced drug loading (Zakeri-Milani et al., 2020).

Ma and associates developed anticancer NPs via pH-responsive self-assembly of a mussel-derived biomimetic peptide (PEP-RGD) with a chemotherapeutic agent, bortezomib (BTZ). The self-assembly of peptide-drug loaded NPs proceeds via the interaction between catechol moiety of peptide and boronic acid (BA) of the drug through a covalent ester linkage is pH-responsive (Fig. 6.7). In vitro drug release studies depicted a 4 times rapid release of BTZ in acidic pH than in basic pH, suggesting a prompted drug release from endosomal space maintained at low pH. Acting as a molecular signature via binding with integrins expressed on the cancer cell, RGD moiety was responsible for an enhanced in vitro uptake of NPs in αvβ3-overexpressed MDA-MB-231 cell line when compared to the negative cell lines. Increased cellular uptake was indicative of an improved accumulation of drug at the target tumor site. A high in vitro apoptotic activity was observed with BTZ-PEP-RGD NPs in the MDA-MB-231cell line. In vivo therapeutic efficacy was established using the MDA-MB-231 cell grafted nude mice model. A higher circulation time, target-receptor binding ability, and rapid drug release functionalities make BTZ-PEP-RGD NPs a superior anticancer agent (Ma et al., 2019).

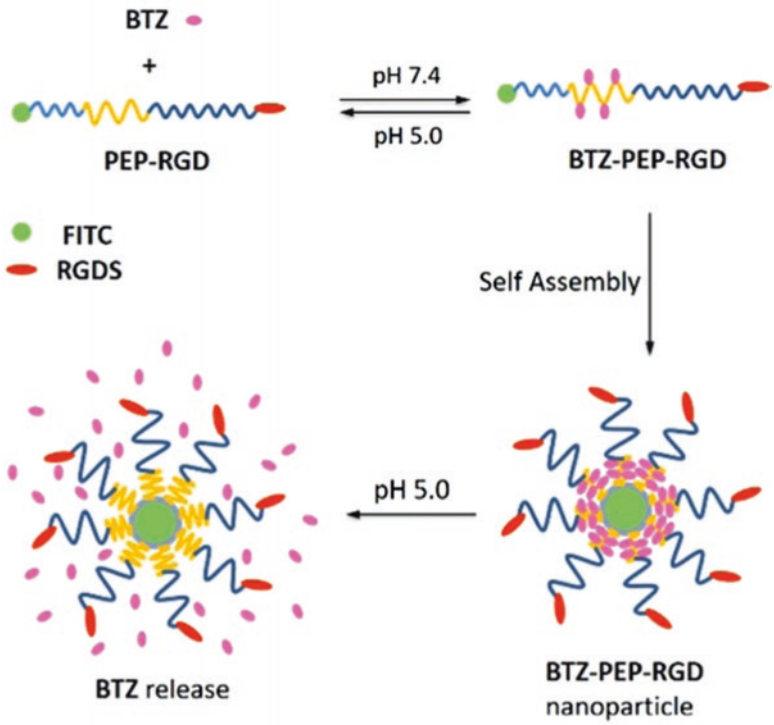

Fig. 6.7 Schematic representation of self-assembly of BTZ-PEP-RGD to nanosized particles with RGD motifs on the outer layer. (Adapted with permission from Ma et al., 2019. Copyright 2019 American Chemical Society)

6.4 Future Prospects

Protein- and peptide-based drug delivery systems are developing as a promising prospect for cancer therapeutics as they possess higher specificity and efficacy. These components can permeate through the cellular membranes and specifically bind to the receptors present on the tumor cells have shown lower toxicity. Peptides are utilized for targeting cellular signaling pathways as well as they cross the blood-brain barrier (BBB) effectively to deliver the therapeutic cargo. Peptides and protein delivery systems face certain shortcomings, such as sensitivity to enzymatic degradation, which decreases the half-life in the circulation. By encapsulating these proteins and peptide-based therapeutics with nanoparticles, it increases their stability, and structural integrity is kept intact so that they can reach the desired targeted region and undergo therapeutic effect.

Protein/peptide engineering is still in its nascent phase as it cannot completely strike out the challenges related to conventional therapy. Many peptides face permeability and stability issues when injected in vivo, as well as few cases of immunogenic responses (Sorolla et al., 2020b). Though the pharmaceutical industry faces many difficulties in manufacturing and scaling up protein-based nanocarriers, a large number of protein-based delivery systems are currently in clinical trials. More experimentations are being carried out with protein and peptide-based delivery systems to design nanotherapeutic components for targeting cancer with due time.

6.5 Conclusion

This article has engrossed a comprehensive study of how proteins and peptides are emerging as nanotherapeutics for cancer therapy. Owing to inherent biocompatibility with the human system, negligible cytotoxicity is observed with protein and peptides drug delivery systems. Ease of fabrication and a huge tendency for surface modification allows proteins and peptides to form a site-specific drug delivery system. Protein- and peptide-based nanomaterials have significantly been explored for their therapeutic efficacy in glioblastoma, breast cancer, gastric cancer, and lung cancer. Receptors overexpressed in cancerous tissues have been targeted with specific proteins and peptide nanoformulations. It has also been observed that anticancer agents bound to protein/peptide NPs accumulate in the cancer tissue to a much greater extent than the free drug. The book chapter also explores the ability of peptides to self-assemble spontaneously via non-covalent interactions. In situ self-assembly of peptide NPs in response to the site environment has been shown to enhance passive drug accumulation in tumor tissue via the EPR effect. Self-assembly provides the nanoformulation a more stable configuration, eventually increasing the blood circulation time and suppressing clearance from the body. Positively charged CPP-based nanomaterials have contributed significantly towards raising the penetrability and cellular uptake across the cancer tissue. Nanovaccines composed of

protein/peptide have also been discussed, which are in the long run towards developing cancer immunotherapy. A plethora of nano-based cancer therapeutics is well flourished in the market. However, the aforementioned applications need a critical clinical evaluation to enable a safe and effective drug delivery for treating cancer. Furthermore, personalized therapeutics can be developed if targets for protein/peptide nanomaterials could be recognized based on the molecular and genetic profile of each patient.

References

Agrawal, S., & Agrawal, J. (2015). Neural network techniques for cancer prediction: A survey. *Procedia Computer Science*. https://doi.org/10.1016/j.procs.2015.08.234

Akbarzadeh, A., et al. (2013). Liposome: Classification, preparation, and applications. *Nanoscale Research Letters*. https://doi.org/10.1186/1556-276X-8-102

Alhakamy, N. A., et al. (2020). Development of lipid membrane based assays to accurately predict the transfection efficiency of cell-penetrating peptide-based gene nanoparticles. *International Journal of Pharmaceutics*. https://doi.org/10.1016/j.ijpharm.2020.119221

Amer, M. H. (2014). Gene therapy for cancer: Present status and future perspective. *Molecular and Cellular Therapies*. https://doi.org/10.1186/2052-8426-2-27

Antoni, S., Soerjomataram, I., Møller, B., Bray, F., & Ferlay, J. (2016). An assessment of GLOBOCAN methods for deriving national estimates of cancer incidence. *Bulletin of the World Health Organization*. https://doi.org/10.2471/blt.15.164384

Balekouzou, A., et al. (2016). Epidemiology of breast cancer: retrospective study in the Central African Republic. *BMC Public Health, 16*, 1–10.

Bangham, A. D., & Horne, R. W. (1964). Negative staining of phospholipids and their structural modification by surface-active agents as observed in the electron microscope. *Journal of Molecular Biology*. https://doi.org/10.1016/S0022-2836(64)80115-7

Bawarski, W. E., Chidlowsky, E., Bharali, D. J., & Mousa, S. A. (2008). Emerging nanopharmaceuticals. *Nanomedicine: Nanotechnology, Biology, and Medicine*. https://doi.org/10.1016/j.nano.2008.06.002

Beaver, K., Williamson, S., & Briggs, J. (2013). Exploring patient experiences of neo-adjuvant chemotherapy for breast cancer. *European Journal of Cancer*. https://doi.org/10.1016/j.ejon.2015.06.001

Behan, F. M., et al. (2019). Prioritization of cancer therapeutic targets using CRISPR–Cas9 screens. *Nature*. https://doi.org/10.1038/s41586-019-1103-9

Bugoye, F. C., Leyna, G. H., Moen, K., & Mmbaga, E. J. (2019). Knowledge, perceived risk and utilization of prostate cancer screening services among men in Dar Es Salaam, Tanzania. *Prostate Cancer*. https://doi.org/10.1155/2019/2463048

Buys, S. S., et al. (2017). A study of over 35,000 women with breast cancer tested with a 25-gene panel of hereditary cancer genes. *Cancer*. https://doi.org/10.1002/cncr.30498

Cai, D., et al. (2005). Highly efficient molecular delivery into mammalian cells using carbon nanotube spearing. *Nature Methods*. https://doi.org/10.1038/nmeth761

Cao, M., Xing, R., Chang, R., Wang, Y., & Yan, X. (2019). Peptide-coordination self-assembly for the precise design of theranostic nanodrugs. *Coordination Chemistry Reviews*. https://doi.org/10.1016/j.ccr.2019.06.013

Cheng, Y., et al. (2018). Deep-level defect enhanced photothermal performance of bismuth sulfide–gold heterojunction nanorods for photothermal therapy of cancer guided by computed tomography imaging. *Angewandte Chemie International Edition*. https://doi.org/10.1002/anie.201710399

Cheng, X., et al. (2020). TfR1 binding with H-ferritin nanocarrier achieves prognostic diagnosis and enhances the therapeutic efficacy in clinical gastric cancer. *Cell Death & Disease*. https://doi.org/10.1038/s41419-020-2272-z

Chhikara, B. S., Rathi, B., & Parang, K. (2019). Critical evaluation of pharmaceutical rational design of nano-delivery systems for doxorubicin in cancer therapy. *Journal of Materials NanoScience, 6*, 47–66.

Chowdhury, S., Chowdhury, I. R., Mazumder, M. A. J., & Al-Suwaiyan, M. S. (2020). Predicting risk and loss of disability-adjusted life years (DALY) from selected disinfection byproducts in multiple water supply sources in Saudi Arabia. *Science of The Total Environment*. https://doi.org/10.1016/j.scitotenv.2020.140296

Daso, R. E., & Banerjee, I. A. (2020). Self-assembled peptide-based biocomposites for near-infrared light triggered drug release to tumor cells. *Biotechnology Journal*. https://doi.org/10.1002/biot.202000128

De Souza, J. A., Hunt, B., Asirwa, F. C., Adebamowo, C., & Lopes, G. (2016). Global health equity: Cancer care outcome disparities in high-, middle-, and low-income countries. *Journal of Clinical Oncology*. https://doi.org/10.1200/JCO.2015.62.2860

DeGregori, J., & Eldredge, N. (2020). Parallel causation in oncogenic and anthropogenic degradation and extinction. *Biological Theory*. https://doi.org/10.1007/s13752-019-00331-9

Egusquiaguirre, S. P., Igartua, M., Hernández, R. M., & Pedraz, J. L. (2012). Nanoparticle delivery systems for cancer therapy: Advances in clinical and preclinical research. *Clinical and Translational Oncology*. https://doi.org/10.1007/s12094-012-0766-6

Fitzmaurice, C., et al. (2017). The burden of primary liver cancer and underlying etiologies from 1990 to 2015 at the global, regional, and national level results from the global burden of disease study 2015. *JAMA Oncology*. https://doi.org/10.1001/jamaoncol.2017.3055

Gaitanis, A., & Staal, S. (2010). Liposomal doxorubicin and nab-paclitaxel: nanoparticle cancer chemotherapy in current clinical use. *Methods in Molecular Biology (Clifton, N.J.)*. https://doi.org/10.1007/978-1-60761-609-2_26

Gil, P. R., & Parak, W. J. (2008). Composite nanoparticles take aim at cancer. *ACS Nano*. https://doi.org/10.1021/nn800716j

Gong, Z., et al. (2020). PH-triggered morphological change in a self-assembling amphiphilic peptide used as an antitumor drug carrier. *Nanotechnology*. https://doi.org/10.1088/1361-6528/ab667c

Gregory, J. V., et al. (2020). Systemic brain tumor delivery of synthetic protein nanoparticles for glioblastoma therapy. *Nature Communications*. https://doi.org/10.1038/s41467-020-19225-7

Guo, X., et al. (2020). Multifunctional nanoplatforms for subcellular delivery of drugs in cancer therapy. *Progress in Materials Science*. https://doi.org/10.1016/j.pmatsci.2019.100599

Habibi, N., Kamaly, N., Memic, A., & Shafiee, H. (2016). Self-assembled peptide-based nanostructures: Smart nanomaterials toward targeted drug delivery. *Nano Today*. https://doi.org/10.1016/j.nantod.2016.02.004

Haume, K., et al. (2016). Gold nanoparticles for cancer radiotherapy: A review. *Cancer Nanotechnology*. https://doi.org/10.1186/s12645-016-0021-x

Hofheinz, R. D., Gnad-Vogt, S. U., Beyer, U., & Hochhaus, A. (2005). Liposomal encapsulated anticancer drugs. *Anti-Cancer Drugs*. https://doi.org/10.1097/01.cad.0000167902.53039.5a

Hoppenz, P., Els-Heindl, S., & Beck-Sickinger, A. G. (2020). Peptide-drug conjugates and their targets in advanced cancer therapies. *Frontiers in Chemistry*. https://doi.org/10.3389/fchem.2020.00571

Hu, X., et al. (2020). Recent advances in short peptide self-assembly: From rational design to novel applications. *Current Opinion in Colloid and Interface Science*. https://doi.org/10.1016/j.cocis.2019.08.003

Ibaraki, H., et al. (2020). Anti-metastatic effects on melanoma via intravenous administration of anti-NF-κB siRNA complexed with functional peptide-modified nano-micelles. *Pharmaceutics*. https://doi.org/10.3390/pharmaceutics12010064

Jiang, Z., Guan, J., Qian, J., & Zhan, C. (2019a). Peptide ligand-mediated targeted drug delivery of nanomedicines. *Biomaterials Science*. https://doi.org/10.1039/c8bm01340c

Jiang, X., et al. (2019b). Self-assembled peptide nanoparticles responsive to multiple tumor microenvironment triggers provide highly efficient targeted delivery and release of antitumor drug. *Journal of Controlled Release*. https://doi.org/10.1016/j.jconrel.2019.10.031

Kadiyala, P., et al. (2019). High-density lipoprotein-mimicking nanodiscs for chemoimmunotherapy against glioblastoma multiforme. *ACS Nano*. https://doi.org/10.1021/acsnano.8b06842

Kurrikoff, K., Aphkhazava, D., & Langel, Ü. (2019). The future of peptides in cancer treatment. *Current Opinion in Pharmacology*. https://doi.org/10.1016/j.coph.2019.01.008

Lau, A. K. T., & Hui, D. (2002). The revolutionary creation of new advanced materials – carbon nanotube composites. *Composites Part B: Engineering*. https://doi.org/10.1016/S1359-8368(02)00012-4

Li, X. Y., et al. (2020). Dual variable of drug loaded micelles in both particle and electrical charge on gastric cancer treatment. *Journal of Drug Targeting*. https://doi.org/10.1080/1061186X.2020.1777419

Lohcharoenkal, W., Wang, L., Chen, Y. C., & Rojanasakul, Y. (2014). Protein nanoparticles as drug delivery carriers for cancer therapy. *BioMed Research International*. https://doi.org/10.1155/2014/180549

Ma, Y., et al. (2019). Mussel-derived, cancer-targeting peptide as pH-sensitive prodrug nanocarrier. *ACS Applied Materials & Interfaces*. https://doi.org/10.1021/acsami.9b09031

Matsumura, Y., et al. (2004). Phase I clinical trial and pharmacokinetic evaluation of NK911, a micelle-encapsulated doxorubicin. *British Journal of Cancer*. https://doi.org/10.1038/sj.bjc.6602204

McCormick, P. J. (2018). Cancer tsunami: Emerging trends, economic burden, and perioperative implications. *Current Anesthesiology Reports*. https://doi.org/10.1007/s40140-018-0294-1

McNamara, K., & Tofail, S. A. M. (2017). Nanoparticles in biomedical applications. *Advances in Physics: X*. https://doi.org/10.1080/23746149.2016.1254570

Mie, M., Matsumoto, R., Mashimo, Y., Cass, A. E. G., & Kobatake, E. (2019). Development of drug-loaded protein nanoparticles displaying enzymatically-conjugated DNA aptamers for cancer cell targeting. *Molecular Biology Reports*. https://doi.org/10.1007/s11033-018-4467-2

Minelli, C., Lowe, S. B., & Stevens, M. M. (2010). Engineering nanocomposite materials for cancer therapy. *Small*. https://doi.org/10.1002/smll.201000523

Mohanraj, V. J., & Chen, Y. (2007). Nanoparticles – a review. *Tropical Journal of Pharmaceutical Research*. https://doi.org/10.4314/tjpr.v5i1.14634

Moyer, T. J., et al. (2019). Self-assembled peptide nanostructures targeting death receptor 5 and encapsulating paclitaxel as a multifunctional cancer therapy. *ACS Biomaterials Science & Engineering*. https://doi.org/10.1021/acsbiomaterials.9b01259

Mulder, W. J. M., et al. (2009). Molecular imaging of tumor angiogenesis using αvβ3-integrin targeted multimodal quantum dots. *Angiogenesis*. https://doi.org/10.1007/s10456-008-9124-2

Nazir, S., Hussain, T., Ayub, A., Rashid, U., & MacRobert, A. J. (2014). Nanomaterials in combating cancer: Therapeutic applications and developments. *Nanomedicine: Nanotechnology, Biology, and Medicine*. https://doi.org/10.1016/j.nano.2013.07.001

Ou, Z., et al. (2009). Functional single-walled carbon nanotubes based on an integrin αvβ3 monoclonal antibody for highly efficient cancer cell targeting. *Nanotechnology*. https://doi.org/10.1088/0957-4484/20/10/105102

Park, J., Sun, B., & Yeo, Y. (2017). Albumin-coated nanocrystals for carrier-free delivery of paclitaxel. *Journal of Controlled Release*. https://doi.org/10.1016/j.jconrel.2016.12.040

Peng, F., et al. (2014). Silicon nanomaterials platform for bioimaging, biosensing, and cancer therapy. *Accounts of Chemical Research*. https://doi.org/10.1021/ar400221g

Plummer, M., et al. (2016). Global burden of cancers attributable to infections in 2012: A synthetic analysis. *The Lancet Global Health*. https://doi.org/10.1016/S2214-109X(16)30143-7

Raju, G. S. R., et al. (2019). Nanomaterials multifunctional behavior for enlightened cancer therapeutics. *Seminars in Cancer Biology*. https://doi.org/10.1016/j.semcancer.2019.08.013

Raucher, D. (2019). Tumor targeting peptides: Novel therapeutic strategies in glioblastoma. *Current Opinion in Pharmacology*. https://doi.org/10.1016/j.coph.2019.01.006

Ren, C., Wang, Z., Wang, Q., Yang, C., & Liu, J. (2020). Self-assembled peptide-based nanoprobes for disease theranostics and disease-related molecular imaging. *Small Methods*. https://doi.org/10.1002/smtd.201900403

Ruan, H., et al. (2021). Stapled RAP12 peptide ligand of LRP1 for micelles-based multifunctional glioma-targeted drug delivery. *Chemical Engineering Journal*. https://doi.org/10.1016/j.cej.2020.126296

Sahoo, S. K., & Labhasetwar, V. (2003). Nanotech approaches to drug delivery and imaging. *Drug Discovery Today*. https://doi.org/10.1016/S1359-6446(03)02903-9

Saifi, M. A., Khan, W., & Godugu, C. (2018). Cytotoxicity of nanomaterials: Using nanotoxicology to address the safety concerns of nanoparticles. *Pharmaceutical Nanotechnology*. https://doi.org/10.2174/2211738505666171023152928

Sandra, F., Khaliq, N. U., Sunna, A., & Care, A. (2019). Developing protein-based nanoparticles as versatile delivery systems for cancer therapy and imaging. *Nanomaterials*. https://doi.org/10.3390/nano9091329

Sapra, P., & Allen, T. M. (2003). Ligand-targeted liposomal anticancer drugs. *Progress in Lipid Research*. https://doi.org/10.1016/S0163-7827(03)00032-8

Siegel, R. L., Miller, K. D., & Jemal, A. (2019). Cancer statistics, 2019. *CA: a Cancer Journal for Clinicians*. https://doi.org/10.3322/caac.21551

Silva, S., Almeida, A. J., & Vale, N. (2019). Combination of cell-penetrating peptides with nanoparticles for therapeutic application: A review. *Biomolecules*. https://doi.org/10.3390/biom9010022

Sorolla, A., et al. (2019). Triple-hit therapeutic approach for triple negative breast cancers using docetaxel nanoparticles, EN1-iPeps and RGD peptides. *Nanomedicine: Nanotechnology, Biology and Medicine*. https://doi.org/10.1016/j.nano.2019.04.006

Sorolla, A., Sorolla, M. A., Wang, E., & Ceña, V. (2020a). Peptides, proteins and nanotechnology: A promising synergy for breast cancer targeting and treatment. *Expert Opinion on Drug Delivery*. https://doi.org/10.1080/17425247.2020.1814733

Sorolla, A., et al. (2020b). Precision medicine by designer interference peptides: Applications in oncology and molecular therapeutics. *Oncogene*. https://doi.org/10.1038/s41388-019-1056-3

Stathopoulos, G. P., & Boulikas, T. (2012). Lipoplatin formulation review article. *Journal of Drug Delivery*. https://doi.org/10.1155/2012/581363

Tiwari, G., et al. (2012). Drug delivery systems: An updated review. *International journal of pharmaceutical investigation*. https://doi.org/10.4103/2230-973x.96920

Torti, S. V., et al. (2007). Thermal ablation therapeutics based on CNx multiwalled nanotubes. *International Journal of Nanomedicine, 2*, 707–714.

Toub, N., Malvy, C., Fattal, E., & Couvreur, P. (2006). Innovative nanotechnologies for the delivery of oligonucleotides and siRNA. *Biomedicine & Pharmacotherapy*. https://doi.org/10.1016/j.biopha.2006.07.093

Trama, A., Botta, L., & Steliarova-Foucher, E. (2018). Cancer burden in adolescents and young adults: A review of epidemiological evidence. *Cancer Journal (United States)*. https://doi.org/10.1097/PPO.0000000000000346

Walter, F. M., Humphrys, E., Tso, S., Johnson, M., & Cohn, S. (2010). Patient understanding of moles and skin cancer, and factors influencing presentation in primary care: A qualitative study. *BMC Family Practice*. https://doi.org/10.1186/1471-2296-11-62

Wang, X., Wang, Y., Chen, Z. G., & Shin, D. M. (2009). Advances of cancer therapy by nanotechnology. *Cancer Research and Treatment*. https://doi.org/10.4143/crt.2009.41.1.1

Wang, Z., et al. (2020). Development of a novel dual-order protein-based nanodelivery carrier that rapidly targets low-grade gliomas with microscopic metastasis in vivo. *ACS Omega*. https://doi.org/10.1021/acsomega.0c03073

Weinberg, R. S., et al. (2015). A phase II dose-escalation trial of perioperative desmopressin (1-desamino-8-d-arginine vasopressin) in breast cancer patients. *Springerplus, 4*, 1–8.

Whitehead, K., Pan, M., Masumura, K. I., Bonneau, R., & Baliga, N. S. (2009). Diurnally entrained anticipatory behavior in archaea. *PLoS One*. https://doi.org/10.1371/journal.pone.0005485

Wiener, L., Shaw Weaver, M., Sansom Daly, U. M., & Bell, C. J. (2015). Threading the cloak: Palliative care education for care providers of adolescents and young adults with cancer. *Clinical Oncology in Adolescents and Young Adults*. https://doi.org/10.2147/coaya.s49176

Yaku, K., Okabe, K., Hikosaka, K., & Nakagawa, T. (2018). NAD metabolism in cancer therapeutics. *Frontiers in Oncology*. https://doi.org/10.3389/fonc.2018.00622

Yan, X., et al. (2020). Arginine-rich peptide based nanoparticles with bridge-like structure: Enhanced cell penetration and tumor therapy effect. *Chemical Engineering Journal*. https://doi.org/10.1016/j.cej.2020.125171

Yang, J., et al. (2020). Nanoparticle-based co-delivery of siRNA and paclitaxel for dual-targeting of glioblastoma. *Nanomedicine*. https://doi.org/10.2217/nnm-2020-0066

Yu, M., Wu, J., Shi, J., & Farokhzad, O. C. (2016). Nanotechnology for protein delivery: Overview and perspectives. *Journal of Controlled Release*. https://doi.org/10.1016/j.jconrel.2015.10.012

Zakeri-Milani, P., et al. (2020). Self-assembled peptide nanoparticles for efficient delivery of methotrexate into cancer cells. *Drug Development and Industrial Pharmacy, 46*, 521–530.

Zhang, L., et al. (2020). Transformable peptide nanoparticles arrest HER2 signalling and cause cancer cell death in vivo. *Nature Nanotechnology*. https://doi.org/10.1038/s41565-019-0626-4

Zhao, J., & Stenzel, M. H. (2018). Entry of nanoparticles into cells: The importance of nanoparticle properties. *Polymer Chemistry*. https://doi.org/10.1039/c7py01603d

Zhao, Z., Ukidve, A., Kim, J., & Mitragotri, S. (2020). Targeting strategies for tissue-specific drug delivery. *Cell*. https://doi.org/10.1016/j.cell.2020.02.001

Zou, Q., Chang, R., Xing, R., Yuan, C., & Yan, X. (2020). Injectable self-assembled bola-dipeptide hydrogels for sustained photodynamic prodrug delivery and enhanced tumor therapy. *Journal of Controlled Release*. https://doi.org/10.1016/j.jconrel.2020.01.002

Chapter 7
Emerging Polymer-Based Nanomaterials for Cancer Therapeutics

Chandan Gupta, Abhay Uthale, Tanuja Teni, Premlata Ambre, and Evans Coutinho

Contents

C. Gupta · P. Ambre (✉) · E. Coutinho
Bombay College of Pharmacy (Autonomous), Kalina, Santacruz (E), Mumbai, India
e-mail: premlata.ambre@bcp.edu.in

A. Uthale · T. Teni
Advanced Centre for Treatment, Research and Education in Cancer (ACTREC), Kharghar, Navi Mumbai, Maharashtra, India

Homi Bhabha National Institute, Anushakti Nagar, Mumbai, India

M. Saravanan, H. Barabadi (eds.), *Cancer Nanotheranostics*, Nanotechnology in the Life Sciences, https://doi.org/10.1007/978-3-030-74330-7_7

7.1 Introduction

The challenge for current cancer treatment modalities is the ability to target tumour cells; this is because of issues related to poor pharmacokinetics, nonspecific biodistribution, adverse drug reactions, development of multiple drug resistance, etc. of the existing chemotherapeutic agents (Dreicer et al., 2004; Agarwal et al., 2019; Chidambaram et al., 2011). As a result, more than 10 million people die every year during the treatment of early to advanced stages of cancers (Siegel et al., 2018; Heidel & Davis, 2011). Surgery is the first choice of treatment when diagnosis is done in the early stage of cancer, whereas chemotherapy and radiation therapy are the second most widely used therapies (Killoran & Moyer, 2006; Minami et al., 2020); sometimes immunotherapy and immune checkpoint therapy have been used as adjuvant therapies; however they have been found to be less effective and reported to target even normal cells (Heidel & Davis, 2011; Betea et al., 2015). Combination therapy is widely used; however due to different pharmacokinetic profiles of the drugs in the combination, this strategy fails in the clinic. Therefore, development of novel drug delivery approaches to overcome the limitation of combination therapy is the need of the hour. Delivering the chemotherapeutic agents specifically to the target site has been attempted with the science of nanotechnology (Kummar et al., 2010).

The last decade has witnessed some remarkable advancements in nanotechnology-based nanocarriers for delivery of drugs. Nanocarriers have been explored with various types of polymers as carrier agents for encapsulation/conjugation of chemotherapeutic agents. These drug carriers are prepared from natural, synthetic or semisynthetic polymers to protect drug payloads from precipitation, renal clearance, protein adsorption and nonspecific cell uptake in major organs such as the liver and spleen. Polymeric nanocarriers (PNCs) are able to deliver hydrophobic as well as hydrophilic drugs to targeted tumour sites, due to the ability of these materials to be rapidly taken up by the reticuloendothelial system (RES), thus prolonging the circulation time in the body (Choi & Kim, 2007). The physicochemical properties of PNCs are directly related to their size, morphology, charge and the type of the polymer used in their preparation. Several advantages like clearance by RES and specific tissue distribution have been achieved through tuning the size of PNCs to 10–100 nm (Masarudin et al., 2015). Similarly, the shape of the nanoparticle, e.g. cylindrical, enables such nanoparticles to remain longer in circulation; on the other hand, a spherical shape imparts increased cellular uptake (Geng et al., 2007). The surface charge on the nanomaterial can interfere with cell membrane penetration; thus a positive charge on PNCs helps easy entry of the drug into tumour cells, in contrast to negatively charged and non-ionic materials; however the downside of positively charged nanomaterials is that they are cleared quickly from circulation, as their positive charge contributes to rapid filtration by the glomerular apparatus. Thus, properties like size, shape and charge are important factors to be considered while engineering and designing suitable PNCs for cancer treatment.

In this chapter, we will discuss different polymeric nanomaterials as drug carriers and their current clinical status, with suitable examples.

7.2 Types of Polymeric Nanomaterials as Drug Carriers (PNC)

Polymer-based nanomaterials have been classified as depicted in Fig. 7.1 on the basis of their size, shape and type of polymer.

7.2.1 Polymeric Nanoparticles

The polymeric nanoparticles are submicron (size range 10–1000 nm) solid colloidal particles. Based on the method of preparation, they have been categorized as nanocapsules or nanospheres. Nanocapsular polymeric nanoparticles encapsulate the drug in the central cavity with a liquid medium (i.e. aqueous or lipid medium depending on the solubility of the drug), and the boundary of the capsule is controlled by tuning the polymerization between the disperse and continuous phases. When the drug is susceptible to degradation, then it is loaded onto the nanoparticles by adsorption in case of nanospheres (Fig. 7.1a). The structure of the surface of the nanoparticles can be fine-tuned using suitable polymer(s) to provide for higher drug loading and maximum drug delivery. A layered approach (Johnston et al., 2006) has been widely explored for loading drug/antigen to achieve sustained delivery at the targeted site in case of nanocapsules. Traditionally an emulsification approach was used for preparation of nanoparticles, but due to use of harsh chemicals and being a time-consuming process, it is not the method of choice today. Some techniques like solvent evaporation/solvent extraction, nanoprecipitation, anti-solvent method,

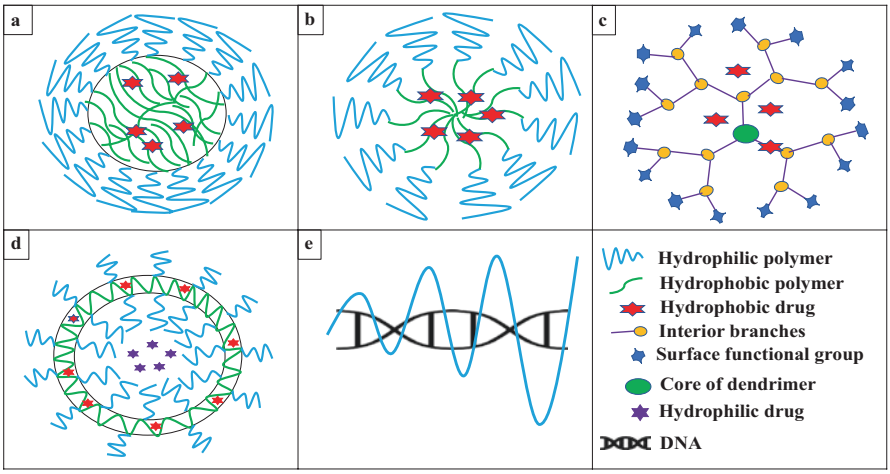

Fig. 7.1 Types of polymer nanomaterials for cancer drug delivery. (**a**) Polymeric nanoparticles (size: 10–1000 nm), (**b**) polymer micelle (size: 10–200 nm), (**c**) polymeric dendrimer (size: 3–20 nm), (**d**) polymersomes (size: 5–50 nm) (**e**) Polyplexes (size: 30–100 nm)

salting out and particle replication in not wetting templates (PRINT) have been developed to produce nanocapsules on a pilot scale (Sah & Sah, 2015; Perry et al., 2011).

Both passive and active targeting methods have been followed for delivering drug-loaded polymeric nanoparticles in the treatment of cancer; however, passive targeting has been widely adopted for clinical therapy. It has some drawbacks, such as lack of diffusion through the solid tumours, poor permeability through blood vessels in the tumour region, chances of drug escaping from the leaky vasculature and the likelihood of healthy cells uptaking the antitumour drug due to nonspecificity. Because of these drawbacks, active targeting has been preferred for delivering drugs by polymer-based nanoparticles. Polyethylene glycol (PEG), 2-hydroxypropyl methacrylate, copolymer poly(lactic-*co*-glycolic) acid (PLGA), polylactic acid (PLA), poly(ε-caprolactone) (PCL), chitosan, dextran, etc. have been generally used in the preparation of polymeric nanomaterials.

Fabienne Danhier et al. have reported paclitaxel (PTX) loaded on PEGylated PLGA polymeric nanoparticles with enhanced permeability and retention (EPR). It was more cytotoxic compared to PTX in cremophor EL (IC_{50} 5.5 vs 15.5μg/ ml) in HeLa cells. The latter, cremophor EL, has been used as a vehicle for improving solubility and modifying interfacial tension; however several adverse effects have been reported with the cremophor EL**.**PTX combination [a dot sign (.) indicates a physical mixture of drug and polymer in the formulation] (Danhier et al., 2009).

Similarly, Hyuk Sang et al. have reported nanoparticles made from poly(D,L-lactic-*co*-glycolic acid (PLGA) and polyethylene glycol (PEG) and conjugated with folate and doxorubicin (Dox) [PLGA-PEG-Folate-Dox, wherein a dash sign (-) indicates a conjugate between the polymer and the drug] for actively targeting the folate receptor-positive cell lines (Yoo & Park, 2004), since folate is a nonimmunogenic vitamin (vitamin B_9) with high affinity for the folate receptors which play crucial role in synthesis of DNA and production of WBC and RBC. The functionalization of nanoparticles with folate guided the nanosystem to the overexpressed folate receptors via receptor-mediated endocytosis pathway. Nanoparticles made from the natural polymer chitosan functionalized by trastuzumab (anti-HER2 humanized antibody) and conjugated with Dox for active target of cancer cells were fabricated by Yousefpour P. et al. These nanoparticles demonstrated a higher uptake for HER2+ breast cell line (Yousefpour et al., 2011; Haghighi et al., 2019).. Table 7.1 lists some more examples of nanoparticles and their applications.

7.2.2 Polymeric Micelles

Polymeric micelles are nanosize (10–200 nm) self-assemblies made up of di- or tri-block amphiphilic copolymers. Micelles are formed when an amphiphilic molecule is added to an aqueous solution at a specific concentration that is known as critical micelle concentration (CMC). At CMC, the amphiphilic di- or tri-block polymer tries to roll the hydrophilic head into the core while orienting the hydrophobic tail

Table 7.1 Representative examples of polymer-based nanomaterial for cancer therapy

Class of nanomaterial	Composition of polymer-based nanocarrier	Drug	Cell lines	Targeted site of tumour	Outcome of study	Ref
Nanoparticles	PEGylated hyaluronic acid (HA)	Doxorubicin (DOX)	SCC7, HCT116, and CV-1 cell	OverexpressCD44 receptors of lung and colon cancer cells, pancreas	In vivo biodistribution study demonstrated improved uptake in tumour cell with prolonged circulation time and reduced liver toxicity	Choi et al. (2011)
	Glycyrrhetinic acid (GA)-modified alginate (AA)	DOX	HepG2 cells	Liver tumour cells	It selectively induced cell death in live tumour cell than healthy liver cells with reduced cardiac toxicity	Zhang et al. (2012)
	Single chain fragment variable against epidermal growth factor receptor Heparin nanoparticle (ScFv-EGFR/Heparin)	Cisplatin	EGFR expressing non-small cell lung cancer H292 cell	Overexpress EGFR receptors of non-small cell lung cancer	In-vitro/in-vivo study indicated efficiency to selectively internalize in EGFR overexpress H292 lung tumour cells with improved antitumour efficacy and reduced side-effects	Peng et al. (2011)

(continued)

Table 7.1 (continued)

Class of nanomaterial	Composition of polymer-based nanocarrier	Drug	Cell lines	Targeted site of tumour	Outcome of study	Ref
Micelles	Folic acid conjugated poly(styrene-co-maleic anhydride) (FA-SMA)	Curcumin-difluorinated (CDF)	HeLa, SKOV3, and A549	Overexpress folate receptors of ovarian and cervical tumour cells	Confocal microscopic study of developed formulation showed comparatively higher uptake than the non-targeted formulation in both the cell lines with excellent anticancer activity	Luong et al. (2017)
	Poly(histidine-co-phenylalanine)-*b*-poly(ethylene glycol) and poly(L-lactic acid)-*b*-PEG-folate	DOX	Wild-type-sensitive (A2780) and DOX-resistant ovarian carcinoma cell lines	Overexpress folate receptors of ovarian cancer	Developed nanoparticles showed burst released of drug in endosomal pH of tumour cells and drug effectively kill both wild-type-sensitive (A2780) and DOX-resistant ovarian MDR cancer- cell	Kim et al. (2008)
	Pluronic-F127	Miltefosine (MTF)	HeLa and H-358 cells	Cervical carcinoma, bronchioalveolar carcinoma	The developed therapeutic formulation showed high potential for cancer treatment and improved the pharmacotherapy by reducing side effects	Valenzuela-Oses et al. (2017)
	Monomethyl poly (ethylene glycol)-poly (ε-caprolactone)-poly (trimethylene carbonate) [MPEG-P(CL-*co*-TMC)]	Curcumin	CT26 colon carcinoma cells	Colon cancer	The developed curcumin micelles showed improved cellular uptake in CT26 cell lines and increased the efficacy of inhibition growth of CT26 colon tumour	Yang et al. (2015a)

Class of nanomaterial	Composition of polymer-based nanocarrier	Drug	Cell lines	Targeted site of tumour	Outcome of study	Ref
Dendrimer	Hyaluronic acid-modified amine-terminated-polyamidoamine dendrimer nanoparticles [HA-PAMAM (G4)]	Platinates (Pt), DOX	MCF-7 and MDA-MB-231 breast cancer cell	Overexpress CD44 receptors of lungs, breast	Significantly inhibited tumour cells due to accumulation of HA@PAMAM-Pt-Dox and exhibited synergistic effects of Pt and Dox in breast cancer cell lines	Guo et al. (2019)
	Folic acid modified generation 5 (G5) PAMAM dendrimers	DOX	KB cells	Overexpress folate receptors of tumour cells	The developed formulation exhibited folic acid receptor-mediated endocytosis in cancer cells and demonstrated enhanced antitumour efficiency	Zhang et al. (2018)
	AS1411 aptamer-functionalized/PEGylated PAMAM dendrimer (G4)	5-Fluorouracil with BODIPY dye (fluoresces dye generally used for cell imaging study)	MKN45 gastric cancer cells	Overexpress nucleolin receptors of gastric tumour cells	The biodistribution study showed an enhanced accumulation of the drug complex in the tumour region of nucleolin receptor	Barzegar Behrooz et al. (2017)

(continued)

Table 7.1 (continued)

Class of nanomaterial	Composition of polymer-based nanocarrier	Drug	Cell lines	Targeted site of tumour	Outcome of study	Ref
Polymersomes	Peptide CGGGHKYLRW (TBP)-PEG-P(TMC-DTC) [Poly(ethylene glycol)-*b*-poly(trimethylene carbonate-*co*-dithiolane trimethylene carbonate) conjugated with transferrin binding peptide(TBP) functionalized polymersomes]	DOX HCl	Transferrin receptor (TfR) overexpressing HCT-116 colorectal cancer cells	Overexpress transferrin receptors of colorectal tumour cells	It significantly enhanced the antitumour efficacy in mice bearing HCT-116 tumours when compared with polymersomes without Tf binding	Wei et al. (2020)
	AS1411 aptamer-conjugated, SN38-loaded PEG-pep-PLA chimeric nanopolymersomes	SN38 (active metabolite of irinotecan)	C26-tumour	Overexpress fibronectin (FN) of breast tumours	The developed polymersomes exhibited smart controlled release of drug against cancer cells with highest therapeutic index	Bessone et al. (2019)
	Hyaluronan-polycaprolactone	Doxorubicin	4T1 and MCF7	Overexpress CD44 of breast tumour cells	It demonstrated highest loading capacity and excellent drug accumulation efficiency in tumour cells	Shahriari et al. (2019)

Class of nanomaterial	Composition of polymer-based nanocarrier	Drug	Cell lines	Targeted site of tumour	Outcome of study	Ref
Polyplexes	Polyethyleneimine (PEI) and hyaluronic acid (HA)	The cell division cycle protein 20 (CDC20) siRNA, doxorubicin	MCF7 cells, SUM149PT	Overexpress HA receptors of breast cancer	The in vivo study showed inhibition of cell migration and metastasis. It's therefore considered as a potential target to inhibit migration of highly aggressive breast cancer cells	Parmar et al. (2018)
	Chitosan conjugated folic acid	siRNA and doxorubicin	4T1, 4T1-MDR cell lines	Overexpress 4T1 multidrug resistance tumour cells	The developed DOX-loaded polyplexes exhibited enhanced antitumour efficacy with improved circulation time	Butt et al. (2016)
Polymer-lipid hybrid nanoparticles (LPHN)	Folate-conjugated chitosan-lipid hybrid nanoparticles	Cisplatin	SK-OV-3, A2780 and MCF-7 cancer cell lines	Overexpress folate receptors of breast cancer cells	The developed LPHN system enhanced the cellular uptake and increased the anticancer efficacy for the spheroid tumour model as compared to non-targeted LPHN	Khan et al. (2020)

(continued)

Table 7.1 (continued)

Class of nanomaterial	Composition of polymer-based nanocarrier	Drug	Cell lines	Targeted site of tumour	Outcome of study	Ref
Polymer-surfactant	Sodium alginate, dioctyl sodium sulfosuccinate	Methylene blue for photodynamic therapy (PDT)	MCF-7 and 4T1	p-Glycoprotein overexpressing cells of solid tumour, e.g. breast, lung	The developed polymer-based surfactant enhanced the reactive oxygen species (ROS) production and favourable alteration in the subcellular distribution thereby contributing to enhanced PDT efficacy of nanoparticle-encapsulated photosensitizer	Chavanpatil et al. (2007)
	Sodium alginate, dioctyl sodium sulfosuccinate	DOX	MDCK-WT and MDCK-MDR cells	Overexpress P-glycoprotein of tumour cells	The encapsulated polymer surfactant demonstrated improved oral bioavailability compared to the plain drug in solution	Kirtane et al. (2017)
Cyclodextrin polymer conjugate	Polyrotaxanes consisting of cyclodextrin rings, polyethylene glycol	DOX	Cell line L929	Connective fibroblast adhesive cell	The MTT assay demonstrated high antitumour efficacy with reduced side effects	Adeli et al. (2011)
	Alginate (AA), β-cyclodextrin (β-CD)	5-Folourouracil (5-FU)	HT-29 cell line	Colon tumour cell	The developed complexation helped to reduce the initial burst release effect and gave sustained release for long period of time	Hosseinifar et al. (2018)

Class of nanomaterial	Composition of polymer-based nanocarrier	Drug	Cell lines	Targeted site of tumour	Outcome of study	Ref
Polymer-drug conjugate	Poly[N-(2-hydroxypropyl) methacrylamide]-DOX conjugate with Gly-Phe-Leu-Gly cathepsin B-sensitive linker	DOX	4T1 cells	Breast tumour cells	Tumour growth inhibition and immunohistochemical study revealed the enhanced antitumour efficiency with fewer side effect. Ex vivo imaging study showed accumulation of drug in 4T1 tumour cells via EPR effect	Wei et al. (2016)
	Arginine-glycine-aspartic acid (RGD)-decorated polyethylene glycol (PEG)-conjugated paclitaxel	Paclitaxel (PTX)	SGC7901cells, cytokine-induced killer (CIK) cells	αvβ3 integrins of gastric tumour cells	In vivo study indicated the selective delivery of RGD micelles to the tumour cells and inhibition of the tumour growth by triggered releasing PTX inside the tumour cells due to glutathione (GSH) enzyme	Shi et al. (2019)

(continued)

Table 7.1 (continued)

Class of nanomaterial	Composition of polymer-based nanocarrier	Drug	Cell lines	Targeted site of tumour	Outcome of study	Ref
	Poly(glycerol adipate) (PGA)-conjugated methotrexate (MTX)	Methotrexate (MTX)	791T cells, Saos-2 cells	Bone tumour cells (osteosarcoma cells)	It was first PGA conjugated MTX nanomaterial which reveals that in polymer can be conjugated to drug without using any bio responsive linker if PGA like suitable biodegradable polymer can be used. However PGA-MTX conjugate exhibited less cytotoxicity and potency than free methotrexate hence further modification needed for PGA-MTX for improvement in specificity and efficacy for tumour cells	Suksiriworapong et al. (2018)

in such a way so as to form intermolecular polar bonds with the aqueous solution (Fig. 7.1b). The core of the micelle is usually constructed from polyesters or poly ethers, whereas the hydrophilic shells are built from poly (ethylene glycol) (PEG), poly (D, L) lactic acid (PLA) or poly(ε-caprolactone) (PCL). Hydrophobic groups in the core of micelle allow loading of hydrophobic chemotherapeutic drugs. Micelles are generally prepared by techniques such as oil-in-water emulsion, direct dissolution, dialysis or film casting (Tyrrell et al., 2010; Gaucher et al., 2005). David Vetvicka et al. have prepared micelles from [poly(ethylene oxide-*b*-poly(allyl glycidyl ether)] [*b* stands for block] system and loaded the micelles with the drug doxorubicin. The micelles showed improved circulation time and enhanced accumulation at the tumour site with 20 times reduced toxicity compared with free Dox (Vetvicka et al., 2009). Baorui Liu et al. have constructed a micellar system with the composition [poly(N-isopropyl acrylamide-*co*-acryl amide)-*b*-poly(D,L-lactide)] that is both temperature sensitive and biodegradable, loaded with the drug docetaxel. The lower critical solution temperature (LCST) of this micellar system is 41 °C, which is close to the clinical hyperthermia treatment (above 40 °C). These micelles exhibited an excellent antitumour efficacy with reduced toxicity in an in vitro and in vivo study (Liu et al., 2008). In yet another example, Xiaoxia Wen et al. have prepared micelles [^{111}In-DTPA-PEG-C225] where the anti-EGFR antibody (C225) has been conjugated to the polymer PEG-diethylenetriaminepentaacetic acid (DTPA) which has been tagged with the ^{111}In isotope (Wen et al., 2001). The antibody C225 binds with high affinity to overexpressed EGFR receptors on the surface of cancer cells. A selective accumulation of ^{111}In-DTPA-PEG-C225 was observed in tumour cells overexpressing the EGFR receptor where the indium radionuclide isotope ^{111}In was used as the imaging agent for detection of tumour and metastasis in the organ. More recent examples of polymeric micelles are listed in Table 7.1.

7.2.3 Dendrimers

Dendrimers are synthetic monodisperse nanomaterials with three-dimensional tree-like architecture assemblies (Tomalia et al., 2012; Abbasi et al., 2014). Dendrimers have a variety of free functional groups that enable them to conjugate drugs or to encapsulate drugs within their hollow confines (Fig. 7.1c). Dendrimers have unique geometry with high surface density (i.e. high drug loading potential) and are therefore attractive for tethering anticancer drugs, imaging agents and targeting moieties (Noriega-Luna et al., 2014). The ability of dendrimers to passively accumulate and penetrate into solid tumours makes them preferred candidates for treatment of cancer. Dendrimers are prepared either by the divergent or convergent method. In the divergent method, dendrimers are prepared sequentially, expanding from the central core to the periphery, whereas in the convergent method, the dendrimers are made in a reverse fashion, moving from the periphery to the central core (Medina & El-Sayed, 2009). The molecular weight and particle size of dendrimers increase exponentially with increase in the number of generations or branches (Maiti et al.,

2004). Generally, dendritic nanoparticles are in the range of 3–20 nm which makes them suitable for intravenous, intraperitoneal, transdermal and oral delivery (Kobayashi & Brechbiel, 2005). One can grow dendrimers in 1–13 generations using different methods of preparations. The lower generations are light and flexible, whereas higher generations are dense in molecular weight. Dendrimers are suitable nanocarrier systems for targeted drug delivery because of the high volume of internal pores, mono-dispersibility and the ability to modify their surface properties.

Polymers such as polyethylene glycol (PEG), poly(amidoamine) (PAMAM), polyesters, poly (propylene imine) (PPI), melamine, dextrans, poly[2,2-bis(hydroxymethyl) propionic acid], poly(glycerol), phosphor hydrazone, carbo silanes, poly(glycerol-*co*-succinic acid), etc. have been explored for fabrication of dendrimers (Yang et al., 2004; Lee et al., 2005; Shukla et al., 2019).

Xue-Ling Guo et al. have prepared a PAMAM-G4 (G4 stands for 4th generation) dendrimer for loading cisplatin (Pt), doxorubicin (Dox) and hyaluronic acid (HA) [HA@PAMAM-Pt-Dox] and demonstrated the enhanced accumulation of the drugs in MCF-7 and MDA-MB-231 nude mice bearing tumours compared with the free drugs. This dendrimer drug delivery system has been found to be stable and safe (Guo et al., 2019). The researchers Mengen Zhang et al. have prepared PAMAM-G5 dendrimer conjugated with folate and doxorubicin using a pH-sensitive linker (cis-aconityl) and in an in vitro study have shown the slow release and enhanced cellular uptake of the drug doxorubicin (DOX) at physiological pH. The active targeting approach has been investigated by Amir Barzegar Behrooz et al. using aptamer (APT^{AS1411})-based PEGylated PAMAM dendrimer system (PAMAM-PEG) loaded with the drug 5-fluorouracil (5-FU). This system (PAMAM-PEG-APT^{AS1411}.5-FU) demonstrated an enhanced accumulation of the drug 5-FU in gastric cell lines (MKN45) when tested in vitro with a similar effect observed in the in vivo study arising from the interaction of APT^{AS1411} with the nucleolin receptors (Barzegar Behrooz et al., 2017).

7.2.4 Polymersomes

Polymersomes are synthetic self-assembled polymeric vesicles containing a broad aqueous cavity that can hold hydrophilic drugs and a hydrophobic polymeric bilayer that can hold hydrophobic anticancer drugs (Fig. 7.1d) (Liu et al., 2012; Simone et al., 2008). Polymersomes have better stability than liposomes due to the wider bilayer membrane thickness (5–50 nm), entanglement and lateral diffusivity (Rideau et al., 2018). Though they possess high drug loading capacity and prolonged circulation time, the downside is that the stable bilayer membrane restricts immediate release of the drug. Polymersomes have been prepared using methods like solvent switch, film rehydration, solid rehydration and electro-formation (Eissa et al., 2013; Yildiz et al., 2007).

Jing Xu et al. have prepared polymersomes using poly[methoxy-poly(ethylene glycol) and ethyl p- aminobenzoate] graft phosphazenes (PEPs). The graft polymer

was prepared by graft substitution reaction between the terminal amino group of PEG–NH_2, the ester group of ethyl p-aminobenzoate (EAB) and the amino group of ethylene diamine (ED) which specifically forms NH_2–PEG–ED–EAB. This was followed by another substitution reaction with the Cl functional group of poly(dichlorophosphazene) using a ring-open polymerization that produces the PEP graft polymer. PEP was fabricated into polymersomes and loaded with DOX by dialysis. The in vivo studies showed an increase in survival rates with enhanced safety when this polymersome was administered by the intravenous route into nude mice with the MCF-7 tumour xenograft compared to free DOX (Xu et al., 2014).

Current research in this area focuses on functionalization of polymersome with lactoferrin (Lf) and transferrin (Tf) for selectively targeting brain tumours (Pawar et al., 2013; Nicolas et al., 2013). One such study has been reported by Zhiqing Pang et al., where DOX has been loaded into the biodegradable PEG-PCL polymersomes having a vesicle size small enough to cross the blood-brain barrier. PEG-PCL polymersome has been conjugated with transferrin to selectively target glioma cells. This system was found to be more cytotoxic against glioma cells as compared to free DOX. The study also showed a reduction in tumour volume, increased apoptosis and improved survival rate of rats with glioma (Pang et al., 2011). A similar study for delivering DOX was carried out by Yaohua Wei et al. with transferrin functionalized polymersomes made from maleimide functionalized poly(ethylene glycol)-*b*-poly(trimethylene carbonate-*co*-dithiolane trimethylene carbonate) [Mal-mPEG-P(TMC-DTC)]. The functionalized polymersomes exhibited receptor-mediated delivery of DOX in tumour cells and have revealed high binding affinity for overexpressed transferrin receptors (Wei et al., 2020). The recent developments in polymersome have been discussed with their outcomes in Table 7.1.

7.2.5 Polyplexes

Polyplexes are the yet another novel non-vector-type nanocarrier systems with size range of 30 to 100 nm for the effective and safe delivery of a specific gene or a nucleic acid (Linhardt 2015). They have been synthesized by conjugating cationic polymers and anionic nucleic acid (single-stranded DNA or RNA) through electrostatic interactions (Fig. 7.1e and Table 7.1). The conjugate protects the nucleic acid from degradation, thereby enhancing cellular uptake of drug into tumour cells (Uchida et al., 2016). However, application of polyplexes is limited due to degradation by serum nucleases in the blood when administered intravenously and also due to its repulsive interaction with the anionic membrane of tumour cells, which reduces the cellular uptake of the drug.

Lina Chen et al. (2013) have reported 12-acryloyloxy dodecyl phosphorylcholine-polyethyleneimine**:**DNA [ADPC-PEI**:**DNA {a colon sign (:) indicates ionic bond between the polymer and DNA}] polyplex for improved delivery of DNA for cancer gene therapy. The ADPC-PEI**:**DNA polyplex has shown excellent cellular uptake in HepG2 tumour cells (Chen et al., 2013). Adeel Masood Butt et al. have made a

polyplex of chitosan-coated (CS) PF127 (which is a block copolymer of [poly(ethylene oxide) and poly(propylene oxide)] and TPGS (water-soluble derivative of vitamin E) with siRNA and DOX. In vivo and ex vivo optical imaging data revealed an enhanced accumulation of DOX in 4T1-MDR tumour cells with improved pharmacokinetic properties like improvement in circulation time and reduced clearance by RES (Butt et al., 2016).

7.2.6 Polymer Hybrid Systems

Polymer hybrid systems are combinations of polymer and a macromolecule like lipid or surfactant or cyclodextrin or a drug. The resultant system improves stability, circulation time and drug loading capacity and provides control over drug release kinetics, etc. Figure 7.2 illustrates classification of polymer hybrid systems.

7.2.6.1 Polymer-Lipid Hybrid System

Polymeric nanoparticles when conjugated with liposomes produce polymer-lipid hybrid nanoparticles (LPHN). They typically possess synergistic properties of both materials and are also labelled as the next-generation drug delivery system. Size of LPHNs has generally been recorded in the range of 150–400 nm and has been targeted for cancer therapy. Furthermore, LPHNs have excellent biodegradability and biocompatibility properties and can therefore overcome the drawbacks of liposomes like instability in long-term storage and undesirable drug leakage. They can generate stable nanoparticles, capable of loading both hydrophobic and hydrophilic drugs (Fig. 7.2a). Ruifeng Wu et al. have developed an aptamer (APT)-decorated LPHN [i.e. poly(L-lactide)-poly(ethylene glycol) or PLA-PEG nanoparticle] for the co-delivery of a prodrug of docetaxel (DTXp) and cisplatin (Pt) to treat non-small cell lung cancer (NSCLC). The DTXp.Pt.APT-LPHN demonstrated significantly enhanced cytotoxicity and profound tumour inhibition ability compared to the non-aptamer-decorated LPHN and single drug-loaded LPHNs (Wu et al., 2020). In another study, Muhammad Muzamil Khan et al. have synthesized LPHN conjugate of folate with chitosan and Lipoid 75 (type of phospholipid) for loading cisplatin. The in vitro study revealed that a significant amount of cisplatin accumulated in SK-OV-3, A2780 ovarian cancer cell lines and MCF-7 breast cancer cell lines (Khan et al., 2020) and enhanced therapeutic activity.

7.2.6.2 Polymer-Surfactant Nanoparticles

A combination of polymer and surfactant forms a stable polymer-surfactant micelle (PSM) at low CMC (Fig. 7.2b). The size of PSM is dependent on the concentration of both surfactant and polymer; usually the size of PSM is in the range of 10–1000 nm

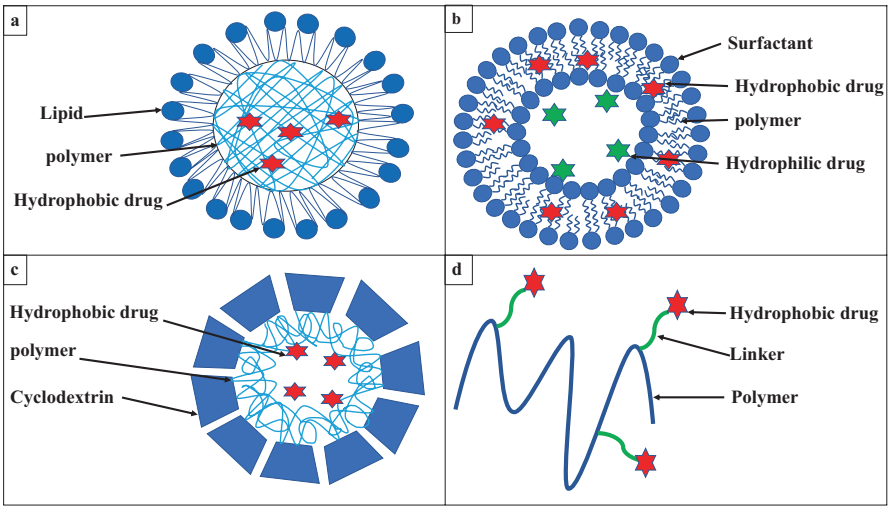

Fig. 7.2 Classification of polymer-hybrid nanomaterials. (**a**) Polymer-lipid hybrid nanoparticle (size: 150–400 nm), (**b**) polymer-surfactant (size 10–1000 nm), (**c**) cyclodextrin polymer conjugates (size 10–1000 nm), (**d**) polymer-drug conjugate (size 2–20 nm)

(Nasef et al., 2015). Nanoprecipitation is the common technique used for preparation of polymer-surfactant nanoparticles (PSNPs). The PSNP formulation helps to decrease the interfacial surface tension between two or more systems (liquid-liquid, gas-liquid or solid-liquid) at CMC – a property that is crucial for drug delivery; hence PSNPs are a promising drug delivery system for cancer therapy. Chavanpatil et al. have reported a PSNP by combining the polymer sodium alginate with the surfactant dioctyl sodium sulfosuccinate. This system exhibited enhanced cytotoxicity in P-glycoprotein drug resistance cell lines (Chavanpatil et al., 2007). Similarly, Kirtane et al. have developed a polymer-surfactant-based system for DOX that showed enhanced cellular uptake and oral bioavailability and which inhibits the transporter P-glycoprotein in the epithelial cells (MDCK-MDR) of the gastrointestinal tract. The PSNP was prepared from a complex of the polymer sodium alginate with DOX in the core of the nanomaterial, and the PSNP was stabilized with the sodium bis(2-ethylhexyl) sulfosuccinate (aerosol OT) surfactant (Kirtane et al., 2017).

7.2.6.3 Polymer Cyclodextrins (pCDs)

pCDs are cyclic oligosaccharides made up of linkage of glucose subunits and α-1,4-glycosidic bonds. pCDs have been explored for improving the solubility of Class II BCS (biopharmaceutics classification systems) drugs. These drugs typically contain a carboxylic acid with pK_a values between 4 and 5 and are insoluble at fasted gastric pH but soluble at intestinal pH. The pCDs are cone-shaped macromolecules with a

hydrophilic exterior and the interior being hydrophobic; the latter is often utilized for encapsulating hydrophobic drugs (Fig. 7.2c). Moreover, pCDs exhibit dose-dependent toxicity which can be overcome by surface conjugation with polymers like chitosan, alginic acid (AA), hyaluronic acid (HA), etc. The pCDs form hollow nanoparticles with size range of 10–1000 nm (Zarepour et al., 2019). These systems help to enhance biocompatibility, stability, retention time and permeability of the drug payload. pCDs conjugated with AA and loaded with 5-fluorouracil (5-FU) when tested in the HT-29 cell line exhibited significant accumulation of 5-FU in HT-29 cells compared to free 5-FU (Hosseinifar et al., 2018) and good therapeutic activity. All said and done, pCDs have not been extensively investigated, although the system has a good potential for success.

7.2.6.4 Polymer-Drug Conjugates (PDC)

Polymer-drug conjugate (PDC) is an approach for passive as well as active target drug delivery and is capable of preventing premature drug release into the blood circulation, improving aqueous solubility, enhancing stability, extending plasma half-life and altering biodistribution. It selectively aids delivery of anticancer drugs to the targeted tumour site without affecting normal healthy cells. Selection of the overexpressed receptor and the receptive ligand plays a crucial role in the design of the PDC so that it can discriminate between the host cell and the tumour cell. Several PDCs have been successfully translated into clinical trials. PDC is prepared by reacting a hydrophobic anticancer drug with a high molecular weight hydrophilic polymer by forming a hydrolysable covalent bond (Fig. 7.2d). Usually the size of PDC falls in the range of 2–20 nm (Linhardt 2015). The PDC system is designed to undergo hydrolysis by endogenous enzymes present at the targeted site like phosphatases, esterases, amidases, peptidases, cathepsin, etc. In addition, these conjugates can be designed to release the drug within the lysosomal compartment (lysosomotropic delivery).

The first approved PDC clinical trial study was reported with N-(2-hydroxypropyl) methacrylamide (HPMA) copolymer conjugated with DOX. HPMA is a promising synthetic polymer due to presence of multi-functionality for conjugation and is biocompatible and non-immunogenic towards host cells. Preclinical studies have revealed the HMPA-DOX conjugate has an improved pharmacokinetic property and enhanced plasma half-life of 1 hour compared to free DOX which is just 5 minutes. However, phase II trial was discontinued due to poor anticancer efficacy; attempts were made to enhance the activity by conjugating the PDC with a galactosamine targeted for liver hepatocytes. Unfortunately, this modification exhibited accumulation of the drug in healthy liver cells with serious toxicity in the clinical study and was discontinued after the phase I study. Recent in vivo study by Tomas et al. of a high molecular weight HPMA copolymer conjugated with DOX via a pH-sensitive linker (6-methacrylamidohexanohydrazide) on 38C13 B-cell or EL4 mice showed

an enhanced accumulation of DOX in the cells with prolonged circulation time. The initial promising results have necessitated further research which is in progress (Etrych et al., 2008).

7.3 Strategies Used for selection of Polymers for Site-Directed and Site-Triggered Drug Delivery Systems

In recent times, developing a personalized medication using suitable polymeric nanomaterials for delivering the anticancer drug at the specific targeted tumour has become an important mission for researchers. Strategies to discover such personalized medications have been explored either by site targeting approach or site triggered approach. In the former approach of site targeting strategy, the nanocarrier actively searches for or attaches itself to the metastasized tumour cells through an antibody, aptamer, enzyme or receptor. In the case of site triggered strategy, a rapid release of the drug payload occurs due to a trigger or an applied external stimuli like pH, temperature, enzyme, magnetic field or sound waves while delivering the formulation to the targeted tumour tissues (Nelemans & Gurevich, 2020).

7.3.1 Stimuli-Responsive/Site-Triggered Drug Delivery Systems

A defective vascular fenestration, an inefficient lymphatic drainage, extensive angiogenesis and hypervasculature are the characteristics of the tumour microenvironment as depicted in Fig. 7.3a (Danhier, 2011). The polymer nanocarriers (PNC) have the ability to accumulate in the solid tumours by the enhanced permeation and retention (EPR) mechanism, thereby enhancing accumulation of drugs in the tumour (Maeda, 2013; Ngoune et al., 2016). Moreover, a specific design strategy can also be implemented for releasing the drug payload from the encapsulated nanomaterial at the tumour site utilizing altered pH, temperature and redox homeostasis in the extracellular matrix (ECM) or by external stimuli such as a magnetic field, light, ultrasonic sound, etc. as shown in Fig. 7.3b, c, respectively.

The following section covers different types of stimuli-responsive polymers and their application in cancer treatment.

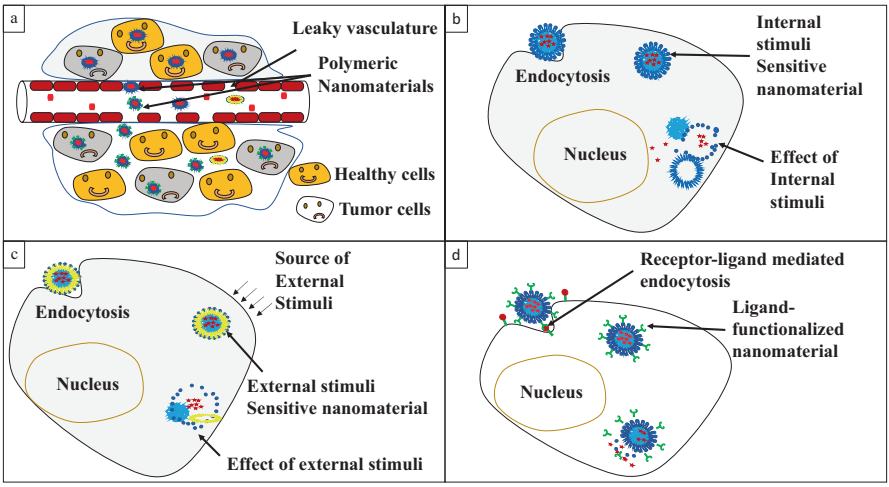

Fig. 7.3 Strategies used for selection of polymers for site-directed and site-triggered drug delivery systems. (**a**) Characteristics of tumour microenvironment. (**b**) Internal stimuli based drug delivery. (**c**) External stimuli-based drug delivery. (**d**) Site-directed drug delivery

7.3.1.1 Internal Stimuli

7.3.1.1.1 pH

Most of the solid cancers meet their extensive energy needs by increasing the glycolysis rate which leads to reduction in the extracellular pH (slightly acidic). The pH-responsive polymers are composed of charge shifting functional groups which under the influence of an acidic pH cause the polymer to swell and undergo a conformational change, thus releasing the drug payload. These polymers are synthesized by incorporating acid-cleavable bonds in the polymer backbone such that in an acidic pH, the drug payload is released. Recent studies demonstrated that anionic and cationic groups in the pH-responsive polymers are responsible for the drug release. Liang et al. have synthesized a pH-responsive polymer for delivering DOX; this was accomplished by incorporating arginine and histamine as a cell-penetrating peptide (CPP) into the poly(2-diisopropylaminoethyl methacrylate) (PDPA) homopolymer. The resultant assembly showed almost 90% release of DOX from the polymer in response to change in the pH at the tumour site (Ye et al., 2014).

A three-layered micelle formulation has been reported using cationic copolymers from poly (N,N-diethylaminoethyl methacrylate)-*b*-poly(poly(ethylene glycol) methylether methacrylate) (PDEAEMA-PPEGMA) and polycaprolactone-*b*-poly(poly(ethylene glycol) methylether methacrylate) (PCL-PPEGMA) and conjugated with DOX (Chen et al., 2017). The synthesized micelles swelled in an acidic pH due to protonation of the tertiary amino groups in the polymers. The pH-responsive polymer showed it is insoluble at physiological pH 7.4; however due to the tertiary ammonium group, the polymer solubilized with a change in the pH from

7.4 to 5.0 (intracellular endosomal and lysosomal pH is 5.0 and 4.5, respectively) which accelerated the release of the payload drug DOX (Theerasilp et al., 2017).

Anionic polymers viz.poly (acrylic acid) (PAA) and poly(methyl acrylate) (PMA) become more hydrophobic with a reduction in pH (Das et al., 2020) and hence are suitable carriers for delivering drugs like DOX or PTX. The copolymeric system of PAA and poly(N-isopropylacrylamide) (pNIPAAm) has been reported for DOX delivery (Mahmoodzadeh et al., 2018), whereas β-cyclodextrin-modified chitosan-PAA polymer has been used for PTX delivery (Mohapatra et al., 2018).

Often, synthetic polymers have been fabricated with acid-cleavable bonds such as hydrazone, imine, acetal and the cis-aconityl linkage. Different drugs like PTX, DOX and Pt have been either encapsulated or conjugated to polymers [N-(2-hydroxypropyl) methacrylamide (HPMA), poly(ethylene glycol)-block-poly(D,L-lactic acid) (PEG-*b*-PLA), poly(amidoamine) (PAMAM), etc.] via such linkages (Zhang et al., 2019; Feng et al., 2017; Zhai et al., 2017; Zhu et al., 2010; Lin et al., 2016). These acid labile bonds are stable at physiological pH but undergo hydrolysis at tumour-specific pH thereby releasing the drugs of DOX and cisplatin (Etrych et al., 2001; Aryal et al., 2010).

YuJe *Che* et al. have demonstrated the application of pH-responsive polymers, viz. acrylic acid and dimethylaminoethyl methacrylate (DMAEMA) with modified chitosan for delivering 5-fluorouracil (5-FU) and bovine serum albumin (BSA) (George et al., 2019). Likewise carboxymethyl chitosan-layered Pluronic® F68/poly(lactic-*co*-glycolic acid) (PF/PLGA) nanoparticles have been explored for delivering the poorly soluble drug gefitinib, orally to tumours (Das et al., 2020).

7.3.1.1.2 Redox Potential

Cancer cells have a high reducing potential in the cytosol compared to normal cells due to the overexpression of glutathione (GSH) to oxidized glutathione (GSSH) ratio in the cytosol. This reducing potential has been exploited for delivering drugs at the targeted site. PNCs with either the disulphide linkage or diselenide linkage are cleaved in a reducing environment (Cheng et al., 2011). Disulphide linkers like L-cysteine, dithiodiglycolic acid and pyridyl disulphide when cross linked with the core of the micelles demonstrated improved drug release. Song, N. and co-workers have loaded PTX onto nanoparticles made from methylpolyethyleneglycol-S-S-poly(D, L-lactide) (mPEG-SS-PLA) formulated as an oil in water emulsion by the solvent evaporation method. In vitro cytotoxicity and cellular uptake study of the redox-sensitive nanoparticles on A549, MCF-7 HeLa cells have demonstrated rapid penetration and excellent migration towards the tumour cells (Song et al., 2011). Additionally, Junping Xia et al. have also reported PTX-loaded nanoparticles using a graft polymer of hyaluronic acid and tocopherol succinate (TOS) using the disulphide linker (HA-ss-TOS**.**PTX) (Xia et al., 2018). In vitro cellular uptake study on overexpressed CD44 in B16F10 cell lines demonstrated enhanced cellular uptake compared to free PTX. Nanoparticles labelled with the fluorescent dye 1,1′-dioctadecyl-3,3,3′,3′-tetramethylindotricarbocyanine iodide

(DiR)-HA-ss-TOS.PTX were used for in vivo imaging studies. It showed greater accumulation of drug in the tumour cells (Xia et al., 2018).

Similarly Peijian Sun et al. have described redox-sensitive micelles made from the block polymer poly(ethylene oxide)-*b*-poly(N-methacryloyl-N′-(t-butyloxycarbonyl) cystamine) (PEO-*b*-PMABC) and loaded with DOX. The block polymer PEO-*b*-PMABC was prepared by the RAFT polymerization technique and fabricated into self-assemblies by dialysis. The in vitro cytotoxicity and cellular uptake studies on T24 human bladder cancer cells showed release of DOX that was triggered under the reducing environment, with higher anticancer efficacy (Sun et al., 2011).

All the above quoted examples corroborate the great potential of redox-sensitive polymers in nanomaterials for site-directed targeted drug delivery in cancer treatment.

7.3.1.1.3 Hypoxia

Hypoxia is considered as one of the prominent features of solid tumour and plays a major role in enhanced angiogenesis, therapy resistance and tumour metastasis (Ruan et al., 2009). Hypoxia-responsive polymers are designed by incorporating azo and nitro linkages. These linkages undergo cleavage in the hypoxic condition, thereby releasing the drug payload. Methoxy poly(ethylene glycol)-*b*-poly(glutamic acid)-graft-6-(2-nitroimidazole)hexylamine (mPEG-*b*-PLG-*g*-NID) nanoparticles have been modified using nitro functional group to selectively deliver DOX in hypoxic cancer cells (Ahmad et al., 2016). Similarly hypoxia-responsive polymersomes, ionizable liposomes and silica-based polymers have been exploited for delivering siRNA and chemotherapeutics (Kulkarni et al., 2016; Liu et al., 2017; Yan et al., 2019; Son et al., 2018; Kang et al., 2016).

7.3.1.1.4 Enzyme

Cancer cells show remarkable changes in metabolic pathways and expression of enzymes; some of which are esterase, matrix metalloproteases (MMPs), lipases, etc. Therefore, researchers have explored polymeric nanomaterials with enzyme-sensitive linkers which undergo cleavage due to presence of specific enzymes in the ECM. Table 7.2 lists linkers that have been used for designing polymeric nanocarriers.

7.3.1.1.5 Temperature

Tumours are slightly “warmer” than normal tissue, thus providing another pathway for site-specific and target delivery. Thermoresponsive polymers can change their phase above a certain temperature; this phenomenon is known as critical solution

Table 7.2 Examples of enzyme responsive polymeric nanocarrier-based drug delivery systems

Enzyme	Polymer	Drug	Linker	Ref
Trypsin/ hyaluronidase	Polymeric nanocapsule [polypeptide protamine (PRM), glycosaminoglycan chondroitin sulphate (CS)]	DOX	Polypeptide protaine/ chondroitin sulphate	Radhakrishnan et al. (2014)
MMP2	Poly(ethylene glycol)-*b*-poly(L-lysine) (PEG-*b*-PLL)	DOX	MMP2-sensitive peptide Ac-CPLGLAGG	Chen et al. (2015)
	Polyethylene glycol-peptide-polyethylenimine-1,2-dioleoyl-sn-glycero-3--phosphoethanolamine (PEG-pp-PEI-PE)	siRNA and PTX	Octapeptide (GPLGIAGQ)	Zhu et al. (2015)
	Co polymer of D-α-tocopheryl polyethylene glycol 3350 succinate ($TPGS_{3350}$) with poly (lactic-*co*-glycolic acid) (PLGA) with MMP2-sensitive peptide (pp) ($TPGS_{3350}$-pp-PLGA)	PTX	GPLGIAGQ peptide	Pan et al. (2018)
Cathepsin B	Dendrimer-methoxy poly(ethylene glycol) (mPEG)	DOX; gemcitabine	GFLG peptide	Lee et al. (2015) and Zhang et al. (2017)
	PEGylated dendrimer	BIM peptide	FKFL peptide	Kern et al. (2017)

temperature (CST). Change in the physicochemical properties and phase separation of polymers solely depend on the CST. Thermoresponsive polymers are categorized into upper critical solution temperature polymers (UCST; phase separation at temperature below critical temperature) and lower critical solution temperature polymers (LCST; phase separation at temperature above critical temperature) (Bordat et al., 2019). These polymers are soluble at physiological temperature (~37 °C), and a shift in the temperature to ~40–42 °C (hyperthermia) acts as a stimulus for the polymers to release the drugs. Hyperthermia can be achieved through temperature-controlled water sacks, radiofrequency oscillators or miniature annular-phased array microwave applicators (Mura et al., 2013). In the LCST category are polymers like poly-N-isopropylacrylamide (PNIPAAm), elastin like polypeptide (ELPs), chitosan-based polymers and poly(N-vinylcaprolactam) (PNVCL), while the UCST category includes polymers like poly(N-acryloylglycinamide) (PNAGA), poly(acrylamide-*co*-acrylonitrile) P(AAm-*co*-AN) and poly(N-acryloyl glycinamide-*co*-butyl acrylate) P(NAGA-*co*-BA) which have been explored for delivery of different drugs (Bordat et al., 2019).

7.3.1.2 External Stimuli

Synthetic and natural polymers have been fabricated to release drugs in response to various external stimuli such as light, magnetism and ultrasound.

7.3.1.2.1 Magnetism

Magnetic polymeric nanoparticles contain either supermagnetic or paramagnetic material like magnetite or superparamagnetic iron oxide nanoparticles (SPIONs) entrapped in the core of the polymer. Magnetic NPs work by either hyperthermia-induced release of the drug or by a magnetic field that gravitates the NPs at the tumour site. SPIONs when encapsulated with DOX and a heat-sensitive matrix like PLGA, on application of a magnetic field, the heat generated, trigger the release of DOX at the tumour site (Thirunavukkarasu et al., 2018). Similarly a magnetite embedded in the shell of pluronic/polyethylenimine (PEI) was used to deliver siRNA to the cancer cells (Lee et al., 2010). Ghamkhari et al. have made a triblock polymer of poly[(2-succinyloxyethylmethacrylate)-*b*-(*N*-isopropylacrylamide)-*b*-(dimethylaminoethyl methacrylate) [poly(SEMA-*b*-NIPAM-*b*-DMAEMA)] and adsorbed Fe_3O_4 on the surface of the nanoparticles and then encapsulated the nanoparticles with DOX. . The polymeric nanoparticles have demonstrated a high loading capacity for DOX; hence they can be used as a theranostic agent and anti-cancer drug delivery (Ghamkhari et al., 2018).

7.3.1.2.2 Light

Light-responsive polymers have been widely used for controlled drug release because of excellent tissue penetration capacity. Light-responsive polymers with linkers like azo or spiropyrans and coumarin undergo cleavage at a specific wavelength of light. A novel coumarin-functionalized copolymeric block of poly(ethyleneoxide)-*b*-poly(n-butylmethacrylate-*co*-4-methyl)-[7-(methacryloyl) oxyethyloxy] coumarin) has been used to deliver the anticancer drug 5-FU in response to 254 nm of light irradiation (Jin et al., 2011).

7.3.1.2.3 Ultrasound

Nanoparticles of polymers responsive to ultrasound [sound waves of low frequency (<100 kHz) or high frequency (>100 kHz and MHz range)] release the payload drug either by mechanical or thermal mechanism. The mechanical mechanism involves pressure created by the ultrasound, shockwaves, or ultrasound oscillations to release the payload, while the thermal mechanism involves absorption of sound energy to release the payload (Couture et al., 2014). PNC systems such as micelles,

microbubbles, nanobubbles, liposomes and liquid perfluorocarbon nanodroplets all have been exploited for drug release at targeted sites. On application of ultrasound, the disrupted micelles, nanodroplets or liposomes reform after ultrasound treatment but with a smaller diameter, and during this process they expel most of the payload in the initial burst (Couture et al., 2014). Promising results have been revealed using ultrasound stimuli (20 kHz frequency) on responsive polymeric nanocarriers like pluronic micelles for the release of DOX/curcumin (Husseini et al., 2011). Likewise, PTX release was seen when 1 MHz ultrasound frequency was applied to a microbubble formulation made of PEO-*co*-PCL (Wu et al., 2017). Using nanobubbles in the polymeric shell, DOX release was seen to double compared to the non-sonicated samples (Zhou et al., 2019). Similarly co-delivery of a therapeutic drug and siRNA/shRNA (sh is short hairpin RNA) was achieved using nanobubbles against different cancer cell lines (Yin et al., 2014; Yang et al., 2015b). Release of several anticancer drugs using ultrasound technology from preparations involving nanobubbles, nanodroplets, micelles and nanoliposomes have been reported in the literature (Acharya et al., 2009; Kim et al., 2018; Alshaer et al., 2018).

7.3.2 Site-Directed Drug Delivery Systems

Polymeric nanocarriers are very efficient at active targeting of specific drugs. Targeting agents could be cell surface receptors such as folate receptors, transferrin receptors and $\alpha_V\beta 3$ receptors (integrin receptor) or proteins, aptamers, nucleic acids, vitamins, glycoproteins, peptides, etc. as shown in Fig. 7.3d. Majority of site-directed drug delivery systems have been covered in Sect. 7.2.6.4. Hence here we cover the different types of targets in brief.

7.3.2.1 Antibodies

Nanocarriers have been conjugated with antibodies and targeted to tumours expressing a specific antigen. This type of work is still in the infancy stage with few examples. One such example is HER-2 antibodies conjugated with poly(2-methyl-2-carboxytrimethylene carbonate-*co*-D,L-lactide)-graft-poly(ethylene glycol)-furan (P(TMCC-*co*-LA)-*g*-PEG-furan) used for releasing DOX at the targeted receptor with promising results (Shi et al., 2009). It has been observed that epithelial growth factor (EGFR) is often overexpressed in solid tumours. With this knowledge, the EGFR antibody was functionalized onto the surface of rapamycin loaded PLGA/poly(vinyl alcohol) nanoparticles; the result was 17 times higher uptake by MCF-7 cells compared to the non-targeted nanoparticles (Peng et al., 2011; Danhier et al., 2015; Acharya et al., 2009).

7.3.2.2 Nucleic Acids

A short strand of DNA and RNA is known as an aptamer. These have been explored as targeting agents for binding cytosolic proteins, transmembrane proteins, carbohydrates, viruses and cells. Aptamers have been found to be more accepted over protein antibodies because of the multiple advantages such as ease of synthesis, resistance to different physiological conditions, lower immunogenicity, ease of modification to increase surface specificity, ease of denaturation and renaturation without loss of activity (Kim et al., 2018). A number of cancer-related biomarkers have been explored as targeting moieties with the help of aptamer-conjugated polymeric nanoparticles (Alshaer et al., 2018).

7.3.2.3 Transferrin

Transferrin transports iron to proliferating cancer cells. It is an iron-binding glycoprotein with affinity to bind the transferrin receptor on the surface of the cell and consequent release of iron into the acidic compartment of the cancer cell (Tortorella & Karagiannis, 2014). Different polymeric micelles using [poly(amine-ester)-*co*-D,L-lactide (HPAE-*co*-PLA) (Xu et al., 2012), poly(methoxy-polyethyleneglycol cyanoacrylate-*co*-n-hexadecyl cyanoacrylate) (PEG-PHDCA) (Hong et al., 2009), poly(lactide)-d-α-tocopheryl polyethylene glycol 1000 succinate (PLA-TPGS) (Gan & Feng, 2010) and polymersomes using [PEG-PCL] (Pang et al., 2011) have been conjugated with transferrin for targeted delivery (Zhong et al., 2014).

7.3.2.4 Peptides

Conjugation of peptides with polymers has been found to be a promising approach to address the intrinsic drawbacks of peptides such as short half-life and rapid hydrolysis in an acidic environment. Jingwen Shi et al. have demonstrated poly(ethylene) conjugated with paclitaxel via disulphide bond as linker along with the arginine-glycine-aspartic acid (RGD) peptide as the active moiety (RGD-PEG**.**PTX) is an effective method for selective delivery of the drug to tumour cells (Shi et al., 2019). In vitro/in vivo study on the RGD-PEG.PTX micelles revealed a longer circulation time and improved antitumour efficacy with reduced side effects. Likewise, Huili Guan et al. have reported polyglutamic acid conjugated with DOX and decorated with the H2009.1 peptide for targeting the αvβ6 receptor. The H2009.1 peptide helped the conjugate to selectively internalize the payload (DOX) in αvβ6-positive tumour cells (Guan et al., 2008).

7.4 Current Updates on the Clinical Status of Polymeric Nanomedicines

The use of polymeric nanoparticles (PNCs) for targeted drug delivery has seen an exponential growth during the past four decades. Rapid advancements made in polymeric nanomedicines are evident from the reported literature, patents and clinical trials. With the help of this technology, issues of patient safety, drug toxicity, problems regarding difficulty in formulating drugs and target specificity have been resolved successfully. In preclinical and clinical trials, polymeric nanomedicines have been evaluated for improvement in the half-life of the medicine, bioavailability, biodistribution and reduction in adverse effects if any after the release of the drug either by passive or active mechanism. Preclinical and clinical technological experts are putting extensive efforts in designing personalized medication using combination therapy as a "magic bullet" for treating cancer. However, due to several challenges in clinical trials, the ratio of the number of polymeric nanomedicines in clinical trials versus the number of research papers and patents published in this area is in microscopic numbers. In the last two decades, the FDA has approved almost 50 different nanodrugs; however they failed to come into the market due to poor efficacy. The following section covers examples of clinically approved and under investigational PNCs.

7.5 Clinically Approved and Under Investigational Polymeric Nanomedicines for Cancer Therapy

The first FDA-approved polymer-based nanomedicine, Eligard (Tolmar), was approved in 2002 for treatment of prostate cancer. Eligard was made of biodegradable poly(lactic-*co*-glycolic acid) polymer in which leuprolide was loaded for sustained delivery (Wex et al., 2013). Another polymer-based nanomedicine, polyethylene glycol (PEGyl) conjugated filgrastim (pegfilgrastim or Amgen or Neulasta), was approved in 2002 for reducing neutropenic complication during chemotherapy. This PEGylated nanocarrier has been reported for enhancing the shelf life of loaded drugs (15–80 hours) and to reduce the frequency of the administration of the drug (Biganzoli et al., 2004). XyotaxTM (CT-2103) has entered in phase III clinical trials for treatment of ovarian cancer and non-small cell lung cancer (NSCLC) with the combination of gemcitabine by CTI BioPharma. XyotaxTM (CT-2103), as a potential chemotherapeutic agent, is expected to be approved in the near future (Boddy et al., 2002; Langer, 2004; He et al., 2019).

Few more examples of polymeric nanomedicines under clinical investigation are given in Table 7.3.

Table 7.3 Clinical status of polymeric nanomedicines

Commercial name	Polymer type	Drug encapsulated/ conjugated	Cancer type	Clinical trial identifier	Ref
AZD2811	Polymeric nanoparticle accurin platform composed of [block copolymers poly-D, L-lactide (PLA) and poly(ethylene glycol) (PEG)]	Aurora B kinase inhibitor	Advanced solid tumours	NCT02579226 (phase I) NCT03217838 (phase I recruiting) NCT03366675 (phase II terminated)	Della Corte et al. (2019), Donnellan et al. (2019), and Park et al. (2019)
BIND-014	PSMA targeted [((*S*)-2-(3-((*S*)-5-amino-1-carboxypentyl) ureido) pentanedioic acid (ACUPA)] poly (ethylene glycol)-poly(L-lactide) (PEG-PLA)	Docetaxel	Advanced urothelial carcinoma, cervical cancer, cholangiocarcinoma or carcinomas of the biliary tree and squamous cell carcinoma of the head and neck, KRAS-positive patients with non-small cell lung cancer (NSCLC), squamous cell NSCLC, prostate cancer, metastatic NSCLC	NCT02479178 (terminated), NCT02283320 (phase II), NCT01812746 (phase II), NCT01792479 (phase II), NCT01300533 (phase I)	Pushpalatha et al. (2017), Wang et al. (2018), Autio et al. (2016), Kannan et al. (2014), and Xu et al. (2015)
Cynviloq or IG-001	Polymeric micelle of methoxy poly (ethylene glycol)-poly (lactide)	Paclitaxel (PTX)	Breast cancer	NCT02064829 (not provided)	Allen (2016)
Genexol-PM	Polymeric micelle of methoxy poly (ethylene glycol)-poly (lactide)	Paclitaxel (PTX)	Locally advanced head and neck squamous cell carcinoma, metastatic breast cancer, hepatocellular carcinoma	NCT01689194 (phase II), NCT02263495 (phase II), NCT00912639 (phase IV), NCT02739633 (phase II), NCT03008512 (phase II)	Zhou et al. (2018) and Jung et al. (2017)

Commercial name	Polymer type	Drug encapsulated/ conjugated	Cancer type	Clinical trial identifier	Ref
NC-6004 Nanoplatin	PAA-PEG micelle	Cisplatin	Advanced solid tumours or non-small cell lung, biliary tract, and bladder cancer, pancreatic neoplasm, recurrent or metastatic squamous cell carcinoma of the head and neck	NCT02240238 (phase I/II) NCT02043288 (phase III), NCT03771820 (phase II), NCT03109158 (phase I/II), NCT02817113 (phase I terminated), NCT00910741 (phase I/II)	Zhou et al. (2018)
NC-4016	PAA-PEG micelle	Oxaloplatin	Advanced solid tumours or lymphoma	NCT03168035 (phase I)	Poursharifi et al. (2020)
NK105	Polymeric micelle: block copolymer of PEG and modified polyaspartate	Paclitaxel (PTX)	Breast cancer	NCT01644890 (phase III)	Fujiwara et al. (2019)
Docetaxel-PM DOPNP201 Nanoxel®M	Polymeric micelle: methoxy-poly(ethyleneglycol)-*b*-poly(d,l-lactide) (mPEG-PDLLA)	Docetaxel	Head and neck squamous cell carcinoma, non-muscle invasive bladder cancer, breast cancer, non-small cell lung cancer, prostate cancer, ovarian cancer, head and neck cancer, gastric cancer, oesophageal cancer, advanced solid tumour	NCT02639858 (phase II), NCT02982395 (phase III), NCT04066335 (not given), NCT02274610 (phase I), NCT03585673 (phase II)	Madamsetty et al. (2019) and Fraguas-Sánchez et al. (2019)
CriPec	Polymeric micelle: poly (ethylene glycol)-*b*-poly[N-(2-hydroxypropyl) methacrylamidelactate]	Docetaxel	Solid tumours, ovarian cancer	NCT02442531 (phase I) NCT03712423 (phase I) NCT03742713 (phase II)	Atrafi et al. (2019) and Van Eerden et al. (2019)

(continued)

Table 7.3 (continued)

Commercial name	Polymer type	Drug encapsulated/ conjugated	Cancer type	Clinical trial identifier	Ref
CRLX101	Cyclodextrin-based nanoformulation	Camptothecin	Ovarian cancer, solid tumours, renal cell carcinoma, rectal cancer, NSCLC, urothelial cancer, lung neoplasms, small cell lung cancer, prostate cancer	NCT02187302 (phase II), NCT02010567 (phase I/II), NCT02389985 (phase I terminated), NCT01803269 (phase II terminated), NCT01652079 (phase II) NCT02769962 (phase I) NCT03531827 (phase II) NCT02648711(phase I) terminated NCT01380769 (phase II) NCT01612546 (phase II) NCT00333502 (phase II) NCT01625936 (phase I) NCT00753740 (phase II) withdrawn	Voss et al. (2015), Phase I (2015), and Schmidt (2020)
CRLX301	Cyclodextrin-based nanoformulation	Docetaxel	Advanced solid tumours	NCT02380677 (phase I/II) terminated	Markman et al. (2016)
NK012	Polymeric micelle: poly(ethylene glycol)–poly(glutamate) [PEG-PGlu]	CPT-11, 7-ethyl-10-hydroxy-camptothecin (SN-38)	Advanced solid tumours, metastatic colorectal cancer, triple negative breast cancer, SCLC	NCT00951613 (phase II) NCT00951054 (phase II) NCT00542958 (phase I) NCT01238952 (phase I) NCT01238939 (phase I)	Svenson (2012, 2014) and Saravanakumar et al. (2019)
SMANCS	Styrene-maleic acid polymer	Neocarzinostatin (NCS)	Hepatocellular carcinoma	NCT01327521 (phase III) withdrawn	Vacchelli et al. (2012)
Eligard	PLGH (poly(D, L-lactide-coglycolide))	Leuprolide acetate	Prostate cancer	More than 100 registries for clinical trial with phases I–IV	Hernandez and Exner (2017)

Commercial name	Polymer type	Drug encapsulated/ conjugated	Cancer type	Clinical trial identifier	Ref
Neulasta	Poly(ethylene glycol) [PEG]	Recombinant human G-CSF	To treat chemotherapy-induced neutropenia in cancer	More than 100 registries for clinical trial with phases I–IV	Piedmonte and Treuheit (2008)
NK911	Polymeric micelle: block copolymer of PEG and poly(aspartic acid)	Doxorubicin	Solid tumour	Clinical trial govt. registry number (NCT) not available phase I	Matsumura et al. (2004)
Imx-110	Polymeric nanoparticle - polyethylene glycol-phosphatidylethanolamine (PEG-PE)	Curcumin and doxorubicin	Advanced solid tumours	NCT03382340 (phase I/II)	Vishnoi et al. (2020)
IT-141	Polymeric nanoparticle: triblock copolymer of poly(ethylene) glycol (PEG), glutamic acid hydroxamate and polypeptide block	SN-38	Advanced cancer	NCT03096340 (phase I)	Carie et al. (2011)

7.6 Concluding Remarks

A major challenge in achieving improved survival outcomes post cancer therapy is the successful delivery of anticancer therapeutics specifically to the tumour tissues. This chapter highlights the different polymer-based materials and their applications for cancer therapy. The polymer-based nanomaterials exhibit several advantages due to excellent biocompatibility, ease of fabrication, great drug loading capacity, control over drug release and favourable physicochemical properties. These unique properties have prompted researchers to explore their wide-ranging applications in the development of potential drug delivery systems, providing promising strategies to fight cancer. A good number of reported polymeric nanomaterials have passed through several stages of clinical trials and may soon become an alternative and superior option for cancer therapy. However, it is a challenging task to obtain approval for clinically tested formulations because researchers are still struggling with the precise control of drug release, uniformity in drug content, stability of the chemical structure, etc. Hence to address these limitations, there is a need to develop superior polymeric nanocarrier systems while designing formulations to overcome these challenges during clinical trials in the future.

References

Abbasi, E., Aval, S. F., Akbarzadeh, A., Milani, M., Nasrabadi, H. T., Joo, S. W., Hanifehpour, Y., Nejati-Koshki, K., & Pashaei-Asl, R. (2014). Dendrimers: Synthesis, applications, and properties. *Nanoscale Research Letters, 9*(1), 247.

Acharya, S., Dilnawaz, F., & Sahoo, S. K. (2009). Targeted epidermal growth factor receptor nanoparticle bioconjugates for breast cancer therapy. *Biomaterials, 30*(29), 5737–5750.

Adeli, M., Kalantari, M., Parsamanesh, M., Sadeghi, E., & Mahmoudi, M. (2011). Synthesis of new hybrid nanomaterials: Promising systems for cancer therapy. *Nanomedicine: Nanotechnology, Biology and Medicine, 7*(6), 806–817.

Agarwal, S., Dominic, A., & Wasnik, S. (2019). An overview of polymeric nanoparticles as potential cancer therapeutics. In *Polymeric nanoparticles as a promising tool for anti-cancer therapeutics* (pp. 21–34). Elsevier.

Ahmad, Z., Lv, S., Tang, Z., Shah, A., & Chen, X. (2016). Methoxy poly (ethylene glycol)-block-poly (glutamic acid)-graft-6-(2-nitroimidazole) hexyl amine nanoparticles for potential hypoxia-responsive delivery of doxorubicin. *Journal of Biomaterials Science, Polymer Edition, 27*(1), 40–54.

Allen, C. (2016). Why I'm holding onto hope for nano in oncology. *Molecular Pharmaceutics, 13*(8), 2603–2604.

Alshaer, W., Hillaireau, H., & Fattal, E. (2018). Aptamer-guided nanomedicines for anticancer drug delivery. *Advanced Drug Delivery Reviews, 134*, 122–137.

Aryal, S., Hu, C.-M. J., & Zhang, L. (2010). Polymer– cisplatin conjugate nanoparticles for acid-responsive drug delivery. *ACS Nano, 4*(1), 251–258.

Atrafi, F., Dumez, H., Mathijssen, R. H., Menke, C. W., Costermans, J., Rijcken, C. J., Hanssen, R., Eskens, F., & Schoffski, P. (2019). *A phase I dose-finding and pharmacokinetics study of CPC634 (nanoparticle entrapped docetaxel) in patients with advanced solid tumors*. American Society of Clinical Oncology, Alexandria.

Autio, K. A., Garcia, J. A., Alva, A. S., Hart, L. L., Milowsky, M. I., Posadas, E. M., Ryan, C. J., Summa, J. M., Youssoufian, H., & Scher, H. I. (2016). *A phase 2 study of BIND-014 (PSMA-targeted docetaxel nanoparticle) administered to patients with chemotherapy-naïve metastatic castration-resistant prostate cancer (mCRPC)*. American Society of Clinical Oncology.

Barzegar Behrooz, A., Nabavizadeh, F., Adiban, J., Shafiee Ardestani, M., Vahabpour, R., Aghasadeghi, M. R., & Sohanaki, H. (2017). Smart bomb AS 1411 aptamer-functionalized/PAMAM dendrimer nanocarriers for targeted drug delivery in the treatment of gastric cancer. *Clinical and Experimental Pharmacology and Physiology, 44*(1), 41–51.

Bessone, M. I. D., Simón-Gracia, L., Scodeller, P., de los Angeles Ramirez, M., Huvelle, M. A. L., Soler-Illia, G. J., & Simian, M. (2019). iRGD-guided tamoxifen polymersomes inhibit estrogen receptor transcriptional activity and decrease the number of breast cancer cells with self-renewing capacity. *Journal of Nanobiotechnology, 17*(1), 1–14.

Betea, D., Potorac, I., & Beckers, A. (2015). Parathyroid carcinoma: challenges in diagnosis and treatment. *Annales d'Endocrinologie, Elsevier, 76*, 169–177.

Biganzoli, L., Untch, M., Skacel, T., & Pico, J.-L. (2004). Neulasta (pegfilgrastim): a once-per-cycle option for the management of chemotherapy-induced neutropenia. *Seminars in Oncology, Elsevier, 31*, 27–34.

Boddy, A., Todd, R., Verrill, M., Sludden, J., Fishwick, K., Robson, L., Cassidy, J., Bisset, D., Garzone, P., & Calvert, A. (2002). Pharmacological study of CT-2103 (XyotaxTM), a poly (L-glutamic acid)-paclitaxel conjugate administered every 3 weeks or every 2 weeks in a phase I study. *European Journal of Cancer, 38*, 98.

Bordat, A., Boissenot, T., Nicolas, J., & Tsapis, N. (2019). Thermoresponsive polymer nanocarriers for biomedical applications. *Advanced Drug Delivery Reviews, 138*, 167–192.

Butt, A. M., Amin, M. C. I. M., Katas, H., Abdul Murad, N. A., Jamal, R., & Kesharwani, P. (2016). Doxorubicin and siRNA codelivery via chitosan-coated pH-responsive mixed micellar polyplexes for enhanced cancer therapy in multidrug-resistant tumors. *Molecular Pharmaceutics, 13*(12), 4179–4190.

Carie, A., Rios-Doria, J., Costich, T., Burke, B., Slama, R., Skaff, H., & Sill, K. (2011). IT-141, a polymer micelle encapsulating SN-38, induces tumor regression in multiple colorectal cancer models. *Journal of Drug Delivery, 2011*, 869027.

Chavanpatil, M. D., Khdair, A., Gerard, B., Bachmeier, C., Miller, D. W., Shekhar, M. P., & Panyam, J. (2007). Surfactant–polymer nanoparticles overcome P-glycoprotein-mediated drug efflux. *Molecular Pharmaceutics, 4*(5), 730–738.

Chen, L., Wang, H., Zhang, Y., Wang, Y., Hu, Q., & Ji, J. (2013). Bioinspired phosphorylcholine-modified polyplexes as an effective strategy for selective uptake and transfection of cancer cells. *Colloids and Surfaces B: Biointerfaces, 111*, 297–305.

Chen, W. H., Yang, C. X., Qiu, W. X., Luo, G. F., Jia, H. Z., Lei, Q., Wang, X. Y., Liu, G., Zhuo, R. X., & Zhang, X. Z. (2015). Multifunctional theranostic nanoplatform for cancer combined therapy based on gold nanorods. *Advanced Healthcare Materials, 4*(15), 2247–2259.

Chen, Q., Li, S., Feng, Z., Wang, M., Cai, C., Wang, J., & Zhang, L. (2017). Poly (2-(diethylamino) ethyl methacrylate)-based, pH-responsive, copolymeric mixed micelles for targeting anticancer drug control release. *International Journal of Nanomedicine, 12*, 6857.

Cheng, R., Feng, F., Meng, F., Deng, C., Feijen, J., & Zhong, Z. (2011). Glutathione-responsive nano-vehicles as a promising platform for targeted intracellular drug and gene delivery. *Journal of Controlled Release, 152*(1), 2–12.

Chidambaram, M., Manavalan, R., & Kathiresan, K. (2011). Nanotherapeutics to overcome conventional cancer chemotherapy limitations. *Journal of Pharmacy & Pharmaceutical Sciences, 14*(1), 67–77.

Choi, S.-W., & Kim, J.-H. (2007). Design of surface-modified poly (D, L-lactide-co-glycolide) nanoparticles for targeted drug delivery to bone. *Journal of Controlled Release, 122*(1), 24–30.

Choi, K. Y., Min, K. H., Yoon, H. Y., Kim, K., Park, J. H., Kwon, I. C., Choi, K., & Jeong, S. Y. (2011). PEGylation of hyaluronic acid nanoparticles improves tumor targetability in vivo. *Biomaterials, 32*(7), 1880–1889.

Couture, O., Foley, J., Kassell, N. F., Larrat, B., & Aubry, J.-F. (2014). Review of ultrasound mediated drug delivery for cancer treatment: Updates from pre-clinical studies. *Translational Cancer Research, 3*(5), 494–511.

Danhier, F. (2011). *Comparison between two anti-tumoral strategies: passive and active targeting of nanoencapsulated anti-cancer drugs*. UCL-Université Catholique de Louvain.

Danhier, F., Lecouturier, N., Vroman, B., Jérôme, C., Marchand-Brynaert, J., Feron, O., & Préat, V. (2009). Paclitaxel-loaded PEGylated PLGA-based nanoparticles: In vitro and in vivo evaluation. *Journal of Controlled Release, 133*(1), 11–17.

Danhier, F., Messaoudi, K., Lemaire, L., Benoit, J.-P., & Lagarce, F. (2015). Combined anti-Galectin-1 and anti-EGFR siRNA-loaded chitosan-lipid nanocapsules decrease temozolomide resistance in glioblastoma: In vivo evaluation. *International Journal of Pharmaceutics, 481*(1–2), 154–161.

Das, S. S., Bharadwaj, P., Bilal, M., Barani, M., Rahdar, A., Taboada, P., Bungau, S., & Kyzas, G. Z. (2020). Stimuli-responsive polymeric nanocarriers for drug delivery, imaging, and theragnosis. *Polymers, 12*(6), 1397.

Della Corte, C. M., Ajpacaja, L., Cardnell, R., Gay, C., Wang, Q., Shen, L., Ramkumar, K., Stewart, A., Fan, Y.-H., & Adelman, C. (2019). Activity of the novel Aurora kinase B inhibitor AZD2811 in biomarker-defined models of small cell lung cancer. *Annals of Oncology, 30*, v716.

Donnellan, W. B., Atallah, E. L., Asch, A. S., Patel, M. R., Yang, J., Eghtedar, A., Borthakur, G. M., Charlton, J., MacDonald, A., & Korzeniowska, A. (2019). *A Phase I/II study of AZD2811 nanoparticles (NP) as monotherapy or in combination in treatment-naïve or relapsed/refractory AML/MDS patients not eligible for intensive induction therapy*. American Society of Hematology.

Dreicer, R., Manola, J., Roth, B. J., See, W. A., Kuross, S., Edelman, M. J., Hudes, G. R., & Wilding, G. (2004). Phase III trial of methotrexate, vinblastine, doxorubicin, and cisplatin versus carboplatin and paclitaxel in patients with advanced carcinoma of the urothelium: A trial of the Eastern Cooperative Oncology Group. *Cancer: Interdisciplinary International Journal of the American Cancer Society, 100*(8), 1639–1645.

Eissa, A. M., Smith, M. J., Kubilis, A., Mosely, J. A., & Cameron, N. R. (2013). Polymersome-forming amphiphilic glycosylated polymers: Synthesis and characterization. *Journal of Polymer Science Part A: Polymer Chemistry, 51*(24), 5184–5193.

Etrych, T., Jelínková, M., Říhová, B., & Ulbrich, K. (2001). New HPMA copolymers containing doxorubicin bound via pH-sensitive linkage: Synthesis and preliminary in vitro and in vivo biological properties. *Journal of Controlled Release, 73*(1), 89–102.

Etrych, T., Chytil, P., Mrkvan, T., Šírová, M., Říhová, B., & Ulbrich, K. (2008). Conjugates of doxorubicin with graft HPMA copolymers for passive tumor targeting. *Journal of Controlled Release, 132*(3), 184–192.

Feng, X., Li, D., Han, J., Zhuang, X., & Ding, J. (2017). Schiff base bond-linked polysaccharide–doxorubicin conjugate for upregulated cancer therapy. *Materials Science and Engineering: C, 76*, 1121–1128.

Fraguas-Sánchez, A., Martín-Sabroso, C., Fernández-Carballido, A., & Torres-Suárez, A. (2019). Current status of nanomedicine in the chemotherapy of breast cancer. *Cancer Chemotherapy and Pharmacology*, 1–18.

Fujiwara, Y., Mukai, H., Saeki, T., Ro, J., Lin, Y.-C., Nagai, S. E., Lee, K. S., Watanabe, J., Ohtani, S., & Kim, S. B. (2019). A multi-national, randomised, open-label, parallel, phase III non-inferiority study comparing NK105 and paclitaxel in metastatic or recurrent breast cancer patients. *British Journal of Cancer, 120*(5), 475–480.

Gan, C. W., & Feng, S.-S. (2010). Transferrin-conjugated nanoparticles of poly (lactide)-D-α-tocopheryl polyethylene glycol succinate diblock copolymer for targeted drug delivery across the blood–brain barrier. *Biomaterials, 31*(30), 7748–7757.

Gaucher, G., Dufresne, M.-H., Sant, V. P., Kang, N., Maysinger, D., & Leroux, J.-C. (2005). Block copolymer micelles: Preparation, characterization and application in drug delivery. *Journal of Controlled Release, 109*(1–3), 169–188.

Geng, Y., Dalhaimer, P., Cai, S., Tsai, R., Tewari, M., Minko, T., & Discher, D. E. (2007). Shape effects of filaments versus spherical particles in flow and drug delivery. *Nature Nanotechnology, 2*(4), 249–255.

George, A., Shah, P. A., & Shrivastav, P. S. (2019). Natural biodegradable polymers based nanoformulations for drug delivery: A review. *International Journal of Pharmaceutics, 561*, 244–264.

Ghamkhari, A., Ghorbani, M., & Aghbolaghi, S. (2018). A perfect stimuli-responsive magnetic nanocomposite for intracellular delivery of doxorubicin. *Artificial Cells, Nanomedicine, and Biotechnology, 46*(sup3), S911–S921.

Guan, H., McGuire, M. J., Li, S., & Brown, K. C. (2008). Peptide-targeted polyglutamic acid doxorubicin conjugates for the treatment of αvβ6-positive cancers. *Bioconjugate Chemistry, 19*(9), 1813–1821.

Guo, X.-L., Kang, X.-X., Wang, Y.-Q., Zhang, X.-J., Li, C.-J., Liu, Y., & Du, L.-B. (2019). Co-delivery of cisplatin and doxorubicin by covalently conjugating with polyamidoamine dendrimer for enhanced synergistic cancer therapy. *Acta Biomaterialia, 84*, 367–377.

Haghighi, A. H., Faghih, Z., Khorasani, M. T., & Farjadian, F. (2019). Antibody conjugated onto surface modified magnetic nanoparticles for separation of HER2+ breast cancer cells. *Journal of Magnetism and Magnetic Materials, 490*, 165479.

He, H., Liu, L., Morin, E. E., Liu, M., & Schwendeman, A. (2019). Survey of clinical translation of cancer nanomedicines—Lessons learned from successes and failures. *Accounts of Chemical Research, 52*(9), 2445–2461.

Heidel, J. D., & Davis, M. E. (2011). Clinical developments in nanotechnology for cancer therapy. *Pharmaceutical Research, 28*(2), 187–199.

Hernandez, C., & Exner, A. A. (2017). *Predicting in vivo behavior of injectable, in situ-forming drug-delivery systems*. Future Science.

Hong, M., Zhu, S., Jiang, Y., Tang, G., & Pei, Y. (2009). Efficient tumor targeting of hydroxycamptothecin loaded PEGylated niosomes modified with transferrin. *Journal of Controlled Release, 133*(2), 96–102.

Hosseinifar, T., Sheybani, S., Abdouss, M., Hassani Najafabadi, S. A., & Shafiee Ardestani, M. (2018). Pressure responsive nanogel base on alginate-Cyclodextrin with enhanced apoptosis mechanism for colon cancer delivery. *Journal of Biomedical Materials Research Part A, 106*(2), 349–359.

Husseini, G. A., Abdel-Jabbar, N. M., Mjalli, F. S., & Pitt, W. G. (2011). Optimizing the use of ultrasound to deliver chemotherapeutic agents to cancer cells from polymeric micelles. *Journal of the Franklin Institute, 348*(7), 1276–1284.

Jin, Q., Mitschang, F., & Agarwal, S. (2011). Biocompatible drug delivery system for photo-triggered controlled release of 5-fluorouracil. *Biomacromolecules, 12*(10), 3684–3691.

Johnston, A. P., Cortez, C., Angelatos, A. S., & Caruso, F. (2006). Layer-by-layer engineered capsules and their applications. *Current Opinion in Colloid & Interface Science, 11*(4), 203–209.

Jung, K. H., Park, Y. H., Im, S.-A., Sohn, J., Lee, K.-S., Chae, Y. S., Lee, K. H., Kim, J. H., Im, Y.-H., & Kim, J.-Y. (2017). *A phase II, multicenter, randomized trial of eribulin plus gemcitabine (EG) vs. paclitaxel plus gemcitabine (PG) in patients with HER2-negative metastatic breast cancer (MBC) as first-line chemotherapy (KCSG BR13-11, NCT02263495)*. American Society of Clinical Oncology.

Kang, L., Fan, B., Sun, P., Huang, W., Jin, M., Wang, Q., & Gao, Z. (2016). An effective tumor-targeting strategy utilizing hypoxia-sensitive siRNA delivery system for improved anti-tumor outcome. *Acta Biomaterialia, 44*, 341–354.

Kannan, R., Nance, E., Kannan, S., & Tomalia, D. A. (2014). Emerging concepts in dendrimer-based nanomedicine: From design principles to clinical applications. *Journal of Internal Medicine, 276*(6), 579–617.

Kern, H. B., Srinivasan, S., Convertine, A. J., Hockenbery, D., Press, O. W., & Stayton, P. S. (2017). Enzyme-cleavable polymeric micelles for the intracellular delivery of proapoptotic peptides. *Molecular Pharmaceutics, 14*(5), 1450–1459.

Khan, M. M., Madni, A., Filipczak, N., Pan, J., Rehman, M., Rai, N., Attia, S. A., & Torchilin, V. P. (2020). Folate targeted lipid chitosan hybrid nanoparticles for enhanced anti-tumor efficacy. *Nanomedicine: Nanotechnology, Biology and Medicine, 28*, 102228.

Killoran, M., & Moyer, A. (2006). Surgical treatment preferences in Chinese-American women with early-stage breast cancer. *Psycho-Oncology: Journal of the Psychological, Social and Behavioral Dimensions of Cancer, 15*(11), 969–984.

Kim, D., Lee, E. S., Oh, K. T., Gao, Z. G., & Bae, Y. H. (2008). Doxorubicin-loaded polymeric micelle overcomes multidrug resistance of cancer by double-targeting folate receptor and early endosomal pH. *Small, 4*(11), 2043–2050.

Kim, M., Kim, D.-M., Kim, K.-S., Jung, W., & Kim, D.-E. (2018). Applications of cancer cell-specific aptamers in targeted delivery of anticancer therapeutic agents. *Molecules, 23*(4), 830.

Kirtane, A. R., Narayan, P., Liu, G., & Panyam, J. (2017). Polymer-surfactant nanoparticles for improving oral bioavailability of doxorubicin. *Journal of Pharmaceutical Investigation, 47*(1), 65–73.

Kobayashi, H., & Brechbiel, M. W. (2005). Nano-sized MRI contrast agents with dendrimer cores. *Advanced Drug Delivery Reviews, 57*(15), 2271–2286.

Kulkarni, P., Haldar, M. K., You, S., Choi, Y., & Mallik, S. (2016). Hypoxia-responsive polymersomes for drug delivery to hypoxic pancreatic cancer cells. *Biomacromolecules, 17*(8), 2507–2513.

Kummar, S., Chen, H. X., Wright, J., Holbeck, S., Millin, M. D., Tomaszewski, J., Zweibel, J., Collins, J., & Doroshow, J. H. (2010). Utilizing targeted cancer therapeutic agents in combination: Novel approaches and urgent requirements. *Nature Reviews Drug Discovery, 9*(11), 843–856.

Langer, C. J. (2004). CT-2103: A novel macromolecular taxane with potential advantages compared with conventional taxanes. *Clinical Lung Cancer, 6*, S85–S88.

Lee, C. C., MacKay, J. A., Fréchet, J. M., & Szoka, F. C. (2005). Designing dendrimers for biological applications. *Nature Biotechnology, 23*(12), 1517–1526.

Lee, K., Bae, K. H., Lee, Y., Lee, S. H., Ahn, C. H., & Park, T. G. (2010). Pluronic/polyethylenimine shell crosslinked nanocapsules with embedded magnetite nanocrystals for magnetically triggered delivery of siRNA. *Macromolecular Bioscience, 10*(3), 239–245.

Lee, S. J., Jeong, Y.-I., Park, H.-K., Kang, D. H., Oh, J.-S., Lee, S.-G., & Lee, H. C. (2015). Enzyme-responsive doxorubicin release from dendrimer nanoparticles for anticancer drug delivery. *International Journal of Nanomedicine, 10*, 5489.

Lin, C.-J., Kuan, C.-H., Wang, L.-W., Wu, H.-C., Chen, Y., Chang, C.-W., Huang, R.-Y., & Wang, T.-W. (2016). Integrated self-assembling drug delivery system possessing dual responsive and active targeting for orthotopic ovarian cancer theranostics. *Biomaterials, 90*, 12–26.

Linhardt, A. (2015). *Synthesis and characterisation of polyphosphazenes with controlled drug release*. Dissertation, University of Maryland

Liu, B., Yang, M., Li, R., Ding, Y., Qian, X., Yu, L., & Jiang, X. (2008). The antitumor effect of novel docetaxel-loaded thermosensitive micelles. *European Journal of Pharmaceutics and Biopharmaceutics, 69*(2), 527–534.

Liu, G.-Y., Chen, C.-J., & Ji, J. (2012). Biocompatible and biodegradable polymersomes as delivery vehicles in biomedical applications. *Soft Matter, 8*(34), 8811–8821.

Liu, H.-M., Zhang, Y.-F., Xie, Y.-D., Cai, Y.-F., Li, B.-Y., Li, W., Zeng, L.-Y., Li, Y.-L., & Yu, R.-T. (2017). Hypoxia-responsive ionizable liposome delivery siRNA for glioma therapy. *International Journal of Nanomedicine, 12*, 1065.

Luong, D., Kesharwani, P., Alsaab, H. O., Sau, S., Padhye, S., Sarkar, F. H., & Iyer, A. K. (2017). Folic acid conjugated polymeric micelles loaded with a curcumin difluorinated analog for targeting cervical and ovarian cancers. *Colloids and Surfaces B: Biointerfaces, 157*, 490–502.

Madamsetty, V. S., Mukherjee, A., & Mukherjee, S. (2019). Recent trends of the bio-inspired nanoparticles in cancer theranostics. *Frontiers in Pharmacology, 10*, 1264.

Maeda, H. (2013). The link between infection and cancer: Tumor vasculature, free radicals, and drug delivery to tumors via the EPR effect. *Cancer Science, 104*(7), 779–789.

Mahmoodzadeh, F., Abbasian, M., Jaymand, M., Salehi, R., & Bagherzadeh-Khajehmarjan, E. (2018). A novel gold-based stimuli-responsive theranostic nanomedicine for chemo-photothermal therapy of solid tumors. *Materials Science and Engineering: C, 93*, 880–889.

Maiti, P. K., Çağın, T., Wang, G., & Goddard, W. A. (2004). Structure of PAMAM dendrimers: Generations 1 through 11. *Macromolecules, 37*(16), 6236–6254.

Markman, B., De Souza, P. L., Dees, E. C., Gangadhar, T. C., Cooper, A., Roohullah, A., Boolell, V., Zamboni, W., Murphy, C., & Senderowicz, A. M. (2016). *A phase 1 study of CRLX301, a novel nanoparticle-drug conjugate (NDC) containing docetaxel (DOC), in patients with refractory solid tumors*. American Society of Clinical Oncology.

Masarudin, M. J., Cutts, S. M., Evison, B. J., Phillips, D. R., & Pigram, P. J. (2015). Factors determining the stability, size distribution, and cellular accumulation of small, monodisperse chitosan nanoparticles as candidate vectors for anticancer drug delivery: application to the passive encapsulation of [14C]-doxorubicin. *Nanotechnology, Science and Applications, 8*, 67.

Matsumura, Y., Hamaguchi, T., Ura, T., Muro, K., Yamada, Y., Shimada, Y., Shirao, K., Okusaka, T., Ueno, H., & Ikeda, M. (2004). Phase I clinical trial and pharmacokinetic evaluation of NK911, a micelle-encapsulated doxorubicin. *British Journal of Cancer, 91*(10), 1775–1781.

Medina, S. H., & El-Sayed, M. E. (2009). Dendrimers as carriers for delivery of chemotherapeutic agents. *Chemical Reviews, 109*(7), 3141–3157.

Minami, C. A., King, T. A., & Mittendorf, E. A. (2020). Patient preferences for locoregional therapy in early-stage breast cancer. *Breast Cancer Research and Treatment*, 1–19.

Mohapatra, S., Ranjan, S., Dasgupta, N., Kumar, R., & Thomas, S. (2018). *Nanocarriers for drug delivery: Nanoscience and nanotechnology in drug delivery*. Elsevier.

Mura, S., Nicolas, J., & Couvreur, P. (2013). Stimuli-responsive nanocarriers for drug delivery. *Nature Materials, 12*(11), 991–1003.

Nasef, A. M., Gardouh, A. R., & Ghorab, M. M. (2015). Polymeric nanoparticles: influence of polymer, surfactant and composition of manufacturing vehicle on particle size. *World Journal of Pharmaceutical Sciences, 3*, 2308–2322.

Nelemans, L. C., & Gurevich, L. (2020). Drug delivery with polymeric nanocarriers—cellular uptake mechanisms. *Materials, 13*(2), 366.

Ngoune, R., Peters, A., von Elverfeldt, D., Winkler, K., & Pütz, G. (2016). Accumulating nanoparticles by EPR: A route of no return. *Journal of Controlled Release, 238*, 58–70.

Nicolas, J., Mura, S., Brambilla, D., Mackiewicz, N., & Couvreur, P. (2013). Design, functionalization strategies and biomedical applications of targeted biodegradable/biocompatible polymer-based nanocarriers for drug delivery. *Chemical Society Reviews, 42*(3), 1147–1235.

Noriega-Luna, B., Godínez, L. A., Rodríguez, F. J., Rodríguez, A., Zaldívar-Lelo de Larrea, G., Sosa-Ferreyra, C., Mercado-Curiel, R., Manríquez, J., & Bustos, E. (2014). Applications of dendrimers in drug delivery agents, diagnosis, therapy, and detection. *Journal of Nanomaterials, 2014*, 507273.

Pan, J., Li, P.-J., Wang, Y., Chang, L., Wan, D., & Wang, H. (2018). Active targeted drug delivery of MMP-2 sensitive polymeric nanoparticles. *Chemical Communications, 54*(79), 11092–11095.

Pang, Z., Gao, H., Yu, Y., Guo, L., Chen, J., Pan, S., Ren, J., Wen, Z., & Jiang, X. (2011). Enhanced intracellular delivery and chemotherapy for glioma rats by transferrin-conjugated biodegradable polymersomes loaded with doxorubicin. *Bioconjugate Chemistry, 22*(6), 1171–1180.

Park, S., Shim, J., Jung, H. A., Sun, J.-M., Lee, S.-H., Park, W.-Y., Ahn, J. S., Ahn, M.-J., & Park, K. (2019). *Biomarker driven phase II umbrella trial study of AZD1775, AZD2014, AZD2811 monotherapy in relapsed small cell lung cancer*. American Society of Clinical Oncology.

Parmar, M. B., Sundaram, D. N. M., Remant Bahadur, K. C., Maranchuk, R., Aliabadi, H. M., Hugh, J. C., Löbenberg, R., & Uludağ, H. (2018). Combinational siRNA delivery using hyaluronic acid modified amphiphilic polyplexes against cell cycle and phosphatase proteins to

inhibit growth and migration of triple-negative breast cancer cells. *Acta Biomaterialia, 66*, 294–309.

Pawar, P. V., Gohil, S. V., Jain, J. P., & Kumar, N. (2013). Functionalized polymersomes for biomedical applications. *Polymer Chemistry, 4*(11), 3160–3176.

Peng, X.-H., Wang, Y., Huang, D., Wang, Y., Shin, H. J., Chen, Z., Spewak, M. B., Mao, H., Wang, X., & Wang, Y. (2011). Targeted delivery of cisplatin to lung cancer using ScFvEGFR-heparin-cisplatin nanoparticles. *ACS Nano, 5*(12), 9480–9493.

Perry, J. L., Herlihy, K. P., Napier, M. E., & DeSimone, J. M. (2011). PRINT: A novel platform toward shape and size specific nanoparticle theranostics. *Accounts of Chemical Research, 44*(10), 990–998.

Phase I. (2015). *NCI alliance for nanotechnology in cancer*.

Piedmonte, D. M., & Treuheit, M. J. (2008). Formulation of Neulasta®(pegfilgrastim). *Advanced Drug Delivery Reviews, 60*(1), 50–58.

Poursharifi, M., Wlodarczyk, M. T., & Mieszawska, A. J. (2020). How does access to this work benefit you? Let us know! *The FASEB Journal, 34*(S1), 1.

Pushpalatha, R., Selvamuthukumar, S., & Kilimozhi, D. (2017). Nanocarrier mediated combination drug delivery for chemotherapy–a review. *Journal of Drug Delivery Science and Technology, 39*, 362–371.

Radhakrishnan, K., Tripathy, J., Gnanadhas, D. P., Chakravortty, D., & Raichur, A. M. (2014). Dual enzyme responsive and targeted nanocapsules for intracellular delivery of anticancer agents. *RSC Advances, 4*(86), 45961–45968.

Rideau, E., Dimova, R., Schwille, P., Wurm, F. R., & Landfester, K. (2018). Liposomes and polymersomes: A comparative review towards cell mimicking. *Chemical Society Reviews, 47*(23), 8572–8610.

Ruan, K., Song, G., & Ouyang, G. (2009). Role of hypoxia in the hallmarks of human cancer. *Journal of Cellular Biochemistry, 107*(6), 1053–1062.

Sah, E., & Sah, H. (2015). Recent trends in preparation of poly (lactide-co-glycolide) nanoparticles by mixing polymeric organic solution with antisolvent. *Journal of Nanomaterials, 2015*, 794601.

Saravanakumar, K., Hu, X., Ali, D. M., & Wang, M.-H. (2019). Emerging strategies in stimuli-responsive nanocarriers as the drug delivery system for enhanced cancer therapy. *Current Pharmaceutical Design, 25*(24), 2609–2625.

Schmidt, K. T. (2020). *Novel therapeutic approaches to overcome acquired resistance to enzalutamide in patients with advanced prostate cancer*. Utrecht University.

Shahriari, M., Taghdisi, S. M., Abnous, K., Ramezani, M., & Alibolandi, M. (2019). Synthesis of hyaluronic acid-based polymersomes for doxorubicin delivery to metastatic breast cancer. *International Journal of Pharmaceutics, 572*, 118835.

Shi, M., Ho, K., Keating, A., & Shoichet, M. S. (2009). Doxorubicin-conjugated immunonanoparticles for intracellular anticancer drug delivery. *Advanced Functional Materials, 19*(11), 1689–1696.

Shi, J., Liu, S., Yu, Y., He, C., Tan, L., & Shen, Y.-M. (2019). RGD peptide-decorated micelles assembled from polymer–paclitaxel conjugates towards gastric cancer therapy. *Colloids and Surfaces B: Biointerfaces, 180*, 58–67.

Shukla, R., Singh, A., Pardhi, V., Kashyap, K., Dubey, S. K., Dandela, R., & Kesharwani, P. (2019). Dendrimer-based nanoparticulate delivery system for cancer therapy. In *Polymeric nanoparticles as a promising tool for anti-cancer therapeutics* (pp. 233–255). Elsevier.

Siegel, R. L., Miller, K. D., & Jemal, A. (2018). Cancer statistics, 2018. *CA: a Cancer Journal for Clinicians, 68*(1), 7–30.

Simone, E. A., Dziubla, T. D., & Muzykantov, V. R. (2008). Polymeric carriers: Role of geometry in drug delivery. *Expert Opinion on Drug Delivery, 5*(12), 1283–1300.

Son, S., Rao, N. V., Ko, H., Shin, S., Jeon, J., Han, H. S., Thambi, T., Suh, Y. D., & Park, J. H. (2018). Carboxymethyl dextran-based hypoxia-responsive nanoparticles for doxorubicin delivery. *International Journal of Biological Macromolecules, 110*, 399–405.

Song, N., Liu, W., Tu, Q., Liu, R., Zhang, Y., & Wang, J. (2011). Preparation and in vitro properties of redox-responsive polymeric nanoparticles for paclitaxel delivery. *Colloids and Surfaces B: Biointerfaces, 87*(2), 454–463.

Suksiriworapong, J., Taresco, V., Ivanov, D. P., Styliari, I. D., Sakchaisri, K., Junyaprasert, V. B., & Garnett, M. C. (2018). Synthesis and properties of a biodegradable polymer-drug conjugate: Methotrexate-poly (glycerol adipate). *Colloids and Surfaces B: Biointerfaces, 167*, 115–125.

Sun, P., Zhou, D., & Gan, Z. (2011). Novel reduction-sensitive micelles for triggered intracellular drug release. *Journal of Controlled Release, 155*(1), 96–103.

Svenson, S. (2012). Clinical translation of nanomedicines. *Current Opinion in Solid State and Materials Science, 16*(6), 287–294.

Svenson, S. (2014). What nanomedicine in the clinic right now really forms nanoparticles? *Wiley Interdisciplinary Reviews: Nanomedicine and Nanobiotechnology, 6*(2), 125–135.

Theerasilp, M., Chalermpanapun, P., Ponlamuangdee, K., Sukvanitvichai, D., & Nasongkla, N. (2017). Imidazole-modified deferasirox encapsulated polymeric micelles as pH-responsive iron-chelating nanocarrier for cancer chemotherapy. *RSC Advances, 7*(18), 11158–11169.

Thirunavukkarasu, G. K., Cherukula, K., Lee, H., Jeong, Y. Y., Park, I.-K., & Lee, J. Y. (2018). Magnetic field-inducible drug-eluting nanoparticles for image-guided thermo-chemotherapy. *Biomaterials, 180*, 240–252.

Tomalia, D. A., Christensen, J. B., & Boas, U. (2012). *Dendrimers, dendrons, and dendritic polymers: Discovery, applications, and the future*. Cambridge University Press.

Tortorella, S., & Karagiannis, T. C. (2014). The significance of transferrin receptors in oncology: The development of functional nano-based drug delivery systems. *Current Drug Delivery, 11*(4), 427–443.

Tyrrell, Z. L., Shen, Y., & Radosz, M. (2010). Fabrication of micellar nanoparticles for drug delivery through the self-assembly of block copolymers. *Progress in Polymer Science, 35*(9), 1128–1143.

Uchida, S., Kinoh, H., Ishii, T., Matsui, A., Tockary, T. A., Takeda, K. M., Uchida, H., Osada, K., Itaka, K., & Kataoka, K. (2016). Systemic delivery of messenger RNA for the treatment of pancreatic cancer using polyplex nanomicelles with a cholesterol moiety. *Biomaterials, 82*, 221–228.

Vacchelli, E., Galluzzi, L., Fridman, W. H., Galon, J., Sautès-Fridman, C., Tartour, E., & Kroemer, G. (2012). Trial watch: Chemotherapy with immunogenic cell death inducers. *Oncoimmunology, 1*(2), 179–188.

Valenzuela-Oses, J. K., García, M. C., Feitosa, V. A., Pachioni-Vasconcelos, J. A., Gomes-Filho, S. M., Lourenço, F. R., Cerize, N. N., Bassères, D. S., & Rangel-Yagui, C. O. (2017). Development and characterization of miltefosine-loaded polymeric micelles for cancer treatment. *Materials Science and Engineering: C, 81*, 327–333.

Van Eerden, R. A., Atrafi, F., vanHylckama Vlieg, M. A., Oomen-de Hoop, E., de Bruijn, P., Moelker, A., Lolkema, M. P., Rijcken, C. J., Hanssen, R., & Eskens, F. (2019). Comparison of intratumoral docetaxel exposure in cancer patients between nanoparticle entrapped docetaxel (CPC634) and conventional docetaxel (Cd): The CriTax study. *Annals of Oncology, 30*, v184.

Vetvicka, D., Hruby, M., Hovorka, O., Etrych, T., Vetrik, M., Kovar, L., Kovar, M., Ulbrich, K., & Rihova, B. (2009). Biological evaluation of polymeric micelles with covalently bound doxorubicin. *Bioconjugate Chemistry, 20*(11), 2090–2097.

Vishnoi, K., Viswakarma, N., Rana, A., & Rana, B. (2020). Transcription factors in cancer development and therapy. *Cancers, 12*(8), 2296.

Voss, M. H., Coates, A., Garmey, E. G., Haas, N. B., Hutson, T., Keefe, S. M., Motzer, R., Piscitelli, A., Vogelzang, N. J., & Figlin, R. A. (2015). *Randomized phase 2 study to assess the safety and efficacy of CRLX101 in combination with bevacizumab in patients (pts.) with metastatic renal cell carcinoma (RCC) versus standard of care (SOC)*. American Society of Clinical Oncology.

Wang, J., Bai, J., & Al-Jamal, K. (2018). Applications of magnetic nanoparticles in multi-modal imaging. *Theranostics and Image Guided Drug Delivery, 63*, 53.

Wei, X., Luo, Q., Sun, L., Li, X., Zhu, H., Guan, P., Wu, M., Luo, K., & Gong, Q. (2016). Enzyme- and pH-sensitive branched polymer–doxorubicin conjugate-based nanoscale drug delivery system for cancer therapy. *ACS Applied Materials & Interfaces, 8*(18), 11765–11778.

Wei, Y., Gu, X., Sun, Y., Meng, F., Storm, G., & Zhong, Z. (2020). Transferrin-binding peptide functionalized polymersomes mediate targeted doxorubicin delivery to colorectal cancer in vivo. *Journal of Controlled Release, 319*, 407–415.

Wen, X., Wu, Q.-P., Lu, Y., Fan, Z., Charnsangavej, C., Wallace, S., Chow, D., & Li, C. (2001). Poly (ethylene glycol)-conjugated anti-EGF receptor antibody C225 with radiometal chelator attached to the termini of polymer chains. *Bioconjugate Chemistry, 12*(4), 545–553.

Wex, J., Sidhu, M., Odeyemi, I., Abou-Setta, A. M., Retsa, P., & Tombal, B. (2013). Leuprolide acetate 1-, 3-and 6-monthly depot formulations in androgen deprivation therapy for prostate cancer in nine European countries: Evidence review and economic evaluation. *ClinicoEconomics and Outcomes Research: CEOR, 5*, 257.

Wu, P., Jia, Y., Qu, F., Sun, Y., Wang, P., Zhang, K., Xu, C., Liu, Q., & Wang, X. (2017). Ultrasound-responsive polymeric micelles for sonoporation-assisted site-specific therapeutic action. *ACS Applied Materials & Interfaces, 9*(31), 25706–25716.

Wu, R., Zhang, Z., Wang, B., Chen, G., Zhang, Y., Deng, H., Tang, Z., Mao, J., & Wang, L. (2020). Combination chemotherapy of lung cancer–co-delivery of docetaxel prodrug and cisplatin using aptamer-decorated lipid–polymer hybrid nanoparticles. *Drug Design, Development and Therapy, 14*, 2249–2261.

Xia, J., Du, Y., Huang, L., Chaurasiya, B., Tu, J., Webster, T. J., & Sun, C. (2018). Redox-responsive micelles from disulfide bond-bridged hyaluronic acid-tocopherol succinate for the treatment of melanoma. *Nanomedicine: Nanotechnology, Biology and Medicine, 14*(3), 713–723.

Xu, Q., Liu, Y., Su, S., Li, W., Chen, C., & Wu, Y. (2012). Anti-tumor activity of paclitaxel through dual-targeting carrier of cyclic RGD and transferrin conjugated hyperbranched copolymer nanoparticles. *Biomaterials, 33*(5), 1627–1639.

Xu, J., Zhao, Q., Jin, Y., & Qiu, L. (2014). High loading of hydrophilic/hydrophobic doxorubicin into polyphosphazene polymersome for breast cancer therapy. *Nanomedicine: Nanotechnology, Biology and Medicine, 10*(2), 349–358.

Xu, X., Ho, W., Zhang, X., Bertrand, N., & Farokhzad, O. (2015). Cancer nanomedicine: From targeted delivery to combination therapy. *Trends in Molecular Medicine, 21*(4), 223–232.

Yan, Q., Guo, X., Huang, X., Meng, X., Liu, F., Dai, P., Wang, Z., & Zhao, Y. (2019). Gated mesoporous silica nanocarriers for hypoxia-responsive cargo release. *ACS Applied Materials & Interfaces, 11*(27), 24377–24385.

Yang, H., Morris, J. J., & Lopina, S. T. (2004). Polyethylene glycol–polyamidoamine dendritic micelle as solubility enhancer and the effect of the length of polyethylene glycol arms on the solubility of pyrene in water. *Journal of Colloid and Interface Science, 273*(1), 148–154.

Yang, X., Li, Z., Wang, N., Li, L., Song, L., He, T., Sun, L., Wang, Z., Wu, Q., & Luo, N. (2015a). Curcumin-encapsulated polymeric micelles suppress the development of colon cancer in vitro and in vivo. *Scientific Reports, 5*, 10322.

Yang, H., Cai, W., Xu, L., Lv, X., Qiao, Y., Li, P., Wu, H., Yang, Y., Zhang, L., & Duan, Y. (2015b). Nanobubble–Affibody: Novel ultrasound contrast agents for targeted molecular ultrasound imaging of tumor. *Biomaterials, 37*, 279–288.

Ye, W. L., Du JB, N. R., Song, Y. F., Mei, Q. B., Zhao, M. G., & Zhou, S. Y. (2014). Cellular uptake and antitumor activity of DOX-hyd-PEG-FA nanoparticles. *PLoS One, 9*(5), e97358.

Yildiz, M., Prud'homme, R. K., Robb, I., & Adamson, D. (2007). Formation and characterization of polymersomes made by a solvent injection method. *Polymers for Advanced Technologies, 18*(6), 427–432.

Yin, T., Wang, P., Li, J., Wang, Y., Zheng, B., Zheng, R., Cheng, D., & Shuai, X. (2014). Tumor-penetrating codelivery of siRNA and paclitaxel with ultrasound-responsive nanobubbles hetero-assembled from polymeric micelles and liposomes. *Biomaterials, 35*(22), 5932–5943.

Yoo, H. S., & Park, T. G. (2004). Folate receptor targeted biodegradable polymeric doxorubicin micelles. *Journal of Controlled Release, 96*(2), 273–283.

Yousefpour, P., Atyabi, F., Vasheghani-Farahani, E., Movahedi, A.-A. M., & Dinarvand, R. (2011). Targeted delivery of doxorubicin-utilizing chitosan nanoparticles surface-functionalized with anti-Her2 trastuzumab. *International Journal of Nanomedicine, 6*, 1977.

Zarepour, A., Zarrabi, A., & Larsen, K. L. (2019). Fabricating B-cyclodextrin based pH-responsive nanotheranostics as a programmable polymeric nanocapsule for simultaneous diagnosis and therapy. *International Journal of Nanomedicine, 14*, 7017.

Zhai, Y., Zhou, X., Jia, L., Ma, C., Song, R., Deng, Y., Hu, X., & Sun, W. (2017). Acetal-linked paclitaxel polymeric prodrug based on functionalized mPEG-PCL diblock polymer for pH-triggered drug delivery. *Polymers, 9*(12), 698.

Zhang, C., Wang, W., Liu, T., Wu, Y., Guo, H., Wang, P., Tian, Q., Wang, Y., & Yuan, Z. (2012). Doxorubicin-loaded glycyrrhetinic acid-modified alginate nanoparticles for liver tumor chemotherapy. *Biomaterials, 33*(7), 2187–2196.

Zhang, C., Pan, D., Li, J., Hu, J., Bains, A., Guys, N., Zhu, H., Li, X., Luo, K., & Gong, Q. (2017). Enzyme-responsive peptide dendrimer-gemcitabine conjugate as a controlled-release drug delivery vehicle with enhanced antitumor efficacy. *Acta Biomaterialia, 55*, 153–162.

Zhang, M., Zhu, J., Zheng, Y., Guo, R., Wang, S., Mignani, S., Caminade, A.-M., Majoral, J.-P., & Shi, X. (2018). Doxorubicin-conjugated PAMAM dendrimers for pH-responsive drug release and folic acid-targeted cancer therapy. *Pharmaceutics, 10*(3), 162.

Zhang, X., Kang, Y., Liu, G.-T., Li, D.-D., Zhang, J.-Y., Gu, Z.-P., & Wu, J. (2019). Poly (cystine–PCL) based pH/redox dual-responsive nanocarriers for enhanced tumor therapy. *Biomaterials Science, 7*(5), 1962–1972.

Zhong, Y., Meng, F., Deng, C., & Zhong, Z. (2014). Ligand-directed active tumor-targeting polymeric nanoparticles for cancer chemotherapy. *Biomacromolecules, 15*(6), 1955–1969.

Zhou, Q., Zhang, L., Yang, T., & Wu, H. (2018). Stimuli-responsive polymeric micelles for drug delivery and cancer therapy. *International Journal of Nanomedicine, 13*, 2921.

Zhou, X., Guo, L., Shi, D., Duan, S., & Li, J. (2019). Biocompatible chitosan nanobubbles for ultrasound-mediated targeted delivery of doxorubicin. *Nanoscale Research Letters, 14*(1), 24.

Zhu, S., Hong, M., Zhang, L., Tang, G., Jiang, Y., & Pei, Y. (2010). PEGylated PAMAM dendrimer-doxorubicin conjugates: In vitro evaluation and in vivo tumor accumulation. *Pharmaceutical Research, 27*(1), 161–174.

Zhu, L., Yu, H., Liu, S.-Y., Xiao, X.-S., Dong, W.-H., Chen, Y.-N., Xu, W., & Zhu, T. (2015). Prognostic value of tissue inhibitor of metalloproteinase-2 expression in patients with non–small cell lung cancer: A systematic review and meta-analysis. *PLoS One, 10*(4), e0124230.

Chapter 8
Emerging Metal-Organic Framework Nanomaterials for Cancer Theranostics

Elham Asadian, Mahnaz Ahmadi, Rüstem Keçili, and Fatemeh Ghorbani-Bidkorbeh

Contents

E. Asadian
Department of Medical Physics and Biomedical Engineering, School of Medicine, Shahid Beheshti University of Medical Sciences, Tehran, Iran

M. Ahmadi · F. Ghorbani-Bidkorbeh (✉)
Department of Pharmaceutics, School of Pharmacy, Shahid Beheshti University of Medical Sciences, Tehran, Iran
e-mail: f.ghorbani@sbmu.ac.ir

R. Keçili
Yunus Emre Vocational School of Health Services, Department of Medical Services and Techniques, Anadolu University, Eskişehir, Turkey

M. Saravanan, H. Barabadi (eds.), *Cancer Nanotheranostics*, Nanotechnology in the Life Sciences, https://doi.org/10.1007/978-3-030-74330-7_8

List of Acronyms and Abbreviations

5-Fu	5-Fluorouracil
BDC	Benzene dicarboxylic acid
BTC	1,3,5-Benzenetricarboxylic acid (trimesic acid)
CD	Cyclodextrin
CDT	Chemodynamic therapy
CT	X-ray computed tomography
Cur	Curcumin
DEF	N,N-Diethylformamide
DMF	N,N-Dimethylformamide
DOX	Doxorubicin
EPR	Enhanced permeability and retention
FL	Fluorescence
HKUST	Hong Kong University of Science and Technology
IRMOF	Isoreticular metal-organic framework
LBL	Layer-by-layer
MIL	Material of Institute Lavoisier
MIm	2-Methylimidazole
MOFs	Metal-organic frameworks
MRI	Magnetic resonance imaging
MW	Microwave
MWCNTs	Multiwalled carbon nanotubes
NIR	Near infrared
nMOFs	NanoMOFs
NPs	Nanoparticles
PAI	Photoacoustic imaging
PB	Prussian blue
PCN	Porous coordination network
PDA	Polydopamine
PDT	Photodynamic therapy
PEG	Polyethylene glycol
PET	Positron emission tomography
Ppy	Polypyrrole
PS	Photosensitizer
PTT	Photothermal therapy
RhB	Rhodamine B
ROS	Reactive oxygen species
SAM	Self-assembled monolayer
TCPP	Tetrakis (4-carboxyphenyl) porphyrin
UiO	Universitetet i Oslo
ZIF	Zeolitic imidazolate framework

8.1 Introduction

Cancer, which is used as a generic term for a large group of diseases associated with the abnormal cell growth and subsequent invasion to other parts of the body, is one of the major public health threats and accounts for millions of deaths worldwide. Two main challenges concerning cancer diagnosis and treatment correspond to the (1) late diagnosis of the disease due to the lack of early symptoms which resulted in spread to other sites in the body (metastasis) and (2) nonspecific distribution of highly toxic chemotherapeutic drugs that affect normal tissues. On the other hand, agents which are used for diagnostic and therapeutic purposes come up with some limitations including low bioavailability, undesirable side effects, and rapid clearance from the body. Hence, designing novel strategies seems to be inevitable in order to address these challenges. In this regard, nanoparticle-based systems such as polymeric, magnetic, iron oxide, and gold nanoparticles are considered as intriguing candidates to overcome these problems (Peer et al., 2007; Cho et al., 2008; Huang & Lovell, 2017). Nanomaterials have been widely investigated for drug/cargo delivery owing to their small size, high surface area, and enhanced loading capacities along with improving pharmacokinetics and biocompatibility (Hossen et al., 2019; Alexis et al., 2008). They can be also exploited as carriers of targeting ligands to target a specific tissue and reduce the toxicity of the drug molecules by on-site control release mechanisms (Singh & Lillard, 2009; Petros & DeSimone, 2010). In addition to therapeutic applications, nanoparticles are advantageous as diagnostic agents for biomedical imaging. Nanoparticles, pristine or conjugated with diagnosis agents, can be traced and detected in the body and, therefore, provide us with the opportunity not only to develop the imaging modalities to assist with disease detection but also to investigate the biodistribution (Nune et al., 2009; Choi & Frangioni, 2010; Han et al., 2019). In the meantime, simultaneous integration of therapeutic potentials of nanoparticles with their diagnostic capabilities, named *theranostic* approaches, has been the subject of interest in the past few years (Huang & Lovell, 2017; Xie et al., 2010). In this regard, various kinds of nanomaterials such as polymeric (Qian et al., 2017; Indoria et al., 2020), gold (Guo et al., 2017; Gharatape & Salehi, 2017), magnetic (Yoo et al., 2011; Gul et al., 2019), carbon (Gupta et al., 2019), and iron oxide (Dadfar et al., 2019) nanoparticles have been widely used for theranostic applications. Among them, porous nanomaterials are of great importance due to their intrinsic properties as cargo carriers.

Metal-organic frameworks (MOFs), also called coordination polymers, are an emerging class of crystalline materials with uniform porous structure. Although they have been first discovered in 1965, the further development of MOFs was hampered by the collapse of their porous structure in the absence of solvent or other guest molecules (Yaghi et al., 1998; Kepert & Rosseinsky, 1999). In the late 1990s, Yaghi et al. reported on the synthesis of a highly stable metal-organic framework which maintained its crystallinity while fully desolvated and even after heating up to 300 °C (Li et al., 1999). Their simple and potentially universal synthetic route has opened up new horizons toward various design strategies which resulted in the

synthesis of more than 20,000 different MOFs with diverse size, morphology, and functionality within the past two decades.

MOFs are literally organic-inorganic hybrid materials composed of transition metal cations (or clusters) linked together by organic linkers through strong coordination bonds based on reticular chemistry (Fig. 8.1a). The versatility of organic building blocks and the diversity of metal-ligand combinations along with various adoptable synthesis methods have led to development of MOFs with structural flexibility. So far, a wide variety of MOFs with tunable chemical properties and ample functionalities have been prepared by different research groups, some of which are shown in Fig. 8.1b. As can be seen, the repetition of MOF building blocks forms a periodic cage-like framework with well-defined pore apertures where the pore size and structure can be controlled through wise choices of organic linkers (Lu et al., 2014).

MOF family possess fascinating properties stemmed from their unique structure such as extremely high specific surface area (up to 10,000 m^2g^{-1}), large pore volumes with well-defined pore aperture, tunable pore size, shape and dimensionality, and versatile functionality along with structural diversity. These superior

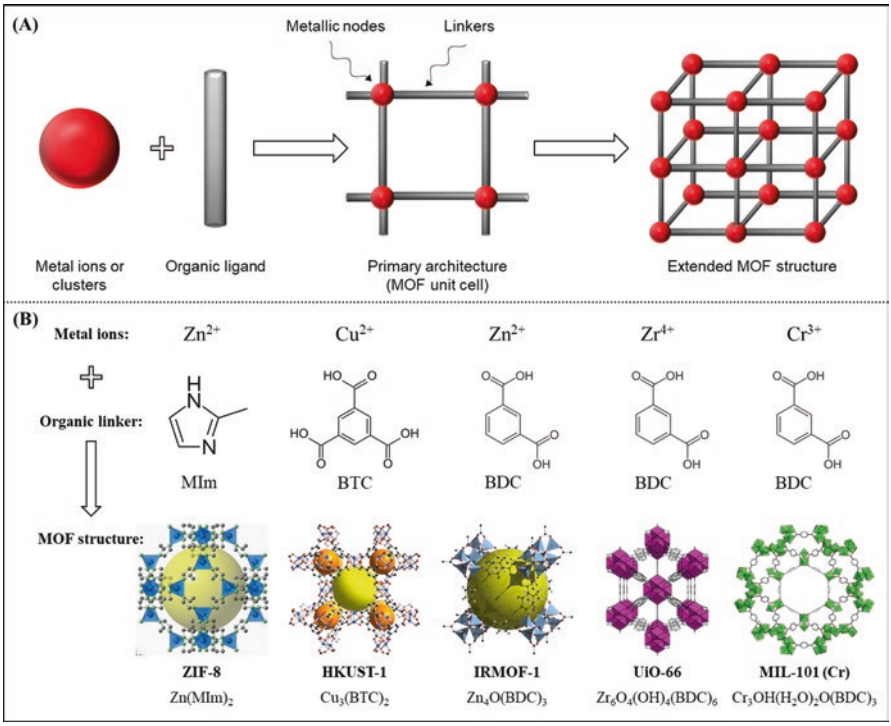

Fig. 8.1 (**a**) Schematic illustration of MOF structure composed of metallic nodes and organic linkers. (**b**) Some representative MOF structures (the yellow spheres represent the highest volume of the free pore in the structure)

characteristics turn them into potential candidates for a wide range of applications from gas storage, separation and purification (Li et al., 2018a; Xue et al., 2019a; Dhainaut et al., 2020), catalysis (Wang & Astruc, 2019; Zhu et al., 2020), and sensing (Kumar et al., 2015; Dolgopolova et al., 2018; Amini et al., 2020) to biomedical ones (Lu et al., 2018; Luo et al., 2019; Yang & Yang, 2020; Zhang et al., 2020). The fact that MOFs provide extremely high loading capacities as a result of their extraordinary porosities as well as their improved biocompatibility paves the way for their use as promising cargo delivery systems for drugs and therapeutic agents and even biomacromolecules such as proteins, genes, and nucleic acids (Wu & Yang, 2017; Cheng et al., 2018; Liu et al., 2019). On the other hand, MOFs are appealing candidates for biomedical imaging purposes (Della Rocca et al., 2011; Li et al., 2019a). They can be exploited as carriers for delivering imaging contrast agents or even serve as contrast agents themselves through appropriate selection of structural components. Moreover, the incorporation of superparamagnetic metal centers (i.e., Mn^{2+}, Fe^{3+}, and Gd^{3+}) in the framework makes it possible for the MR imaging applications. As a result, recent years have witnessed an increasing interest in the implementation of metal-organic frameworks as tools for cancer diagnosis and therapy (theranostics) by integrating their imaging and therapy capabilities into a single formulation (Cai et al., 2015; Zhao et al., 2016; Cai et al., 2017; Zhou et al., 2018; Pandey et al., 2020).

In the present chapter, the synthesis and modification methods of MOFs will be first addressed. Then, the therapeutic and imaging applications of MOFs will be highlighted. The next section will focus on nanoMOF-based theranostic platforms followed by the future perspectives toward the development of efficient theranostic systems.

8.2 MOF: Synthesis and Surface Modification

As mentioned previously, metal-organic frameworks are formed by the self-assembly of polynuclear metal clusters (named as "secondary building units, SBUs") and multitopic organic linkers as the structural key components and within the realm of reticular chemistry[1] (Kalmutzki et al., 2018). One of the fascinating features of MOFs is their synthetic flexibility, which allows the possibility of designing various kinds of topologies via rational choice of precursors. This capability makes it possible not only to control the pore size but also to regulate their internal environment. In addition to the structure and type of precursor used, the structural and functional tunability can be achieved by choosing the appropriate synthesis method along with controlling the synthetic parameters such as concentration of reagents, solvent polarity, temperature, pH of the solution, and the reaction time

[1] The term reticular derived from Latin *reticulum* which means "small net" and referred to the formation of an extended netlike structure through linking the molecular building blocks by means of strong coordination bonds.

(Meek et al., 2011; Stock & Biswas, 2012; Safaei et al., 2019; Al Amery et al., 2020). So far and as shown in Fig. 8.2, different synthetic approaches have been adopted to prepare MOFs with diverse morphologies which will be presented in the following sections.

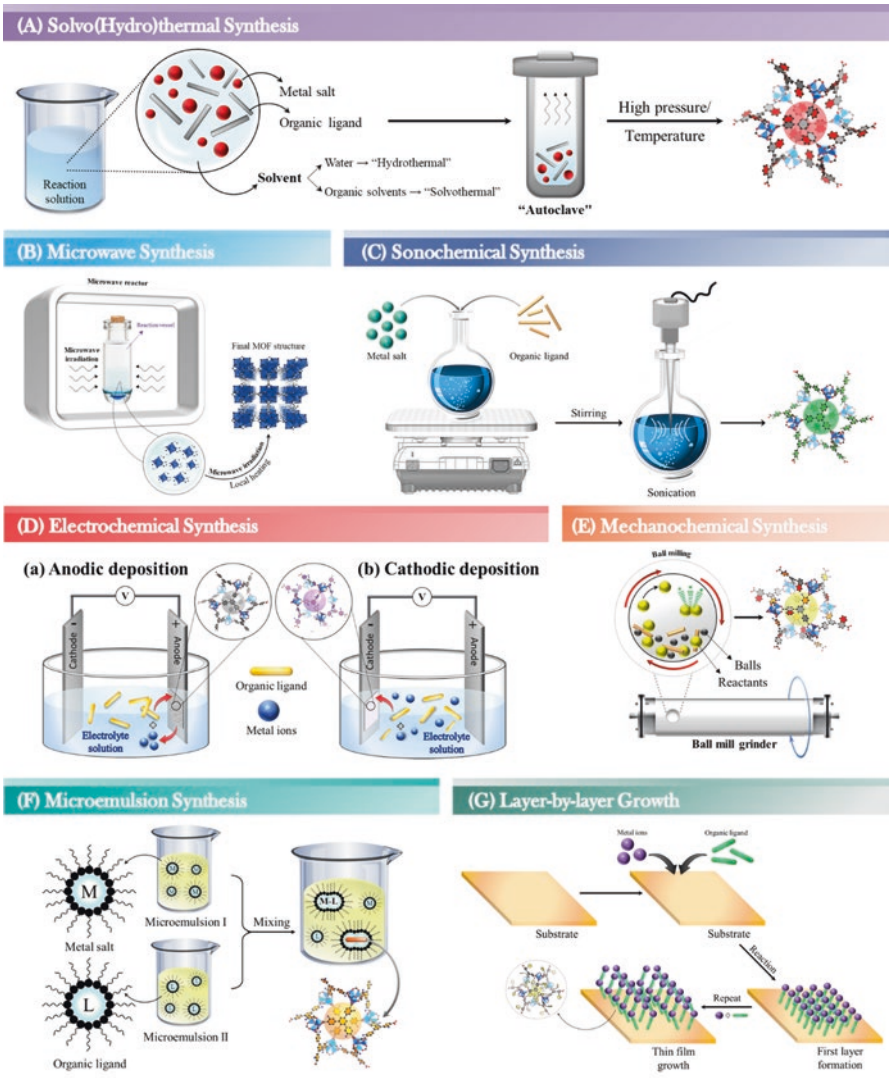

Fig. 8.2 Schematic representation of some synthetic methods widely applied for the preparation of MOF structures. (*The MOF crystal structures which relate to MOF-177 are adopted from Ref. Zhang et al. (2015) and only used as a schematic representative for MOFs prepared through various methods)

8.2.1 Direct Precipitation Reaction

Early efforts for producing MOFs have generally focused on low-temperature methods (Hoskins & Robson, 1990). These conventional techniques have been mainly relied on the simple mixing of the starting materials (i.e., metal salts and organic ligands) which have already been dissolved in suitable solvents followed by nucleation and crystal growth processes which finally result in precipitation of MOF structures. Once the precursors are mixed together and the critical nucleation concentration is exceeded, the initial nuclei are formed. The reaction solution will be then aged at constant low temperature (often room temperature) during which the solution mixture is concentrated by slow evaporation of the solvent and primary nuclei are consequently grown. As a result, tuning the reaction conditions, i.e., the rate of nucleation and growth processes, has a direct impact on controlling the size of the final product (Stock & Biswas, 2012; Rowsell & Yaghi, 2004). On the other hand, chemical and structural properties of the solvents including solubility, reactivity, polarity, dielectric constant, donor number, and the boiling point temperature play a key role in such liquid phase synthesis reactions (Al Amery et al., 2020). In the meantime, certain ligands contain functional groups (like carboxylic acid) which should be deprotonated prior to coordination, while so many polar solvents can compete with the organic linkers to coordinate with the available metal centers. Hence, the choice of solvent used is essential in achieving the desired MOF product. The direct precipitation approach has been utilized to prepare some prominent MOFs like MOF-5, MOF-74, MOF-177, MOF-199, and IRMOF-0 at room temperature (Tranchemontagne et al., 2008). It is noteworthy to mention that with this method, the MOF crystals not only can be synthesized in the solution phase but also can be grown on the surface of suitable substrates through nucleation and growth processes. For instance, ZIF-8 nanoparticles were synthesized on the surface of 3D graphene networks (Cao et al., 2014) or carbon cloth (Asadian et al., 2020) by immersing the substrate in methanolic solutions of $Zn(NO_3)_2$ and MIm for a specific period of time followed by thorough washing the substrate with appropriate solvent. The slow evaporation method is suitable for thermally sensitive starting materials; however when kinetically inert ions are used or in the case of MOFs with higher crystallinity degrees, high-temperature synthetic methods such as solvothermal/hydrothermal techniques are more desirable.

8.2.2 Solvothermal/Hydrothermal Synthesis

With the increasing tendency to synthesize MOF structures with improved crystallinity, techniques at higher operational temperatures became mandatory. In this regard, hydrothermal/solvothermal methods were found to be convenient synthetic routes. These techniques refer to the chemical reactions performed in a closed vessel at relatively high temperature (generally above the boiling point of solvent). In

the case of water as the solvent and when the reaction proceeds in an aqueous medium, the method is called "hydrothermal," while in "solvothermal" technique, the solvents used are non-aqueous (organic solvents). Regardless of the type of solvent, in both the aforementioned techniques, the reactants are first thoroughly dissolved in an appropriate solvent. The resulting homogeneous solution is then transferred to a Teflon lined stainless steel autoclave (Fig. 8.2a). Since the reaction proceeds at elevated temperature and in a sealed container, the pressure under which the MOF nanoparticles are formed is relatively high resulting in structures with higher degrees of crystallinity suitable for power X-ray diffraction (PXRD) analysis.

In 1995, Yaghi and Li proposed hydrothermal synthesis as a viable route to produce copper MOF with crystalline porous structure composed of extended channel network (Yaghi & Li, 1995). Their method involved exposing the reactants ($Cu(NO_3)_2 \cdot 2/5H_2O$, 4,4′-bpy and 1,3,5-triazine) to a specified temperature program in which the autoclave was kept at 140 °C for 24 h, then cooled to 90 °C, and held for 12 h followed by another 12 h at 70 °C and final cooling to the room temperature. Their results revealed that the hydrothermal conditions were essential to achieve the product as the same reaction did not succeed through refluxing even after 24 h. Although hydrothermal technique has been applied to synthesis certain kinds of MOFs (Chalati et al., 2011; Qian et al., 2012), its further implementation was hindered by poor water solubility of organic linkers and the stability issues of MOF structures in aqueous medium. From this respect, the solvothermal method is more convenient so that taking a glance at literature reveals that it is the most widely used technology for the synthesis of this family of nanomaterials (Park et al., 2006; Cheng et al., 2013; Sun et al., 2020; Hu et al., 2014; Esrafili et al., 2019; Xue et al., 2019b; Chen et al., 2020; Wang et al., 2019a). The solvents used in solvothermal synthesis could be protic such as ethanol, methanol, and acetic acid as well as aprotic ones like DMF (N,N-dimethylformamide), DEF (N,N-diethylformamide), and acetonitrile and should be carefully selected based on the polarity and dielectric constant to achieve the desired product.

Zeolitic imidazolate frameworks (ZIFs), as one of the most extensively studied subclasses of MOFs, are composed of tetrahedrally coordinated transition metal ions (i.e., Fe, Co, Cu, Zn) linked by imidazolate organic ligands. ZIFs borrowed their name from zeolites as a result of their zeolite-like topologies and integrate the advantages of their inorganic counterparts (namely, high chemical and thermal stability of zeolites) with those of MOF family (i.e., high porosity and surface area). Yaghi's group was the first to synthesize ZIF-8 using $Zn(NO_3)_2 \cdot 4H_2O$ and 2-methylimidazole (2-MIm) dissolved in DMF and via a solvothermal method at 140 °C (Park et al., 2006). The prepared ZIF-8 demonstrated high permanent porosity (1810 m^2/g) and extraordinary thermal rigidity (up to 550 °C) along with remarkable chemical stability (even in boiling alkaline aqueous solution and organic solvents).

The solvothermal technique has attracted a great deal of attention since it can be used to not only synthesize different types of MOFs but also provide us with the ability of tuning the size and morphology. The size and shape of MOF

nanostructures can be altered by varying the synthesis conditions including the type of solvents, the concentrations of reactants, and the presence of surfactants (Cheng et al., 2013; Sun et al., 2020; Hu et al., 2014; Esrafili et al., 2019). For instance, by controlling the degree of deprotonation of NH_2-BDC via adjusting the water content in a DMF-water mixed solvent system, Guo et al. synthesized a series of NH_2-MIL-53 (Al) crystals with different sizes and morphologies (Cheng et al., 2013). The results demonstrated the effect of water on modulating the nucleation and crystal growth process in such a way that differs the morphology from cube-like to rhomboid monocrystals. The same solvent-adjustment solvothermal strategy was also applied to prepare bimetallic NiCo frameworks (Sun et al., 2020). As shown in Fig. 8.3a, the size and shape of the resulting MOFs strongly depend on the composition of the solvent. It was revealed that the presence of water plays an important role in the formation of nanosheet-like structures by lowering the rate of ligand deprotonation and, as a consequent, the nucleation step. The concentration of the reactants is another critical parameter that affects the morphology during crystallization (Hu et al., 2014; Esrafili et al., 2019). Due to the crystalline structure of MOFs, changing the concentration of precursors as well as the presence of surfactants can orient their growth along specific crystal plates and, as a result, the formation of different morphologies.

Moreover, preparing MOF composites through combination of MOFs with various functional materials which are capable of introducing improved or rather novel properties has been the focus of interest during the past few years (Xue et al., 2019b; Chen et al., 2020). Considering the synthesis techniques of MOF-based composites, solvothermal method is regarded as a suitable approach in which the composite nanostructures can be achieved in a one-pot synthesis and through careful adjusting of the reaction conditions. As an example, Wang and coworkers introduced a flower-string-like NiCo MOF@MWCNT composites by utilizing carboxylated MWCNTs as a substrate for the in situ growth of binary NiCo MOF with the aid of solvothermal method (Wang et al., 2019a). The reaction proceeded in an autoclave by mixing $Ni(NO_3)_2{\cdot}6H_2O$, $Co(NO_3)_2{\cdot}6H_2O$, and 4,4′-biphenyldicarboxylic acid (BPDC) as organic ligand in a DMF-EtOH solution and in the presence of MWCNTs with different wt% (Fig. 8.3b). The MWCNTs not only act as a guiding agent on the MOF growth but also increase the conductivity of the composite material. In general, if the reaction parameters are properly controlled and, in the meantime, the nucleation process on the substrate and then the subsequent growth occur efficiently, MOF composites can be synthesized with high yield using a solvothermal method.

Nevertheless, the solvothermal technique generally requires long reaction times (from hours to weeks) at high temperatures and needs organic solvents which are toxic and pose environmental concerns. These challenges along with operational limitations (setup fabrication at large scale) are obstacles which should be addressed for scaling-up and commercialization of solvothermal synthesis.

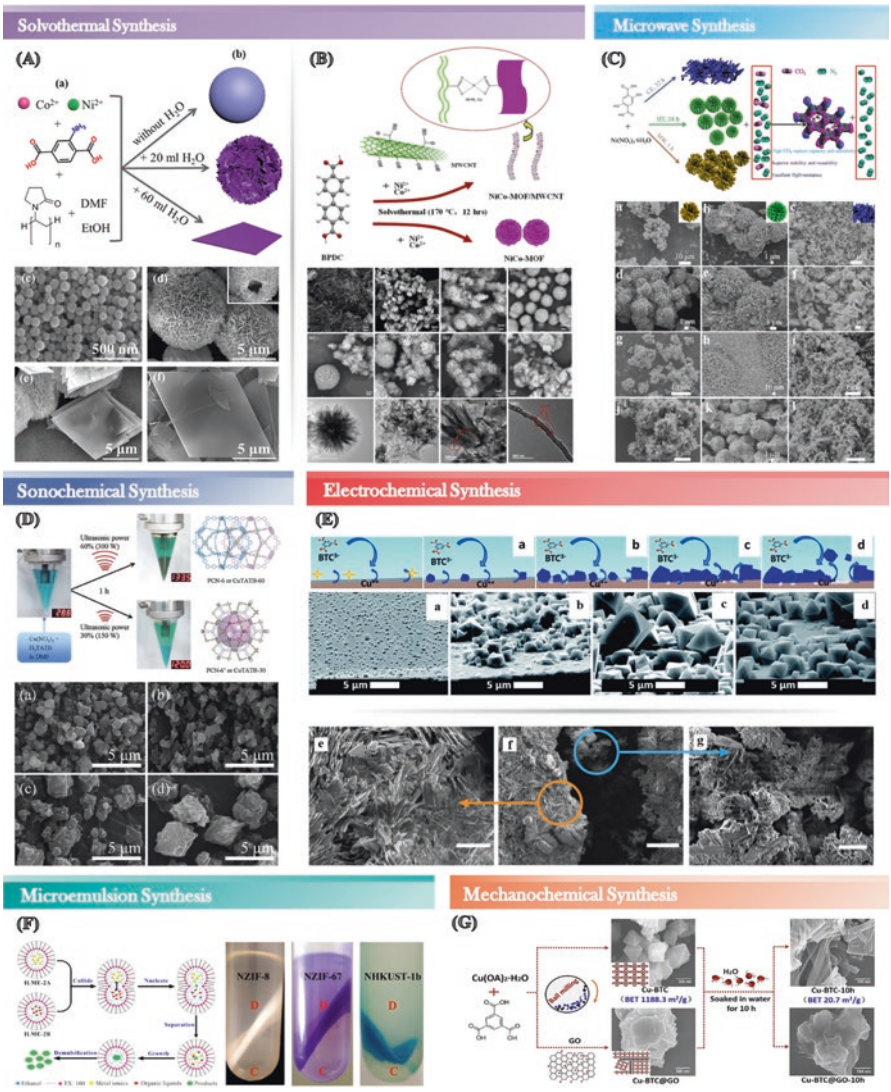

Fig. 8.3 (**A**) Schematic illustration of solvothermal synthesis of NiCo MOF nanostructures with different morphologies (a, b) and SEM images of (c) NiCo-MOF nanosheets (NSs), (d) nanosheet-assembled hollow spheres (NSHS), (e) mixed NSHS and rhombus sheets (RSs), and (f) RSs (*Reprinted with permission from* Sun et al. (2020)), (**B**) SEM and TEM images of carboxylated MWCNTs (a), NiCo-MOF nanostructures (d, j), and NiCo-MOF@MWCNTs particles (b, c, e–h, k–m) (*Reprinted with permission from* Wang et al. (2019a)), (**C**) SEM images of MOF-74 (Ni) nanostructures prepared by MW at (a, d) 125 and (g, j) 140 °C for 60 min, by hydrothermal at (b, e) 125 and (h, k) 140 °C for 24 h and by condensation reflux at (c, f) 125 and (i, l) 140 °C for 32 h (*Reprinted with permission from* Chen et al. (2019a)), (**D**) SEM micrographs of CuTATB nanostructures synthesized sonochemically under different ultrasonic power levels; (a) 30%, (b) 40%, (c) 50%, and (d) 60% (*Reprinted with permission from* Kim et al. (2011)), (**E**) SEM pictures of four phases involved in the anodic electrodeposition of HKUST-1: (I) initial nucleation (a), (II)

(continued)

growth of islands (b), (III) intergrowth (c), and (III) detachment (d) (*Reprinted with permission from* Campagnol et al. (2016)) and cathodic electrodeposition of biphasic metal-organic framework thin film produced by sequential growth at −1.10 and −1.50 V (f), displaying the characteristic feather-like morphology of $(Et_3NH)_2Zn_3(BDC)_4$ in the top layer (e, orange arrow) and the small crystallites associated with the Zn/MOF-5 composite in the layer closer to the electrode surface (g, blue arrow) (*Reprinted with permission from* Li and Dincă (2014)), (**F**) Schematic representation of the growth mechanism of HKUST-1 nanoparticles synthesized through ionic liquid microemulsion technique along with the digital images of ternary system after demulsification and centrifugation (*Reprinted with permission from* Zheng et al. (2017)), (**G**) Mechanochemical synthesis of Cu-BTC and Cu-BTC@GO nanostructures which depicts the BET and water stability of each sample (*Reprinted with permission from* Li et al. (2016b))

8.2.3 Microwave-Assisted Synthesis

Although the solvothermal method comes up with numerous advantages as mentioned in the last section, it is considered as an energy-intensive approach since it requires high temperatures and pressures for a long period of time. To overcome this issue, microwave-assisted synthesis has been proposed as a mechanism of rate enhancement through accelerating the rate of reactions (Meek et al., 2011). In the MW synthesis, a mixture of reactants is transferred to a sealed MW tube and placed in a MW reactor as schematically shown in Fig. 8.2b. Once the reaction vessel is exposed to the MW irradiation, the permanent dipole moment of the molecules or ions in polar solvents can be coupled with the oscillating electric field. Hence, by applying an appropriate frequency, the molecules in the synthesis medium collide which leads to an increase in the temperature of the system. The rapid heating of the solution reduces the reaction time to a great extent (from several days in the solvothermal technique to several minutes for MW method). Moreover, since the rise in the temperature occurs as a result of direct interaction between the electromagnetic waves and electric charges of molecules, homogeneous heating throughout the whole medium is possible which in turn accelerates the crystallization and improves the product purity (Stock & Biswas, 2012). MIL-100(Cr) was the first nanoporous MOF synthesized through the MW route in 2005 (Jhung et al., 2005). The XRD pattern of the as-synthesized chromium trimesate revealed that the particles prepared under MW irradiation at 220 °C for 4 h are comparable in crystallinity with those of synthesized by solvothermal technique at 220 °C for 4 days. So far, numerous MOF nanostructures have been synthesized by means of MW method including MIL-101(Fe) (Taylor-Pashow et al., 2009), Co-MOF-74 (Cho et al., 2012), MOF-205 (Babu et al., 2016), and MOF-74(Ni) (Chen et al., 2019a).

To elucidate the mechanism of the rate enhancement induced by MW conditions, a systematic study was conducted by Jhung group on different MOFs prepared by MW method, and the results were compared with other synthetic routes such as conventional electric heating and solvothermal (Khan et al., 2010; Haque et al., 2010). Their investigations indicated that the mechanism of rate acceleration strongly depends on the type of MOF and can be due to the enhancement in the kinetics of either the nucleation step or the crystal growth. For instance, in the case of HKUST-1 (Cu-BTC MOF), even though both stages are enhanced, the observed

acceleration is mainly due to the nucleation step (Khan et al., 2010). This is while for iron terephthalate (MIL-53(Fe)), the enhancement in the crystal growth plays a more critical role (Haque et al., 2010). It is noteworthy to mention that to obtain high crystalline MOFs with narrow size distribution and desired morphologies, it is essential to control the reaction parameters. Increasing the reaction parameters such as MW irradiation time, power level, and concentration of substrates beyond an optimal condition would result in reduction of the synthesis time at the expense of products' crystallinity. As an example, the results of a study performed on MW-assisted synthesis of MOF-5 showed that prolonging the microwave irradiation time led to a sharp deterioration in its physicochemical properties (Choi et al., 2008). In a recent article published by Chen and coworkers, the effect of synthesis conditions (i.e., hydrothermal (HT), microwave-assisted (MW), and condensation reflux (CE)) on the morphology and physicochemical properties of a series of MOF-74(Ni) was thoroughly investigated (Chen et al., 2019a). It was shown that the MW method is a facile and rapid (within 60 min) approach for preparing MOF-74(Ni) particles compared to those of HT (24 h) and CE (32 h) techniques. Furthermore, the materials prepared via MW route demonstrated smaller and relatively more uniform particle size as well as higher thermal stability as depicted in Fig. 8.3c.

8.2.4 Sonochemical Synthesis

Sonochemical synthesis refers to the use of high-energy ultrasound to a liquid that generates bubbles in the reaction mixture in which ultrasonic energy is accumulated. The formed bubbles start to grow gradually and, once reaching a certain size, collapse instantaneously. The process of formation, growth, and implosive collapse of the microbubbles in the medium is called "acoustic cavitation." This phenomenon results in the formation of localized "hot spots" with extremely high temperatures (~5000 K) and pressures (~1000 bar) throughout the solution (Suslick et al., 1986). Hence, free radicals are formed through the remarkable increase in the reaction conditions (i.e., temperature and pressure), and as a consequence, homogeneous nucleation centers are generated (Al Amery et al., 2020). As a result, a sonochemical method can be applied to produce small MOF nanocrystals with higher degree of crystallinity within considerably shorter reaction times (compared to conventional solvothermal technique). Various experimental conditions such as type of solvents, concentration of the substrates, pH of solution, the applied ultrasound power, as well as reaction time and duration of ultrasonication should be considered to achieve MOFs with desired structures (Cho et al., 2013; Abdollahi et al., 2018; Armstrong et al., 2017; Kim et al., 2011). Different equipment with adjustable power outputs including reactors equipped with high-power ultrasonic horns (Fig. 8.2c) or ultrasonic baths (with relatively lower power intensities) can be utilized in this regard. The choice of the instrument used is important since the ultrasound frequency and intensity has a direct influence on the crystallization. For instance, CuTATB-n where TATB is 4,4′,4″-s-triazine-2,4,6-triyltribenzoate and n

represents the power level were synthesized in 1 h by adjusting the ultrasonic power level (Kim et al., 2011). As clearly shown in the SEM images of Fig. 8.3d, by increasing the power level from 30% to 60%, a progressive increase was observed in the particle size. After precise characterizations, it was concluded that at 30% ultrasonic power, PCN-6′ was produced, while at 60% power intensity, PCN-6 (the catenated form) with higher surface area and enhanced stability of the network was obtained. In the past few years, as an environmentally friendly method, sonochemical route has been used for synthesizing numerous MOF structures (Cho et al., 2013; Abdollahi et al., 2018; Armstrong et al., 2017; Kim et al., 2011; Son et al., 2008; Jung et al., 2010; Dastbaz et al., 2019) due to its advantages, namely, rapidity, facility, and energy-efficiency which allows the scale up of MOF's production. This is while more investigations are yet needed to be done for better comprehension of the involved mechanism.

8.2.5 Electrochemical Synthesis

Electrochemical method is another promising technique which is suitable for deposition of MOF thin films on the surface of conductive substrates. In electrochemical deposition of MOFs, the substrate of interest is immersed in an electrolyte solution containing organic ligands. Subsequently, by applying appropriate conditions (voltage or current density), a thin layer of MOF is grown on the surface of the substrate. The electrodeposition technique can be performed via two different routes: anodic and cathodic deposition in a two-electrode cell configuration (Al-Kutubi et al., 2015; Campagnol et al., 2016; Li et al., 2016a).

In anodic deposition, the metal ions are electrochemically produced through anodic dissolution of anode material which then react with the deprotonated organic ligands in the electrolyte solution. The result is the formation of a thin MOF layer on the surface of anode as schematically shown in Fig. 8.2D-a. Since the metallic electrodes (such as Cu and Zn) are utilized in anodic deposition as the source of metal ions, the use of metal salts is avoided during the synthesis which in turn eliminates the formation of hazards associated with anions such as nitrates, perchlorate, or chloride (Stock & Biswas, 2012; Lee et al., 2013; Dey et al., 2014). The first report on electrochemical synthesis of MOFs was published in 2005 by researchers of BASF (Mueller et al., 2007). They made use of copper plates as both cathode and anode electrodes in a methanol electrolyte containing H_3BTC as the organic ligand. By applying a voltage of 12–19 V for a duration of 150 min followed by an activation step, copper (II) trimesate framework of HKUST-1 was prepared through anodic deposition. From then on, their pioneering work was further extended to synthesis various metal-organic frameworks such as ZIF-8, MIL-100 (Al), MIL-53 (Al), and NH_2-MIL-53 (Al) via anodic electrodeposition (Martinez Joaristi et al., 2012; Hauser et al., 2019; Stassen et al., 2015).

Another approach for the formation of MOF thin film is based on providing the metal centers from an electrolyte solution containing metal salts rather than metallic

oxidation. The metal ions present in the solution coordinate with the deprotonated organic ligands near the cathodic electrode which are generated either by OH^- ions produced through reduction of water at the surface of cathode or anions such as NO_3^- from the nitrate salts. In the other words, the increase in the pH of the electrolyte solution near the cathodic electrode surface as a result of OH^- ions formation led to the deprotonation of neutral organic linkers which then react with the metal ions and subsequent deposition of MOF layer on the surface of cathode. This approach which is known as "cathodic deposition" (Fig. 8.2D-b) was adopted to synthesis MOF nanostructures on the electrode surface (Li & Dincă, 2014; Zhu et al., 2015; Wei et al., 2020; Xiao et al., 2020). Figure 8.3E depicts the scanning electron micrographs of MOF layers grown on the surface of electrodes via anodic and cathodic deposition (Campagnol et al., 2016; Li & Dincă, 2014). In order to obtain an adherent microporous layer of MOF with textural properties, the effect of synthesis parameters including type of the solvent, type and concentration of the electrolyte, the applied voltage or current-density, and temperature and duration of the electrodeposition should be precisely controlled.

Electrochemical deposition method has several advantages including the possibility of synthesizing thin films of metal-organic frameworks under mild preparation conditions (compared to solvothermal technique, it operates at relatively low temperatures within a short period of time). In addition, it is of great interest for direct growth of MOF layers on a conductive substrate. Moreover, by altering the reaction parameters (i.e., voltages and current density) along with the deposition time, it is possible to tune the thickness of deposited MOF coatings with controlled phase and morphology. All these properties together turn electrochemical synthesis into an appropriate approach for large-scale production processes. However, the mechanisms of growth should be yet investigated to achieve a deeper insight for further design and preparation of MOF nanostructures.

8.2.6 Microemulsion Synthesis

Microemulsions are thermodynamically stable dispersions of water and oil mixtures in the presence of surfactants molecules. When a surfactant is added to an immiscible water/oil mixture, small droplets (size <100 nm) are formed spontaneously due to the self-assembly of these amphiphilic molecules in which the dispersed phase is retained. There are three main types of microemulsions including "direct" as for oil dispersed in water, "reversed" which refer to dispersed water in a continuous organic phase, and "bicontinuous." These droplets can act as nanocontainers inside which the dissolved starting materials react together within a confined area. From this perspective, microemulsion synthesis approach is of great value for preparing nanoparticles with small size and narrow size distribution (Flügel et al., 2012). Various approaches have been adopted for the formation of microemulsion in order to synthesis nanoMOFs (Sun et al., 2016; Zheng et al., 2017; Shang et al., 2013; Ye et al., 2018). For instance, ZIF nanocrystals were synthesized through

reverse microemulsion technique as well as ionic liquid microemulsion (Sun et al., 2016; Zheng et al., 2017). In reverse microemulsion, as schematically shown in Fig. 8.2F, the precursors are dissolved separately in appropriate solvents, and then, the solutions are mixed together to form a stable water in oil dispersion. As an example, Sun et al. synthesized monodispersed ZIF nanostructures (ZIF-8 and ZIF-67) with extremely small size (<5 nm) at room temperature and through reverse microemulsion (Sun et al., 2016). Their synthetic route is based on the addition of solutions containing the starting materials (i.e., $Zn(NO_3)_2{\cdot}6H_2O$ in water as solution I and 2-MIm/triethylamine in water as solution II) to the CTAB/1-haexanol/heptane mixture. The prepared ZIF nanoparticles showed high surface area and thermal stability. On the other hand, Zheng and coworkers synthesized nanoscale ZIFs by the ionic liquid-containing microemulsion system of H_2O/BmimPF$_6$/TX-100 (Zheng et al., 2017). As depicted in Fig. 8.3F, HKUST-1 nanoparticles could be also synthesized by adding ethanol into the H_2O/TX-100/BmimPF$_6$ system in order to improve the dissolution of organic ligands. These examples demonstrate that by careful adjustment of the reaction composition, different MOFs with controlled shape and morphology are achievable.

8.2.7 Layer-by-Layer Growth

The layer-by-layer (LBL) growth is an approach composed of immersing a substrate in the solutions of metal salt and organic linker, respectively. After each immersion step, a molecular layer is formed on the surface (Fig. 8.2G). As its name implies, a homogeneous nanoscale film of MOF can be grown by successive deposition steps. The thickness of MOF layer can be controlled through the number of repeated cycles of immersion in the solutions of precursors, while its crystal direction is tunable via using modified substrates with special functional groups (Shekhah et al., 2007; Zacher et al., 2009; Shekhah, 2010; Yuan & Zhu, 2020).

The step-by-step route was developed for the growth of various MOF thin films (Shekhah et al., 2009; So et al., 2013; Li et al., 2014). Shekhah et al. reported on the formation of a highly ordered and oriented HKUST-1 layer on the surface of gold substrate (Shekhah et al., 2009). To this end, well-defined organic surfaces were prepared by fabricating self-assembled monolayers (SAMs), namely, COOH- and OH-terminated SAMs, on the surface of Au substrates as the growth templates. It was found that the growth direction strongly depends on the type of functional groups since for COOH-functionalized surface, the growth of [Cu_3-(btc)$_2$] proceeded along the (Shang et al., 2013) direction, while an OH-terminated surface favors the formation of a MOF layer with (Biswal et al., 2013) orientation. Compared to direct growth method, the layer-by-layer approach allows for obtaining homogeneous films with preferred orientation at mild conditions (i.e., room temperature). However, it can be classified as a time-consuming process since it needs pre-functionalized substrates with SAMs as well as immersion/washing repetitive cycles to obtain MOF layers with a certain thickness.

8.2.8 Mechanochemical Synthesis

Mechanochemistry refers to the chemical reactions which are induced by mechanical forces that break the intramolecular bonds. Unlike all the abovementioned methods which rely on solvents, mechanochemical synthesis is a solid-state reaction which means that it is a solvent-free technique. As schematically represented in Fig. 8.2E, in the mechanochemical method, the precursors (i.e., metal salts and organic ligands) are mixed together and then ground in a ball mill grinder. Pichon et al. were the first to report solvent-free synthesis of a microporous $[Cu(INA)_2]$ metal-organic framework by grinding $Cu(OAc)_2{\cdot}3H_2O$ and isonicotinic acid (INA) (Pichon et al., 2006). From then on, various MOFs have been synthesized through mechanochemical methods (Klimakow et al., 2010; Biswal et al., 2013; Li et al., 2016b; Chen et al., 2019b; Wang et al., 2020). This technique can be used not only to synthesize pure MOF crystals but also to prepare MOF hybrid structures. For instance, Cu-BTC@GO composites were mechanochemically synthesized within 30 min (Li et al., 2016b). As shown in the SEM images of Fig. 8.3G, the water stability of Cu-BTC framework was remarkably enhanced after compositing with graphene oxide nanosheets.

In order to increase the reactivity of mechanochemical synthesis, organic reactants with low melting point along with hydrated metal salts (such as metal acetates or carbonates) are preferred. The mechanochemical is advantageous for synthesizing MOF structures from different perspectives: it is an environmentally friendly approach compared to liquid-phase reactions, because the organic solvents are avoided in such a solvent-free technique. Moreover, porous MOF nanocrystals can be obtained at room temperatures within short reaction times with quantitative yields which makes it appropriate for scaling up.

8.3 Biomedical Applications of MOF Nanoparticles

Recent years have witnessed a dynamic development in early diagnosis and treatment of diseases. The emergence of nanotechnology has undoubtedly played a pivotal role in this regard and opened up new horizons in various fields of nanomedicine specially for early detection and targeted therapy of cancers. As mentioned previously, cancer treatment strongly depends on detection of the disease at primary stages followed by localized therapy in such a way that healthy tissues and organs are not affected. With the intense evolution of imaging modalities, nanoparticle probes have been utilized for molecular imaging to assist with the cancer diagnosis. Typical contrast agents such as iodine, barium, and gadolinium, although providing valuable information, are associated with certain drawbacks including nonspecific biodistribution, short blood half-life, fast clearance from the body, and slight renal toxicity (Naseri et al., 2018). Therefore, developing targeted contrast agents with high sensitivity and specificity for noninvasive diagnosis purposes is of tremendous

importance. Nanoparticles represent a promising strategy for biomedical imaging which encompass prolonged circulation half-lives and higher in vitro and/or in vivo stabilities.

Moreover, nanoscale cargo delivery systems which can be used to deliver drugs, nucleic acids, ligands, or antibodies show great potential in cancer treatment (Mi et al., 2020). Compared to conventional cancer therapies such as chemotherapy and radiotherapy which suffer from nonspecific biodistribution and targeting as well as poor oral bioavailabilities, cancer nanotherapeutics make use of nanoparticles not only to improve pharmacokinetics and biodistribution but also to increase the blood circulation time. Moreover, nanoparticles are beneficial for increased concentration in the target site by passive accumulation at the tumor microenvironments due to the enhanced permeability and retention (EPR) effect. These properties reduce the toxicity and side effects and, as a result, enhance their therapeutic efficiency (Shi et al., 2017).

Among various kinds of nanostructures, MOFs have attracted considerable attention for nanomedical applications because of their unique characteristics such as tunable pore size and structure, large surface areas, biodegradability, and functionalization versatility. In one hand, their high specific surface area allows for functionalization with various small molecules such as drugs and therapeutic agents, while on the other hand, the wise selection of metal ions (like those of paramagnetic or superparamagnetic) and organic ligands (such as luminescent ones) makes them prone for imaging applications. These features have led to the emergence of MOF-based theranostic nanoplatforms which enable the integration of both diagnostic and therapeutic functions at the same time and in one entity (Cai et al., 2015). In addition to the advantages of nanoMOFs (nMOFs) for drug delivery and imaging applications, incorporating extra materials into a MOF structure or preparing MOF composites can also enhance the efficacy of MOF systems in biomedical applications (Osterrieth & Fairen-Jimenez, 2020). In the following sub-sections, we first enumerate the applications of MOFs for biomedical imaging as well as for drug delivery purposes. Then, various MOF-based nanostructures with potential for theranostic goals will be discussed.

8.3.1 Biomedical Imaging

Nanoparticles are proved to be promising candidates for biomedical imaging due to their capabilities in producing signals or even enhancing the signal contrast at tumor sites. In the realm of bioimaging, nanoMOFs offer numerous advantages as contrast agents which relates to the fact that their composition and structure and, as a result, their physicochemical properties can be tuned by reasonable choice of metal ions/clusters as well as organic linkers (Yang & Yang, 2020; Li et al., 2019a). For this reason, nMOFs have been exploited as powerful diagnostic tools for magnetic resonance imaging (MRI), X-ray computed tomography (CT), positron emission tomography (PET), and photoacoustic (PA) and optical imaging techniques (Deng et al.,

2017; Yang et al., 2019; Robison et al., 2019; Peller et al., 2018; Taylor et al., 2008; Horcajada et al., 2010; Pereira et al., 2010; Tian et al., 2015; Chen et al., 2017; Shang et al., 2017; Zhang et al., 2018a).

In 2017, Deng et al. designed a fluorescent probe composed of encapsulated Rhodamine B (RhB) into nanoscale ZIF-90 particles for mitochondrial ATP sensing and imaging in living cells (Deng et al., 2017). The competitive coordination between ATP molecules and the metal centers of ZIF-90 decomposes the zeolitic framework structure and, as a consequence, releases the RhB. It was argued that through this ATP-triggered release mechanism, monitoring of ATP molecules which are mainly produced in mitochondria is possible which is of value to study the process of cellular respiration and disease diagnosis. A two-photon Zr-based MOF (PCN-58) was also applied as a sensing platform for intracellular sensing and deep tissue imaging (Yang et al., 2019). The incorporation of a target-responsive two-photon organic moiety into the MOF structure through click chemistry resulted in a fluorescent probe with high signal-to-noise ratio, photostability, and deep tissue penetration. The structure was designed in such a way that ensures large enough cavities for loading fluorophores. As schematically shown in Fig. 8.4A (a and b), PCN-58 was covalently cross-linked with two-photon fluorescent organic probes via Cu(I)-catalyzed azide-alkyne cycloaddition (CuAAC) without any cross-reactivity toward the MOF structure or other functional groups. The synthesized probe retained its fluorescence-responsive properties corresponding to the two-photon organic moiety with a penetration depth up to 130 μm (Fig. 8.4A-c and d).

X-ray computed tomography (CT) is another common diagnostic method used in the medical field. A new cluster-based bismuth metal-organic framework (Bi-NU-901) which consists of eight connected Bi_6 nodes and tetratopic pyrene-based linkers was synthesized solvothermally and tested as a CT contrast agent (Robison et al., 2019). The results revealed that the prepared Bi-MOF with robust chemical and thermal stability demonstrated ∼7 times better contrast intensity compared to the zirconium analogue (Zr-NU-901) and ∼14 times superior than that of a commercially available CT contrast agent (idixanol).

In addition, metal-organic frameworks have also paved their way toward magnetic resonance imaging as one of the most versatile imaging modalities being used in routine clinical examinations that provides high spatial resolution images (Peller et al., 2018). Regarding the contrast agents used in MRI such as gadolinium, the safety issue is a major concern since Gd ions can leak from the chelate complex during their application. In this respect, three different approaches have been adopted to construct MRI active MOF nanoparticles (Peller et al., 2018). In the first concept, the metallic centers are responsible for MRI contrast such as in Gd-, Mn-, and Fe-based MOFs (Taylor et al., 2008; Horcajada et al., 2010; Pereira et al., 2010; Tian et al., 2015). The high chemical stability of MOF complexes minimizes the metal leakage to a great extent and leads to biocompatibility issues. The second concept is based on growing a MOF shell on the surface of MRI-active metal oxide nanoparticles, while in the third strategy, post-synthetic modification procedures are used to functionalize the external surface of MOFs with contrast agents (Peller et al., 2018). The latter two cases are generally utilized for theranostic applications

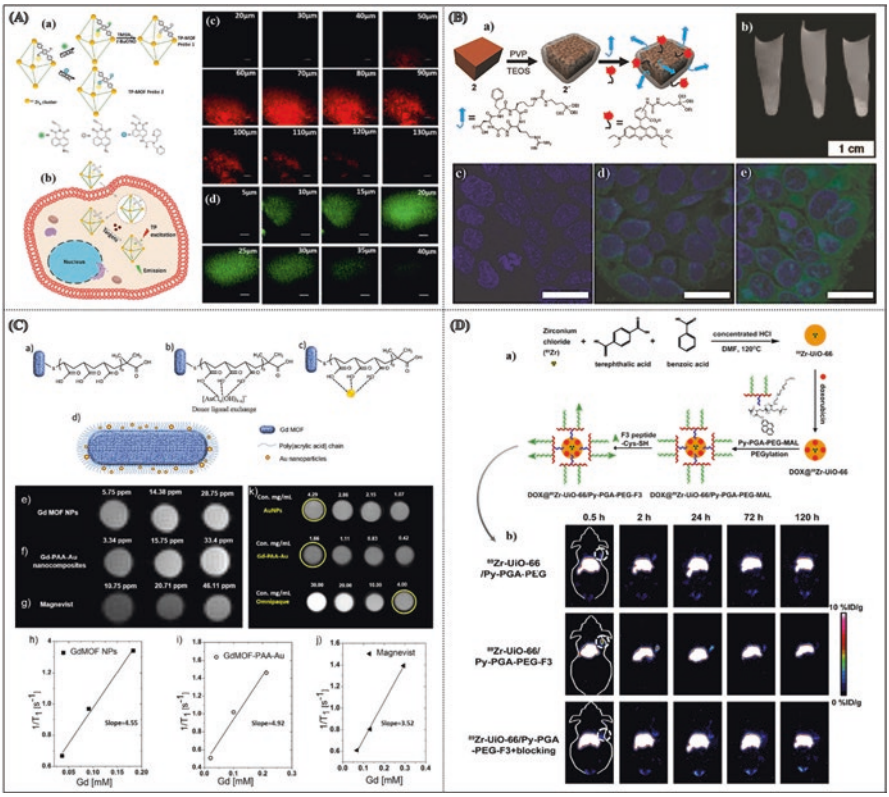

Fig. 8.4 Examples of nMOFs for various biomedical imaging applications; (**A**) Schematic illustration for the preparation of two photon (TP)-MOF sensing platform and the process of intracellular sensing (a, b); Depth fluorescence images of TP-MOF probe 1 in rat liver tissue in which the change of FL intensity with scan depth was determined by spectral confocal multiphoton microscopy (c) or one-photon microscopy (d) in the z-scan mode (the scale bar is 50 μm) (*Reprinted with permission from* Yang et al. (2019)); (**B**) Mn-based MOF nanoparticles synthesized via MW method were coated with a thin silica shell (denoted as 2′) in order to stabilize them as well as facilitating their functionalization with a fluorophore and c(RGDfK) cell-targeting peptide (a), In vitro MR images of HT-29 cells incubated with 2′ (left), nontargeted 2′ (middle) and c(RGDfK)-targeted 2′ (right) (b), Merged confocal images of HT-29 cells that were incubated with 2′ (c), nontargeted 2′ (d) and c(RGDfK)-targeted 2′ (e); The blue color was from DRAQ5 used to stain the cell nuclei while the green color was from RhB. The bars represent 20 μm (*Reprinted with permission from* Taylor et al. (2008)), (**C**) Schematic representation of the Gd-MOF/PAA/Au nanocomposite preparation (a-d), T_1-weighted MRI images and relaxation rate ($1/T_1$) as a function of the Gd concentration for unmodified Gd-MOF nanoparticles (e, h), Gd-MOF/PAA/Au nanocomposite (f, i), and chelate-based Gd contrast agent (Magnevist) (g, j) at various Gd concentrations in DIUF water, CT images of plain AuNPs, Gd-MOF/PAA/Au nanocomposite, and the iodine-based contrast agent Omnipaque with different Au or iodine concentration (k) (*Reprinted with permission from* Tian et al. (2015)), (**D**) Schematic synthesis route of ^{89}Zr-UiO-66/Py-PGA-PEG-F3 conjugates (a) and representative coronal PET images of MDA-MB-231 tumor bearing mice at different time points post-injection for various nanostructures with excessive amount of F3 peptide blocking; The location of tumors was identified by dashed circles (b) (*Reprinted with permission from* Chen et al. (2017))

as they can merge the advantages of potentially MRI active agents for imaging purposes with extremely high porosity of MOFs as drug carriers for therapeutic goals. Mn-containing nMOFs with various morphologies were synthesized through reverse-phase microemulsion method at room temperature and MW-assisted synthesis at 120 °C (Taylor et al., 2008). The as-prepared particles demonstrated very high in vitro and in vivo longitudinal relaxivity (r_1) with excellent MR contrast enhancement. The surface of MW-synthesized MOF nanoparticles was further modified with a thin silica shell which made it possible to covalently attach a cyclic RGD peptide (c(RGDfK)) and an organic fluorophore, as schematically depicted in Fig. 8.4B-a. In one hand, the cell-targeting molecules (c(RGDfK)) enhanced the delivery of the prepared core-shell hybrid nanostructures to the cancer cells, while on the other hand, the silica shell provided an adequate protection until reaching the tumor site where Mn^{2+} ions are released to give T_1-weighted contrast enhancement (Fig. 8.4B, b-e). Nontoxic iron-based MOFs (MIL-88A) were also used as contrast agents for MR imaging (Horcajada et al., 2010). As raised by the authors, the efficiency of the prepared MIL nMOFs in MRI is directly related to their relaxivity by modifying the relaxation times of the water protons in the surrounding medium in the presence of a magnetic field, since MIL nanoparticles not only possess paramagnetic iron atoms in their matrix but also offer an interconnected porous network filled with metal coordinated and/or free water molecules. MOFs containing Ln^{3+} ions with high transverse relaxivity (r_2) were also reported as potential MRI contrast agents for T_2-weighted imaging (Pereira et al., 2010). Gd is one of the most used rare earth elements in MRI medical diagnosis due to its seven unpaired electrons and a large magnetic moment. Tian et al. proposed the Gd MOF nanoparticles synthesized through microemulsion process as an efficient MRI contrast agent (Tian et al., 2015). In the next step and in order to achieve MRI/CT bimodal imaging, Gd MOF nanoparticles were covered with a thin polymeric layer of poly (acrylic acid) (PAA) via reversible addition-fragmentation chain transfer (RAFT) polymerization which is used as a linker between Gd MOF and Au nanoparticles. Finally, Au nanoparticles were deposited on the surface to obtain Gd MOF-PAA-Au nanocomposites, as schematically shown in Fig. 8.4C (a-d). Hence, the prepared nanocomposite can be also exploited as a CT imaging agent. The T_1-weighted MR images as well as relaxation rate ($1/T_1$) studies (Fig. 8.4C, e-j) demonstrated that even at lower concentration, Gd MOF nanoparticles offered brighter images compared to the clinically used chelate-based Gd contrast agent (i.e., Magnevist) and its performance was not hindered by the surface modification procedure. Moreover, the results of CT were also compared to that of clinically used iodine-based contrast agent (Omnipaque), and the results showed higher X-ray attenuation for Gd-PAA-Au nanocomposites than Omnipaque with similar concentrations (Fig. 8.4C-k).

Positron emission tomography (PET) scan is another functional imaging technique with superior detection sensitivity (down to picomolar range) that utilizes radioactive substances (radiotracers) to visualize the biomedical functions of tissues. MOFs with intrinsically radioactive metal nodes can be used for PET imaging. For instance, UiO-66 nMOF (^{89}ZrUiO-66) composed of positron-emitting isotope zirconium-89 (^{89}Zr) was synthesized by a solvothermal method (Chen et al., 2017).

The prepared MOF nanoparticles were loaded with doxorubicin (DOX) with high payload followed by further functionalization with pyrene-derived polyethylene glycol (Py-PGA-PEG) and conjugation with a peptide ligand (F3) to nucleolin for targeting of triple-negative breast tumors (Fig. 8.4D-a). The ability of functionalized UiO-66 conjugates was investigated for PET-guided cargo delivery to cancerous sites. Figure 8.4D-b depicts the representative coronal PET images of MDA-MB-231 tumor-bearing mice regarding the distribution/clearance profile at different time points post-injection for various UiO-66 structures. The results revealed that ^{89}Zr-UiO-66/Py−PGA-PEG-F3 can serve as a potential image-guidable, tumor-selective cargo delivery nanoplatform.

It is noteworthy to mention that in some certain cases, single-modality imaging cannot provide sufficient features on its own. Moreover, each of the previously mentioned techniques is associated with some inherent defects such as low tissue penetration rate, poor special resolution, and low sensitivity. Therefore, multimodal imaging techniques have been proposed to overcome these issues over the past few years. Various MOF nanoarchitectures were used for this purpose by integrating materials with different functionalities (Cai et al., 2017; Shang et al., 2017; Zhang et al., 2018a). For instance, core-shell Au@MIL-88(Fe) nanoparticles were prepared through a microemulsion method and further used for multimodality imaging-based glioma diagnosis (Shang et al., 2017). The potential of the as-prepared Au@MIL-88(Fe) nanocomposites as a triple-modality CT/MR/PA-imaging contrast agent was investigated using a U87 MG-subcutaneous tumor-bearing mice. The CT, T_2-weighted MR, and in vivo PA images of mice before and after intravenous injection as well as the bioluminescent image of tumor demonstrate a remarkable enhancement after injection with the nanocomposite. The results represent that Au@MIL-88(Fe) nanoparticles with low cytotoxicity provide a contrast agent with substantial enhancement of imaging sensitivity, high depth of penetration, and spatial resolution for imaging of glioma. Other multimodal imaging such as FL/PA/T_2-weighted MR imaging based on hyaluronic acid and ICG-engineered MIL-100(Fe) NPs (Cai et al., 2017) or doxorubicin (DOX)@Gd MOFs-glucose nanocarrier for CT/T_1-weighted MR imaging (Zhang et al., 2018a) were also reported.

8.3.2 MOF-Based Therapeutic Systems

The development of controllable drug delivery systems (DDSs) capable of transporting therapeutic agents as well as their subsequent release in a targeted manner (without reaching the nontarget cells, organs, or tissues) is indispensable to reduce the side effects and enhance the therapeutic efficacy of drugs (Sousa et al., 2019; Mir et al., 2017). In the meantime, phototherapy techniques including photodynamic therapy (PDT) and photothermal therapy (PTT) have attracted a great deal of attention for treating cancer due to their minimally invasive nature and minor collateral damages to the surrounding normal tissues (Dolmans et al., 2003; Doughty et al., 2019). In PDT, photoactive molecules called photosensitizer (PS) generate

reactive oxygen species (ROS) through a series of photochemical reactions upon absorbing light with a specific wavelength which will consequently lead to cell death. Photothermal therapy refers to the use of photothermal agents which can convert light (most often in infrared wavelengths) to heat energy for local hyperthermia and tumor treatment. When a photosensitizer is stimulated by an electromagnetic radiation, it can absorb energy through excitation and then release the vibrational energy (heat). This photon-mediated process results in elevating the local temperature to 41–47 °C which ultimately can kill the targeted cells.

Conventional carriers such as liposomes, micelles, or nanoparticles are commonly associated with low drug capacity and, as a result, poor loading. This is while nMOFs hold great promise for drug storage and delivery considering their highly porous topology along with the possibility of designing these structures with suitable biocompatibility (Sun et al., 2013; Wang et al., 2018a; Cao et al., 2020). Moreover, their structural robustness prevents undesirable decomposition and burst release.

There exist three different approaches for loading the drug molecules on nMOFs based on the location of the drug as well as the host-guest interactions (Fig. 8.5A) (Wang et al., 2018a). In the first approach, drug molecules are encapsulated in the void volume (channels, pores, and cavities) of porous nMOFs (Fig. 8.5A-a). To this end, MOF nanoparticles are first synthesized through an appropriate method and then exploited for loading of drugs via either covalent or noncovalent interactions. The efficiency of encapsulation strategy strongly depends on the size of therapeutic substances compared to the pore size and structure of MOF carriers and should be carefully adjusted to obtain high loading capacities. Direct assembly is another method for incorporation of drug molecules into MOF structures. As shown in Fig. 8.5A-b, in the direct assembly method, the drug molecules or their prodrug formulations with suitable functional groups are used as linkers between metallic centers through coordination bonds. Under physiological conditions, the MOF nanoparticles are decomposed slowly which in turn release the active therapeutic components. Compared to the encapsulation technique, direct assembly is of advantage since inserting the drug molecule as a ligand into the structure results in more uniform distribution with higher loadings. However, controlling the reaction parameters in order to achieve the expected MOF structures is more challenging. The direct assembly approach has been successfully used for incorporation of some chemotherapeutic drugs such as methotrexate (MTX) (Huxford et al., 2012), bisphosphonates like pamidronate (Pam) (Liu et al., 2012), and cisplatin and oxaliplatin prodrugs (Liu et al., 2014a; Rieter et al., 2008) into MOF matrix. The third strategy for drug loading proceeds via a post-synthetic modification in which the guest molecules are covalently attached to a pre-synthesized MOF through formation of coordination bonds with metal centers or covalent bonds with the functional sites of the organic linkers (Fig. 8.5A-c) (Wang et al., 2018a).

Furthermore, the application of nanoscale MOFs in phototherapy, as a clinically approved technique for treatment of cancer, has been also investigated (Guan et al., 2018; Lan et al., 2019; Boddula et al., 2020; Hu et al., 2018; Wang et al., 2018b, 2019b; Li et al., 2019b; Li et al., 2020). The characteristic features of these porous

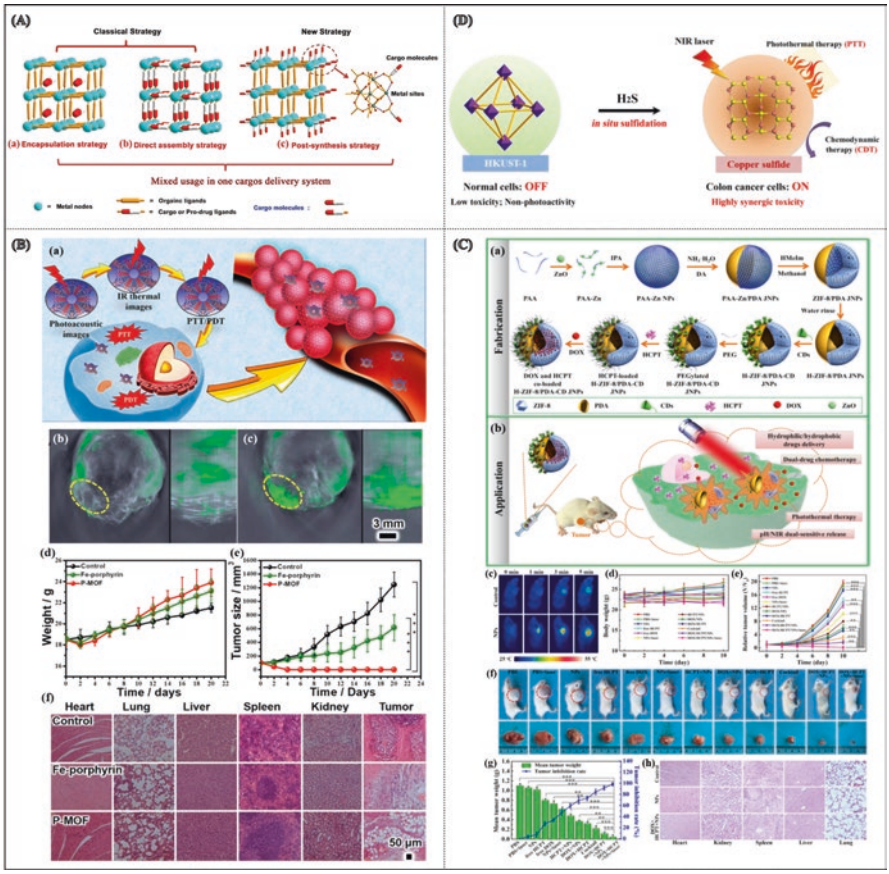

Fig. 8.5 Therapeutic applications of nMOFs; (**A**) Three different cargo-loading strategies for MOFs: "Encapsulation" in which drug molecules are entered into the pores or channels of MOF and maintained via noncovalent interactions (a), "Direct assembly" which uses drug/prodrug molecules as ligands to partly participate in the formation of MOFs via coordination bonds (b) and "Post-synthesis" that comprises the formation of coordination bonds between cargo molecules and unsaturated metal sites or ligand defect sites of pre-synthesized MOF structures (*Reprinted with permission from* Wang et al. (2018a)), (**B**) Schematic representation of PDT/PTT cancer cotherapy as well as PA imaging based on NIR-stimulation of single atom iron centers in PMOF (a), 3D multispectral photoacoustic tomography (MSOT) image and enlarged orthogonal views of tumor after the injection of PBS (b), PMOF under 808 nm laser irradiation (c), Body weights of various mice groups after the therapy (d), Tumor growth curves under different treatments (Statistical analysis, $^{***}p < 0.001$), (e) and H&E-stained main organs and tumor slices obtained from different groups of mice following different therapies (f) (*Reprinted with permission from* Wang et al. (2019b)), (**C**) Fabrication process of H-ZIF-8/PDA-CD JNPs used in dual-drug chemotherapy and photothermal therapy (a, b), IR thermal images of tumor-bearing mice administrated with PBS and H-ZIF-8/PDA-CD JNPs under 808 nm laser irradiation (c), The body weight of mice (d), Tumor growth curves of mice (e), Digital images of mice and excised tumors in the groups with various treatments (f), The mean tumor weight and the tumor inhibition rate of each group on the last day of experiments (g), and H&E stained histological sections of major organs (Statistical significance: $^{**}p < 0.01$, $^{***}p < 0.001$) (h) (*Reprinted with permission from* Li et al. (2019b)), (**D**) Schematic of the H_2S-triggered transformation of non-photoactive HKUST-1 nanoenzyme into an NIR-activatable photothermal agent by in situ sulfidation reaction used for synergic photothermal and chemodynamic therapy for colon cancer (*Reprinted with permission from* Li et al. (2020))

crystalline materials turn them into potential candidates for photo-induced therapeutic purposes. MOFs can be either used as photosensitizers themselves or exploited as a carrier for exogenous photosensitizers due to their porous structure with high specific surface area. Since PSs have low water solubility and tend to aggregate easily as a result of their organic nature with high degree of conjugation, the encapsulation strategy assists in increasing their solubility, hence improving their cellular uptake. Last but not least, these nanoplatforms can be used for phototherapies in combination with the loading and release of chemotherapy drugs which will reduce the long-term morbidity (Boddula et al., 2020).

Hu et al. encapsulated different kinds of PSs (i.e., Ce6, TPEDC, and TPETCF) in MIL-100(Fe) as a general inert carrier (Hu et al., 2018). The encapsulation process blocked the photosensitizing capability of the aforementioned compounds as a result of their isolation from oxygen (O_2). After reaching the tumor site with excess H_2O_2 secretion, the framework collapsed and released the encapsulated PSs which led to recovered photosensitization and activated PDT. In addition, it was observed that in comparison to the original PSs, the recovered photosensitization underwent enhanced PDT due to the relieving of hypoxia by O_2 generated from the reaction between Fe (III) and H_2O_2. In another study conducted by Wang and coworkers, a multifunctional MOF-based hybrid nanogel was synthesized through in situ polymerization of dopamine monomers encapsulated in the pores of a MnCo MOF structure ($Mn_3[Co(CN)_6]_2$) and named as MCP nanoparticles (Wang et al., 2018b). Polydopamine (PDA) is found to be a promising PTT agent due to its NIR absorption. The prepared MCP nanoparticles were further modified with polyethylene glycol (PEG) in order to increase the in vivo stability, biocompatibility, and blood circulation time of MCP as well as with thiol terminal cyclic arginine-glycine-aspartic acid peptide to ensure the tumor accumulation of MCP-PEG nanoparticles and improve their therapeutic efficiency as photothermal agent. The resulting hybrid nanostructure could also have served as a positive T_1 MR contrast agent as well due to the high-spin Mn-N_6 ($S = 5/2$) in the skeleton of MnCo. The results revealed that the obtained nanocomposite offers numerous advantages over commonly explored photothermal agents including uniform size distribution, long-term solution stability, enhanced photothermal conversion efficiency, and higher tumor accumulation.

Dual photodynamic and photothermal (PDT/PTT) co-therapy is another way of exploiting the therapeutic potential of nMOFs. For instance, a porphyrin-like single atom Fe(III)-containing MOF (denoted as PMOF) was synthesized and evaluated for PDT/PTT co-therapy under NIR (808 nm) irradiation as well as for PA imaging (Fig. 8.5B-a) (Wang et al., 2019b). The prepared PMOF nanocrystals demonstrated not only excellent performance for modulation of the hypoxic tumor microenvironment of HeLa cell tumors in mice but also good properties as a photoacoustic imaging (PAI) agent which were attributed to the abundant single atom Fe(III) centers (as shown in Fig. 8.5B, b-f). The results of density functional theory (DFT) calculations revealed that this superior performance is related to the narrow HOMO-LUMO band gap energy of 1.31 eV which enabled strong absorption of NIR photons while irradiated and resulted in promoted PTT. Moreover, the presence of porphyrin-like Fe(III) nodes assists in generating singlet oxygen ($^1O_2$) from triplet one ($^3O_2$), hence

benefiting PDT. In another attempt, spherical zeolitic imidazolate framework-8/polydopamine Janus nanoparticles with hollow structure (H-ZIF-8/PDA JNPs) were first prepared through a mild synthesis strategy, and then, PDA chains were further functionalized with β-cyclodextrins (CDs) (Li et al., 2019b). The resultant composite was explored as a multifunctional platform for cancer treatment via synergistic dual-drug chemotherapy and PTT as schematically depicted in Fig. 8.5C-a, b. The obtained results can be attributed to the following characteristics: (i) CDs with hydrophobic cavities can encapsulate hydrophobic drug, while ZIF-8 can serve as reservoirs for loading hydrophilic drug molecules, (ii) strong NIR absorption of PDA chains results in high photothermal conversion capacity from laser energy to heat, (iii) H-ZIF-8/PDA-CD JNPs are featured with pH/NIR dual-responsive drug release behaviors due to the presence of pH-sensitive ZIF-8 nanoparticles, and (iv) the cytotoxicity tests as well as histological and biochemical blood assays all prove the high biocompatibility of the proposed hybrid nanostructure (Fig. 8.5C, c-h). Although this report was the first one to introduce the construction of MOF-polymer nanoparticles for synergetic dual-drug chemo- and photothermal therapy, it promised the potential of MOF-based hybrid materials for further therapeutic-imaging applications.

Recently, Li et al. have designed an endogenous H_2S-activated Cu-MOF (HKUST-1) nanoenzyme for synergic NIR PTT and chemodynamic therapy (CDT) for colon cancer treatment (Li et al., 2020). It has been long found that the dysregulated H_2S production from the catalysis process of overexpressed cystathionine β-synthase (CBS) can be utilized as a specific target for early diagnosis of some certain cancers such as colon and ovarian. Accordingly, the transformation of non-photoactive HKUST-1 nanoenzyme into an NIR-activatable copper sulfide which was triggered by endogenous H_2S species produced from in situ sulfidation reaction was adopted for construction of a smart theranostics nanoplatform for synergic colon cancer treatment.

As schematically illustrated in Fig. 8.5D, for photothermal therapy, an "ON-OFF" strategy was used therein in which the non-photoactive HKUST-1 nanoparticles are in their "OFF" state in normal tissues with no obvious adsorption within the NIR region. This is while near the microenvironment of colon tumor tissues they turned into "ON" state as a consequence of reacting with overexpressed endogenous H_2S and in situ production of photoactive CuS as a photothermal agent with stronger UV-Vis absorption. On the other hand, the prepared HKUST-1 nanoparticles are favorable for CDT due to their horseradish peroxidase (HRP)-mimicking activity which can provoke the effective conversion of overexpressed H_2O_2 within cancer cells into more toxic OH radicals.

Altogether, various strategies and approaches can be applied using MOF-based nanoarchitectures for the design and fabrication of smart therapeutic systems capable of targeting tumor sites and enhance the therapeutic efficacy while reducing the side effects.

8.3.3 Nanoscale MOFs for Cancer Theranostics

As mentioned previously, the design and fabrication of platforms which can potentially integrate therapeutic and diagnostic features in a single platform is of great significance. The versatility of MOFs and their high potential for multifunctionality have turned them swiftly into promising candidates for such theranostics applications. In this regard, theranostic MOFs have developed rapidly, and it is anticipated that these systems play an important role in personalized medicine in the near future. Advantages of nanoscale MOFs for tumor theranostics include desirable biocompatibility, high drug loading capacity, active tumor targeting, and image-guided smart drug delivery. Using these characteristics allows managing the treatment process through monitoring the biodistribution and accumulation of drugs, controlling their release and dose adjustment to patients (Lu et al., 2018; Wu & Yang, 2017).

For any biomedical investigation, in vivo toxicity is a key factor which should be taken into consideration. Accordingly, one of the main goals of developing theranostic nMOFs is to design a low-toxicity nanosystem in the body. To reach this goal, it is important to select appropriate metal centers and organic ligands that both show adequate biocompatibility. In 2015, Maspoch group found out a direct correlation between the in vitro cytotoxicity with that of in vivo toxicity of 16 representative uncoated nMOFs using powder X-ray diffraction and ICP-OES quantification of the corresponding metal ions in the solutions upon incubation at 37 °C (Ruyra et al., 2015). They systematically investigated the stability of nMOFs in the culture medium as well as their in vitro cytotoxicity to HepG2 and MCF7 cells along with their in vivo toxicity in zebrafish (*Danio rerio*) embryos. Their results revealed that certain MOFs including UiO-66 and UiO-67, MIL-100 and MIL-101, and ZIF-7 were mostly stable even after 24 h of incubation, while others such as ZIF-8 and some of MOF-74 nMOFs showed slight degradation; however their respective crystal structures remained unaltered. Some special nMOFs (i.e., MOF-5, HKUST-1, NOTT-100, and most of MOF-74 nMOFs) exhibited great degradation accompanied by a loss of crystallinity. Based on these findings, the authors suggested that the toxicity of nMOFs is strongly related to the toxicity of their metallic nodes and organic ligands which are released into the media upon the degradation of nMOFs. This is while numerous studies have demonstrated that metals such as Ca, Mg, Zn, Fe, Ti, or Zr have safe toxicity as estimated by oral lethal dose 50 (LD50) (Imaz et al., 2010).

Besides, in order to decrease the cytotoxicity and endow the biological compatibility to these porous materials, biological MOFs, also called "BioMOFs," can be utilized. BioMOFs are a class of metal-organic frameworks in which biomolecules such as amino acids, proteins, peptides, nucleobases, carbohydrates, cyclodextrins, and porphyrin (or metalloporphyrin) are used as bio-ligands instead of organic linkers (Imaz et al., 2011; Rojas et al., 2017; Cai et al., 2019).

In the following sections, the various nMOF systems used for theranostic purposes will be discussed in detail. For better understanding, nanoMOF theranostic systems were categorized into iron, zinc, copper, and manganese-based MOFs.

8.3.3.1 Iron-Based MOFs

Nontoxic iron (III) carboxylate metal-organic framework (Fig. 8.6A) is one of the promising subclass of nMOFs which has been widely explored in the theranostic field owing to their biocompatibility and high loading capacities. Moreover, their iron-based core with good relaxivity makes them applicable as a suitable magnetic resonance imaging contrast agent. These properties along with the potential of co-incorporating the therapeutic and diagnostic agents open up new opportunities for smoothing the way for theranostic purposes (Liu et al., 2020).

In 2009, amino-modified iron terephthalate MIL-101 nanoparticles were used to load an anticancer drug (i.e., ethoxysuccinato-cisplatin (ESCP) prodrug) and an organic fluorophore via covalent modifications of the as-prepared nanoparticles, then covered with silica shell to increase the stability as well as enhance the controlled-release property. The adopted post-synthetic modification strategy of highly porous nMOFs provided a platform for optical imaging and anticancer therapy to obtain theranostic purposes (Taylor-Pashow et al., 2009). Horcajada et al. investigated the efficiency of various MIL MOF nanoparticles synthesized through green chemistry (in aqueous or ethanolic solutions) as nontoxic and biocompatible drug nanocarriers (Horcajada et al., 2010). For this purpose, porous MILs with engineered cores and surfaces were loaded with different anticancer or antiviral drugs, namely, busulfan (Bu), azidothymidine triphosphate (AZT-TP), cidofovir (CDV), and doxorubicin (DOX). The results revealed that the prepared nanoMOFs act as remarkable *molecular sponges* capable of encapsulating drugs with different polarities, sizes, and functional groups through simple immersion in the corresponding solutions. Furthermore, they came up with good magnetic resonance imaging properties due to the presence of paramagnetic iron atoms with good relaxivities in their matrix. Another work displayed a functionalized MOF through post-synthetic modification designed for cancer cell imaging and dual chemo-photodynamic therapy (Liu et al., 2017). Camptothecin drug was encapsulated into iron(iii) carboxylate MOFs (NH_2-MIL-101(Fe)) and then integrated with folic acid as targeting moiety as well as chlorine e6-labeled peptide (Ce6-peptide) as a diagnostic agent. The detachment of Ce6-peptide from the MOF surface as a result of its specific cleavage reaction with intracellular cathepsin B (CaB) recovered the fluorescence of Ce6. This CaB-activable fluorescence property was used as a signal switch for imaging applications, while combining Ce6 as the photosensitizer with the camptothecin drug made it operational for chemo-photodynamic dual therapy. Likewise, MIL-88B nanoparticles were loaded with curcumin (Cur) as a hydrophobic anticancer drug followed by coating with folic acid-chitosan conjugate (FC) on the surface of the carrier via electrostatic interactions to attain smart targeted cancer therapy properties (Dehghani et al., 2020). The prepared multifunctional MIL-Cur@FC nanoparticle exhibited simultaneous noninvasive cancer diagnosis with enhanced dual contrast T_1- and T_2-weighted MR imaging features owing to its pH-responsive MRI characteristic due to the degradation of framework in the mild acidic microenvironment of tumor as well as efficient cancer treatment properties through efficient intracellular anticancer drug delivery.

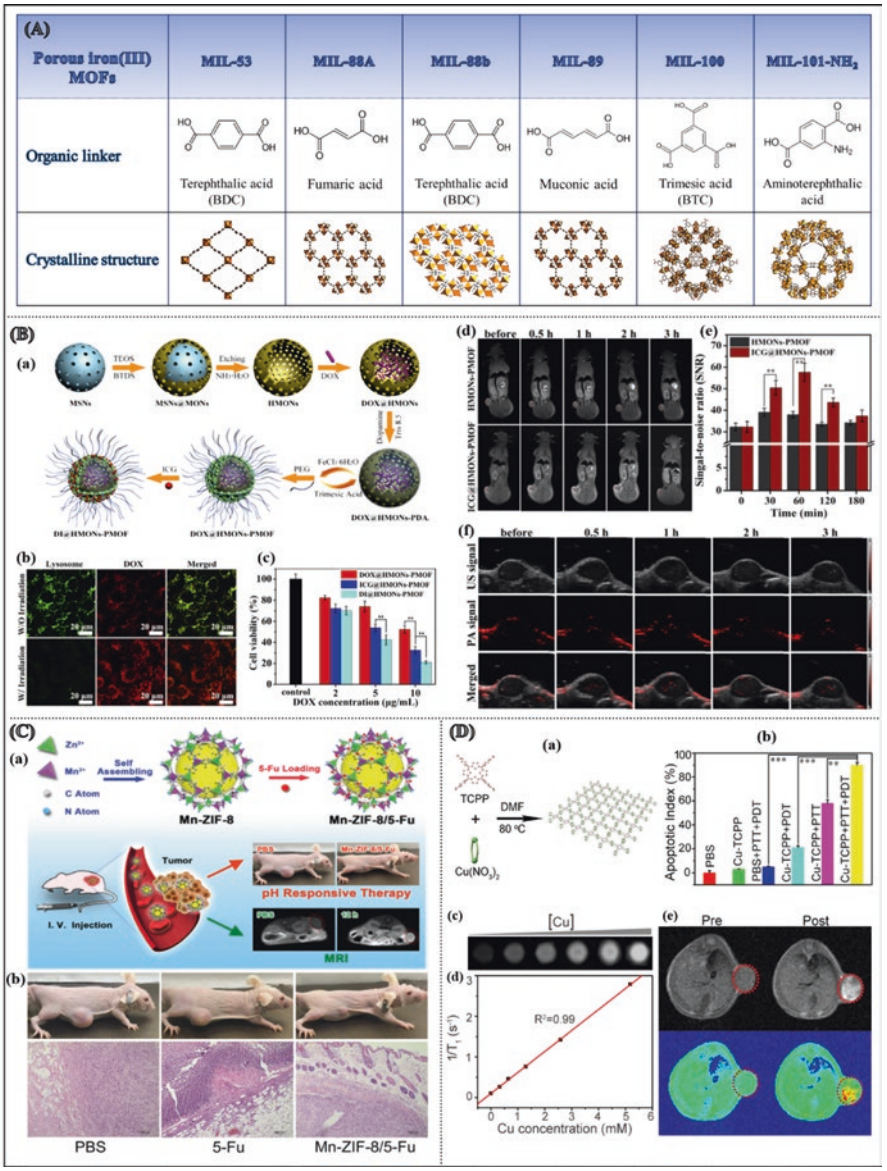

Fig. 8.6 Theranostic MOF nanoplatforms used for imaging-guided cancer therapy; (**A**) Structural description of MIL family composed of iron (III) metal nodes, (**B**) Schematic representation of general procedure of fabricating dual drug-loaded HMONs-PMOF nanoplatform (a), The CLSM images of lysosome-stained 4T1 cells exposed to DI@HMONs-PMOF for 2 h with or without laser irradiation (b), Cell viability of 4T1 cells subjected to chemotherapy and PT therapy alone and the combination therapy (c), MR images (d) and the corresponding signal-to-noise value of tumor-bearing mice at different time intervals of HMONs-PMOF and ICG@HMONs-PMOF post-injection (e), PA images at the tumor site obtained from the tumor-bearing mice in different time intervals of post-injection of ICG@HMONs-PMOF (f) (*Reprinted with permission from* Chen

(continued)

et al. (2019c)), (**C**) Synthetic procedure of Mn-ZIF-8/5-Fu with the application in targeted therapy and MR imaging for glioma (a), H&E staining sections of tumor tissues 14 days after treatment (*Reprinted with permission from* Pan et al. (2019)), (**D**) Schematic illustration of the synthesis process of Cu-TCPP MOF (a), Cancer cell apoptosis after treatment with Cu-TCPP MOF nanosheets (P values: $***p < 0.001$, $**p < 0.01$, or $*p < 0.05$) (b), In vitro T_1-weighted MR images of the Cu-TCPP MOF nanosheets with different concentrations (c) and the corresponding plots of the $1/T_1$ value of the Cu-TCPP MOF nanosheets as a function of concentration (d), *In vivo* T_1-weighted MR views of a mouse before and after intra-tumoral injection of the Cu-TCPP MOF nanosheets solution (e) (*Reprinted with permission from* Li et al. (2018c))

Additionally, the integration of metal-organic frameworks with other functional nanomaterials has resulted in nanoformulations with superior properties and synergistic performance which is not available from any of these nanostructures alone. In this regard, a well-defined hollow structure was formed by successful merging of MOF(Fe) with hollow mesoporous organosilica nanoparticles (HMONs) using a thin layer of polydopamine (PDA) (Chen et al., 2019c). The resulting molecularly organic/inorganic hybridized nanocomposite (HMONs-PMOF) with extraordinary loading capacity (resulted from large cavity of HMONs along with highly porous network of metal-organic framework) was exploited as a nanocontainer inside which the doxorubicin hydrochloride (DOX) drug was loaded. In the meantime, indocyanine green (ICG) with the ability of cooperatively enhancing the MR imaging capability was bound to the outer porous shell of MOF with high loading efficacy. The fabrication process of the dual drug-loaded nanocomposite (DI@HMONs-PMOF) is schematically shown in Fig. 8.6B-a. The killing efficacy of DI@HMONs-PMOF nanocomposite toward cancer cells arose from not only the presence of the chemotherapeutic drug (DOX) that exhibited a pH/NIR laser dual-responsive intracellular release behavior but also the incorporated ICG which provided reasonable photothermal effect and photostability. Moreover, the prepared nanoarchitecture revealed desirable magnetic resonance (MR) and photoacoustic (PA) dual-modality imaging properties benefited from the coordination interaction of iron ions and PDA interlayer as MRI contrast agent as well as the ICG shell with PA imaging capability. Hence, simultaneous chemo-photothermal combination therapy and MR/PA dual-modality imaging were realized with the aid of the prepared nanoplatform with favorable biocompatibility (Fig. 8.6B, b-f).

Conducting polymer-MOF composite/hybrid nanostructures are another intriguing option for nanotheranostic applications. For instance, Zhu and coworkers have proposed a core-shell structure composed of uniform polypyrrole (PPy) nanoparticles with adequate biodegradability as core covered with a mesoporous MIL-100 shell (Zhu et al., 2016). The PPy@MIL-100 composite showed synergistically enhanced therapeutic efficacy by the combination of chemotherapy and PTT. The results were attributed to the high loading capacity of porous MIL shell as DOX drug nanocarrier which exhibited a pH-controlled drug release behavior as well as the role of PPy core as an organic photothermal agent under NIR irradiation.

In another research work, PPy@MIL-53 nanocomposite was prepared through in situ growth of PPy nanoparticles inside MIL-53 MOF as a microreactor in which Fe^{3+} ions played the role of an intrinsic oxidizing agent for polymerizing pyrrole

monomers to PPy nanoparticles (Huang et al., 2018). PPy@MIL-53 nanocomposite integrated the intrinsic photothermal therapy (PTT) of PPy nanoparticles with MR imaging ability of Fe^{3+}. As a consequence, the prepared nanocomposite presented in vitro and in vivo tools for MRI-guided photothermal therapy of cancer. The integration of diagnostic and therapeutic agents was also observed in the core-shell structure of PB@MIL-100(Fe) dual MOFs nanoparticles (dMOFs) (Wang et al., 2016). dMOFs were prepared by layer-by-layer deposition of MIL-100(Fe) MOF shell on the surface of Prussian blue nanocubes and were shown to be useful as a T_1-T_2 dual-modal MRI and fluorescence optical imaging agent. The inner PB core was advantageous for imaging and phototherapy due to strong absorbance in the NIR region, while the porous MOF shell provided great potential for targeted intracellular artemisinin drug delivery as a result of its pH-responsive degradation nature in the acidic pH of lysosomes in the tumor microenvironment.

8.3.3.2 Zinc-Based MOFs

ZIF-8 nanoparticles which are composed of Zn^{2+} ions and 2-methylimidazole (2-MIm) ligands are among the most widely used metal-organic frameworks due to their ease of synthesis via a wide range of methods, excellent in vivo stability and structural robustness, pH responsiveness, as well as high porosity. In this regard, numerous studies have focused on the use of ZIF-8 hybrid nanomaterials for cancer theranostics (He et al., 2014; Li et al., 2018b; Pan et al., 2019; Zhu et al., 2019a; Chowdhuri et al., 2016; Zhu et al., 2019b; Nejadshafiee et al., 2019). He et al. utilized encapsulated fluorescent carbon nanodots (C-dots) in porous ZIF-8 nanoparticles (C-dots@ZIF-8) as a platform for simultaneous pH-responsive anticancer drug delivery and cell fluorescence imaging (He et al., 2014). The encapsulated C-dots, as a new class of nanocarbons which present strong fluorescence intensity, paved the way for fluorescence imaging of cancer cells, while ZIF-8 porous network was exploited as a potential carrier for the loading of 5-fluorouracil (5-Fu) as a representative anticancer drug. In another study, Cy@ZIF-8 nanoparticles were obtained by loading cyanine (Cy) as a NIR-active dye into the zeolitic imidazolate framework-8, and the resulting nanoparticles were used for NIR imaging-guided photothermal therapy (Li et al., 2018b). Cy@ZIF-8 nanoparticles showed notable cytotoxicity toward cancer cells under a specific wavelength of laser with an increase of Cy concentration. Moreover, in order to assess the antitumor efficacy of the system, NIR fluorescence imaging was performed using calcein AM and propidium iodide. The results demonstrated that Cy@ZIF-8 nanoparticles were mostly located in the tumor and liver. Altogether, the prepared Cy@ZIF-8 composite demonstrated NIR absorbance, photothermal transformation, and NIR imaging capability which made it suitable for theranostic applications.

Determination of tumor uptake and diagnosis of glioma rely on the MRI results as a recognition method for detecting tumor anatomical details with high quality. In a research conducted by Pan and coworkers, the bimetallic zeolitic imidazolate framework (Mn-ZIF-8) was used as a drug delivery system of 5-Fu and applied for

the first time for in vivo magnetic resonance imaging (Pan et al., 2019). As schematically illustrated in Fig. 8.6C-a, the synthesized Mn-ZIF-8/5-Fu nanoparticles were served as a multifunctional theranostic nanomedical platform which combined the MR imaging capability of accumulated Mn^{2+} in the tumor sites, ultrahigh antiglioma drug loading into ZIF-8 nanoparticles with high specific surface area, and pH-responsive drug release in a single system. The hematoxylin and eosin (H&E) staining sections of tumor tissues obtaining 14 days after treatment are shown in Fig. 8.6C-b. As can be seen, excellent therapeutic effects and prolonged survival time was obtained for the Mn-ZIF-8/5-Fu group. These observations were attributed to the augmented drug concentrations in the tumors as a result of longer circulation time of blood with higher concentration of drug. Another ZIF-8 multifunctional MOF with the composition of DOX/Pd@ZIF-8 was also constructed as a theranostic nanoplatform (Zhu et al., 2019a). The fabricated nanosystem indicated photothermal and optoacoustic effects due to the high NIR absorption of Pd nanoparticles loaded into MOFs. Also, DOX showed a pH-dependent release that enabled successful chemotherapy.

Zn-based nMOFs other than ZIF-8 were also investigated for theranostic applications. As an example, magnetic Fe_3O_4@IRMOF-3 nanostructures were fabricated by the incorporation of Fe_3O_4 nanoparticles into isoreticular metal organic frameworks (IRMOF-3) and used as the first targeted magnetic nMOFs for the delivery of hydrophobic drugs and MR imaging (Chowdhuri et al., 2016). Fe_3O_4 is a T_2 contrast agent for magnetic resonance imaging. Furthermore, rhodamine B isothiocyanate (RITC) was conjugated to the nMOFs as the fluorescent agent for biomedical imaging. As an anticancer drug, paclitaxel was incorporated into the prepared nanocarriers with high loading capacity. Finally, folic acid was conjugated to the surface of nMOFs to obtain a targeted drug delivery system. Two-dimensional nMOFs with much larger surface area compared to their particulate counterparts are another emerging class of MOFs with attractive features for theranostic purposes. For instance, 2D nanosheets based on Zn^{2+} metal centers and tetrakis (4-carboxyphenyl) porphyrin (TCPP) organic linkers were synthesized and further functionalized with polyethylene glycol (PEG) (Zhu et al., 2019b). The Zn-TCPP@PEG nanoparticles not only exhibited enhanced photodynamic therapeutic effect due to the more efficient light-triggered singlet oxygen production but also showed higher drug loading capacity for DOX chemotherapy drugs as a result of their sheet structure. The porphyrin structure of TCPP made it possible for the 2D nMOFs to be labeled with ^{99m}Tc as a diagnostic radioisotope and consequently used for single photon emission computed tomography (SPECT) imaging. It is noteworthy to mention that the prepared nanosheets showed efficient antitumor chemo-PDT effect with low biotoxicity which results from their rapid renal clearance. Similarly, another magnetic metal-organic framework, namely, Fe_3O_4@Bio-MOF, which was coated with folic acid and conjugated with chitosan (FC) was also reported for delivery of curcumin (Cur) and 5-fluorouracil (5-FU) in cancer targeted therapy (Nejadshafiee et al., 2019). In this study, MOF nanocarriers loaded by anticancer drugs demonstrated high toxicity against the cancer cells. MRI investigations indicated negative signal improvement in the in vitro and in vivo tumor studies, which revealed the capability

of using the nanoparticles as a diagnostic agent. Accordingly, the performance of these nanocarriers in T_2 MRI and their cytotoxicity effect on cancer cells proved the potential of these nMOFs as promising agents in cancer theranostics.

8.3.3.3 Cu- and Mn-Based MOFs

Cu-containing MOFs have attracted a great deal of attention during the past few years due to their inherent properties: (i) Cu^{2+} sites show strong binding attraction to some anions such as S^{2-} which present in high concentration in some certain cancer as a result of high overexpression of H_2S in the tumor microenvironment, (ii) Cu-MOFs are convenient for chemodynamic therapy (CDT) since they exhibit peroxidase-mimicking activity which can catalyze the formation of toxic hydroxyl radicals (•OH) from H_2O_2 secreted by cancer cells, and (iii) compared to Fe^{2+}, the Cu^{2+}/Cu^{+} pair has lower redox potential (~0.16 eV) and, as a result, offers higher catalytic activity as Fenton agents (Li et al., 2020; Ma et al., 2018; Zhang et al., 2018b; Ke et al., 2011; Li et al., 2018c). HKUST-1 MOF, which is composed of dimeric copper metal units connected by benzene-1,3,5-tricarboxylate (BTC) linker molecules, is an example of appropriate nMOFs for theranostics purposes (Li et al., 2020; Ke et al., 2011). In 2011, a magnetic Cu-based MOF composite was prepared via incorporation of Fe_3O_4 nanorods with nanocrystals of HKUST-1 (Fe_3O_4/$Cu_3(BTC)_2$) and was further investigated for targeted delivery of nimesulide (NIM) as an anticancer drug for pancreatic cancer treatment along with MR imaging (Ke et al., 2011). The prepared three-dimensional MOF with a 3D channel system showed high loading capacity (up to 0.2 g of NIM) due to its extraordinary porosity as well as prolonged release duration of as long as 11 days in physiological saline at 37 °C. This theranostic nanoplatform was one of the very first examples of MOF materials for targeted drug delivery goals.

Copper-tetrakis (4-carboxyphenyl) porphyrin (Cu-TCPP) nanosheet (Fig. 8.6D-a) is another example which not only exhibited strong NIR absorption and capability for magnetic resonance imaging as a result of copper centers but also showed synergistic effect of photothermal and photodynamic therapy due to the presence of TCCP with the ability of producing singlet oxygen (SO) as a characteristic photosensitizer (Li et al., 2018c). Two-dimensional (2D) nanosheets demonstrated better photothermal effect than bulk materials because of more rapid response to light. As can be seen in Fig. 8.6D-b which shows the cancer cell apoptosis, the cell mortality rates for the Cu-TCPP under PDT and the Cu-TCPP group under PTT were ~21% and ~58%, respectively. This is while for the cells treated with Cu-TCPP MOF under PD/PTT condition, the cell mortality demonstrated a remarkable increase up to ~90%. The obtained combination index (CI) of 0.778 revealed the synergetic PDT/PTT effect which is originated from the photosensitizing effect of TCPP capable of generating toxic singlet oxygen for PDT plus the ability of converting light energy into heat under NIR irradiation for PTT that cause hyperthermia in the tumor environment. In addition, these nanosheets showed T_1-weighted MR imaging ability due to the unpaired 3D electrons in copper. The in vitro and in vivo MR images are

shown in Fig. 8.6D, c-e which illustrate a sharp color contrast after injection of MOF nanosheets compared with that of before injection. The obtained results confirmed that ultrathin Cu-TCPP MOF nanosheets could be utilized as a theranostic agent for imaging and phototherapy of cancer.

Mn-based nMOFs present another interesting nanoplatforms for bioimaging implementations due to the ability of Mn^{2+} ions as an efficient T_1-weighted contrast agent when binding to intracellular proteins (Wang et al., 2018b; Liu et al., 2014b; Zhao et al., 2017). Theranostic features were observed in a multifunctional Mn-containing nanoscale coordination polymer as a result of high capacity for loading an anticancer agent (zoledronate) along with the presence of Mn^{2+} centers as MRI contrast agent (Liu et al., 2014b). Surface pegylation followed by functionalization with anisamide as a targeting group was adopted to control the kinetics of the drug release and to endow the specificity to cancer cells, respectively. The results demonstrated the ability of the as-prepared Mn-bisphosphonate particles with physiological stability and biocompatibility for imaging-guided targeted cancer therapy. Intelligent and logical design of nMOF structures is a key parameter in obtaining the desired results. As an example, a redox-sensitive MOF was synthesized from Mn^{2+} nodes and dithiodiglycolic acid as the disulfide (SS)-containing organic ligand (Zhao et al., 2017). The yielded nanoparticles were loaded with DOX and then coated with a PDA layer. In such a redox-active structure, the release of drug can be triggered by the cleavage of disulfide bonds (S-S) within dithiodiglycolic acid in the presence of excessive glutathione (GSH) and the subsequent decomposition of MOF. This is while the manganese centers offer a strong T_1 contrast in MRI. Similar strategies can be adopted for constructing various stimuli-responsive theranostic nanoplatforms susceptible to different exogenous and/or endogenous environmental stimuli such as pH, reactive oxygen species, and even light and temperature.

8.3.3.4 Other MOFs

Apart from the aforementioned transition metals which were widely used in the construction of theranostic nMOFs, certain frameworks with unusual metallic centers were also reported (Zhang et al., 2018a; Meng et al., 2020; Rowe et al., 2009).

A novel biocompatible MOF composed of UiO-66 (Zr) with carboxylic acid (COOH) groups was incorporated with Mn^{2+} and doxorubicin as diagnostic and therapeutic compounds, respectively (Meng et al., 2020). The prepared multifunctional MOF-based nanosystem showed promoted T_1-weighted relaxivity and pH-responsive drug release. The simultaneous incorporation of diagnosis and therapeutic agents led into a platform with the ability of tracing the accumulation of nanoparticles, assisted in diagnosis, allowing evaluation of therapy through magnetic resonance imaging along with eradicating tumor cells by the aid of doxorubicin. Mn^{2+}-DOX@MOF showed significant dose-dependent cytotoxicity for breast cancer and demonstrated high survival rate for lung metastasis as well. The MR images exhibited high sensitivity of Mn^{2+}-DOX@MOF in probing tumors and the potential for tumor detection of the fabricated nanocarrier.

As another MOFs for theranostic applications, polymer-modified Gd(III) nMOFs were introduced as a multifunctional device (Rowe et al., 2009). In this research, the surface of Gd MOF nanoparticles was modified for the first time with biocompatible polymers. These nMOFs were loaded with anticancer drug methotrexate (MTX) and then functionalized with a fluorescent dye and targeting peptide. The modified nMOFs exhibited bimodal imaging ability (fluorescence and MRI). The incorporation of FMA (fluorescein-O-methacrylate) into the backbone of the copolymer allowed the cellular level imaging via fluorescence microscopy. On the other hand, the Gd centers acted as a contrast agent for MRI. These two features could provide diagnostic imaging at the clinical level accompanied by treatment through MTX.

Furthermore, MOFs could be also used in X-ray computed tomography imaging as mentioned previously. For example, Yb-MOFs-Glu with 3-dicarboxylic acid (BBDC) as ligand and glucose as a biocompatibility enhancer provided a platform for CT imaging. Yb is an element with a high molecular weight that exhibited X-ray attenuation. Thus, DOX@Yb-MOFs-Glu indicated great potential for chemotherapy and CT imaging and represented theranostic capability (Zhang et al., 2018a).

8.4 Future Perspectives and Conclusion

Since their discovery in 1989, MOFs have attracted a great deal of attention not only as a result of their versatile molecular architectures and topologies but also due to their wide range of applications. Compared to advanced composites and hybrid materials, MOFs present both properties of being prepared in a single step via various strategies and by simply mixing the components as well as the ability of tuning the structural features through controlling the reaction conditions (i.e., temperature, solvent polarity, pressure, the presence of additives, the concentration of metal salts/organic linkers, and their ratio). Furthermore, a wide variety of secondary building units (SBUs) and on-demand synthesized organic linkers can be introduced to provide the scientific community with infinite properties. Therefore, the past few years have witnessed an increasing development in the exploitation of MOFs for diverse applications including bioimaging, drug delivery, and diagnosis purposes. Their beneficial characteristics such as tunable porosity, ease of surface modification, biocompatibility, biodegradability, bioavailability, high drug loading capacity, and controlled release manner have paved the way for their utilization in cancer theranostics which potentially integrate therapeutic and diagnostic features in a single platform. In this regard, MOFs are considered as promising nanomedical systems for cancer theranostic applications in order to achieve a faster diagnosis and more efficient treatment of cancer. As a result, theranostic nanoMOFs have developed rapidly, and it is expected that these systems play a vital role in personalized medicine in the near future. However, there are limitations such as low selectivity and high cost of certain organic ligands that should be considered to improve the efficacy of MOFs as theranostic platforms. The in vitro and in vivo stability of nanoMOFs against degradation and aggregation stay still challenging and need to be investigated. Their

degradation behavior, the toxicity of the components, as well as the possible elimination roots from the body should be well identified for their further development as theranostic systems. New MOFs can be engineered for biomedical applications by gaining in-depth knowledge on their degradation behavior in biological fluids. For MOFs to be applied in real biomedicine and clinical use, their biodistribution, efficacy, health risks, in vitro/in vivo biosafety, and environmental issues have to be investigated in more detail. More emphasis should be paid on the optimization and design of safe and stable multifunctional stimuli-responsive nanoMOFs based on green, environmentally friendly, and energy-efficient approaches with demonstration of sufficient biodegradability and biocompatibility of the as-prepared nanoparticles. Although there exists many challenges and further progress is still needed for practical applications, MOFs are still attractive candidates with a bright future and promising capabilities in various fields owing to their outstanding properties. Hence, it is anticipated that an increasing number of researches will appear in the near future exploiting the full potential of nanoMOFs in various biomedical fields.

References

Abdollahi, N., Masoomi, M. Y., Morsali, A., Junk, P. C., & Wang, J. (2018). Sonochemical synthesis and structural characterization of a new Zn (II) nanoplate metal-organic framework with removal efficiency of Sudan red and Congo red. *Ultrasonics Sonochemistry, 45*, 50–56.

Al Amery, N., Abid, H. R., Al-Saadi, S., Wang, S., & Liu, S. (2020). Facile directions for synthesis, modification and activation of MOFs. *Materials Today Chemistry, 17*, 100343.

Alexis, F., Pridgen, E., Molnar, L. K., & Farokhzad, O. C. (2008). Factors affecting the clearance and biodistribution of polymeric nanoparticles. *Molecular Pharmaceutics, 5*(4), 505–515.

Al-Kutubi, H., Gascon, J., Sudhölter, E. J., & Rassaei, L. (2015). Electrosynthesis of metal-organic frameworks: Challenges and opportunities. *ChemElectroChem, 2*(4), 462–474.

Amini, A., Kazemi, S., & Safarifard, V. (2020). Metal-organic framework-based nanocomposites for sensing applications – A review. *Polyhedron, 177*, 114260.

Armstrong, M. R., Senthilnathan, S., Balzer, C. J., Shan, B., Chen, L., & Mu, B. (2017). Particle size studies to reveal crystallization mechanisms of the metal organic framework HKUST-1 during sonochemical synthesis. *Ultrasonics Sonochemistry, 34*, 365–370.

Asadian, E., Shahrokhian, S., & Zad, A. I. (2020). ZIF-8/PEDOT@flexible carbon cloth electrode as highly efficient electrocatalyst for oxygen reduction reaction. *International Journal of Hydrogen Energy, 45*(3), 1890–1900.

Babu, R., Roshan, R., Kathalikkattil, A. C., Kim, D. W., & Park, D. W. (2016). Rapid, microwave-assisted synthesis of cubic, three-dimensional, highly porous MOF-205 for room temperature CO_2 fixation via cyclic carbonate synthesis. *ACS Applied Materials & Interfaces, 8*(49), 33723–33731.

Biswal, B. P., Chandra, S., Kandambeth, S., Lukose, B., Heine, T., & Banerjee, R. (2013). Mechanochemical synthesis of chemically stable isoreticular covalent organic frameworks. *Journal of the American Chemical Society, 135*(14), 5328–5331.

Boddula, R., Ahamed, M. I., & Asiri, A. M. (Eds.). (2020). *Applications of metal-organic frameworks and their derived materials*. John Wiley & Sons.

Cai, W., Chu, C. C., Liu, G., & Wáng, Y. X. J. (2015). Metal-organic framework-based nanomedicine platforms for drug delivery and molecular imaging. *Small, 11*(37), 4806–4822.

Cai, W., Gao, H., Chu, C., Wang, X., Wang, J., Zhang, P., Lin, G., Li, W., Liu, G., & Chen, X. (2017). Engineering photo-theranostic nanoscale metal-organic frameworks for multimodal imaging-guided cancer therapy. *ACS Applied Materials & Interfaces, 9*(3), 2040–2051.

Cai, H., Huang, Y. L., & Li, D. (2019). Biological metal-organic frameworks: Structures, host–guest chemistry and bio-applications. *Coordination Chemistry Reviews, 378*, 207–221.

Campagnol, N., Van Assche, T. R., Li, M., Stappers, L., Dincă, M., Denayer, J. F., Binnemans, K., De Vos, D. E., & Fransaer, J. (2016). On the electrochemical deposition of metal-organic frameworks. *Journal of Materials Chemistry A, 4*(10), 3914–3925.

Cao, X., Zheng, B., Rui, X., Shi, W., Yan, Q., & Zhang, H. (2014). Metal oxide-coated three-dimensional graphene prepared by the use of metal–organic frameworks as precursors. *Angewandte Chemie International Edition, 53*(5), 1404–1409.

Cao, J., Li, X., & Tian, H. (2020). Metal-organic framework (MOF)-based drug delivery. *Current Medicinal Chemistry, 27*(35), 5949–5969.

Chalati, T., Horcajada, P., Gref, R., Couvreur, P., & Serre, C. (2011). Optimization of the synthesis of MOF nanoparticles made of flexible porous iron fumarate MIL-88A. *Journal of Materials Chemistry, 21*(7), 2220–2227.

Chen, D., Yang, D., Dougherty, C. A., Lu, W., Wu, H., He, X., Cai, T., Van Dort, M. E., Ross, B. D., & Hong, H. (2017). In vivo targeting and positron emission tomography imaging of tumor with intrinsically radioactive metal-organic frameworks nanomaterials. *ACS Nano, 11*(4), 4315–4327.

Chen, C., Feng, X., Zhu, Q., Dong, R., Yang, R., Cheng, Y., & He, C. (2019a). Microwave-assisted rapid synthesis of well-shaped MOF-74 (Ni) for CO_2 efficient capture. *Inorganic Chemistry, 58*(4), 2717–2728.

Chen, D., Zhao, J., Zhang, P., & Dai, S. (2019b). Mechanochemical synthesis of metal-organic frameworks. *Polyhedron, 162*, 59–64.

Chen, L., Zhang, J., Zhou, X., Yang, S., Zhang, Q., Wang, W., You, Z., Peng, C., & He, C. (2019c). Merging metal organic framework with hollow organosilica nanoparticles as a versatile nano-platform for cancer theranostics. *Acta Biomaterialia, 86*, 406–415.

Chen, L., Zhang, X., Cheng, X., Xie, Z., Kuang, Q., & Zheng, L. (2020). The function of metal-organic frameworks in the application of MOF-based composites. *Nanoscale Advances, 2*, 2628–2647.

Cheng, X., Zhang, A., Hou, K., Liu, M., Wang, Y., Song, C., Zhang, G., & Guo, X. (2013). Size- and morphology-controlled NH_2-MIL-53 (Al) prepared in DMF-water mixed solvents. *Dalton Transactions, 42*(37), 13698–13705.

Cheng, G., Li, W., Ha, L., Han, X., Hao, S., Wan, Y., Wang, Z., Dong, F., Zou, X., Mao, Y., & Zheng, S. Y. (2018). Self-assembly of extracellular vesicle-like metal-organic framework nanoparticles for protection and intracellular delivery of biofunctional proteins. *Journal of the American Chemical Society, 140*(23), 7282–7291.

Cho, K., Wang, X. U., Nie, S., & Shin, D. M. (2008). Therapeutic nanoparticles for drug delivery in cancer. *Clinical Cancer Research, 14*(5), 1310–1316.

Cho, H. Y., Yang, D. A., Kim, J., Jeong, S. Y., & Ahn, W. S. (2012). CO_2 adsorption and catalytic application of Co-MOF-74 synthesized by microwave heating. *Catalysis Today, 185*(1), 35–40.

Cho, H. Y., Kim, J., Kim, S. N., & Ahn, W. S. (2013). High yield 1-L scale synthesis of ZIF-8 via a sonochemical route. *Microporous and Mesoporous Materials, 169*, 180–184.

Choi, H. S., & Frangioni, J. V. (2010). Nanoparticles for biomedical imaging: Fundamentals of clinical translation. *Molecular Imaging, 9*(6), 7290–2010.

Choi, J. S., Son, W. J., Kim, J., & Ahn, W. S. (2008). Metal-organic framework MOF-5 prepared by microwave heating: Factors to be considered. *Microporous and Mesoporous Materials, 116*(1–3), 727–731.

Chowdhuri, A. R., Bhattacharya, D., & Sahu, S. K. (2016). Magnetic nanoscale metal organic frameworks for potential targeted anticancer drug delivery, imaging and as an MRI contrast agent. *Dalton Transactions, 45*(7), 2963–2973.

Dadfar, S. M., Roemhild, K., Drude, N. I., von Stillfried, S., Knüchel, R., Kiessling, F., & Lammers, T. (2019). Iron oxide nanoparticles: Diagnostic, therapeutic and theranostic applications. *Advanced Drug Delivery Reviews, 138*, 302–325.

Dastbaz, A., Karimi-Sabet, J., & Moosavian, M. A. (2019). Sonochemical synthesis of novel decorated graphene nanosheets with amine functional Cu-terephthalate MOF for hydrogen adsorption: Effect of ultrasound and graphene content. *International Journal of Hydrogen Energy, 44*(48), 26444–26458.

Dehghani, S., Hosseini, M., Haghgoo, S., Changizi, V., Akbari Javar, H., Khoobi, M., & Riahi Alam, N. (2020). Multifunctional MIL-Cur@FC as a theranostic agent for magnetic resonance imaging and targeting drug delivery: In vitro and in vivo study. *Journal of Drug Targeting, 28*(6), 668–680.

Della Rocca, J., Liu, D., & Lin, W. (2011). Nanoscale metal-organic frameworks for biomedical imaging and drug delivery. *Accounts of Chemical Research, 44*(10), 957–968.

Deng, J., Wang, K., Wang, M., Yu, P., & Mao, L. (2017). Mitochondria targeted nanoscale zeolitic imidazole framework-90 for ATP imaging in live cells. *Journal of the American Chemical Society, 139*(16), 5877–5882.

Dey, C., Kundu, T., Biswal, B. P., Mallick, A., & Banerjee, R. (2014). Crystalline metal-organic frameworks (MOFs): Synthesis, structure and function. *Acta Crystallographica Section B: Structural Science, Crystal Engineering and Materials, 70*(1), 3–10.

Dhainaut, J., Bonneau, M., Ueoka, R., Kanamori, K., & Furukawa, S. (2020). Formulation of metal-organic framework inks for the 3D printing of robust microporous solids toward high-pressure gas storage and separation. *ACS Applied Materials & Interfaces, 12*(9), 10983–10992.

Dolgopolova, E. A., Rice, A. M., Martin, C. R., & Shustova, N. B. (2018). Photochemistry and photophysics of MOFs: Steps towards MOF-based sensing enhancements. *Chemical Society Reviews, 47*(13), 4710–4728.

Dolmans, D. E., Fukumura, D., & Jain, R. K. (2003). Photodynamic therapy for cancer. *Nature Reviews Cancer, 3*(5), 380–387.

Doughty, A. C., Hoover, A. R., Layton, E., Murray, C. K., Howard, E. W., & Chen, W. R. (2019). Nanomaterial applications in photothermal therapy for cancer. *Materials, 12*(5), 779.

Esrafili, L., Tehrani, A. A., Morsali, A., Carlucci, L., & Proserpio, D. M. (2019). Ultrasound and solvothermal synthesis of a new urea-based metal-organic framework as a precursor for fabrication of cadmium (II) oxide nanostructures. *Inorganica Chimica Acta, 484*, 386–393.

Flügel, E. A., Ranft, A., Haase, F., & Lotsch, B. V. (2012). Synthetic routes toward MOF nanomorphologies. *Journal of Materials Chemistry, 22*(20), 10119–10133.

Gharatape, A., & Salehi, R. (2017). Recent progress in theranostic applications of hybrid gold nanoparticles. *European Journal of Medicinal Chemistry, 138*, 221–233.

Guan, Q., Li, Y. A., Li, W. Y., & Dong, Y. B. (2018). Photodynamic therapy based on nanoscale metal-organic frameworks: From material design to cancer nanotherapeutics. *Chemistry–An Asian Journal, 13*(21), 3122–3149.

Gul, S., Khan, S. B., Rehman, I. U., Khan, M. A., & Khan, M. I. (2019). A comprehensive review of magnetic nanomaterials modern day theranostics. *Frontiers in Materials, 6*, 179.

Guo, J., Rahme, K., He, Y., Li, L. L., Holmes, J. D., & O'Driscoll, C. M. (2017). Gold nanoparticles enlighten the future of cancer theranostics. *International Journal of Nanomedicine, 12*, 6131.

Gupta, N., Rai, D. B., Jangid, A. K., & Kulhari, H. (2019). A review of theranostics applications and toxicities of carbon nanomaterials. *Current Drug Metabolism, 20*(6), 506–532.

Han, X., Xu, K., Taratula, O., & Farsad, K. (2019). Applications of nanoparticles in biomedical imaging. *Nanoscale, 11*(3), 799–819.

Haque, E., Khan, N. A., Park, J. H., & Jhung, S. H. (2010). Synthesis of a metal-organic framework material, iron terephthalate, by ultrasound, microwave, and conventional electric heating: A kinetic study. *Chemistry–A European Journal, 16*(3), 1046–1052.

Hauser, J. L., Tso, M., Fitchmun, K., & Oliver, S. R. (2019). Anodic electrodeposition of several metal organic framework thin films on indium tin oxide glass. *Crystal Growth & Design, 19*(4), 2358–2365.

He, L., Wang, T., An, J., Li, X., Zhang, L., Li, L., Li, G., Wu, X., Su, Z., & Wang, C. (2014). Carbon nanodots@ zeolitic imidazolate framework-8 nanoparticles for simultaneous pH-responsive drug delivery and fluorescence imaging. *CrystEngComm, 16*(16), 3259–3263.

Horcajada, P., Chalati, T., Serre, C., Gillet, B., Sebrie, C., Baati, T., Eubank, J. F., Heurtaux, D., Clayette, P., Kreuz, C., & Chang, J. S. (2010). Porous metal-organic-framework nanoscale carriers as a potential platform for drug delivery and imaging. *Nature Materials, 9*(2), 172–178.

Hoskins, B. F., & Robson, R. (1990). Design and construction of a new class of scaffolding-like materials comprising infinite polymeric frameworks of 3D-linked molecular rods. A reappraisal of the zinc cyanide and cadmium cyanide structures and the synthesis and structure of the diamond-related frameworks $[N(CH_3)_4][CuIZnII(CN)_4]$ and CuI [4, 4′, 4″, 4‴-tetracyanotetraphenylmethane]$BF_4.xC_6H_5NO_2$. *Journal of the American Chemical Society, 112*(4), 1546–1554.

Hossen, S., Hossain, M. K., Basher, M. K., Mia, M. N. H., Rahman, M. T., & Uddin, M. J. (2019). Smart nanocarrier-based drug delivery systems for cancer therapy and toxicity studies: A review. *Journal of Advanced Research, 15*, 1–18.

Hu, S., Liu, M., Li, K., Zuo, Y., Zhang, A., Song, C., Zhang, G., & Guo, X. (2014). Solvothermal synthesis of NH_2-MIL-125 (Ti) from circular plate to octahedron. *CrystEngComm, 16*(41), 9645–9650.

Hu, F., Mao, D., Wang, Y., Wu, W., Zhao, D., Kong, D., & Liu, B. (2018). Metal-organic framework as a simple and general inert nanocarrier for photosensitizers to implement activatable photodynamic therapy. *Advanced Functional Materials, 28*(19), 1707519.

Huang, H., & Lovell, J. F. (2017). Advanced functional nanomaterials for theranostics. *Advanced Functional Materials, 27*(2), 1603524.

Huang, J., Li, N., Zhang, C., & Meng, Z. (2018). Metal-organic framework as a microreactor for in situ fabrication of multifunctional nanocomposites for photothermal-chemotherapy of tumors in vivo. *ACS Applied Materials & Interfaces, 10*(45), 38729–38738.

Huxford, R. C., deKrafft, K. E., Boyle, W. S., Liu, D., & Lin, W. (2012). Lipid-coated nanoscale coordination polymers for targeted delivery of antifolates to cancer cells. *Chemical Science, 3*(1), 198–204.

Imaz, I., Rubio-Martínez, M., García-Fernández, L., García, F., Ruiz-Molina, D., Hernando, J., Puntes, V., & Maspoch, D. (2010). Coordination polymer particles as potential drug delivery systems. *Chemical Communications, 46*(26), 4737–4739.

Imaz, I., Rubio-Martínez, M., An, J., Sole-Font, I., Rosi, N. L., & Maspoch, D. (2011). Metal-biomolecule frameworks (MBioFs). *Chemical Communications, 47*(26), 7287–7302.

Indoria, S., Singh, V., & Hsieh, M. F. (2020). Recent advances in theranostic polymeric nanoparticles for cancer treatment: A review. *International Journal of Pharmaceutics, 582*, 119314.

Jhung, S. H., Lee, J. H., & Chang, J. S. (2005). Microwave synthesis of a nanoporous hybrid material, chromium trimesate. *Bulletin of the Korean Chemical Society, 26*(6), 880–881.

Jung, D. W., Yang, D. A., Kim, J., Kim, J., & Ahn, W. S. (2010). Facile synthesis of MOF-177 by a sonochemical method using 1-methyl-2-pyrrolidinone as a solvent. *Dalton Transactions, 39*(11), 2883–2887.

Kalmutzki, M. J., Hanikel, N., & Yaghi, O. M. (2018). Secondary building units as the turning point in the development of the reticular chemistry of MOFs. *Science Advances, 4*(10), eaat9180.

Ke, F., Yuan, Y. P., Qiu, L. G., Shen, Y. H., Xie, A. J., Zhu, J. F., Tian, X. Y., & Zhang, L. D. (2011). Facile fabrication of magnetic metal-organic framework nanocomposites for potential targeted drug delivery. *Journal of Materials Chemistry, 21*(11), 3843–3848.

Kepert, C. J., & Rosseinsky, M. J. (1999). Zeolite-like crystal structure of an empty microporous molecular framework. *Chemical Communications, 4*, 375–376.

Khan, N. A., Haque, E., & Jhung, S. H. (2010). Rapid syntheses of a metal-organic framework material $Cu_3(BTC)_2(H_2O)_3$ under microwave: A quantitative analysis of accelerated syntheses. *Physical Chemistry Chemical Physics, 12*(11), 2625–2631.

Kim, J., Yang, S. T., Choi, S. B., Sim, J., Kim, J., & Ahn, W. S. (2011). Control of catenation in CuTATB-n metal–organic frameworks by sonochemical synthesis and its effect on CO_2 adsorption. *Journal of Materials Chemistry, 21*(9), 3070–3076.

Klimakow, M., Klobes, P., Thunemann, A. F., Rademann, K., & Emmerling, F. (2010). Mechanochemical synthesis of metal-organic frameworks: A fast and facile approach toward quantitative yields and high specific surface areas. *Chemistry of Materials, 22*(18), 5216–5221.

Kumar, P., Deep, A., & Kim, K. H. (2015). Metal organic frameworks for sensing applications. *TrAC Trends in Analytical Chemistry, 73*, 39–53.

Lan, G., Ni, K., & Lin, W. (2019). Nanoscale metal-organic frameworks for phototherapy of cancer. *Coordination Chemistry Reviews, 379*, 65–81.

Lee, Y. R., Kim, J., & Ahn, W. S. (2013). Synthesis of metal-organic frameworks: A mini review. *Korean Journal of Chemical Engineering, 30*(9), 1667–1680.

Li, M., & Dincă, M. (2014). Selective formation of biphasic thin films of metal-organic frameworks by potential-controlled cathodic electrodeposition. *Chemical Science, 5*(1), 107–111.

Li, H., Eddaoudi, M., O'Keeffe, M., & Yaghi, O. M. (1999). Design and synthesis of an exceptionally stable and highly porous metal-organic framework. *Nature, 402*(6759), 276–279.

Li, L., Sun, K. K., Fan, L., Hong, W., Xu, Z. S., & Liu, L. (2014). Layer by layer assembly synthesis of Fe_3O_4@ MOFs/GO core–shell nanoparticles. *Materials Letters, 126*, 197–201.

Li, W. J., Tu, M., Cao, R., & Fischer, R. A. (2016a). Metal-organic framework thin films: Electrochemical fabrication techniques and corresponding applications & perspectives. *Journal of Materials Chemistry A, 4*(32), 12356–12369.

Li, Y., Miao, J., Sun, X., Xiao, J., Li, Y., Wang, H., Xia, Q., & Li, Z. (2016b). Mechanochemical synthesis of Cu-BTC@GO with enhanced water stability and toluene adsorption capacity. *Chemical Engineering Journal, 298*, 191–197.

Li, H., Wang, K., Sun, Y., Lollar, C. T., Li, J., & Zhou, H. C. (2018a). Recent advances in gas storage and separation using metal-organic frameworks. *Materials Today, 21*(2), 108–121.

Li, Y., Xu, N., Zhou, J., Zhu, W., Li, L., Dong, M., Yu, H., Wang, L., Liu, W., & Xie, Z. (2018b). Facile synthesis of a metal–organic framework nanocarrier for NIR imaging-guided photothermal therapy. *Biomaterials Science, 6*(11), 2918–2924.

Li, B., Wang, X., Chen, L., Zhou, Y., Dang, W., Chang, J., & Wu, C. (2018c). Ultrathin Cu-TCPP MOF nanosheets: A new theragnostic nanoplatform with magnetic resonance/near-infrared thermal imaging for synergistic phototherapy of cancers. *Theranostics, 8*(15), 4086.

Li, X., Cai, Z., Jiang, L. P., He, Z., & Zhu, J. J. (2019a). Metal-ligand coordination nanomaterials for biomedical imaging. *Bioconjugate Chemistry, 31*(2), 332–339.

Li, S., Zhang, L., Liang, X., Wang, T., Chen, X., Liu, C., Li, L., & Wang, C. (2019b). Tailored synthesis of hollow MOF/polydopamine Janus nanoparticles for synergistic multi-drug chemo-photothermal therapy. *Chemical Engineering Journal, 378*, 122175.

Li, Y., Zhou, J., Wang, L., & Xie, Z. (2020). Endogenous hydrogen sulfide-triggered MOF-based nanoenzyme for synergic cancer therapy. *ACS Applied Materials & Interfaces, 12*(27), 30213–30220.

Liu, D., Kramer, S. A., Huxford-Phillips, R. C., Wang, S., Della Rocca, J., & Lin, W. (2012). Coercing bisphosphonates to kill cancer cells with nanoscale coordination polymers. *Chemical Communications, 48*(21), 2668–2670.

Liu, D., Poon, C., Lu, K., He, C., & Lin, W. (2014a). Self-assembled nanoscale coordination polymers with trigger release properties for effective anticancer therapy. *Nature Communications, 5*(1), 1–11.

Liu, D., He, C., Poon, C., & Lin, W. (2014b). Theranostic nanoscale coordination polymers for magnetic resonance imaging and bisphosphonate delivery. *Journal of Materials Chemistry B, 2*(46), 8249–8255.

Liu, J., Zhang, L., Lei, J., Shen, H., & Ju, H. (2017). Multifunctional metal-organic framework nanoprobe for cathepsin B-activated cancer cell imaging and chemo-photodynamic therapy. *ACS Applied Materials & Interfaces, 9*(3), 2150–2158.

Liu, B., Hu, F., Zhang, J., Wang, C., & Li, L. (2019). A biomimetic coordination nanoplatform for controlled encapsulation and delivery of drug-gene combinations. *Angewandte Chemie, 131*(26), 8896–8900.

Liu, X., Jin, Y., Liu, T., Yang, S., Zhou, M., Wang, W., & Yu, H. (2020). Iron-based theranostic nanoplatform for improving chemodynamic therapy of cancer. *ACS Biomaterials Science & Engineering, 6*(9), 4834–4845.

Lu, W., Wei, Z., Gu, Z. Y., Liu, T. F., Park, J., Park, J., Tian, J., Zhang, M., Zhang, Q., Gentle, T., III, & Bosch, M. (2014). Tuning the structure and function of metal-organic frameworks via linker design. *Chemical Society Reviews, 43*(16), 5561–5593.

Lu, K., Aung, T., Guo, N., Weichselbaum, R., & Lin, W. (2018). Nanoscale metal-organic frameworks for therapeutic, imaging, and sensing applications. *Advanced Materials, 30*(37), 1707634.

Luo, Z., Fan, S., Gu, C., Liu, W., Chen, J., Li, B., & Liu, J. (2019). Metal-organic framework (MOF)-based nanomaterials for biomedical applications. *Current Medicinal Chemistry, 26*(18), 3341–3369.

Ma, B., Wang, S., Liu, F., Zhang, S., Duan, J., Li, Z., Kong, Y., Sang, Y., Liu, H., Bu, W., & Li, L. (2018). Self-assembled copper–amino acid nanoparticles for in situ glutathione "and" H_2O_2 sequentially triggered chemodynamic therapy. *Journal of the American Chemical Society, 141*(2), 849–857.

Martinez Joaristi, A., Juan-Alcañiz, J., Serra-Crespo, P., Kapteijn, F., & Gascon, J. (2012). Electrochemical synthesis of some archetypical Zn^{2+}, Cu^{2+}, and Al^{3+} metal organic frameworks. *Crystal Growth & Design, 12*(7), 3489–3498.

Meek, S. T., Greathouse, J. A., & Allendorf, M. D. (2011). Metal-organic frameworks: A rapidly growing class of versatile nanoporous materials. *Advanced Materials, 23*(2), 249–267.

Meng, Z., Huang, H., Huang, D., Zhang, F., & Mi, P. (2020). Functional metal-organic framework-based nanocarriers for accurate magnetic resonance imaging and effective eradication of breast tumor and lung metastasis. *Journal of Colloid and Interface Science, 581*, 31–43.

Mi, P., Cabral, H., & Kataoka, K. (2020). Ligand-installed nanocarriers toward precision therapy. *Advanced Materials, 32*(13), 1902604.

Mir, M., Ishtiaq, S., Rabia, S., Khatoon, M., Zeb, A., Khan, G. M., Ur Rehman, A., & Ud Din, F. (2017). Nanotechnology: From in vivo imaging system to controlled drug delivery. *Nanoscale Research Letters, 12*(1), 500.

Mueller, U., Puetter, H., Hesse, M., & Wessel, H. (2007). WO 2005/049892, 2005. *BASF Aktiengesellschaft*.

Naseri, N., Ajorlou, E., Asghari, F., & Pilehvar-Soltanahmadi, Y. (2018). An update on nanoparticle-based contrast agents in medical imaging. *Artificial Cells, Nanomedicine, and Biotechnology, 46*(6), 1111–1121.

Nejadshafiee, V., Naeimi, H., Goliaei, B., Bigdeli, B., Sadighi, A., Dehghani, S., Lotfabadi, A., Hosseini, M., Nezamtaheri, M. S., Amanlou, M., & Sharifzadeh, M. (2019). Magnetic bio-metal–organic framework nanocomposites decorated with folic acid conjugated chitosan as a promising biocompatible targeted theranostic system for cancer treatment. *Materials Science and Engineering: C, 99*, 805–815.

Nune, S. K., Gunda, P., Thallapally, P. K., Lin, Y. Y., Laird Forrest, M., & Berkland, C. J. (2009). Nanoparticles for biomedical imaging. *Expert Opinion on Drug Delivery, 6*(11), 1175–1194.

Osterrieth, J. W., & Fairen-Jimenez, D. (2020). Metal-organic framework composites for theragnostics and drug delivery applications. *Biotechnology Journal, 16*(2), 2000005.

Pan, Y. B., Wang, S., He, X., Tang, W., Wang, J., Shao, A., & Zhang, J. (2019). A combination of glioma in vivo imaging and in vivo drug delivery by metal-organic framework based composite nanoparticles. *Journal of Materials Chemistry B, 7*(48), 7683–7689.

Pandey, A., Dhas, N., Deshmukh, P., Caro, C., Patil, P., García-Martín, M. L., Padya, B., Nikam, A., Mehta, T., & Mutalik, S. (2020). Heterogeneous surface architectured metal-organic frameworks for cancer therapy, imaging, and biosensing: A state-of-the-art review. *Coordination Chemistry Reviews, 409*, 213212.

Park, K. S., Ni, Z., Côté, A. P., Choi, J. Y., Huang, R., Uribe-Romo, F. J., Chae, H. K., O'Keeffe, M., & Yaghi, O. M. (2006). Exceptional chemical and thermal stability of zeolitic imidazolate frameworks. *Proceedings of the National Academy of Sciences, 103*(27), 10186–10191.

Peer, D., Karp, J. M., Hong, S., Farokhzad, O. C., Margalit, R., & Langer, R. (2007). Nanocarriers as an emerging platform for cancer therapy. *Nature Nanotechnology, 2*(12), 751–760.

Peller, M., Böll, K., Zimpel, A., & Wuttke, S. (2018). Metal-organic framework nanoparticles for magnetic resonance imaging. *Inorganic Chemistry Frontiers, 5*(8), 1760–1779.

Pereira, G. A., Peters, J. A., Almeida Paz, F. A., Rocha, J., & Geraldes, C. F. (2010). Evaluation of [Ln (H_2cmp)(H_2O)] metal organic framework materials for potential application as magnetic resonance imaging contrast agents. *Inorganic Chemistry, 49*(6), 2969–2974.

Petros, R. A., & DeSimone, J. M. (2010). Strategies in the design of nanoparticles for therapeutic applications. *Nature Reviews Drug Dscovery, 9*(8), 615–627.

Pichon, A., Lazuen-Garay, A., & James, S. L. (2006). Solvent-free synthesis of a microporous metal-organic framework. *CrystEngComm, 8*(3), 211–214.

Qian, J., Sun, F., & Qin, L. (2012). Hydrothermal synthesis of zeolitic imidazolate framework-67 (ZIF-67) nanocrystals. *Materials Letters, 82*, 220–223.

Qian, C. G., Chen, Y. L., Feng, P. J., Xiao, X. Z., Dong, M., Yu, J. C., Hu, Q. Y., Shen, Q. D., & Gu, Z. (2017). Conjugated polymer nanomaterials for theranostics. *Acta Pharmacologica Sinica, 38*(6), 764–781.

Rieter, W. J., Pott, K. M., Taylor, K. M., & Lin, W. (2008). Nanoscale coordination polymers for platinum-based anticancer drug delivery. *Journal of the American Chemical Society, 130*(35), 11584–11585.

Robison, L., Zhang, L., Drout, R. J., Li, P., Haney, C. R., Brikha, A., Noh, H., Mehdi, B. L., Browning, N. D., Dravid, V. P., & Cui, Q. (2019). A bismuth metal-organic framework as a contrast agent for X-ray computed tomography. *ACS Applied Bio Materials, 2*(3), 1197–1203.

Rojas, S., Devic, T., & Horcajada, P. (2017). Metal organic frameworks based on bioactive components. *Journal of Materials Chemistry B, 5*(14), 2560–2573.

Rowe, M. D., Thamm, D. H., Kraft, S. L., & Boyes, S. G. (2009). Polymer-modified gadolinium metal-organic framework nanoparticles used as multifunctional nanomedicines for the targeted imaging and treatment of cancer. *Biomacromolecules, 10*(4), 983–993.

Rowsell, J. L., & Yaghi, O. M. (2004). Metal-organic frameworks: A new class of porous materials. *Microporous and Mesoporous Materials, 73*(1–2), 3–14.

Ruyra, À., Yazdi, A., Espín, J., Carné-Sánchez, A., Roher, N., Lorenzo, J., Imaz, I., & Maspoch, D. (2015). Synthesis, culture medium stability, and in vitro and in vivo zebrafish embryo toxicity of metal-organic framework nanoparticles. *Chemistry–A European Journal, 21*(6), 2508–2518.

Safaei, M., Foroughi, M. M., Ebrahimpoor, N., Jahani, S., Omidi, A., & Khatami, M. (2019). A review on metal-organic frameworks: Synthesis and applications. *TrAC Trends in Analytical Chemistry, 118*, 401–425.

Shang, W., Kang, X., Ning, H., Zhang, J., Zhang, X., Wu, Z., Mo, G., Xing, X., & Han, B. (2013). Shape and size-controlled synthesis of MOF nanocrystals with the assistance of ionic liquid mircoemulsions. *Langmuir, 29*(43), 13168–13174.

Shang, W., Zeng, C., Du, Y., Hui, H., Liang, X., Chi, C., Wang, K., Wang, Z., & Tian, J. (2017). Core-shell gold Nanorod@metal-organic framework nanoprobes for multimodality diagnosis of glioma. *Advanced Materials, 29*(3), 1604381.

Shekhah, O. (2010). Layer-by-layer method for the synthesis and growth of surface mounted metal-organic frameworks (SURMOFs). *Materials, 3*(2), 1302–1315.

Shekhah, O., Wang, H., Kowarik, S., Schreiber, F., Paulus, M., Tolan, M., Sternemann, C., Evers, F., Zacher, D., Fischer, R. A., & Wöll, C. (2007). Step-by-step route for the synthesis of metal-organic frameworks. *Journal of the American Chemical Society, 129*(49), 15118–15119.

Shekhah, O., Wang, H., Zacher, D., Fischer, R. A., & Wöll, C. (2009). Growth mechanism of metal-organic frameworks: Insights into the nucleation by employing a step-by-step route. *Angewandte Chemie International Edition, 48*(27), 5038–5041.

Shi, J., Kantoff, P. W., Wooster, R., & Farokhzad, O. C. (2017). Cancer nanomedicine: Progress, challenges and opportunities. *Nature Reviews Cancer, 17*(1), 20.

Singh, R., & Lillard, J. W. (2009). Nanoparticle-based targeted drug delivery. *Experimental and Molecular Pathology, 86*(3), 215–223.

So, M. C., Jin, S., Son, H. J., Wiederrecht, G. P., Farha, O. K., & Hupp, J. T. (2013). Layer-by-layer fabrication of oriented porous thin films based on porphyrin-containing metal–organic frameworks. *Journal of the American Chemical Society, 135*(42), 15698–15701.

Son, W. J., Kim, J., Kim, J., & Ahn, W. S. (2008). Sonochemical synthesis of MOF-5. *Chemical Communications, 47*, 6336–6338.

Sousa, D., Ferreira, D., Rodrigues, J. L., & Rodrigues, L. R. (2019). Nanotechnology in targeted drug delivery and therapeutics. In *Applications of targeted nano drugs and delivery systems* (pp. 357–409). Elsevier.

Stassen, I., Styles, M., Van Assche, T., Campagnol, N., Fransaer, J., Denayer, J., Tan, J. C., Falcaro, P., De Vos, D., & Ameloot, R. (2015). Electrochemical film deposition of the zirconium metal–organic framework UiO-66 and application in a miniaturized sorbent trap. *Chemistry of Materials, 27*(5), 1801–1807.

Stock, N., & Biswas, S. (2012). Synthesis of metal-organic frameworks (MOFs): Routes to various MOF topologies, morphologies, and composites. *Chemical Reviews, 112*(2), 933–969.

Sun, C. Y., Qin, C., Wang, X. L., & Su, Z. M. (2013). Metal-organic frameworks as potential drug delivery systems. *Expert Opinion on Drug Delivery, 10*(1), 89–101.

Sun, W., Zhai, X., & Zhao, L. (2016). Synthesis of ZIF-8 and ZIF-67 nanocrystals with well-controllable size distribution through reverse microemulsions. *Chemical Engineering Journal, 289*, 59–64.

Sun, J., Yu, X., Zhao, S., Chen, H., Tao, K., & Han, L. (2020). Solvent-controlled morphology of amino-functionalized bimetal metal-organic frameworks for asymmetric supercapacitors. *Inorganic Chemistry, 59*(16), 11385–11395.

Suslick, K. S., Hammerton, D. A., & Cline, R. E. (1986). Sonochemical hot spot. *Journal of the American Chemical Society, 108*(18), 5641–5642.

Taylor, K. M., Rieter, W. J., & Lin, W. (2008). Manganese-based nanoscale metal-organic frameworks for magnetic resonance imaging. *Journal of the American Chemical Society, 130*(44), 14358–14359.

Taylor-Pashow, K. M., Della Rocca, J., Xie, Z., Tran, S., & Lin, W. (2009). Postsynthetic modifications of iron-carboxylate nanoscale metal-organic frameworks for imaging and drug delivery. *Journal of the American Chemical Society, 131*(40), 14261–14263.

Tian, C., Zhu, L., Lin, F., & Boyes, S. G. (2015). Poly (acrylic acid) bridged gadolinium metal-organic framework-gold nanoparticle composites as contrast agents for computed tomography and magnetic resonance bimodal imaging. *ACS Applied Materials & Interfaces, 7*(32), 17765–17775.

Tranchemontagne, D. J., Hunt, J. R., & Yaghi, O. M. (2008). Room temperature synthesis of metal-organic frameworks: MOF-5, MOF-74, MOF-177, MOF-199, and IRMOF-0. *Tetrahedron, 64*(36), 8553–8557.

Wang, Q., & Astruc, D. (2019). State of the art and prospects in metal-organic framework (MOF)-based and MOF-derived nanocatalysis. *Chemical Reviews, 120*(2), 1438–1511.

Wang, D., Zhou, J., Chen, R., Shi, R., Zhao, G., Xia, G., Li, R., Liu, Z., Tian, J., Wang, H., & Guo, Z. (2016). Controllable synthesis of dual-MOFs nanostructures for pH-responsive artemisinin delivery, magnetic resonance and optical dual-model imaging-guided chemo/photothermal combinational cancer therapy. *Biomaterials, 100*, 27–40.

Wang, L., Zheng, M., & Xie, Z. (2018a). Nanoscale metal-organic frameworks for drug delivery: A conventional platform with new promise. *Journal of Materials Chemistry B, 6*(5), 707–717.

Wang, D., Wu, H., Zhou, J., Xu, P., Wang, C., Shi, R., Wang, H., Wang, H., Guo, Z., & Chen, Q. (2018b). In situ one-pot synthesis of MOF-Polydopamine hybrid Nanogels with enhanced Photothermal effect for targeted Cancer therapy. *Advanced Science, 5*(6), 1800287.

Wang, X., Yang, N., Li, Q., He, F., Yang, Y., Wu, B., Chu, J., Zhou, A., & Xiong, S. (2019a). Solvothermal synthesis of flower-string-like NiCo-MOF/MWCNT composites as a high-performance supercapacitor electrode material. *Journal of Solid State Chemistry, 277*, 575–586.

Wang, L., Qu, X., Zhao, Y., Weng, Y., Waterhouse, G. I., Yan, H., Guan, S., & Zhou, S. (2019b). Exploiting single atom iron centers in a porphyrin-like MOF for efficient cancer phototherapy. *ACS Applied Materials & Interfaces, 11*(38), 35228–35237.

Wang, Z., Li, Z., Ng, M., & Milner, P. J. (2020). Rapid mechanochemical synthesis of metal-organic frameworks using exogenous organic base. *Dalton Transactions, 49*(45), 16238–16244. https://doi.org/10.1039/D0DT01240H

Wei, R., Chi, H. Y., Li, X., Lu, D., Wan, Y., Yang, C. W., & Lai, Z. (2020). Aqueously cathodic deposition of ZIF-8 membranes for superior propylene/propane separation. *Advanced Functional Materials, 30*(7), 1907089.

Wu, M. X., & Yang, Y. W. (2017). Metal-organic framework (MOF)-based drug/cargo delivery and cancer therapy. *Advanced Materials, 29*(23), 1606134.

Xiao, Y., Wu, Z., Zhang, Q., Li, P., Yu, H., & Lu, G. (2020). Oxygen-assisted cathodic deposition of copper-carboxylate metal–organic framework films. *Crystal Growth & Design, 20*(6), 3997–4004.

Xie, J., Lee, S., & Chen, X. (2010). Nanoparticle-based theranostic agents. *Advanced Drug Delivery Reviews, 62*(11), 1064–1079.

Xue, D. X., Wang, Q., & Bai, J. (2019a). Amide-functionalized metal-organic frameworks: Syntheses, structures and improved gas storage and separation properties. *Coordination Chemistry Reviews, 378*, 2–16.

Xue, Y., Zheng, S., Xue, H., & Pang, H. (2019b). Metal-organic framework composites and their electrochemical applications. *Journal of Materials Chemistry A, 7*(13), 7301–7327.

Yaghi, O. M., & Li, H. (1995). Hydrothermal synthesis of a metal-organic framework containing large rectangular channels. *Journal of the American Chemical Society, 117*(41), 10401–10402.

Yaghi, O. M., Li, H., Davis, C., Richardson, D., & Groy, T. L. (1998). Synthetic strategies, structure patterns, and emerging properties in the chemistry of modular porous solids. *Accounts of Chemical Research, 31*(8), 474–484.

Yang, J., & Yang, Y. W. (2020). Metal-organic frameworks for biomedical applications. *Small, 16*(10), 1906846.

Yang, C., Chen, K., Chen, M., Hu, X., Huan, S. Y., Chen, L., Song, G., & Zhang, X. B. (2019). Nanoscale metal-organic framework based two-photon sensing platform for bioimaging in live tissue. *Analytical Chemistry, 91*(4), 2727–2733.

Ye, R., Ni, M., Xu, Y., Chen, H., & Li, S. (2018). Synthesis of Zn-based metal-organic frameworks in ionic liquid microemulsions at room temperature. *RSC Advances, 8*(46), 26237–26242.

Yoo, D., Lee, J. H., Shin, T. H., & Cheon, J. (2011). Theranostic magnetic nanoparticles. *Accounts of Chemical Research, 44*(10), 863–874.

Yuan, Q., & Zhu, G. (2020). A review on metal organic frameworks (MOFs) modified membrane for remediation of water pollution. *Environmental Engineering Research, 26*(3), 190435.

Zacher, D., Shekhah, O., Wöll, C., & Fischer, R. A. (2009). Thin films of metal-organic frameworks. *Chemical Society Reviews, 38*(5), 1418–1429.

Zhang, Y. B., Furukawa, H., Ko, N., Nie, W., Park, H. J., Okajima, S., Cordova, K. E., Deng, H., Kim, J., & Yaghi, O. M. (2015). Introduction of functionality, selection of topology, and enhancement of gas adsorption in multivariate metal-organic framework-177. *Journal of the American Chemical Society, 137*(7), 2641–2650.

Zhang, H., Shang, Y., Li, Y. H., Sun, S. K., & Yin, X. B. (2018a). Smart metal-organic framework-based nanoplatforms for imaging-guided precise chemotherapy. *ACS Applied Materials & Interfaces, 11*(2), 1886–1895.

Zhang, W., Lu, J., Gao, X., Li, P., Zhang, W., Ma, Y., Wang, H., & Tang, B. (2018b). Enhanced photodynamic therapy by reduced levels of intracellular glutathione obtained by employing a Nano-MOF with Cu(II) as the active center. *Angewandte Chemie, 130*(18), 4985–4990.

Zhang, S., Pei, X., Gao, H., Chen, S., & Wang, J. (2020). Metal-organic framework-based nanomaterials for biomedical applications. *Chinese Chemical Letters, 31*(5), 1060–1070.

Zhao, H. X., Zou, Q., Sun, S. K., Yu, C., Zhang, X., Li, R. J., & Fu, Y. Y. (2016). Theranostic metal-organic framework core-shell composites for magnetic resonance imaging and drug delivery. *Chemical Science, 7*(8), 5294–5301.

Zhao, J., Yang, Y., Han, X., Liang, C., Liu, J., Song, X., Ge, Z., & Liu, Z. (2017). Redox-sensitive nanoscale coordination polymers for drug delivery and cancer theranostics. *ACS Applied Materials & Interfaces, 9*(28), 23555–23563.

Zheng, W., Hao, X., Zhao, L., & Sun, W. (2017). Controllable preparation of nanoscale metal-organic frameworks by ionic liquid microemulsions. *Industrial & Engineering Chemistry Research, 56*(20), 5899–5905.

Zhou, J., Tian, G., Zeng, L., Song, X., & Bian, X. W. (2018). Nanoscaled metal-organic frameworks for biosensing, imaging, and cancer therapy. *Advanced Healthcare Materials, 7*(10), 1800022.

Zhu, H., Liu, H., Zhitomirsky, I., & Zhu, S. (2015). Preparation of metal-organic framework films by electrophoretic deposition method. *Materials Letters, 142*, 19–22.

Zhu, Y. D., Chen, S. P., Zhao, H., Yang, Y., Chen, X. Q., Sun, J., Fan, H. S., & Zhang, X. D. (2016). PPy@MIL-100 nanoparticles as a pH-and near-IR-irradiation-responsive drug carrier for simultaneous photothermal therapy and chemotherapy of cancer cells. *ACS Applied Materials & Interfaces, 8*(50), 34209–34217.

Zhu, W., Chen, M., Liu, Y., Tian, Y., Song, Z., Song, G., & Zhang, X. (2019a). A dual factor activated metal-organic framework hybrid nanoplatform for photoacoustic imaging and synergetic photo-chemotherapy. *Nanoscale, 11*(43), 20630–20637.

Zhu, W., Yang, Y., Jin, Q., Chao, Y., Tian, L., Liu, J., Dong, Z., & Liu, Z. (2019b). Two-dimensional metal-organic-framework as a unique theranostic nano-platform for nuclear imaging and chemo-photodynamic cancer therapy. *Nano Research, 12*(6), 1307–1312.

Zhu, D., Qiao, M., Liu, J., Tao, T., & Guo, C. (2020). Engineering pristine 2D metal-organic framework nanosheets for electrocatalysis. *Journal of Materials Chemistry A, 8*(17), 8143–8170.

Chapter 9
Porphyrin-Based Nanomaterials for Cancer Nanotheranostics

Md. Habban Akhter, Javed Ahmad, Md. Noushad Javed, Rafiul Haque, Habibullah Khalilullah, Manish Gupta, and Javed Ali

Contents

Md. H. Akhter (✉)
Faculty of Pharmacy, DIT University, Dehradun, India
e-mail: habban.akhter@dituniversity.edu.in

J. Ahmad
Department of Pharmaceutics, Najran University, Najran, Saudi Arabia

Md. N. Javed · J. Ali
Department of Pharmaceutics, School of Pharmaceutical Education and Research, Jamia Hamdard, New Delhi, India

R. Haque
Principle Champaran College of Pharmacy, Purbi Champaran, Motihari, Bihar, Bihar, India

H. Khalilullah
Department of Pharmaceutical Chemistry and Pharmacognosy, Unaizah College of Pharmacy, Qassim University, Qassim, Kingdom of Saudi Arabia

M. Gupta
Department of Pharmaceutical Sciences, School of Health Sciences, University of Petroleum and Energy Studies (UPES), Dehradun, Uttarakhand, India

M. Saravanan, H. Barabadi (eds.), *Cancer Nanotheranostics*, Nanotechnology in the Life Sciences, https://doi.org/10.1007/978-3-030-74330-7_9

9.1 Introduction

The integration of diagnosis and therapy in one platform as theranostic agent has shown growing interest worldwide in the therapeutic intervention of annihilating cancer disease (Chen et al., 2017; Nabil et al., 2019). The design and development of the theranostic agent is challenging as it is expected to perform the multiple therapeutic modalities from a single entity. Thus, unmet challenges could be addressed by utilizing the nanotechnology approach designing the theranostic agent into nanosize objects that preferentially accumulate and retain in the tumor by enhancing permeation and retention (EPR) effect. Further, surface modification has been carried out for multiple functions to identify tumor cell overexpressed receptor or diagnose the tumor cells and deliver therapeutics to them (Akhter, Beg, et al., 2020, Akhter et al., 2020; Akhter, Alam, & Minhaj, 2018, Akhter, Madhav, & Ahmad, 2018; Akhter & Amin, 2017; Akhter, 2017 multifunctional). The imaging agent helps in detection and diagnosis of disease. Together, nanotheranostic agents treat the tumor via distinguished mechanism, viz., specific recognition and real-time monitoring due to accumulation of therapeutics, and help in assessment of benefits as well as risk of the treatment (Zhang et al., 2016).

Of late, porphyrin and their derivatives have shown tremendous interest in the field of biomedical sciences and theranostic application because of the photosensitizing, imaging properties, and specific accumulation in tumor tissues for predefined time period (Yuan et al., 2001). Porphyrins is a pyrrole-derived molecule composed of 4-pyrrole subunits bonded together with α-carbon atoms by 4-methine bridges (=CH−) (Paszko et al., 2011). It also bears magnetic and metal chelator properties (Takehara et al., 2002). It has unique optical properties due to which it is used in imaging of biological cells and theranostic utility. The application of porphyrin is not limited to photosensitizer only rather having other applications of fluorescence imaging, photodynamic therapy (PDT), magnetic resonance imaging (MRI) (Zhang et al., 2007), sonodynamic therapy (SDT), boron neutron capture therapy (BNCT) (Hua et al., 2020; Renner et al., 2006), and radiation therapy (Chen & Zhang, 2006; Zhang et al., 2007).

The diagnosis and therapy together as nanotheranostic based on nanotechnologies embracing the patients though high quality imaging, diagnosis, personalized treatment that lead to better prediction of disease progress and therapy (Blau et al., 2016). Theranostic system is able to monitor their performance due to high sensitivity, tumor detection across various loci, specific targeting, and non-toxic at therapeutic concentration (Zhou et al., 2016). Thus, porphyrin could be a promising theranostic agent compared with conventional treatment modalities such as chemotherapy, radiotherapy, and surgery. In defiance of poor aqueous solubility and high

degree of aggregation in aqueous medium, two porphyrin-based medicine has been approved, namely, Photofrin and Visudyne as PDT drugs by US-FDA. The limited solubility of porphyrin in water and toxicity hinders their wide biomedical uses and therapeutic efficacy in vivo, although it preferably accumulate in the tumor tissue due to potential vascular permeability and high affinity with endothelial cells and poor lymphatic drainage in the tumors (Chen et al., 2005; Obaid et al., 2015).

9.2 Conventional Cancer Therapy

Cancer is an uncontrolled cell division resulting from gene mutation or other causes that has capacity to proliferate rapidly and metastasize at the distant part of the body if it is not treated and monitored properly in an early period of time (Akhter, Nomani, & Kumar 2020; Soni et al., 2020). The conventional treatment with chemotherapy results in unspecified delivery of drug, poor biodistribution, and low bioavailability and efficacy owing to the great biological barrier as well as dose-related side effects (Kievit & Zhang, 2011).

Surgery is preferred for eradication of cancer cells/tissues in some types of tumor, and for this procedure, it is required to anaesthetize the patient, and during this process, heavy blood loss and soft tissue trauma could result. In some cases disease recurrence takes place after the surgical resection process. Therefore, developing innovative technology is more helpful and efficacious to meet the challenges in conventional therapies in cancer to overall improve the therapeutic modalities of disease conditions and prevent the undesirable side effects.

9.3 Porphyrins as Emerging Nanomaterials in Cancer Theranostic

The theranostic agent is generally image-guided therapeutic intervention in cancer. It consists of both therapeutic and imaging (diagnostic) agents for the treatment of cancer. Another way we can say is it is a precise treatment of cancer or related areas due to imaging and selective killing of cells that leads to improved patient survival rate. The biomedical utility of porphyrin and its related compound rises in the field of photodynamic therapy. The current advances in nanoscale engineering of porphyrin in certain carrier systems potentially improve human health. For example, porphyrin associated with metal, viz., metalloporphyrin, has been extensively employed as diagnosis and therapy in cancer. Since, few decades back, the emergence of cancer therapy based on diagnosis was put forwarded to overcome the shortcomings in the past treatment approach. It is a photodynamic therapy which involves the use of photosensitizer that absorbs radiation at particular wavelength and thereby generates the reactive oxygen species that led to molecular vibration

and produce hyperthermia. The generation of reactive oxygen molecules depends upon the wavelength of light which activates the photosensitizer.

The nanocarreir, viz., polymeric nanoparticle, silica nanoparticle, lipid-based vesicles, and organic and inorganic nanoparticle, is explored widely as photosensitizer in photodynamic therapy of cancer. The porphyrin nanostructures are smart nanomaterials capable of releasing off their medicaments at the site of targeting. Assembling the nanomaterials with photosensitizer activity with functional nanomoieties such as protein, peptides, aptamers, antibodies, m-RNA, and DNA to deliver them in disease site is highly anticipated. The complex structure of porphyrin with multiple functional moieties can possibly reduce the side effects and improve the efficacy in phototherapeutics (Imran et al., 2018; Tsolekile et al., 2019).

9.4 Porphyrin-Based Nanomedicine

9.4.1 Porphyrin-Based Lipidic Nanoparticles

The liposome is of particular interest and widely explored for delivery of porphyrin in PDT therapy owing to the high flexibility, drug entrapment capacity, and high retention of drug in tumor cells. Visudyne clinically approved liposomal preparation of verteporfin (Schmidt-Erfurth & Hasan, 2000). Porphyrin substantially improved cancer therapy and safety profile based on PDT utilizing liposomal nanocarrier compared to non-liposomal photosensitizing carriers under similar conditions. For example, Photofrin is a complex oligomeric structure of porphyrin (up to 9 rings) linked with ether bonds. Loading into liposomal vesicles resulted in potential therapeutic outcomes against the implanted glioma tumor in animal brains compared with non-liposomal Photofrin due to excellent uptake of nanocarriers by tumor tissues (Jiang et al., 1998).

To combat the systemic capture of conventional liposomes by macrophagic system, viz., liver and spleen, and improve circulation time in the blood surface modification using polyethylene glycol (PEG), a hydrophilic polymer is an exciting approach to implement in drug delivery systems for effective therapeutic concentration in blood. This modified liposome has got advantages of minimal toxicity, non-immunogenicity, and hindrance to protein layering (Kepczyński et al., 2006).

Nawalany and coworkers designed pegylated liposomes to disseminate aggregation of tetrakis 4-hydroxyphenyl porphyrin (p-THPP) for effective treatment in prostate carcinoma and human colon carcinoma. Moreover, it was observed the specific accrual of p-THPP around carcinoma cells and thus improved the therapeutic efficacy of PDT. Subsequently Nawalany et al. in Nawalany et al., 2012 investigated PEG-chain length impact on photodynamic activity of various PEG-modified tetraarylporphyrin liposomes. The observation led to increasing PEG-chains length from 350 to 5000 Da showing marked reduction in cytotoxicity opposed to (DU 125 and HCT 116) cell line by the use of parent porphyrin. Further, cell viability

evaluation established pegylated systems bearing PEG chain of 2000 Da showing highest phototoxicity and induced pronounced apoptosis in abovementioned cell lines compared with plain pegylated porphyrin in vitro (Nawalany et al., 2012).

Theranostic agent (A) has a Gd3 + −texaphyrin core disulfide bonded to DOX prodrug. This conjugate 1 cleaved easily with glutathione (GSH) which is upregulated in tumor cells. The free DOX release was examined in presence of excess of GSH due to raised fluorescence intensity at 592 nm. Moreover, the conjugate 1 is loaded into a folate functionalized liposome assigned as FL-1. In vitro cytotoxicity studies confirmed FL-1 undergone selective uptake by folate receptor and cleavage of conjugate release free DOX dominantly into KB and CT26 cell lines. FL-1 also monitored the metastatic progress of tumors by magnetic resonance imaging in vivo. It was concluded that tumor therapy was time dependent and greatly reduced the progress of tumor in mouse model of liver cancer (Lee et al., 2016).

Rizvi et al. (2019)) developed photodynamic therapy to target lethal tumors as well as reducing toxicity to normal cells. PDT therapy based on the activation of photosensitizer when exposed to light resulting in the generation of reactive molecular species which is toxic to target tissue. The photodamage of targeted cellular and subcellular tissues to this therapy depends upon the presence of photosensitizer to the affected domain.

Here they prepared two liposomal formulation benzoporphyrin derivatives (BPD) Visudyne and lipid conjugate of BPD with photosensitizer for targeting the different loci in mitochondria, lysosome, and endoplasmic reticulum using single light wavelength. The groups studied the photodamage of three organs mediated via BPD liposomal preparation and compared with photodamage caused by alone photosensitizer and found that BPD-mediated photodestruction was significantly higher than photosensitizer formulation alone (Rizvi et al., 2019).

Sadzuka et al. illustrated the Zn-complexed coproporphyrin I (ZnCPI) liposomalization that act as PDT photosensitizer. It was suggested that the ZnCPI liposome with laser irradiation had effective anti-tumor efficacy at pH 4.6 with minimal side effects (Sadzuka et al., 2007).

9.4.2 Porphyrosome

Lipid-based nanocarriers, viz., liposomes, are deliberated to be one of the most flourishing nanomedicines in tumor therapy. A number of liposomes based on nanomedicine have been developed and commercialized so far, viz., DaunoXome, Doxil, Marqibo, Depocyte, Mepact, etc. The building block of liposomes are phospholipids, viz., phosphatidylcholine, which provides high biodegradation and hence biocompatibility to the nanocarrier. However, the applicability of unmodified nanocarriers or conventional liposomes is limited in providing therapy to heterogeneous tumors. For surface modification, liposomes typically require incorporation of ligand/diagnostic agent or fluorescent tag to trace the tumor locality and precise targeting and tracing their pharmacokinetic and biodistribution (Xue et al., 2019).

In this perspective, Lovell and associate developed porphyrosome which was a porphyrin-based multifunctional liposome. The porphyrin-lipid conjugate assembly demonstrated mean particle size of 100 nm for drug delivery in vitro. The porphyrosome demonstrated excellent photoacoustic imaging and near-infrared (NIR) fluorescent imaging properties that allowed sensitive visualization of tumors on the lymphatic system in animal models. The NIR fluorescence property of porphyrin restored after liposome dissociation and helpful in low fluorescent imaging. The organic nature of porphyrosomes makes them degradable enzymatically and cause low acute toxicity at a dose of 1000 mg/kg administered intravenously. The tumor cell accumulation of porphyrosomes was traced out in xenograft-mice model and caused tumor eradication by induction of laser irradiation thereby photothermal tumor ablation. Therefore, optical properties and biodegradability and biocompatibility of porphyrosomes as organic nanoparticles were potential in multimodal imaging and therapy (Lovell et al., 2011).

9.5 Porphyrin Polymeric Drug Delivery

To overcome the drawback of conventional photosensitizer (PS), several studies integrated PS into nanoparticles. As a rule most of the PDT nano-fabrications require potential uptake by the target cell for causing the lethal effect to the cancer cells. Therefore, the PDT efficacy generally largely depends on the % cell uptake and translocation of PS within the cells. Typically, the poor efficacy of anti-cancer therapeutics could be due to either low or inadequate cell uptake or drug efflux from cancer cells. In this concern, a functional plasma membrane exhibiting the control of transporting drug substances is used as a barrier layer for PDT-assisted cancer therapy. The surface modification of nanoparticles with ligands greatly enhances cell uptake process due to specific interaction of ligands with cell surface receptors. However, therapeutic efficacy is still limited owing to receptor density and overexpressed receptor-ligand binding (Rosenkranz et al., 2000; Wang & Thanou, 2010). Using PS, the possibility of efficient cancer cell death is more due to diverse subcellular location of PS in lysosome, Golgi apparatus, cell membrane, mitochondrion, and nucleus (Benov, 2015). Therefore, Jia et al. addressed the problem of low cell uptake by designing PEG-chitosan by conjugating with protoporphyrin IX (PpIX) as photosensitizer with nanodrug release controlled by plasma membrane. The resulting nano-conjugate formed GC-PEG-PpIX that self-assembled into core-shell nanoparticles (NPs).The porphyrin (PpIX) moieties show fluorescence due to π-π bond quenching under laser irradiation in aqueous solution and produce oxygen singlet. The enormous production of oxygen singlet enables the leakage of plasma membrane resulting in an influx of extracellular nanodrug into cells which govern cell death. Moreover, the injection of GC-PEG-PpIX particles produces the physical interaction with tumor cells and shows pronounced fluorescence in vivo at the target tumor site. Additionally, accumulation of nanoparticles at tumor site and enhanced

tumor retention of GC-PEG-PpIX nanoparticles indicated potential imaging-guided PDT (Jia et al., 2017).

9.6 Porphyrin-Based Upconversion Nanoparticle

Rieffel et al. designed a novel theranostic paradigm of nanoparticles having two active entities that could be used to examine the imaging in diverse modalities. Owing to the versatility and deep, low background imaging, ultraconversions (UCNPs) have appealed considerable concern nowadays. Recently, they demonstrated that porphyrin-phospholipid (PoP)-coated multimodal UCNPs can be used as theranostic nanocarriers. The designed upconversion nanoparticle claimed to possess the both fluorescence and photoacoustic properties (Rieffel et al., 2015). Further based on the porphyrins copper affinity, nanoparticles can be made as PET and CL imaging by incubating nanoparticle copper (Liu et al., 2012). The UCNP was rationally designed for near-infrared luminescence imaging and computed tomography. Due to their great diversity and inclination and strong imaging at low background, PoP-UCNPs were developed via surfacing oleic acid covered UCNPs, through phospholipids mediated thermal biodegradation to disseminate in aqueous solutions (Boyer et al., 2006). Moreover, thin layer of PoP-UCNPs accompanying different ratios of PoP to PEG-lipid was hydrated with aqueous solution and developed stable and dispersible nanoparticles with controlled sonication. The PoP-UCNPs surface coating with 80% PoP and 20% PEG-lipid indicated mean particle size of 74 ± 3.6 nm using transmission electron microscopy; low polydispersity index (0.12) showed minimal aggregation post surface modification process. The electron micrograph studies without negative staining not observing PEG coating demonstrated particle diameter near to 60 nm. The other electron micrographs revealed clearly shell (core) structure and X-ray spectrum of the UCNP. The UCNPs showed NIR emission to ~800 nm and excitation wavelengths at 980 nm.

9.7 Porphyrin-Based Inorganic Nanoparticle for Photodynamic Therapy

9.7.1 Porphyrin-Based Silica Nanoparticles

Cao et al. developed pH-sensitive DOX-loaded mesoporous hollow silica nanoparticle (HMSN) functionalized with folic as a nanocarrier for photothermal therapy (PTT) of liver cancer. The in vitro characterization of TEM revealed that nanoparticles were spherical, hollow, and monodispersed and the average particle size was ~140 nm (Fig. 9.1). In vitro drug release experiments were conducted in phosphate buffer saline (PBS) pH 4 and 7.4 at a temperature of 37 °C. The DOX concentration

in the withdrawn samples was estimated by UV-spectrophotometer (UV-2000, Unico, Franksville, WI) 490 nm of set wavelength. For another group exhibiting laser irradiation (NIR), the sample was subjected to 808 nm laser beam 2.0 W/cm^2 for a time interval of 10 min, and the release profile was investigated. All experiments were repeated in triplicate ($n = 3$). The drug release experiment showed pH-triggered release behavior. The HMSN and HPCF preparation cytotoxicity was evaluated by MTT assay indicated in Fig. 9.2a, indicating 90% of cell viability post 48 h treatment with HMSN and HPCF. It was also indicated that these preparations are biologically safe (Cao et al., 2020).

In the cytotoxicity study as shown in Fig. 9.2b, apoptosis of cells caused by DOX-HPC and DOX-HPCF were significantly higher than plain DOX. At DOX concentration of 250 ng/ml, the cell viabilities were 64.5 ± 2.9% and 43.2 ± 1.9% corresponding to formulation DOX-HPC and DOXHPCF compared to plain DOX 71.9 ± 1.3% at the same concentration. The cell viabilities through NIR-laser irradiation-mediated DOX-HPC and DOX-HPCF formulation were reduced to 53.7 ± 1.9% and 41.4 ± 1.0%, respectively. Further, results demonstrated these formulations showed concentration-dependent cell viabilities and NIR laser radiation-assisted DOX-HPCF and indicated strongest inhibition of cell growth and

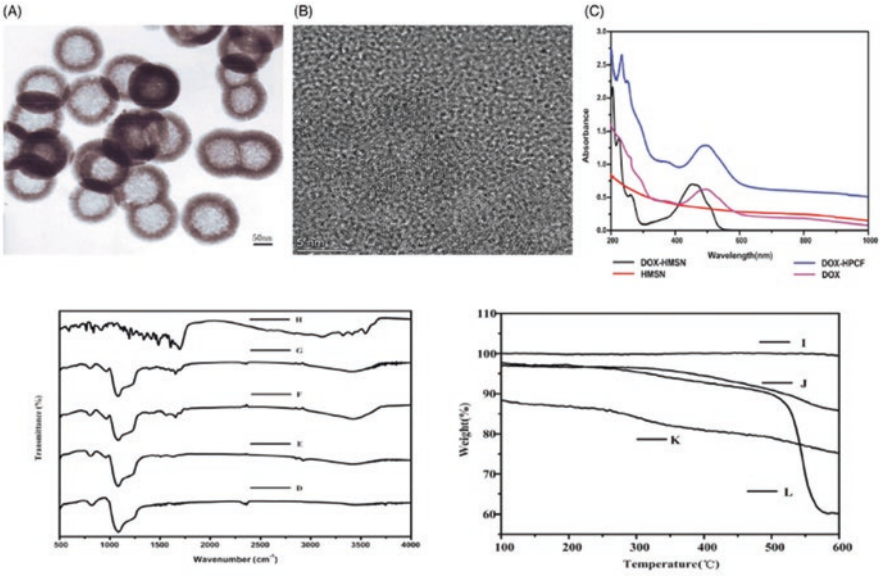

Fig. 9.1 The TEM image of HMSN (**a**); The TEM image of Carbon Quantum Dots (**b**); UV absorption spectrum of DOX, HMSN, DOX-HMSN, and PTT-assisted DOX-hollow mesoporous silica nanoparticle (DOX-HPCF) aqueous dispersion (**c**). The FTIR spectrum of HMSN (**d**); HP (**e**); HPC (**f**); HPCF (**g**); Folic acid (**h**); TGA curves of HMSN (**i**); HP (**j**); HPC (**k**); HPCF (**l**). (Reproduced from Open Access Journal under the term of Creative Commons Creative Commons Attribution License (Cao et al., 2020))

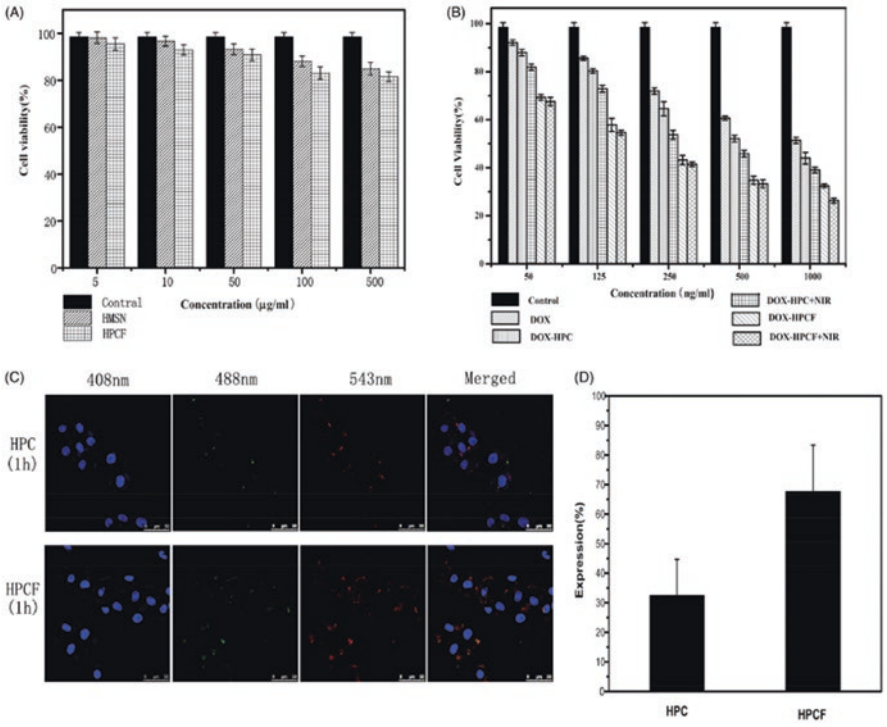

Fig. 9.2 The cell viability of SMMC-7721 cells incubated with HMSN, HPCF (**a**). The cell viability of SMMC-7721 cells incubated with DOX, DOX-HPC, DOXHPCþNIR, DOX-HPCF, and DOX-HPCFþNIR for 48 h (**b**). Data represented as mean ± SD ($n = 6$). Confocal laser scanning microscopy (CLSM) images of SMMC-7721 cells treated with HPC and HPCF for 1 h, respectively (**c**). The fluorescence intensity of SMMC-7721 cells treated with HPC and HPCF (**d**). (Reproduced from Open Access journal under the term of Creative Commons Creative Commons Attribution License (Cao et al., 2020))

proliferation and better therapeutic efficacy. DOX-HPCF-mediated NIR-laser radiation demonstrated potential cytotoxic effect by concomitant folate targeting and photothermal action.

In Fig. 9.2c, the cell uptake study established that DOX-HPCF is efficiently delivered to SMMC-7721 cells and inhibited their growth significantly. The SMMC-7721 cell fluorescence intensity posttreatment with HPC and HPCF are shown in Fig. 9.2d. The anti-tumor study indicated that laser light-assisted DOX-HPCF inhibited tumor growth significantly in vivo. Thus, HPCF could be promising in photothermal therapy of liver cancer (Cao et al., 2020).

9.8 Nanoemulsion-Based Porphyrin Shell in Cancer Theranostic

Hou and associates developed a nanoemulsion with a porphyrin shell (NewPS) by assembling porphyrin salt surrounding the oil core of nanoemulsion. The in vitro characterization observed splendid colloidal stability against alteration in temperature, pH, and agitation. The droplet size of NewPS was ~100 nm with spherical geometry. The NewPS system was compiled to various salts of porphyrin and low, high density oils, able to co-load various chemotherapeutic agents including paclitaxel. The optical tune up could only be achieved from nanostructure of porphyrin salt shell NewPS composed of pyropheophorbide a mono-salt (PyroNewPS) had an uniform aggregates shell of porphyrin which enable to generate a narrow absorbance in the wavelength range of 671–715 nm. The fluorescence and photodynamic activity of porphyrin shells restored post dissociation of nanostructure. Due to the excellent photoacoustic imaging at 715 nm by intact NewPS as well as fluorescence at 671 nm by dissociated NewPS of porphyrin shell nanostructure, it was prosperously traced the accumulation of NewPS and their disruption in mice carrying KB tumors for efficacious photodynamic therapy. Additionally replacing the oil core novel component Lipiodol® gave CT contrast, while encapsulating paclitaxel into NewPS facilitates drug release. Thus, the NewPS system could be a novel nanoplatform for multimodal cancer therapy-associated cancer diagnosis, image-guided drug release, and phototherapy (Hou et al., 2019).

9.9 Porphyrin-Armored Gold Nanoparticle

The therapeutics from the nanocarrier selectively internalize inside the target cells accompanied with endocytosis and thus deliver the drug to the nucleus of the target cells. The engraft of TPPS on the gold nanoparticle surface furnish them excellent biostability and biocompatibility of nanoparticle. Porphyrin forms co-ordinate bond between the nitrogen of pyrrole ring with gold metal yielding a strong association complex. DOX-loaded nanocomposite (DOX@TPPS-AuNPs) showed potential cell uptake with minimized drug efflux in multidrug resistance brain tumor, thus enhancing the retention and efficacy of DOX within tumor cells. It has been reported that therapy was ~9 times more potent in cell apoptosis mediated via acidic pH. The porphyrin gold core exhibited 90% encapsulation efficacy with DOX in which drug was non-covalently associated with nano-surface and tightly linked under physiological conditions but efficiently delivered up to ~81% of DOX at lower pH environment. The finding suggested that DOX-loaded TPPS-AuNPs was potential to prevent tumor metastasis, invasion, and proliferation and could ameliorate DOX efficacy against the target tumor. Therefore, under high drug entrapment and precise targeting under acidic pH and the intracellular release of DOX made the gold

nanoparticle TPPS-AuNPs an excellent magic bullet for therapeutic intervention in cancer therapy (Bera et al., 2018).

9.10 Porphyrin Metal Nanoshell

The current growing interest for biomedical uses of metal nanoshell toward targeted therapy of cancer employing nano-photothermal approaches. This study synthesized folic acid (FA)-tagged silica@gold core shell nanoparticle (FA-SiO_2@AuNPs) to make better melanoma cancer therapy. The developed nanomaterials characterized in vitro. The characterization study expressed that FA-SiO_2@AuNPs was consistent, spherical morphology with particle size of ~73.7 nm. The cell uptake of FA-SiO_2@AuNPs was measured 47.7% into melanoma cells, A375 by application of the inductively coupled-plasma technique. The cell line study of the nanoparticles on human dermal fibroblast (A375 and HDF) was investigated that showed pronounced cytotoxicity against HDF cell line. The cytotoxicity and flow cytometry study observed that A375 cell viability posttreatment with SiO_2@Au and FA-SiO_2@AuNPs significantly decreased to 31% and 16%, respectively. The higher toxicity of said cells were observed after near-infrared (NIR) laser exposure to 808 nm when the cells incubated with targeted FA-SiO_2@AuNPs compared to untargeted SiO_2@AuNPs. Moreover, the about 64% higher cell death was recorded for A-375 cells applying FA-SiO_2@AuNPs and photothermal treatment compared to photothermal therapy alone. It was concluded that FA-SiO_2@AuNPs has shown significant impact of photothermal therapy in melanoma treatment.

9.11 Carbon Dots (CDs)

In the recent past, carbon nanomaterials have received extensive attraction for valuable application in biomedical imaging (Zhu et al., 2013), fluorescence ink (Qu et al., 2012), and optoelectronic devices (Qu et al., 2016). The physicochemical properties of the material are of very much interest due to the excellent biocompatibility, tunable fluorescence properties, high quantum yield, tunable fluorescence properties, as well as nanosize; carbon dots (CDs) are considered as the emerging nanomaterials for bioimaging and in cancer therapy.

The conventionally developed CDs had shown emissions triggered by ultraviolet, visible, blue light in shorter wavelengths less than 800 nm, thus limiting the in-depth imaging in vivo. Li et al. (2019) design novel carbon dots (CDs) that has shown luminescence at 900–1200 nm region with high yield, lower toxicity, high photostability, and provided desirable biological and optical imaging as well as proven effective for in vivo NIR-II bioimaging. In vivo study that more than 60% of CDs were eliminated from mouse urine post 6 h of administration showed rapid renal clearance of CDs. Moreover, the developed CDs exhibited 30.6%

photothermal efficiency, creating them excellent nanomaterials as thermal ablation therapy of cancer. The findings suggested that designing a multifunctional CD-based theranostic platform integrated with advanced NIR-II bioimaging could be potential for diagnosis and photothermal cancer therapy (Li et al., 2019).

Wu and associates fabricated a surface functionalized with cetuximab of porphyrin-engrafted CDs that enable to identify and target cancer-specific cells which has shown overexpression of epidermal growth factor receptor. The developed CDs could improve amplitude of PA signals and conserve substantial signal animal bodies for 12 h. Therefore, the CDs could be promising to provide sustained long-term effect and precise monitoring in efficient photodynamic therapy in breast cancer (Wu et al., 2018).

9.12 Porphyrin Carbon Nanodots

Wu F and associates synthesized multifunctional nanoparticle integrating the light-absorbing moiety porphyrins for imaging and therapeutic efficacy against cancer cells. They designed synthetic approach for porphyrin-implanted carbon nanodots (PNDs) modified pyrolysis of 5,10,15,20-tetrakis (4- aminophenyl) porphyrin (TAPP) with citric acid (CA) at ambient temperature. The developed carbon nanodots apart from showing good biocompatibility and stability also demonstrated unique characteristics of strong absorption in ultraviolet, infrared absorption due to porphyrin macrocycle ultimately effective photodynamic therapy. The unique property of the PNDs, i.e., absorption in near-infrared regions, led to a good contrast agent due to photoacoustic imaging and deeper penetration of cancer cells. The nanodots further conjugated with cetuximab, i.e., cetuximab-ligated porphyrin-based carbon nanodots (C225-PNDs) for precise targeting of overexpressed receptor EGFR led to potential photodynamic therapy at excitation wavelength of 800 nm. The study of photoacoustic tumor ablation capability of C225-PNDs evaluated in vivo and confirmed complete tumor ablation in mice MDA-MB-231 cells (Wu et al., 2018).

The PNDs were developed with selective pyrolysis of TAPP with citric acid as shown in Fig. 9.3 (Hu et al., 2015). The porphyrin macrocycle ring was entrapped into developed carbon nanodots without modification in the structural integrity as the reaction temperature rose to 200 °C from normal room temperature. The encapsulation amount of porphyrin was 232μg per mg of PNDs obtained from the calibration plot of the optical density of TAPP using UV-Visible spectrophotometry. The aqueous solution of PNDs remains stable at ambient temperature for 60 days of storage and did not precipitate out or show aggregation suggesting their awesome colloidal stability. The developed PND surface was functionalized using PEG diamine; PEG1500N make PEG-layered nanodots (NH2-PNDs) with free NH_2 groups. Thereafter, cetuximab bonded covalently to NH_2-PNDs applying a modified EDC-NHS reaction and yielded the C225-PNDs.

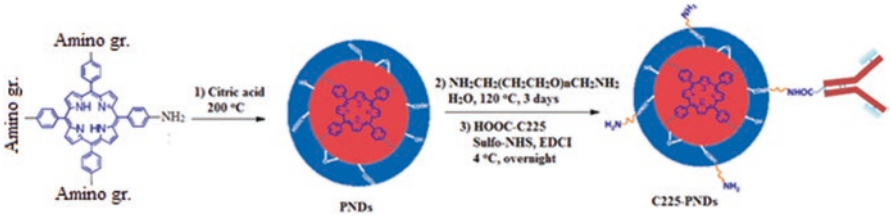

Fig. 9.3 Pathway and synthesis of PNDs and C225-PNDs. (Reprinted with permission (Wu et al., 2018). Copyright © 2018, American Chemical Society)

The particle size and morphology of PNDs was investigated by using transmission electron microscopy (TEM). The PNDs were well dispersed and spherical nanocomposites structure as shown in Fig. 9.4a with mean diameter of 3.3 nm. The HRTEM image particle size has a distinct lattice fringes as indicated in Fig. 9.4b. The TEM indicated the average particle size of C225-PNDs were 11 nm as shown in Fig. 9.4c were in agreement with results obtained from dynamic light scattering analysis 12.1 ± 3.5 nm Fig. 9.4d.

As indicated in Fig. 9.5a, b, the PA signals of PNDs and C225-PNDs in water increased with increase in concentrations. Due to pH-dependent absorption of PNDs in the NIR region, the PA response with varying pH of buffer solutions was also investigated. In Figs. 9.4d and 9.5c, the PNDs showed strong PA signals at 686 nm in a slightly acidic environment, and the intensity of PA signal showed fragile decline with increase in pH from 6 to 7.

As the pH rises from 7 to 8, the amplitude of PA signal of PNDs reduced by 7 times; this could be attributed to deprotonation of the porphyrin in PNDs within alkaline medium. Thus, the pH-responsive nanoprobe with PNDs concept could be potential for PA imaging of tumor acidic microenvironment. The results clearly demonstrate that both PNDs and C225-PNDs could be used as photoacoustic imaging.

The C225-PNDs cell viabilities at concentration of 100μg/mL subjected to irradiation were estimated 22.3% and 15.2% cell line of HCC827 and MDA-MB-231, respectively. Moreover, the treatment of both the cell lines with C225-PNDs at these concentrations lacking irradiation enabled them to survive 85% of cells, demonstrating that C225-PNDs had insignificant cytotoxicity alone against these cells.

Adversely, after incubation of H23 or HBL-100 cells with 0–100μg/mL concentration of C225-PNDs for 8 h along with exposing light irradiation, the cytotoxicity % were similar as earlier without irradiation. The results precisely demonstrated that lack of potential uptake of C225-PNDs by these cells probably due to lack of overexpressed receptor EGFR, which was in agreement with LSCM study of C225-PNDs in these cells as indicated in Fig. 9.6e, f. Further, overexpression level of the EGFR receptor on cell membrane allowed selective uptake of C225-PNDs in HCC827 and MDAMB-231 cancer cells owing to specific drug targeting into tumor cells, and light irradiation led to image monitored tumor ablation. HCC827 cells are shown in Fig. 9.6e, and MDA-MB-231 cells in Fig. 9.6f on the first row exhibited

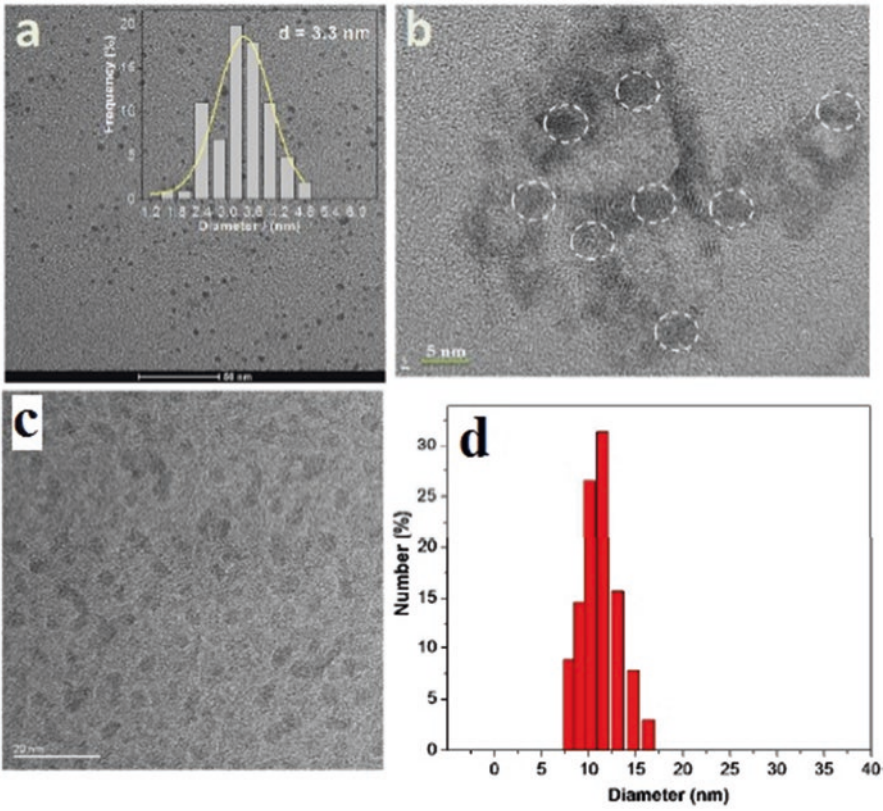

Fig. 9.4 (**a**) TEM image of PNDs with a corresponding size distribution histogram; (**b**) HRTEM images of PNDs; (**c**) TEM image of C225-PNDs and (**d**) TEM image of C225-PNDs. (Adapted with permission (Wu et al., 2018). Copyright © 2018, American Chemical Society)

strong fluorescent signals (red) post 8 h of incubation with C225-PNDs. Conversely, red fluorescent signals were observed very weak in H23 and HBL-100 cells under the similar condition as indicated in the second row of Fig. 9.6e, f.

The prepared C225-PNDs indicated an absorption band in extended NIR region, and their photoacoustic imaging property estimated further in vivo employing breast tumor MDA-MB-23 in mice. For induction of cancer, mice were treated with intratumoral C225-PNDs injection at dose of (7 mg/mL, 100μL). The photoacoustic images of tumors recorded when their volume achieved at 500 mm^3 at various time intervals. The results interpreted that in the complete imaging process, C225-PNDs maintained uniform PA signal post long-term systemic circulation (Fig. 9.7a). The signal intensity of the desirable region demonstrated that signal with strong intensity that ended for 24 h intimating contrast and enhanced photoacoustic imaging and diagnostic application.

When treatment given individually by C225-PNDs/PBS/irradiation with NIR laser growth of all the tumor remains interrupted, one mice died due to tumor

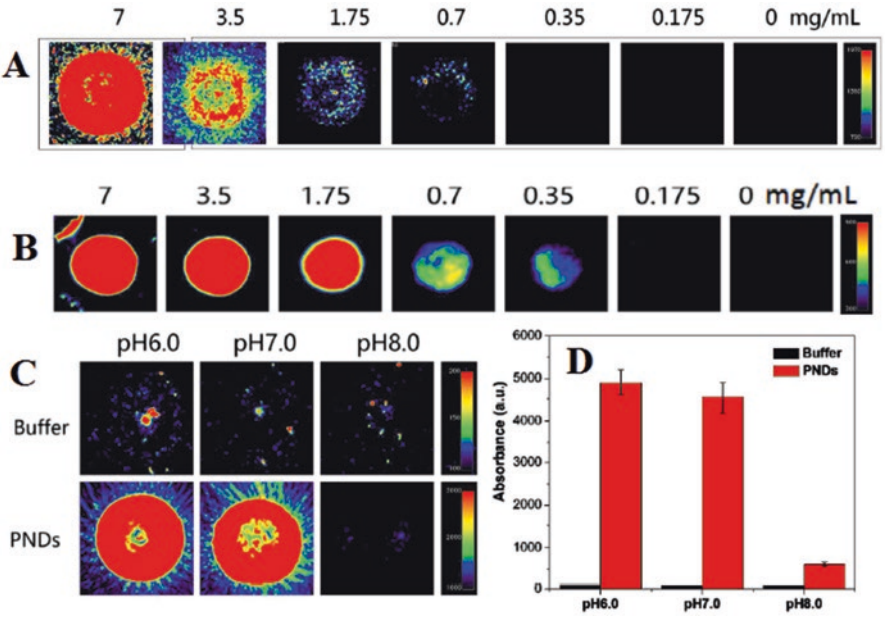

Fig. 9.5 (**a**) The photoacoustic signal (PA) imaging of PNDs aqueous solution with different concentrations (0–7 mg/mL) under 686 nm; (**b**) PA imaging of the aqueous solution of C225-PNDs with different concentrations (0–7 mg/mL) under 686 nm; (**c**) PA imaging of PNDs dispersed in buffer solution (1.75 mg/mL) with different pH values (pH = 6.0, 7.0 and 8.0); (**d**) PA signal intensity of PNDs dispersed in buffer solution (1.75 mg/mL) with different pH values (pH = 6.0, 7.0 and 8.0). (Adapted with permission (Wu et al., 2018). Copyright © 2018, American Chemical Society)

burden after 1 month post receiving PBS + irradiation as shown in Fig. 9.7b. One of the three mice in PBS plus irradiation group died of tumor burden on the 30th treatment day. After 40 days of treatment, tumor volume was increased up to 25 times than initial stage demonstrating that impact of C225-PNDs/laser irradiation alone was negligible in retarding tumor growth. Further, tumor efficacy of C225-PNDs, PBS, or irradiation with NIR laser was evaluated and found that single treatment with either of the above had effectively regressed the tumor growth. However, treatment with combinatorial C225-PNDs and laser irradiation at 808 nm showed significant inhibition in tumor growth (Fig. 9.7c). Post combinatorial treatment two mice recovered within 1 month (Fig. 9.7d).

The porphyrin macrocycle-loaded carbon nanodots generated laser irradiation which damages the tumor. Posttreatment schedule the mice were sacrificed and different organs examined after staining with dyes. As indicated in Fig. 9.7e, the tumor cells were significantly damaged, while treatment with C225-PNDs + laser irradiation and normal cells/tissues were unaffected confirmed by examination of different organs and no conspicuous side effects over the PBS group. The study suggested

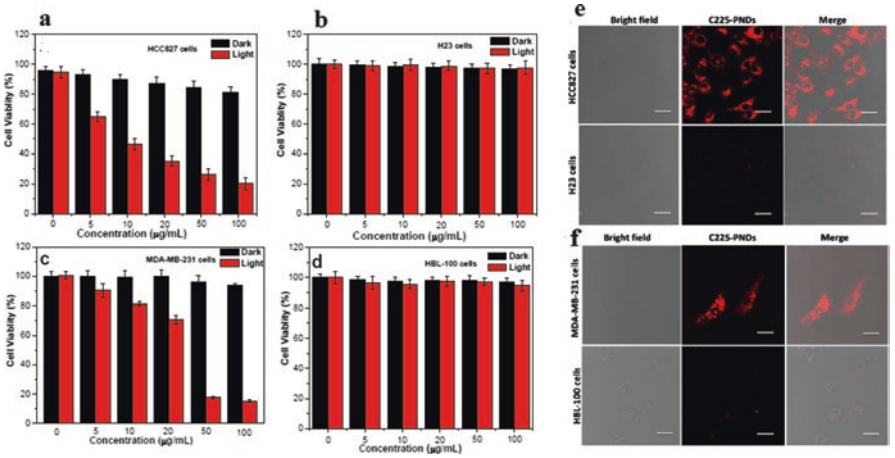

Fig. 9.6 HCC827 (**a**), H23 (**b**), MDA-MB-231 (**c**), HBL-100 (**d**) cells viability at different concentrations (0, 5, 10, 20, 50, and 100μg/mL) of C225-PNDs for 8 hours at 37 °C without or with irradiation for 30 min with a white light (6.5 mW/cm^2). (**e**) Laser scanning confocal microscopy images (excited at 488 nm laser) of HCC827 and H23 cells (**a**); and MDA-MB-231 and HBL-100 cells (**f**) incubated with C225-PNDs at a concentration of 0.5 mg/mL in the cell culture medium for 8 h at 37 °C (Scale bar = 20μm). (Adapted with permission (Wu et al., 2018). Copyright © 2018, American Chemical Society)

that C225-PNDs could provide excellent photoacoustic contrast, photodynamic, and therapeutic effect for cancer theranostic promisingly.

9.13 Porphyrin Loaded Self-Assembled Nanosheet

Yuan et al. developed drug delivery system which lacked excipients for potential diagnosis and therapy in cancer as nanotheranostics. Herein they used infrared photosensitizer with naked chemotherapeutic agents. The building block of the delivery system designed conjugating 4-chemotherapeutic agent (7-ethyl-10-hydroxy-camp tothecin, SN-38) via covalent bond with photosensitizer (porphyrin) through ester linkage, which furnished 100% drug delivery with excellent imaging and therapy in cancer. In synthesis process, (23.7 mg, 0.03 mmol) of TCPP, (61 mg, 0.36 mmol) of 6-Cl-HOBt, (55.9 mg, 0.36 mmol) of EDC, and (63μL, 0.36 mmol) of DIEA were dissolved in 10 ml of dried N,N-dimethylformamide (DMF), and the mixture agitated at room temperature for half an hour for terminal carboxyl group activation. Then (117.6 mg, 0.3 mmol) solution of SN-38 was added in 5 mL dried DMF. The final mixture was agitated at room temperature, and esterification reaction was examined by thin layer chromatography (TLC). The reaction mixture was washed with H_2O/CH_2Cl_2 for 3 times and the organic phase evaporated till dried. Further, the resulting substance was purified using column chromatography to get the purple

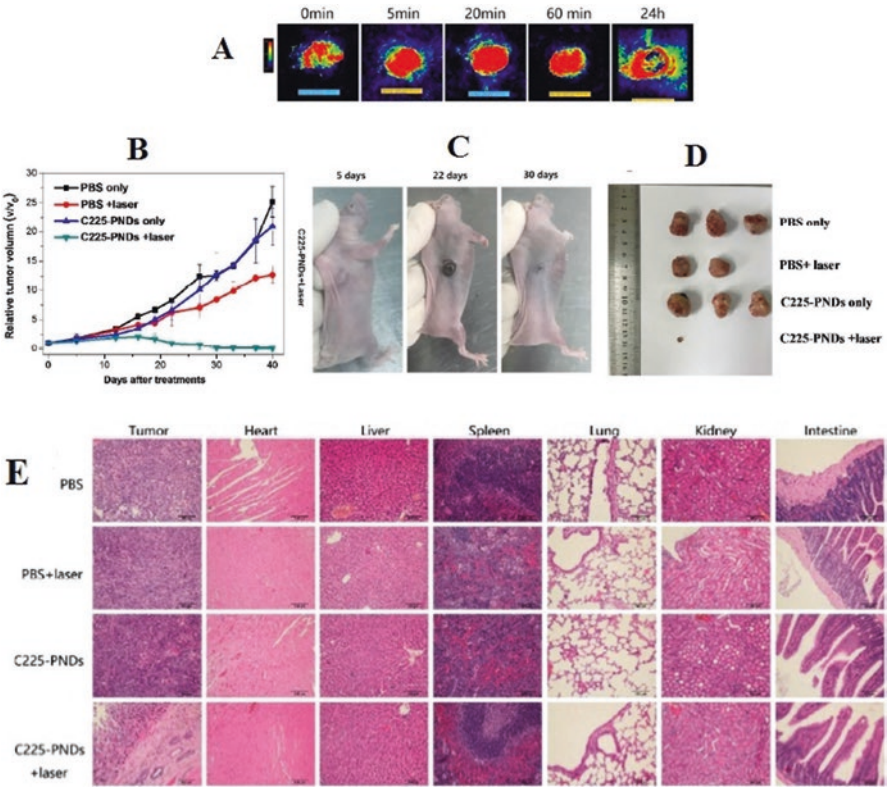

Fig. 9.7 (**a**) PA Imaging of C225-PNDs in tumor at 0, 5, 20, 60 min, and 24 h after intratumoral injection (7 mg/mL, 100μL); (**b**) Relative PA intensity of C225-PNDs in tumor at 0, 5, 20, 60 min, and 24 h after intratumoral injection (7 mg/mL, 100μL); (**c**) Relative tumor volume of the tumor-bearing mice of the different groups after treatment ($n = 3$, $P < 0.05$ for each group); (**d**) Photographs of the tumor-bearing mice after different days (5, 22, and 30 days) of treatments with C225-PNDs+laser (λex = 808 nm); (**e**) Tumor size of the different groups after treatment for 30 days; (**f**) Hematoxylin and eosin (H&E)-stained slices of the tumor, heart, liver, spleen, lung, kidney, and intestines in mice after treatments. Scar bar: 100μm. (Reproduced with permission (Wu et al., 2018). Copyright © 2018, American Chemical Society)

TCPP (SN-38)4 prodrug. The molecular structure of the compound was estimated using proton nuclear magnetic resonance and mass spectroscopy, and thereafter nanoformulation of conjugate was developed. The conjugates were self-assembled into nanosheets (PS NSs), and excellent stability was recorded for 20 days in aqueous solution. The drug release phenomena from PS NSs monitored via fluorescence of SN-38. In vitro fluorescent system indicated excellent anti-cancer activity owing to potential uptake along with synergistic diagnosis and chemotherapy (Yuan et al., 2001).

9.14 Conclusion

The cancer nanotheranostics has acquired rapid growth by exploiting smart nanocarriers in drug delivery and biomedical application. The aim of the nanotheranostic development is based on improving therapeutic efficacy through precise diagnosis and treatment of the cancer along with providing safety and reducing the adverse effects of the therapeutic regimen. Moreover, this area should further be comprehensively explored based on the various novel porphyrin-based drug delivery nanocarriers to see the long-term biological effect and therapeutic advantages. This chapter briefly discussed uses of porphyrin-based smart nanomaterials and their delivery for diagnosis and simultaneous therapy of most devastating disease cancer.

The pharmacokinetics, biodistribution, biocompatibility, biodegradability, cell uptake, and chronic toxicology profile of porphyrin tagged nanoparticle should be investigated in detail. This is of course challenging for scientists worldwide to design and develop the theranostic nanomaterials that enable to bring bench to the bedside and translate in clinics. The work on various porphyrin nanocarriers discussed here looks promising as indicated in their therapeutic outcomes and yet more to be needed in the future to explore their potential utility in cancer therapy.

References

Akhter, M. H.. (2017). Multifunctional nanocargo in the treatment modalities in tumor microenvironment. Pharma Focus Asia [cited 2017 April]. Available from: https://www.pharmafocusasia.com/articles/multifunctional-nano-cargo-for-drugdelivery-to-tumor-cells.

Akhter, M. H., Alam, M. S., & Minhaj, M. A.. (2018). Smart nano-enabled drug carrier in combating tumor development and progress. *Pharma Focus Asia* [cited 2018b September]. Available from: https://www.pharmafocusasia.com/articles/smart-nanoenabled-drug-carrier-in-combating-tumor-development.

Akhter, M. H., & Amin, S. (2017). An investigative approach to the treatment modalities of squamous cell carcinoma. *Current Drug Delivery, 14*, 597–612.

Akhter, M. H., Beg, S., Tarique, M., Malik, A., Afaq, S., & Choudhry, H. (2020). Receptor-based targeting of engineered nanocarrier against solid tumors: Recent progress and challenges ahead. *Biochimica et Biophysica Acta (BBA) – General Subjects, 1865*(2), 129777. Available online 29 October 2020a.

Akhter, M. H., Madhav, N. S., & Ahmad, J. (2018). Epidermal growth factor based active targeting: A paradigm shift towards advance tumor therapy. *Artif Cells Nanomed Biotech, 46*(2), 1–11.

Akhter, M. H., Nomani, S., & Kumar, S. (2020). Sonication tailored enhance cytotoxicity of naringenin nanoparticle in pancreatic cancer: Design, optimization, and in vitro studies. *Drug Development and Industrial Pharmacy, 46*(4), 1–14.

Akhter, M. H., et al. (2020). Molecular targets and nanoparticulate systems designed for the improved therapeutic intervention in glioblastoma multiforme. *Drug Research, 71*(3), 122–137. Accepted, 19 October, 2020b.

Benov, L. (2015). Photodynamic therapy: Current status and future directions. *Medical Principles and Practice, 24*, 14–28.

Bera, K., Maiti, S., Maity, M., Mandal, C., & Maiti, N. C. (2018). Porphyrin–gold nanomaterial for efficient drug delivery to cancerous cells. *ACS Omega, 3*(4), 4602–4619.

Blau, R., Krivitsky, A., Epshtein, Y., & Satchi-Fainaro, R. (2016). Are nanotheranostics and nanodiagnostics-guided drug delivery stepping stones towards precision medicine? *Drug Resistance Updates, 27*, 39–58.

Boyer, J.-C., Vetrone, F., Cuccia, L. A., & Capobianco, J. A. (2006). Synthesis of colloidal upconverting NaYF4 nanocrystals doped with Er^{3+}, Yb^{3+} and Tm^{3+}, Yb^{3+} via thermal decomposition of lanthanide trifluoroacetate precursors. *Journal of the American Chemical Society, 128*, 7444.

Cao, Y., Wu, C., Liu, Y., Hu, L., Shang, W., Gao, Z., & Xia, N. (2020). Folate functionalized pH-sensitive photothermal therapy traceable hollow mesoporous silica nanoparticles as a targeted drug carrier to improve the antitumor effect of doxorubicin in the hepatoma cell line SMMC-7721. *Drug Delivery, 27*(1), 258–268.

Chen, B., Pogue, B. W., & Hasan, T. (2005). Liposomal delivery of photosensitising agents. *Expert Opinion on Drug Delivery, 2*(3), 477–487.

Chen, H., Zhang, W., Zhu, G., Xie, J., & Chen, X. (2017). Rethinking cancer nanotheranostics. *Nature Reviews Materials, 2*, 17024.

Chen, W., & Zhang, J. (2006). Using nanoparticles to enable simultaneous radiation and photodynamic therapies for cancer treatment. *Journal of Nanoscience and Nanotechnology, 6*(4), 1159–1166.

Hou, W., Lou, J. W. H., Bu, J., Chang, E., Ding, L., & Valic, M. (2019). Nanoemulsion with porphyrin shell for cancer theranostics. *Angewandte Chemie, International Edition, 58*(42), 14974–14978.

Hu, S., Trinchi, A., Atkin, P., & Cole, I. (2015). Tunable photoluminescence across the entire visible spectrum from carbon dots excited by white light. *Angewandte Chemie, International Edition, 54*, 2970–2974.

Hua, K., Yangab, Z., Zhang, L., Xie, L., Wang, L., Xu, H., Lee Josephson, L., Liang, S. H., & Zhang, M.-R. (2020). Boron agents for neutron capture therapy. *Coordination Chemistry Reviews, 405*, 213139.

Imran, M., Ramzan, M., Qureshi, A. K., Khan, M. A., & Tariq, M. (2018). Emerging applications of porphyrins and Metalloporphyrins in biomedicine and diagnostic magnetic resonance imaging. *Biosensors (Basel), 8*(4), 95. Published 2018 Oct 19.

Jia, H.-R., Jian, Y.-W., Zhua, Y.-X., Lia, Y.-H., Wang, H.-Y., Han, X., et al. (2017). Plasma membrane activatable polymeric nanotheranostics with self-enhanced light-triggered photosensitizer cellular influx for photodynamic cancer therapy. *Journal of Controlled Release, 255*, 231–241.

Jiang, F., Lilge, L., Grenier, J., Li, Y., Wilson, M. D., & Chopp, M. (1998). Photodynamic therapy of U87 human glioma in nude rat using liposome-delivered photofrin. *Laser in Surgery and Medicine, 22*(2), 74–80.

Kepczyński, M., Nawalany, K., Jachimska, B., Romek, M., & Nowakowska, M. (2006). Pegylated tetraarylporphyrin entrapped in liposomal membranes. A possible novel drug-carrier system for photodynamic therapy. *Colloids and Surfaces. B, Biointerfaces, 49*(1), 22–30.

Kievit, F. M., & Zhang, M. (2011). Cancer nanotheranostics: Improving imaging and therapy by targeted delivery across biological barriers. *Advanced Materials, 23*, H217–H247.

Lee, M. H., Kim, E.-J., Lee, H., Kim, H. M., Chang, M. J., Park, S. Y., Hong, K. S., Kim, J. S., & Sessler, J. L. (2016). Liposomal Texaphyrin Theranostics for metastatic liver cancer. *Journal of the American Chemical Society, 138*(50), 16380–16387.

Li, Y., Bai, G., Zeng, S., & Hao, J. (2019). Theranostic carbon dots with innovative NIR-II emission for in vivo renal-excreted optical imaging and Photothermal therapy. *ACS Applied Materials & Interfaces, 11*(5), 4737–4744.

Liu, T. W., MacDonald, T. D., Shi, J., Wilson, B. C., & Zheng, G. (2012). Intrinsically copper-64-labeled organic nanoparticles as radiotracers. *Angewandte Chemie, International Edition, 51*, 13128.

Lovell, J. F., Jin, C. S., Huynh, E., Jin, H., Kim, C., Rubinstein, J. L., Chan, W. C. W., Cao, W., Wang, L. V., & Zheng, G. (2011). Porphysome nanovesicles generated by porphyrin bilayers for use as multimodal biophotonic contrast agents. *Nature Materials, 10*, 324–332.

Nabil, G., Bhise, K., Sau, S., Atef, M., El-Banna, H. A., & Iyer, A. K. (2019). Nano-engineered delivery systems for cancer imaging and therapy: Recent advances, future direction and patent evaluation. *Drug Discovery Today, 24*, 462–491.

Nawalany, K., Rusin, A., Kepczynski, M., Filipczak, P., Kumorek, M., Kozik, B., Weitman, H., Ehrenberg, B., Krawczyk, Z., & Nowakowska, M. (2012, July 1). Novel nanostructural photosensitizers for photodynamic therapy: In vitro studies. *International Journal of Pharmaceutics, 430*(1–2), 129–140.

Obaid, G., Chambrier, I., Cook, M. J., & Russell, D. A. (2015). Cancer targeting with biomolecules: A comparative study of photodynamic therapy efficacy using antibody or lectin conjugated phthalocyanine-PEG gold nanoparticles. *Photochemical & Photobiological Sciences, 14*, 737–747.

Paszko, E., Ehrhardt, C., Senge, M. O., Kelleher, D. P., & Reynolds, J. V. (2011). Nanodrug applications in photodynamic therapy. *Photodiagnosis and Photodynamic Ther, 8*, 14–29.

Qu, S., Wang, X., Lu, Q., Liu, X., & Wang, L. (2012). A biocompatible fluorescent ink based on water-soluble luminescent carbon Nanodots. *Angewandte Chemie, International Edition, 51*, 12215–12218.

Qu, S., Zhou, D., Li, D., Ji, W., Jing, P., Han, D., Liu, L., Zeng, H., & Shen, D. (2016). Toward efficient orange emissive carbon Nanodots through conjugated sp2 -domain controlling and surface charges engineering. *Advanced Materials, 28*, 3516–3521.

Renner, M. W., Miura, M., Easson, M. W., & Vicente, M. G. (2006). Recent progress in the syntheses and biological evaluation of boronated porphyrins for boron neutron-capture therapy. *Anti-Cancer Agents in Medicinal Chemistry, 6*(2), 145–157.

Rieffel, J., Chen, F., Kim, J., Chen, G., Shao, W., Shao, S., et al. (2015). Hexamodal imaging with porphyrin-phospholipid-coated Upconversion nanoparticles. *Advanced Materials, 27*(10), 1785–1790.

Rizvi, I., Nath, S., Obaid, G., Ruhi, M. K., Moore, K., Bano, S., Kessel, D., & Hasan, T. (2019). A combination of Visudyne and a lipid-anchored liposomal formulation of benzoporphyrin derivative enhances photodynamic therapy efficacy in a 3D model for ovarian cancer. *Photochemistry and Photobiology, 95*(1), 419–429.

Rosenkranz, A. A., Jans, D. A., & Sobolev, A. S. (2000). Targeted intracellular delivery of photosensitizers to enhance photodynamic efficiency. *Immunology and Cell Biology, 78*, 452–464.

Sadzuka, Y., Iwasaki, F., Sugiyama, I., Horiuchi, K., Hirano, T., Ozawa, H., Kanayama, N., & Sonobe, T. (2007). Study on liposomalization of zinc-coproporphyrin I as a novel drug in photodynamic therapy. *International Journal of Pharmaceutics, 338*(1–2), 306–309.

Schmidt-Erfurth, U., & Hasan, T. (2000). Mechanisms of action of photodynamic therapy with verteporfin for the treatment of age-related macular degeneration. *Survey of Ophthalmology, 45*, 195–214.

Soni, K., Mujtaba, A., Akhter, M. H., et al. (2020). Optimisation of ethosomal nanogel for topical nano-CUR and sulphoraphane delivery in effective skin cancer therapy. *Journal of Microencapsulation, 37*(2), 91–108.

Takehara, Y., Sakahara, H., Masunaga, H., et al. (2002). Assessment of a potential tumor-seeking manganese metalloporphyrin contrast agent in a mouse model. *Magnetic Resonance in Medicine, 47*(3), 549–553.

Tsolekile, N., Nelana, S., & Oluwafemi, O. S. (2019). Porphyrin as diagnostic and therapeutic agent. *Molecules, 24*(14), 2669.

Wang, M., & Thanou, M. (2010). Targeting nanoparticles to cancer. *Pharmacological Research, 62*, 90–99.

Wu, F., Su, H., Cai, Y., Wong, W.-K., Jiang, W., & Zhu, X. (2018). Porphyrin-implanted carbon Nanodots for photoacoustic imaging and in vivo breast Cancer ablation. *ACS Applied Bio Materials, 1*, 110–117.

Xue, X., Lindstrom, A., & Li, Y. (2019). Porphyrin-based nanomedicines for cancer treatment. *Bioconjugate Chemistry, 30*(6), 1585–1603.

Yuan, Y., Bo, R., Jing, D., Ma, Z., Wang, Z., Lin, T.-Y., Dong, L., Xue, X., Li, Y., & Vicente, M. G. (2001). Porphyrin-based sensitizers in the detection and treatment of cancer: Recent progress. *Current Medicinal Chemistry – Anti-Cancer Agents, 1*(2), 175–194.

Zhang, P., Hu, C., Ran, W., Meng, J., Yin, Q., & Li, Y. (2016). Recent progress in light-triggered Nanotheranostics for cancer treatment. *Theranostics, 6*(7), 948–968.

Zhang, X., Lovejoy, K. S., Jasanoff, A., & Lippard, S. J. (2007). Water-soluble porphyrins as a dual-function molecular imaging platform for MRI and fluorescence zinc sensing. *Proceedings of the National Academy of Sciences of the United States of America, 104*(26), 10780–10785.

Zhou, Y., Liang, X., & Dai, Z. (2016). Porphyrin-loaded nanoparticles for cancer theranostic. *Nanoscale, 8*, 12394–12405.

Zhu, S., Meng, Q., Wang, L., Zhang, J., Song, Y., Jin, H., Zhang, K., Sun, H., Wang, H., & Yang, B. (2013). Highly Photoluminescent carbon dots for multicolor patterning, sensors, and bioimaging. *Angewandte Chemie, International Edition, 52*, 3953–3957.

Chapter 10
The Emerging Role of Exosomes as Cancer Theranostics

Gilar Gorji-Bahri and Atieh Hashemi

Contents

10.1 Introduction

Exosomes are emerging cellular nano-structures greatly considered for cancer therapeutics and diagnostics. They are double lipid layered products of the cell's endosomal compartment containing biological active molecules such as DNA, RNA, proteins, and lipids that come from exosomes' parent cells. Exosomes are secreted from almost all cells of the human body and exist in several biofluids like plasma, urine, saliva, cerebrospinal fluid, and breast milk. They are well-recognized as cell-cell communicators in which they are able to functionally deliver their content to recipient cells (Gorji-Bahri et al., 2018; O'Brien et al., 2020). Thereby, tumor cell-derived exosomes can transfer and spread their oncogenic features between cells in the tumor microenvironment. In this way, evidence has shown that exosomes facilitate tumor metastasis, progression, and drug resistance via transferring active molecules such as *MET* proto-oncogene (He et al., 2015; Yu et al., 2019), mir-501 (Liu, Lu, et al., 2019a), long noncoding RNA (lncRNAs) CCAL (Deng et al., 2020), STAT3, and FAS (Dorayappan et al., 2018). Thus, researchers have increasingly

G. Gorji-Bahri · A. Hashemi (✉)
Department of Pharmaceutical Biotechnology, School of Pharmacy, Shahid Beheshti University of Medical Sciences, Tehran, Iran
e-mail: gorji.b-pharma@sbmu.ac.ir; at_hashemi@sbmu.ac.ir

M. Saravanan, H. Barabadi (eds.), *Cancer Nanotheranostics*, Nanotechnology in the Life Sciences, https://doi.org/10.1007/978-3-030-74330-7_10

focused on mechanisms and factors that blockade the exosomes secretion to fight cancer malignancies. Exosomes are formed after passing the following four steps: first, intraluminal cell membrane budding resulted from endocytosis; second, the generation of multivesicular bodies (MVB) in the cytoplasm; third, the fusion of MVBs with the cell membrane; and fourth, the release of vesicles that are named exosomes into the intracellular space (Gorji-Bahri et al., 2018). Up to now, many genes of three different pathways, namely, Endosomal Sorting Complex Required for Transport (ESCRT) dependent, ESCRT independent, and Rab GTPases, are found to affect exosome biogenesis at each above step. For example, *ARF6* and *PLD2*, ESCRT independent molecules, control cell membrane budding and MVB formation (Ghossoub et al., 2014) as well as the cooperation of ESCRT I and II members that regulate the latter step (Gorji-Bahri et al., 2018). Moreover, Rab GTPases such as *RAB35* (Hsu et al., 2010) and *RAB27A* (Sinha et al., 2016) have been reported to affect the last step of exosome biogenesis that is docking and exosome secretion. Hence, targeting these genes via gene therapy approaches is considered a therapeutic method to decrease exosome secretion that results in the inhibition of tumor progression and metastasis. Moreover, several well-known drugs are also recognized to reduce exosome secretion such as ketoconazole, climbazole (Datta et al., 2018), and simvastatin (Kulshreshtha et al., 2019).

On the other hand, exosome content particularly RNAs and miRNAs is growingly and successfully considered as cancer biomarkers. Since exosomes are frequently accessible through biofluids in a noninvasive manner, they could be an applicable and useful source of biomarkers. Indeed, two lipid layers of tumor-derived exosomes protect their composition against degrading intracellular enzymes which result in reflecting their parent cells condition (O'Brien et al., 2020). The use of exosomal biomarkers has not only led to in vitro experiments but has also successfully entered the clinical stages. For instance, exosomal mir221-3p for early detection of cervical squamous cell carcinoma (Zhou et al., 2019), exosomal mir-122 as a diagnostics and prognostics biomarker for colorectal cancer (CRC) with liver metastasis (Sun et al., 2020), and exosomal mir-21 and mir-155 for discrimination of pancreatic ductal adenocarcinoma from chronic pancreatitis (Nakamura et al., 2019) are some of these exosomal-based discoveries in the field of cancer diagnosis. Moreover, ExoDx Prostate (Intelliscore) which assays the expression of specific mRNAs in urinary exosomes is now developed for the detection of patients with high-grade prostate cancer (Tutrone et al., 2020).

In this review, firstly we will explain exosomes biogenesis and composition followed by their roles in cancer progression. Thereafter, we will summarize recent efforts that focus on exosome secretion as a new therapeutic target. Next, exosomal cancer biomarkers will be discussed.

10.2 Exosome Biogenesis and Composition

Exosomes are natural lipidic bilayer nanovesicles with a size range of 30–150 nm and a density gradient of 1.13–1.19 g/ml (Gorji-Bahri et al., 2018). Johnstone and colleagues named these nanovesicles "exosome" for the first time in 1987 when they were working on reticulocyte maturation (Johnstone et al., 1987). During about two last decades, various aspects of exosomes have been studied growingly. As shown in Fig. 10.1, exosome generation begins with endocytosis in the cell plasma membrane which may occur via different mechanisms such as clathrin-mediated, caveolae/caveolin1 dependent, phagocytosis, macropinocytosis, and ARF6 and flotillin dependent (Doherty & McMahon, 2009). After endocytosis being processed, an early endosome is formed in the cytoplasm. Subsequently, MVBs that contain several nanovesicles are generated. These MVBs may fuse with lysosomes which cause degradation and recycling of the vesicles or they may fuse with the plasma membrane to release their nanovesicles that are called exosomes (Gorji-Bahri et al., 2018; Raposo & Stoorvogel, 2013).

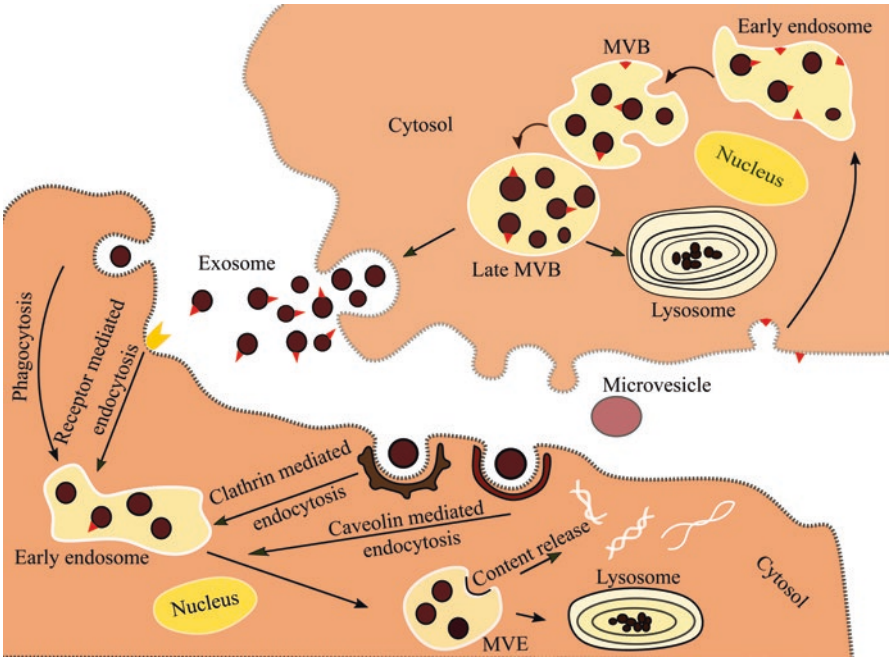

Fig. 10.1 Processes of exosome generation inside the parental cell and their uptake by a recipient cell. After fusion of late MVBs with the plasma membrane, the contained nanovesicles secrete into the extracellular space which are called exosomes. Internalization of exosomes into the recipient cell results in their accumulation in the early endosome. Subsequently, multivesicular endosomes may release their content or may be degraded by lysosomal function (Gorji-Bahri et al., 2018). *MVB* multivesicular bodies, *MVE* multivesicular endosomes

Evidence has demonstrated the major role of ESCRT dependent, ESCRT independent, and Rab GTPases family in exosome biogenesis. The ESCRT machinery is combined of four associated complexes that are named ESCRT 0, I, II, and III along with several accessory proteins that control and regulate cellular trafficking (Saksena et al., 2007). Colombo and colleagues have comprehensively studied the impact of 23 ESCRT components on exosome biogenesis by shRNA sequences. They indicated that contrary to *HGS*, *STAM1* (ESCRT 0), and *TSG101* (ESCRT I), silencing of *CHMP4C* (ESCRT III), *VPS4B*, *PDCD6IP* (*ALIX*), and *VTA1* (Accessory proteins) genes in HeLa-CIITA-OVA cells increase exosome secretion (Colombo et al., 2013). Similar results were also obtained by Chen and colleagues for *TSG101* and *HGS* in AML12 hepatocytes. However, si-*PDCD6IP* reduced exosome secretion (Chen et al., 2018). In this way, it has been reported that inhibition of *VPS34*, a regulatory kinase enzyme of ESCRT machinery, in primary cortical neurons raises exosome secretion (Miranda et al., 2018). Further to ESCRT dependent molecules, there are also several independent ones such as *SIRT1* (Latifkar et al., 2019), *GIPC1* (Bhattacharya et al., 2014), *SRC* (Hikita et al., 2019), *ARF6*, and *PLD2* (Ghossoub et al., 2014) which were reported to affect exosomes secretion. Moreover, the Rab GTPases family, principal players of cellular trafficking, are extensively associated with exosome biogenesis. *RAB27A* and *RAB27B* are two well-known members of the Rab GTPases family which function in the docking of MVBs at plasma membrane causing exosome secretion (Ostrowski et al., 2010). Likewise, downregulation of *RAB5A*, a master regulator of early endocytosis, decreased exosome secretion from HeLa and Huh7 cells (Ostrowski et al., 2010; Gorji-bahri et al., 2020). More molecules which affect exosome biogenesis are summarized in Table 10.1.

Analyzing the exosomal cargo not only would help the determination of new mechanisms involving their biogenesis but also show the importance of exosomal composition in the diagnosis and prognosis of various diseases specifically cancers. Many studies have reported that exosomes contain proteins, mRNAs, miRNAs, lncRNAs, and lipids (Sun et al., 2018; Skotland et al., 2019). Several studies have comprehensively reviewed the exosome composition as in refs Sun et al. (2018); Skotland et al. (2019); Ferguson and Nguyen (2016); and Deng et al. (2018)). Thereby, here we introduce several exosome-based databases that are established to cover all kinds of exosome cargos.

The first and maybe the well-known database of exosomal content is ExoCarta, in which proteins and mRNAs are the most recognized contents of exosomes with approximately more than 9000 and 3000 different proteins and mRNAs, respectively. However, the last update of ExoCarta is from 4 years ago, 2016 (http://www.exocarta.org/). Another database, VesiclePedia (http://microvesicles.org/#), is similar to ExoCarta in terms of the included extracellular vesicle cargos, except that VesiclePedia consists of more data derived from 1254 studies compared with 286 studies for ExoCarta, and it is also synchronized with the FunRich, functional enrichment and network analysis software that provides bioinformatics and statistical analysis of exosomal content. Indeed, VesiclePedia supports the content of all types of extracellular vesicles such as ectosomes, apoptotic bodies, exosomes, and

Table 10.1 The genes/proteins and lipid molecules which have been reported to affect exosomes biogenesis

Genes/lipid	Studied cells	References
ESCRT dependent		
ESCRT 0		
HRS	HeLa-CIITA-OVA cells, AML12 hepatocytes, SCC61 cells, SCC25-H1047R cells	Colombo et al. (2013); Chen et al. (2018); Hoshino et al. (2013)
STAM1	HeLa-CIITA-OVA cells	Colombo et al. (2013)
ESCRT I		
TSG101	HeLa-CIITA-OVA cells, AML12 hepatocytes	Colombo et al. (2013); Chen et al. (2018)
ESCRT II		
VPS22	MCF7	Baietti et al. (2012)
ESCRT III		
CHMP4C	H1299 (TP53 null), HeLa-CIITA-OVA cells	Colombo et al. (2013); Yu et al. (2009)
Accessory proteins		
VTA1	HeLa-CIITA-OVA cells	Colombo et al. (2013)
ALIX	HeLa-CIITA-OVA cells, AML12 hepatocytes	Colombo et al. (2013); Chen et al. (2018)
VPS4B	HeLa-CIITA-OVA cells	Colombo et al. (2013)
VPS34	Primary cortical neurons	Miranda et al. (2018)
ESCRT independent		
SYT7	SCC61 cells, SCC25-H1047R cells	Hoshino et al. (2013)
NISCH	MCF7, MDA-MB-231	Maziveyi et al. (2019)
ATG5	Mouse embryonic fibroblast, MDA-MB-231	Guo et al. (2017)
ATG16L	HCT116	Guo et al. (2017)
ARF6	MCF7	Ghossoub et al. (2014)
PLD2	MCF7, RBL-2H3	Ghossoub et al. (2014); Laulagnier et al. (2004)
STX6	C4-2B and CWR-R1 enzalutamide-resistant cells	Peak et al. (2020)
Rab GTPases family		
RAB27A	SCC61 cells, SCC25-H1047R cells, HeLa, B16F10, SK-Mel28	Ostrowski et al. (2010); Hoshino et al. (2013); Peinado et al. (2012)
RAB27B, RAB2B, RAB9A, RAB5A	HeLa	Ostrowski et al. (2010)
RAB5A	Huh7	Gorji-bahri et al. (2020)
RAB14	MDA-MB-231	Maziveyi et al. (2019)
RAB35	Oli-neu	Hsu et al. (2010)
RAB3D	MCF7, MDA-MB-231	Yang et al. (2015)

(continued)

Table 10.1 (continued)

Genes/lipid	Studied cells	References
RAB11	K562	Savina et al. (2002)
Lipid		
Ceramide	SCC61 cells, Oli-neu	Hoshino et al. (2013); Trajkovic et al. (2008)

oncosomes from 41 organisms through the FunRich software (Pathan et al., 2019; Pathan et al., 2015). Further to the above databases which collect almost all content of exosomes including proteins, mRNAs, miRNAs, and lipids, EVmiRNA is one of the first databases focusing on miRNA content of extracellular vesicles (i.e., exosome and microvesicle) that was developed by the College of Life Science and Technology, HUST, of China and allows users to search based on miRNA ID or sample type simply (Liu, Zhang, et al., 2019b). Similarly, exRNA Atlas has been created by the NIH Extracellular RNA Communication Consortium (ERCC) which contains exRNA sequences and exRNA qPCR profiles from 19 studies on five types of human biofluids including cerebrospinal fluid, serum, saliva, plasma, and urine (Murillo et al., 2019). In this regard, human exosomal proteins are annotated manually by UniProt curators at the EBI to serve reliable and authoritative datasets of human exosomal proteins (https://www.ebi.ac.uk/GOA/EXOSOME). Undoubtedly, the expansion and utilization of these databases would accelerate the finding of new biomarkers for various diseases.

10.3 Roles of Exosomes in Cancer Progression

It has been reported that exosomes can stimulate and potentiate cancer progression (Wortzel et al., 2019; Yu et al., 2015). But how? Upon exosome uptake by the cell via receptor-mediated (specified) or unspecified pathways such as micropinocytosis or macropinocytosis, exosomes share and transfer their content to the recipient cells functionally. mRNA content of extracellular vesicles can translate in recipient cells to generate functional proteins (O'Brien et al., 2020). Ridder and colleagues demonstrated that Cre mRNA containing exosomes are able to change the miRNA profile of non-recombined recipient Purkinje neurons (Ridder et al., 2014). Moreover, Maugeri and colleagues reported that human Erythropoietin (hEPO) mRNA-loaded extracellular vesicles not only transfer their content to HTB-177 cells but also result in hEPO protein expression in recipient cells in vitro along with its protein expression 2 hours after intravenously mice injection in vivo (Maugeri et al., 2019). Hence, given the fact that exosomes actively transfer their content to the other cells, it is not unexpected to call tumor-derived exosomes "tumorigenic mediators."

10.3.1 Roles of Exosomes in Cancer Metastasis

A report by Nakamura et al. indicated that epithelial ovarian cancer cell-derived exosomes which are enriched in CD44, have been uptaken by human peritoneal mesothelial cells (HPMC), result in cell morphology changes and induction of CD44-mediated MMP9 secretion, promoting cancer invasion (Nakamura et al., 2017). Dutta and colleagues also reported that exosomes derived from KKU-M213, a well-differentiated cholangiocarcinoma (CCA) cell line, are able to enhance migration and invasion of H69, a normal human cholangiocyte cell line via increasing and decreasing β-catenin and E-cadherin, respectively. Moreover, the proteomics profiling showed that exosomes of the CCA cell line carry several cancer-related proteins such as Integrin β1 and β4 and Galectin 3 binding protein that are not detected in normal cholangiocyte exosomes (Dutta et al., 2015). Gene expression profile of mice lung tissues that were injected with exosomes derived from B16-F10, a highly metastatic mouse melanoma cell line, 24 and 48 h after injection has shown that several differentially expressed genes belong to extracellular remodeling and inflammation pathways. In this comprehensive study published by Peinado et al., proteomics profiling of exosomes derived from highly metastatic human and mouse melanoma cell lines also indicated that MET oncoprotein, CD44, HSP70, and Annexin A6 have been carried by exosomes. Moreover, transfer of MET oncoprotein to bone marrow progenitor cells via melanoma cell-derived exosomes induced metastasis capability in vivo (Peinado et al., 2012).

Moreover, many studies have determined the association of exosomal miRNAs in cancer metastasis. It has been reported that exosomes derived from gastric cancer cell lines (AGS, SGC7901, and BGC823) are enriched in mir-1290 the same as serum-derived exosomes of gastric cancer patients. Besides that, exosomes derived from miR-1290 overexpressing AGS and SGC7901 cells promote gastric cancer (GC) cell proliferation, migration, and invasiveness via targeting NKD1 (Huang et al., 2019). In this regard, Ding et al. showed that breast cancer was associated with the mir-222-NF-κB pathway and the aggressivity was transferred by exosomes. In contrast to normal controls, mir-222 was overexpressed in exosomes extracted from the serum of breast cancer patients and was correlated with the lymph node metastasis. Following the incubation of MCF7 cells with MDA-MB-231 cells (a high invasive triple-negative breast cancer cell line)-derived exosomes, it was shown that the levels of mir-222 as well as *RELA* and *RELB*, two major NF-κB family members in the recipient cells, were increased significantly which resulted in the enhancement of invasion and migration capacities of the recipient cells (Ding et al., 2018). Transfer of several lncRNAs via tumor-derived exosomes has also been reported. For example, *LINC01559* that in silico and experimental analyses have proved its association with gastric cancer cells proliferation, migration, and stemness is transferred by exosomes. *LINC01559* activates PI3K/AKT pathway via sponging mir-1343-3p which results in alteration of PGK1 and PTEN expression levels (Wang et al., 2020). Similar documents were obtained for *ASMTL-AS1* for hepatocellular carcinoma (HCC) malignancy (Ma et al., 2020), *CCAT2* for glioma

cells angiogenesis (Lang et al., 2017), and *MALAT1* for lung cancer cell migration and tumor growth (Zhang et al., 2017).

10.3.2 Roles of Exosomes in Drug Resistance

One of the critical obstacles in cancer treatment is chemotherapeutics resistance that slows down the improvement processes and therefore would be life-threatening. Several mechanisms have been recognized to be involved in chemoresistance such as inactivation of chemotherapeutics, the implication of ABC transporters, changes in the metabolization mechanisms of chemotherapeutics, and alteration in chemotherapeutic targets due to mutations (Mowla & Hashemi, 2021; Nikolaou et al., 2018). In this regard, it has been delineated that exosomes can potentiate chemoresistance. For example, exosomes are able to convey chemotherapeutics into extracellular space. Li et al. have recently reported that the expression of *RAB27B*, which is greatly considered as a regulator of exosome secretion, is increased in 5-fluorouracil-resistant Bel7402 cells (Bel/5Fu), and notably its knockdown showed a significant decrease in secreted exosomes derived from Bel/5Fu cells, triggering an accumulation of the drug in cells. Moreover, Nanosight particle tracking analysis (NTA) and gas chromatography-mass spectrometry (GC-MS) analyses demonstrated that the number of secreted exosomes from the same number of Bel/5Fu was 4.5-fold more than Bel7402 cells and 5Fu is entrapped in exosomes derived from 5Fu-treated Bel/5Fu cells (Li et al., 2020). It has also been reported that co-culture of docetaxel-sensitive MCF7 cells with exosomes derived from MCF7-resistant cells significantly decreased chemosensitivity. Importantly, a higher level of P-gp expression, a product of the MDR1 gene, in MCF7-resistant exosomes than MCF7-sensitive exosomes have been detected (M-m et al., 2014). *EPHA2*, a member of the EphA receptor tyrosine kinase family, is transmitted via exosomes derived from gemcitabine-resistant pancreatic cancer cells, i.e., PANC-1 cell line (exo-PANC1), resulting in an enhancement in the cell viability of pancreatic-gemcitabine-sensitive cells which means the lower chemosensitivity of exo-PANC1-treated recipient cells (Fan et al., 2018). Chemoresistance transmission by exosomes has been reported in several other studies such as *ZEB1*, an EMT transcription factor, transfer via exosomes of oncogenically transformed mesenchymal lung cells (Lobb et al., 2017) or *SNHG14* transfer via exosomes of HER2-positive trastuzumab-resistant cell lines (Dong et al., 2018).

10.3.3 Roles of Exosomes in Anti-immune Responses

Exosomes can aid tumor cells to escape from the responses of the immune cells in which the immune cells become inefficient to recognize and fight with tumor cells. For instance, scientists believe that low responses to the PD-L1/PD-1 treatment are

attributed to the tumor-derived exosomes (Poggio et al., 2019; Theodoraki et al., 2018). It has been reported that exosomes derived from tumor cells such as lung and head and neck carcinoma express PD-L1 the same as their parent cells, whose receptor is on T-cells (Theodoraki et al., 2018; Kim et al., 2019). Kim and colleagues showed that exosomes containing PD-L1 could decrease IFNγ secretion from Jurkat T-cells and induce apoptosis in $CD8^+$ T-cells. Compared with PD-L1 expressing cells, exosomes containing PD-L1 can go farther easily and reduce the effect of immune cell activity (Kim et al., 2019). In this way, the NKG2D receptor is expressed on the surface of immune cells such as natural killer (NK) cells and cytotoxic T-cells, having an important role in the recognition and elimination of inflamed, DNA damaged, and malignant cells. The ligands of NKG2D receptor, i.e., NKG2DLs, include the polymorphic MHC I-related proteins, MICA and MICB, along with members of the Unique long protein 16 (UL16)-binding proteins (ULBP) family. It has been reported that NKG2DLs are expressed on tumor-derived exosomes, resulting in impairment of the function of NK cells regarding their cytotoxicity and tumor cell recognition (Clayton & Tabi, 2005; Ashiru et al., 2010).

Taken together, it is not unexpected that efforts being paid to peruse the exosomes secretion pathways to find new compounds inhibiting exosomes secretion such as *RAB27A* inhibitors, neutral sphingomyelinase inhibitors, and proton pump inhibitors (PPI). For example, Ketoconazole, an imidazole antifungal drug which is approved for the treatment of prostate cancer patients, reduces exosome secretion from C4-2B and PC3 cell lines at 5 μM concentration and expression of *RAB27A*, *ALIX*, nSMase, and pERK in a dose-dependent manner (Datta et al., 2018). Similar results were also reported for Manumycin A, a natural metabolite of *Streptomyces parvulus*. It has been shown that Manumycin A decreases exosome secretion from C4-2B, PC3, and 22Rv1 cell lines along with reducing the expression of *RAB27A*, *ALIX*, and *HRS* in C4-2B cells. Ras activation was also hindered in C4-2B cells, while no significant changes were observed for RWPE1, a normal prostate epithelial cell line. Accordingly, Datta and colleagues have suggested Manumycin A as a new drug candidate for prostate cancer treatment (Datta et al., 2017). Moreover, melanoma cells treated with lansoprazole, a PPI drug, not only reduced exosome secretion via lowering the pH of tumor cells microenvironment but also improved cisplatin uptake by melanoma cells and decreased the amount of accumulated cisplatin in exosomes (Federici et al., 2014). Thereby, studying the exosome secretion pathways would help scientists either to find novel compounds as a new drug or utilize previously approved drugs for new therapeutic purposes.

10.4 Exosomal Content as Cancer Biomarkers

Always use of noninvasive, abundant, and easily accessible sources can be valuable for disease diagnosis and monitoring of patients' treatment. Tissue biopsy for cancer diagnosis is invasive as well as difficult and discomfort which can be associated with further problems for patients (Ilié & Hofman, 2016; Pisapia et al., 2019).

Moreover, it is not always feasible to be performed (Barlebo Ahlborn & Østrup, 2019). Thus, the potential of exosomal content as a new source of cancer biomarkers has been considered. Exosomal content remains intact against extracellular degradation due to the bilayer phospholipid membranes of exosomes. Besides that, the abundance of exosomes in biofluids such as urine, plasma, and saliva provides easy access to this useful and valuable source of cancer biomarkers.

Up to now, many studies have been focused on plasma-derived exosomes for cancer diagnosis and prognosis. Here, we will review the recently published articles regarding this issue. Zhang et al. have analyzed the small RNA profile of serum exosomes derived from gastric cancer patients using next-generation sequencing (NGS) and proposed mir-10b-5p, mir-101-3p, and mir-143-5p as new biomarkers for gastric cancer with lymph node metastasis, ovarian metastasis, and liver metastasis, respectively (Zhang et al., 2020). Besides, it has been demonstrated that analyzing the expression of three lncRNAs, namely, *PCAT1*, *UBC1*, and *SNHG16*, in plasma exosomes of bladder cancer (BC) patients can be more accurately replaced with the traditional urine cytology as a diagnostic and prognostic method. RT-qPCR analysis with a three-step case-control strategy showed that the above three lncRNAs were upregulated in plasma exosomes of BC patients. Among them, *UBC1* expression was correlated with recurrence-free survival (RFS) in non-muscle-invasive BC. Thereby it has been proposed as a prognostic factor for BC recurrence prediction (Zhang et al., 2019). In this way, RNA sequencing of serum exosomes derived from CRC patients and ROC curve analysis by Xie et al. have shown that the expression of circ-PNN in serum exosomes of CRC patients is associated with early-stage CRC (Xie et al., 2020). Moreover, it has been reported that the lncRNAs, *SOX2-OT* and ENSG00000245648 (KLRK1-AS1), are upregulated in plasma exosomes of lung squamous cell carcinoma (LSCC) and notably exosomal *SOX2-OT* expression is significantly decreased in postoperative plasma exosome compared with preoperative ones. ROC curve analysis finally showed that *SOX2-OT* could potentially discriminate LSCC from non-LSCC patients with an AUC of 0.815 (Teng et al., 2019). Further to RNA and miRNA, exosomal proteins are also considered as cancer biomarkers. For instance, it has been reported that CPNE3 protein expression in plasma exosomes of CRC patients is significantly more than healthy controls. Moreover, its expression is enhanced in plasma exosomes derived from stage III–IV of CRC and patients with distant metastasis compared with stage I–II and no metastasis, respectively (Sun et al., 2019).

Compared with plasma that is minimally invasive, the exosome collection from urine samples is completely noninvasive. Recently it has been shown that mir-3940-5p/mir-8069 expression ratio is elevated in urinary exosomes of pancreatic ductal adenocarcinoma (PDAC) which is higher than plasma exosomes. Moreover, it has been indicated that the positive predictive value for the combination of mir-3940-5p/mir-8069 ratio with CA19-9, a known pancreatic tumor marker, can reach 100%. Thus, their combination can be used as a novel useful biomarker for PDAC (Yoshizawa et al., 2020). But the most serious study on urinary exosomes is ExoDx Prostate (Intelliscore) (EPI) (https://www.exosomedx.com/), in which the

expression of three mRNAs, namely, *ERG*, *PCA*, and *SPDEF*, in urinary exosomes is analyzed and following the calculation of EPI score, patients with EPI score >15.6 are considered to have a higher risk of high-grade prostate cancer. Besides the PSA test, the results of EPI can help urologists to decide on the patient biopsy (Tutrone et al., 2020).

Salivary exosomes are also an interesting cancer biomarker source due to its noninvasive collection approach as it is considered for detection of lung cancer, head and neck carcinoma, pancreatic cancer, and oral squamous cell carcinoma (Chiabotto et al., 2019). Moreover, Lin et al. have recently analyzed the potential of *GOLM1-NAA35* chimeric RNA (*G-N*chiRNA) expression in salivary exosomes (se*G-N*chiRNA) of esophageal squamous cell carcinoma (ESCC) as a new biomarker for early detection, disease recurrence, and prognosis in a prospective study. Clinically it has been shown that se*G-N*chiRNA can discriminate early stage and advanced ESCC patients with high sensitivity and specificity (>80%). Moreover, alteration in se*G-N*chiRNA expression was correlated with response to chemoradiation treatments as well as post-resection condition (Lin et al., 2019). Similarly, it has been reported that mir-24-3p is upregulated in salivary exosomes derived from oral squamous cell carcinoma (OSCC) patients which provides detection of OSCC patients accurately (He et al., 2020). Despite many studies about salivary exosomes, the saliva collection method is still variable in the published articles (Michael et al., 2010; Zheng et al., 2017). Collection of saliva in large volumes can be performed by stimulating the parotid, submandibular, and sublingual salivary glands using gum or citric acid which triggers a more complicated salivary content than unstimulated ones (Hyun et al., 2018). Thereby, it is important to report the collection method of saliva in the related articles for future experiments and literature review. Further exosomal biomarkers are listed in Table 10.2.

10.5 Future Prospective

Searches on exosomes are continuing increasingly as evidenced by the registered clinical trials regarding exosomes that reach over one hundred studies up to now. Given the published crucial findings of the importance of exosomes function due to their valuable content, recent studies are focused on novel exosomes isolation techniques that provide high pure exosomes rapidly as well as the high yield of isolation resulting in the acceleration of clinical studies. The latest methods include size-based and immunoaffinity-based microfluidics (Yang et al., 2020). Taken together, it is expected that the exosome-based therapeutics and diagnostics would enter the treatment and diagnosing programs of patients suffering from cancer in the coming years.

Table 10.2 The identified exosomal biomarkers for different cancer types

Cancer type	Exosomal biomarkers	Source	Potentials	Reference
Pancreatobiliary tract cancer	mir-1246, mir-4644	Saliva	Diagnosis of advanced stage	Machida et al. (2016)
Pancreatic cancer	ZIP4	Serum	Diagnosis of malignant pancreatic cancer (PC)	Jin et al. (2018)
Colorectal cancer (CRC)	mir-19a	Serum	Diagnosis of early and advanced stage, association with clinicopathological characteristics	Matsumura et al. (2015)
	CRNDE	Serum	Diagnosis and prognosis of CRC[a], association with clinicopathological characteristics	Liu et al. (2016)
	mir-548c-5p	Serum	Diagnosis (stages III and IV), association with clinicopathological characteristics	Peng et al. (2019)
	mir-320d	Serum	Diagnosis of metastatic CRC	Tang et al. (2019)
Prostate cancer (PC)	SURVIVIN	Plasma	Diagnosis of early and advanced stage	Khan et al. (2012)
	mir-196a-5p, mir-501-3p	Urine	Diagnosis[a]	Rodríguez et al. (2017)
	Phosphatidylserine 18:1/18:1, Lactosylceramide (d18:1/16:0), Phosphatidylserine 18:0–18:2	Urine	Diagnosis[a]	Skotland et al. (2017)
Gastric cancer (GC)	lnc-UEGC1	Plasma	Early stage diagnosis	Lin et al. (2018)
	HOTTIP	Serum	Diagnosis[a], association with clinicopathological characteristics	Zhao et al. (2018)
	mir-23b	Plasma	Prognosis of all stages and GC recurrence, association with clinicopathological characteristics	Kumata et al. (2018)
	mir-19b-3p, mir-106a-5p	Serum	Diagnosis[a], association with clinicopathological characteristics	Wang et al. (2017)

(continued)

Table 10.2 (continued)

Cancer type	Exosomal biomarkers	Source	Potentials	Reference
Breast cancer	mir-223-3p	Plasma	Diagnosis of early invasion in breast cancer patients, association with clinicopathological characteristics, distinguishing the invasive ductal carcinoma (IDC) and upstage IDC from ductal carcinoma in situ (DCIS)	Yoshikawa et al. (2018)
Non-small cell lung cancer (NSCLC)	mir-21, mir-4257	Plasma	Diagnosis of NSCLC recurrence, association with clinicopathological characteristics	Dejima et al. (2017)

[a]The cancer stage was not mentioned in the article

References

Gorji-Bahri, G., Hashemi, A., & Moghimi, H. R. (2018). ExomiRs: A novel strategy in cancer diagnosis and therapy. *Current Gene Therapy, 18*(6), 336–350. https://doi.org/10.2174/1566523218666181017163204

O'Brien, K., Breyne, K., Ughetto, S., Laurent, L. C., & Breakefield, X. O. (2020). RNA delivery by extracellular vesicles in mammalian cells and its applications. *Nature Reviews Molecular Cell Biology.*, 1–22. https://doi.org/10.1038/s41580-020-0251-y

He, M., Qin, H., Poon, T. C., Sze, S.-C., Ding, X., Ngai, S.-M., et al. (2015). Hepatocellular carcinoma-derived exosomes promote motility of immortalized hepatocyte through transfer of oncogenic proteins and RNAs. *Carcinogenesis, 36*(9), 1008–1018. https://doi.org/10.1093/carcin/bgv081

Yu, Y., Abudula, M., Li, C., Chen, Z., Zhang, Y., & Chen, Y. (2019). Icotinib-resistant HCC827 cells produce exosomes with mRNA MET oncogenes and mediate the migration and invasion of NSCLC. *Respiratory Research, 20*(1), 217. https://doi.org/10.1186/s12931-019-1202-z

Liu, X., Lu, Y., Xu, Y., Hou, S., Huang, J., Wang, B., et al. (2019a). Exosomal transfer of miR-501 confers doxorubicin resistance and tumorigenesis via targeting of BLID in gastric cancer. *Cancer Letters, 459*, 122–134. https://doi.org/10.1016/j.canlet.2019.05.035

Deng, X., Ruan, H., Zhang, X., Xu, X., Zhu, Y., Peng, H., et al. (2020). Long noncoding RNA CCAL transferred from fibroblasts by exosomes promotes chemoresistance of colorectal cancer cells. *International Journal of Cancer, 146*(6), 1700–1716. https://doi.org/10.1002/ijc.32608

Dorayappan, K. D. P., Wanner, R., Wallbillich, J. J., Saini, U., Zingarelli, R., Suarez, A. A., et al. (2018). Hypoxia-induced exosomes contribute to a more aggressive and chemoresistant ovarian cancer phenotype: A novel mechanism linking STAT3/Rab proteins. *Oncogene, 37*(28), 3806–3821. https://doi.org/10.1038/s41388-018-0189-0

Ghossoub, R., Lembo, F., Rubio, A., Gaillard, C. B., Bouchet, J., Vitale, N., et al. (2014). Syntenin-ALIX exosome biogenesis and budding into multivesicular bodies are controlled by ARF6 and PLD2. *Nature Communications, 5*(1), 1–12. https://doi.org/10.1038/ncomms4477

Hsu, C., Morohashi, Y., Yoshimura, S.-I., Manrique-Hoyos, N., Jung, S., Lauterbach, M. A., et al. (2010). Regulation of exosome secretion by Rab35 and its GTPase-activating proteins TBC1D10A–C. *Journal of Cell Biology., 189*(2), 223–232. https://doi.org/10.1083/jcb.200911018

Sinha, S., Hoshino, D., Hong, N. H., Kirkbride, K. C., Grega-Larson, N. E., Seiki, M., et al. (2016). Cortactin promotes exosome secretion by controlling branched actin dynamics. *Journal of Cell Biology., 214*(2), 197–213. https://doi.org/10.1083/jcb.201601025

Datta, A., Kim, H., McGee, L., Johnson, A. E., Talwar, S., Marugan, J., et al. (2018). High-throughput screening identified selective inhibitors of exosome biogenesis and secretion: A drug repurposing strategy for advanced cancer. *Scientific Reports, 8*(1), 1–13. https://doi.org/10.1038/s41598-018-26411-7

Kulshreshtha, A., Singh, S., Ahmad, M., Khanna, K., Ahmad, T., Agrawal, A., et al. (2019). Simvastatin mediates inhibition of exosome synthesis, localization and secretion via multicomponent interventions. *Scientific Reports, 9*(1), 1–10. https://doi.org/10.1038/s41598-019-52765-7

Zhou, C.-F., Ma, J., Huang, L., Yi, H.-Y., Zhang, Y.-M., Wu, X.-G., et al. (2019). Cervical squamous cell carcinoma-secreted exosomal miR-221-3p promotes lymphangiogenesis and lymphatic metastasis by targeting VASH1. *Oncogene, 38*(8), 1256–1268. https://doi.org/10.1038/s41388-018-0511-x

Sun, L., Liu, X., Pan, B., Hu, X., Zhu, Y., Su, Y., et al. (2020). Serum exosomal miR-122 as a potential diagnostic and prognostic biomarker of colorectal cancer with liver metastasis. *Journal of Cancer., 11*(3), 630–637. https://doi.org/10.7150/jca.33022

Nakamura, S., Sadakari, Y., Ohtsuka, T., Okayama, T., Nakashima, Y., Gotoh, Y., et al. (2019). Pancreatic juice exosomal microRNAs as biomarkers for detection of pancreatic ductal adenocarcinoma. *Annals of Surgical Oncology., 26*(7), 2104–2111. https://doi.org/10.1245/s10434-019-07269-z

Tutrone, R., Donovan, M. J., Torkler, P., Tadigotla, V., McLain, T., Noerholm, M., et al. (2020). Clinical utility of the exosome based ExoDx Prostate (IntelliScore) EPI test in men presenting for initial Biopsy with a PSA 2–10 ng/mL. *Prostate Cancer and Prostatic Diseases.*, 1–8. https://doi.org/10.1038/s41391-020-0237-z

Johnstone, R. M., Adam, M., Hammond, J., Orr, L., & Turbide, C. (1987). Vesicle formation during reticulocyte maturation. Association of plasma membrane activities with released vesicles (exosomes). *Journal of Biological Chemistry., 262*(19), 9412–9420.

Doherty, G. J., & McMahon, H. T. (2009). Mechanisms of endocytosis. *Annual Review of Biochemistry, 78*, 857–902. https://doi.org/10.1146/annurev.biochem.78.081307.110540

Raposo, G., & Stoorvogel, W. (2013). Extracellular vesicles: Exosomes, microvesicles, and friends. *Journal of Cell Biology., 200*(4), 373–383. https://doi.org/10.1083/jcb.201211138

Saksena, S., Sun, J., Chu, T., & Emr, S. D. (2007). ESCRTing proteins in the endocytic pathway. *Trends in Biochemical Sciences., 32*(12), 561–573. https://doi.org/10.1016/j.tibs.2007.09.010

Colombo, M., Moita, C., van Niel, G., Kowal, J., Vigneron, J., Benaroch, P., et al. (2013). Analysis of ESCRT functions in exosome biogenesis, composition and secretion highlights the heterogeneity of extracellular vesicles. *Journal of Cell Science., 126*(24), 5553–5565. https://doi.org/10.1242/jcs.128868

Chen, L., Chen, R., Kemper, S., & Brigstock, D. R. (2018). Pathways of production and delivery of hepatocyte exosomes. *Journal of Cell Communication and Signaling., 12*(1), 343–357. https://doi.org/10.1007/s12079-017-0421-7

Miranda, A. M., Lasiecka, Z. M., Xu, Y., Neufeld, J., Shahriar, S., Simoes, S., et al. (2018). Neuronal lysosomal dysfunction releases exosomes harboring APP C-terminal fragments and unique lipid signatures. *Nature Communications, 9*(1), 1–16. https://doi.org/10.1038/s41467-017-02533-w

Latifkar, A., Ling, L., Hingorani, A., Johansen, E., Clement, A., Zhang, X., et al. (2019). Loss of Sirtuin 1 alters the secretome of breast cancer cells by impairing lysosomal integrity. *Developmental Cell, 49*(3), 393–408. e7. https://doi.org/10.1016/j.devcel.2019.03.011

Bhattacharya, S., Pal, K., Sharma, A. K., Dutta, S. K., Lau, J. S., Yan, I. K., et al. (2014). GAIP interacting protein C-terminus regulates autophagy and exosome biogenesis of pancreatic cancer through metabolic pathways. *PLoS One, 9*(12). https://doi.org/10.1371/journal.pone.0114409

Hikita, T., Kuwahara, A., Watanabe, R., Miyata, M., & Oneyama, C. (2019). Src in endosomal membranes promotes exosome secretion and tumor progression. *Scientific Reports, 9*(1), 1–14. https://doi.org/10.1038/s41598-019-39882-z

Ostrowski, M., Carmo, N. B., Krumeich, S., Fanget, I., Raposo, G., Savina, A., et al. (2010). Rab27a and Rab27b control different steps of the exosome secretion pathway. *Nature Cell Biology., 12*(1), 19–30. https://doi.org/10.1038/ncb2000

Gorji-bahri, G., Moghimi, H. R., & Hashemi, A. (2020). RAB5A is associated with genes involved in exosome secretion: Integration of bioinformatics analysis and experimental validation. *Journal of Cellular Biochemistry*. https://doi.org/10.1002/jcb.29871

Hoshino, D., Kirkbride, K. C., Costello, K., Clark, E. S., Sinha, S., Grega-Larson, N., et al. (2013). Exosome secretion is enhanced by invadopodia and drives invasive behavior. *Cell Reports, 5*(5), 1159–1168. https://doi.org/10.1016/j.celrep.2013.10.050

Baietti, M. F., Zhang, Z., Mortier, E., Melchior, A., Degeest, G., Geeraerts, A., et al. (2012). Syndecan–syntenin–ALIX regulates the biogenesis of exosomes. *Nature Cell Biology., 14*(7), 677–685. https://doi.org/10.1038/ncb2502

Yu, X., Riley, T., & Levine, A. J. (2009). The regulation of the endosomal compartment by p53 the tumor suppressor gene. *The FEBS Journal., 276*(8), 2201–2212. https://doi.org/10.1111/j.1742-4658.2009.06949.x

Maziveyi, M., Dong, S., Baranwal, S., Mehrnezhad, A., Rathinam, R., Huckaba, T. M., et al. (2019). Exosomes from Nischarin-expressing cells reduce breast cancer cell motility and tumor growth. *Cancer Research., 79*(9), 2152–2166. https://doi.org/10.1158/0008-5472.CAN-18-0842

Guo, H., Chitiprolu, M., Roncevic, L., Javalet, C., Hemming, F. J., Trung, M. T., et al. (2017). Atg5 disassociates the V1V0-ATPase to promote exosome production and tumor metastasis independent of canonical macroautophagy. *Developmental Cell, 43*(6), 716–30. e7. https://doi.org/10.1016/j.devcel.2017.11.018

Laulagnier, K., Grand, D., Dujardin, A., Hamdi, S., Vincent-Schneider, H., Lankar, D., et al. (2004). PLD2 is enriched on exosomes and its activity is correlated to the release of exosomes. *FEBS Letters., 572*(1–3), 11–14. https://doi.org/10.1016/j.febslet.2004.06.082

Peak, T. C., Panigrahi, G. K., Praharaj, P. P., Su, Y., Shi, L., Chyr, J., et al. (2020). Syntaxin 6-mediated exosome secretion regulates enzalutamide resistance in prostate cancer. *Molecular Carcinogenesis., 59*(1), 62–72. https://doi.org/10.1002/mc.23129

Peinado, H., Alečković, M., Lavotshkin, S., Matei, I., Costa-Silva, B., Moreno-Bueno, G., et al. (2012). Melanoma exosomes educate bone marrow progenitor cells toward a pro-metastatic phenotype through MET. *Nature Medicine., 18*(6), 883–891. https://doi.org/10.1038/nm.2753

Yang, J., Liu, W., Xin'an Lu, Y. F., Li, L., & Luo, Y. (2015). High expression of small GTPase Rab3D promotes cancer progression and metastasis. *Oncotarget, 6*(13), 11125. https://doi.org/10.18632/oncotarget.3575

Savina, A., Vidal, M., & Colombo, M. I. (2002). The exosome pathway in K562 cells is regulated by Rab11. *Journal of Cell Science., 115*(12), 2505–2515.

Trajkovic, K., Hsu, C., Chiantia, S., Rajendran, L., Wenzel, D., Wieland, F., et al. (2008). Ceramide triggers budding of exosome vesicles into multivesicular endosomes. *Science, 319*(5867), 1244–1247. https://doi.org/10.1126/science.1153124

Sun, Z., Yang, S., Zhou, Q., Wang, G., Song, J., Li, Z., et al. (2018). Emerging role of exosome-derived long non-coding RNAs in tumor microenvironment. *Molecular Cancer., 17*(1), 1–9. https://doi.org/10.1186/s12943-018-0831-z

Skotland, T., Hessvik, N. P., Sandvig, K., & Llorente, A. (2019). Exosomal lipid composition and the role of ether lipids and phosphoinositides in exosome biology. *Journal of Lipid Research., 60*(1), 9–18. https://doi.org/10.1194/jlr.R084343

Ferguson, S. W., & Nguyen, J. (2016). Exosomes as therapeutics: The implications of molecular composition and exosomal heterogeneity. *Journal of Controlled Release, 228*, 179–190. https://doi.org/10.1016/j.jconrel.2016.02.037

Deng, H., Sun, C., Sun, Y., Li, H., Yang, L., Wu, D., et al. (2018). Lipid, protein, and microRNA composition within mesenchymal stem cell-derived exosomes. *Cellular Reprogramming, 20*(3), 178–186. https://doi.org/10.1089/cell.2017.0047

Pathan, M., Fonseka, P., Chitti, S. V., Kang, T., Sanwlani, R., Van Deun, J., et al. (2019). Vesiclepedia 2019: A compendium of RNA, proteins, lipids and metabolites in extracellular vesicles. *Nucleic Acids Research., 47*(D1), D516–D5D9. https://doi.org/10.1093/nar/gky1029

Pathan, M., Keerthikumar, S., Ang, C. S., Gangoda, L., Quek, C. Y., Williamson, N. A., et al. (2015). FunRich: An open access standalone functional enrichment and interaction network analysis tool. *Proteomics, 15*(15), 2597–2601. https://doi.org/10.1002/pmic.201400515

Liu, T., Zhang, Q., Zhang, J., Li, C., Miao, Y.-R., Lei, Q., et al. (2019b). EVmiRNA: A database of miRNA profiling in extracellular vesicles. *Nucleic Acids Research., 47*(D1), D89–D93. https://doi.org/10.1093/nar/gky985

Murillo, O. D., Thistlethwaite, W., Rozowsky, J., Subramanian, S. L., Lucero, R., Shah, N., et al. (2019). exRNA atlas analysis reveals distinct extracellular RNA cargo types and their carriers present across human biofluids. *Cell, 177*(2), 463–77. e15. https://doi.org/10.1016/j.cell.2019.02.018

Wortzel, I., Dror, S., Kenific, C. M., & Lyden, D. (2019). Exosome-mediated metastasis: Communication from a distance. *Developmental Cell., 49*(3), 347–360. https://doi.org/10.1016/j.devcel.2019.04.011

Yu, S., Cao, H., Shen, B., & Feng, J. (2015). Tumor-derived exosomes in cancer progression and treatment failure. *Oncotarget, 6*(35), 37151. https://doi.org/10.18632/oncotarget.6022

Ridder, K., Keller, S., Dams, M., Rupp, A.-K., Schlaudraff, J., Del Turco, D., et al. (2014). Extracellular vesicle-mediated transfer of genetic information between the hematopoietic system and the brain in response to inflammation. *PLoS Biology., 12*(6), e1001874. https://doi.org/10.1371/journal.pbio.1002623

Maugeri, M., Nawaz, M., Papadimitriou, A., Angerfors, A., Camponeschi, A., Na, M., et al. (2019). Linkage between endosomal escape of LNP-mRNA and loading into EVs for transport to other cells. *Nature Communications, 10*(1), 1–15. https://doi.org/10.1038/s41467-019-12275-6

Nakamura, K., Sawada, K., Kinose, Y., Yoshimura, A., Toda, A., Nakatsuka, E., et al. (2017). Exosomes promote ovarian cancer cell invasion through transfer of CD44 to peritoneal mesothelial cells. *Molecular Cancer Research., 15*(1), 78–92. https://doi.org/10.1158/1541-7786.MCR-16-0191

Dutta, S., Reamtong, O., Panvongsa, W., Kitdumrongthum, S., Janpipatkul, K., Sangvanich, P., et al. (2015). Proteomics profiling of cholangiocarcinoma exosomes: A potential role of oncogenic protein transferring in cancer progression. *Biochimica et Biophysica Acta (BBA)-Molecular Basis of Disease, 1852*(9), 1989–1999. https://doi.org/10.1016/j.bbadis.2015.06.024

Huang, J., Shen, M., Yan, M., Cui, Y., Gao, Z., & Meng, X. (2019). Exosome-mediated transfer of miR-1290 promotes cell proliferation and invasion in gastric cancer via NKD1. *Acta Biochimica et Biophysica Sinica., 51*(9), 900–907. https://doi.org/10.1093/abbs/gmz077

Ding, J., Xu, Z., Zhang, Y., Tan, C., Hu, W., Wang, M., et al. (2018). Exosome-mediated miR-222 transferring: An insight into NF-κB-mediated breast cancer metastasis. *Experimental Cell Research., 369*(1), 129–138. https://doi.org/10.1016/j.yexcr.2018.05.014

Wang, L., Bo, X., Yi, X., Xiao, X., Zheng, Q., Ma, L., et al. (2020). Exosome-transferred LINC01559 promotes the progression of gastric cancer via PI3K/AKT signaling pathway. *Cell Death & Disease., 11*(9), 1–14. https://doi.org/10.1038/s41419-020-02810-5

Ma, D., Gao, X., Liu, Z., Lu, X., Ju, H., & Zhang, N. (2020). Exosome-transferred long non-coding RNA ASMTL-AS1 contributes to malignant phenotypes in residual hepatocellular carcinoma after insufficient radiofrequency ablation. *Cell Proliferation., 53*(9), e12795. https://doi.org/10.1111/cpr.12795

Lang, H.-L., Hu, G.-W., Zhang, B., Kuang, W., Chen, Y., Wu, L., et al. (2017). Glioma cells enhance angiogenesis and inhibit endothelial cell apoptosis through the release of exosomes that contain long non-coding RNA CCAT2. *Oncology Reports., 38*(2), 785–798. https://doi.org/10.3892/or.2017.5742

Zhang, R., Xia, Y., Wang, Z., Zheng, J., Chen, Y., Li, X., et al. (2017). Serum long non coding RNA MALAT-1 protected by exosomes is up-regulated and promotes cell proliferation and migration in non-small cell lung cancer. *Biochemical and Biophysical Research Communications., 490*(2), 406–414. https://doi.org/10.1016/j.bbrc.2017.06.055

Mowla, M., & Hashemi, A. (2021). Functional roles of exosomal miRNAs in multi-drug resistance in cancer chemotherapeutics. *Experimental and Molecular Pathology., 118*. https://doi.org/10.1016/j.yexmp.2020.104592

Nikolaou, M., Pavlopoulou, A., Georgakilas, A. G., & Kyrodimos, E. (2018). The challenge of drug resistance in cancer treatment: A current overview. *Clinical & Experimental Metastasis., 35*(4), 309–318. https://doi.org/10.1007/s10585-018-9903-0

Li, R., Dong, C., Jiang, K., Sun, R., Zhou, Y., Yin, Z., et al. (2020). Rab27B enhances drug resistance in hepatocellular carcinoma by promoting exosome-mediated drug efflux. *Carcinogenesis, 41*(11), 1583–1591. https://doi.org/10.1093/carcin/bgaa029

M-m, L., Zhu, X.-y., W-x, C., Zhong S-l, H. Q., Ma, T.-f., et al. (2014). Exosomes mediate drug resistance transfer in MCF-7 breast cancer cells and a probable mechanism is delivery of P-glycoprotein. *Tumor Biology, 35*(11), 10773–10779. https://doi.org/10.1007/s13277-014-2377-z

Fan, J., Wei, Q., Koay, E. J., Liu, Y., Ning, B., Bernard, P. W., et al. (2018). Chemoresistance transmission via exosome-mediated EphA2 transfer in pancreatic cancer. *Theranostics., 8*(21), 5986–5994. https://doi.org/10.7150/thno.26650

Lobb, R. J., van Amerongen, R., Wiegmans, A., Ham, S., Larsen, J. E., & Möller, A. (2017). Exosomes derived from mesenchymal non-small cell lung cancer cells promote chemoresistance. *International Journal of Cancer., 141*(3), 614–620. https://doi.org/10.1002/ijc.30752

Dong, H., Wang, W., Chen, R., Zhang, Y., Zou, K., Ye, M., et al. (2018). Exosome-mediated transfer of lncRNA-SNHG14 promotes trastuzumab chemoresistance in breast cancer. *International Journal of Oncology., 53*(3), 1013–1026. https://doi.org/10.3892/ijo.2018.4467

Poggio, M., Hu, T., Pai, C.-C., Chu, B., Belair, C. D., Chang, A., et al. (2019). Suppression of exosomal PD-L1 induces systemic anti-tumor immunity and memory. *Cell, 177*(2), 414–27. e13. https://doi.org/10.1016/j.cell.2019.02.016

Theodoraki, M.-N., Yerneni, S. S., Hoffmann, T. K., Gooding, W. E., & Whiteside, T. L. (2018). Clinical significance of PD-L1+ exosomes in plasma of head and neck cancer patients. *Clinical Cancer Research., 24*(4), 896–905. https://doi.org/10.1158/1078-0432.CCR-17-2664

Kim, D. H., Kim, H., Choi, Y. J., Kim, S. Y., Lee, J.-E., Sung, K. J., et al. (2019). Exosomal PD-L1 promotes tumor growth through immune escape in non-small cell lung cancer. *Experimental & Molecular Medicine., 51*(8), 1–13. https://doi.org/10.1038/s12276-019-0295-2

Clayton, A., & Tabi, Z. (2005). Exosomes and the MICA-NKG2D system in cancer. *Blood Cells, Molecules, and Diseases., 34*(3), 206–213. https://doi.org/10.1016/j.bcmd.2005.03.003

Ashiru, O., Boutet, P., Fernández-Messina, L., Agüera-González, S., Skepper, J. N., Valés-Gómez, M., et al. (2010). Natural killer cell cytotoxicity is suppressed by exposure to the human NKG2D ligand MICA* 008 that is shed by tumor cells in exosomes. *Cancer Research., 70*(2), 481–489. https://doi.org/10.1158/0008-5472.CAN-09-1688

Datta, A., Kim, H., Lal, M., McGee, L., Johnson, A., Moustafa, A. A., et al. (2017). Manumycin A suppresses exosome biogenesis and secretion via targeted inhibition of Ras/Raf/ERK1/2 signaling and hnRNP H1 in castration-resistant prostate cancer cells. *Cancer Letters., 408*, 73–81. https://doi.org/10.1016/j.canlet.2017.08.020

Federici, C., Petrucci, F., Caimi, S., Cesolini, A., Logozzi, M., Borghi, M., et al. (2014). Exosome release and low pH belong to a framework of resistance of human melanoma cells to cisplatin. *PLoS One, 9*(2), e88193. https://doi.org/10.1371/journal.pone.0088193

Ilié, M., & Hofman, P. (2016). Pros: Can tissue biopsy be replaced by liquid biopsy? *Translational Lung Cancer Research, 5*(4), 420. https://doi.org/10.21037/tlcr.2016.08.06

Pisapia, P., Malapelle, U., & Troncone, G. (2019). Liquid biopsy and lung cancer. *Acta Cytologica., 63*(6), 489–496. https://doi.org/10.1159/000492710

Barlebo Ahlborn, L., & Østrup, O. (2019). Toward liquid biopsies in cancer treatment: Application of circulating tumor DNA. *APMIS, 127*(5), 329–336. https://doi.org/10.1111/apm.12912

Zhang, Y., Han, T., Feng, D., Li, J., Wu, M., Peng, X., et al. (2020). Screening of non-invasive miRNA biomarker candidates for metastasis of gastric cancer by small RNA sequencing of plasma exosomes. *Carcinogenesis, 41*(5), 582–590. https://doi.org/10.1093/carcin/bgz186

Zhang, S., Du, L., Wang, L., Jiang, X., Zhan, Y., Li, J., et al. (2019). Evaluation of serum exosomal Lnc RNA-based biomarker panel for diagnosis and recurrence prediction of bladder cancer. *Journal of Cellular and Molecular Medicine., 23*(2), 1396–1405. https://doi.org/10.1111/jcmm.14042

Xie, Y., Li, J., Li, P., Li, N., Zhang, Y., Binang, H., et al. (2020). RNA-seq profiling of serum exosomal circular RNAs reveals Circ-PNN as a potential biomarker for human colorectal cancer. *Frontiers in Oncology., 10*, 982. https://doi.org/10.3389/fonc.2020.00982

Teng, Y., Kang, H., & Chu, Y. (2019). Identification of an exosomal long noncoding RNA SOX2-OT in plasma as a promising biomarker for lung squamous cell carcinoma. *Genetic Testing and Molecular Biomarkers., 23*(4), 235–240. https://doi.org/10.1089/gtmb.2018.0103

Sun, B., Li, Y., Zhou, Y., Ng, T. K., Zhao, C., Gan, Q., et al. (2019). Circulating exosomal CPNE3 as a diagnostic and prognostic biomarker for colorectal cancer. *Journal of Cellular Physiology., 234*(2), 1416–1425. https://doi.org/10.1002/jcp.26936

Yoshizawa, N., Sugimoto, K., Tameda, M., Inagaki, Y., Ikejiri, M., Inoue, H., et al. (2020). miR-3940-5p/miR-8069 ratio in urine exosomes is a novel diagnostic biomarker for pancreatic ductal adenocarcinoma. *Oncology Letters., 19*(4), 2677–2684. https://doi.org/10.3892/ol.2020.11357

Chiabotto, G., Gai, C., Deregibus, M. C., & Camussi, G. (2019). Salivary extracellular vesicle-associated exRNA as cancer biomarker. *Cancers, 11*(7), 891. https://doi.org/10.3390/cancers11070891

Lin, Y., Dong, H., Deng, W., Lin, W., Li, K., Xiong, X., et al. (2019). Evaluation of salivary exosomal chimeric GOLM1-NAA35 RNA as a potential biomarker in esophageal carcinoma. *Clinical Cancer Research., 25*(10), 3035–3045. https://doi.org/10.1158/1078-0432.CCR-18-3169

He, L., Ping, F., Fan, Z., Zhang, C., Deng, M., Cheng, B., et al. (2020). Salivary exosomal miR-24-3p serves as a potential detective biomarker for oral squamous cell carcinoma screening. *Biomedicine & Pharmacotherapy., 121*, 109553. https://doi.org/10.1016/j.biopha.2019.109553

Michael, A., Bajracharya, S. D., Yuen, P. S., Zhou, H., Star, R. A., Illei, G. G., et al. (2010). Exosomes from human saliva as a source of microRNA biomarkers. *Oral Diseases., 16*(1), 34–38. https://doi.org/10.1111/j.1601-0825.2009.01604.x

Zheng, X., Chen, F., Zhang, Q., Liu, Y., You, P., Sun, S., et al. (2017). Salivary exosomal PSMA7: A promising biomarker of inflammatory bowel disease. *Protein & Cell., 8*(9), 686–695. https://doi.org/10.1007/s13238-017-0413-7

Hyun, K.-A., Gwak, H., Lee, J., Kwak, B., & Jung, H.-I. (2018). Salivary exosome and cell-free DNA for cancer detection. *Micromachines, 9*(7), 340. https://doi.org/10.3390/mi9070340

Machida, T., Tomofuji, T., Maruyama, T., Yoneda, T., Ekuni, D., Azuma, T., et al. (2016). miR-1246 and miR-4644 in salivary exosome as potential biomarkers for pancreatobiliary tract cancer. *Oncology Reports., 36*(4), 2375–2381. https://doi.org/10.3892/or.2016.5021

Jin, H., Liu, P., Wu, Y., Meng, X., Wu, M., Han, J., et al. (2018). Exosomal zinc transporter ZIP4 promotes cancer growth and is a novel diagnostic biomarker for pancreatic cancer. *Cancer Science., 109*(9), 2946–2956. https://doi.org/10.1111/cas.13737

Matsumura, T., Sugimachi, K., Iinuma, H., Takahashi, Y., Kurashige, J., Sawada, G., et al. (2015). Exosomal microRNA in serum is a novel biomarker of recurrence in human colorectal cancer. *British Journal of Cancer., 113*(2), 275. https://doi.org/10.1038/bjc.2015.201

Liu, T., Zhang, X., Gao, S., Jing, F., Yang, Y., Du, L., et al. (2016). Exosomal long noncoding RNA CRNDE-h as a novel serum-based biomarker for diagnosis and prognosis of colorectal cancer. *Oncotarget, 7*(51), 85551–85563. https://doi.org/10.18632/oncotarget.13465

Peng, Z. Y., Gu, R. H., & Yan, B. (2019). Downregulation of exosome-encapsulated miR-548c-5p is associated with poor prognosis in colorectal cancer. *Journal of Cellular Biochemistry, 120*(2), 1457–1463. https://doi.org/10.1002/jcb.27291

Tang, Y., Zhao, Y., Song, X., Song, X., Niu, L., & Xie, L. (2019). Tumor-derived exosomal miRNA-320d as a biomarker for metastatic colorectal cancer. *Journal of Clinical Laboratory Analysis., 33*(9), e23004. https://doi.org/10.1002/jcla.23004

Khan, S., Jutzy, J. M., Valenzuela, M. M. A., Turay, D., Aspe, J. R., Ashok, A., et al. (2012). Plasma-derived exosomal survivin, a plausible biomarker for early detection of prostate cancer. *PLoS One, 7*(10), e46737. https://doi.org/10.1371/journal.pone.0046737

Rodríguez, M., Bajo-Santos, C., Hessvik, N. P., Lorenz, S., Fromm, B., Berge, V., et al. (2017). Identification of non-invasive miRNAs biomarkers for prostate cancer by deep sequencing analysis of urinary exosomes. *Molecular Cancer., 16*(1), 156. https://doi.org/10.1186/s12943-017-0726-4

Skotland, T., Ekroos, K., Kauhanen, D., Simolin, H., Seierstad, T., Berge, V., et al. (2017). Molecular lipid species in urinary exosomes as potential prostate cancer biomarkers. *European Journal of Cancer., 70*, 122–132. https://doi.org/10.1016/j.ejca.2016.10.011

Lin, L.-Y., Yang, L., Zeng, Q., Wang, L., Chen, M.-L., Zhao, Z.-H., et al. (2018). Tumor-originated exosomal lncUEGC1 as a circulating biomarker for early-stage gastric cancer. *Molecular Cancer., 17*(1), 84. https://doi.org/10.1186/s12943-018-0834-9

Zhao, R., Zhang, Y., Zhang, X., Yang, Y., Zheng, X., Li, X., et al. (2018). Exosomal long noncoding RNA HOTTIP as potential novel diagnostic and prognostic biomarker test for gastric cancer. *Molecular Cancer., 17*(1), 1–5. https://doi.org/10.1186/s12943-018-0817-x

Kumata, Y., Iinuma, H., Suzuki, Y., Tsukahara, D., Midorikawa, H., Igarashi, Y., et al. (2018). Exosome-encapsulated microRNA-23b as a minimally invasive liquid biomarker for the prediction of recurrence and prognosis of gastric cancer patients in each tumor stage. *Oncology Reports., 40*(1), 319–330. https://doi.org/10.3892/or.2018.6418

Wang, N., Wang, L., Yang, Y., Gong, L., Xiao, B., & Liu, X. (2017). A serum exosomal microRNA panel as a potential biomarker test for gastric cancer. *Biochemical and Biophysical Research Communications., 493*(3), 1322–1328. https://doi.org/10.1016/j.bbrc.2017.10.003

Yoshikawa, M., Iinuma, H., Umemoto, Y., Yanagisawa, T., Matsumoto, A., & Jinno, H. (2018). Exosome-encapsulated microRNA-223-3p as a minimally invasive biomarker for the early detection of invasive breast cancer. *Oncology Letters., 15*(6), 9584–9592. https://doi.org/10.3892/ol.2018.8457

Dejima, H., Iinuma, H., Kanaoka, R., Matsutani, N., & Kawamura, M. (2017). Exosomal microRNA in plasma as a non-invasive biomarker for the recurrence of non-small cell lung cancer. *Oncology Letters., 13*(3), 1256–1263. https://doi.org/10.3892/ol.2017.5569

Yang, D., Zhang, W., Zhang, H., Zhang, F., Chen, L., Ma, L., et al. (2020). Progress, opportunity, and perspective on exosome isolation-efforts for efficient exosome-based theranostics. *Theranostics., 10*(8), 3684–3707. https://doi.org/10.7150/thno.41580

Chapter 11
Emerging Theragnostic Metal-Based Nanomaterials to Combat Cancer

Sivasubramanian Manikandan, Ramasamy Subbaiya, Muthupandian Saravanan, Hamed Barabadi, and Ramaswamy Arulvel

Contents

S. Manikandan (✉) · R. Arulvel
Department of Biotechnology, Saveetha School of Engineering, Saveetha Institute of Medical and Technical Sciences (SIMATS), Thandalam, Chennai, Tamil Nadu, India

R. Subbaiya
Department of Biological Sciences, School of Mathematics and Natural Sciences, The Copperbelt University, Riverside, Jambo Drive, Kitwe, Zambia

M. Saravanan
Department of Microbiology and Immunology, Division of Biomedical Sciences, School of Medicine, College of Health Sciences, Mekelle University, Mekelle, Ethiopia

AMR and Nanomedicine Laboratory, Department of Pharmacology, Saveetha Dental College, Saveetha Institute of Medical and Technical Sciences (SIMATS), Chennai, Tamil Nadu, India

H. Barabadi
Department of Pharmaceutical Biotechnology, School of Pharmacy, Shahid Beheshti University of Medical Sciences, Tehran, Iran

M. Saravanan, H. Barabadi (eds.), *Cancer Nanotheranostics*, Nanotechnology in the Life Sciences, https://doi.org/10.1007/978-3-030-74330-7_11

11.1 Introduction

Uncontrolled tissue development and rapid invasion are cancer without proper growth and distinguishment. The six biological capacities have been known as 'carcinogenic marks' proliferative signalling, avoidance of growth suppression, cell death resistance, replicating angiogenesis intolerance, metastasis and invasion (Murray et al., 2020). Cancer is a significant source of catastrophic results in human health and of financial restrictions. Cancer rates are rising at a distressing pace worldwide. It's predicted that 1,660,290 new cases of cancer are new, as seen in the Cancer Facts, although only 580,350 deaths are expected in the USA (Fan et al., 2014). A large number of cancer research projects have already been conducted, leading to a number of available diagnosis and treatment options such as magnetic resonance imaging, biosensor, radiation therapy, chemotherapy, gene therapy, immunotherapy, etc. (Li et al., 2020)

Nanotechnology in cancer medicine could have a significant effect on tumour diagnosis and treatment. The development of treatment or diagnostic platforms is a primary objective of nanomedicine (Fadeel & Alexiou, 2020; Wu et al., 2020). Use of chemotherapeutic combinations specially designed cancer theranostics nanocarriers. The use of nanomedicine by highly complex physiology networks allows for maximum supply of chemotherapy to the tumour. Hybrid nanoparticles (HNPs) use multimodal nanoplastics with outstanding surface functionality that can boost the anticancer activity directly in the tumour site by boosting drug release (Shetty & Chandra, 2020; Chen et al., 2020; Ghitman et al., 2020). HNPs may be very promising for cancer theranostic treatment by taking advantage of nanostructures and chemotherapies: (i) HNPs have efficient accumulation and retention at tumour sites as well as current active or passive targeting processes (Chen et al., 2020; Andrade et al., 2019; Ferreira Soares et al., 2020), (ii) functional nanocarriers have a high pervasiveness comparable with those of small tumour molecules (Liu et al., 2019), and (iii) HNPs hold and release. This analysis summarises the variety of commonly used HNPs that are underlying their recent cancer theranostics applications (Shetty & Chandra, 2020; Ghitman et al., 2020; Thorat et al., 2020; Cheng et al., 2020). Figure 11.1 describes and outlines the developmental stages for the diagnosis and treatment of cancer.

Numerous antitumour drugs have been licensed, and some are in clinical research. Nevertheless, most are unhealthy and chemical-based and have several side effects. Nanotechnology advancement allowed numerous therapeutic and diagnostic agents to be integrated into the nanostructures (Ghazy et al., 2020; Barani et al., 2021). Therefore, for cancer detection, hybrid nanostructures are the most effective option. Researchers have developed various hybrid nanostructures that can blend and tune to cancers in the blood. In the initial stages of the growth, the optical and magnetic properties of different hybrid nanostructures provide a basis for diagnostic cancer (Sharma et al., 2020; Ranjan et al., 2020; Dar et al., 2019; Zhang et al., 2020). Likewise, fluorescence imaging is given by the quantum confining effect of hybrid semiconducting materials. In addition, a variety of other hybrid structures

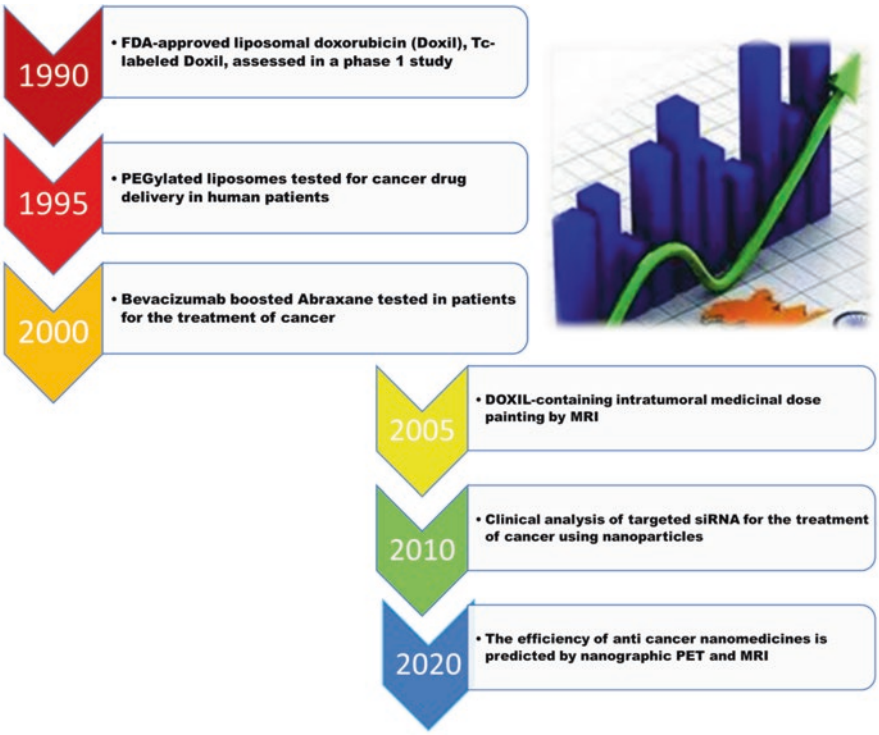

Fig. 11.1 Development stadiums for cancer diagnosis and care

may deliver high-load anticancer medicines to the tumour site. Many inorganic hybrid structures in biological sciences are used for the transport of diagnostic and healing instruments.

A variety of cancer research has already been performed, which has led to many available diagnostic and therapeutic options, including MRI, CT, biosensory medicine, radiation therapy, chemotherapy, gene therapies and immunotherapy (Dhas et al., 2021; Nandini et al., 2020; Wooster et al., 2021). The treatment of cancer with ionising radiation, including high-energy X-rays, gamma rays or particle beam radiation, requires radiation therapy or radiation therapy to delete the target tissue by destroying their DNA. The use of heat is also tested for hyperthermia for its efficacy in sensitising radiation tissue. Further research in recent years has concentrated on the use of radiation mark antibodies to supply radiation to the cancer site (radioimmunotherapy) (Das, Alkahtani, et al., 2020; Levitzki & Klein, 2010; Teates & Parekh, 1993). Radiotherapy can be used either alone or with chemotherapy or surgery in combination. While painless, the radiation itself induces mutations in healthy genes and may produce cancer, and it has some serious side impacts, such as permanent hair loss, foetal damage, skin problems and secondary malignancies. In comparison, chemotherapy requires numerous cytotoxic medications, including vinblastine, doxorubicin and taxol (Allan et al., 2012; Tewari et al., 2019; Adelberg

& Bishop, 2009). Multidrug resistance (MDR) is not at least one representative of each of the three groups of a chosen antimicrobial compound family who is susceptible to antibiotic-resistant conditions. Highly drug-resistant at least one individual of all, but very few antimicrobial compound families is susceptible (Imran et al., 2019). In addition, they degrade into toxicity, which contributes to nephrotoxicity and cardiotoxicity. To develop an effective treatment scheme, the key disadvantages of several treatments, such as inadequate solubility, fast disabling, adverse pharmacokinetics and restricted biodiversity, must be taken into account. In order to establish more extensive and diverse diagnosis and treatment options for malignancies, a wide variety of nanomaterials has been implemented. We are hereby systematically reviewing state-of-the-art developments in the field of new-generation nanomedicines in the clinical level, cancer theranostics for the diagnosis, therapy and monitoring of therapy. In particular, hybrid formulations, new bioconjugation methods and the potential for clinical translation of advanced multimodal therapies are a reasonable design.

11.2 Nanotheranostic Approach to Advanced Cancer Care Practical Smart Hybrid Nanostructures

Clinicians develop protocols for cancer therapy based on cancer tumour size, level, location and grade. Current nanomedicines are usually used as the monotherapy method in the preclinical settings, as well as surgery, radiotherapy and chemotherapy, alone or with the use of radiation + chemotherapy protocols. Having monotherapies has shown very limited results in terms of efficacy, and lamination is therefore difficult to achieve high therapeutic effectiveness in the clinical stage. The intrinsic potential of nanomedicine formulations with additional therapy choice is, however, utilised optimally by the advanced approach of nanomedicine and nanotheranostics (therapy + diagnostics) (Thorat & Bauer, 2020; Xiao & Chen, 2020). Indeed, nanotheranostics combine well with traditional medical therapies, such as chemotherapy and radiation. The newly proposed HNCs are capable of encapsulating multiple chemotherapy cargos, targeting moieties in solitary formulation and promoting more powerful than typical nanomedicine interactions with external physical stimulus. Advanced nanomedicine relies on nanotheranostics which therefore has many advantages: (i) nanotheranostics promote efficient vascular perfusion and drug permeability (Prasad et al., 2020; Malla et al., 2020); (ii) the high functionality characteristics of HNCs on faces gain from multi-trail loading (Mottaghitalab et al., 2019; Cazares-Cortes et al., 2019; Rawal & Patel, 2019); and (iii) locally applied physical energies further stimulate increased cargo spreads in the microenvironmental tumour environment. These aspects are exploited in combination therapy by more innovative and efficient cancer nanomedicine (Malla et al., 2020; Lagopati et al., 2021; Hatami et al., 1874; Pereira-Silva et al., 2020).

11.2.1 Hybrid Nanoplatforms in Modular Architecture

The field of cancer nanomedicine was modified to multiple modes of theranostic nanoplatforms with combined functions, including diagnoses/images; stimuli for controlled chemotherapy delivery; solid tumour treatments, following the demonstration of surface functions; geometries (spherical, rod shaped, etc.); and bioconjugation strategies in different types of HNC (Chen et al., 2020; Bueloni et al., 2020). Previous preparation protocols and methods of HNC synthesis use an approach of bulk chemistry solution that restricts the large-scale monolithic and homogenous nanostructures. Stimulating products, focused on hybrid platforms, pledge this purpose. A hybrid nanoplatform presumes that the nanocarriers are multifunctional and can respond internally or externally to stimuli from the tumour. You will also require strong stability in the circulatory system for effective passive targeting. HNPs are able to bring several medications to improve their ability to help treat cancer. The ability to diagnose HNP-dependent cancer theranostics may treat cancer. This non-traditional approach to cancer treatment allows drug release control and visualisation of medication released into the tumour. Hybrid nanocarriers and targeted polypeptides in combat cancer treatment has been tabulated and explained in Table.11.1.

The potential for use of HNP in customised care is demonstrated in these properties. Next-generation HNPs provide therapeutic molecules and therapeutic energy with double determination. Usually, the concept of theranostics belongs to the combination of medication, diagnostics and imaging in one cancer treatment protocol. In addition, nanomedicine is also called nanotheranostics, paired with theranostics on a solitary platform. Similarly to theranostics, nanotheranostics integrate nanoscale properties of nanomaterials such as surface nanoscale function and contrast improvement physics with biology to facilitate therapy and cancer diagnosis. Nanotheranostics provides broad coverage, both in preclinical and clinical trials, for the primary and secondary stage cancer detection and therapy. Thus, researchers in recent years have been exceptionally influential and widely acknowledged. Experts in cancer and researchers conclude that nanotheranostics can produce higher clinical results than the existing protocol for imaging and therapy. In addition, nanotheranostics can be incorporated into future-generation cancer therapies including PTT, MH, PDT and external regulation, enabling an excellent temporal response.

Nanostructures are easily extracted from blood circulation and therefore have low tumour penetration, despite recent progress in HNPs to improve their therapeutic efficacy. In historical terms, the enhanced permeability and retention (EPR) effect has contributed to the position of a nanocarrier in tumours. More recently, however, more criticism has been directed at the EPR principle, and some nanomedicine scientists say that the impact of EPR is only available in mouse tumours and not in humans. The engineering nanocarriers with anti-sulphur surfaces that resist unspecified serum protein adsorption and extended circulation time are the easy solution to meet maximal tumour accumulation by passive targeting. The low EPR and tumour heterogeneity can be partial and overcome by developing

Table 11.1 Hybrid nanocarriers and targeted polypeptides in combat cancer treatment

Nanocarriers	Targeted polypeptides	Targeted drug	Cancer disease targeted	Ref.
Magnetite (Fe_3O_4) nanoparticles	Serum albumin (C123H193N35O37)	DOXORUBICIN	Magnetic hyperthermia and combined chemotherapy	Natesan et al. (2017)
Magnetite (Fe_3O_4) nanoparticles	Serum albumin (C123H193N35O37)	shRNA GEMCITABINE	Magnetic hyperthermia and combined chemotherapy	Peng et al. (2016)
Magnetite (Fe_3O_4) nanoparticles	Serum albumin (C123H193N35O37)	5-Fu (FLUOROURACIL)	Magnetic targeting and combined chemotherapy	Panda et al. (2019)
Magnetite (Fe_3O_4) nanoparticles	Gelatin (C102H151O39N31)	PLATINUM (IV) PRODRUG	Magnetic targeting and combined chemotherapy	Saxena et al. (2020)
Gold (au) nanoparticles	Serum albumin (C123H193N35O37)	PACLITAXEL	Photothermal therapy and combined chemotherapy	Karthika et al. (2018)
Gold (au) nanoparticles	Serum albumin (C123H193N35O37)	SORAFENIB	Photothermal therapy and combined chemotherapy	Karthika et al. (2018); Fatematossadat et al. (2019)
Gadolinium (III) nanoparticles	Serum albumin (C123H193N35O37)	CHLARINEe6	Radiotherapy and combined chemotherapy	Usman et al. (2020)

stealth-coated HNPs and by large targeted payloads. A targeted nanosponge enveloped by the RBC membrane would be a choice. The nanosponge functions as a light under near-infrared (NIR). Photo-penetrative and photolytic agents that further damage the localised heat energy in the deep tumour tissues. The prospect for a more successful cancer cure is combined with drug use and thermal therapy, such as magnetic hyperthermia (MH), photothermic treatment (PTT) and photodynamic therapy (PDT. Local heating's duplex effect monitors the sum of medications discharged and spatial discharge control. Furthermore, due to synergetic thermo-chemo, the high temperature will boost the efficacy of the medication. Based on these interesting dual modalities of HNPs, preclinical reports demonstrated efficient photothermal damage to primary tumours and hyperthermal, immunostimulatory effect in tumour deposits, under guidance from the photoacoustic MRI method. Imaging-led light and magnetically reacting immunostimulatory nanoagents (MINPs) are suggested for primary and remotely treated tumours to cause cancer immunotherapy. HNPs undertake a photothermal effect under laser irradiation to disrupt the primary cells of the tumour and further achieve robust immune responses under light and magnetic triggers to suppress tumours for a longer time. Another

approach is to enhance circulation stabilisation and permit chemical therapeutic drug release on demand by means of a far-red-light-induced reactive oxygen species (ROS) generation, a cross-relinking HNP micellar system ROS. Spatially and temporally, non-invasive magnetic fields of hybrid superparamagnetic nanoparticles drug delivery regulated stimulus reaction. Interestingly, not only do HNP cancer theranostics include theranostic agents to assist in tumour imaging and treatment, but they also provide an opportunity to develop combination theranostic agent RMR, chemotherapeutics in an advanced cancer platform.

Hybrid nanoparticles can rationally be built to improve the accessibility of chemotherapeutic drugs to cancer tissues through deeper understanding of molecular biology of tumours. Currently, HNPs are based on the supply and release of highly cytotoxic chemodrugs in the tumour microenvironment to selectively destroy cells of cancer through cellular apoptosis or necrosis. While this selective therapy is advantageous, the penetration of the tumour and its microenvironment is restricted due to its complex exterior structure. This can be further overcome using next-generation HNPs by forming, catalysing or causing complex chemical reactions within a tumour that can produce special localised chemical compounds and products to cause a range of biological and pathological unique effects. The cancer therapy may take place via tumour-specific enzymes, for example, which may extend the exposure of the drug and establish intracellular nanoassembling. A similar strategy of intracellular tumour-specific HNPs uses a biomass composition that promotes the access to tumour cells by anticancer drugs and contributes to a successful antitumour thermal photothermia. More than one pragmatic analysis report has indicated the next-generation HNPs for the prevention of primary and metastatic cancer of the breast and therapeutic cancer colon. Such methods can be expected to improve the position and sensitivity of anticancer drugs while reducing toxicity.

11.3 Catalysis for Treating Combat Cancer Using Multidrug Resistance Free Radical Species

Modern chemotherapy with various small therapeutic molecules and their combinations is used most frequently to overcome cancer recurrence following surgery or radiation therapy (Kankala et al., 2020). However, due to a MDR that has acquired in cells through the synthesis of anti-apoptotic cascades and the overexpression of drug efflux pumps based on the cell membrane, such as P-glycoproteins (P-gp), the MDR proteins (MRP1) and Breast Cancer Resistance Protein (BCRP), which is significant, the applicability of this conventional chemotherapeutic approach is largely restricted (Sinha et al., 2019) These effects also contribute to the use of high-dose therapeutic regimens or multiple synergistic medications. In this sense, the use of nanotechnology-based drug supply systems has been able to overcome such constraints by providing various advantages of regulated and active and passive target supply patterns, making the availability of medicines more intracellular and

simpler. Moreover, multiple efflux pump inhibitors have also been immobilised, particularly limiting P-gp action, to silence MDR through nanocarriers. In this context, several efforts were made, among other things, in order to co-deliver therapeutic agents capable of combating obstacles associated with MDR through synergistic action, to develop different hybrid multifunctional nanoformulation products based on polymers, liposomes and layered double hydroxides (Miller et al., 2021).

11.3.1 Advances in Treating Combat Cancer with Multiple Break Through Nanocarriers

Advances made by numerous creative nanocarriers are based primarily on improving bioavailability and still face numerous issues including lower cargo and distribution performance, an effective battle against MDR and the restricted efficiency of penetration into solid tumours. Mesoporous silica (MSN) nanoparticles have gathered among many drug carriers based on inorganic nanomaterials. Huge interest from drug researchers because of their advantageous morphological features, such as wide surface area, adaptable pore volume and pores for efficient medical carriage of mesopores. These highly stable silica frameworks have been modifiable to deal with this limitation by doping the first-transition metals such as copper nanoparticles and iron nanoparticles to enhance the charging efficiency of medicament molecules via pH-responsive coordination interactions and allow their substantial release in the acidic tumour microenvironment.

11.3.2 Tumour Penetration Efficacy of Nanocarriers

With respect to the effectiveness of the tumour penetration, it is exceedingly difficult to enhance nanocarrier accessibility to all solid tumours due to a lack of blood perfusion. Given the challenges of an increased heterogeneous vascular network of interstitial fluid pressure and dense extracellular matrix, rational designs to boost their tumour penetration efficiency on demand are highly appropriate. However, two highly successful methods may be used to overcome this vulnerability of the nanocarriers. One is the regulation of the physicochemical features of nanometrics, such as altered sizes and shapes and the alteration of the surface by means of ligands. On the other side, tumour vasculature modulation and tumour microenvironment remodelling may be used to increase the efficacy of tumour penetration successfully. In these techniques, it would be most convenient to modify and strictly optimise the formulation and to install stimulation response on the basis of your therapeutic needs by controlling physicochemical properties with exceptional surface modification. For example, He and colleagues manufactured a size-switchable poly-L-lysine (PCL) micelle-smell dendrigrafted nano-platform, a highly

responsive, MMP-2-sensitive, MMP-1 (MMP-2) matrix-sensitive peptide. The shrinkage effect induced by these composites with the size-switchable capacity via the MMP-2 has increased penetration and conservation in vivo. In another case, Wang and colleagues formed platinum (PT) drug-dependent superstructures of the combined dendrimers (PAMAM) with ionised tertiary amine groups in the amphiphilic polymer that showed a pH response in which the size of the composite in the acidic environment decreased to less than 10 nm, from ~80 nm in the neutral pH.

11.4 Fabrication Strategies of Hierarchical Zinc-Doped Mesoporous Silica Nanocarriers (Zn-MSNs) for Combating MDR

Based on this evidence, the manufacture of hierarchical MSNs for the battle against the MDR is stated. The MSN was initially conveniently doped with Zn metal, so that in the mesoporous silica setting, they could be well co-impregnated (Zn-MSNs). Such metal-doped nanocontainers could significantly enhance the efficiency of the drug encapsulation, via coordination with amine-based drugs, which are especially suited to the acidic environment, thus facilitating the accuracy of tumour site delivery. The applications of zinc-doped mesoporous silica nanocarriers in nanomedicine have been shown in Fig. 11.2.

Doxorubicin (Dox) is chosen as a model medicine because of its amine role, as transition metals can well coordinate interactions with guest species in silica frameworks and facilitate their release through rapid protonation in the tumour microacid environment. In addition, it is an acceptable candidacy for the MDR examination. Furthermore, the design was extended by wrapping Zn-MSNs with a composite layer based on a platinum (Pt) nanoparticulate-embedded chitosan layer, which is also responsive to an acidic environment. The decorated Pt nanoparticles are one of the most fascinating characteristics of this hierarchical design. They greatly encourage the deep tumour penetration efficiency by adherence to cell interfaces due to its ultrasmic dimensions. In addition, the Pt nanoparticles can also be used to reduce cancer by means of free radical catalysis of species supported by hydrogen peroxide molecules from delivered Dox species, transforming Pt (II) ions into their Pt (II). Various in vitro experiments in MDR cells and in vivo in nude mice have been routinely carried out to show all this. In vitro pH-responsive releases of Dox molecules as well as the effectiveness of tumour penetration into a stable 3D culture of MDR cells were further investigated as well as the pericellular actin staining approach to show the effect of the engineered nanocomposites on the adhering cell junctions.

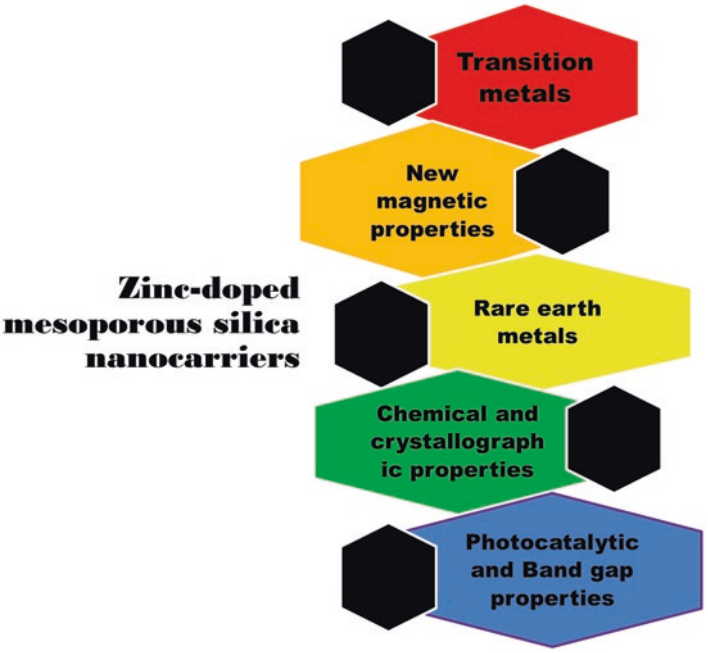

Fig. 11.2 Applications of zinc-doped mesoporous silica nanocarriers in nanomedicine

11.5 Diagnostic and Integrated Approach to Fight Against Combat Cancer Using Hybrid Nanostructures

Numerous licenced antitumour drugs and clinical trials are carried out. But, others are toxic and chemically based and have various side effects. Nanotechnology developments have allowed many therapeutic and diagnostic agents to be integrated into nanostructures. Hybrid nanostructures therefore are the most appropriate choice for diagnosing cancer. Researchers have produced a variety of hybrid nanostructures that can mix and bind to blood and cancer. Both optical and magnetic properties of different hybrid nanostructures provide a diagnostic resource for cancers at their early growth stage. The superparamagnetic characteristics of materials allow the tissue to visualise. Likewise, fluorescence imaging provides the quantum containment effect of hybrid semiconducting materials. In addition, some other hybrids may provide tumour sites with high loading capabilities with anticancer drugs. Many inorganic hybrid structures are used in the field of biological science for diagnosis and healing.

11.5.1 Nanotechnology-Based Combat Cancer Diagnosis

Due to their exceptional physicochemical features, nanostructures give some prospects for diagnosis. The nanostructures may work with various chemical agents that may allow the precise identification of cancer cells and can be used for compact identification processes. Nanoparticles can achieve effective, targeted and managed drug delivery. These systems can be tuned to improve availability of drugs in cancer cells, increase absorption and diffusion through membranes and protect medicines against degradation. Various hybrid nanostructures have been used in cancer cell diagnostic techniques. Nanostructuring is bio-conjugated to improve diagnosis with peptides, aptamers, oligonucleotides and antibodies (Sun et al., 2019; Prasher et al., 2020; Zhou, Latchoumanin, et al., 2018; Zhou, Liu, & Jiang, 2018b). Several papers on the application of nanotechnology for cancer diagnoses are available in recent literature. A simple method for labelling a cancer cell is to mix molecules with the nanoparticles with cancer-affected or transportable effects of tumours.

Golden nanoparticles and quantum dots hybrid nanostructures have gained considerable interest in cancer cell biosensors due to their higher efficiency in the use of golden nanoparticles and the radius of Forster compared with traditional organic resonance energy transfer acceptors. Targeted human breast cancer SK-BR-3 cell line is successful to aptamer S 6 conjugated hybrid nanomaterial based on SERS assay and is able to differentiate it from regular cells of the skin and other untouched M.D. Cancer cells of MDA-MB and Anderson Breast. They find that short 1.5 W/cm^2 photothermal healing with 785 nm laser is adequate to kill S6 cells with hybrid nanomaterials combined. They identified likely mechanisms and principles for targeted sensing by using photothermal treatment of hybrid materials in a breast cancer celestial cell line, with Au-single-walled carbon nanotubes (Au-SWCNT). Hybrid nanomaterials are able to produce higher temperatures that lead to a far more effective photothermal process.

11.5.2 Hybrid Nanomaterials in the Diagnosis and Treatment to Combat Cancer

In addition to polymer, non-polymeric, nanoparticles, metal-nanoparticles, AuNPs, quantity densities, spionage cells, nano-pips and nano-biomedicines, recent research activities have led to groundbreaking nanostructures. Due to the specific properties of nanomaterials, numerous nanostructures and strategies have been developed for use performance, including in vitro, in vitro analytics, targeting, drug delivery and therapeutics (Anoop et al., 2020; Alfaifi et al., 2020; Badıllı et al., 2020). A number of hybrid nanostructures have been developed by the researchers which can pass through the blood and bind to tumours. The optical and magnetic nanostructures are an early stage of development for imaging cancers. The overexpression and the delivery of image predictor and therapeutics to cancer cells are also an extra

approach. A targeted cancer surrounding with fluorescent teeth paired with anticancer antibodies that then excite the teeth from visible or NIR light sources helps to image cancer cells with fluorescence. In photodynamic therapy (PDT), however, a photosensitising medicine (PS) is used to irradiate tumour cells with light (Du et al., 2021; Wang et al., 2021; Janas et al., 2021; Yi et al., 2020). PDT's fundamental mechanism is to distribute energy or electrons to the photoactivated PS drug to oxygen or other molecules and to produce reactive oxygen species which react with the cell immediately and kill essential organelle biomolecules that lead to cell death. Fluorescence image's primary value is that visible and NIR excitement is nonionised and less dangerous in fluorescence imaging than other biomedical techniques, such as CT, X-raying and PET.

In plasma gold nanoparticles, the cooperative waves of free electrons show optical and photothermal properties in their size (Wu et al., 2017; Yang et al., 2021; Beik et al., 2019). The absorption and scattering efficiency of gold nanoparticles depending on their size, shape and structure compared to organic dyes are very high. These properties are useful when using gold as contrast agents in imagery. For cancer sensing and healing applications, the gold-containing plasmonic nanostructures are commonly used. Targeted approach for molecular imaging that enables cancer to be discovered in cells and molecular stages using gold nanorods, using conventional medical CT. In simultaneous biological imaging and photothermal therapy, hybrid nanostructures were au-ancrated. Gold nanostructures with different methods have been synthesised. For their plausible uses in cancer treatment, magnetic nanoparticles (MNPs) have been overexpressed. MNPs are based on their properties of scale, shape and surface. Hybrid nanostructures with superparamagnetic iron oxide have superior magnetic properties, which enable them to serve as potential biomedical candidates. They may serve as contrasting agents for RMI, malignant cell destructors and colloidal drug carriers for treating cancer. Various modifications were used to increase strength and circulation of MNPs such as dextran, polysaccharides, PEG and polyethylene oxide which are half-life and biocompatible.

Graphene is a recently found material. These carbonic substances are viewed as more environmental and biological than inorganic compounds, as carbon is one of the common features of our atmosphere. Due to their unique physicochemical properties, carbon nanostructured materials were especially important and led to the great potential for diagnostics and cancer treatment (Su et al., 2020; Das, Mudigunda, et al., 2020; Deepa & Pundir, 2020; Alemi et al., 2020). For sensing, diagnosis, magnetics and MRI in recent years, carbon allotropes like carbon nanotubes, graphene, fullerenes and nanodiamonds have been produced as magnetic hybrid carbon-based nanostructures. Graphene was recently found to use biosensors for its specific properties, including biomonitoring, low cytotoxicity, mechanical, electrical, optical characteristics such as stability, conductiveness, fluorescence and photoluminescence. Graphene is used individually or in conjunction with other effective cargo-selective nanomaterials, fluorescent dyes and other signalling molecules as a basic component. Different chemical or physical methods such as chemical steam deposition, mechanical exfoliation and chemical or electrochemical GO reductions can be used to obtain graphene. In a recent development, the researchers have

incorporated pH-sensitive chitosan and fluorescent CDs into a single nanostructure and developed chitosan carbon dot (CD) hybrid nanogels (CCHNs, B65 nm) (Mehra & Jain, 2016). This nanostructure is used to improve the therapeutic use of parallel NIR and NIR/pH dual-responsive delivery.

11.6 Combating Cancer Is a Heterogeneous Disorder Related to Different Cell Populations

Combat cancer is a heterogeneous disorder related to different cell populations. Understanding tumour biology is important for effective theranostic applications because cancer cells are capable of growing, differentiating, drug-resisting and forming metastases in different ways. One of the main problems in cancer theranostics is precise drug delivery to a target tumour site. While current theranostic nanomaterials have great potential, concepts and efficient implementation strategies of the next generation are important. Numerous nanoplatforms for treatment for tumours have been tested, some of which have been approved by the FDA and are used in clinics on a regular basis. However, in late-stage preclinical trials or early-stage clinical trials, the majority have failed. In future efforts, it will also be necessary to understand subcellular interactions between cancer cells and nanomaterials and not simply to manufacture more and more nanomaterials. Mechanisms of targeted theranostic nanomaterial interactions with tumour cells and the tumour microenvironment must be understood. Furthermore, future nanosystems can pass bio-barriers to any tumour site of the body.

11.7 Conclusion

Efficient nanoplatforms have their principal purpose as the reduction of the drug dose necessary to achieve a particular therapeutic effect and thereby minimise costs and side effects. Organic nanocarriers provide the strongest examples of bioconsistent nanocarriers and have properties that better conform to the physicochemical conditions in biological tissues. Inorganic materials, on the other hand, are complementary in diagnosis and calculation in the disease tissue. In preclinical characterisation, the principal challenge is the need to grasp the nanoformulation in full. For an advanced assessment of nanomedicine, particularly at the preclinical stage, a multidisciplinary expert team is needed. A broad range of data is currently available for various nanosystems at the preclinical analytical level; however, unless studies are systemically scheduled due to heterogeneity in cell lines and animal models, a firm conclusion would be difficult to achieve. It is thus possible to predict in vivo effects with nanoformulation approaches and to decide whether in vivo experiments are warranted or need to be redesigned. Further study of the in vivo immunological answer of nanoformulations is now required in vitro studies to assess the immune response.

References

Murray, F. J., Monnot, A. D., Jacobson-Kram, D., et al. (2020). A critical review of the acetaminophen preclinical carcinogenicity and tumor promotion data and their implications for its carcinogenic hazard potential. *Regulatory Toxicology and Pharmacology*, 104801.

Fan, Z., Fu, P. P., Yu, H., et al. (2014). Theranostic nanomedicine for cancer detection and treatment. *Journal of Food and Drug Analysis*, 3–17.

Li, Y., Gao, Y., Zhang, X., et al. (2020). Nanoparticles in precision medicine for ovarian cancer: From chemotherapy to immunotherapy. *International Journal of Pharmaceutics*, 119986.

Fadeel, B., & Alexiou, C. (2020). Brave new world revisited: Focus on nanomedicine. *Biochemical and Biophysical Research Communications, 533*, 36–49. Available from: http://www.sciencedirect.com/science/article/pii/S0006291X20316429.

Wu, P., Zhang, B., Ocansey, D. K. W., et al. (2020). Extracellular vesicles: A bright star of nanomedicine. *Biomaterials*, 120467. Available from: http://www.sciencedirect.com/science/article/pii/S0142961220307134.

Shetty, A., & Chandra, S. (2020). Inorganic hybrid nanoparticles in cancer theranostics: Understanding their combinations for better clinical translation. *Materials Today Chemistry, 18*, 100381. Available from: http://www.sciencedirect.com/science/article/pii/S2468519420301415.

Chen, H.-Y., Deng, J., Wang, Y., et al. (2020). Hybrid cell membrane-coated nanoparticles: A multifunctional biomimetic platform for cancer diagnosis and therapy. *Acta Biomaterialia, 112*, 1–13. Available from: http://www.sciencedirect.com/science/article/pii/S1742706120302981.

Ghitman, J., Biru, E. I., Stan, R., et al. (2020). Review of hybrid PLGA nanoparticles: Future of smart drug delivery and theranostics medicine. *Materials and Design, 193*, 108805. Available from: http://www.sciencedirect.com/science/article/pii/S0264127520303397

Andrade, K. N., Pérez, A. M. P., & Arízaga, G. G. C. (2019). Passive and active targeting strategies in hybrid layered double hydroxides nanoparticles for tumor bioimaging and therapy. *Applied Clay Science, 181*, 105214. Available from: http://www.sciencedirect.com/science/article/pii/S0169131719302728

Ferreira Soares, D. C., Domingues, S. C., Viana, D. B., et al. (2020). Polymer-hybrid nanoparticles: Current advances in biomedical applications. *Biomedicine & Pharmacotherapy, 131*, 110695. Available from: http://www.sciencedirect.com/science/article/pii/S075333222030888X

Liu, Y., Meng, X., & Bu, W. (2019). Upconversion-based photodynamic cancer therapy. *Coordination Chemistry Reviews, 379*, 82–98. Available from: http://www.sciencedirect.com/science/article/pii/S001085451730351X

Thorat, N. D., Townley, H. E., Patil, R. M., et al. (2020). Comprehensive approach of hybrid nanoplatforms in drug delivery and theranostics to combat cancer. *Drug Discovery Today, 25*, 1245–1252. Available from: http://www.sciencedirect.com/science/article/pii/S1359644620301665

Cheng, Y., Jiao, X., Fan, W., et al. (2020). Controllable synthesis of versatile mesoporous organosilica nanoparticles as precision cancer theranostics. *Biomaterials [Internet], 256*, 120191. Available from: http://www.sciencedirect.com/science/article/pii/S0142961220304373

Ghazy, E., Kumar, A., Barani, M., et al. (2020). Scrutinizing the therapeutic and diagnostic potential of nanotechnology in thyroid cancer: Edifying drug targeting by nano-oncotherapeutics. *Journal of Drug Delivery Science and Technology, 17*, 102221. Available from: http://www.sciencedirect.com/science/article/pii/S1773224720315100

Barani, M., Bilal, M., Sabir, F., et al. (2021). Nanotechnology in ovarian cancer: Diagnosis and treatment. *Life Sciences, 266*, 118914. Available from: http://www.sciencedirect.com/science/article/pii/S0024320520316738

Sharma, S., Kumari, R., Varshney, S. K., et al. (2020). Optical biosensing with electromagnetic nanostructures. *Physical Review, 5*, 100044. Available from: http://www.sciencedirect.com/science/article/pii/S2405428320300071

Ranjan, P., Parihar, A., Jain, S., et al. (2020). Biosensor-based diagnostic approaches for various cellular biomarkers of breast cancer: A comprehensive review. *Analytical Biochemistry, 610*, 113996. Available from: http://www.sciencedirect.com/science/article/pii/S0003269720305285

Dar, G. I., Zubair Iqbal, M., & Wu, A. (2019). Multifunctional biocompatible Janus nanostructures for biomedical applications. *Current Opinion in Biomedical Engineering, 10*, 79–88. Available from: http://www.sciencedirect.com/science/article/pii/S2468451119300017

Zhang, D., Yang, Z., Yu, S., et al. (2020). Diversiform metal oxide-based hybrid nanostructures for gas sensing with versatile prospects. *Coordination Chemistry Reviews, 413*, 213272. Available from: http://www.sciencedirect.com/science/article/pii/S0010854520300904

Dhas, N., Kudarha, R., Garkal, A., et al. (2021). Molybdenum-based hetero-nanocomposites for cancer therapy, diagnosis and biosensing application: Current advancement and future breakthroughs. *Journal of Controlled Release, 330*, 257–283. Available from: http://www.sciencedirect.com/science/article/pii/S0168365920307392

Nandini, D. B., Rao, R. S., Hosmani, J., et al. (2020). Novel therapies in the management of oral cancer: An update. *Disease-a-Month, 66*, 101036. Available from: http://www.sciencedirect.com/science/article/pii/S0011502920300985

Wooster, A. L., Girgis, L. H., Brazeale, H., et al. (2021). Dendritic cell vaccine therapy for colorectal cancer. *Pharmacological Research, 164*, 105374. Available from: http://www.sciencedirect.com/science/article/pii/S1043661820316820

Das, S. S., Alkahtani, S., Bharadwaj, P., et al. (2020a). Molecular insights and novel approaches for targeting tumor metastasis. *International Journal of Pharmaceutics, 585*, 119556. Available from: http://www.sciencedirect.com/science/article/pii/S0378517320305408

Levitzki, A., & Klein, S. (2010). Signal transduction therapy of cancer. *Molecular Aspects of Medicine, 31*, 287–329. Available from: http://www.sciencedirect.com/science/article/pii/S0098299710000348

Teates, C. D., & Parekh, J. S. (1993). New radiopharmaceuticals and new applications in medicine. *Current Problems in Diagnostic Radiology, 22*, 231–266. Available from: http://www.sciencedirect.com/science/article/pii/036301889390013J

Allan, N., Siller, C., & Breen, A. (2012). Anaesthetic implications of chemotherapy. *Continuing Education in Anesthesia, Critical Care and Pain, 12*, 52–56. Available from: http://www.sciencedirect.com/science/article/pii/S1743181617301695

Tewari, D., Rawat, P., & Singh, P. K. (2019). Adverse drug reactions of anticancer drugs derived from natural sources. *Food and Chemical Toxicology, 123*, 522–535. Available from: http://www.sciencedirect.com/science/article/pii/S0278691518308433

Adelberg, D. E., & Bishop, M. R. (2009). Emergencies related to cancer chemotherapy and hematopoietic stem cell transplantation. *Emergency Medicine Clinics of North America, 27*, 311–331. Available from: http://www.sciencedirect.com/science/article/pii/S0733862709000170

Imran, M., Das, K. R., & Naik, M. M. (2019). Co-selection of multi-antibiotic resistance in bacterial pathogens in metal and microplastic contaminated environments: An emerging health threat. *Chemosphere, 215*, 846–857. Available from: http://www.sciencedirect.com/science/article/pii/S0045653518319751

Thorat, N. D., & Bauer, J. (2020). Functional smart hybrid nanostructures based nanotheranostic approach for advanced cancer treatment. *Applied Surface Science, 527*, 146809. Available from: http://www.sciencedirect.com/science/article/pii/S016943322031566X

Xiao, S., & Chen, L. (2020). The emerging landscape of nanotheranostic-based diagnosis and therapy for osteoarthritis. *Journal of Controlled Release, 328*, 817–833. Available from: http://www.sciencedirect.com/science/article/pii/S0168365920306568

Prasad, R., Jain, N. K., Conde, J., et al. (2020). Localized nanotheranostics: Recent developments in cancer nanomedicine. *Materials Today Advances, 8*, 100087. Available from: http://www.sciencedirect.com/science/article/pii/S2590049820300345

Malla, R. R., Kumari, S., Kgk, D., et al. (2020). Nanotheranostics: Their role in hepatocellular carcinoma. *Critical Reviews in Oncology/Hematology, 151*, 102968. Available from: http://www.sciencedirect.com/science/article/pii/S1040842820301062

Mottaghitalab, F., Farokhi, M., Fatahi, Y., et al. (2019). New insights into designing hybrid nanoparticles for lung cancer: Diagnosis and treatment. *Journal of Controlled Release, 295*, 250–267. Available from: http://www.sciencedirect.com/science/article/pii/S0168365919300276

Cazares-Cortes, E., Cabana, S., Boitard, C., et al. (2019). Recent insights in magnetic hyperthermia: From the "hot-spot" effect for local delivery to combined magneto-photo-thermia using magneto-plasmonic hybrids. *Advanced Drug Delivery Reviews, 138*, 233–246. Available from: http://www.sciencedirect.com/science/article/pii/S0169409X18302849f

Rawal, S., & Patel, M. M. (2019). Threatening cancer with nanoparticle aided combination oncotherapy. *Journal of Controlled Release, 301*, 76–109. Available from: http://www.sciencedirect.com/science/article/pii/S0168365919301646

Lagopati, N., Evangelou, K., Falaras, P., et al. (2021). Nanomedicine: Photo-activated nanostructured titanium dioxide, as a promising anticancer agent. *Pharmacology & Therapeutics, 222*, 107795. Available from: http://www.sciencedirect.com/science/article/pii/S0163725820303260

Hatami, E., Jaggi, M., Chauhan, S. C., et al. (1874). Gambogic acid: A shining natural compound to nanomedicine for cancer therapeutics. *Biochimica et Biophysica Acta – Reviews on Cancer, 2020*, 188381. Available from: http://www.sciencedirect.com/science/article/pii/S0304419X20301001

Pereira-Silva, M., Alvarez-Lorenzo, C., Concheiro, A., et al. (2020). Nanomedicine in osteosarcoma therapy: Micelleplexes for delivery of nucleic acids and drugs toward osteosarcoma-targeted therapies. *European Journal of Pharmaceutics and Biopharmaceutics, 148*, 88–106. Available from: http://www.sciencedirect.com/science/article/pii/S0939641120300175

Bueloni, B., Sanna, D., Garribba, E., et al. (2020). Design of nalidixic acid-vanadium complex loaded into chitosan hybrid nanoparticles as smart strategy to inhibit bacterial growth and quorum sensing. *International Journal of Biological Macromolecules, 161*, 1568–1580. Available from: http://www.sciencedirect.com/science/article/pii/S0141813020340630

Natesan, S., Ponnusamy, C., Sugumaran, A., et al. (2017). Artemisinin loaded chitosan magnetic nanoparticles for the efficient targeting to the breast cancer. *International Journal of Biological Macromolecules, 104*, 1853–1859. Available from: https://www.sciencedirect.com/science/article/pii/S0141813016327222

Peng, H., Hu, C., Hu, J., et al. (2016). Fe_3O_4@mZnO nanoparticles as magnetic and microwave responsive drug carriers. *Microporous Mesoporous Mater. [Internet]., 226*, 140–145. Available from: https://www.sciencedirect.com/science/article/pii/S1387181115007179

Panda, J., Satapathy, B. S., Majumder, S., et al. (2019). Engineered polymeric iron oxide nanoparticles as potential drug carrier for targeted delivery of docetaxel to breast cancer cells. *Journal of Magnetism and Magnetic Materials, 485*, 165–173. Available from: https://www.sciencedirect.com/science/article/pii/S0304885318327185

Saxena, N., Agraval, H., Barick, K. C., et al. (2020). Thermal and microwave synthesized SPIONs: Energy effects on the efficiency of nano drug carriers. *Materials Science and Engineering: C, 111*, 110792. Available from: https://www.sciencedirect.com/science/article/pii/S0928493119340068

Karthika, V., Kaleeswarran, P., Gopinath, K., et al. (2018). Biocompatible properties of nano-drug carriers using TiO_2-Au embedded on multiwall carbon nanotubes for targeted drug delivery. *Materials Science and Engineering: C, 90*, 589–601. Available from: https://www.sciencedirect.com/science/article/pii/S0928493117334173

Fatematossadat, P. A., Mohammadi, M., & Roozmeh, S. E. (2019). Fe@(Au/Ag)n (n=1,12,54) core-shell nanoparticles as effective drug delivery vehicles for anti-cancer drugs: The computational study. *Journal of Molecular Graphics and Modelling [Internet]., 90*, 33–41. Available from: https://www.sciencedirect.com/science/article/pii/S1093326319300257

Usman, M. S., Hussein, M. Z., Kura, A. U., et al. (2020). Chlorogenic acid intercalated Gadolinium–Zinc/Aluminium layered double hydroxide and gold nanohybrid for MR imaging and drug

delivery. *Materials Chemistry and Physics [Internet], 240*, 122232. Available from: https://www.sciencedirect.com/science/article/pii/S0254058419310478

Kankala, R. K., Liu, C.-G., Yang, D.-Y., et al. (2020). Ultrasmall platinum nanoparticles enable deep tumor penetration and synergistic therapeutic abilities through free radical species-assisted catalysis to combat cancer multidrug resistance. *Chemical Engineering Journal, 383*, 123138. Available from: http://www.sciencedirect.com/science/article/pii/S1385894719325501

Sinha, B. K., Perera, L., & Cannon, R. E. (2019). Reversal of drug resistance by JS-K and nitric oxide in $ABCB_1$- and $ABCG_2$-expressing multi-drug resistant human tumor cells. *Biomedicine & Pharmacotherapy, 120*, 109468. Available from: http://www.sciencedirect.com/science/article/pii/S0753332219331464

Miller, E. M., Samec, T. M., & Alexander-Bryant, A. A. (2021). Nanoparticle delivery systems to combat drug resistance in ovarian cancer. *Nanomedicine: Nanotechnology, Biology and Medicine, 31*, 102309. Available from: http://www.sciencedirect.com/science/article/pii/S1549963420301635

Sun, D., Lu, J., Zhang, L., et al. (2019). Aptamer-based electrochemical cytosensors for tumor cell detection in cancer diagnosis: A review. *Analytica Chimica Acta, 1082*, 1–17. Available from: http://www.sciencedirect.com/science/article/pii/S0003267019308785

Prasher, P., Sharma, M., Mudila, H., et al. (2020). Emerging trends in clinical implications of bio-conjugated silver nanoparticles in drug delivery. *Colloid and Interface Science Communications, 35*, 100244. Available from: http://www.sciencedirect.com/science/article/pii/S2215038220300248

Zhou, G., Latchoumanin, O., Hebbard, L., et al. (2018a). Aptamers as targeting ligands and therapeutic molecules for overcoming drug resistance in cancers. *Advanced Drug Delivery Reviews, 134*, 107–121. Available from: http://www.sciencedirect.com/science/article/pii/S0169409X18300577

Zhou, Z., Liu, M., & Jiang, J. (2018b). The potential of aptamers for cancer research. *Analytical Biochemistry, 549*, 91–95. Available from: http://www.sciencedirect.com/science/article/pii/S0003269718302641

Anoop, V., Cutinho, L. I., Mourya, P., et al. (2020). Approaches for encephalic drug delivery using nanomaterials: The current status. *Brain Research Bulletin, 155*, 184–190. Available from: http://www.sciencedirect.com/science/article/pii/S036192301830950X

Alfaifi, A. A., Heyder, R. S., Bielski, E. R., et al. (2020). Megalin-targeting liposomes for placental drug delivery. *Journal of Controlled Release, 324*, 366–378. Available from: http://www.sciencedirect.com/science/article/pii/S0168365920303102

Badılı, U., Mollarasouli, F., Bakirhan, N. K., et al. (2020). Role of quantum dots in pharmaceutical and biomedical analysis, and its application in drug delivery. *TrAC Trends in Analytical Chemistry, 131*, 116013. Available from: http://www.sciencedirect.com/science/article/pii/S0165993620302429

Du, J., Shi, T., Long, S., et al. (2021). Enhanced photodynamic therapy for overcoming tumor hypoxia: From microenvironment regulation to photosensitizer innovation. *Coordination Chemistry Reviews, 427*, 213604. Available from: http://www.sciencedirect.com/science/article/pii/S0010854520307189

Wang, H., Guo, Y., Wang, C., et al. (2021). Light-controlled oxygen production and collection for sustainable photodynamic therapy in tumor hypoxia. *Biomaterials, 269*, 120621. Available from: http://www.sciencedirect.com/science/article/pii/S0142961220308681

Janas, K., Boniewska-Bernacka, E., Dyrda, G., et al. (2021). Porphyrin and phthalocyanine photosensitizers designed for targeted photodynamic therapy of colorectal cancer. *Bioorganic & Medicinal Chemistry, 30*, 115926. Available from: http://www.sciencedirect.com/science/article/pii/S0968089620307562

Yi, C., Yu, Z., Ren, Q., et al. (2020). Nanoscale ZnO-based photosensitizers for photodynamic therapy. *Photodiagnosis and Photodynamic Therapy, 30*, 101694. Available from: http://www.sciencedirect.com/science/article/pii/S1572100020300478

Wu, C., Li, D., Wang, L., et al. (2017). Single wavelength light-mediated, synergistic bimodal cancer photoablation and amplified photothermal performance by graphene/gold nanostar/photosensitizer theranostics. *Acta Biomaterialia, 53*, 631–642. Available from: http://www.sciencedirect.com/science/article/pii/S1742706117300879

Yang, K., Zhang, S., He, J., et al. (2021). Polymers and inorganic nanoparticles: A winning combination towards assembled nanostructures for cancer imaging and therapy. *Nano Today, 36*, 101046. Available from: http://www.sciencedirect.com/science/article/pii/S1748013220302164

Beik, J., Khateri, M., Khosravi, Z., et al. (2019). Gold nanoparticles in combinatorial cancer therapy strategies. *Coordination Chemistry Reviews, 387*, 299–324. Available from: http://www.sciencedirect.com/science/article/pii/S0010854518305393

Su, Y., Wang, N., Liu, B., et al. (2020). A phototheranostic nanoparticle for cancer therapy fabricated by BODIPY and graphene to realize photo-chemo synergistic therapy and fluorescence/photothermal imaging. *Dyes and Pigments, 177*, 108262. Available from: http://www.sciencedirect.com/science/article/pii/S0143720819323782

Das, P., Mudigunda, S. V., Darabdhara, G., et al. (2020b). Biocompatible functionalized AuPd bimetallic nanoparticles decorated on reduced graphene oxide sheets for photothermal therapy of targeted cancer cells. *Journal of Photochemistry and Photobiology B: Biology, 212*, 112028. Available from: http://www.sciencedirect.com/science/article/pii/S1011134420304784

Deepa, N. B., & Pundir, C. S. (2020). An electrochemical CD59 targeted noninvasive immunosensor based on graphene oxide nanoparticles embodied pencil graphite for detection of lung cancer. *Microchemical Journal, 156*, 104957. Available from: http://www.sciencedirect.com/science/article/pii/S0026265X20301831

Alemi, F., Zarezadeh, R., Sadigh, A. R., et al. (2020). Graphene oxide and reduced graphene oxide: Efficient cargo platforms for cancer theranostics. *Journal of Drug Delivery Science and Technology, 60*, 101974. Available from: http://www.sciencedirect.com/science/article/pii/S1773224720312636

Mehra, N. K., & Jain, N. K. (2016). Multifunctional hybrid-carbon nanotubes: New horizon in drug delivery and targeting. *Journal of Drug Targeting*, 294–308.

Chapter 12
Emerging Lipid-Coated Silica Nanoparticles for Cancer Therapy

Achraf Noureddine, Joseph D. Butner, Wei Zhu, Paulina Naydenkov, María J. Peláez, Shreya Goel, Zhihui Wang, C. Jeffrey Brinker, Vittorio Cristini, and Prashant Dogra

Contents

Achraf Noureddine and Prashant Dogra contributed equally with all other contributors.

A. Noureddine · P. Naydenkov
Department of Chemical and Biological Engineering, The University of New Mexico, Albuquerque, NM, USA

J. D. Butner · M. J. Peláez · P. Dogra (✉)
Mathematics in Medicine Program, Houston Methodist Research Institute, Houston, TX, USA
e-mail: pdogra@houstonmethodist.org

W. Zhu
MOE International Joint Research Laboratory on Synthetic Biology and Medicines, School of Biology and Biological Engineering, South China University of Technology, Guangzhou, People's Republic of China

M. Saravanan, H. Barabadi (eds.), *Cancer Nanotheranostics*, Nanotechnology in the Life Sciences, https://doi.org/10.1007/978-3-030-74330-7_12

12.1 Introduction

Challenges associated with systemic cancer chemotherapy have prompted the need for novel drug delivery systems that are capable of reducing collateral damage to healthy cells while overcoming the physical limitations that often result in failure of traditional cancer therapies (Brocato et al., 2014). This may be accomplished by delivering therapeutic concentrations of the drug specifically to the tumor site via nanoparticles (NPs) capable of targeted delivery of chemotherapeutics to solid tumors via passive (Goel et al., 2019; Attia et al., 2019; Patel & Patel, 2019) or active targeting strategies (Hosoya et al., 2016; Villegas et al., 2018; Mackowiak et al., 2013). NPs offer an additional advantage as well, in that they may be imaged in real time in vivo (Patitsa et al., 2017), thereby enabling detailed quantification of the delivered cargo, and may even be used to deliver multiple therapeutic agents simultaneously (Palanikumar et al., 2017). Thus, NPs have emerged as a highly desirable clinical tool, and nanomedicine has found applications in diagnostic imaging (Phillips et al., 2014), biosensing (Sarihi et al., 2019), and, more recently, immune stimulation for cancer and infectious diseases (Fusciello et al., 2019; Gheibi Hayat & Darroudi, 2019; Sahin et al., 2020; Staquicini et al., 2020; Shin et al., 2020; Dogra et al., 2020a). The advancements made in the field of nanomedicine have been made possible largely due to improved understanding of the pharmacological behavior of NPs (Wilhelm et al., 2016; Dogra et al., 2018; Tsoi et al., 2016; Beltrán-Gracia et al., 2019; Townson et al., 2013), which has been supported by data-driven mathematical modeling efforts that provide mechanistic insights into the pharmacokinetics of nanomaterials (Dogra et al., 2020b; Dogra et al., 2020c; Dogra, Butner, et al., 2020; Goel et al., 2020; Brachi et al., 2020; Dogra et al., 2019; Cristini et al., 2017; Wang et al., 2016; Brocato et al., 2018; Pascal et al., 2013). These predictive models are becoming increasingly useful as advancements in techniques that allow for precise control in the synthesis of NPs and accuracy of their characterization (Wang et al., 2011; Shen et al., 2014) have increased the reliability of the data used to inform the models while also increasing the precision of targeted in vivo drug delivery.

S. Goel
Department of Cancer Systems Imaging, University of Texas, MD Anderson Cancer Center, Houston, TX, USA

Z. Wang · V. Cristini
Mathematics in Medicine Program, Houston Methodist Research Institute, Houston, TX, USA

Weill Cornell Medicine, New York, NY, USA

C. J. Brinker
Department of Chemical and Biological Engineering, The University of New Mexico, Albuquerque, NM, USA

UNM Comprehensive Cancer Center, The University of New Mexico, Albuquerque, NM, USA

In the quest of the "magic bullet" for cancer therapy, nanoscale particles of various materials and physicochemical attributes have been engineered to deliver drugs and other payloads to the pathological tissue. The first NP to be used clinically was the doxorubicin-loaded liposomal formulation Doxil® (1995, Sequus Pharmaceuticals), marketed for anti-ovarian and anti-breast cancer applications. Liposomes consist of a spherical lipid bilayer vesicle enclosing an aqueous medium, and due to their dual domain, liposomes can accommodate hydrophilic drugs in their cavity and lipophilic molecules in the lipid bilayer. As of January 2020, there are nine FDA-approved liposomal formulations for clinical applications in cancer (Beltrán-Gracia et al., 2019). For over 20 years, liposomes have continued to thrive, and the most recent approved formulations are indicated for metastatic pancreatic ductal adenocarcinoma (irinotecan-based Onivyde® (2015, Merrimack)) and acute myeloid leukemia (daunorubicin/cytarabine-based Vyxeos® (2017, Jazz Pharmaceuticals)).

The success of liposomes in drug delivery is mainly driven by their biocompatibility and low immunogenicity, in addition to their ease of preparation, which allows for surface functionalization with various ligands of interest, e.g., cell-targeting agents and hydrophilic copolymers such as polyethylene glycol (PEG). However, liposomes suffer from uncontrolled drug release due to cargo leakage before arrival at the desired site of action that can potentially induce nonspecific cell death or can cause sub-therapeutic drug accumulation at the tumor site (Akbarzadeh et al., 2013). Also, due to their *soft* character, the fundamental physicochemical characteristics (e.g., size, dispersity, and surface charge) are susceptible to variation when loaded with multiple cargos of different physicochemical properties (Sarfraz et al., 2018; Sen et al., 2019) (Table 12.1).

In parallel, inorganic nanomaterial-based NPs are being increasingly developed and have shown tremendous potential in overcoming the weaknesses of liposomes and therefore are driving the progress of cancer nanomedicine. Inorganic bulky structures (such as superparamagnetic iron oxide NPs (SPIONs) (Sen et al., 2012), gold (Sugikawa et al., 2016), calcium phosphate (Wang et al., 2017), carbon (Mandlmeier et al., 2015)) are primarily used to harness their intrinsic features in applications like plasmonic heating and photothermal and photodynamic cancer therapies, as well as in bioimaging applications (Schmid et al., 2017; Gondan et al., 2018; Lee et al., 2018; Han et al., 2019), but have also been used as drug carriers through surface modifications. Porous matrices (e.g., MOFs (Cheng et al., 2018; Zhu et al., 2018; Zhu et al., 2019a) and siliceous NPs (Goel et al., 2019; Shenoi-Perdoor et al., 2016; LaBauve et al., 2018; Noureddine & Brinker, 2018; Li et al., 2014; Lei et al., 2020)) are ideally suited for cargo delivery, as their inner pores may be loaded with the cargo of interest. These benefit from controllable structure and dimensions, along with fine-tunable pore size and morphology that results in an exceptionally high surface area (>500 m^2/g) (Mohammadi et al., 2017; Zhu et al., 2019b), thereby improving payload carrying capacity. Nonetheless, both porous and non-porous inorganic nanomaterials can possess significant cytotoxicity (Soenen et al., 2015) and colloidal instability due to aggregation; however these effects may be reduced through the use of surface coatings (Guerrini et al., 2018). Owing to the clinical success of liposomal drug delivery systems, it is anticipated that lipid-coated inorganic NPs will offer advantages over

Table 12.1 Physicochemical properties, lipid coating composition, and biomedical applications of lipid-coated silica nanoparticle formulations

Hydrodynamic diameter (nm)	Zeta potential (mV)	Biomedical applications	Lipid coating composition	References
Drug delivery				
~100	–	Controllable release of drug (calcein)	DOPC/DOTAP DOPC/DOPS	Liu, Stace-Naughton, Jiang, & Brinker (2009)
50	–	Depolymerization of microtubules with enhanced efficiency using colchicine	DOPC POPC DOTAP/DOPC	Cauda et al. (2010)
~60 to 150	~ −66 to −13	Controlled release of fluorescein molecules	Phosphorylated lipid	Roggers et al. (2012)
~ 128 to 129	−25 to −22	Reduce toxicity of irinotecan drug for PDAC	DSPC/Chol/D SPE-PEG_{2000}	Liu et al. (2016)
101 to 112	−27 to −5	PDAC	DPPC/cholesterol/DSPE-PEG	Meng et al. (2015)
~80	−40 to +25	Synergistic lung cancer therapy	SPC/HHG2C18/Chol	He et al. (2016)
Gene delivery				
8 to 130	~ −20 to +35	Transfect plasmid DNA into cells	DOTAP/cholesterol	Liu, Stace-Naughton, & Brinker (2009)
60 to 150	−40 to +40	Multifunctional delivery platform	DOTAP	Möller et al. (2016)
~100 to 235	~ − 50 to +17	Loading of CRISPR and release within cancer cells	DOTAP/cholesterol/DOPE/ DSPE- PEG_{2000}	Noureddine et al. (2020)
Enhancing cargo retention				
8 to 130	~ −20 to +35	Load negatively charged calcein in negatively charged MSNs with positively charged DOTAP liposomes	DOTAP/cholesterol	Liu, Stace-Naughton, & Brinker (2009)
~50 to 300	~ −60 to +20	Load calcein using a cationic amine-modified silane	DOPS/DOTAP/DOTAP	Liu, Jiang, Ashley, & Brinker (2009)

Hydrodynamic diameter (nm)	Zeta potential (mV)	Biomedical applications	Lipid coating composition	References
101	−25 ± 1	Use of QDs for molecular imaging	DPPC/Chol/DSPE-PEG_{2000}	Pan et al. (2011b)
150	~ − 17 to +10	First MRI contrast agent and therapeutic peptide delivery system	DPPC/DSPE-PEG_{200}/Chol	Jin et al. (2017)
Tumor targeting				
165	~ − 32 to +12	Protocells as delivery platforms for siRNAs	DOPC/DOPE/Chol/ 18:1 PEG_{2000}PE	Ashley et al. (2012)
160	~ −15 to +12	Drug delivery system with spatial and temporal release control	DOPC:DOTAP	Mackowiak et al. (2013)
75–100	–	Efficient delivery of nanocarriers into solid tumors	DSPC/Chol/ /DSPE-PEG_{2000}-NH2/ DSPE- PEG_{2000}-COOH	Villegas et al. (2018)
Immunotherapy				
191 ± 3	~ − 24 to +11	Novel intradermal antigen delivery system	DOPC/DOPS/Chol	Tu et al. (2017)
~83	−5 ± 1.	Induce immunogenic cell death on PDAC	IND-PL/Chol/DSPE-PEG_{2000}	Lu et al. (2017)

other surface coatings. Coating the surface of hard NPs with various lipids imparts the NPs with the biocompatibility of lipids and improves their colloidal stability, thereby improving their prospects for clinical translation. In this chapter, we will discuss the physical principles governing the use of lipids as surface coating for siliceous nanomaterials, along with the biological and pharmacological activity of these lipid-coated NPs, and their applications in cancer therapy.

12.2 Principles of Applying Lipid Coatings to Nanomaterials

It is known that lipid fusion onto flat silica surfaces (Cha et al., 2006; Jing et al., 2014) involves a cascade of steps including adsorption through electrostatic or van der Waals interactions, rupture, self-spreading via hydrophobic interaction of lipid tails to form a lipid bilayer separated from the surface by a water layer with ~1 nm thickness, and finally the ejection of excess lipid, water, and salts back into the solution. Mornet et al. (Mornet et al., 2005) pioneered the study of the fusion of small unilamellar vesicles/liposomes (SUVs) onto sub-200 nm silica NPs via cryo-transmission electron microscopy. They observed that vesicle fusion on the curved surfaces (of spherical silica NPs) generally follows the same principles as the interactions between lipid vesicles and flat surfaces, but with additional effects due to differences in surface area, curvature, and surface charge distribution induced by the NPs. Vesicle fusion onto the NP surface starts by adsorption of entire vesicles (though deformed) onto the NP surface, followed by vesicle rupture to form discontinuous lipid patches. These catalyze the rupture of other adsorbed vesicles, leading to full surface coverage through the *active edge effect (*Reviakine & Brisson*,* 2000*)* wherein the coating strictly follows the surface roughness/contour. We summarize the parameters that dictate the fusion of lipids on the NP surface below.

12.2.1 Effect of Surface Area Ratio

The coating of NPs with lipids is a surface phenomenon, and thus the accessible surface area of the two entities of interest (i.e., liposomal surface area (S_L) and silica NP surface area (S_P)) plays a key role in their fusion. The effect of surface area ratios ($\mathbf{R} = S_L/S_P$) was first studied by Nordlund et al., who used flow cytometry to quantify the fraction of silica NPs (~600 nm) coated with DOPC/fluorescein-DHPE 200/1 lipids upon incubation with lipid vesicles (Nordlund et al., 2009). They demonstrated that the fraction of fully coated NPs gradually increased with increase in **R**. As **R** increased from 0 to 1, the percentage of coated NPs sharply increased to 60% (at $\mathbf{R} = 1$) and then grew slowly to reach 75% at $\mathbf{R} = 3$. Importantly, beyond this point, the percentage of coated NPs saturates at about 85–90% (tested across a wide range of $\mathbf{R} \sim 15$ to 290).

The above trend was also observed by Durfee et al. (Durfee et al., 2016) who additionally showed that at least $\mathbf{R} = 1$ is necessary to achieve complete fusion of

liposomes on monosized mesoporous silica NPs (MSNs) of size ~100 nm. At $\mathbf{R} < 1$, incomplete coating was verified by observation of the presence of MSN aggregates as monitored by dynamic light scattering (at a constant ionic strength). Also, for $1 \leq \mathbf{R} \leq 4$, NPs maintained a constant hydrodynamic size in 1xPBS, indicating a successful lipid coating that avoided particle aggregation in salt-rich solution. Note that the nature/size of silica NPs and the fusion conditions (buffer, sonication) were different between the two studies, which may explain the observed differences in coverage extent.

12.2.2 Effects of Surface Charge

In line with studies on flat surfaces, the surface charge plays a key role in successful lipid fusion onto the curved NP surface. Effective coverage onto negatively charged silica surfaces was only achieved with the use of lipids with positive (DOTAP) or neutral charges (DOPC, DMPC, POPC, or DOPC/DOPS 4/1), whereas a mix of DOPC/DOPS (1:1) with high negative charge resulted in deformed coatings and discontinued patches. Of note, Wang et al. have shown that surface chemistry has an even stronger effect than the absolute surface charge (Wang & Liu, 2015). This was demonstrated by using neutral DOPC and its homologous reversed-head DOCP, which possess zwitterionic headgroups with terminal ammonium and phosphate, respectively. With a terminal phosphate, DOCP fails to fuse on a negatively charged silica surface due to steric hindrance, as opposed to DOPC which binds readily to the surface.

12.2.3 Effects of Surface Curvature (Particle Size and Roughness)

NP surface curvature affects the formation of a supported lipid bilayer (SLB); these effects are greatest when NP size is comparable to the size of the lipid vesicle. If the NPs are significantly larger, the curvature effect will be minimal, and the lipid coating will locally follow a flat surface-like disposition. With respect to this, Savarala et al. showed that at a constant ionic strength and $\mathbf{R} = 1$, 50–100 nm, silica nanobeads are more efficient to form DMPC SLB than their smaller counterparts (5–25 nm) (Savarala et al., 2010) (see Fig. 12.1a). It is worth noting that 5 nm NPs could not form SLB as the lipids may form bridges between many NPs, resulting in their aggregation. The same group made use of FTIR (Ahmed & Wunder, 2009) and Raman spectroscopy (Ahmed, Nikolov, & Wunder, 2011) to confirm that both conformation and packing of DSPC, DPPC, and DMPC change as a function of the particle size (5–100 nm) and subsequently the curvature. They observed an interdigitation process of lipids (hydrophobic chains in the bilayer get closer and more

compact) that increases as the size of NP decreases (higher curvature) and is also more pronounced with longer chain lipids.

Further, Durfee et al. showed that DOTAP lipids do not fuse on small, dense silica NPs (<20 nm) and that successful fusion occurred only on particles with tested sizes with range of 30–130 nm (Liu, Stace-Naughton, & Brinker, 2009). They also showed that MSNs with 2–8 nm pore sizes were successfully coated by DSPC/cholesterol/DSPE-PEG2K (77.5:20:2.5), as opposed to 18 nm pore-MSNs (Durfee et al., 2016). In this case, cryo-EM showed that fully intact vesicles were present adjacent to the particles; this was attributed to the sharp curvature induced by the large pore size that inhibited the deposition and induced rupture of the vesicles on the particle surface (i.e., the large pore size relative to the NP diameter results in large concave regions on the NP surface, thereby disrupting the expected interaction between lipid vesicles and the NP).

12.2.4 Effect of Dispersant Ionic Strength

The liposomes are typically fused on silica NPs in an aqueous solution that is called dispersant where the final particles are suspended and "dispersed." Savarala et al. (Savarala et al., 2010; Savarala et al., 2011) showed that a higher concentration of NaCl ([NaCl]) in the dispersant promotes the formation of SLB when DMPC SUVs were incubated with silica nanobeads (of 5, 25, 45, and 100 nm hydrodynamic size) at a fixed **R** = 1 (Fig. 12.1a). While none of the beads showed formation of SLB at [NaCl] = 0 mM (pure water), they all presented SLB at 0.75 mM [NaCl]. Similarly, Durfee et al. (Durfee et al., 2016) conducted the first experiments on MSNs with a complex lipid formulation (containing multiple lipids of variable molecular weights). They showed that from 20 mM to 160 mM [NaCl], the lipid coated (LC)-MSNs were homogeneous without significant effects from the increasing salt concentration. In contrast, in pure water, fusion of liposomes on the MSNs induced a larger hydrodynamic size in the LC-MSNs, which is indicative of destabilization in the lipid coating. Although it is not clear if there is a threshold of ionic strength required for lipid fusion, especially because different cores and lipid formulations were used in the studies discussed here, all published data supports the necessity of salts in the fusion of liposomes on NPs. Additional studies can evaluate the effects of salt type, relation between the dispersant ionic strength with the surface area ratio (**R**), and the surface curvature (presented in the sections before).

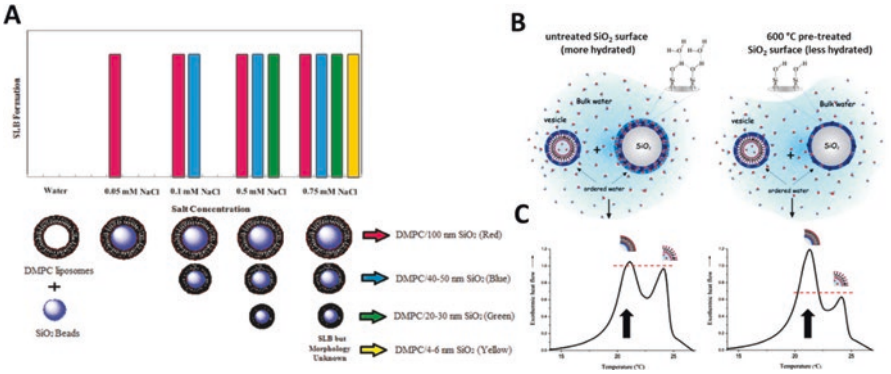

Fig. 12.1 Effect of particle size, ionic strength, and surface hydration on lipid coating of silica NPs. (**a**) Histogram depicting lipid coating as a function of NP size and ionic strength for silica nanobeads. (**b**) Schematic showing effects of surface hydration on lipid fusion: (left) untreated surface had a higher silanol density and more bound water than the (right) sample treated at 600 °C. The increased hydration repulsion results from thermal removal of bound water, increasing supported lipid bilayer (SLB) formation rate relative to the more hydrated SiO_2 that demonstrated decreased rate of SLB formation. (**c**) The nano-DSC thermograms at comparable times for the two SiO_2 surface conditions show more SLB formation (black arrow) for the less hydrated SiO_2. (Adapted with permissions from Savarala et al. (2010) and Ahmed, Madathingal, et al. (2011))

12.2.5 Effect of Hydration Repulsion

The fusion of lipid vesicles onto silica surfaces requires the removal of the hydration layers between the two surfaces, namely, the hydrophilic headgroups of the lipid and the silanol of the siliceous surface, thus inducing the "hydration repulsion effect." Ahmed et al. studied this effect on the formation of SLB (DMPC) (Ahmed, Madathingal, et al., 2011) on silica NPs via differential scanning calorimetry (DSC), cryo-EM, and FTIR (Fig. 12.1b). They demonstrated that heat-treating NPs (600 °C) reduced silanol extent and the NPs showed more effective and faster SLB formation than untreated silica NPs. This was attributed to the fact that fewer silanols on the surface exhibited fewer interactions with water molecules and therefore reduced the hydration repulsion energy required to fuse the lipid bilayer, rendering the mechanism energetically favorable. Importantly, NPs heat-treated to 1000 °C did not show coherent behavior, most likely because dehydration resulted in aggregation of the NPs that favored the formation of lipid sheaths instead of defined SLB contours.

In summary, the efficiency of the lipid bilayer shell formation over silica NP surface is dictated by the (1) liposome to silica NP surface area ratio (of at least one), (2) presence of salt in the dispersant where the fusion of liposomes and silica NPs is taking place, (3) electrostatic interaction between the liposomes and the silica surface, and (4) surface roughness and curvature that limits the lipid to follow the surface contour.

12.3 Biocompatibility, Pharmacokinetics, and Cellular Uptake

Biocompatibility and predictable in vivo pharmacokinetics (PK) is critical for the successful clinical translation of nanovectors that are intended for delivery of cytotoxic agents or other applications. In this direction, Schooneveld et al. investigated for the first time the cytotoxicity and PK of quantum dot containing silica NPs (Q-SiPaLC), which were coated with a physically adsorbed (non-covalent) monolayer of paramagnetic and PEGylated phospholipids (van Schooneveld et al., 2008). Incubation of murine macrophages with either bare- or lipid-coated silica NPs in a cell viability assay demonstrated significantly lowered toxicity of lipid-coated particles over their bare-silica counterparts (Fig. 12.2a). Lipid-coated particles also demonstrated significant improvement in in vivo circulation half-life (162 ± 34 min) compared to bare-silica NPs (14 ± 2 min). Furthermore, they studied the whole-body biodistribution of the particles in mice at various spatial scales using analytical and imaging techniques and demonstrated slower and lesser total uptake of lipid-coated particles in the mononuclear phagocytic system (MPS) organs (liver, spleen) compared to bare-silica NPs. Importantly, aggregates of bare silica NPs in the lungs and other tissues were observed through TEM imaging, while uniform distribution of lipid-coated particles were observed, highlighting the greater stability of the latter against aggregation in physiological conditions.

Durfee et al. demonstrated that their crafted monosized MSNs coated with DSPC/Chol/DSPE-PEG_{2000} 77.5:20:2.5 showed excellent safety (<5% toxicity of REH-EGFR cells at 200 μg/mL) and hemocompatibility (<5% hemolysis at 400 μg/mL) in comparison to bare MSNs that exhibited 30% and 100% hemolysis at 50 and 400 μg/mL, respectively (Fig. 12.2b) (Durfee et al., 2016). In the same year, Liu et al. (Liu et al., 2016) published a systematic study comparing the efficiency of irinotecan-bearing liposomal carriers against LC-MSNs for pancreatic ductal adenocarcinoma (PDAC), a slowly growing aggressive tumor (Zaid et al., 2020), and also showed that LC-MSNs are safer over a liposomal formulation made by Merrimack (MM-398).

Roggers et al. studied the effect of NP surface coating with four different dipalmitoyl phospholipids with different polar head groups (Roggers et al., 2012), namely, DPPC, DPPE, DPPA, and DPCL, with a focus on establishing their effects on NP cytotoxic potential. As lipid-coated NPs have a biomimetic lipid shell with headgroups oriented outward, the latter are expected to influence the interaction with cells. Interestingly, HeLa and normal liver cells showed no toxicity for all headgroups except slight cell death (<10%) in the case of DPCL. This highlighted the safety of the most common polar headgroups vis-à-vis the intended bioapplications. Further, they also conducted studies on the interaction between red blood cells (RBCs) and large mesoporous silica NPs (MSNs) (~800 nm) coated with DPPC (DPPC-l-MSN) or an RBC-mimicking lipid mixture (mRBC-l-MSN; DPPC/DPPE/cholesterol is 28:7:65) by using electron microscopy coupled with hemolysis assays and flow cytometry (Fig. 12.2c–e) (Roggers et al., 2014). Interestingly,

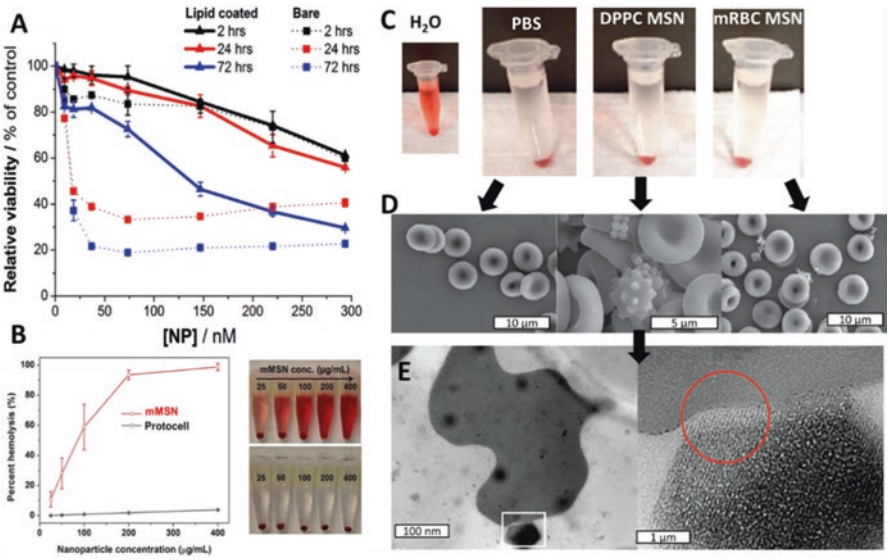

Fig. 12.2 Biocompatibility of lipid-coated silica NPs. (**a**) PEGylated phospholipid coatings lowered the cytotoxicity of silica particles on J744A cells. (**b**) The presence of lipid bilayer on monosized mesoporous silica NPs (mMSNs) to form protocells removes their hemolytic activity. (**c**) Results of hemolysis assays showing RBCs under the influence of water, PBS, PBS with DPPC-l-MSNs, and PBS with mRBC-l-MSNs (50 μg mL^{-1}). (**d**) SEM images showing RBCs exposed to no MSNs (left), DPPC-l-MSNs at 50 μg mL^{-1} (center), and mRBC-l-MSNs at 50 μg mL^{-1} (right). RBCs associated with DPPC-l-MSNs show a large amount of damage in the form of spikes; however RBCs exposed to mRBC-l-MSNs appear largely undamaged even when clearly associated with particles. (**e**) l-MSNs coated with only DPPC are shown to be in contact with a spiculated cell. A clear bending of the RBC membrane is also observed at the corner of the particle. The right panel shows a magnified image of the area marked by the white box in left panel. Notice the marked curvature of the RBC membrane. (Reproduced with permissions from van Schooneveld et al. (2008), Durfee et al. (2016), and Roggers et al. (2014))

although both nanosystems showed hemocompatibility, the SEM and TEM images revealed that unlike RBC-mimicking lipid coated-MSNs (LC-MSNs), DPPC-coated MSNs damaged the cells, leading to "spiculated" RBCs upon their interaction with the NPs.

Jin and coworkers reported a gadolinium-laden LC-MSN as an MRI contrast agent (Jin et al., 2017). The authors showed that lipid bilayer (DPPC/Chol/DSPE-PEG_{2000} (77.5:20:2.5)) enhanced the hemo- and biocompatibility of the construct. Lipid-coated Gd-MSNs showed a nearly 100% cell survival up to 100 μg/mL, whereas only 50% cell viability was obtained with lipid-free NPs, which could be attributed to Gd leaching from bare MSNs. With regard to hemocompatibility, whereas lipid-free NPs showed 40% to 75% hemolysis (at 200 and 800 μg/mL, respectively), the lipid-coated NPs demonstrated excellent hemocompatibility with no detectable lysis even at the highest reported concentration (800 μg/mL).

Paving the way to better understand NP toxicity, a biocompatibility assessment of (160–180 nm) cargo-free core-shell magnetic iron oxide-mesoporous silica NPs

(M-MSNs) uncoated or coated by a grafted PEG layer or a (DMPC) supported lipid bilayer was conducted in human liver HepaRG cells by Pisani et al. (Pisani et al., 2017). Using colorimetric MTT assay, the lowest toxicity was found with lipid-coated NPs (20%), whereas a slightly higher toxicity (25%) was induced by the other two NPs at 400 μg/mL NP concentration. In line with the latter assay, real-time cell impedance (RTCA, xCELLigence®) shows that the cell morphology and viability was less affected by DMPC-coated NPs than its counterparts (this time with NP concentration at 300 μg/mL). On the other hand, a transcriptomic analysis[1] showed that fewer genes were disrupted by lipid-coated NPs than their uncoated counterparts after 48 h exposure at 300 μg/mL (DMPC = 2606, PEG = 2800, Bare = 3440). Importantly, based on the results of the above experiments, the authors were able to identify the cellular internalization pathways involved (by using Ingenuity Pathway Analysis (IPA) software, Qiagen) and inferred that M-MSNs are engulfed by a receptor-mediated mechanism instead of the conventional clathrin- or caveolin-mediated pathways. It is noteworthy that, in this study, PEGylated NPs that were barely modulating these internalization pathways (only 10–40% compared to DMPC and MMSNs at 24 h) drastically increased to nearly the same modulation level as DMPC at 48 h. This study highlights the effects of PEG insertion into the lipid bilayer on modulation of the toxicity and response of (liver) cells toward administered nanosystems.

To understand the cellular internalization efficiency of LC-MSNs, Rosenbrand et al. compared the in vitro internalization of LC-MSNs to unmodified MSNs in patient-derived mesenchymal stem cells (Rosenbrand et al., 2018) and observed that LC-MSNs had 17 times higher internalization compared to their unmodified counterparts, without affecting the differentiation of stem cells. Clathrin-mediated endocytosis was later identified by LaBauve et al. as the mechanism of cellular uptake of LC-MSNs (LaBauve et al., 2018).

12.4 Biomedical Applications

12.4.1 Drug Delivery

Delivery of chemotherapeutics and biomolecules is one of the most important applications of nanomaterials. To this end, lipid-coated silica NPs have shown promise due to their ability to protect cargo and prevent its leakage (Jin et al., 2017; Pan et al., 2011a), permit loading of molecules through hydrophobic imprisoning or charge interaction (Liu, Jiang, Ashley, & Brinker, 2009; Noureddine et al., 2020), and, importantly, allow targeted delivery of cargo to cancerous cells via surface

[1] This is a technology that detects subtle molecular changes that occur before macroscopic physiological changes are visible. The obtained gene expression profile shows the number of differentially expressed transcripts that reflects the disruption level induced by exogenous systems (herein, NPs).

functionalization with ligands specific to cell surface receptors (Villegas et al., 2018; Mackowiak et al., 2013; Kang et al., 2016).

Pioneering work on the implementation of novel drug delivery systems based on evaporation-induced self-assembly (EISA)-produced MSNs (Lu et al., 1999; Brinker et al., 1999) encapsulated within liposomal composites were carried out by Liu and Brinker (Liu, Jiang, Ashley, & Brinker, 2009; Liu, Stace-Naughton, Jiang, & Brinker, 2009) in 2009 (Fig. 12.3a–d). They showed that LC-MSNs were able to deliver calcein, which is membrane-impermeable in its free form, into hamster ovary cells (CHO). They also showed that doxorubicin (DOX) loaded in MSNs was delivered with the same efficiency as free DOX, whereas LC-MSNs showed higher delivery efficiency of DOX through endocytosis of the carrier.

In the following year, Cauda et al. (Cauda et al., 2010) presented the first example of cargo-loaded LC-MSNs prepared via hydrolytic sol-gel (Fig. 12.3e–h). The nanosystem in this study was colchicine-loaded (microtubule polymerization inhibitor) coated with one of three lipid formulations (zwitterionic POPC, DOPC, and mix of DOTAP/DOPC 3:7) through the solvent exchange method. The system was

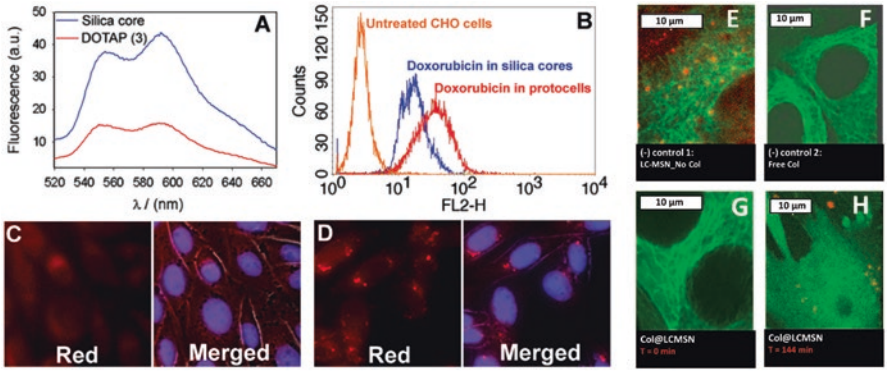

Fig. 12.3 Drug delivery applications of lipid-coated silica NPs. (**a**) Doxorubicin fluorescence spectra of the supernatant after mixing of the F-12 K medium with doxorubicin-loaded anionic silica cores or cores mixed successively with three liposomes (DOTAP/DOPS/DOTAP) for 20 min, followed by centrifugation. (**b**) Flow cytometry histogram (doxorubicin fluorescence) of CHO cells incubated with different particles. (**c**, **d**) Fluorescence microscopy studies of CHO cells incubated with (**c**) doxorubicin-loaded silica cores or (**d**) cores mixed with the three liposomes. Intense red dots in (d) indicate endocytosis instead of nonspecific uptake. Cell nuclei were stained by Hoechst 33342 (blue). (**e**–**h**) Drug delivery by colchicine loaded POPC-SLB@CMS NPs to HuH7 liver cancer cells. (**e**) Spinning disk confocal live cell imaging of untreated HuH7 cells showed a GFP-labeled well-structured microtubule network (green). (**f**) Dissolved colchicine from POPC-SLB@CMS confined into the dialysis-capped tube on the cell culture holder. After 6 h, the microtubule network of the HuH7 cells was still intact as shown by live cell imaging. (**g**) HuH7 cells with GFP-labeled microtubules (green) were exposed to colchicine-loaded POPC-SLB@CMS (CMS labeled with ATTO 633, shown in red) for <15 minutes. The microtubule network still appears to be intact. (**h**) After 144 min, the cell morphology was disintegrated, confirming cell death. (Reproduced with permissions from Liu, Jiang, Ashley, & Brinker, (2009) and Cauda et al. (2010))

dual-labeled (MSN-ATTO633 and DOPC-BODIPY) and imaged by fluorescence microscopy to study colocalization. 120 minutes post incubation with colchicine-loaded LC-MSNs, cells showed disappearance of the microtubular network, which was followed by disintegration of cell morphology 144 minutes post incubation, confirming cell death (Fig. 12.3h). However, intact microtubular network were still observed in cells incubated with unloaded LC-MSNs (up to 2 h post incubation) or with free colchicine (up to 6 h post incubation), thus highlighting the superior cellular uptake of LC-MSNs leading to efficient drug delivery.

In a novel approach, Roggers et al. covalently conjugated a dipalmitoyl (DP) monolayer to thiol-bearing MSNs via disulfide bonding (Roggers et al., 2012). The Brunauer-Emmett-Teller (BET) surface area (or simply, specific surface area) dropped from 1050 m^2/g to 49 m^2/g upon DP grafting, thus indicating the potential of this strategy in capping and controllably blocking the pores. Further, another monolayer of one of four dipalmitoyl phosphorylated lipids with different polar head groups, namely, DPPC, DPPE, DPPA, and DPCL, was then successfully added through hydrophobic interaction between the dipalmitoyl tails. This supported lipid monolayer system was developed to have an efficient triggered release behavior, where it showed controlled release of the cargo (fluorescein) upon exposure to dithiothreitol (DTT, 0.5–2 mM), an agent that mimics the reducing tumor environment, for potential drug delivery applications in tumors.

Liu et al. (Liu et al., 2016), showed that LC-MSNs exhibit improved safety and efficacy over a liposomal formulation developed by Merrimack (MM-398) and marketed as Onivyde® (usually administered when gemcitabine therapy regimen fails on PDAC patients). IVIS® imaging on IV-injected transgenic KPC mice (B6/129) and ex vivo confocal imaging on collected organs (24 h post injection) showed that NIR-labeled LC-MSNs were more stable, minimized systemic drug leakage, and enhanced accumulation in the tumor as compared to liposomes (both injected at 100 μg/mg in mice). In addition, the plasma half-life of irinotecan was found to be 1 h, 8.7 h, and 11 h in free form and liposome- and LC-MSN-encapsulated formulation, respectively, and LC-MSNs exhibited reduced toxicity to the liver, bone marrow, and gastrointestinal tract, decreased leakage, and slower release rate of drug compared to liposomal encapsulation. Importantly, LC-MSNs exhibited more potent antitumor effects and better control of local tumor spread and metastases.

Further, Meng et al. reported a highly efficient system against pancreatic cancer based on gemcitabine (GEM)-loaded LC-MSNs (Meng et al., 2015). They took advantage of the hydrophobic layer of the SLB to co-load paclitaxel (PTX) that enhanced the efficacy of GEM by inhibiting its inactivating enzyme (cytidine deaminase), which is secreted by the tumor. They assessed the efficacy of the novel platform in vivo in PANC-1 xenograft mice where tumor development was tracked after iv administration of dual-loaded LC-MSNs and compared to free drugs. Importantly, it was found that 12 doses of Abraxane were necessary to reach the same tumor shrinkage obtained by 25 μg of LC-MSNs (with 40% wt and 4% wt GEM and PTX loading, respectively). In addition, the co-release of PTX with GEM increased the DNA-related GEM metabolite 13-fold and decreased the GEM inactivating enzyme by 4-fold compared to free GEM. Later on, they also reported an oxaliplatin- and

indoximod-co-loaded immunogenic nanosytem (Jing et al., 2014); this will be detailed in the "immunotherapy" section.

Similarly, He et al. exploited the ability of LC-MSNs to co-load drugs with synergistic effects in different compartments. They reported a dual loaded nanosystem of DOX and erlotinib incorporated in positively charged MSNs coated with a lipid bilayer containing a synthetic pH-sensitive (PHS) component (He et al., 2016). As this nanosystem is internalized by tumor cells, the pH drops, and the lipid shell (DSPC/PHS/Chol is 67:21:11) gradually transitions from negative (−40 mV) to positive (+25 mV) charge, resulting in a charge repulsion mechanism with aminated MSNs. This causes the interaction between MSNs and lipid coating to weaken, allowing for a better release of retained cargo compared to a zwitterionic (DSPC/Chol is 91:9) lipid coating. Both systems were tested in vivo in C57/BL6 Lewis lung carcinoma tumor xenograft models; the PHS-containing LC-MSN restricted the tumor growth at 1 cm^3 after 17 days, whereas in the case of PHS-free LC-MSN, a tumor volume of 2.5 cm^3 was observed. Additionally, the authors showed that the cell uptake mechanism is likely an energy-dependent micropinocytosis.

12.4.2 Gene Delivery

Liu and Brinker demonstrated, for the first time, the capability of lipid-coated dense silica NPs (LC-DSNs) to transfect plasmid DNA (encoding for DsRed FP) into cells (CHO) (Liu, Stace-Naughton, & Brinker, 2009). By studying a matrix of various SLB formulations on dense silica NPs of different sizes, they established that carrier-mediated transfection efficiency highly depends on the size of the particles; while smaller LC-DSNs (30–80 nm) showed successful plasmid delivery, there was no transfection with larger used particles LC-DSN >130 nm even at higher doses. They also showed that transfecting plasmid DNA into cells via LC-DSNs strongly depends on the lipid composition, such that the best results were obtained for DOTAP/cholesterol (1:1), while reducing the cholesterol amount or inserting DOPE resulted in reduced transfection efficiency.

Moller et al. (Möller et al., 2016) utilized DOTAP coating to transfect cells with 5 nm pore-sized MSNs loaded with up to 38% wt luciferase siRNA. High gene knockdown by the system was observed in a KB wild-type cell line, but this efficacy strongly decreased when tested inMCF-7 cells.

Noureddine et al. introduced a monosized LC-MSN delivery vehicle that enables loading of CRISPR components (145 μg ribonucleoprotein (RNP) or 40 μg plasmid/mg NPs) and achieves efficient release within cancer cells (70%) (Fig. 12.4a). The RNP-loaded LC-MSN exhibited 10% gene editing in in vitro reporter cancer cell lines. In vivo data showed that RNP-loaded LC-MSN injected in the brain neurons of an Ai9-tdTomato reporter mouse model also exhibited around 10% tdTomato expression (Noureddine et al., 2020) (Ai9 mice are designed to exhibit a STOP cassette that prevents the transcription of the red-fluorescent protein tdTomato).

12.4.3 Enhancing Cargo Retention

Cargo loading is highly driven by host-guest electrostatic interactions. In this context, drugs with opposite charge relative to their carrier will be preferentially loaded. However, this feature reduces the capacity of the cargo to "leave the surface" of the nanocarrier upon arrival at the intended drug delivery location. A solution to this problem was the introduction of lipid coatings with charge opposite to both cargo and the core so that cargo loading will be driven by the lipid coating and easily released (through electrostatic repulsion with the core) once the lipids are removed. For instance, in 2009 Liu et al. (Liu, Stace-Naughton, & Brinker, 2009) were able to load a negatively charged membrane-impermeable calcein into negatively charged MSNs only after adding positively charged DOTAP liposomes that drive the loading of calcein into the surface.

In efforts to use LC-NPs for imaging applications, Pan et al. reported that lipid bilayer sealing can potentially present a solution to the bio-related toxicity of cadmium (Cd)-based quantum dots (QDs), which is caused by the leaching of Cd due to oxidation (Pan et al., 2011b). QDs of CdSe/ZnS core in a mesoporous silica shell coated with an outer layer of DPPC/Chol/DSPE-PEG_{2000} (60:33:7) decreased Cd leaching by 15-fold compared to silica-coated QDs without lipid coatings. This successful sealing of the nanocomposite avoided water and oxygen to enter deep into the system to oxidize metallic core, thereby increasing the potential of QD-core systems for in vitro and in vivo applications. More recently, the first MRI contrast agent-bearing LC-MSN was reported by Jin et al., who incorporated gadolinium (Gd) within the silica matrix (Jin et al., 2017). These NPs were loaded with the KLA peptide that is responsible for regulating mitochondrial apoptosis, and the whole system was sealed by a lipid bilayer made up of DPPC/Chol/DSPE-PEG (77.5:20:2.5). The authors demonstrated that LC-MSNs showed superior performance (stability, biocompatibility) than their lipid-free counterparts, which allowed for successful MRI on nude mice after tumors were injected by Gd-LC-MSN. The capacity of the lipids to seal the system and retain toxic Gd within the framework was demonstrated by 100% cell survival in the presence of Gd-LC-MSN as opposed to only 50% with lipid-free NPs, attributed mainly to Gd leaching. These studies show that lipid coating of NPs can reduce the heavy metal-associated toxicity in cancer imaging.

12.4.4 Tumor Targeting

Targeted delivery of cargo to cancer cells via LC-MSN was first introduced by Ashley et al. (Ashley et al., 2012) where various targeting ligands including SP-94 peptides, EGFR, transferrin, and CHALV-1 antibodies (through cross-linking thiolated ligands (terminal cysteine or sulfhydryl addition kit)) were conjugated to aminated lipids via $SM(PEG)_{24}$ bridge and lead to enhanced particle uptake by targeted

cells. Later, Mackowiak et al. also demonstrated the targeting capacity of LC-MSNs, where folate (FA) and epidermal growth factor (EGF) were introduced a posteriori by diffusion of DSPE-PEG-TL (TL, targeting ligand) onto a preformed lipid coating (DOPC/DOTAP is 7:3) (Mackowiak et al., 2013). Targeting activity was assessed by competition experiments where the internalization of LC-MSN-TL was imaged with or without incubation of KB or HuH7 cells with their corresponding overexpressed receptors, i.e., folic acid and EGFR, respectively. This step resulted in saturation of the cell receptors before exposure to the targeting ligands of the NPs. While almost no NP internalization occurred when cells were preincubated with free FA or EGF, confocal microscopy images show that targeted particles were significantly internalized (incubation 3 h, 37 °C) through receptor-mediated endocytosis without preincubation.

Paving the way for more efficient delivery of nanocarriers into solid tumors with dense extracellular matrix, Villegas Dias et al. developed a multifunctional LC-MSN platform housing an anti-cancer drug and sealed by a lipid coating (Fig. 12.4b) (Villegas et al., 2018). The particle surface was passivated by EGFR antibody (through NeutrAvidin-biotin interaction) which also functionalized the surface for cell targeting and also by pH-sensitive collagenase polymeric nanocapsules (grafted onto LC-MSNs through EDC-NHS chemistry) for loosening the dense extracellular matrix of the tumor, in order to achieve better penetration of the nanocarrier into the tumor. Collagenase-conjugated LC-MSNs loaded with chemotherapeutics were proven to be more efficient in reaching cancer cells embedded within a 3D matrix of collagen (40% cell death) in comparison to collagenase-free LC-MSNs (showing negligible effect on cells (<2% cell death)).

12.4.5 Immunotherapy

NP-induced immunotherapy is gaining much attention in recent years. In this context, lipid-coatings can be harnessed by researchers to find solutions to some complexities required to induce NP-mediated immune response. In a novel approach to implement innovative vaccination methods, ovalbumin (OVA)-loaded large pore MSN-SLBs were attached by Tu et al. on microneedle arrays devices in the efforts to develop a novel intradermal antigen delivery system (Fig. 12.5) (Tu et al., 2017). Silicon microneedles were modified with pyridine groups presenting a prominent positive charge at pH < 6. OVA-containing aminated MSN coated by a negatively charged lipid composition DOPC/DOPS/Chol (7:1:2) was used to seal the system, as it electrostatically interacts with positive the microneedles at pH 5.8. Once the microneedles pierce the human skin ex vivo where the pH is 7.4, the LCMSN will be *freed*, and the model antigen is released into the milieu. In addition to its aforementioned role, the lipid coating also extended the stability of the nanosystem to at least 1 week and lowered the OVA burst release profile compared to lipid-free MSN.

In the same year, Lu et al. reported a pioneering work on the possibility to induce an immunogenic cell death (ICD) by using immunogenic (I)-LC-MSNs on PDAC

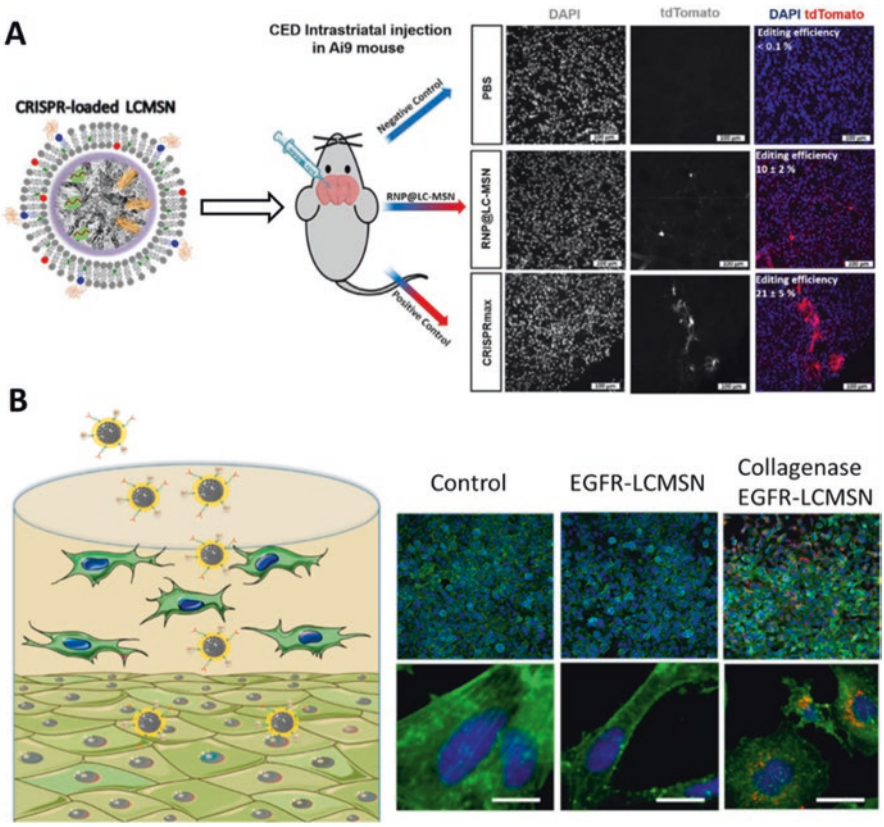

Fig. 12.4 Gene delivery and tumor targeting applications of lipid-coated silica NPs. (**a**) In vivo gene editing of RNP-loaded LC-MSNs. Confocal microscopy images of the striatum injected by PBS, RNP@LCMSN, and CRISPRmax 14 days post injection. DAPI and tdTomato alone are seen in fluorescent monochromatic images and merged (DAPI, blue; TdTomato, red). The ratio of red/blue was used to estimate the TdTomato expression upon gene editing. (**b**) Evaluation of penetration and internalization capacity of EGFR LCMSN and Collagenase EGFR LCMSN nanodevices, employing 3D tumoral tissue models. Cell nuclei are stained in blue, actin filaments were stained in green, and protocells were labeled in red (white bars correspond to 25 μm). (Reproduced with permissions from Noureddine et al. (2020) and Villegas et al. (2018))

(Lu et al., 2017). I-LC-MSNs were loaded with an ICD-inducing agent oxaliplatin (OX), and the lipid bilayer coating was engineered to incorporate indoximod moieties that interfere with the immunosuppressive indoleamine dioxygenase overexpressed in PDAC. KPC cells (a murine PDAC model cell line) were implanted in B6/129 mice, and after tumors were established, mice were IV-injected by free or ILC-MSN-co-loaded drugs (5 mg/Kg OX; 50 mg/Kg IND, corresponding to about 110 mg/Kg ILC-MSN). Mature dendritic cells (messenger cells between mammalian innate and adaptive immune systems) were enhanced to 32% when dual-loaded nanocarriers were delivered, while their concentrations remained below 18% in all other treatments. This induced significantly more tumor shrinkage (up to 8 times)

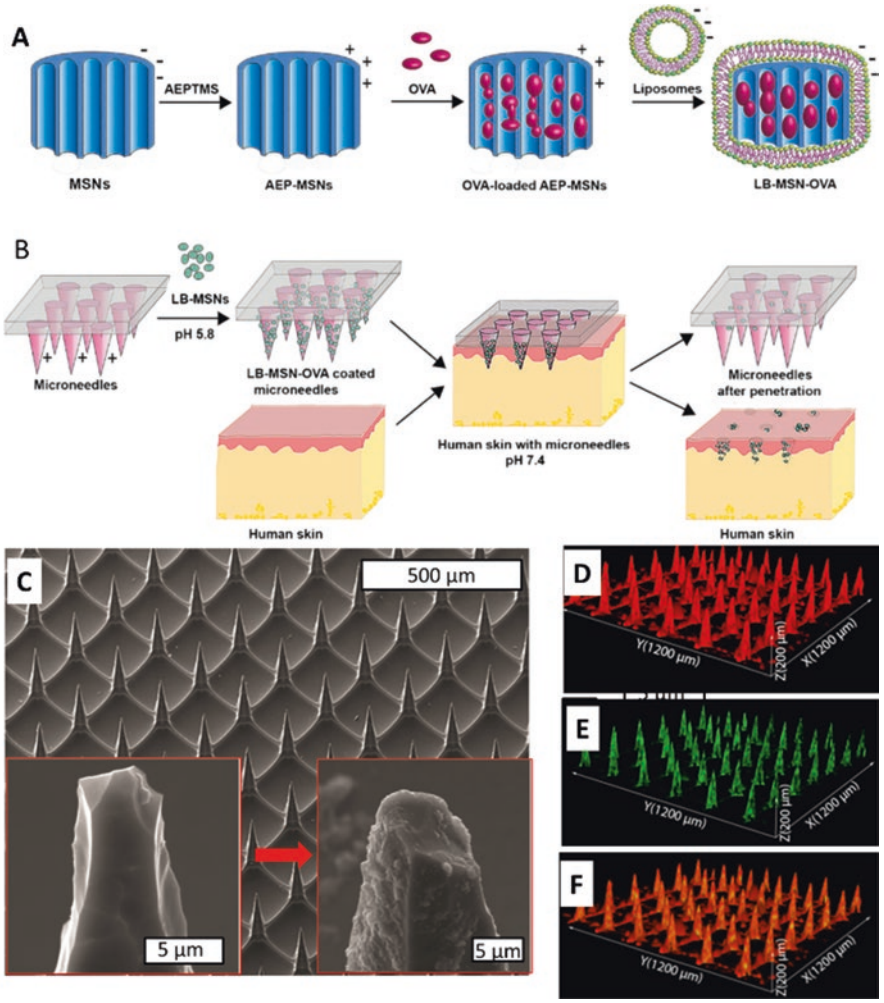

Fig. 12.5 Intradermal vaccination with microneedles covered with lipid-coated silica NPs. (**a**) Preparation and application of pH-sensitive microneedle arrays coated with LB-MSN-OVA. Encapsulation of OVA into AEP-MSNs, followed by fusion of liposomes (composed of DOPC/DOPS/cholesterol), resulting in LB-MSN-OVA. (**b**) Adsorption of LB-MSN-OVA onto pH-sensitive microneedles and penetration of microneedles into human skin, resulting in a pH shift and delivery of LB-MSN-OVA into the viable epidermis and dermis. (**c**) SEM images of pyridine-modified microneedle arrays before the adsorption of LB-MSN-OVA. Insets show a zoomed microneedle before (left) and after (right) NPs adsorption. (**d**–**f**) CLSM images of LB-MSNOVA coated microneedles. Red, DOPE-LR (**d**); Green, OVAAF488 (**e**); Merged (**f**). The x and y arrows show that the scanning area is 1200 µm × 1200 µm large. The z arrow indicates the scanning depth of 200 µm. (Reproduced with permission from Tu et al. (2017))

than free or liposome-loaded drugs and at least double the tumor shrinkage OX-loaded LC-MSN w/o IND used, thus outlining the synergistic (and somewhat unexpected) effects of IND on ICD when used along with OX.

12.5 Conclusions

In order for nanomaterials to be used as stable, safe, and efficacious agents for clinical applications, they must be synthesized reproducibly, provide predictable pharmacokinetics, and protect and deliver therapeutic concentrations of the drugs specifically to the target tumor site. Lipid-coated siliceous nanomaterials have emerged as promising candidates for drug delivery and diagnostic imaging applications due to the biocompatibility and colloidal stability conferred to NPs by lipid surface coatings and the high cargo loading capacity and structural stability provided by the inorganic siliceous core. In this chapter, we discussed the physicochemical principles of lipid coating applied to siliceous nanomaterials; the result improved nanomaterial biocompatibility, cellular internalization, and pharmacokinetics in vivo and highlighted the cancer therapy applications of these nanomaterials. The ability to combine multiple cargoes makes these nanomaterials multifunctional, and going forward, better understanding of the effects of interplay between their physicochemical properties and the biological microenvironment on their in vivo activity is necessary to support their clinical translation. Although the Cornell Dots (Phillips et al., 2014) (<7 nm) are the only siliceous NPs currently in clinical trials, we believe that the chemical versatility of bigger siliceous NPs should be better exploited to induce enhanced particle dissolution in vivo. Also, additional and complete investigations of the fate of administered NPs in correlation with their physicochemical properties and the administration route should be undertaken.

12.6 Appendix

Acronym	Definition	Acronym	Definition
BET surface area	The Brunauer-Emmett-teller surface area	**IPA**	Ingenuity pathway analysis
BL6	Mouse cell line derived from melanoma	**KB cells**	Subline of the ubiquitous KERATIN-forming tumor cell line HeLa
Cd	Cadmium	**Kg**	Kilograms
CdSe	Cadmium selenide	**KLA**	Acetyl-(KLAKLAK)2-NH2

Acronym	Definition	Acronym	Definition
C57	A common inbred strain of laboratory mouse	**KPC**	Mouse is an established and clinically relevant model of pancreatic ductal adenocarcinoma
CHALV-1 antibodies	Hepatocellular carcinoma antibody	**LC**	Lipid coated
CHO	Hamster ovary cells	**MCF-7**	Human breast cancer cell line with estrogen, progesterone, and glucocorticoid receptors
Chol	Cholesterol	**mg**	Milligrams
Cryo-em	Cryogenic electron microscopy	**MMSN**	Magnetic-silica nanoparticles
DHPE	N-(Fluorescein-5-Thiocarbamoyl)-1,2-dihexadecanoyl-*sn*-glycero-3--phosphoethanolamine, triethylammonium salt	**MPS**	Mononuclear phagocytic system
DMPC	1,2-dimyristoyl-sn-glycero-3--phosphocholine	**MOFs**	Metal-organic frameworks
DOCP	2-((2,3-Bis(oleoyloxy)propyl) dimethylammonio)ethyl hydrogen phosphate	**MRI**	Magnetic resonance imaging
DOPC	1,2-Dioleoyl-sn-glycero-3--phosphocholine	**MSN**	Mesoporous silica nanoparticles
DOPE	1,2-Dioleoyl-sn-glycero-3--phosphoethanolamine	**mV**	Millivolt
DOPS	1,2-Dioleoyl-*sn*-glycero-3--phosphocholine	**NPs**	Nanoparticles
DOTAP	Dioleoyl-3-trimethylammonium propane	**OVA**	Ovalbumin
DOX	Doxorubicin	**OX**	Oxaliplatin
DP	Covalently conjugated dipalmitoyl	**PANC-1**	Human pancreatic cancer cell line isolated from a pancreatic carcinoma of ductal cell origin
DPCL	Cardiolipin/N-dodecylpyridinium chloride	**PDAC**	Pancreatic ductal adenocarcinoma
DPPA	1,2-Distearoyl-sn-glycero-3--phosphoethanolamine-N-diethylenetriaminepentaacetic acid	**PEG**	Polyethylene glycol
DPPC	1,2-Dipalmitoyl-sn-glycero-3--phosphocholine	**PHS**	pH-sensitive
DPPE	Phosphatidylethanolamine/ 1,2-Bis(diphenylphosphino)ethane	**PK**	Pharmacokinetics
DSC	Differential scanning calorimetry	**POPC**	1-Palmitoyl-2-oleoyl-sn--glycero-3-phosphocholine
DSN	Ocetaxel-loaded solid lipid nanoparticles	**PTX**	Paclitaxel
DSPC	1,2-Distearoyl-sn-glycero-3--phosphocholine	**QDs**	Quantum dots

Acronym	Definition	Acronym	Definition
DSPE	1,2-Distearoyl-sn-glycero-3--phosphoethanolamine	**Q-SiPaLC**	Quantum dot containing silica nanoparticles
DTT	Dithiothreitol	**RBCs**	Red blood cells
EGF	Epidermal growth factor	**RNP**	Ribonucleoprotein
EGFR	Epidermal growth factor receptor	**siRNA**	Small interfering RNA
EISA	Evaporation-induced self-assembly	**SEM**	Scanning electron microscope
FA	Folate	**SLB**	Supported lipid bilayer
FDA	Food and Drug Administration	**SM(PEG)24**	(Succinimidyl-[(N-maleimidopropionamido)-tetracosaethyleneglycol] ester) cross-linker
FTIR	Fourier-transform infrared spectroscopy	**SP-94**	Targeting peptide for hepatocellular carcinoma
Gd	Gadolinium(III)	**SUVs**	Small unilamellar vesicles/liposomes
GEM	Gemcitabine	**TEM**	Transmission electron microscopy
HuH7 cells	Derived cellular carcinoma cell line that was originally taken from a liver tumor	**TL**	Targeting ligand
I	Immunogenic	**ZnS**	Zinc sulfide

References

Ahmed, S., Madathingal, R. R., Wunder, S. L., Chen, Y., & Bothun, G. (2011). Hydration repulsion effects on the formation of supported lipid bilayers. *Soft Matter, 7*, 1936–1947. https://doi.org/10.1039/C0SM01045F

Ahmed, S., Nikolov, Z., & Wunder, S. L. (2011). Effect of curvature on nanoparticle supported lipid bilayers investigated by Raman spectroscopy. *The Journal of Physical Chemistry B, 115*, 13181–13190. https://doi.org/10.1021/jp205999p

Ahmed, S., & Wunder, S. L. (2009). Effect of high surface curvature on the main phase transition of supported phospholipid bilayers on SiO2 nanoparticles. *Langmuir, 25*, 3682–3691. https://doi.org/10.1021/la803630m

Akbarzadeh, A., et al. (2013). Liposome: Classification, preparation, and applications. *Nanoscale Research Letters, 8*. https://doi.org/10.1186/1556-276X-8-102

Ashley, C. E., et al. (2012). Delivery of small interfering RNA by peptide-targeted mesoporous silica nanoparticle-supported lipid bilayers. *ACS Nano, 6*, 2174–2188. https://doi.org/10.1021/nn204102q

Attia, M. F., et al. (2019). An overview of active and passive targeting strategies to improve the nanocarriers efficiency to tumour sites. *Journal of Pharmacy and Pharmacology, 71*, 1185–1198.

Beltrán-Gracia, E., et al. (2019). Nanomedicine review: Clinical developments in liposomal applications. *Cancer Nanotechnology, 10*. https://doi.org/10.1186/s12645-019-0055-y

Brachi, G., et al. (2020). Intratumoral injection of hydrogel-embedded nanoparticles enhances retention in glioblastoma. *Nanoscale*.

Brinker, C. J., Lu, Y., Sellinger, A., & Fan, H. (1999). Evaporation-induced self-assembly: Nanostructures made easy. *Advanced Materials, 11*, 579–585. https://doi.org/10.1002/(SICI)1521-4095(199905)11:7<579::AID-ADMA579>3.0.CO;2-R

Brocato, T., et al. (2014). Understanding drug resistance in breast cancer with mathematical oncology. *Current Breast Cancer Reports, 6*, 110–120.

Brocato, T. A., et al. (2018). Understanding the connection between nanoparticle uptake and cancer treatment efficacy using mathematical modeling. *Scientific Reports, 8*, 7538.

Cauda, V., et al. (2010). Colchicine-loaded lipid bilayer-coated 50 nm mesoporous nanoparticles efficiently induce microtubule depolymerization upon cell uptake. *Nano Letters, 10*, 2484–2492. https://doi.org/10.1021/nl100991w

Cha, T., Guo, A., & Zhu, X. Y. (2006). Formation of supported phospholipid bilayers on molecular surfaces: Role of surface charge density and electrostatic interaction. *Biophysical Journal, 90*, 1270–1274. https://doi.org/10.1529/biophysj.105.061432

Cheng, G., et al. (2018). Self-assembly of extracellular vesicle-like metal-organic framework nanoparticles for protection and intracellular delivery of biofunctional proteins. *Journal of the American Chemical Society, 140*, 7282–7291. https://doi.org/10.1021/jacs.8b03584

Cristini, V., Koay, E., & Wang, Z. (2017). *An introduction to physical oncology: How mechanistic mathematical modeling can improve cancer therapy outcomes*. CRC Press.

Dogra, P., Butner, J. D., Ramírez, J. R., Cristini, V., & Wang, Z. (2020). *2020 42nd Annual International Conference of the IEEE Engineering in Medicine & Biology Society (EMBC)* (pp. 2447–2450).

Dogra, P., et al. (2018). Establishing the effects of mesoporous silica nanoparticle properties on in vivo disposition using imaging-based pharmacokinetics. *Nature Communications, 9*, 4551.

Dogra, P., et al. (2019). Mathematical modeling in cancer nanomedicine: A review. *Biomedical Microdevices, 21*, 40.

Dogra, P., et al. (2020a). Innate immunity plays a key role in controlling viral load in COVID-19: mechanistic insights from a whole-body infection dynamics model. *medRxiv*.

Dogra, P., et al. (2020b). Image-guided mathematical modeling for pharmacological evaluation of nanomaterials and monoclonal antibodies. *Wiley Interdisciplinary Reviews. Nanomedicine and Nanobiotechnology*, e1628. https://doi.org/10.1002/wnan.1628

Dogra, P., et al. (2020c). A mathematical model to predict nanomedicine pharmacokinetics and tumor delivery. *Computational and Structural Biotechnology Journal, 18*, 518–531.

Durfee, P. N., et al. (2016). Mesoporous silica nanoparticle-supported lipid bilayers (protocells) for active targeting and delivery to individual leukemia cells. *ACS Nano, 10*, 8325–8345. https://doi.org/10.1021/acsnano.6b02819

Fusciello, M., et al. (2019). Artificially cloaked viral nanovaccine for cancer immunotherapy. *Nature Communications, 10*, 5747. https://doi.org/10.1038/s41467-019-13744-8

Gheibi Hayat, S. M., & Darroudi, M. (2019). Nanovaccine: A novel approach in immunization. *Journal of Cellular Physiology, 234*, 12530–12536. https://doi.org/10.1002/jcp.28120

Goel, S., et al. (2019). Size-optimized ultrasmall porous slica nanoparticles depict vasculature-based differential targeting in triple negative breast cancer. *Small*, e1903747. https://doi.org/10.1002/smll.201903747

Goel, S., et al. (2020). Sequential deconstruction of composite drug transport in metastatic breast cancer. *Science Advances, 6*, eaba4498.

Gondan, A. I. B., et al. (2018). Effective cancer immunotherapy in mice by polyIC-imiquimod complexes and engineered magnetic nanoparticles. *Biomaterials, 170*, 95–115.

Guerrini, L., Alvarez-Puebla, R. A., & Pazos-Perez, N. J. M. (2018). Surface modifications of nanoparticles for stability in biological fluids. *Materials (Basel), 11*, 1154.

Han, C., et al. (2019). Multifunctional iron oxide-carbon hybrid nanoparticles for targeted fluorescent/MR dual-modal imaging and detection of breast cancer cells. *Analytica Chimica Acta, 1067*, 115–128.

He, Y., Su, Z., Xue, L., Xu, H., & Zhang, C. (2016). Co-delivery of erlotinib and doxorubicin by pH-sensitive charge conversion nanocarrier for synergistic therapy. *Journal of Controlled Release, 229*, 80–92. https://doi.org/10.1016/j.jconrel.2016.03.001

Hosoya, H., et al. (2016). Integrated nanotechnology platform for tumor-targeted multimodal imaging and therapeutic cargo release. *Proceedings of the National Academy of Sciences, 113*, 1877. https://doi.org/10.1073/pnas.1525796113

Jin, Y., et al. (2017). Nanosystem composed with MSNs, gadolinium, liposome and cytotoxic peptides for tumor theranostics. *Colloids and Surfaces B: Biointerfaces, 151*, 240–248. https://doi.org/10.1016/j.colsurfb.2016.12.024

Jing, Y., Trefna, H., Persson, M., Kasemo, B., & Svedhem, S. (2014). Formation of supported lipid bilayers on silica: Relation to lipid phase transition temperature and liposome size. *Soft Matter, 10*, 187–195. https://doi.org/10.1039/c3sm50947h

Kang, J., et al. (2016). Self-sealing porous silicon-calcium silicate core-shell nanoparticles for targeted siRNA delivery to the injured brain. *Advanced Materials, 28*, 7962–7969. https://doi.org/10.1002/adma.201600634

LaBauve, A. E., et al. (2018). Lipid-coated mesoporous silica nanoparticles for the delivery of the ML336 antiviral to inhibit encephalitic alphavirus infection. *Scientific Reports, 8*, 13990. https://doi.org/10.1038/s41598-018-32033-w

Lee, B., et al. (2018). Nanoparticle delivery of CRISPR into the brain rescues a mouse model of fragile X syndrome from exaggerated repetitive behaviours. *Nature Biomedical Engineering, 2*, 497–507.

Lei, Q., et al. (2020). Sol–gel-based advanced porous silica materials for biomedical applications. *Advanced Functional Materials, 30*. https://doi.org/10.1002/adfm.201909539

Li, X., et al. (2014). Anisotropic growth-induced synthesis of dual-compartment janus mesoporous silica nanoparticles for bimodal triggered drugs delivery, Journal of the American Chemical Society*., 136*, 15086–15092. https://doi.org/10.1021/ja508733r

Liu, J., Jiang, X., Ashley, C., & Brinker, C. J. (2009). Electrostatically mediated liposome fusion and lipid exchange with a nanoparticle-supported bilayer for control of surface charge, drug containment, and delivery. *Journal of the American Chemical Society, 131*, 7567–7569. https://doi.org/10.1021/ja902039y

Liu, J., Stace-Naughton, A., & Brinker, C. J. (2009). Silica nanoparticle supported lipid bilayers for gene delivery. *Chemical Communications*, 5100–5102. https://doi.org/10.1039/B911472F

Liu, J., Stace-Naughton, A., Jiang, X., & Brinker, C. J. (2009). Porous nanoparticle supported lipid bilayers (protocells) as delivery vehicles. *Journal of the American Chemical Society, 131*, 1354–1355. https://doi.org/10.1021/ja808018y

Liu, X., et al. (2016). Irinotecan delivery by lipid-coated mesoporous silica nanoparticles shows improved efficacy and safety over liposomes for pancreatic cancer. *ACS Nano, 10*, 2702–2715. https://doi.org/10.1021/acsnano.5b07781

Lu, J., et al. (2017). Nano-enabled pancreas cancer immunotherapy using immunogenic cell death and reversing immunosuppression. *Nature Communications, 8*, 1811. https://doi.org/10.1038/s41467-017-01651-9

Lu, Y., et al. (1999). Aerosol-assisted self-assembly of mesostructured spherical nanoparticles. *Nature, 398*, 223–226. https://doi.org/10.1038/18410

Mackowiak, S. A., et al. (2013). Targeted drug delivery in cancer cells with red-light photoactivated mesoporous silica nanoparticles. *Nano Letters, 13*, 2576–2583. https://doi.org/10.1021/nl400681f

Mandlmeier, B., et al. (2015). Lipid-bilayer coated nanosized bimodal mesoporous carbon spheres for controlled release applications. *Journal of Materials Chemistry B, 3*, 9323–9329. https://doi.org/10.1039/c5tb01635e

Meng, H., et al. (2015). Use of a lipid-coated mesoporous silica nanoparticle platform for synergistic gemcitabine and paclitaxel delivery to human pancreatic cancer in mice. *ACS Nano, 9*, 3540–3557. https://doi.org/10.1021/acsnano.5b00510

Mohammadi, M. R., et al. (2017). Nanomaterials engineering for drug delivery: A hybridization approach. *Journal of Materials Chemistry B, 5*, 3995–4018. https://doi.org/10.1039/c6tb03247h

Möller, K., et al. (2016). Highly efficient siRNA delivery from core–shell mesoporous silica nanoparticles with multifunctional polymer caps. *Nanoscale, 8*, 4007–4019. https://doi.org/10.1039/C5NR06246B

Mornet, S., Lambert, O., Duguet, E., & Brisson, A. (2005). The formation of supported lipid bilayers on silica nanoparticles revealed by cryoelectron microscopy. *Nano Letters, 5*, 281–285. https://doi.org/10.1021/nl048153y

Nordlund, G., Lönneborg, R., & Brzezinski, P. (2009). Formation of supported lipid bilayers on silica particles studied using flow cytometry. *Langmuir, 25*, 4601–4606. https://doi.org/10.1021/la8036296

Noureddine, A., & Brinker, C. J. (2018). Pendant/bridged/mesoporous silsesquioxane nanoparticles: Versatile and biocompatible platforms for smart delivery of therapeutics. *Chemical Engineering Journal, 340*, 125–147. https://doi.org/10.1016/j.cej.2018.01.086

Noureddine, A., et al. (2020). Engineering of monosized lipid-coated mesoporous silica nanoparticles for CRISPR delivery. *Acta Biomaterialia, 114*, 358–368. https://doi.org/10.1016/j.actbio.2020.07.027

Palanikumar, L., et al. (2017). Spatiotemporally and sequentially-controlled drug release from polymer gatekeeper–hollow silica nanoparticles. *Scientific Reports, 7*, 46540.

Pan, J., Wan, D., & Gong, J. (2011a). PEGylated liposome coated QDs/mesoporous silica core-shell nanoparticles for molecular imaging. *Chemical Communications, 47*, 3442–3444. https://doi.org/10.1039/C0CC05520D

Pan, J., Wan, D., & Gong, J. (2011b). PEGylated liposome coated QDs/mesoporous silica core-shell nanoparticles for molecular imaging. *Chemical Communications (Camb), 47*, 3442–3444. https://doi.org/10.1039/c0cc05520d

Pascal, J., et al. (2013). Mechanistic modeling identifies drug-uptake history as predictor of tumor drug resistance and nano-carrier-mediated response. *ACS Nano, 7*, 11174–11182.

Patel, J. K., & Patel, A. P. (2019). *Surface modification of nanoparticles for targeted drug delivery* (pp. 125–143). Springer.

Patitsa, M., et al. (2017). Magnetic nanoparticles coated with polyarabic acid demonstrate enhanced drug delivery and imaging properties for cancer theranostic applications. *Scientific Reports, 7*, 1–8.

Phillips, E., et al. (2014). Clinical translation of an ultrasmall inorganic optical-PET imaging nanoparticle probe. *Science Translational Medicine, 6*, 260ra149–260ra149.

Pisani, C., et al. (2017). Biocompatibility assessment of functionalized magnetic mesoporous silica nanoparticles in human HepaRG cells. *Nanotoxicology, 11*, 871–890. https://doi.org/10.1080/17435390.2017.1378749

Reviakine, I., & Brisson, A. (2000). Formation of supported phospholipid bilayers from unilamellar vesicles investigated by atomic force microscopy. *Langmuir, 16*, 1806–1815.

Roggers, R. A., Joglekar, M., Valenstein, J. S., & Trewyn, B. G. (2014). Mimicking red blood cell lipid membrane to enhance the hemocompatibility of large-pore mesoporous silica. *ACS Applied Materials & Interfaces, 6*, 1675–1681. https://doi.org/10.1021/am4045713

Roggers, R. A., Lin, V. S. Y., & Trewyn, B. G. (2012). Chemically reducible lipid bilayer coated mesoporous silica nanoparticles demonstrating controlled release and HeLa and normal mouse liver cell biocompatibility and cellular internalization. *Molecular Pharmaceutics, 9*, 2770–2777. https://doi.org/10.1021/mp200613y

Rosenbrand, R., et al. (2018). Lipid surface modifications increase mesoporous silica nanoparticle labeling properties in mesenchymal stem cells. *International Journal of Nanomedicine, 13*, 7711.

Sahin, U., et al. (2020). COVID-19 vaccine BNT162b1 elicits human antibody and TH 1 T cell responses. *Nature, 586*, 594–599.

Sarfraz, M., et al. (2018). Development of dual drug loaded nanosized liposomal formulation by a reengineered ethanolic injection method and its pre-clinical pharmacokinetic studies. *Pharmaceutics, 10*. https://doi.org/10.3390/pharmaceutics10030151

Sarihi, P., et al. (2019). Nanoparticles for biosensing. *Nanomaterials for Advanced Biological Applications*, 121–143. https://doi.org/10.1007/978-3-030-10834-2_5

Savarala, S., Ahmed, S., Ilies, M. A., & Wunder, S. L. (2010). Formation and colloidal stability of DMPC supported lipid bilayers on SiO2 nanobeads. *Langmuir, 26*, 12081–12088. https://doi.org/10.1021/la101304v

Savarala, S., Ahmed, S., Ilies, M. A., & Wunder, S. L. (2011). Stabilization of soft lipid colloids: Competing effects of nanoparticle decoration and supported lipid bilayer formation. *ACS Nano, 5*, 2619–2628. https://doi.org/10.1021/nn1025884

Schmid, D., et al. (2017). T cell-targeting nanoparticles focus delivery of immunotherapy to improve antitumor immunity. *Nature Communications, 8*, 1–12.

Sen, K., et al. (2019). Dual drug loaded liposome bearing apigenin and 5-Fluorouracil for synergistic therapeutic efficacy in colorectal cancer. *Colloids and surfaces B: Biointerfaces, 180*, 9–22. https://doi.org/10.1016/j.colsurfb.2019.04.035

Sen, T., et al. (2012). Simple one-pot fabrication of ultra-stable core-shell superparamagnetic nanoparticles for potential application in drug delivery. *RSC advances, 2*, 5221–5228. https://doi.org/10.1039/c2ra20199b

Shen, D., et al. (2014). Biphase stratification approach to three-dimensional dendritic biodegradable mesoporous silica nanospheres. *Nano Letters, 14*, 923–932.

Shenoi-Perdoor, S., et al. (2016). Click functionalization of sol–gel materials. In *Handbook of sol-gel science and tchnology* (pp. 1–40). https://doi.org/10.1007/978-3-319-19454-7_95-1

Shin, M. D., et al. (2020). COVID-19 vaccine development and a potential nanomaterial path forward. *Nature Nanotechnology, 15*, 646–655.

Soenen, S. J., Parak, W. J., Rejman, J., & Manshian, B. J. (2015). (Intra) cellular stability of inorganic nanoparticles: effects on cytotoxicity, particle functionality, and biomedical applications. *Chemical Reviews, 115*, 2109–2135.

Staquicini, D. I., et al. (2020). Targeted phage display-based pulmonary vaccination in mice and non-human primates. *Medicine*.

Sugikawa, K., et al. (2016). Anisotropic self-assembly of citrate-coated gold nanoparticles on fluidic liposomes. *Angewandte Chemie International Edition in English (1962–1997), 128*, 4127–4131. https://doi.org/10.1002/ange.201511785

Townson, J. L., et al. (2013). Re-examining the size/charge paradigm: Differing in vivo characteristics of size-and charge-matched mesoporous silica nanoparticles. *Journal of the American Chemical Society, 135*, 16030–16033.

Tsoi, K. M., et al. (2016). Mechanism of hard-nanomaterial clearance by the liver. *Nature Materials, 15*, 1212–1221.

Tu, J., et al. (2017). Mesoporous silica nanoparticle-coated microneedle arrays for intradermal antigen delivery. *Pharmaceutical Research, 34*, 1693–1706. https://doi.org/10.1007/s11095-017-2177-4

van Schooneveld, M. M., et al. (2008). Improved biocompatibility and pharmacokinetics of silica nanoparticles by means of a lipid coating: A multimodality investigation. *Nano Letters, 8*, 2517–2525. https://doi.org/10.1021/nl801596a

Villegas, M. R., et al. (2018). Multifunctional protocells for enhanced penetration in 3D extracellular tumoral matrices. *Chemistry of Materials, 30*, 112–120. https://doi.org/10.1021/acs.chemmater.7b03128

Wang, F., & Liu, J. (2015). A stable lipid/TiO2 interface with headgroup-inversed phosphocholine and a comparison with SiO2. *Journal of the American Chemical Society, 137*, 11736–11742. https://doi.org/10.1021/jacs.5b06642

Wang, J., Byrne, J. D., Napier, M. E., & DeSimone, J. M. (2011). More effective nanomedicines through particle design. *Small, 7*, 1919–1931.

Wang, X., et al. (2017). Designed synthesis of lipid-coated polyacrylic acid/calcium phosphate nanoparticles as dual pH-responsive drug-delivery vehicles for cancer chemotherapy. *Chemistry, 23*, 6586–6595. https://doi.org/10.1002/chem.201700060

Wang, Z., et al. (2016). Theory and experimental validation of a spatio-temporal model of chemotherapy transport to enhance tumor cell kill. *PLoS Computational Biology, 12*, e1004969.

Wilhelm, S., et al. (2016). Analysis of nanoparticle delivery to tumours. *Nature Reviews Materials, 1*, 16014.

Zaid, M., et al. (2020). Imaging-based subtypes of pancreatic ductal adenocarcinoma exhibit differential growth and metabolic patterns in the pre-diagnostic period: Implications for early detection. *Frontiers in Oncology, 10*, 2629.

Zhu, W., et al. (2018). Versatile surface functionalization of metal–organic frameworks through direct metal coordination with a phenolic lipid enables diverse applications. *Advanced Functional Materials, 28*. https://doi.org/10.1002/adfm.201705274

Zhu, W., et al. (2019a). Modular metal–organic polyhedra superassembly: From molecular-level design to targeted drug delivery. *Advanced Materials, 31*. https://doi.org/10.1002/adma.201806774

Zhu, W., et al. (2019b). Conversion of metal-organic cage to ligand-free ultrasmall noble metal nanocluster catalysts confined within mesoporous silica nanoparticle supports. *Nano Letters, 19*, 1512–1519. https://doi.org/10.1021/acs.nanolett.8b04121